

**COMPARISON OF FLAME SPREAD
MEASUREMENTS USING THE ASTM E
1321 LIFT AND A REDUCED SCALE
ADAPTATION OF THE CONE
CALORIMETER APPARATUS**

BY

GEOFFREY MERRYWEATHER

SUPERVISED BY

MICHAEL SPEARPOINT

A thesis submitted in partial fulfilment of the requirements for the
Degree of Masters of Engineering in Fire Engineering
at the University of Canterbury

Department of Civil Engineering

University of Canterbury

Private Bag 4800

Christchurch, New Zealand

Phone: +64 3 364 2250

Fax: +64 3 364 2758

March 2006

Abstract

A full-scale ASTM E 1321 Lateral ignition and Flame Transport (LIFT) apparatus was constructed and compared with a Reduced scale Ignition and Flame spread Test apparatus (RIFT) adaptation of the cone calorimeter in the vertical position. The objective was to find a low cost and simple alternative to the LIFT apparatus for measuring opposed flow flame spread.

Ignition tests were conducted using the LIFT, RIFT and ISO 5657 ignitability apparatus and flame spread experiments were conducted in the LIFT and RIFT. Nine different types of timber based products were tested for ignition and flame spread, and Quintiere's flame spread model was applied to the results to obtain material properties, such as thermal inertia, flame spread parameter and the minimum heat flux required for flame spread. These materials included plywood, medium density fibreboard (MDF), hardboard, particle board flooring, Melamine (Melteca) covered MDF, New Zealand Rimu, and Beech and New Zealand grown Macrocarpa and Radiata (Monterey) Pine. Further limited tests were conducted on Melteca covered particle board, and a second brand of particle board. The materials in the RIFT were tried with and without preheating to equilibrium. In addition, a view factor for the RIFT was developed, based on earlier work for the cone calorimeter element. The view factor equation was experimentally tested against measured values, and the calculated value was consistently lower than the experimental values, with similar flux profile.

The standard procedure is for the material to be preheated before ignition, so that the surface is at equilibrium. The spread of the flame front past points on the sample surface after ignition is recorded, and from the flame front velocity and the model by Quintiere, material specific properties can be derived. The lack of preheating was found to affect the final results, by reducing the flame spread velocity and increasing the scatter in the experimental results.

The RIFT gives comparable results to the same materials tested in the LIFT and to the published literature. The results the flame spread parameter and the minimum flux for flame spread are usually higher for the RIFT against the same material in the LIFT.

There proved to be an effective limit on suitable materials able to be successfully tested in the RIFT to those that have a minimum flux for flame spread of less than 7kW/m^2 , with this limitation is dictated by the flux profile along the sample, and the lower resolution dictated by the smaller size. It is approximately equivalent to a minimum ignition flux of 18kW/m^2 .

Contents

Abstract	iii
Contents	v
Mathematical symbols	xvi
Acknowledgements.....	xviii
1 Introduction	1
1.1 The history of flame spread testing.....	1
1.2 Research objectives.....	2
1.3 Materials chosen	4
2 The theory of flame spread.....	8
2.1 Ignition.....	9
2.1.1 Definition of ignition results	10
2.1.2 Effect of sample orientation on ignition	13
2.1.3 Effect of sample size.....	14
2.1.4 Effect of pilot ignition source	15
2.1.5 Effect of moisture content on ignition	15
2.1.6 Effect of Sample thickness.....	17
2.2 Theories of ignition.....	19
2.2.1 Quintiere, Harkleroad and Walton (1983) and Quintiere and Harkleroad (1984)	20
2.2.2 Janssens.....	24
2.3 Opposed flow (lateral) flame spread.....	26
2.3.1 Principles of opposed flow flame spread.....	26
3 The ASTM E1321-97a Lateral ignition and flame transport (LIFT) test apparatus	32
3.1 History.....	32
3.2 Requirements of the ASTM E 1321-97a LIFT apparatus.....	32
3.3 The University of Canterbury LIFT apparatus	35
3.3.1 Apparatus description	35
3.3.2 Fuel and air supply.....	37
3.3.3 Flux measurement and calibration	40
3.3.4 Heat flux from the pilot flame	44
3.4 LIFT Operating Procedure.....	44

3.4.1	Ignition test	44
3.4.2	Analysis of the ignition test	47
3.4.3	Flame spread test.....	49
3.4.4	Analysis of flame spread results	50
4	The cone calorimeter	52
5	ISO 5657-1987 Ignition test	55
6	Reduced Scale ignition and flame test (RIFT) method	57
6.1	Comparison between RIFT and LIFT	58
6.2	Procedure for using RIFT	59
6.2.1	Setup of RIFT	59
6.2.2	Sample preparation	60
6.2.3	Flux measurement.....	61
6.3	Heat flux and sample angle in the RIFT	63
6.4	The effect of different element temperatures.....	63
6.5	The effect of changing the sample angle	64
6.6	The effect of increasing the separation distance between the sample and element.....	66
6.7	Optimum angle of sample in RIFT	67
6.8	RIFT test methods.....	69
6.8.1	Ignition test	69
6.8.2	Flame spread test.....	71
6.9	Calculation of the view factor for the reduced scale LIFT test (RIFT)	72
6.9.1	Wilson et al, 2002	72
7	Literature on the LIFT, RIFT and lateral flame spread.....	77
7.1	LIFT literature.....	77
7.1.1	Quintiere, J. A simplified theory for generalizing the results from a radiant panel rate of flame spread apparatus. 1981	77
7.1.2	Quintiere, J. Harkleroad, M, Walton D. Measurement of material flame spread properties. 1983	77
7.1.3	Quintiere, J. Harkleroad, M. New concepts for Measuring flame Spread Properties, 1984.....	78
7.1.4	Fowell, A. Interlaboratory test program on ASTM E 1321: Standard test method for measuring material ignition and flame spread properties. Second edition, November 1994.....	78

7.1.5	Dietenberger, M. Experimental and analytical protocol for ignitability of common materials. 1995	79
7.1.6	Dietenberger, M. Ignitability of siding materials using a modified protocol for LIFT apparatus. 1995	80
7.1.7	Dietenberger, M. Ignitability analysis using the LIFT apparatus and cone calorimeter. 1995	80
7.1.8	Jianmen, Q. Prediction of flame spread test results using the test data from the cone calorimeter. 1990	81
7.1.9	Goransson U. Using the cone calorimeter to predict flame spread, 1991	81
7.1.10	Persson G. Predicting lateral flame spread with cone calorimeter, 1993	81
7.1.11	Babrauskas, V. Wetterlund, I. Comparative data from LIFT and cone calorimeter tests for 6 materials, including flame flux measurements. 1999.....	82
7.1.12	Nisted, T. Flame spread experiments in bench scale; project 5 of the EUREFIC research program. 1991	83
7.2	RIFT literature	84
7.2.1	Azhakesan, A. Shields, T. Silcock, G. Ignition and opposed flow flame spread using a reduced scale attachment to the cone calorimeter. 1998	84
7.2.2	Azhakesan, A. Shields, T. Silcock, G. Combustibility parameters for enclosure lining materials obtained during surface flame spread using reduced scale ignition and flame spread technique. 1998.....	84
7.2.3	Huynh, VCM. Flame spread measurements of New Zealand timber using an adaptation of the cone calorimeter apparatus. 2003	84
8	Material test results for manufactured boards	86
8.1	Medium density fibreboard.....	86
8.1.1	Ignition of MDF	87
8.1.2	Flame spread of MDF	90
8.2	Particle Board (Chipboard).....	96
8.2.1	Ignition of particle board	96
8.2.2	Flame spread for particle board	102
8.3	Plywood	108
8.3.1	Ignition of plywood.....	108
8.3.2	Flame spread of plywood.....	110
8.4	Hardboard	115

8.4.1	Ignition of hardboard	115
8.4.2	Flame spread of hardboard.....	117
8.4.3	Melteca.....	121
8.4.4	Ignition of Melteca faced boards	122
8.4.5	Flame spread of Melteca	125
9	Material test results for natural timbers.....	131
9.1	New Zealand Beech	131
9.1.1	Ignition of Beech.....	131
9.1.2	Flame spread of Beech.....	133
9.2	Macrocarpa	139
9.2.1	Ignition of Macrocarpa	139
9.2.2	Flame spread of Macrocarpa.....	141
9.3	Radiata Pine	146
9.3.1	Ignition of Radiata Pine	146
9.3.2	Flame spread of Radiata Pine	148
9.4	Rimu.....	153
9.4.1	Ignition of Rimu.....	153
9.4.2	Flame spread of Rimu	155
10	Discussion of results	159
10.1	Equipment specific issues	159
10.1.1	LIFT	159
10.1.2	RIFT	161
10.2	Comparison of LIFT, ISO 5657 and RIFT ignition results	163
10.2.1	The effect of data reduction of ignition data.....	164
10.2.2	Time to ignition.....	164
10.2.3	Thermal inertia kpc.....	168
10.2.4	Minimum ignition flux.....	168
10.2.5	Comparison of correlation values and measured minimum ignition flux " $\dot{q}_{ig,min}$	169
10.2.6	Apparatus and flame spread.....	172
10.2.7	Comparison of ignition parameter "b".....	173
10.2.8	Flame spread parameter Φ	174

10.2.9	Minimum heat flux for flame spread	176
10.3	Material and operational differences	178
10.3.1	Effect of preheating.....	178
10.3.2	Effect of substrates on Melteca and facings on boards.....	180
10.3.3	Effect of thickness.....	180
10.4	Proposal for improved apparatus	182
11	Comparison of data with published literature	184
11.1	Comparison of Ignition results with published literature	185
11.1.1	Thermal inertia ($k\rho c$)	185
11.2	Comparison of published flame spread results	190
11.2.1	Flame spread parameter	190
12	Conclusions.....	193
Appendix 1:	Procedure for operating University of Canterbury LIFT	205
Appendix 2:	Electrical power and current requirements for an electric LIFT radiant panel	207
Appendix 3:	Results of material tests	210
Appendix 4	Flame spread results.....	222
12.1	Summary of flame spread results.....	222
12.2	Flame spread data and correlation results.....	228
Appendix 5	Comparison with published results in the literature	357

List of figures

Figure 1: Lateral flame spread	8
Figure 2: Minimum ignition flux	11
Figure 3: Critical heat flux	12
Figure 4: Effect of moisture content on ignition time for redwood in LIFT and cone calorimeter. Adapted from Diitenberger (1996)	16
Figure 5: Heat flux vs. ignition temperature for Radiata Pine. From Moghtaderi et. al (2005).....	16
Figure 6: Control volume for ignition.....	20
Figure 7: Ignition data plot to find preheating time t^* (from Cleary, 1992)	23
Figure 8: Opposed flow flame spread	27
Figure 9: Main components of LIFT apparatus	33
Figure 10: Schematic of LIFT apparatus	34
Figure 11: LIFT showing angled gas radiant panel (left) and sample holder (right)...	34
Figure 12: Standard ASTM E 1321 LIFT heat flux distribution for calibration	35
Figure 13: University of Canterbury LIFT apparatus with measuring template in sample holder	36
Figure 14: UC LIFT burner position adjustment showing rails and leadscrew	37
Figure 15: Heat flux variation without preloaded air regulator	39
Figure 16: Effect of preloading air regulator to minimum of 8psi on heat flux variation	40
Figure 17: Flux gauge and template.....	41
Figure 18: LIFT calibration profile.....	42
Figure 19: Comparison to UC LIFT calibration flux to ASTM E 1321 standard.....	43
Figure 20: Variation from standard for calibration of LIFT	43
Figure 21: Ignition test of particle board in LIFT	46
Figure 22: Flame spread test.....	49
Figure 23: Flame spread correlation graph	51
Figure 24: Cone calorimeter (reproduced from Babrauskas, 2002)	53
Figure 25: ISO 5657 ignition apparatus.....	56
Figure 26: Australasian RIFT test, showing location of sample to the cone (reproduced from Huynh, 2003)	57
Figure 27: Heat flux for LIFT vs. RIFT (both at 15 degree angle).....	58

Figure 28: RIFT setup – plan view	60
Figure 29: RIFT with flux measurement template.....	62
Figure 30: RIFT sample holder from rear.....	62
Figure 31: RIFT irradiance curve for a sample separation of 45mm, 850°C element temperature and 60° sample angle	63
Figure 32: Effect of changing cone element temperature on received heat flux (70mm separation, 30 degree sample angle)	64
Figure 33: Irradiance for a constant 850° element temperature, 70mm separation and changing sample angle	65
Figure 34: Irradiance with constant peak heat flux of 35kW/m ² and 70mm sample separation	66
Figure 35: Change in heat flux with constant element temperature and angle	67
Figure 36: Limitations for flame spread measurement	67
Figure 37: Rift used for ignition testing - rear view	69
Figure 38: RIFT used for ignition testing	70
Figure 39: Flame spread along sample	71
Figure 40: Cone calorimeter view factor geometry (from Wilson, 2002)	73
Figure 41: RIFT geometry	74
Figure 42: Comparison of theoretical heat flux – Equation (38) vs. measured	75
Figure 43: Time to ignition for MDF.....	87
Figure 44: Comparison of time to ignition of MDF in ISO 5657 apparatus with Ngu (2002).....	88
Figure 45: Critical flux for 18mm MDF	89
Figure 46: Ignition parameters from ASTM e1321-97a for MDF	90
Figure 47: LIFT heat flux profile for MDF flame spread test.	91
Figure 48: Flame spread of 18mm MDF in RIFT.....	92
Figure 49: Flame spread parameter for 18mm MDF in RIFT using ISO ignition data and 40s preheat	93
Figure 50: Flame spread correlation for 18mm MDF in RIFT and LIFT.....	94
Figure 51: Flame spread for 9mm and 18mm MDF in RIFT with low (60s) preheating time	95
Figure 52: Ignition time for 2 brands of particle board in ISO 5657 apparatus.....	96
Figure 53: Comparison of ignition times for particle board	97

Figure 54: Time to ignition for Pynefloor particle board	98
Figure 55: Time to ignition for Superflake particle board.....	98
Figure 56: Ignition parameter for Pynefloor particle board.....	99
Figure 57: Ignition parameter for Superflake particle board	99
Figure 58: Critical ignition flux for Pynefloor particle board.....	100
Figure 59: Critical ignition flux for Superflake particle board	100
Figure 60: Janssen's critical ignition flux for Pynefloor particle board.....	101
Figure 61: Janssen's critical ignition flux for Superflake particle board	102
Figure 62: Comparison of flame spread of 2 brands of particle board – low preheat time	103
Figure 63: Comparison of flame spread for 2 brands of particle board - full preheat time	103
Figure 64: Flame spread parameter for Superflake and Pynefloor particle board in RIFT with a 80s preheat time.....	104
Figure 65: Flame spread correlation for 20mm Particle board in RIFT with full pre- heating time.....	105
Figure 66: Heat flux profile for LIFT flame spread tests on particle board.....	106
Figure 67: Flame spread in LIFT for Pynefloor particle board	106
Figure 68: Flame spread correlation for 20mm Pynefloor particle board in LIFT and RIFT	107
Figure 69: Time to ignition for 17mm plywood.....	108
Figure 70: Critical ignition flux for plywood	109
Figure 71: Ignition parameter for plywood.....	110
Figure 72: Flame spread of 17mm plywood in RIFT	111
Figure 73: Comparison of flame spread with different thicknesses of plywood	112
Figure 74: Flame spread correlation for 17mm plywood in RIFT.....	112
Figure 75: LIFT heat flux profile for plywood and hardboard flame spread tests	113
Figure 76: Flame spread for 17mm plywood in LIFT	113
Figure 77: Flame spread correlation for 17mm plywood in RIFT and LIFT	114
Figure 78: Flame spread correlation for plywood in LIFT	114
Figure 79: Time to ignition of hardboard	115
Figure 80: Critical heat flux for hardboard.....	116
Figure 81: Ignition parameters for hardboard.....	116
Figure 82: Cracking behind the flame front on hardboard	118

Figure 83: Flame spread of hardboard in RIFT – full preheat time	118
Figure 84: Flame spread for hardboard in RIFT – low preheat time	119
Figure 85: Flame spread correlation for hardboard in RIFT.....	119
Figure 86: Flame spread of hardboard in LIFT	120
Figure 87: Flame spread correlation for hardboard in RIFT and LIFT	120
Figure 88: Flame spread behaviour of Melteca faced board.....	122
Figure 89: Time to ignition vs. heat flux of Melteca/MDF board	123
Figure 90: Time to ignition for Melteca faced particle board.....	123
Figure 91: Critical ignition flux for Melteca faced MDF	124
Figure 92: Ignition parameter for Melteca/ MDF board	124
Figure 93: Time to ignition vs. heat flux for Melteca faced boards	125
Figure 94: Flame spread of Melteca faced boards in RIFT	126
Figure 95: Comparison of flame spread time to point for MDF vs. particle board, with and without Melteca facing in RIFT	127
Figure 96: Flame spread correlation for Melteca faced board in RIFT	128
Figure 97: Flame spread correlation for Melteca/ MDF	128
Figure 98: Flame spread correlation for Melteca-MDF with a low preheating period	129
Figure 99: LIFT heat flux profile for Melteca faced MDF flame spread test.....	130
Figure 100: Flame spread correlation for Melteca-MDF in LIFT	130
Figure 101: Time to ignition vs. heat flux for NZ Beech	131
Figure 102: Ignition parameter for Beech.....	132
Figure 103: Critical ignition flux for NZ Beech	133
Figure 104: Flame spread of Beech in RIFT with 55 second preheating period	134
Figure 105: Flame spread for Beech in RIFT with full preheat.....	135
Figure 106: Flame spread correlation for NZ Beech in RIFT - low preheat time	135
Figure 107: Heat flux profile for LIFT tests for NZ Beech	136
Figure 108: Flame spread for NZ Beech in LIFT	137
Figure 109: Flame spread correlation for NZ Beech in LIFT.....	137
Figure 110: Flame spread correlation of Beech in RIFT and LIFT.....	138
Figure 111: Time to ignition for Macrocarpa	139
Figure 112: Ignition parameter for Macrocarpa.....	140
Figure 113: Critical heat flux for Macrocarpa	140
Figure 114: Flame spread of Macrocarpa in RIFT with low (40s) preheat time	141

Figure 115: Flame spread of Macrocarpa in RIFT – full preheat of 436 seconds	142
Figure 116: Flame spread correlation for Macrocarpa in RIFT	142
Figure 117: Flame spread for Macrocarpa in LIFT	143
Figure 118: Flame spread correlation for Macrocarpa in LIFT	144
Figure 119: Flame spread correlation for Macrocarpa	145
Figure 120: Time to ignition of Radiata Pine	146
Figure 121: Critical ignition flux for Radiata Pine	147
Figure 122: Ignition parameter for Radiata Pine	147
Figure 123: Flame spread for Radiata Pine in RIFT – low (40s) preheat.....	148
Figure 124: Flame spread for Radiata Pine in RIFT - full preheat	149
Figure 125: Comparison of flame spread of Radiata Pine	149
Figure 126: Flame spread correlation for Radiata Pine in RIFT – low preheat time.	150
Figure 127: Flame spread correlation for Radiata Pine in RIFT - full preheat.....	150
Figure 128: Flame spread of Radiata Pine in LIFT	151
Figure 129: Flame spread correlation for Radiata Pine in LIFT	151
Figure 130: Flame spread correlation for RIFT and LIFT.....	152
Figure 131: Time to ignition of Rimu.....	153
Figure 132: Critical ignition flux for Rimu.....	154
Figure 133: Ignition parameter of Rimu	154
Figure 134: Flame spread along NZ Rimu in RIFT with a low preheat time of 67-80 seconds.....	155
Figure 135: Flux profile of LIFT flame spread test for Rimu and Radiata Pine	156
Figure 136: Flame spread for Rimu in LIFT	157
Figure 137: Flame spread correlation for Rimu in RIFT with ISO 5657 ignition “b” value – 67-90 seconds preheat time	157
Figure 138: Flame spread correlation for Rimu in LIFT	158
Figure 139: Marker pins in RIFT	163
Figure 140: Comparison of time to ignition for ISO 5657 and LIFT ignition test....	165
Figure 141: Comparison of time to ignition for tests in RIFT and LIFT.....	166
Figure 142: Comparison of time to ignition for tests in RIFT and ISO 5657 ignition apparatus	167
Figure 143: Comparison of thermal inertia ($k\rho c$) in LIFT, ISO 5657 and RIFT.....	168
Figure 144: Comparison of minimum ignition flux $q_{ig,min}^*$	169

Figure 145: Comparison of RIFT flame spread correlation and ISO 5657 ignition test results for minimum ignition flux $\dot{q}_{ig,min}''$	170
Figure 146: Comparison of LIFT correlation and LIFT ignition test results for minimum ignition flux	171
Figure 147: RIFT irradiance curve	172
Figure 148: Comparison of ignition parameter "b" in ISO 5657 and LIFT.....	174
Figure 149: Comparison between flame spread parameter for LIFT and RIFT (using ISO 5657 ign data for RIFT).....	175
Figure 150: Comparison of flame spread parameter for LIFT and RIFT (using RIFT ignition data)	176
Figure 151: Comparison of minimum flux for flame spread \dot{q}_s'' in LIFT and RIFT ..	177
Figure 152: Minimum ignition flux from ISO 5657 test vs. minimum flux for spread for RIFT	178
Figure 153: Effect of preheating on the flame spread correlation for Pynefloor in RIFT	180
Figure 154: Comparison of ignition times for plywood in RIFT test.....	181
Figure 155: Comparison of thermal inertia of plywood	185
Figure 156: Comparison of thermal inertia of particle board	186
Figure 157: Comparison of thermal inertia of MDF.....	187
Figure 158: Comparison of thermal inertia of hardboard	188
Figure 159: Comparison of thermal inertia of Radiata (Monterey) Pine.....	189
Figure 160: Comparison of thermal inertial of Macrocarpa and NZ Rimu	189
Figure 161: Flame spread parameter for plywood.....	190
Figure 162: Comparison of flame spread parameter for MDF	191
Figure 163: Flame spread parameter for particle board.....	192
Figure 164: Regulator and ball valve.....	206
Figure 165: LIFT settings	206

List of tables

Table 1: Materials tested.....	5
Table 2: Pilot flame flux to sample.....	44
Table 3: RIFT setup dimensions.....	60
Table 4: RIFT polynomial coefficients.....	61

Mathematical symbols

<i>Symbol</i>	<i>Name</i>	<i>Units</i>
b	Ignition parameter	$s^{-1/2}$
Bi	Biot number	-
c	Specific heat	J/kgK
C	Flame spread modulus	$m^{3/2}/kW s^{1/2}$
D	Thermal penetration depth	m
Fo	Fourier number	-
h	Heat transfer coefficient	kW/m^2K
k	Thermal conductivity	kW/mK
$k\rho c$	Thermal inertia	$(kW/m^2K)^2s$
q	Heat flux	kW/m^2
t	Time	s
t^*	Time for thermal equilibrium	s
T	Temperature	$^{\circ}C$
V	Velocity	m/s
x	Distance along sample	mm
α	Thermal absorptivity	-
δ	Length heated in front of flame	m
ε	Emissivity	-
Φ	Flame spread parameter	kW^2/m^3
ρ	Density	kg/m^3
σ	Stefan- Boltzmann constant	$5.67 \times 10^{-8} kW/m^2K^4$

θ Angle between sample and °
element

Subscripts

crit	Critical ignition value
c	Convective
e	Incident on surface
f	Flame
ig	At ignition
min	Minimum value
r	Radiative
peak	Peak value
s	Required for flame spread
surf	Surface
t	At t seconds
xmm	Measured at the x mm position on the sample
∞	Ambient

Acknowledgements

There are a large number of people who have made this project and the completion of the Masters possible.

In particular, I would like to thank the following people for their assistance and support in helping me to complete this project:

- My parents, Beth and David Merryweather, without their support I could not have done the Masters.
- My wife, Stephanie, who kept the home together by herself while I was away for 2 years.
- Michael Spearpoint, my supervisor, for his help and support over the course of the Masters and particularly this thesis.
- The New Zealand Fire Service Commission who provided a much needed scholarship, and for their ongoing support of the M.E. Fire program.
- The technicians at the University of for their help in various ways and for letting me have use of the workshop for building the LIFT, with particular thanks to the Fire Engineering technicians - Grant and Bob.
- Elizabeth Young and Pauline Anderson, for help, food and coffee.

This report is dedicated to my son Robert.

1 Introduction

1.1 The history of flame spread testing

The study of flame spread along the surface of materials is a key part to fire modelling and prediction of fire behaviour. It forms the underlying basis for many predictions of flashover and room fire growth (Cleary and Quintiere, 1991).

It has long been recognised that the rate of flame spread on the surface is an indication of how quickly conditions in a compartment become hazardous. As a result, most building codes require building surfaces to meet minimum flame spread requirements, and the failure to do so has resulted in tragic fires in the past. A well known example is the Stardust Disco fire in Dublin in 1981, which killed 48 people. The wall linings of an alcove were lined with flammable carpet tiles, and the fire rapidly spread once they ignited. (Rasbash, et al 2004). Most of the code requirements are based on an index figure, based on the performance in a test. The formulation of the index, and what is considered to be “acceptable” performance is largely arbitrary and of little use for further modelling or comparison to other standards. A typical example of this is the ASTM E 84 “tunnel test” where the flame spread over a surface is given an index value depending on the performance of the material compared with red oak (Janssens, 2005). Such a result allows ranking compared with other materials tested in the same manner, but cannot be easily compared with results from other jurisdictions which have different test methods, and the results cannot also be further developed to give an estimate of the fire behaviour when the material is in use. The wide variety of standards increases the cost and space required in the laboratory, and this is made worse by the fact that many of the tests are similar, but specific to certain materials and situations.

There has been a focus on moving to standardised tests, which achieve the objectives of previous test standards, but which can provide data for modelling fire behaviour. This has largely arisen since the development of the ASTM E 1354 cone calorimeter, which has allowed the development of equivalency correlations to previous test methods.

The research in this report is specifically on the study of lateral flame spread. This is also known as creeping or opposed flow flame spread, and covers the case where the

flame front is moving perpendicularly or against the airflow direction, so that the flame front does not extend over the unburnt material. The airflow is generally buoyancy driven flow, driven by the heat from the fire. The flame spread in this direction is typically in the order of 100 times slower than the case where the flame front is moving in the direction of the fire (Quintiere, 2002) , and hence is less of a concern to life safety in the early stages of fire growth.

The protocol which is covered by this research is the Lateral Ignition and Flame Transport (LIFT) test, adopted as the ASTM E 1321 standard. It gives apparent material properties which can be used in modelling fire growth on a surface (Cleary and Quintiere, 1991). These properties include:

- Thermal inertia $k\rho c$;
- The minimum heat flux for ignition $q''_{ig,min}$ and the resulting minimum surface temperature for ignition, T_{ig}
- The minimum heat flux for flame spread q''_s and the resulting minimum surface temperature for flame spread, T_s
- A material property called the flame spread parameter ϕ which will allow the calculation of the flame spread rate for a material, if the incident heat flux and material properties are known.

1.2 Research objectives

The LIFT apparatus, which forms the basis of the lateral flame spread measurements in the ASTM E 1321-97a standard is bulky, with a footprint of approximately 1.7x0.9m, and requires a gas and compressed air supply for a radiant gas panel.. The numbers of LIFT testing facilities in the world is limited, due to the limited scope of the test. In comparison, the ASTM E 1354 cone calorimeter is the cornerstone of modern fire testing, forming the basis of much of the research into material properties, and hence many of the legislative requirements for materials. Within 10 years of the cone calorimeter being available commercially, nearly 100 were in worldwide service (Babrauskas, 1995). There are at least 3 cone calorimeters in New Zealand, at the University of Canterbury, Building Research Association of New Zealand (BRANZ)

and Canesis - formerly the Wool Research Organisation of New Zealand (WRONZ). By comparison, Babrauskas (1995) put the number LIFT testing facilities in the world at 20 in 1995.

In addition, the time for ignition testing in the cone calorimeter is significantly less than that of the LIFT, with the test duration approximately half as long (Babrauskas, 1999). The thermocouple control of the cone element also give more consistent performance than is achievable than the gas panel used in the LIFT.

Finally, the RIFT and cone calorimeter use smaller sample sizes than the LIFT, allowing more tests to be conducted with a given amount of material.

The cone calorimeter has been shown to give good predictions of fire and test performance for materials, electrical cabling, compartment flashover and a wide variety of other parameters. Efforts to apply cone calorimeter data to modelling lateral flame spread have had limited success (Goranson, 1992).

Initial research at FireSERT at the University of Ulster developed the Reduced scale Ignition and Flame spread (RIFT) apparatus, which showed some success. This used the cone calorimeter as the heat source for flame spread testing, in the same manner as the LIFT. Application of the flame spread procedures and theory, developed by Quintiere (1981, 1983, 1984) in the ASTM E 1321 standard gave the flame spread parameter Φ , not otherwise obtainable from cone calorimeter data. Further work at the University of Newcastle by Pease (2001) and Huynh (2003) was inconclusive due to the experimental apparatus. In all cases, the RIFT results were compared with data previously published in the literature, and not directly against LIFT tests of the same material.

The objectives of this report can be summarised as

- To manufacture and calibrate a full scale LIFT apparatus at the University of Canterbury for the use in this report, and to identify improvements for future research.
- To manufacture and calibrate a RIFT attachment for the cone calorimeter and apply the flame spread theory developed for the LIFT by Quintiere to the results.

- To directly compare the results from the RIFT with the same materials tested in the LIFT, to eliminate a variable in the results. If the research is successful then this will allow laboratories with only the cone calorimeter to derive flame spread properties without new equipment.
- As part of the RIFT research, the development of a view factor for the RIFT, previously developed by Huynh (2003), is to be continued to see if the shortcomings identified in the earlier research can be corrected.

The results that will be compared between the two testing methods include:

- The minimum ignition flux $\dot{q}_{ig,min}''$ for ignition tests in the LIFT, RIFT and ISO 5657 ignitability apparatus
- The thermal inertia value, $k\rho c$ from the ignition results
- The minimum flux for flame spread \dot{q}_s'' for LIFT and RIFT tests
- The flame spread parameter, Φ

Where information in the literature is known, then the values will be compared with previously published data.

1.3 Materials chosen

Nine wood based materials were used in the series of tests conducted for this report, with some limited tests conducted on variations of these materials. Most New Zealand manufactured timber based products are Radiata Pine based, as this is the most common species grown in New Zealand. The materials chosen for the tests in this report were based on the availability of previously published data, particularly Huynh (2003) and Azhakesan et al (1998). A secondary objective was to provide some information on New Zealand materials which was otherwise not available.

The thickness of the natural timbers used in the RIFT was less than the samples used in the LIFT due to difficulties in inserting the thicker samples into the sample holder.

<i>Material</i>	<i>Manufacturer and trade name</i>	<i>Description</i>	<i>Thickness (mm)</i>	<i>Density of tested samples (kg/m³)</i>
Plywood	IPL “Tuffply”	C/D grade untreated radiata Pine	17	487
Particle board (chipboard)	Laminex Corp (Fletcher Wood Panels) “Pynefloor”	Radiata Pine based flooring particle board.	20	745
	Laminex Corp (Fletcher Wood Panels) “Superflake”	Radiata Pine based particle board.	20	673
Medium density fibreboard (MDF)	Fletcher Wood Panels “Customwood”	Radiata Pine based standard MDF.	18	620
Melteca faced medium density fibreboard	Laminex Corp (Fletcher Wood Panels) Melteca	White Melamine faced MDF	18	681
		White Melamine pre - finished and clashed shelving from builders merchants	18	661
Melteca faced particle board	“Regal” pre - finished shelving			
Hardboard	Unbranded	Hardboard fibreboard	5	819
NZ Radiata Pine (Monterey Pine)		Clear grade, kiln dried and untreated	16 (RIFT) 20 (LIFT)	425
NZ Macrocarpa		Clear grade,	16 (RIFT) 20 (LIFT)	514
NZ Rimu		Heart grade	16 (RIFT) 20 (LIFT)	660
NZ Beech			16 (RIFT) 22 (LIFT)	489

Table 1: Materials tested

Particle board is made from wood chips held together with a pressure cured adhesive. It is commonly used for flooring and as a substrate for kitset furniture.

Two boards of the same nominal type were tested. Both boards are made by the same company – the Laminex division of Fletcher Wood Panels and are Radiata Pine based, with the Pynefloor having a higher density than the Superflake board used in these tests. According to the Material Safety Data Sheets provided for both materials, as the flooring material is expected to be exposed to the weather during construction, a different adhesive is used. The Pynefloor uses a polymerised urea formaldehyde adhesive (up to 15% of the board content) (MSDS Pynefloor 2004), to give weather resistance for up to 8 weeks of exposure, whereas Superflake uses a melamine urea formaldehyde adhesive (up to 13% of the board content (MSDS Superflake, 2004)), and is for internal use only

Medium Density Fibreboard (MDF) is a panel product frequently used for cabinetry. It is made from wood fibre, which is exploded with steam before being compressed with a pressure cured adhesive to form a flat, stable wood panel (Youngquist, 1999). The term “fibreboard”, used in the literature is often poorly defined and the density and properties of fibreboard products can vary greatly depending on the end use and manufacturing process. While “fibreboard” may refer to MDF, it may also refer to low density fibreboards, of the type commonly used for pinboards and ceiling tiles. As such, the material properties will be different from MDF and will give different test results.

Plywood is made from layers of wood, with the grain direction of each ply at 90 degrees to the neighbouring plies, and the layers are joined with a pressure cured adhesive. The grade used for these tests is C/D grade, commonly used for construction. One face is sanded and surface knots are secure or filled. The other face is rough and empty knots are allowed.

Plywood can have varying properties, depending on the substrate and surface plies used and the presence of any voids in the material.

Hardboard is a compressed fibreboard sheet product, made from wood pulp and fibres, which is exploded with pressure and steam, similar to MDF and this is then compressed using a thermosetting adhesive to form a thin, high density board (Youngquist, 1999), with a characteristic brown colour. It is commonly used for low

strength applications such as cupboard backs and drawer bottoms. A common brand name which is often used as a generic name for this type of hardboard is Masonite.

Melteca consists of melamine facing on a substrate of either MDF or particle board. It is commonly used for shelving, kitchen cabinets, cupboards and bench tops. Two brands of Melteca faced board were tested, where one uses a MDF substrate, and the other uses particle board.

The manufacturer of each board was different so some variation in the performance of the samples due to the differences of the facing material is expected.

Macrocarpa (Cypresses Macrocarpa) is a member of the cypress family, and is also known in the US as Monterey cypress. It has the typical cypress smell to it, which is especially noticeable when it burns. The timber is used for boat building, furniture, framing and panelling. It is known for the wild grain and knotty timber it produces, and can be resinous. It is prone to sparking when burning due to the resin pockets.

Radiata Pine is a native of California, and is also known there as Monterey Pine. It forms the basis of New Zealand silviculture, making up 95% of the New Zealand timber production in 2004 (anon, MAF statistics, 2005). It forms the basis of almost all New Zealand made framing timber and manufactured wood panels.

Rimu is a native New Zealand timber, although other members of the same family are found through the Pacific Rim. It is best known for the dramatic grain of the heart timber and reddish brown colour, although the other Rimu species from the Pacific, principally Fiji and sold in timber suppliers as Pacific Rimu, tends to be plainer and have a lower density. The colour and density varies between the sap wood, and the heart wood. The sap wood and late growth timber tends to be a plain brown and prone to borer infestation.

It has been widely used for flooring, panelling and furniture making, and was widely used for framing until the introduction of Radiata Pine from the 1960s.

2 The theory of flame spread

Flame spread is divided according to the direction of any forced or buoyancy driven flow in regard to the direction of flame travel. In the case of wind assisted or vertical flame spread, the flame extends over the unburnt area, increasing the area affected by the radiation from the flame and hence the preheating of the material. Opposed flow (also called creeping or lateral flame spread) is where the flame is either over the already burnt material or at right angles to it (Figure 1), so that there is no flame extension over the unpyrolysed area. The LIFT test, and hence the RIFT test, is concerned with opposed flow flame spread. The theory and principles of opposed flow flame spread is developed later in 2.

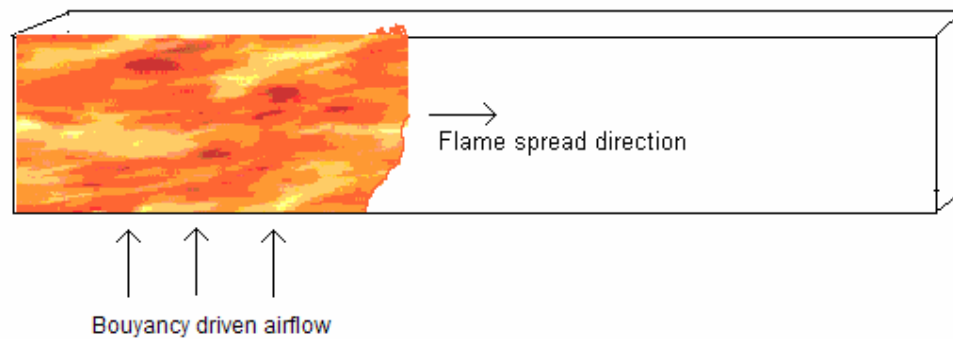


Figure 1: Lateral flame spread

Flame spread is often modelled as a series of piloted ignitions, so that as the area in adjacent to the flame front reaches the critical ignition temperature, then it ignites. This pyrolysis area is heated by gas phase conduction from the flame itself, as well as from the incident heat flux from any external heat source. Therefore, any study of flame spread will involve ignition and ignition theory to at least some degree.

Historically, the study of flame spread has resulted in empirical indices, which allow materials to be compared with each other, for that test procedure, but do not lead to material properties suitable for further calculation or modelling. Such tests involving lateral flame spread include BS478 Part 7 and ASTM E 162 (Surface flammability testing of materials using a radiant heat energy source) (Hilado, 1973). These give an index value, based on the extent of flame spread. The ASTM E 1321-97a LIFT test is

different in that it provides flame spread theory and the required material properties to allow modelling of flame spread.

2.1 Ignition

The study of flame spread and the flame spread rate depends on the ignition properties of the material being tested. The study of ignition can be divided by the means of starting the ignition – either piloted or unpiloted (autoignition). Most of the study of ignition for fire engineering is piloted ignition, as this is more conservative, as the minimum heat flux required for piloted ignition and the resulting minimum surface temperature is less than the unpiloted equivalents. For laboratory testing, the pilot ignition source is generally a spark, hot wire or a gas flame, depending on the apparatus design. Flame spread is a piloted ignition process.

There are a number of models for predicting ignition under varying flux conditions, which are discussed in depth by Babrauskas (2003, 2001), and some of these models have been compared with experimental results by Ngu (2002).

The ASTM E 1321-97a LIFT standard is based on the work by Quintiere et al (1981, 1983, 1984) and hence uses the ignition theory developed there. Other theories on ignition have been developed since, which attempt to give more accurate predictions or address the assumptions and simplifications made by Quintiere et al.

At the simplest level, a material will ignite when a sufficient quantity of material has pyrolysed to reach the lower flammable limit, and in the case of a piloted ignition, a suitable ignition source is available. Using the pyrolysis of the material as an ignition criterion is often not practical, particularly for design purposes. More desirable is a value for the incident heat flux or a temperature at which the item will not ignite, and hence the fire will no longer spread.

To achieve this objective, ignition theory can be divided into several areas, depending on the material properties and thickness. Much ignition theory is based on the concept of heat transfer to and from a quasi steady control volume. The final outcome is a function of the material thickness. At one extreme, a thin material can be effectively at constant temperature throughout and so the temperature from the rear face away from an incident heat flux is the same as the front. The resulting temperature rise, and

hence time to ignition, can be calculated from the material properties and heat transfer boundary conditions.

At the other extreme is a “thick” material, where there is no heat loss from the back of the sample. The development of the ignition theory Quintiere and Harkleroad (1983) which forms the basis of the LIFT test, given later in this report, is based on “thermally thick” heat transfer.

2.1.1 Definition of ignition results

There are some similar but confusing outcomes from ignition tests, regardless which ignition theory is used. A common requirement is to find the lowest heat flux level at which ignition will occur. Based on this, the likelihood of an item made from that material igniting as a result of the radiant heat flux can be calculated. This forms the basis of much of the legislation limiting heat flux from fires across property boundaries (Babrauskas, 2003)

There are 2 “lowest” heat flux from ignition test data - the minimum heat flux for ignition ($\dot{q}_{ig,min}$) and the critical heat flux (\dot{q}_{crit}), and it is important not to confuse the terms.

Minimum ignition flux

The minimum heat flux for ignition is the lowest level at which the material will ignite within some time limit, and this varies depending on the requirements of the test protocol. It is found by a series of ignition tests, until the sample will no longer ignite within the allowed time limit, and so the plot of the time to ignition vs. the incident heat flux asymptotes to the minimum ignition flux. The value for $\dot{q}_{ig,min}$ is found by the average of the highest level where there is no ignition, and the lowest level that caused ignition within the allowable time, e.g. the ASTM E 1321-97a test standard calls for this value to be found by bracketing to within $\pm 2\text{kW/m}^2$.

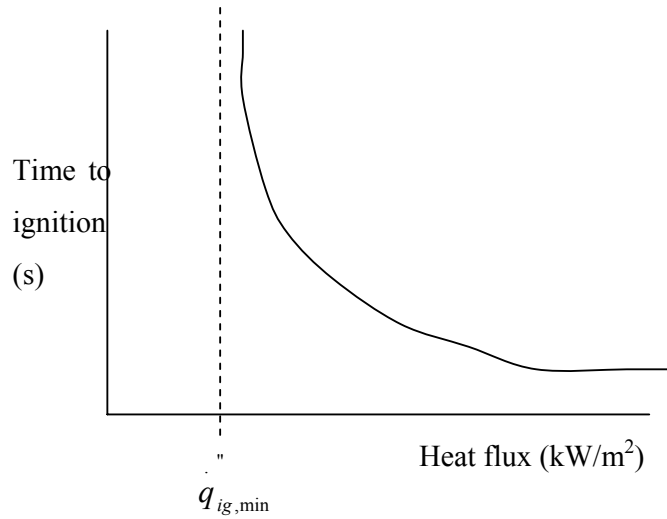


Figure 2: Minimum ignition flux

Critical ignition flux

Unlike the minimum ignition flux, the critical ignition flux is found by correlation, rather than as an experimental value, and different ignition theories can give different results. It is the theoretical lowest flux which will cause ignition, given an infinitely long time. Implicit is that the material properties do not change significantly during that time.

Quintiere's model assumed a thermally thick material, whereby there is no heat loss out of the material through the back of the sample, and the material behaves like an inert solid with no thermal decomposition or reaction. Plotting the ignition flux against $(1/\sqrt{\text{time to ignition}})$ and fitting a straight line to the data (Figure 3) gives the critical heat flux at the intercept at the x- axis.

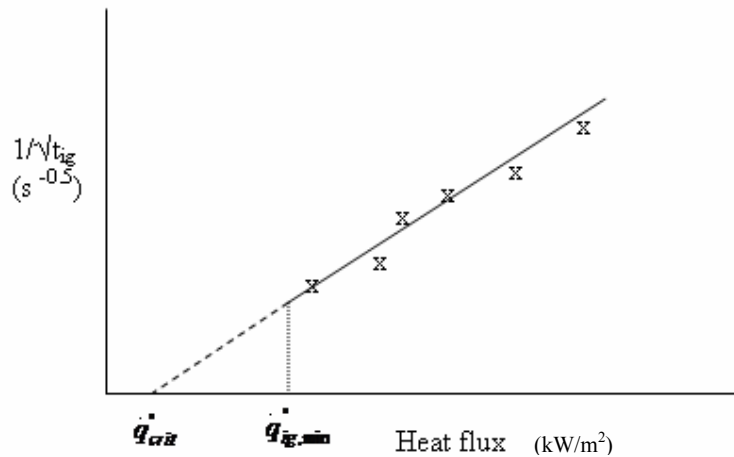


Figure 3: Critical heat flux

An alternative thermal ignition model which gives a value for the critical heat flux and is also widely used is that of Janssens (1991). It is similar to the Quintiere and Harkleroad model, except the basis for the derivation means that the data is plotted as (incident heat flux) q_e vs. (time to ignition)^{0.55}, rather than (time to ignition)^{0.5} as for Quintiere and Harkleroad. The value of the exponent for Janssens theory (0.55) applies if the material is thermally thick. The intercept with the x-axis gives q_{crit} as above. As a result, the value for q_{crit} is often slightly higher than that given by Quintiere and Harkleroad (1983) for the same data set. (Babrauskas, 2003).

Thermal inertia $k\rho c$

Thermal inertia is defined as the product of the specific heat of the material (c), the thermal conductivity (k) and the density (ρ).

It is a measure of how easily the material absorbs energy and hence how quickly the temperature will rise to ignition. A material with a low thermal inertia will ignite sooner than one with a high thermal inertia under the same conditions and ignition temperature, as more energy must be absorbed to raise the surface temperature by the same amount.

A summary of the theories and research into the ignition of wood is given by Babrauskas (2001, 2003). Seven different ignition theories, including the Quintiere and Harkleroad model used in the LIFT standard and that of Janssens, are compared experimentally by Ngu (2002).

2.1.2 Effect of sample orientation on ignition

. The ASTM E 1321 LIFT test uses an ignition test where the sample is held in the vertical plane, whereas the conventional cone calorimeter and ISO 5657 – 1986 test for ignition of samples subjected to thermal irradiance uses a sample in the horizontal orientation. The detail of each test apparatus is discussed later in this report. It is anticipated that the ignition tests for the RIFT will generally use the horizontal orientation in the ISO 5657 ignition testing apparatus or the cone calorimeter, although ignition tests were conducted in the RIFT in the vertical position, in order to compare the results.

Shields, Silcock and Murray (1993) did extensive work on the ISO 5657 ignition apparatus in various orientations, and compared the results to the cone calorimeter. The ISO 5657 apparatus used the “nodding” gas pilot flame applied at 4 second intervals (Babrauskas, 2003), rather than the spark ignition used in this report, and the time to ignition for the cone calorimeter and the ISO 5657 apparatus was similar, allowing for the margin of error due to the interval of the nodding gas pilot ignition system. Ignition times were similar for horizontal and vertical orientation, for heat fluxes between 50-70kW/m², but at lower flux levels (down to 20kW/m²), there was significant difference with orientation, with vertical samples taking longer to ignite, and inverted samples several times longer still.

Babrauskas (2003) notes that the original version of the apparatus developed by the Experimental Building Station (now CSIRO) in Australia had provision for both the gas ignition system and an electric spark ignition system.

Dietenberger (1996) found that the time to ignition for samples in the cone calorimeter, with a horizontal sample, was less than that for the LIFT. This is shown in Figure 4, where the results for the ignition in the cone calorimeter are in the horizontal position, and the others are from the LIFT in the vertical position.

2.1.3 Effect of sample size

The size of the sample can have an effect on the time to ignition, particularly in the vertical orientation. The main difference as the sample height increases is the thickening of the boundary layer and hence the convection coefficient. The main source of heat loss from the sample face is convection, which is proportional to (the height of the sample)^{1/4}. (Babrauskas, 2003)

2.1.4 Effect of pilot ignition source

The pilot source and type is recognised as a source of error in ignition testing. The error can come from the pilot itself, or the manner in which it is applied, where a directly impinging pilot flame will cause ignition sooner than one which is remote from the sample. Similarly, if a gas flame is used, and the pilot flame is sufficiently large, the heat flux from the pilot flame can lead to a local heat flux which is higher than the nominal value. Similarly, if the pilot source is too far away from the sample, or poorly placed, the ignition time will increase, as the pyrolysed material will be diluted with ambient air, decreasing the concentration of flammable gas.

In the original research that looked at the flame spread due to radiant panels, such as the LIFT apparatus, Quintiere (1981) used a “weak” pilot flame. This was formalised experimentally by Quintiere, Harkleroad and Walton (1983) to give the location in the ASTM E 1321 standard. This is mounted above the sample with a backing flange to provide a laminar flow of pyrolysed material to the pilot flame.

The apparatus can have an additional effect. The original ISO 5657 ignitability apparatus, as used by Shields, Silcock and Murray (1993) used a pilot gas flame, applied at 10 second intervals to the sample. This automatically introduces an error in the time to ignition, solely due to the resolution of the pilot flame application. The ISO 5657 apparatus used for this report uses a spark ignition, similar to the cone calorimeter, in order to reduce this systematic error.

Babrauskas (2003) reports several experiments comparing spark and gas ignition. Gas flame pilots are shown to give more inconsistent results than a spark ignition pilot, with generally shorter ignition times, due to local heating, even with “non impinging” pilot flames. Babrauskas recommend a spark ignition as the preferred pilot source.

2.1.5 Effect of moisture content on ignition

The moisture content of the samples, particularly wood, can have a large effect on the time to ignition. This will also then have an effect on the flame spread rate, since this is also affected by the ignition properties of the material. Dietenberger (1996) conducted experiments with the LIFT and cone calorimeter on redwood, with oven dried (0% MC), 30% and 50% moisture content. The resulting increase in the time to ignition for various moisture content levels is shown in Figure 4.

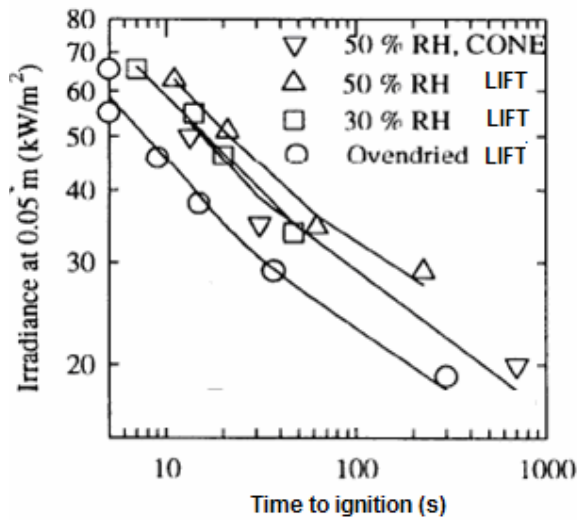


Figure 4: Effect of moisture content on ignition time for redwood in LIFT and cone calorimeter. Adapted from Dietenberger (1996)

The effect on moisture content on the ignition temperature (and hence the heat flux for ignition) can be seen in Figure 5 with the ignition temperature increasing with the moisture content.

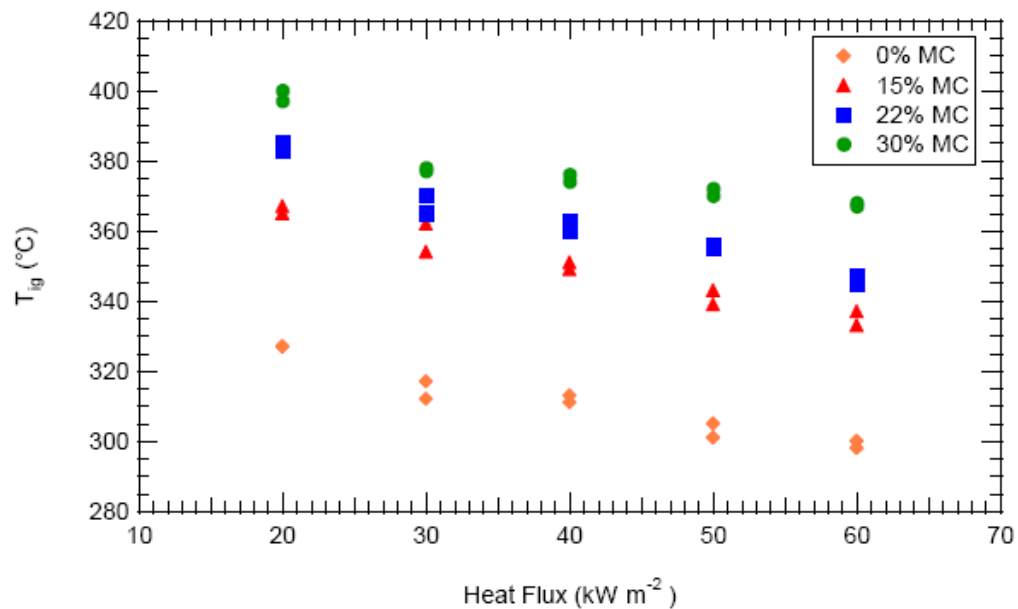


Figure 5: Heat flux vs. ignition temperature for Radiata Pine. From Moghtaderi et. al (2005)

Of greater importance to this report, Babrauskas notes that changes in moisture content of timber at room equilibrium do not make a significant difference to ignition

time (Babrauskas, 2001) and that differences in ignition times for timber moisture contents between 0-12% MC is lost in the data scatter.

2.1.6 Effect of Sample thickness

The thickness of the material affects the time to ignition as it affects the heat loss through the rear of the sample. At one extreme, the material is “thermally thin”, so that the rear of the sample is effectively at the same temperature as the radiated face. The temperature of the sample then depends on the boundary conditions of both the front and rear face, for example if the face is insulated or under natural or forced air flow. At the other extreme, the material is “thermally thick”, where the thickness of the material is such that there is no thermal penetration to the rear of the sample and hence no heat loss from the rear face. Some ignition theories for predicting the time to ignition, such as those used to develop the protocol for the ASTM LIFT test require that the material is thermally thick.

While materials over 1mm in thickness are generally thermally thick or thermally indeterminate, it depends on the flux level and preheating time. (Babrauskas, 2003). A lower flux level will give a longer time until the ignition temperature is reached, leading to greater thermal penetration. Hence, all materials behave as thermally thick for high heat fluxes with a correspondingly short ignition time, but increasingly behave as thermally thin at lower flux levels and longer ignition times.

The time for thermal penetration to depth D is given by Karlsson and Quintiere, (2000) as

$$t_p = \frac{D^2}{4\alpha} \quad (1)$$

Where α is the thermal diffusivity.

$$\alpha = \frac{k}{\rho c} \quad (2)$$

The problem with using Equation (1) to define the minimum thickness is that the properties used to calculate the thermal penetration depth and time are unknown and derived from the ignition test.

For wood products, Babrauskas (2003) summarises many of the findings into this area. For wood products, a rule-of-thumb for the thermal depth D is given by Equation (3) with a comment that several exceptions have been found.

$$\frac{D}{500} = \frac{0.6\rho}{q_e} \quad (3)$$

As the ignition and flame spread theory for the LIFT standard is based on materials being thermally thick, then the thickness of the materials should be chosen to be thermally thick. The ASTM E 1321-97a standard (section X.1.1.1) notes that materials in this category are typically 2-5mm thick, and where the material is less than this, the results apply to the facing and substrate combination as the substrate can have a significant effect on the ignition and flame spread results.

2.2 Theories of ignition

A large number of ignition theories have been developed, in order to predict the likelihood and time to ignition of materials, with varying degrees of complexity. Two common ones which can give the material properties for use in the flame spread model are outlined in the following sections.

The problem of ignition can be treated as a heating problem, with a surface receiving radiation, and losing heat via radiation and convection from the surface (Figure 6), and solving as an energy balance. This also assumes that reactions within the material or on the surface are not significant. This may not always be true if, for example, the production of smoke or water vapour interferes with the received radiation, or alters the material properties.

For an inert solid, an approximate solution is possible for the heat transfer to and from the surface, given in equation (4) (Babrauskas, 2003):

$$T_{ig} - T_{\infty} = \frac{\dot{q}''_e}{h} \left[1 - \exp\left(-\frac{h^2 \alpha t_{ig}}{k\rho c}\right) \operatorname{erfc}\left(\sqrt{\frac{h^2 \alpha t_{ig}}{k\rho c}}\right) \right] \quad (4)$$

Where h is the effective linearised heat transfer coefficient, with both radiative and convection components and α is the surface absorptivity. The radiation losses are proportional to T^4 and hence a linearised heat transfer coefficient can only be accurate over a short range.

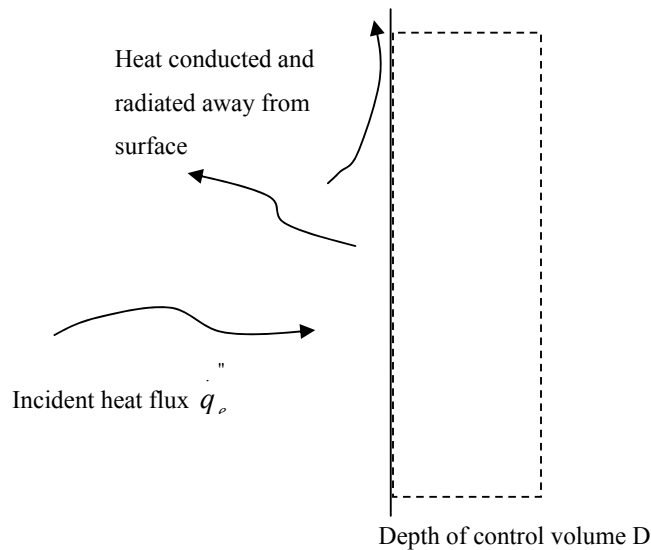


Figure 6: Control volume for ignition

Babrauskas (2003) notes that the application of Equation (4) is difficult, as there are practical difficulties in experimentally calculating the values. It is mathematically complex, and the Gaussian error function complement (erfc) is prone to rounding error when multiplied with the exponent value.

The ignition temperature at ignition is difficult to measure and there is a wide variation in values. Babrauskas (2001) lists a summary of values obtained by various methods, and these range from 228°C to 420°C. The value observed are dependent on the apparatus, orientation, flux level and measurement method (Fangrat et al, 1997). Generally the heat flux is known or more easily measured than the surface temperature at ignition, so any solution should not rely on the ignition temperature for the final result.

2.2.1 Quintiere, Harkleroad and Walton (1983) and Quintiere and Harkleroad (1984)

The ignition theory developed by Quintiere, Harkleroad and Walton (1983) and further developed by Quintiere and Harkleroad (1984) forms the basis for the ignition tests in the ASTM E 1321 LIFT ignition tests, and the basis for the material properties

used in the flame spread part of the test. It is based on an energy balance into a control volume for an infinite 1 dimensional slab (Figure 6).

Some assumptions are made:

- The material under test is modelled as an inert, grey body.
- The temperature in the control volume increases under the received heat flux until it reaches the ignition temperature (T_{ig}), at which point it ignites
- More generally, the sample is assumed to be “well behaved” with homogeneous properties, unaffected by the temperature increase to ignition, and the surface does not melt or blister.

The material is assumed to ignite once the surface temperature (T_{surf}) reaches the minimum temperature for piloted ignition (T_{ig}), and this temperature increase is due to the increase from the external flux and the flame heat flux, i.e.:

$$T_{ig} - T_{surf} = \Delta T_e + \Delta T_f \quad (5)$$

Taking an energy balance on the control volume, the minimum heat flux to raise the temperature of the surface to the ignition temperature is:

$$\dot{q}_{ig,min} = h_c (T_{surf} - T_\infty) + \varepsilon \sigma (T_{surf}^4 - T_\infty^4) \cong h (T_{ig} - T_\infty) \quad (6)$$

Where h = linearised heat transfer coefficient, including the radiation component, and the emissivity $\varepsilon = 1$, as the surface chars before ignition.

The surface temperature required for ignition can be calculated from Equation (6) if a heat transfer coefficient h is known. Experiments by Quintiere, Harkleroad and Walton (1983) showed the heat transfer coefficient was relatively constant across the temperature range of materials commonly tested in the LIFT at 15 kW/m²K. Further work by Dietenberger (1995) showed that in fact the heat transfer coefficient varied along the sample, and that 15 kW/m²K was a simplification. As the surface temperature of the sample varies with position, due to the varying heat flux levels, the heat transfer coefficient will also vary as well. This is further complicated by the effect of the gas fired radiant panel in the LIFT, which provides a turbulent flow due to burning gas from the panel (Babrauskas, 2003).

Treating the control volume as a semi infinite, thermally thick solid with one dimensional heat flow into the solid gives the Newtonian heating equation in Equation (4), rewritten by Quintiere et al (1983) as Equation (7) - Equation (9) for the surface temperature at ignition, where the absorptivity α in Equation (4) is assumed to be equal to 1.

$$\Delta T_e = T_{ig} - T_\infty = \dot{q}_{e,xf}'' [1 - \exp(-at) \operatorname{erfc} \sqrt{at}] / h \quad (7)$$

$$a = \frac{h^2}{k\rho c}$$

or

$$\Delta T_e = T_{ig} - T_\infty = \dot{q}_{e,xf}'' F(t) / h \quad (8)$$

Where $F(t)$ is the time transient term

$$F(t) = 1 - \exp(-at) \operatorname{erfc} \sqrt{at} \quad (9)$$

As the time the sample is exposed to the external flux increases, then the time transient term $F(t)$ tends to zero as the material surface approaches equilibrium.

From ignition tests (Cleary, 1992) the time transient $F(t)$ is related to the flux levels:

$$\frac{\dot{q}_{ig.min}''}{\dot{q}_e''} = F(t) = \begin{cases} b\sqrt{t} & t \leq t^* \\ 1 & t \geq t^* \end{cases} \quad (10)$$

The thermal equilibrium time t^* is calculated from the ignition data, where a plot of the ratio of the (minimum heat flux for ignition $\dot{q}_{ig.min}''$ / incident heat flux \dot{q}_e'') versus (time to ignition)^{0.5} (Figure 7).

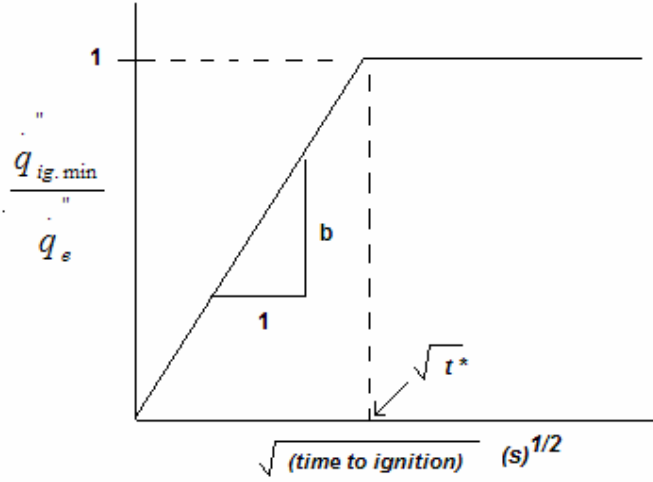


Figure 7: Ignition data plot to find preheating time t^* (from Cleary, 1992)

As the time t increases then $F(t)$ tends to a value of 1 at long ignition times, shown in Equation (11), hence the plateau in Figure 7.

$$F(t) = 1 - \exp(-at) \operatorname{erfc} \sqrt{at} \rightarrow 1 \text{ as } t \rightarrow \infty \quad (11)$$

As the time t tends to 0 – i.e. at high heat fluxes with a correspondingly short ignition time, then the exponential term tends to a value of 1 and as a result $F(t)$ tends to a function dependent on the thermal inertia, shown in Equation (12).

$$F(t) = 1 - \exp(-at) \operatorname{erfc} \sqrt{at} \rightarrow \frac{2h\sqrt{t}}{\sqrt{\pi k \rho c}} \text{ as } t \rightarrow 0 \quad (12)$$

Hence for the period of time when t is small, then the $F(t)$ can also be written as

$$F(t) = \frac{2h}{\sqrt{\pi k \rho c}} \sqrt{t} \text{ as } t \rightarrow 0 \text{ or } \quad (13)$$

$$F(t) = b\sqrt{t}$$

Where b is the ignition parameter, given in Equation (14) and this can be used to derive the effective thermal inertia $k\rho c$.

$$b = \frac{2h}{\sqrt{\pi k \rho c}} \text{ or } k\rho c = \frac{4}{\pi} \left(\frac{h}{b} \right)^2 \quad (14)$$

2.2.2 Janssens

Although the theory by Quintiere et al is specified for the ASTM E 1321 LIFT standard, some researchers have used the ignition theory by Janssens to derive the required physical properties, a summary of which by Babrauskas (2003) is as follows. The basis is derived from Equation (4) however the absorptivity α is not necessarily equal to 1, which is assumed in the work by Quintiere.

Janssens showed that an approximation for the $F(t)$ term in Equation (9) is

$$F(t) = 1 - \exp(-at) \operatorname{erfc} \sqrt{at} \approx \frac{1}{1 + 0.73(at)^{-0.55}} \quad (15)$$

$$a = \frac{h^2}{k\rho c}$$

As the ignition time increases, so that $t_{ig} \rightarrow \infty$ at the critical ignition flux \dot{q}_{crit} then Equation (15) $\rightarrow 1.0$, so then Equation (7) becomes Equation (16) at \dot{q}_{crit} .

$$T_{ig} \approx T_{\infty} + \frac{\alpha \dot{q}_{crit}}{h} \quad (16)$$

And hence the effective heat transfer coefficient can be calculated

$$h = \frac{\alpha \cdot \dot{q}_{crit}}{(T_{ig} - T_{\infty})} \quad (17)$$

Rearranging Equation (8) gives Equation (18) for the energy balance on the surface due to radiant ignition.

$$h (T_{ig} - T_{\infty}) = \alpha \cdot \dot{q}_e \cdot F(t) \quad (18)$$

Equation (15) and Equation (17) are substituted into Equation (18) and the common terms, cancel out and Equation (19) gives the time to ignition at a certain heat flux.

$$\dot{q}_e = \dot{q}_{crit} \left[1 + 0.73 \left(\frac{k\rho c}{h^2 t_{ig}} \right)^{0.55} \right] \quad (19)$$

As a result of Equation (19), the material properties can be found with the following procedure.

Using the time to ignition data for various heat fluxes, as per the Quintiere method,

plot $t_{ig}^{-0.55}$ on the y-axis against \dot{q}_e on the x-axis and fit a straight line to the data

points. The value for the critical ignition flux \dot{q}_{crit} is the intercept with the x-axis.

The ignition temperature T_{ig} is found iteratively from the energy balance at the surface at the minimum ignition flux using Equation (20).

$$\frac{\dot{q}_{min}}{(T_{ig} - T_{\infty})} = \frac{h_c}{\alpha} + \frac{\sigma(T_{ig}^4 - T_{\infty}^4)}{(T_{ig} - T_{\infty})} \quad (20)$$

The value for the absorptivity α is specified as $\alpha = 1$ in the ASTM LIFT standard. More realistically, wood products are around 0.88, and typical plastics range from 0.64 to 0.92 (Babrauskas, 2003).

Given the ignition temperature and absorptivity, then the heat transfer coefficient can be found using Equation (16), and the effective thermal inertia $k\rho c$ can be calculated from Equation (21).

$$k\rho c = h^2 \left[\frac{B_{ig}}{0.73 \dot{q}_{min}} \right]^{1.828} \quad (21)$$

where $B_{ig} = 1/(\text{slope of data fit line})$

2.3 *Opposed flow (lateral) flame spread*

2.3.1 Principles of opposed flow flame spread

Work by Quintiere (1981), Quintiere, Harkleroad and Walton (1983) and Quintiere and Harkleroad (1984) led to the ASTM E 1321 LIFT test for lateral flame spread along thick materials burning in still air (i.e., with natural convection rather than forced flow), where flame spread has been modelled as a series of piloted ignitions. The material ignites when the preheated area reaches the ignition temperature (T_{ig}), and the ignition temperature is assumed to be constant over the temperature range (Quintiere, 2002). The preheating is from the radiation of the flame of already-burning material, any external heat flux and conduction through the material (Delichatsios, 1999), as shown in Figure 8. The heating from the flame is much less than for vertical or wind assisted flame spread, as the flame does not extend over the preheating area, hence there is reduced radiation from the flame to the unpyrolised surface. The main form of heat transfer into the unpyrolised surface is through the gas phase conduction from the flame front (Quintiere, 2002).

The heat loss from the area in front of the flame front which has not yet ignited leads to the requirement for a minimum heat flux impinging on the surface and resulting surface temperature for the flame to spread. Without the heat flux to raise the temperature of the material, either from the flame or from an external source, the surface temperature will not be high enough to reach the ignition temperature, and hence there is a limiting flux for the material to give the ignition temperature required for flame spread. This is given in the LIFT/ RIFT test as the heat flux at the point where the flame front ceases to advance. The analysis by Quintiere (1981) involved a moving control volume, shown in Figure 8.

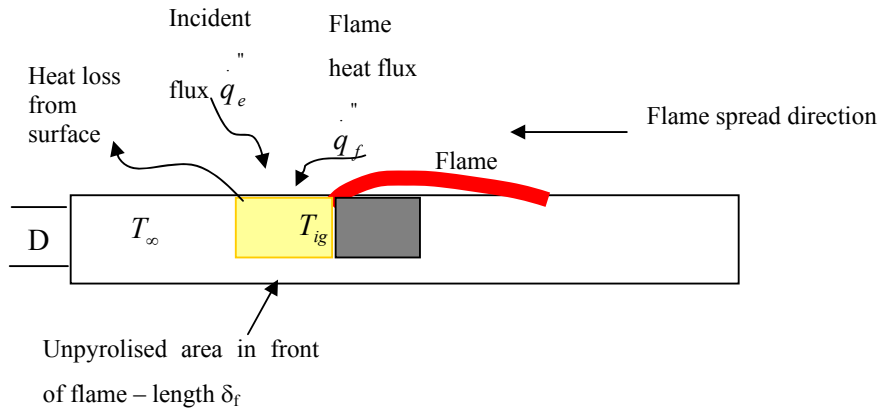


Figure 8: Opposed flow flame spread

The thickness of the material and any backing substrate can have some effect on the rate of flame spread and behaviour (Quintiere 2002). The ASTM E 1321 LIFT test requires the material to be thermally thick, whereby a thermally thick material does not have significant heat loss through the rear or sides of the sample, so that there is no significant temperature rise on the back of the sample.

For thermally thick materials, the flame spread velocity V_f at any point along the sample (Equation (28)) involves an energy balance into the control volume shown ahead of the flame front in Figure 8 (Quintiere et al, 1981) and the energy balance of the control volume can be used to give the material properties, as follows, from Quintiere et al (1983).

The solution depends on a number of simplifying assumptions:

- A key assumption is that the length of the control volume is small. This is valid for opposed flow flame spread, as the flame does not extend over the unpyrolysed area, so the preheated area is limited by conduction from the flame. The length of the control volume is up to 2mm (Quintiere, 1981). The relatively short length of the control volume (δ_f in Figure 8) allows the assumption that the incident flux \dot{q}_e on the sample is constant over that length, allowing energy absorbed to be calculated and a simple energy balance to be used.

- The temperature in the control volume increases under the received heat flux until it reaches the ignition temperature (T_{ig}), at which point it ignites. The flame spread is therefore a series of ignitions along the sample – the flame front is at the position where the surface temperature is greater than or equal to the ignition temperature.
- The external radiation \dot{q}_e varies along the sample, however the radiation from the flame front \dot{q}_f is constant and independent of the external radiation.
- More generally, the sample is assumed to be “well behaved” with homogeneous properties, unaffected by the temperature increase to ignition, and the surface does not melt or blister.

The material is assumed to ignite once the surface temperature reaches the minimum temperature for piloted ignition (T_{ig}), and this temperature increase is due to the increase from the external flux and the flame heat flux:

$$T_{ig} - T_{\infty} = \Delta T_e + \Delta T_f \quad (22)$$

The depth of the control volume into the material (D in Figure 8) is equal to the thermal penetration, which is material dependent, and is given in Equation (23) for an exposure of t seconds. The depth of the control volume is “thin” over the time it takes to heat the length of the control volume from the ambient temperature to the ignition temperature, so the temperature of the control volume is assumed to be the same at any point at a given time.

$$D_t = \sqrt{\frac{kt}{\rho c}} \quad (23)$$

If the surface material is at equilibrium with the external heat flux \dot{q}_e due to a preheating period, then an energy balance on a single unit control volume $D \cdot \delta_f$ in size, moving at the flame front velocity V_f is

$$\rho c D V_f (T_{ig} - T_{\infty}) \cong \dot{q}_f \delta_f \quad (24)$$

Taking an energy balance on the control volume, the critical heat flux to raise the temperature of the surface to the ignition temperature in an “infinite” time is given in Equation (6), reproduced below in Equation (25).

$$\dot{q}_{e,crit} = h_c (T_{ig} - T_{\infty}) + \sigma (T_{ig}^4 - T_{\infty}^4) \cong h (T_{ig} - T_{\infty}) \quad (25)$$

Where h = linearised heat transfer coefficient, including the radiation component, and the emissivity $\varepsilon = 1$, as the surface chars before ignition. Treating the control volume as a semi infinite, thermally thick solid with one dimensional heat flow into the solid gives the Newtonian heating equation in Equation (7), reproduced below in Equation (26) for the surface temperature up until ignition.

$$\Delta T_e = T_{surf} - T_{\infty} = \dot{q}_{e,x_f} [1 - \exp(-at) \operatorname{erfc}(\sqrt{at})] / h \quad (26)$$

$$a = h^2 / k\rho c$$

$$T_{surf} = T_{ig} \text{ at ignition}$$

The surface ignites once it reaches the minimum surface temperature for ignition T_{ig}

The inverse square root of the flame front velocity is found to be proportional to the difference between the critical ignition flux and the incident flux at that point, as shown in Equation (28). Rearranging Equation (24) and Equation (26) and substituting into Equation (22) gives Equation (27)

$$T_{ig} - T_{\infty} = \left[\frac{\dot{q}_f \sqrt{\delta_f}}{\sqrt{k\rho c}} \right] V_f^{-1/2} + \dot{q}_{e,x_f} [1 - \exp(-at) \operatorname{erfc}(\sqrt{at})] / h \quad (27)$$

or the flame front velocity is given as:

$$V_f^{-1/2} = C [h(T_{ig} - T_i) - \dot{q}_{e,x_f} \cdot F(t)] \quad (28)$$

where

$$C = 1 / \dot{q}_f \sqrt{a\delta_f} \quad (29)$$

$$F(t) = 1 - \exp(-at) \operatorname{erfc} \sqrt{at} \quad (30)$$

$$a = \frac{h^2}{k\rho c}$$

where C = a material specific constant referred to as the flame heat transfer modulus.

The solution to Equation (28) requires the accurate measurement of the preheating area in front of the flame front as it progresses along the sample. This is practically difficult, given the objective is to find the properties of the material to solve Equation (23).

As the time the sample is exposed to the external flux increases, then the time transient term $F(t)$ tends to zero as the material surface approaches equilibrium. For this reason, the sample in the LIFT flame spread test is preheated to equilibrium before ignition to simplify Equation (28)

The ignition parameter b , calculated from the ignition tests and equation (14), can be used to calculate the required preheating time t^* to bring the material to thermal equilibrium, which is given by Equation (31) or from reading from the ignition parameter graph (Figure 7)

$$t^* = \left(\frac{1}{b} \right)^2 \quad (31)$$

As the heat flux along the sample is known, the minimum heat flux required for the flame to spread (q_s'') is given by the location of the flame front when it self-extinguishes. Similarly, the minimum temperature for flame spread can be calculated from Equation (25), by setting the critical heat flux value in Equation (32) to that of the minimum flux for spread, and then solving for the temperature.

$$\dot{q}_s'' = h_c (T_s - T_\infty) + \sigma (T_s^4 - T_\infty^4) \cong h(T_s - T_\infty) \quad (32)$$

From Equation (27) and Equation (28), the flame velocity can be calculated. However it is difficult to do in practice as the length of the pyrolysis area δ_f is unknown. However, if the pyrolysis area is assumed to be constant for a given material due to the fact there is no flame impingement on the unpyrolysed area, and the other constants are included in a new value, then equation for flame spread velocity is as below:

$$V_f = \frac{\phi}{k\rho c(T_{ig} - T_\infty)^2} \quad (33)$$

Where the flame spread parameter ϕ can be derived from the experimental results using Equation (34).

$$\phi = \frac{4}{\pi} \frac{\pi}{(Cb)^2} \quad (34)$$

3 The ASTM E1321-97a Lateral ignition and flame transport (LIFT) test apparatus

3.1 *History*

The ASTM E 1321 standards series originated from the ASTM E 1317 Standard for marine surface finishes and work by Quintiere (1981) and Quintiere and Harkleroad (1982, 1984) and uses the same testing apparatus with the addition of a mathematical model of flame spread developed by Quintiere (1981). The difference between the two standards is principally with the pilot flame location and the addition of a 180mm long flange behind the pilot flame at the top of the sample holder. The ASTM E 1317 standard uses a vertical pilot flame at the hot end of the sample, approximately 10mm away from the sample. The ASTM E 1321-97a standard calls for a horizontal pilot flame, above the top edge of the sample with a vertical backing flange, so that the radiation from the burner flame does not affect the time to ignition results by increasing the heat flux received by the sample.

The ASTM E 1317 standard also uses a thermopile in the hood to give basic heat release data, and this is not used in the ASTM E1321-97a test.

3.2 *Requirements of the ASTM E 1321-97a LIFT apparatus*

The standard LIFT testing apparatus uses a gas fuelled diffusion burner and a vertical sample holder, angled at 15 degrees away from each other (Figure 9). The plans for the ASTM E 1317, upon which the ASTM E 1321-97a LIFT test is based, were issued by the National Bureau of Standards and are available from the ASTM as ADJE1317 Adjunct to ASTM1321-97a.

The 155 x 800mm sample holder is angled at $15^{\circ} \pm 0.25^{\circ}$ to the face of the burner (Figure 9). The hot end of the sample is 125mm away from the face of the burner, and offset from the edge of the burner by approximately 125mm (Figure 10). The burner is a flat panel burner 280mm high x 430mm long, with radiant ceramic elements and a reverberant screen. This is mounted so that it allows the burner

assembly to rotate to allow horizontal testing, although this is outside the standard test procedure. The rotating ring assembly can be seen behind the burner in Figure 11. The burner offset can be adjusted to give the best match to the standard flux profile (Figure 12). This gives an almost constant flux level for the first 150mm along the sample for use in ignition testing, and then a decreasing flux level to approximately 2% of the peak heat flux.

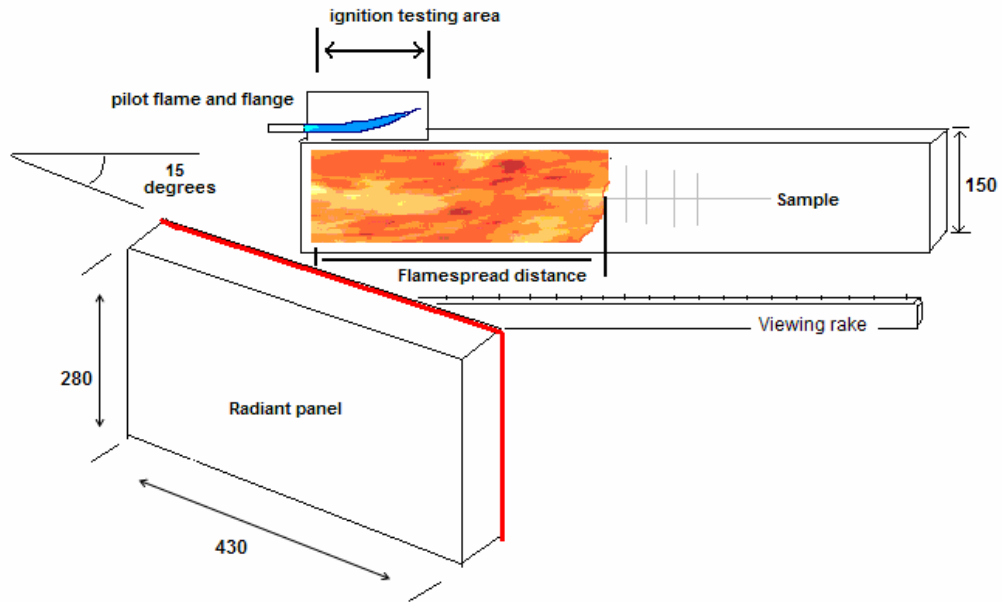


Figure 9: Main components of LIFT apparatus

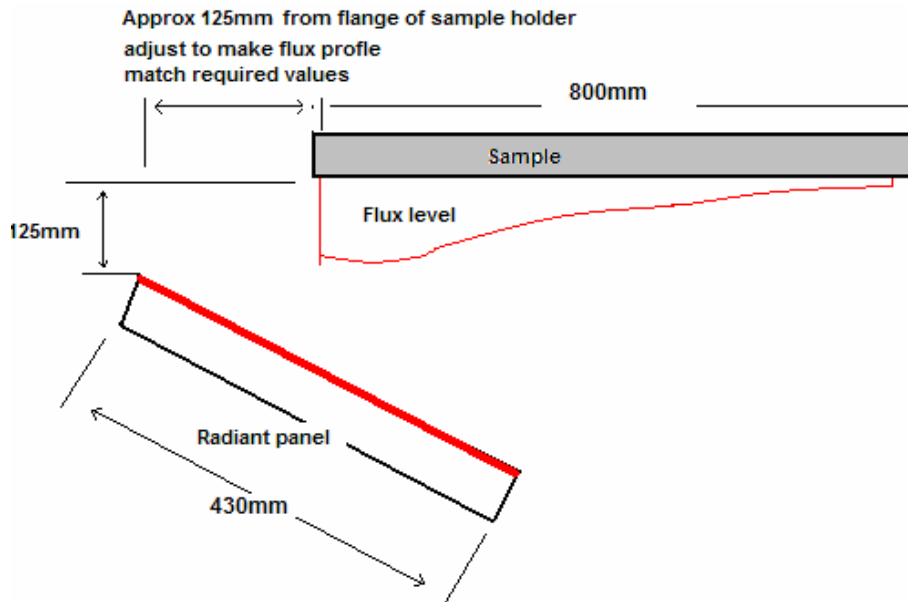


Figure 10: Schematic of LIFT apparatus

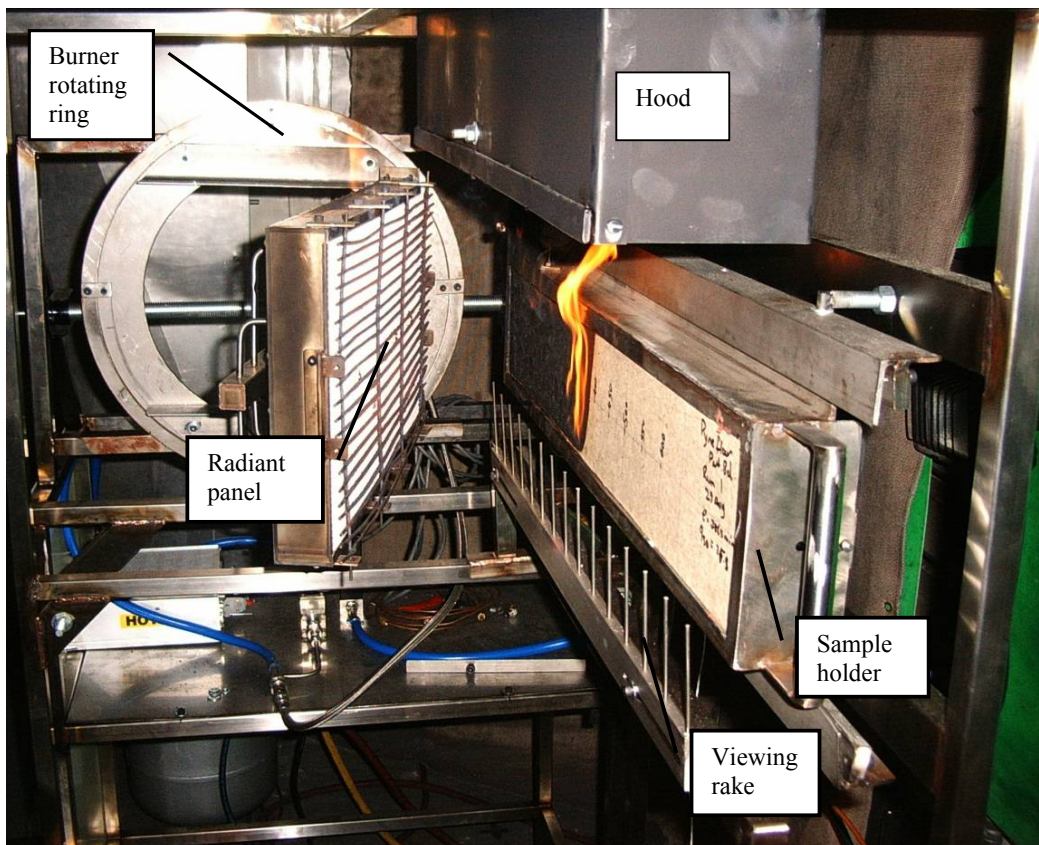


Figure 11: LIFT showing angled gas radiant panel (left) and sample holder (right)

The results from the ignition or flame spread tests can be observed directly or via an observation mirror, which is at the front of the unit and angled to look under the

burner, and this can be seen more clearly in Figure 13. A viewing rake, seen under the sample holder in Figure 11, allows the operator to monitor the flame spread along the face of the sample.

The output of the burner can be varied to suit the desired flux levels by altering the air and gas settings. The standard calibration output, measured at the sample face, is shown in Figure 12.

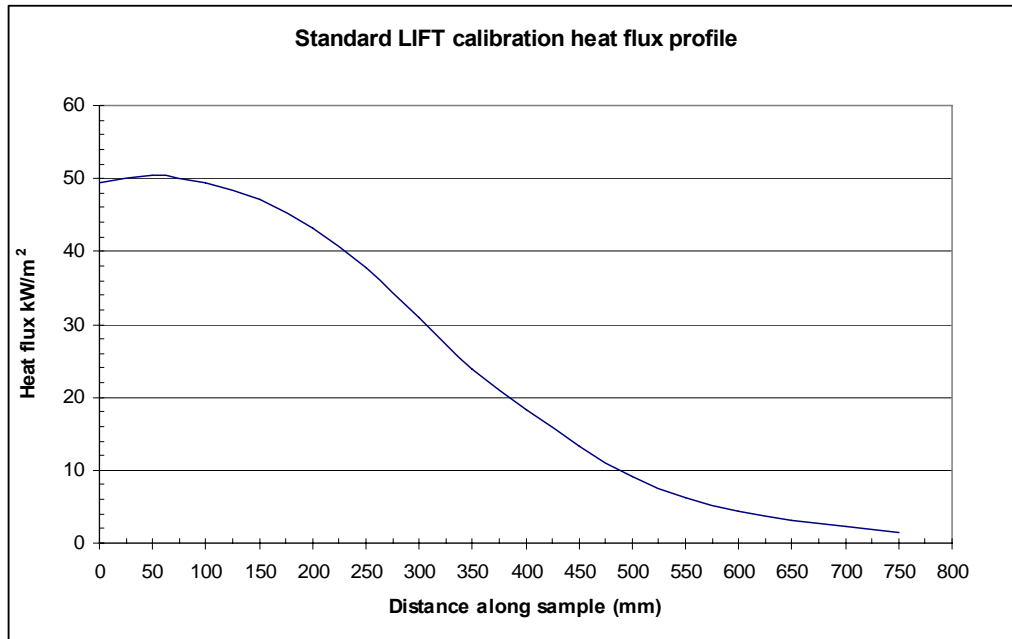


Figure 12: Standard ASTM E 1321 LIFT heat flux distribution for calibration

3.3 *The University of Canterbury LIFT apparatus*

3.3.1 Apparatus description

The LIFT apparatus used in these experiments was built in the University of Canterbury (UC) over a period of 5 months in 2005. While it follows the design for the ASTM E 1317 apparatus (Adjunct to ASTM E 1317), with the modifications listed for the ASTM E 1321-97a standard, there are some variations. The main variation from the ASTM standard is the fuel used for the burners. The ASTM E 1321-97a LIFT standard calls for methane powered main burner with an air-acetylene pilot flame, whereas the University of Canterbury LIFT uses Liquefied Petroleum Gas (LPG) – a mixture of propane and butane - for both burners, controlled via mass flow

controllers and a variable pressure air regulator (Figure 13). The radiant panel also has adjustable spacing using a leadscrew and hand wheel (Figure 14) to allow for lower heat fluxes for the ignition tests than the LPG fuelled burner can provide.

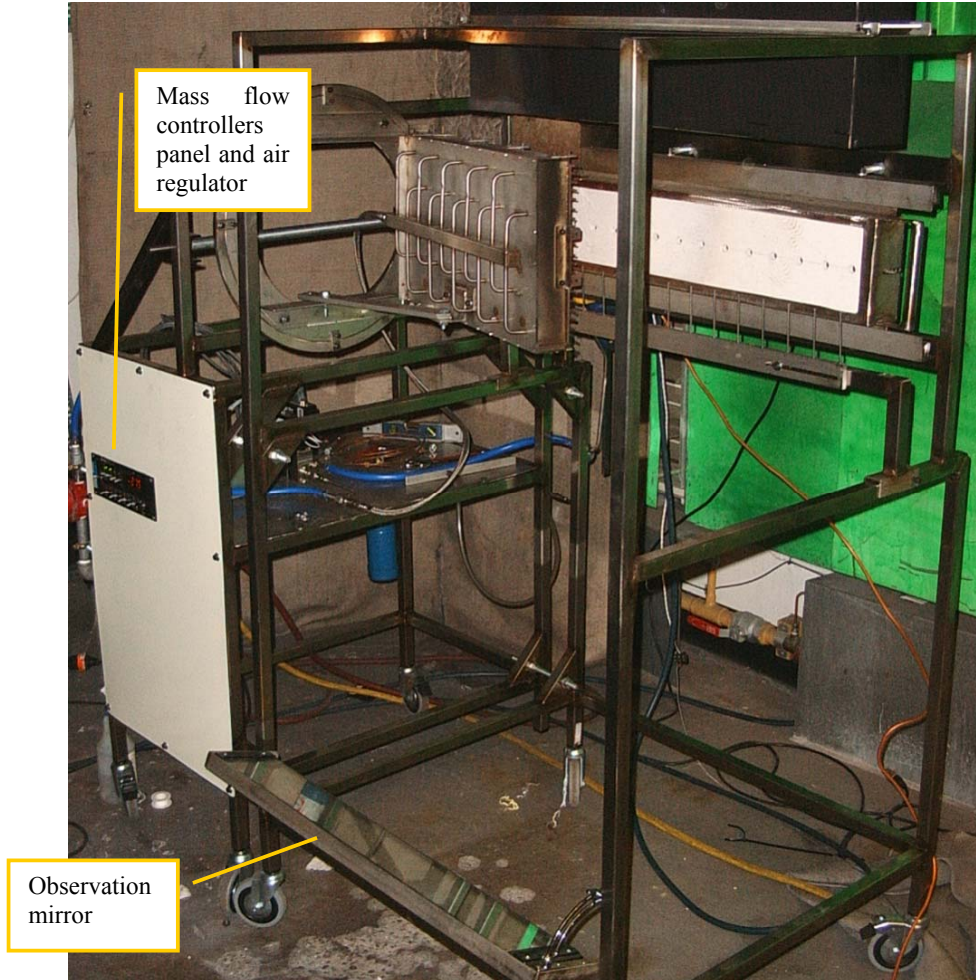


Figure 13: University of Canterbury LIFT apparatus with measuring template in sample holder

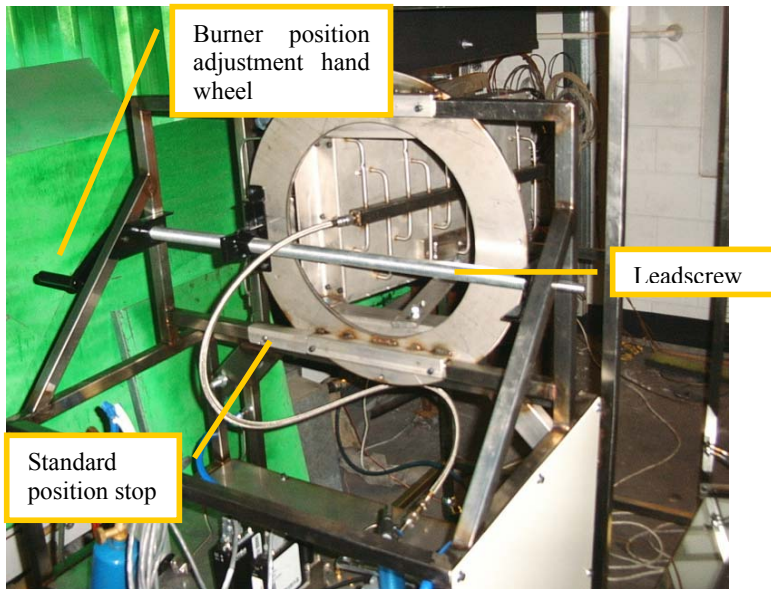


Figure 14: UC LIFT burner position adjustment showing rails and leadscrew

3.3.2 Fuel and air supply

Due to the unavailability of methane, the UC LIFT uses LPG and a compressed air supply for the main radiant panel burner fuel and the pilot flame. The decision to use methane for the burner used in the original research (Quintiere, 1981) and the subsequent ASTM standard was dictated by the wider range of the methane fuelled radiant panel for the ignition test which form part of the experimental procedure. The spacing of the propane fuelled radiant panel used in this case can be adjusted, as the burner can slide on rails and the position is set by using a lead screw (Figure 14) to give the lower flux levels within the limitations of the burner output. This is only for the ignition tests, as the radiant panel can be used with the standard spacing for the flame spread tests.

The use of LPG fuel for the burner is justified by the previously published work in the literature. LPG is a mixture of propane and butane, and propane has been used for ignition experiments with the ASTM E1623 ICAL intermediate scale calorimeter (Grand and Mehrafza 2001), which also normally runs on methane or natural gas. The ICAL procedure also uses a fixed sample, and changes the distance from the burner to alter the flux received by the sample. Similarly, in a round robin test of the IMO Resolution A. 653 (16) marine finishes flame spread test (also known as the ASTM E

1317 standard) which uses the same apparatus as the ASTM E 1321 LIFT test, it was noted that one of the laboratories used propane for the radiant panel burner, although this was later changed to methane. (Pauner, 2003).

The propane powered radiant panel burner used in the UC LIFT has a lower limit of $\dot{q}_{50mm}'' = 25\text{kW/m}^2$ at the 50mm measuring point when set up in accordance to the standard LIFT spacing (Figure 10), as the burner behaviour becomes unstable and has uneven heating below this level. From the observed conditions during the experiments, it appears that a change to the gas manifold to allow a more even entry of gas to the centre of the gas panel would allow a setting lower than the 25kW/m^2 limit currently imposed, by reducing or eliminating the uneven burning across the face of the panel, giving a lower limit of approximately 20kW/m^2 on LPG.

The limitation of $\dot{q}_{50mm}'' = 20\text{-}25\text{kW/m}^2$ for the propane fired panel of the UC LIFT is not generally a limitation for the flame spread tests, as the flux level is usually set to $5\text{-}10\text{kW/m}^2$ over the minimum ignition flux, and for timber based products, the minimum ignition flux is usually in the order of 12kW/m^2 (Babrauskas, 2001), and usually higher for ignition tests conducted in the LIFT (Babrauskas, 2003). The level that the panel is set at is not critical, as it is only to increase the resolution by reducing the step size between each measuring point, and to reduce charring during the preheat period.

An upper limit was found of $\dot{q}_{50mm}'' = 50\text{ kW/m}^2$, due to the air supply to the burner. The air compressor used was unable to supply sufficient air for the burner at higher outputs. In trials using an additional air compressor in parallel with the main air supply, the burner was capable of producing heat fluxes greater than $\dot{q}_{50mm}'' = 60\text{kW/m}^2$, but there was not sufficient air capacity to hold this level for extended periods.

At heat flux settings less than $\dot{q}_{50mm}'' = 30\text{kW/m}^2$, initial tests showed erratic output from the burner, where it cycled in a periodic manner, shown in Figure 15. The

problem was traced to a combination of the air compressor cycling and variation of the output of the air supply regulator. Changing the air compressor set points to increase the running time, and adding a ball valve to allow some preload of the regulator to a minimum of 8psi gauge pressure significantly reduced this problem. It can be seen in Figure 16 that the heat flux output with the regulator preloaded to 8psi is more stable than without any preload.

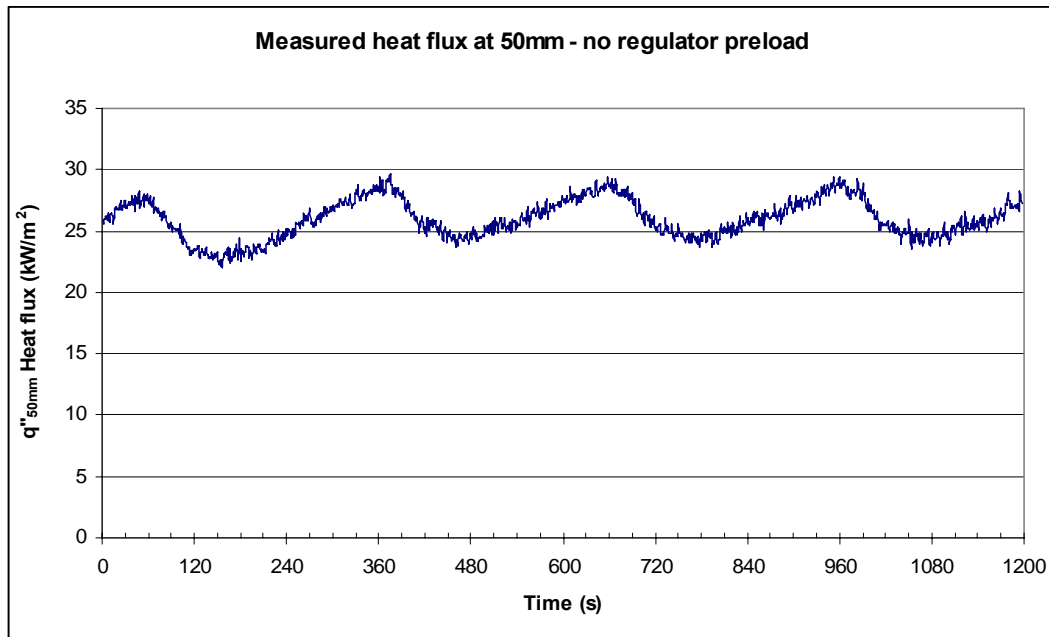


Figure 15: Heat flux variation without preloaded air regulator

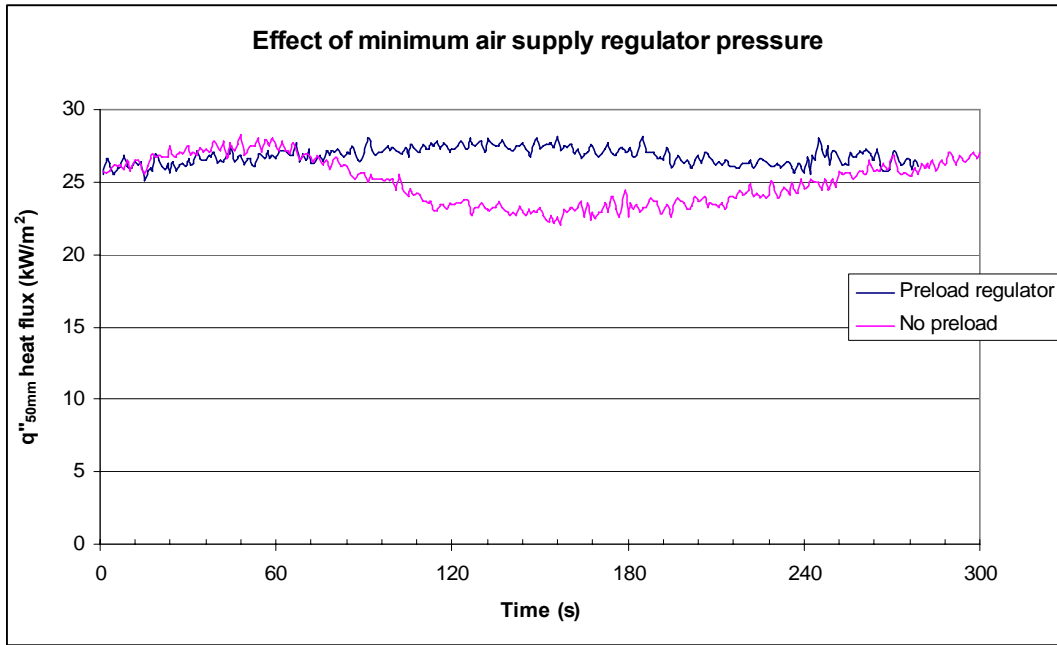


Figure 16: Effect of preloading air regulator to minimum of 8psi on heat flux variation

3.3.3 Flux measurement and calibration

Both the LIFT and the RIFT require a measurement of the heat flux at points along the sample face, to allow the calculation of the flame spread velocity and minimum flux level for flame spread. This is done by using a water cooled flux gauge with a template. The template is made from rigid refractory board, with holes drilled at intervals to suit the head of the flux gauge. The head of the flux gauge is to be a snug fit in the holes, without excess clearance; 12.7mm (1/2 inch) diameter holes were used in the templates. The hole spacing for the LIFT template is at 50mm centres, measured from the edge of the flange of the sample holder.

The heat flux gauge was bent to allow it to be clamped to the rail behind the sample holder (Figure 17), in order to keep the flux gauge in place and at a consistent angle while measurements were taken. In use, it was found that care had to be exercised to ensure that the head of the heat flux gauge was flush with the face of the template and not shielded by being inside the hole. Other work, outlined in Section 10.1, indicates that having the head of the flux meter proud of the surface of the template,

particularly at the cold end of the sample, will improve the accuracy of the measurements.



Figure 17: Flux gauge and template

For the initial calibration for the radiant panel position, the panel was set to the standard angle and position (Figure 10). With the burner output to 50kW/m^2 , measured at the 50mm position, the flux levels were measured at 50mm intervals along the sample template using a calibrated heat flux meter. When compared to the standard values, the measured values must be within 10%. The burner position can be adjusted by moving the burner frame relative to the sample frame to alter the offset to give the desired distribution and so the sample angle remains at 15° and the gap between the sample ($x=0\text{mm}$) and the face of the burner remains at 125mm.

Prior to the flame spread tests, this procedure was repeated for the desired peak heat flux level, so the distribution along the sample was known.

The average of 3 calibration runs over 3 days is shown in Figure 18 and Figure 19. The flux profile matches the standard profile well, although the cause of slightly higher value at 350mm is unknown.

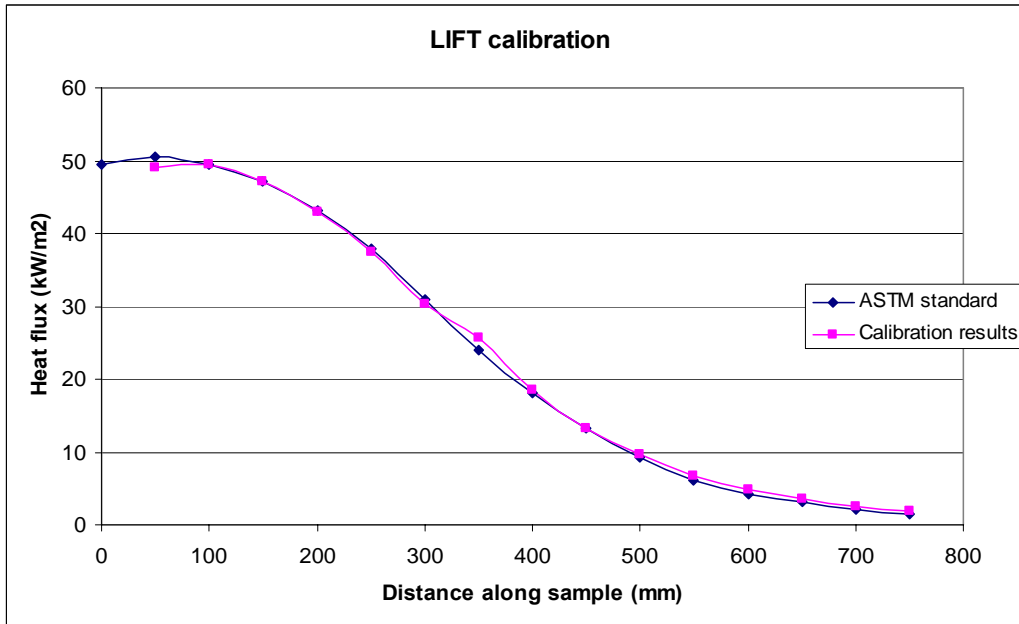


Figure 18: LIFT calibration profile

From 600mm onwards, the calibration results are outside the 10% limit (Figure 20), however this is beyond the limit of flame spread along the sample for the materials tested, so was not considered to be important. The results of the ASTM E 1317/ IMO resolution A.653 (16) interlaboratory round robin comparison (Pauner, 2003) showed a similar level of variation at the cold end of the sample at the same reference q_{50mm} heat flux. The tests published by Nisted (1991) and Babrauskas and Wetterlund (1999) also had this issue and adopted the same approach. Due to the low flux levels at the cold end of the sample, the absolute error is less than the percentage variation would indicate.

Since the heat flux gauge was held flush with the surface of the measuring template, it records the radiative and a convective component to the total heat flux at the point. Dietenberger (1995c) showed the convection coefficient along the sample varied with position, and hence the convective component diminishes along the sample. Dietenberger recorded a bias up to 13% at the 750mm position for this reason.

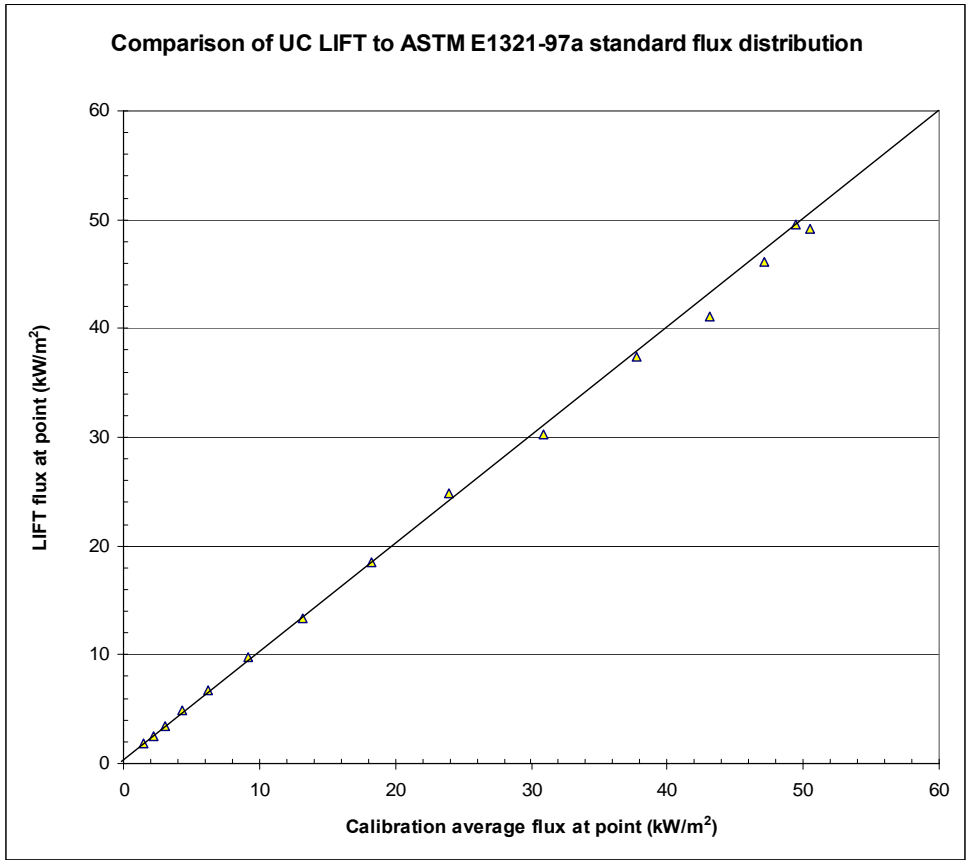


Figure 19: Comparison to UC LIFT calibration flux to ASTM E 1321 standard

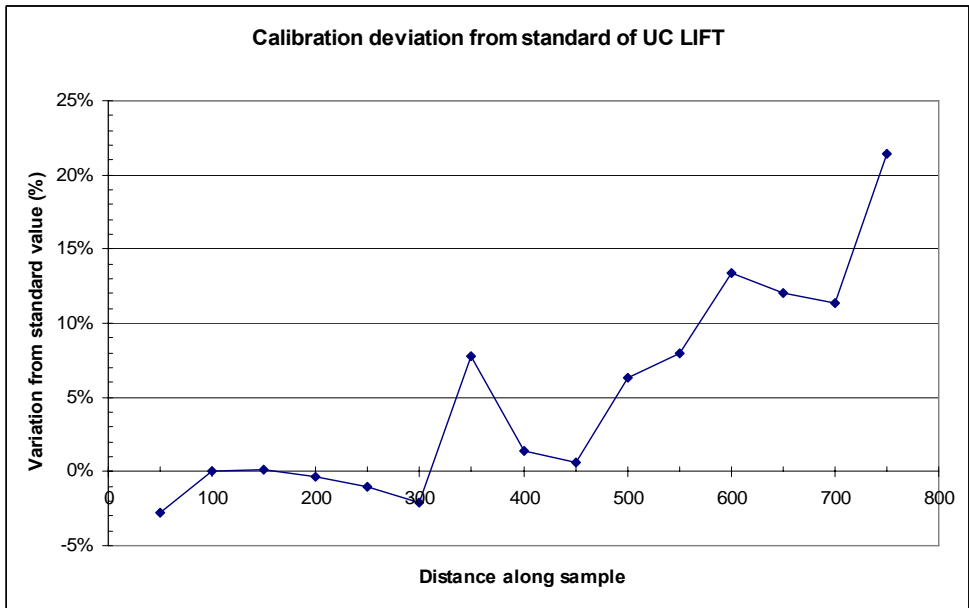


Figure 20: Variation from standard for calibration of LIFT

3.3.4 Heat flux from the pilot flame

The heat flux from the pilot flame to the sample was measured at the \dot{q}_{50mm} position, without the main burner running. The net increase of heat flux to the sample is given in Table 2. The effect of any draft or buoyancy driven updraft was noticeable, with an increase in the net heat flux to the sample of 50%, as the flame moves away from the backing flange. The effect of the pilot burner on the ignition time is within the variation of the experimental error, and variation of the burner output, so cannot be considered a significant source of error.

Average flame heat flux	0.14 kW/m ²
Background flux	0.03 kW/m ²
Net heat flux from flame to sample	0.11 kW/m ²

Table 2: Pilot flame flux to sample

3.4 LIFT Operating Procedure

The operating procedure for the UC LIFT is given in Appendix 1. The effect of moisture content in the LIFT test is controlled by conditioning the samples at 50±5 % RH and 23±3°C until the product weight stabilises so that the change in mass over a 24hour period is less than 0.1% of the sample mass. All materials used in the experiments conducted in this report were conditioned for at least two weeks, with the conditioning room and laboratory conditions being at the lower end of the allowable range. No oven drying calculations were conducted to get the moisture content of the materials; however Simpson and TenWolde (1999) provide data for the typical moisture content of wood in equilibrium with the surrounding air. For the allowable range given in the ASTM LIFT standard, then the moisture content of the natural timber samples would be between 8.5% and 9.9% MC. The data from Simpson and TenWolde (1999) does not specifically address particle board or Meltica boards, where the high adhesive content may cause some difference to the equilibrium moisture content.

3.4.1 Ignition test

The LIFT test comprises of 2 parts, the first is an ignition test where the time to piloted ignition t_{ig} is obtained for various heat fluxes \dot{q}_e , and the minimum heat flux

for ignition ($q_{ig,min}$) is obtained by bracketing the ignition results to find the lowest flux which will cause ignition within 20 minutes. The critical heat flux for ignition (q_{crit}) is obtained by plotting $1/\sqrt{t_{ig}}$ against q_e , and the critical heat flux is given by the intercept with the q_e axis. The minimum heat flux for ignition ($q_{ig,min}$) is given by plotting the time to ignition vs. heat flux and the curve will asymptote at the value for $q_{ig,min}$.

Samples, 155 x 155 (+0,-5)mm were conditioned before the tests so that successive weighings, taken 24 hours apart, did not vary by more than 0.1% of the mass. The readings of the temperature and humidity in the conditioning room during the conditioning period indicated that they were generally at the lower end of the allowable range of $23^{\circ}\text{C} \pm 3^{\circ}\text{C}$ and a relative humidity of $50\% \pm 5\%$. The samples had the edges and back covered in aluminium foil during the test to reduce heat loss, and an insulated backing board is used. (Figure 21)

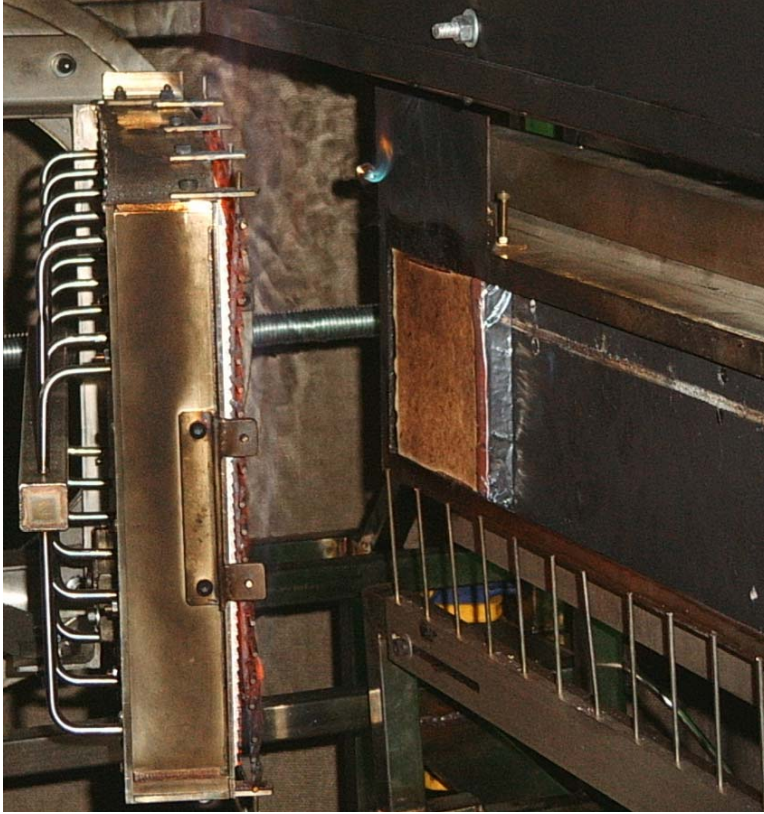


Figure 21: Ignition test of particle board in LIFT

The heat flux level at the sample face was measured using a water cooled heat flux gauge and the measuring template, which was fitted to a sample holder frame. The flux measurements for the ignition tests are conducted at the 50mm position – i.e. 50mm from the edge of the flange on the front face of the sample holder frame. After lighting the pilot burner and main burner, the pilot burner was adjusted to give a flame approximately 180mm long, and after the burner was allowed to equalise for 5 minutes, the flux output was adjusted to give the desired flux level at the 50mm position on the flux measuring template. The equipment was allowed to stabilise to give a constant output prior to testing.

The sample was wrapped with foil on the back and sides and placed with an insulated backing board in a second sample holder. The measuring template was removed and within 10 seconds the sample was slid into place and timing started.

Once the sample ignited, it was removed and extinguished, the burner was adjusted to the next flux level, again using the heat flux gauge and template, and the burner was left to stabilise prior to testing the next sample.

A series of tests was done at varying heat flux levels to bracket the minimum flux for ignition to within 2kW/m^2 , and up to the maximum that the burner could deliver.

3.4.2 Analysis of the ignition test

The basis for the ignition analysis is the ignition theory of Quintiere et al (1983) given in section 2.2.1.

Using the ignition data as above, the time to ignition (t_{ig}) versus heat flux (\dot{q}_e) was plotted. The graph asymptoted to the minimum ignition flux ($\dot{q}_{ig,min}$) with a time to ignition limit of 20 minutes.

The (minimum ignition heat flux / incident heat flux) ($\dot{q}_{ig,min} / \dot{q}_e$) versus $1/\sqrt{t_{ig}}$ was plotted and a best fit line through the origin was overlaid on the data. As discussed in the following section, values where ($\dot{q}_{ig,min} / \dot{q}_e$) > 0.8 were ignored as discussed below, if it significantly improved the fit of the data. This was a matter of engineering judgment as to the effect of these outliers due to the long heating times before ignition.

The point at which the best-fit line passes ($\dot{q}_{ig,min} / \dot{q}_e$) = 1 is the square root of the preheat time t^* for the flame spread test – i.e. $\sqrt{t^*}$. The slope of the best fit line was the ignition parameter “b”, and this was used to solve for $k\rho c$, the thermal inertia using equation (14).

Reduction of ignition data

Since the behaviour of the material changes as the heating time increases, the fit of the data for the correlation to a straight line becomes increasingly less accurate, in particular for the data used in Quintiere et al’s method. The values which best reflect the thermal inertia are those at the higher heat fluxes with the corresponding shorter ignition times. For the most accurate result, some of the data for points close to the minimum ignition flux must be ignored. The problem is that the choice of acceptable

data points is not clearly defined, a problem that has occurred for other researchers in the past:

“From the examples shown in Figure x1.2 of the (ASTM E 1321) standard, it is clear that the sloping-line segment should follow only the initial set of data points. Data points for large values of \sqrt{t} are not to follow the sloping-line segment, but rather should end up fitting the subsequent horizontal line segment. Unfortunately, the standard gives no guidance as to how this is to be done. In our study, we inspected the individual data points and excluded as many from the high end of the time scale as did not follow the same slope as the data points on the left side of the graph...

.... This process is clearly dependent on the judgement of the individual doing the data reduction. This means that, *starting with the same raw data*; two different operators can produce different values of reduced data.”

(Babrauskas and Wetterlund, 1999, page 23)

Attempting to define the limit for this report, based on the thermal penetration depth using equation (3) did not give a definite cut-off for acceptable data, especially if there was some scatter. In order to provide consistency, the data was plotted and a regression fitted to the data and the result was visually inspected. As a guide, points above $(\dot{q}_{ig,min}) / \dot{q}_e > 0.8$ could be discarded if it significantly improved the fit of the data. This value was chosen as it encompassed the values close to the minimum ignition flux where the deviation was the greatest.

The R^2 correlation coefficient calculated by the spreadsheet for the fit of the data was used as a guide to what was deemed a “significant” difference. When considering whether to include a data point, it is again arbitrary, but if the R^2 value improved by more than 0.15 by excluding a data point, then this was deemed to be significant, and the value could be deleted. The difference was generally obvious from visual inspection.

The choice of which data points to include can have a significant effect on the ignition parameter “ b ” and particularly the preheating time t^* .

3.4.3 Flame spread test

Samples, 800 x 155 (+0,-5) mm were conditioned before the test as above. The samples had the edges and back covered in aluminium foil during the test to reduce heat loss, and an insulated backing board was used.

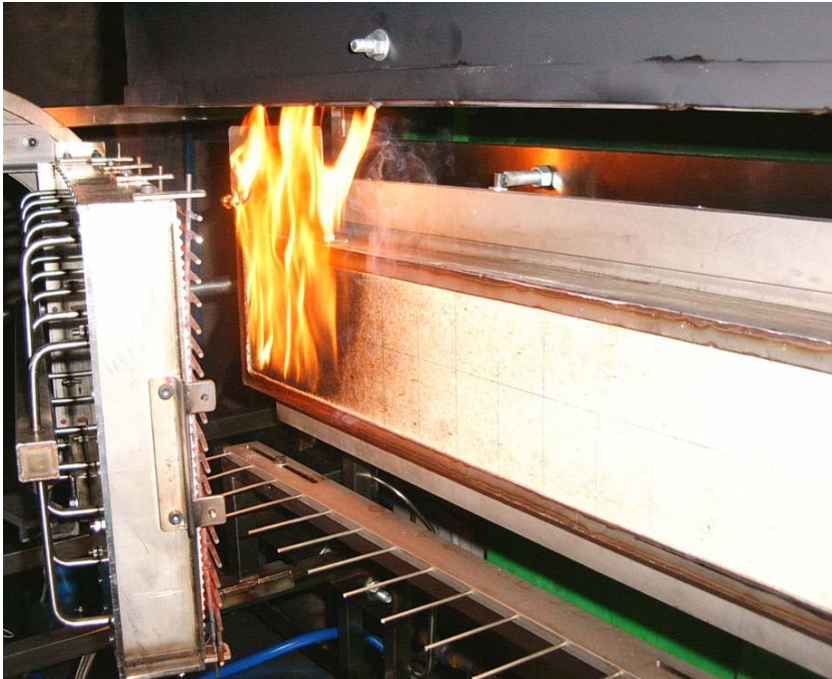


Figure 22: Flame spread test

Using a lead pencil, a line was scribed along the centre of the sample, in the long direction, with intervals marked at 25mm spacing, starting at the flange of the sample holder.

After igniting the pilot burner and main radiant panel burner, the pilot flame was adjusted to approximately 180mm long, and the radiant panel output to approximately 5-10kW/m² over the minimum ignition flux level calculated in the ignition test For the material being tested. The panel was left for 10 minutes to stabilise prior to starting the test. The flux levels at 50mm intervals along the sample were measured, using the flux gauge and measuring template, and then the pilot burner was turned off.

The sample holder containing the measuring template or dummy sample was removed and within 10 seconds the sample holder containing the test specimen was slid into

place and the timing started. If the sample did not ignite within the preheating time t^* calculated from the ignition tests, then the pilot burner was lit or the sample was ignited at the bottom of the hot end using an hand held flame.

The time of ignition was recorded and the spread of the flame front was timed along the sample, using the reference points marked on the sample, or by using the viewing rakes and observation mirror.

As the flux level is effectively constant over the first 150mm of the sample, the flame spread very rapidly over this section. If it was extensively charred from a long preheating period, then it was difficult to ignite using the pilot burner, in which case, a small pilot flame was applied directly to the hot end of the sample.

3.4.4 Analysis of flame spread results

The analysis for the material properties is given in section 2. As noted by Babrasukas (1995), the units used in the flame spread calculations are inconsistent. The sample measuring positions are given in millimetres along the sample, but the calculation of the flame spread parameter value (ϕ) requires the velocity to be in metres/second. The calculation in this case changed the velocities to metres/second.

The velocity of the flame front is calculated using a three point least squares fit calculated from the distance and time results of the nominal point and the points behind and in front – i.e. x_n , x_{n-1} and x_{n+1} using Equation (35) to get the average at the point.

$$V_f = \frac{\Sigma(t.x) - \frac{\Sigma t \Sigma x}{3}}{\Sigma t^2 - \frac{(\Sigma t)^2}{3}} \quad (35)$$

$F(t)$ was calculated for each interval along the sample, where $F(t) = 1$ if the time from inserting the sample was greater than the equilibrium time t^* .

A graph of $1/\sqrt{V_f}$ on the y-axis against ($q_e'' \cdot F(t)$) on the x-axis was plotted and a regression line was fitted to the data (Figure 23)

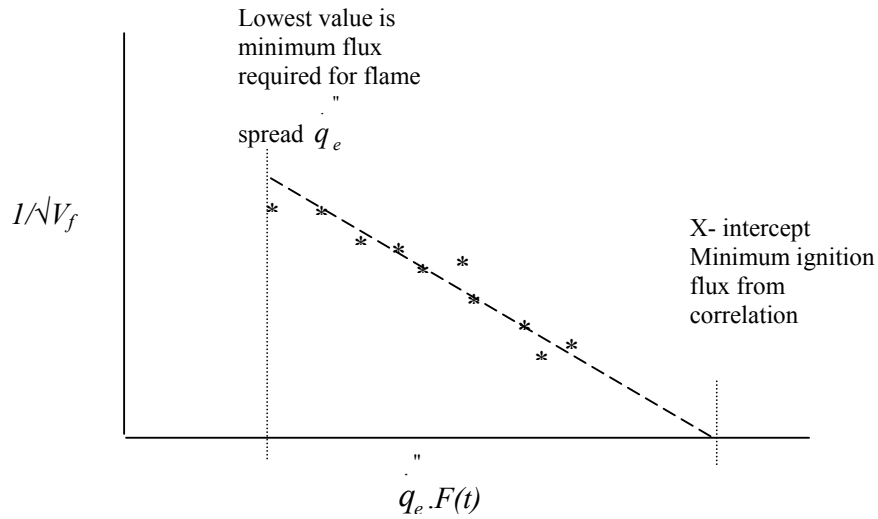


Figure 23: Flame spread correlation graph

The lowest value of $\dot{q}_e.F(t)$ gave the minimum heat flux for flame spread (\dot{q}_s), as an alternative to the heat flux at the point of the extent of flame spread on the sample during the test.

The point at which the regression line crosses the x-axis gave an alternative means of calculating the minimum ignition flux $\dot{q}_{ig,min}$. Note that strictly speaking, the value of $\dot{q}_{ig,min}$ was an experimental result, whereas the value from the graph was a correlation, so some difference in the result was expected.

4 The cone calorimeter

The cone calorimeter was developed by the National Bureau of Standards (now National Institute of Standards and Technology), part of the US Department of Commerce, in 1982. It was a radical departure from previous heat release measuring systems, and attempted to eliminate some of the problems that previous methods had (Babrauskas, 1993). It was adopted as an ISO standard (ISO5660) in 1992, and forms the basis of an increasing number of legislative tests (Babrauskas, 1992) and models of other standards, such as the ISO 9705 room-corner test (Beyler et al, 1999) and the ASTM E 84 “tunnel” flame spread test (White and Dietenberger, 2004).

Conceptually, it is a simple method, but gives the ability to produce a lot of data with a high degree of automation in the data collection. It has a conical element, which gives the device its name. For conventional fire testing, a sample, generally 100mm*100mm is mounted on a load cell, so that the mass loss during burning can be recorded. The sample is exposed to a heat flux, up to 100kW/m², and the heat release rate, mass loss and toxic gas production is recorded. Further enhancements have included measuring the smoke production, opacity and the effect of atmosphere (vitiating or oxygen enriched) on the burning behaviour.

There are a number of key features that make it different from other methods of bench scale fire testing (Figure 24). Most obviously is the use of the conical electric element. Most other devices of this sort at the time used flat panel radiant elements, generally gas fired. Using an electrical element eliminated the need for the fragile refractory ceramic tiles and gas supply, and gave a more consistent control. More importantly, it allowed testing to be done in the horizontal position, particularly for melting materials. The conical shape gave an almost constant heat flux across the face of the sample, yet allowed the smoke and combustion products to escape without interfering with the radiation from the element.

The combustion products are collected in a hood, and sampled to measure the oxygen, carbon monoxide and other gas levels. The heat release rate is calculated using oxygen consumption calorimetry, whereby the amount of oxygen consumed by the combustion is measured. The heat released per mol of oxygen consumed is effectively constant at 13.1kJ/kg and hence by measuring the oxygen consumed, the heat release

rate for the sample can be calculated. As the sample is mounted on a load cell, the heat release rate can be compared with the mass loss and an effective heat of combustion can be determined.

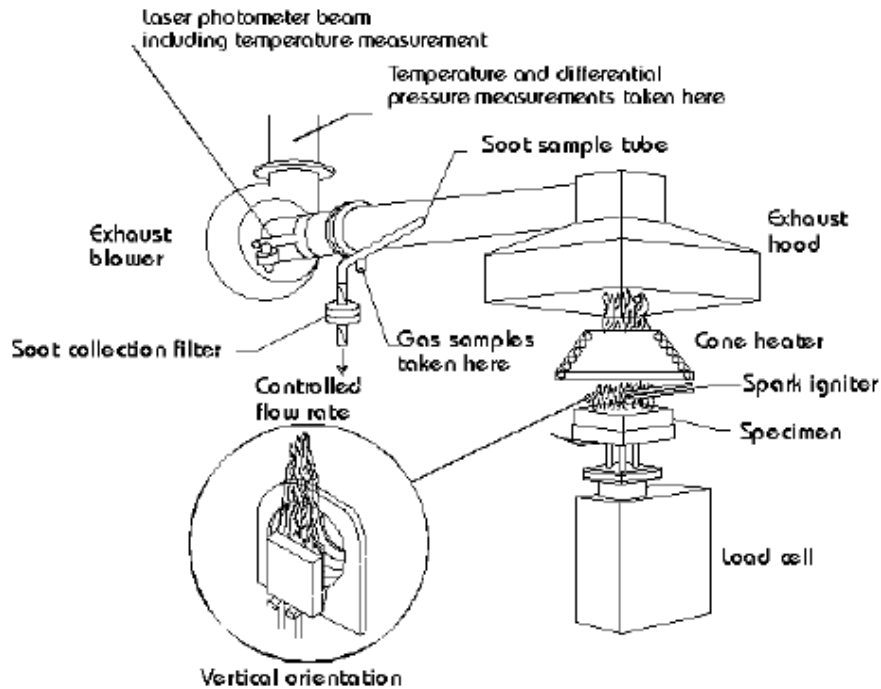


Figure 24: Cone calorimeter (reproduced from Babrauskas, 2002)

The pilot ignition is by a spark gap, and the position of this is adjustable to be centred in the middle of a horizontal specimen, or at the top of a vertical specimen.

A key advantage of the cone calorimeter against tests such as the LIFT is that the data collection is automatic and extensive, hence more data can be collected, the tests are faster and the results do not require as much judgement or manipulation. The cone calorimeter has successfully been used to model a variety of other tests and standards, giving good results for well behaved materials, such as timber products (Janssens, 2005). Thus far, efforts to model lateral flame spread using only cone calorimeter data (Jianmin, 1990) have generally not been successful (Goransson, 1991, Persson, 1993).

While the RIFT as tested here is only concerned with ignition and flame spread, Azhakesan et al (1998) used the RIFT data in conjunction with mass loss readings and calorimetry to give a simultaneous heat release rate as part of a room fire model.

5 ISO 5657-1987 Ignition test

The ISO 5657 apparatus was originally designed in 1970 in the Experimental Building Services in Australia, now part of the CSIRO (Babrauskas, 2003). The ISO 5657-1987 ignition apparatus is similar to the cone calorimeter, in that it uses a conical electrical element, although the size and shape is slightly different. The element is electronically controlled via a thermocouple controller with a maximum heat flux to the sample of 50kW/m^2 .

. The standard ignition method was part of the original British Standard BS 476: 1987: Part 13, from which the ISO 5657-1987 standard is derived. This originally used a small pilot flame, which is dipped above the sample at 4 second intervals – giving a resolution of ± 2 seconds. The ignition in the University of Canterbury ignition apparatus is now a spark, similar to the cone calorimeter, to give a more accurate time for ignition. The pilot flame apparatus, seen on the centre of Figure 25, is still present but was not used for these experiments, or those by Ngu (2002).

The test differs from the cone calorimeter in that it uses a weighted platform with a counterweight (seen on the right side of Figure 25) to hold the sample against a flat plate with a circular cut-out, in order to provide a consistent distance from the sample to the element, even if the top of the sample shrinks away. The sample size is also larger, using a 165mm square sample, instead of the 100mm sample used in the cone calorimeter. In both cases, the sample is backed by an insulating board. Only a circular area of 150mm diameter of the sample is exposed the element, with the remainder of the sample shielded by the flat plate.



Figure 25: ISO 5657 ignition apparatus

The sample is wrapped in aluminium foil. The BS476: 1987 Part 13 standard calls for the top of the sample to be covered with aluminium foil, with a circular cut-out, to prevent the plate from being soiled by residue.

A shield is used while the sample is being placed in position, shown on the bench in Figure 25, which is removed and timing started until the sample ignites, or the test duration is over. Replacing the shield extinguishes the burning sample which can then be removed.

6 Reduced Scale ignition and flame test (RIFT) method

The RIFT method is a result of research published by Azhakesan et al (1998) at FireSERT in Ulster, Northern Ireland. The objective was to provide an alternative to the standard LIFT test for spread-of-flame measurements, by using a modified cone calorimeter, rather than requiring the ASTM1321 LIFT test apparatus. The results published from Azhakesan et al (1998) showed some success.

Further work was done at the University of Newcastle by Pease (2001) and by Huynh (2003) from the University of Canterbury. These results were inconclusive and showed a lack of resolution in the measurements. The principal problem was identified as the location of the sample, where the hot end of the sample was on the centreline of the cone (Figure 26), so only half the heat flux from the cone was available. The resulting flame spread was in the order of 90mm along the sample (Huynh 2003), and the resolution was insufficient to give accurate data.

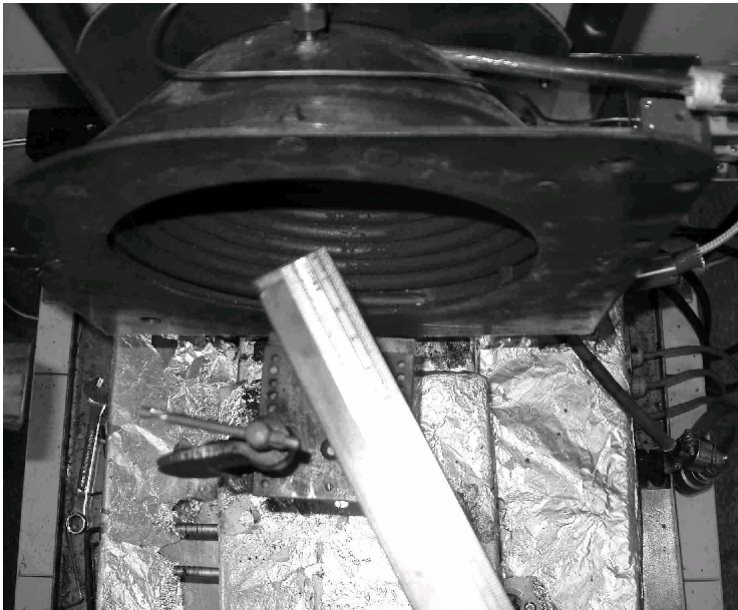


Figure 26: Australasian RIFT test, showing location of sample to the cone (reproduced from Huynh, 2003)

The angle of the sample in the tests in Australia (Huynh 2003, Pease 2001) and Ulster (Azhakesan et al 1998) was at 60 degrees to the cone heater element face, compared

with 15 degrees for the conventional LIFT test, which uses a larger flat panel element. The sample size chosen was 100 x 350mm in Ulster, and 100 x 250mm in Australia.

6.1 Comparison between RIFT and LIFT

The LIFT uses a sample angle of 15 degrees with a flat radiant gas panel instead of the conical element of the RIFT and the LIFT burner panel size and the sample size are in the order of three times larger than those used in the RIFT.

The effect of the smaller scale of the RIFT is shown in Figure 27 where the sample angle and peak heat flux is set at the same values for both sets of apparatus. The heat flux decays more rapidly in the RIFT as the measurement moves away from the element, due to the directional nature and smaller size of the cone and consequently the smaller size of the sample. .

Comparing the heat flux of the RIFT with the LIFT shows that the potential peak heat flux is less (the LIFT has a peak up to 50kW/m²) and the heat flux diminishes more quickly with the RIFT. The peak heat flux for the RIFT is largely dictated by the available cone element temperature. A maximum temperature of approximately 850°C was chosen in the interests of a longer element life. Increasing the peak heat flux level does little to increase the effective flame spread length. This is discussed in more detail in Section 6.3. This is due to the directional nature of the cone element.

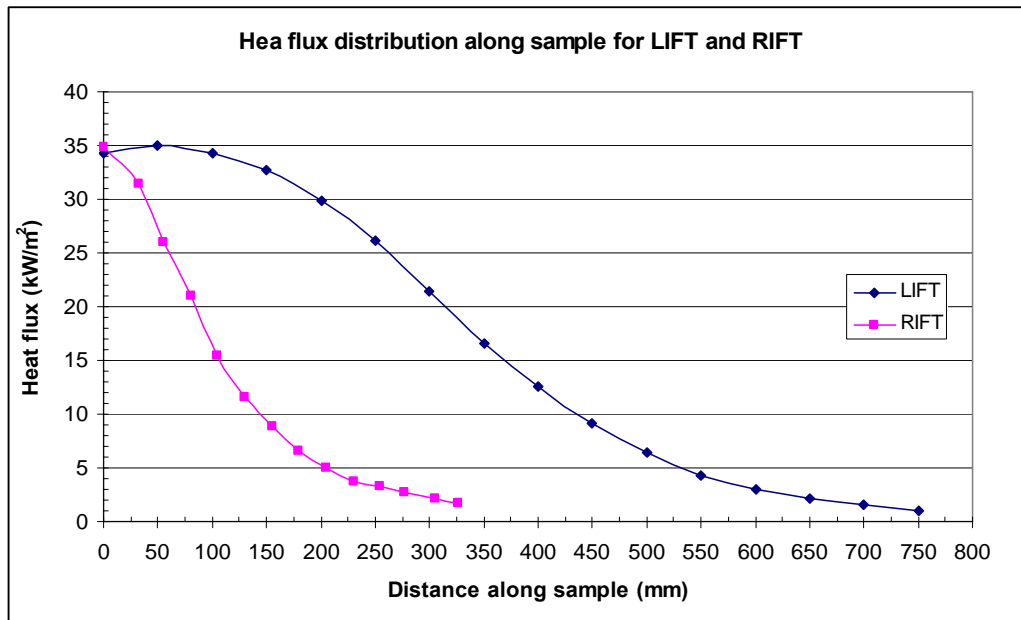


Figure 27: Heat flux for LIFT vs. RIFT (both at 15 degree angle)

6.2 *Procedure for using RIFT*

The procedure for using the RIFT apparatus is based on the ASTM1321 standard and follows the same methodology. The rear and sides of the samples are wrapped in aluminium foil and a 12mm Kaoboard insulating board is used behind the sample. The sample is inserted, with timing starting once the sample is in place against the end of the sample frame. The retaining screws at the rear of the sample frame are tightened to press the sample against the front flange.

6.2.1 Setup of RIFT

The cone calorimeter element was set to the vertical position and the long axis centreline of the RIFT sample holder was inline with the centreline of the cone. The end of the sample closest to the element was in line with the edge of the element, as shown in Figure 28.

The angle and sample separation distance x_0 was set by measuring perpendicularly from the face of the cone to the sample, as shown in Figure 28 and Table 3.

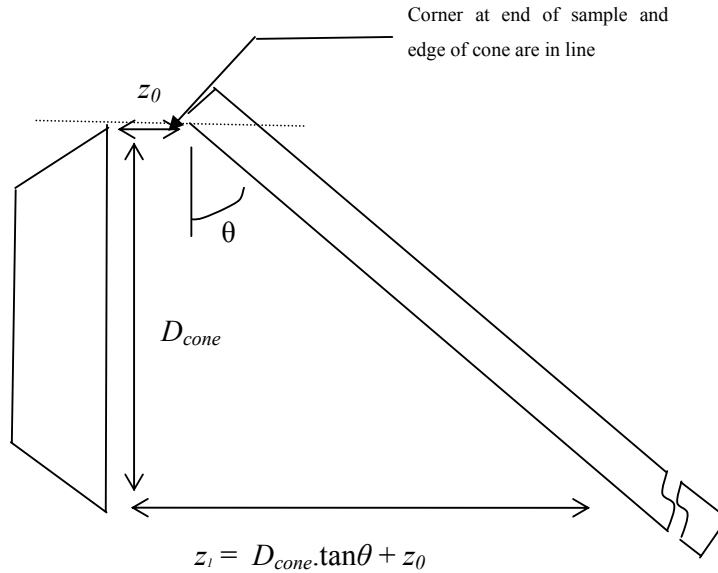


Figure 28: RIFT setup – plan view

The standard RIFT setup is in Table 3.

Angle of sample	60 degrees
Separation of sample from face of element (z_0)	45mm
Peak heat flux (0mm along sample)	35kW/m ²
Typical cone temperature	850°C
Cone diameter D_{cone}	160mm

Table 3: RIFT setup dimensions

The sample holder must be level and parallel to the face of the cone element, when viewed in elevation.

6.2.2 Sample preparation

The same protocol was used as required by the ASTM E1321-97a LIFT standard, which calls for samples to be conditioned at 23°C ±3°C and a relative humidity of 50% ±5% so that successive weighings, taken 24 hours apart, do not vary by more than 0.1% of the mass. For the flame spread test, the samples had the back and sides covered in aluminium foil to limit moisture loss from the sample.

6.2.3 Flux measurement

The heat flux measurement along the sample was conducted using a template made from fibre cement board with location holes at 25mm centres to take the head of a water cooled flux measuring gauge and this was inserted in into the sample holder (Figure 29 and Figure 30).

After turning on the cone element and extraction hood, the cone element was brought up to temperature with 5 minute stabilisation breaks at 400 and 600 degrees, before increasing to the final temperature. The element was running at the final temperature for at least 10 minutes before any readings are taken to allow the temperature of the element and apparatus to stabilise. After checking that there was water flow through the heat flux gauge before taking any heat flux readings, the head of the flux gauge was inserted into the template, ensuring that the face of the heat flux gauge was flush with the face of the template and not inside the hole to ensure accurate readings of the incident flux at each point. The heat flux gauge was left in place for at least 30 seconds to allow an average reading of the heat flux over that time to be taken before moving to the next measuring point. As with the LIFT, and outlined in Section 10.1 having the head of the flux meter proud of the surface of the template at the cold end of the sample will improve the accuracy of the measurements due to the convection boundary layer.

The flux readings were compared with the required values from Figure 31 and the cone temperature was altered to give the best match.

A polynomial match to the final RIFT heat flux profile gives a 5th Degree Polynomial Fit: $y=a+bx+cx^2+dx^3...$ with the coefficients given in Table 4.

a =	34.910273
b =	-0.064334216
c =	-0.0031889273
d =	2.6422166e-005
e =	-8.0288574e-008
f =	8.6335299e-011

Table 4: RIFT polynomial coefficients

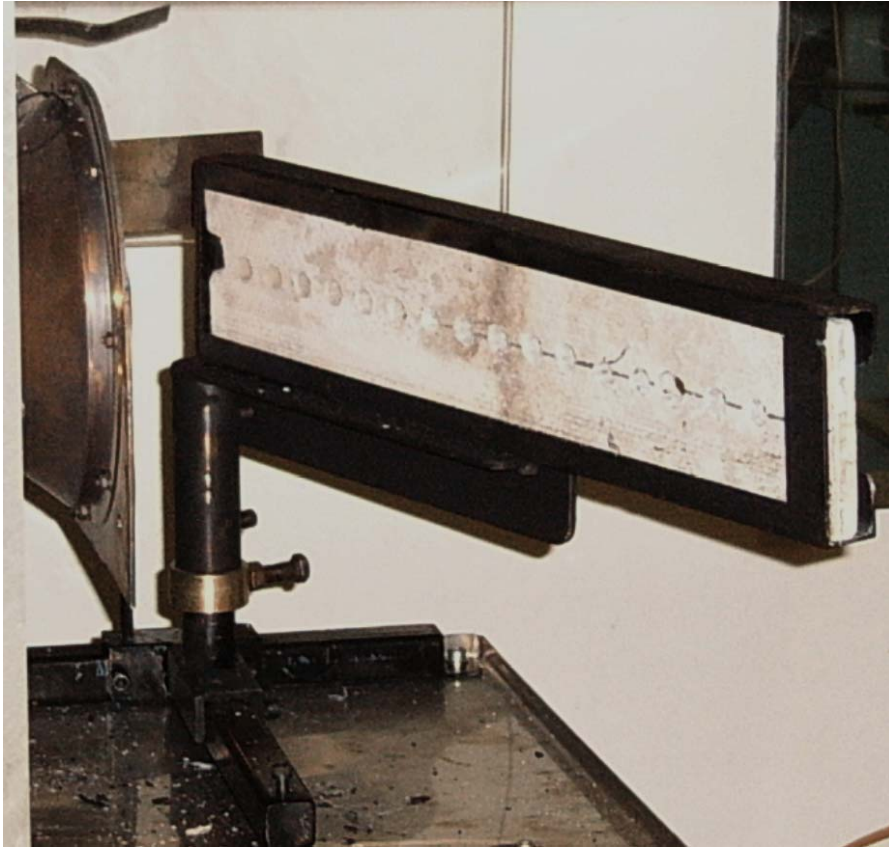


Figure 29: RIFT with flux measurement template

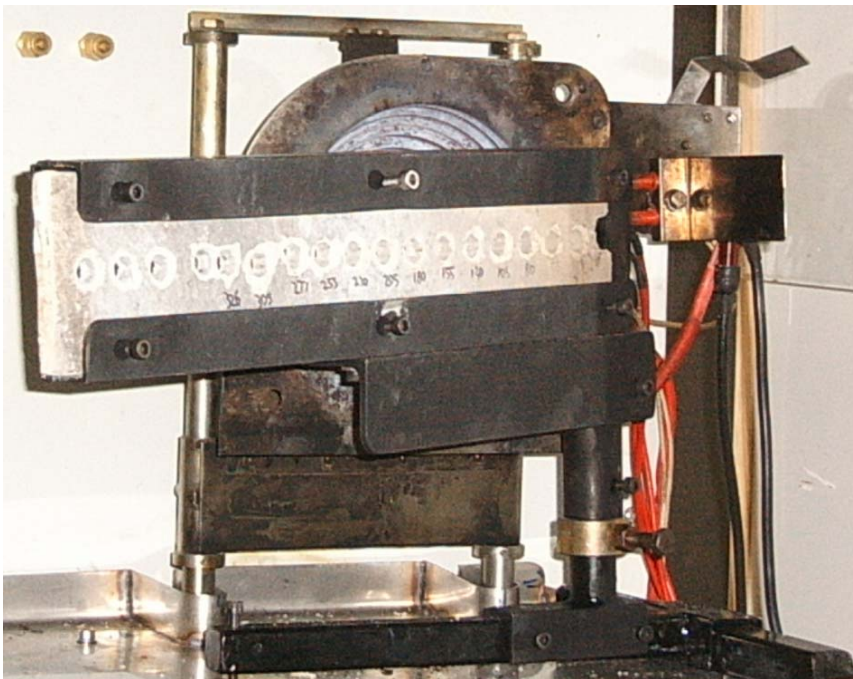


Figure 30: RIFT sample holder from rear

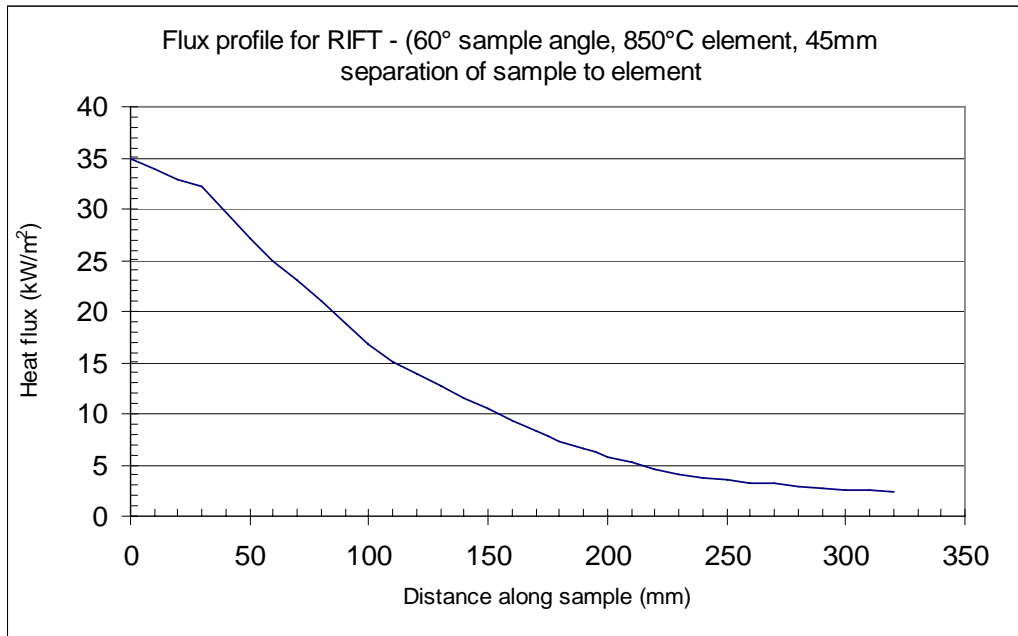


Figure 31: RIFT irradiance curve for a sample separation of 45mm, 850°C element temperature and 60° sample angle

6.3 Heat flux and sample angle in the RIFT

The ASTM E 1321-97a standard test for measuring the spread of flame parameters calls for a peak heat flux 5-10kW/m² over the minimum ignition flux ($\dot{q}_{ig,min}$) from the ignition tests. For timber based products the peak heat flux would then be between 18-28 kW/m², given the minimum ignition flux is in the order of 13-18 kW/m² (Ngu 2002).

Azhakesan et al (1998) used a peak heat flux of 35kW/m², whereas Pease (2000) and Huynh (2003) used a 60kW/m², due to the different experimental setup, which only used half the cone width (Figure 26). The choice in the original tests of 35kW/m² was given as the typical heat flux to walls in a fire (Azhakesan et al (1998)).

6.4 The effect of different element temperatures

The effect of changing the element temperature as a means of altering the received heat flux on the sample can be seen in Figure 32. The main result is the curve is

scaled with a correspondingly lower peak flux value. The point at which the minimum heat flux for flame spread occurs moves slightly towards the hot end of the sample, with little overall difference in the overall length of flame spread, as given in Section 6.7, due to the directional nature of the heat flux profile of the conical element.

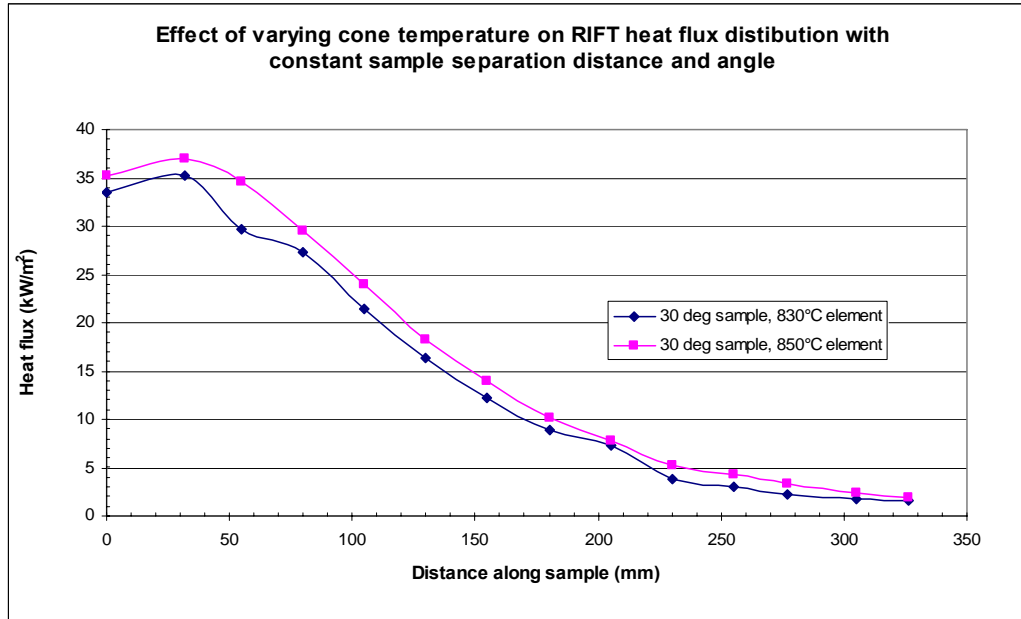


Figure 32: Effect of changing cone element temperature on received heat flux (70mm separation, 30 degree sample angle)

6.5 *The effect of changing the sample angle*

The effect of a changing sample angle for a constant cone temperature on the received heat flux is shown in Figure 33. The decreasing angle increases the peak flux level, however does not significantly alter the minimum flux level or the point at which this occurs, due to the directional output of the cone element.

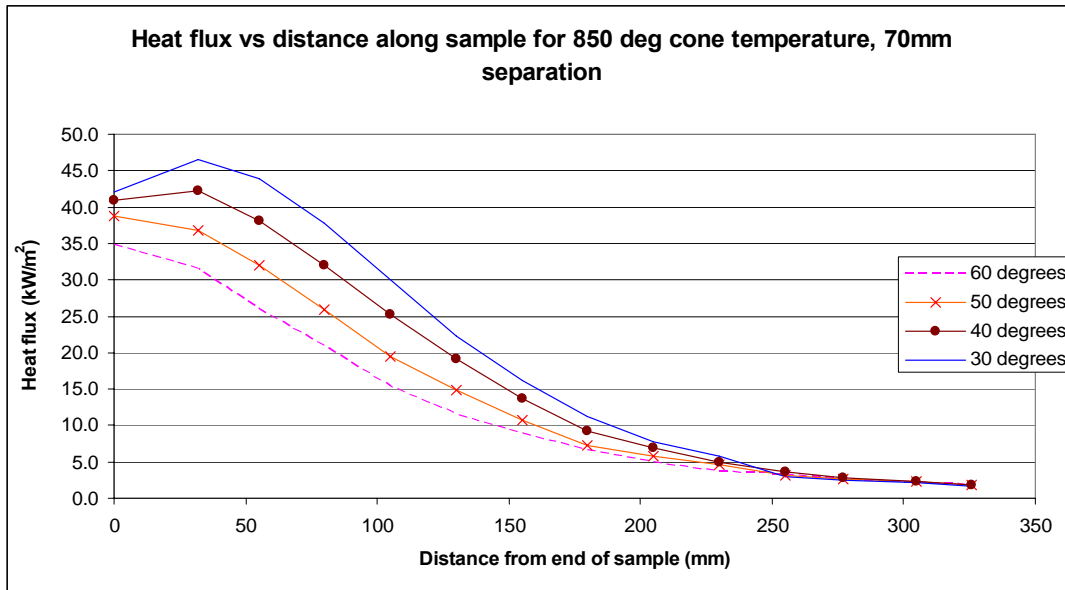


Figure 33: Irradiance for a constant 850° element temperature, 70mm separation and changing sample angle

More usefully, when the peak heat flux is kept constant by changing the cone temperature to suit, then the effect can be seen in Figure 34. The directional nature of the cone element can be seen by the location of the peak flux level along the sample, and the terminal heat flux, which remains relatively constant, despite the changing view factor.

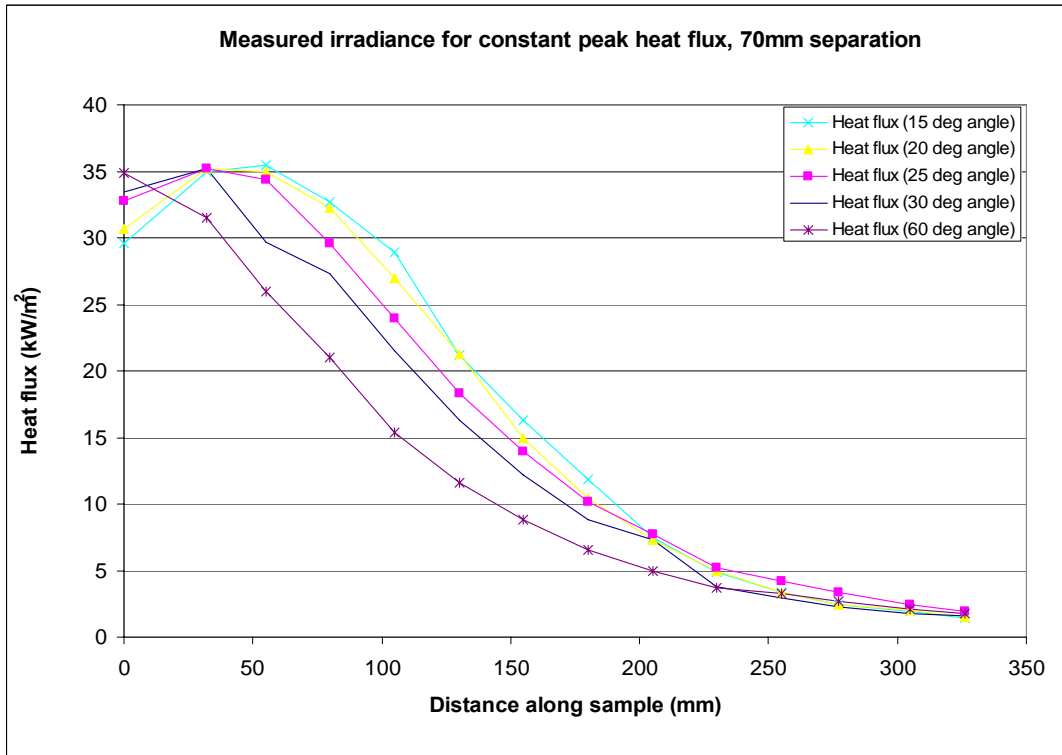


Figure 34: Irradiance with constant peak heat flux of 35kW/m² and 70mm sample separation

6.6 *The effect of increasing the separation distance between the sample and element*

Increasing the distance between the sample and the element should increase the spread of the irradiance along the sample, giving greater resolution by allowing for a greater flame spread, as the minimum flux level for flame spread (\dot{q}_s) is further along the sample. The directional nature of the cone element shows that this does not occur within the limitations of the desired heat flux level and element temperature.

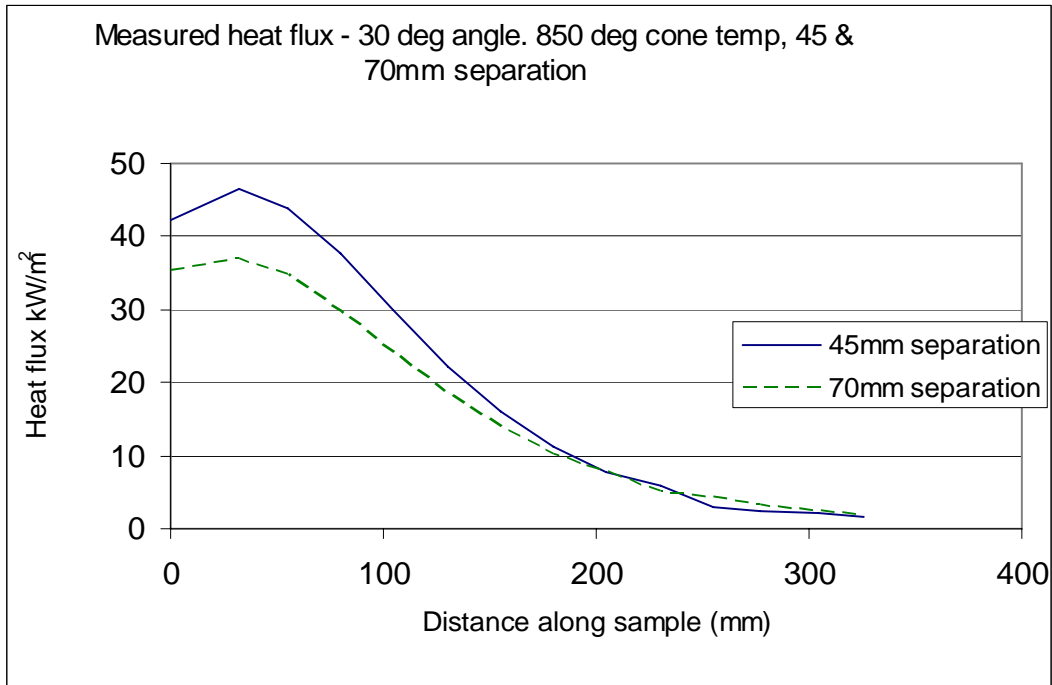


Figure 35: Change in heat flux with constant element temperature and angle

6.7 Optimum angle of sample in RIFT

As the basis of flame spread measurements is to have a series of velocity vs. received heat flux measurements, it follows that the distance along the sample from the point of the peak heat flux (L_{peak}) to the point where the flame spread stops (L_{spread}) due to insufficient received flux, should be as long as possible, as shown in Figure 36

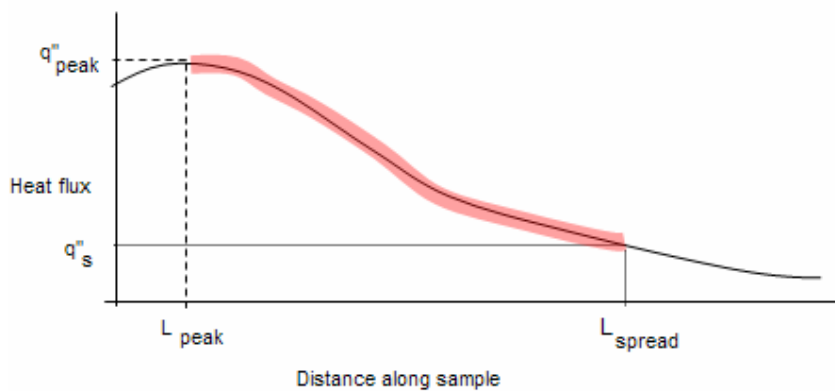


Figure 36: Limitations for flame spread measurement

The profile of the full scale LIFT test allows the apparatus to be used for ignition testing, as there is an almost flat heat flux curve for the first 150mm of the 800mm sample. This feature is not required in the RIFT, as the cone calorimeter or ISO 5657 ignition apparatus can be used for ignition testing in the conventional manner. The maximum distance along the sample, between the points L_{peak} and L_{spread} is when the peak heat flux coincides with the end of the sample, as the location of L_{spread} remains relatively unchanged due to the directional output of the cone element (Figure 34). There is no advantage to having a plateau in the irradiance profile at the beginning of the sample, as the requirement is for different heat fluxes at each measuring point along the sample; hence the optimum angle chosen between the element face and the sample is therefore 60 degrees, as used by Pease (2001), Huynh (2003) and Azhakesan (1998).

6.8 *RIFT test methods*

6.8.1 Ignition test

Previous studies involving the RIFT used either the cone calorimeter in the normal horizontal position (Azhakesan 1998, Huynh, 2003), or the ISO 5657 ignition testing apparatus (Huynh, 2003) to obtain the ignition data. Ignition tests were conducted using the RIFT (Figure 37) to see if it improved the correlation of the data to the LIFT results by having the sample in the same orientation.

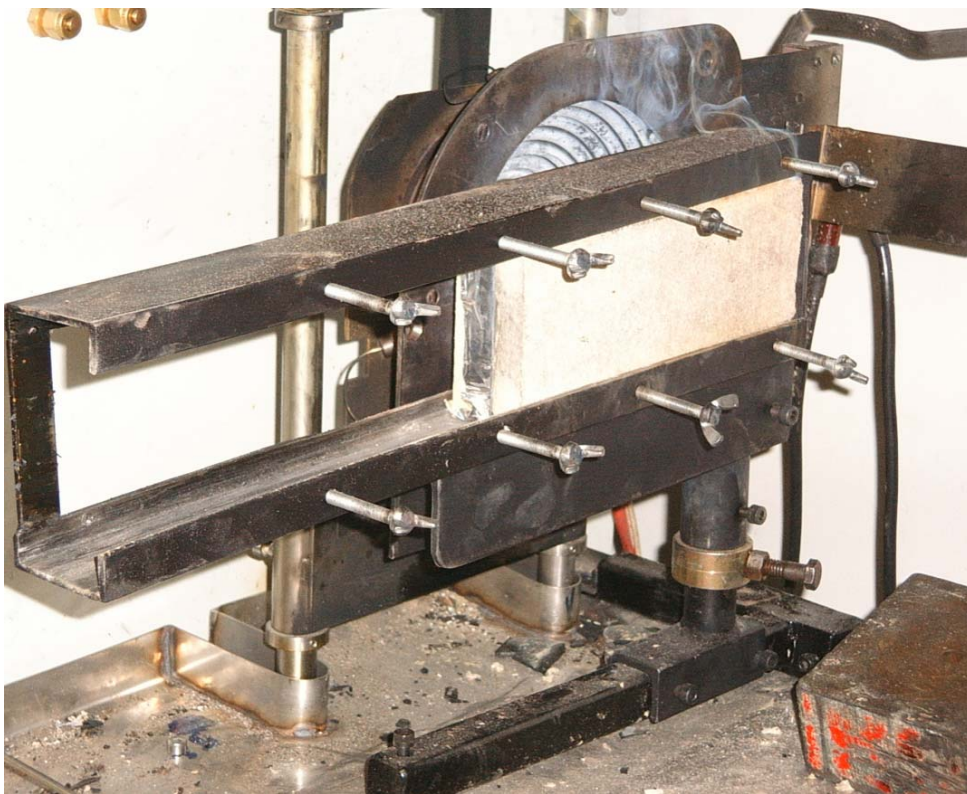


Figure 37: RIFT used for ignition testing - rear view

The ignition test used 200 x 95mm samples with the sample holder mounted parallel with the face of the cone element. The spark igniter was level with the top of the exposed face of the sample, and 13mm from the sample face (Figure 38). The ignition test in the cone calorimeter uses samples 100mm x 100mm, with an insulated backing board and holder, and an electric spark pilot, mounted 13mm above the sample face, and the test is generally conducted with the sample mounted horizontally. The

ISO 5657 ignition apparatus is similar but uses a 165 x 165mm sample. The sample holder in the RIFT ignition test was set to the centreline of the cone, and the cone element set to give the required heat flux, measured with a template in the centreline of the cone element. The required temperatures matched those previously recorded for this cone element when used for ignition testing in the cone calorimeter.

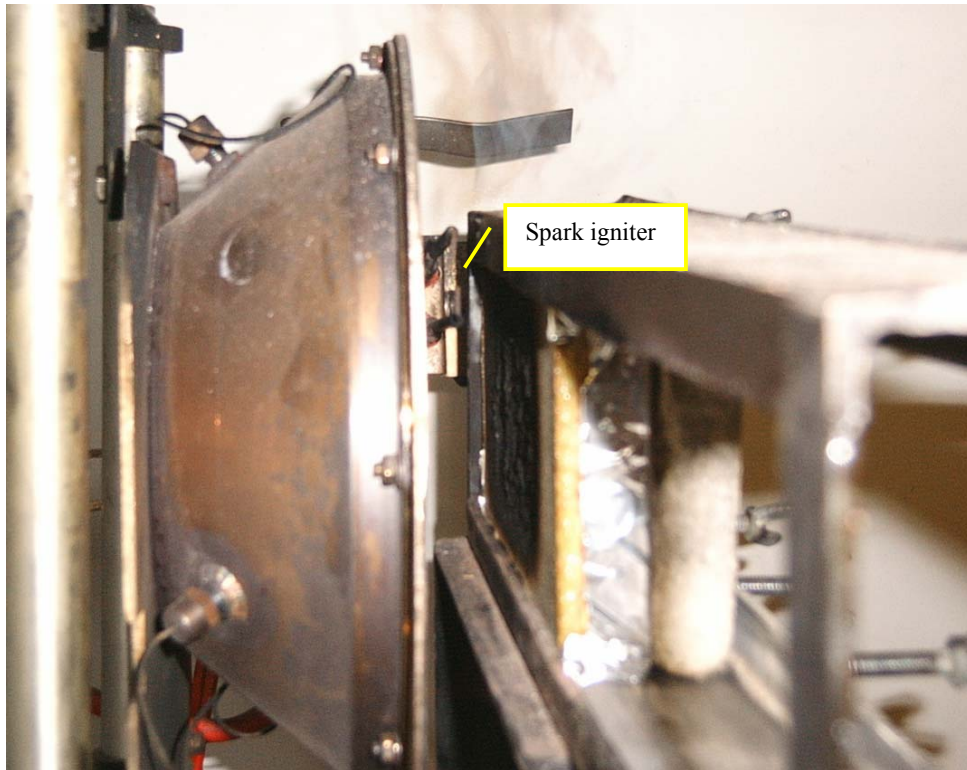


Figure 38: RIFT used for ignition testing

The sample was mounted parallel to the cone element, and exposed to a constant heat flux. In the same manner as ignition testing in the LIFT, cone calorimeter and ISO 5657 apparatus, the time to ignition was recorded, and then another flux level was chosen and the procedure repeated, until the sample did not ignite in 20 minutes.

The external irradiance (\dot{q}_e) was plotted against the time to ignition (t_{ig}) to give the minimum flux for ignition ($\dot{q}_{ig,min}$) where the ignition time is effectively infinite. For thermally thick materials, the x-intercept of \dot{q}_e vs. $1/\sqrt{t_{ig}}$ gave the critical ignition flux (\dot{q}_{crit})

6.8.2 Flame spread test

The samples were marked with a line in the centre of the face in the longitudinal direction, and across the sample every 10mm along the sample, to allow the flame spread to be measured during the test. The distance from the end of the sample was marked on the sample every 20mm, so the flame progress along the sample could be monitored.

The flux measuring template was removed and sample slid into place, with the timing started from the point at which the sample touches the end of the sample holder and the sample holder screws on the back of the sample holder were then tightened so that the face of the sample is pushed against the front flange. If the sample did not within the preheating time t^* , then a 25mm pilot flame was applied to the bottom corner of the hot end of the sample to ignite the sample. The time to ignition and the time taken for the flame front to reach each 10mm gridline, taken at the centreline of the sample was recorded. .

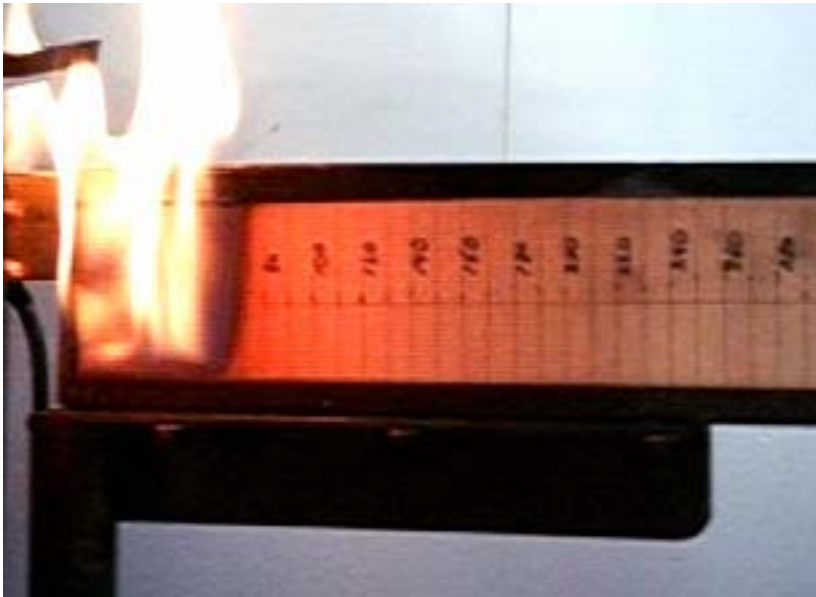


Figure 39: Flame spread along sample

The test was complete once the flame ceases to advance along the sample and extinguishes, or it reaches the end of the sample.

	element (K)
Z	Distance from the lower base of the element frustum to the sample surface
Z_2, Z_4	$Z_2 = 1 + H_2^2 + R_2^2$ $Z_4 = 1 + H_4^2 + R_4^2$
ε	Emissivity of the heating element (0.99)
σ	Stefan-Boltzmann constant, 5.67×10^{-8} (W/(m ² K ⁴))

Figure 40: Cone calorimeter view factor geometry (from Wilson, 2002)

The heat flux to any point on the sample, offset from the centre of the cone element is given by Equation (36)

$$q'' = \frac{1}{2} \left[\left(1 - \frac{1 + H_2^2 - R_2^2}{\sqrt{Z_2^2 - 4R_2^2}} \right) - \left(1 - \frac{1 + H_4^2 - R_4^2}{\sqrt{Z_4^2 - 4R_4^2}} \right) \right] \varepsilon \sigma T^4 \quad (36)$$

The heat flux to a point on the sample centre in the cone calorimeter in normal use is given in equation (37)

$$q'' = \left[\frac{r_2^2}{z^2 + r_2^2} - \frac{r_4^2}{(z + h)^2 + r_4^2} \right] \varepsilon \sigma T^4 \quad (37)$$

where the temperature of the cone element is the average temperature of the element in Kelvin.

In the case of the RIFT, the separation z will vary along the length of the sample, as the sample is at an angle to the face of the element, shown in Figure 41.

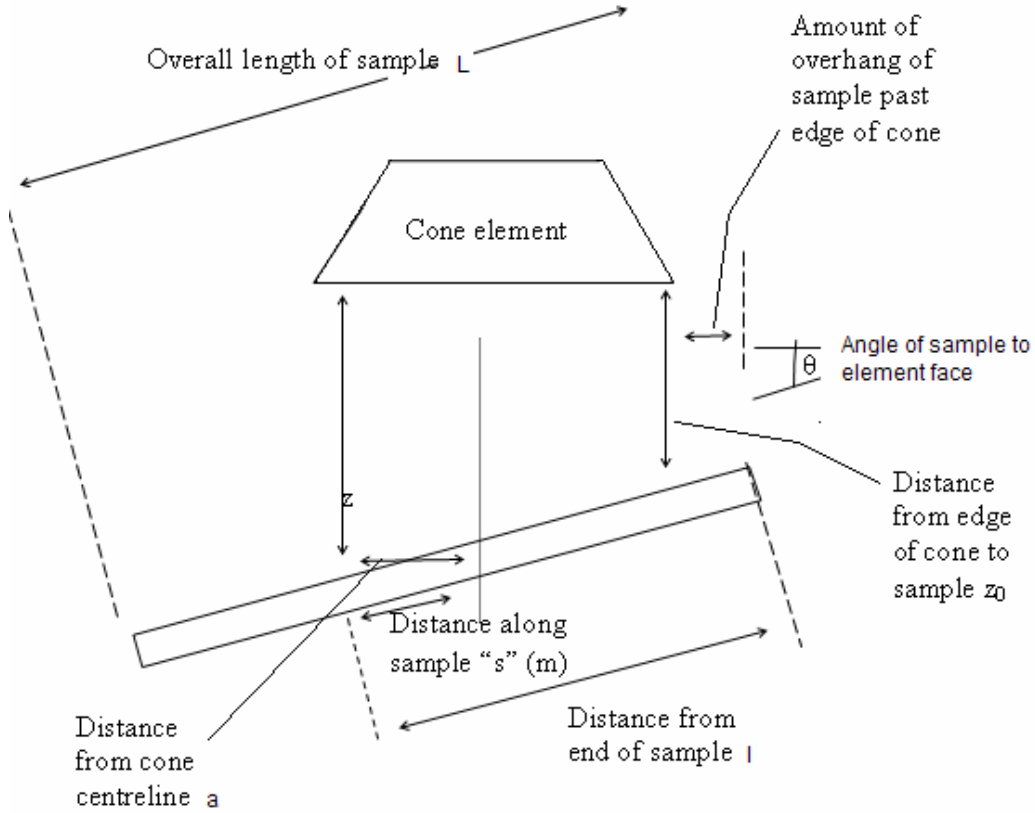


Figure 41: RIFT geometry

As the sample is at an angle to the element face, the heat flux received by the differential element dA_1 is reduced by the cosine of the angle between the sample and the heating element. The heat flux at a point on the sample is therefore given in Equation (38).

$$q'' = \frac{1}{2} \left[\left(1 - \frac{1 + H_2^2 - R_2^2}{\sqrt{Z_2^2 - 4R_2^2}} \right) - \left(1 - \frac{1 + H_4^2 - R_4^2}{\sqrt{Z_4^2 - 4R_4^2}} \right) \right] \varepsilon \sigma T^4 \cdot \cos(\theta) \quad (38)$$

The heat flux on the sample is limited by peak temperature attainable by the element, and this is taken to be 850°C. The distance between the sample and the element (z_0),

measured perpendicular to the face of the element at the closest edge is used as a measure of the separation of the sample from the element.

While Wilson (2002) showed reasonable accuracy for Equation (36) in comparison to measurements taken under the cone calorimeter in the horizontal position, with a sample parallel to the heater face, the relationship becomes increasingly less valid as the sample angle increases. The shape is generally correct, as shown in Figure 42; however the calculated values are significantly lower than the measured values.

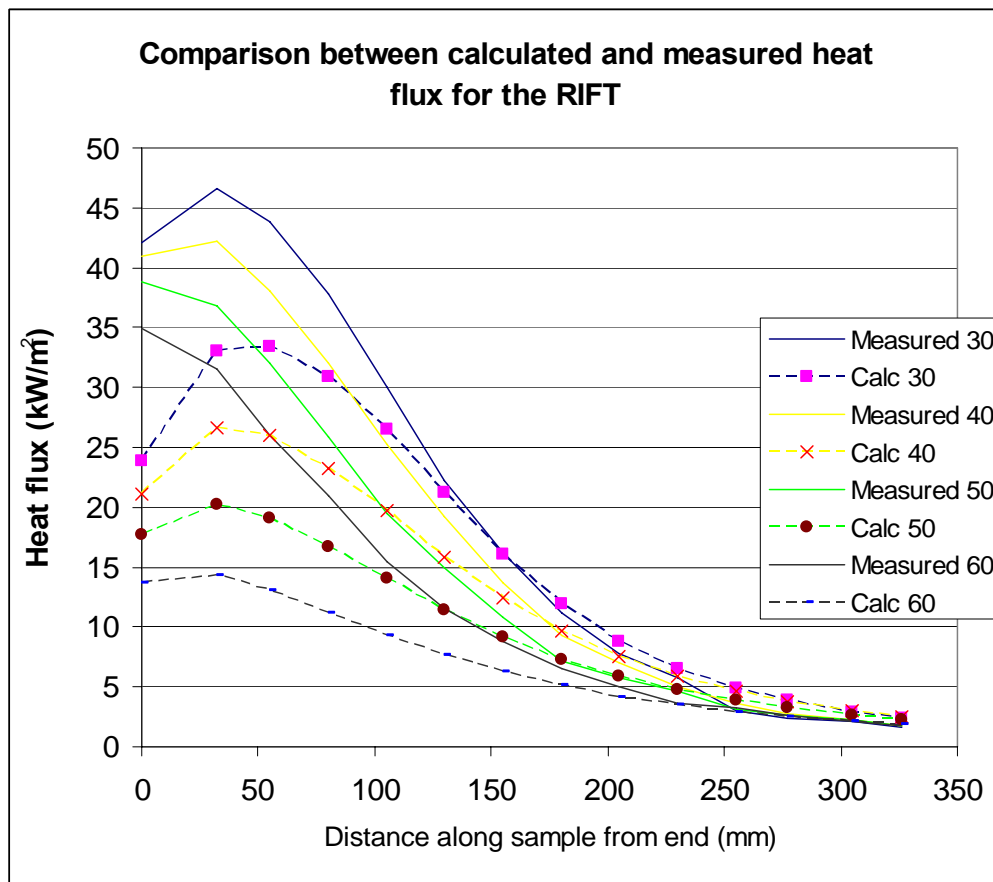


Figure 42: Comparison of theoretical heat flux – Equation (38) vs. measured

The experimental results by Wilson et al (2002) showed reasonable variation between measured element temperature using thermocouples connected to the element, and an optical pyrometer, which used a wider sampling area than the thermocouples. This showed that there was variation between points around the cone element for surface temperature, and consequently a variation in received flux against the expected value given by Equation (38). Visually, it can be seen from the colour when operating the

cone that there is some variation in the element temperature, with the ends of the cone element in the frustum in particular being cooler than the general element temperature. The model is also based on a smooth cone surface as it does not take into account the effect of the spiral element or re-radiation from the supporting elements or the sample holder and takes no account of the element coils.

The view factor calculation is not required for the RIFT, which can be set up empirically, based on flux measurements, so no further work was be done in this area.

7 Literature on the LIFT, RIFT and lateral flame spread

Unlike the cone calorimeter, where a significant number of papers have been published, little has been published on the ASTM 1321 LIFT apparatus. This is largely due to the more limited nature of the test when compared to the cone calorimeter. The cone calorimeter can be used for product comparisons, modelling compartment fire and upholstered furniture behaviour and other legislative tests (Babrauskas, 1992). In comparison, the LIFT is purely a measure of flame spread, and some ignition properties. Some work has been done to model the LIFT using only cone calorimeter data, with mixed success.

The publications given here are most specifically dealing with the LIFT and RIFT. A summary of more general ignition and flame spread research is given by Huynh (2003), Ngu (2002) and Babrauskas (2003).

7.1 *LIFT literature*

7.1.1 Quintiere, J. A simplified theory for generalizing the results from a radiant panel rate of flame spread apparatus. 1981

The basis of the mathematical model for flame spread, which forms the basis of the ASTM E 1321 LIFT and hence the RIFT was initially developed by Quintiere (1981). Although based on the ASTM E 1317 / IMO maritime finishes test apparatus, the derivation makes it generally applicable to any case of opposed flow flame spread under radiant heating, and the resulting equation is that of Equation (28).

The requirement for preheating the material in order to aid data reduction is given, but the method of defining the preheating time is given as “trial and error” by observing the results of the flame spread correlation for linearity.

7.1.2 Quintiere, J. Harkleroad, M, Walton D. Measurement of material flame spread properties. 1983

The work by Quintiere, Harkleroad and Walton in further developing and applying the theories developed by Quintiere (1981) led to the current ASTM LIFT apparatus and procedure. The theory was further developed to be able to calculate the preheating

time required using the ignition parameter. The flame spread theory was further developed and applied to particle board as an example material

The apparatus was further modified to give more consistent results. Amongst these were the location of the pilot flame and the addition of a flange on the top of the sample holder to improve the consistency of the ignition time and reduce the effect of the pilot flame on the material.

7.1.3 Quintiere, J. Harkleroad, M. New concepts for Measuring flame Spread Properties, 1984

The theories developed earlier by Quintiere ET al (1981, 1983) were applied in a series of experiments to obtain material properties for a wide range of materials. This work formed the basis of the ASTM E 1321 standard. Much of the published material properties in the literature (for example, in Quintiere 2000) come from the results published in this paper.

7.1.4 Fowell, A. Interlaboratory test program on ASTM E 1321: Standard test method for measuring material ignition and flame spread properties. Second edition, November 1994

As part of an ongoing research program into the repeatability of various ASTM test methods, a round robin of tests of 6 materials, held in 4 laboratories was conducted by the ASTM, although the results for one material (particle board composite) were withdrawn as one laboratory had received the wrong material. The materials tested were:

- Douglas Fire plywood
- Fire retardant treated Douglas Fir plywood
- Composite panel
- Type X gypsum wall board
- Rigid polystyrene foam
- Rigid polyurethane foam

No detail of the raw experimental data is given, however some statistical analysis was conducted to give some indication of the variability inherent in the ASTM E 1321 test method. Of interest to this research are the results for the flame spread parameter Φ ,

minimum ignition flux and the other properties, which gave an indication of the acceptable range when comparing with other published results in the literature. The results showed large variations in the results for the flame spread parameter, where the highest value was over 2 times the lowest value. The other results showed large variation, but on a smaller scale.

7.1.5 Dietenberger, M. Experimental and analytical protocol for ignitability of common materials. 1995

Dietenberger conducted a number of tests on wood products for the US Forest Service involving the LIFT and cone calorimeter, with the results published in several papers in 1995 and 1996.

This report covers a new protocol for calibration of the LIFT, and recommendations for improving the calibration when aligning the burner to match the required flux profile. The use of at high irradiance level was also recommended, to reduce the error due to the time taken to insert the sample into place. The main result was the development of a function for the actual heat transfer coefficient along the material, given in Equation (39).

$$h = (13.9 - 0.0138x)(q''_{e,50mm}) \text{ kW/m}^2\text{K}, \quad (39)$$

where x is the distance along the sample from the hot end, in metres.

The measured convection coefficient component of the heat transfer coefficient is varies along the sample, and the heat transfer coefficient is significantly higher than the standard value of $0.015\text{kW/m}^2\text{K}$ specified in the ASTM E 1321 standard at points closer than 650mm from the hot end of the sample, and it varies significantly with the panel radiant flux. As a result, using equation (6) and the standard heat transfer coefficient value given in the ASTM E 1321 LIFT standard, gives a higher ignition temperature than experimentally measured values. Using the corrected heat transfer coefficient calculated from equation (39) gave ignition temperatures around 70°C less than predicted for the same materials using the ASTM standard value.

A theory of ignition was developed that interpolated the results between thermally thick and thermally thin materials, to allow for the effect of thermal penetration on the sample.

7.1.6 Dietenberger, M. Ignitability of siding materials using a modified protocol for LIFT apparatus. 1995

The effect of moisture content, apparatus and thickness of the test samples on ignitability were tested for typical US external cladding materials - Cedar, Redwood, Southern Pine, plywood, hardboard and vinyl faced polystyrene foam. A method is proposed to take into account the effect of moisture content on the ignitability of the material, in order to predict the ignition time and thermal properties, given results at an oven dried moisture level.

7.1.7 Dietenberger, M. Ignitability analysis using the LIFT apparatus and cone calorimeter. 1995

The ignition theory for finitely thermally thick materials with radiant heating, convective cooling and an insulated back face was further developed to give a better correlation result. It is a function of the Biot (Bi) and Fourier (Fo) numbers for the material under the test conditions:

$$\frac{\dot{q}''_e}{\dot{q}''_{ig}} = \frac{1}{T_s} = 1 + \frac{1}{(F''_{thick} + F''_{thin})^{1/n}} \quad (40)$$

where

$$\dot{q}''_{ig} = h_{ig}(T_{ig} - T_{\infty}) / \varepsilon \quad (41)$$

$$n = (2.68 + 0.4Bi) / (1 + Bi) \quad (42)$$

$$F''_{thick} = \left(\frac{4}{\pi} Bi^2 Fo \right)^{\frac{1}{2}} \quad (43)$$

$$F''_{thin} = \exp\left(\frac{BiFo}{1 + 0.254Bi} \right) - 1 \quad (44)$$

The advantage of this theory is that the assumption of thermal thickness is not required, and the thermal thickness can change through the test at different irradiances and still give satisfactory results.

The heat transfer coefficient equation was also developed for the cone calorimeter.

7.1.8 Jianmen, Q. Prediction of flame spread test results using the test data from the cone calorimeter. 1990

Jianmen (1990) attempted to model the flame spread on materials using a view factor calculation and material properties derived from cone calorimeter tests. Using the results from the ISO standards LIFT round robin test, the results looked to give a reasonable match, however later work by Goransson (1991) showed poor results in tests of varying materials. The materials tested were chosen to include as wide a range of properties as possible, and the materials were insulating fibreboard, particle board, PVC carpet on gypsum board and transparent PMMA

7.1.9 Goransson U. Using the cone calorimeter to predict flame spread, 1991

Goransson (1991) conducted tests using the LIFT to attempt to verify the flame spread model developed by Jianmen (1990) and had little success. The problems identified included the assumption in the model that the heat transfer from the flame to the unburnt material was via radiation, when gas phase conduction was the main method, and that the choice of values taken from the cone data does not necessarily represent the flame spread accurately.

7.1.10 Persson G. Predicting lateral flame spread with cone calorimeter, 1993

Following the work by Jianmen (1990) and Goransson (1991), Perrson (1993) used a numerical solution to an integral model of surface flame spread, using the experimental data by Goransson. Most of the data required for the model could be obtained from experimental results in the cone calorimeter. These included:

- Heat flux \dot{q}_e along the sample
- Preheating time t^*

- Material thickness
- Thermal inertia $k\rho c$
- Thermal conductivity of the material k
- Ignition temperature T_{ig}
- Flame heat flux parameters called \dot{q}''_{f0} and k_f

The flame heat flux parameters are used to define a decaying heat flux from the flame front on the unburnt material, where the heat flux from the flame is given in equation (45).

$$q''_f = q''_{f0} \exp(-k_f(x - x_f)) \quad (45)$$

A recognised shortcoming was that the flame heat flux parameters are difficult to define experimentally due to the small scale of the heat affected area and a wide combination of \dot{q}''_{f0} and k_f will give similar results. This is explored further by Delichatsios (1999).

The results showed some success in the materials listed for the ASTM E 1317 / IMO marine finishes test, but performed poorly in the LIFT test. While the equipment is similar, apart from the differences in the pilot flame location, the IMO test involves a fixed peak heat flux of 50kW/m² and no preheating time before ignition. The preheating was identified as the main reason why the theory did not perform well against the experimental results. The effect of preheating on the material properties was recognised by Babrauskas and Wetterlund (1999).

7.1.11 Babrauskas, V. Wetterlund, I. Comparative data from LIFT and cone calorimeter tests for 6 materials, including flame flux measurements. 1999

A key part of developing the models of opposed flow flame spread is the heat flux from the flame to the surface of the material. Following an earlier literature review into flame fluxes in opposed flow flame spread (Babrauskas, 1995) where little information had been found, particularly for the LIFT, experiments were conducted at

SP in Sweden on 6 materials with both the LIFT and cone calorimeter. These materials included

- particle board,
- fire retardant polyurethane foam,
- black PMMA,
- insulating fibreboard,
- cotton fabric with a Kevlar liner over polyurethane foam,
- acrylic pile fabric over polyurethane foam.

In addition to measuring the heat flux from the passing flame front to the material, the report covers the requirements of the ASTM standard, and discusses the problems with the standard regarding clarity and definition of some of the terms, and the effect of preheating on the material. Some tests were done without preheating and the data is included, but no calculations were done or conclusions drawn, as it is outside the Standard requirements. The effect of preheating on the material properties was found to affect some of the materials, in particular the foams.

It was found that the flame flux is essentially constant between the materials tested, and hence this should not be a major variant in flame spread modelling.

7.1.12 Nisted, T. Flame spread experiments in bench scale; project 5 of the EUREFIC research program. 1991

Nisted conducted a series of LIFT tests, as part of the wider “European Reaction to Fire Classification” research program, where the 11 materials covered a range of material properties. The report covered only the LIFT tests, the experimental procedure and results obtained.

Of particular interest to this report were the tests for “ordinary” plywood. The raw test data is included by Nisted, which was used to confirm the calculations used in the post experimental processing in this report.

7.2 *RIFT literature*

7.2.1 Azhakesan, A. Shields, T. Silcock, G. Ignition and opposed flow flame spread using a reduced scale attachment to the cone calorimeter. 1998

The paper by Azhakesan et al in 1998 was the first publication on the RIFT method, and all the resulting work stems from it. The method is described, and four materials are tested – fibreboard, hardboard, plywood and melamine faced particle board. The results are compared with published data for the LIFT and the BS476 part 6 Surface spread of flame test, rather than testing the same material in these tests. The conclusion was that the RIFT produced similar results to the tests and could give a comparative result to the BS476 part 6 test, with the flame spread parameter slightly higher than the LIFT results produced.

7.2.2 Azhakesan, A. Shields, T. Silcock, G. Combustibility parameters for enclosure lining materials obtained during surface flame spread using reduced scale ignition and flame spread technique. 1998

This publication is a continuation of the previous paper, and expands the use of the RIFT. Heat release rate and mass loss rate data was gathered during the flame spread test in the RIFT, allowing the calculation of heat of gasification and the heat release per unit area burnt to be calculated in addition to the opposed flow flame spread properties calculated in the conventional test.

7.2.3 Huynh, VCM. Flame spread measurements of New Zealand timber using an adaptation of the cone calorimeter apparatus. 2003

Some earlier work by Pease (2000) at the University of Newcastle in Australia to replicate the work of the work of Azhakesan et al led to Huynh (2003) using the University of Newcastle apparatus to attempt to derive some properties for New Zealand timber using the RIFT. Huynh used ignition data, which forms part of the flame spread analysis, from Ngu (2002) which used the ISO 5657-1987 ignitability apparatus. Both the work by Pease and Huynh suffered from a shortcoming in the test

apparatus, where the sample was exposed to only half the available element area, and consequently the results were inconclusive. A summary of this research is also given by Spearpoint, et al 2005.

8 Material test results for manufactured boards

This chapter describes the ignition and flame spread results obtained in the tests on manufactured boards with both the LIFT and the RIFT.

Ignition tests for each material were conducted at different heat flux in the ISO 5657 apparatus, the LIFT and the RIFT to obtain the material properties required for the flame spread tests. The flame spread tests were conducted in the RIFT and LIFT. A minimum of 4 samples of each material was tested in the RIFT, with 6 samples if allowed by the available material. Three samples of each material were tested for flame spread in the LIFT.

Some additional flame spread and RIFT ignition tests were conducted on different thickness materials of the same nominal type, to gauge an indication that the effect of material thickness may have on the results.

As particle board is a common material used for research in the literature, two brands of particle board were tested in the RIFT to show the variation within a material and hence some indication of the error when comparing the experimental results to those published in the literature.

The effect of preheating the sample on flame spread was investigated by conducting tests in the RIFT with full preheating, given by the ISO 5657 ignition tests, and a low preheating period of a few seconds.

The results for manufactured board were generally more consistent with less variation between tests on the same material than those for natural timbers, as expected from their more consistent composition. The results are summarised in Appendix 3 along with the ignition data, and the raw data from the flame spread tests is in Appendix 4

8.1 Medium density fibreboard

The MDF used in these tests was 18mm “Customwood” brand by Carter Holt Harvey and six samples of 18mm “Customwood” MDF were tested in the RIFT with a low preheat and a full preheat time, and the same material was used in the LIFT to compare results. The ignition results in the LIFT, RIFT and ISO 5657 apparatus used samples of the 18mm MDF. The extent of flame spread along the sample is shown in

Figure 48. Some flame spread tests were conducted on 9mm MDF to look at the effect of thickness on the flame spread rate and variation.

8.1.1 Ignition of MDF

MDF showed very consistent ignition and flame spread properties when tested, with little variation between runs. The time to ignition for MDF in the LIFT, RIFT and ISO 5657 tests is shown in Figure 43.

The results for ignition in the ISO 5657 ignition apparatus are compared with those obtained by Ngu (2002), who also used the ISO 5657 ignition apparatus to test various New Zealand timbers, shown in Figure 44. The ignition results in these tests are within the error limits of the tests by Ngu, showing the material is very consistent.

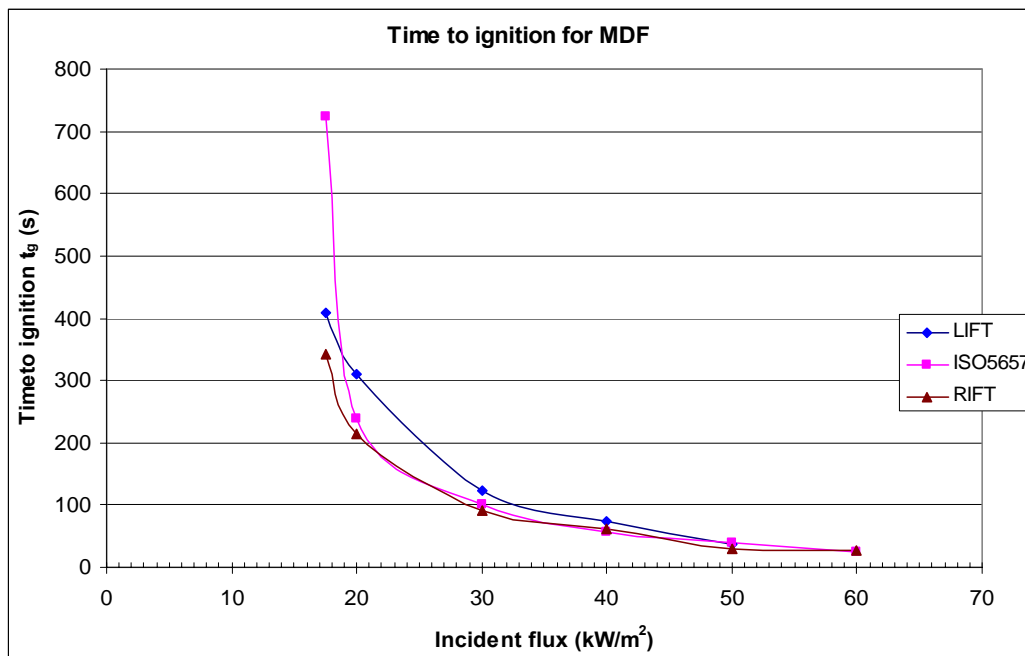


Figure 43: Time to ignition for MDF

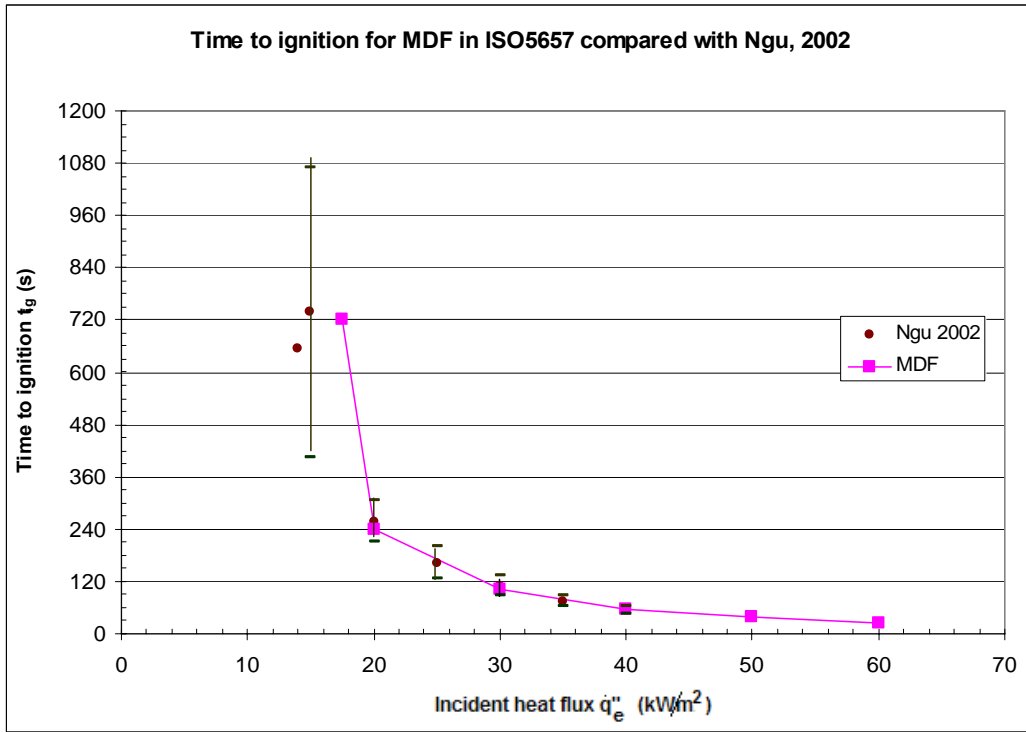


Figure 44: Comparison of time to ignition of MDF in ISO 5657 apparatus with Ngu (2002)

Plotting the incident heat flux (\dot{q}_e'') vs. $1/\sqrt{t_{ig}}$, shown in Figure 45, gives the critical heat flux (\dot{q}_{crit}'') from the intercept with the x-axis.

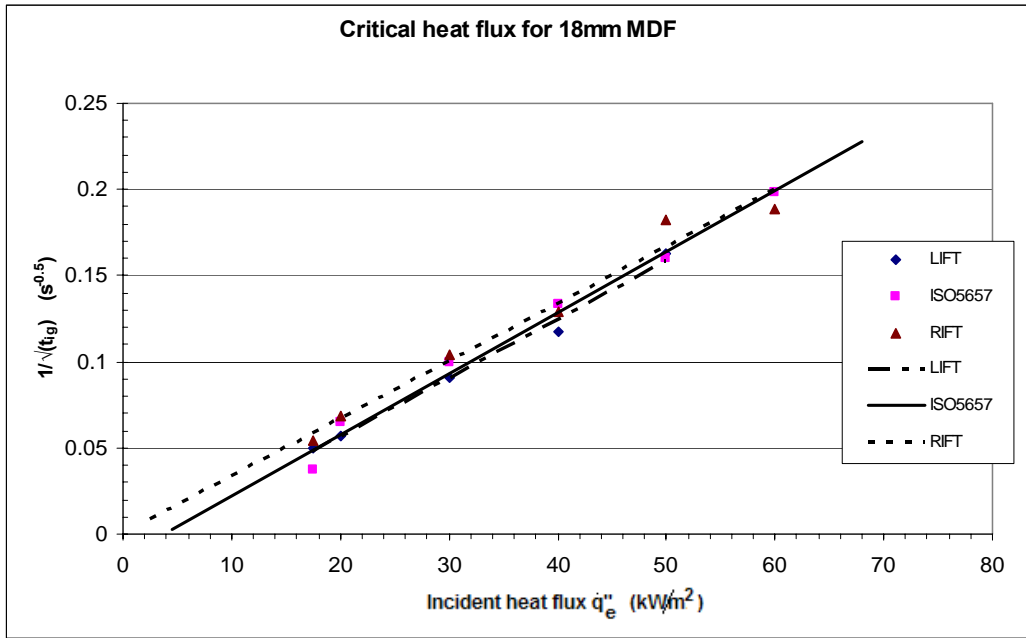


Figure 45: Critical flux for 18mm MDF

Using the protocol from ASTM E 1321-97a, the ignition parameter is calculated (Figure 46) by plotting $(\dot{q}_{ig,min})/(\dot{q}_e)$ vs. $\sqrt{t_{ig}}$. The intercept of a best fit line with $(\dot{q}_{ig,min})/(\dot{q}_e) = 1$ gives the square root of the preheating time $\sqrt{t^*}$ for the time for the sample to reach thermal equilibrium (t^*). The slope is the ignition parameter “ b ”.

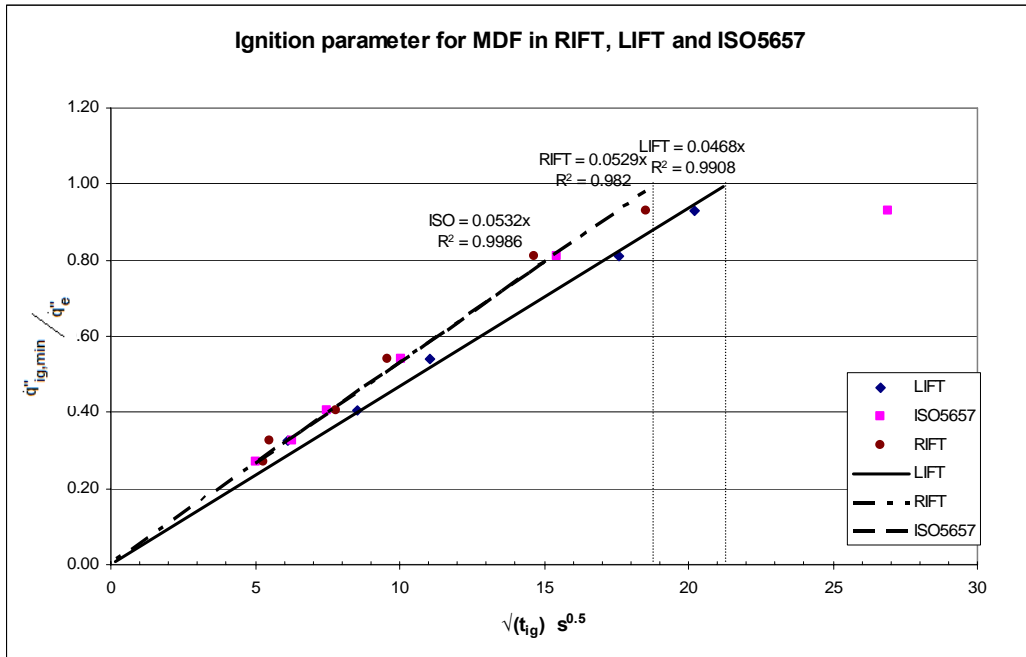


Figure 46: Ignition parameters from ASTM e1321-97a for MDF

8.1.2 Flame spread of MDF

The LIFT was set to a q''_{50mm} heat flux of 24kW/m^2 and the profile measured using the flux gauge and template, with the resulting profile shown in Figure 47. The RIFT was setup as outlined in section 6.2.

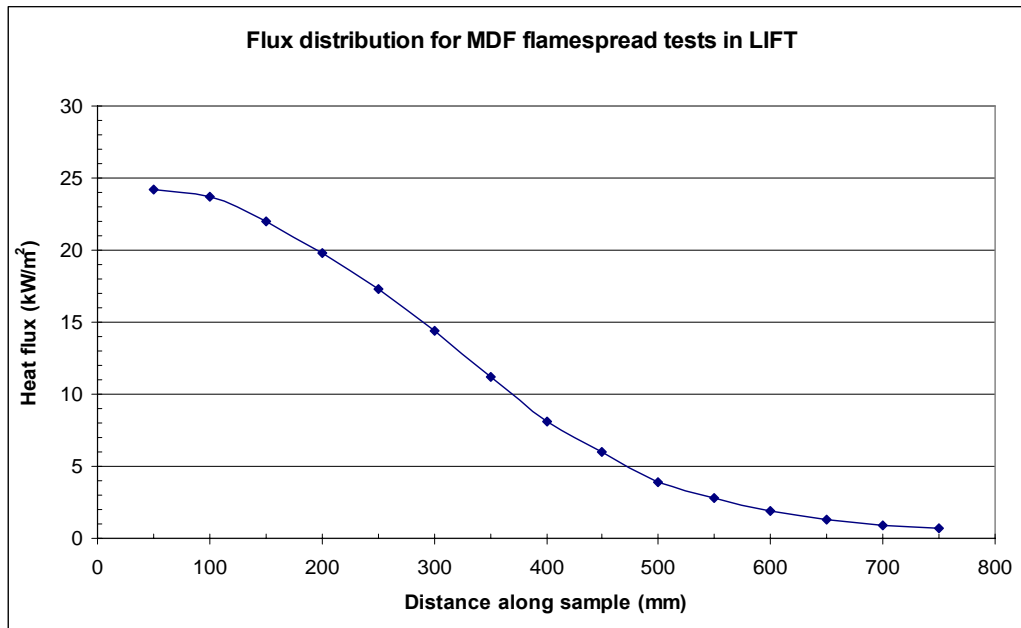


Figure 47: LIFT heat flux profile for MDF flame spread test.

The effect of preheating

MDF was compared in the RIFT with and without preheating the material fully to thermal equilibrium prior to ignition. The comparison of distance along the sample against time from ignition is shown in Figure 48, where the unpreheated sample has a lower flame spread rate, and the extent of flame spread is less. The lesser extent of flame spread means that the value for \dot{q}_s – the minimum heat flux for flame spread - is higher for the unpreheated sample. It shows that the flame front progressed faster than the material could heat to the minimum ignition temperature, and hence the flame self extinguished before the maximum flame spread distance could be achieved.

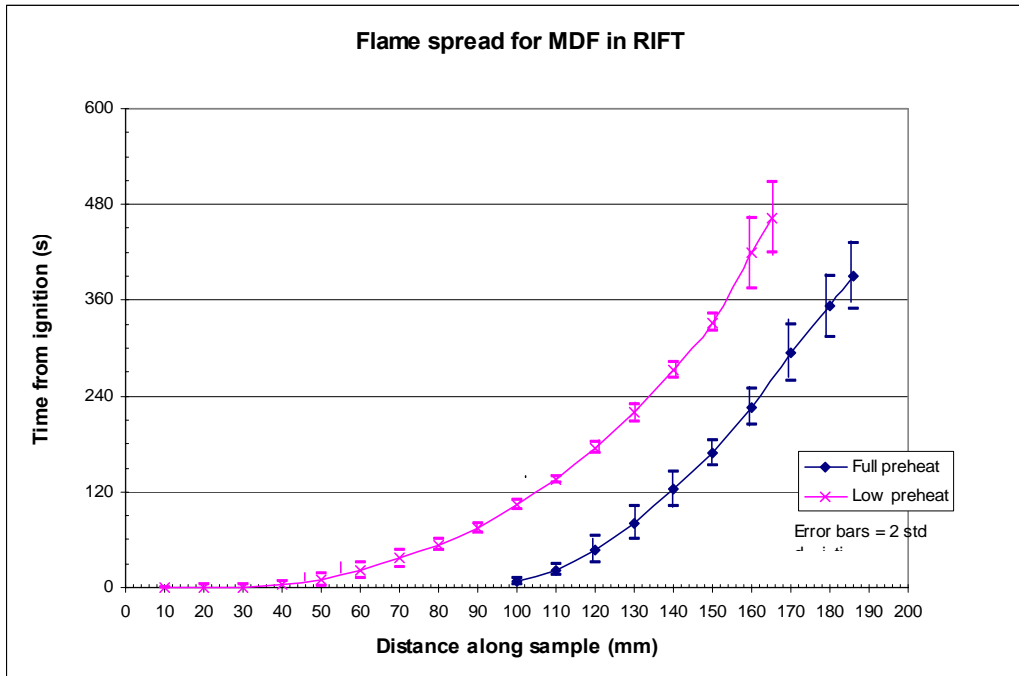


Figure 48: Flame spread of 18mm MDF in RIFT

The effect of preheating can be seen from Figure 49 and Figure 50, where the slope of the data fit line of the flame spread correlation decreases until the material reaches equilibrium, reflecting the slower flame spread rate of the unpreheated material, due to a lower surface temperature. Tests with varying preheating times were not conducted in the LIFT.

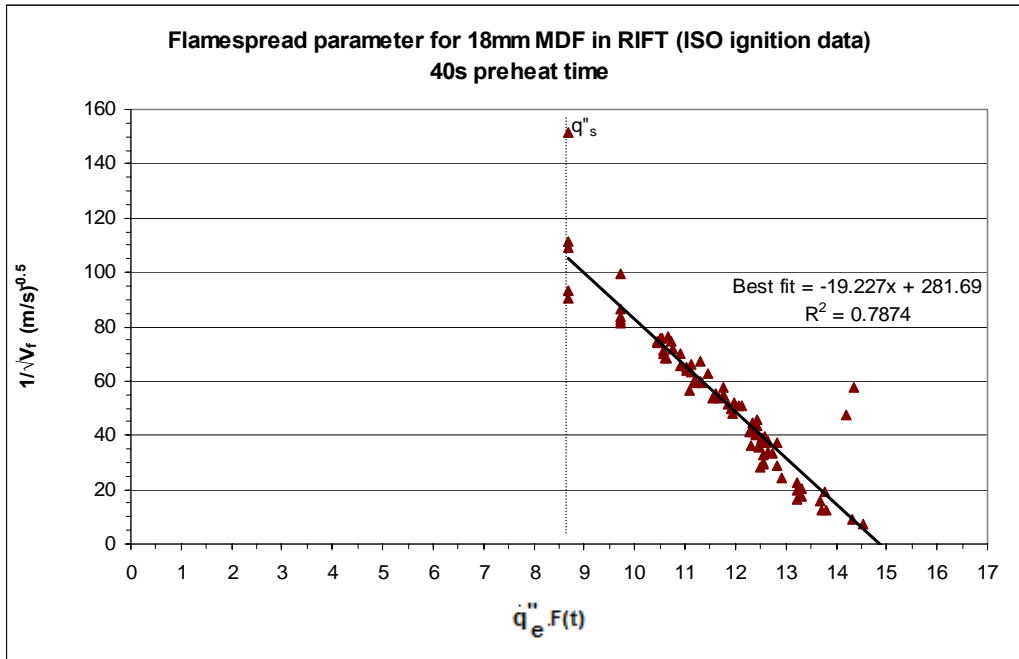


Figure 49: Flame spread parameter for 18mm MDF in RIFT using ISO ignition data and 40s preheat

Comparison of MDF in RIFT and LIFT

The flame spread correlations for the LIFT and RIFT are compared in Figure 50. The RIFT and LIFT produce similar results for both the slope of the data fit line, which leads to the flame spread parameter, and for the values of the minimum flux for flame spread. The RIFT gives a higher value for the minimum ignition flux from the correlation.

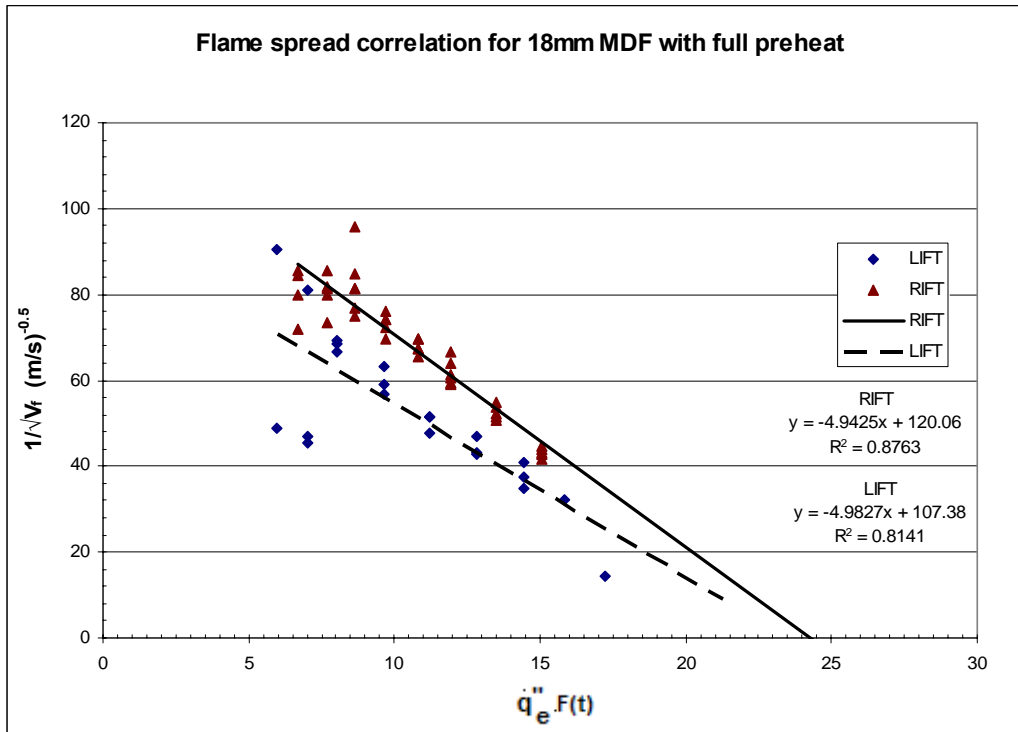


Figure 50: Flame spread correlation for 18mm MDF in RIFT and LIFT

The effect of sample thickness on flame spread

As a check on the effect of sample thickness on the flame spread, the flame spread for 6 pieces each of 9mm and 18mm MDF is compared in the RIFT with no preheating, shown in Figure 51. This shows that for this material, the two thicknesses have similar flame spread results, with the 18mm MDF having a slightly slower flame spread rate than the 9mm MDF.

This is expected to be due to thermal penetration of the thinner material, which is backed by a lightweight insulating board, allowing the material to reach a higher temperature at a given time than the thinner material. The 9mm MDF also had a far higher variation between the runs than the thicker material.

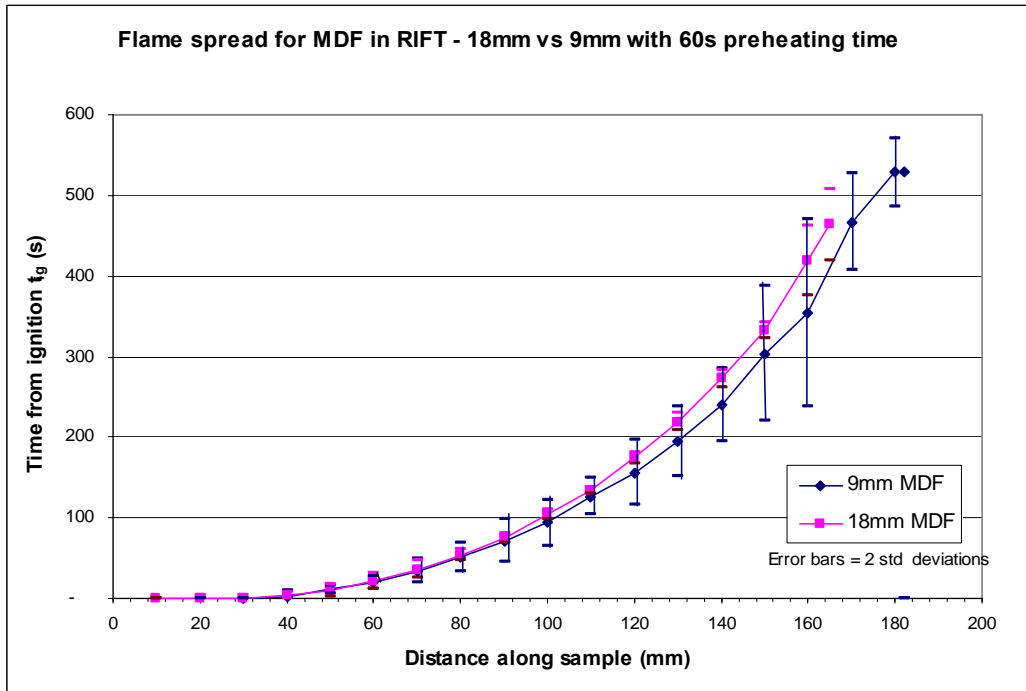


Figure 51: Flame spread for 9mm and 18mm MDF in RIFT with low (60s) preheating time

8.2 Particle Board (Chipboard)

Samples of 20mm “Pynefloor” flooring grade particle board were tested in the ISO 5657 ignition testing apparatus, the RIFT and the LIFT. In addition, a different brand (20mm “Superflake”), of nominally the same material, was also tested in the RIFT and ISO 5657 apparatus to compare the time to ignition and the flame spread rate in the RIFT, and hence the variation between materials of the same nominal type.

The results are summarised in Appendix 3

8.2.1 Ignition of particle board

As particle board is a commonly used material in the research literature, the two brands of particle board were compared for ignition, to see if there was significant variation between two samples of the same nominal material, and hence gauge the expected variation with published results. The ignition results in the ISO 5657 ignition apparatus is shown in Figure 52 and Figure 53

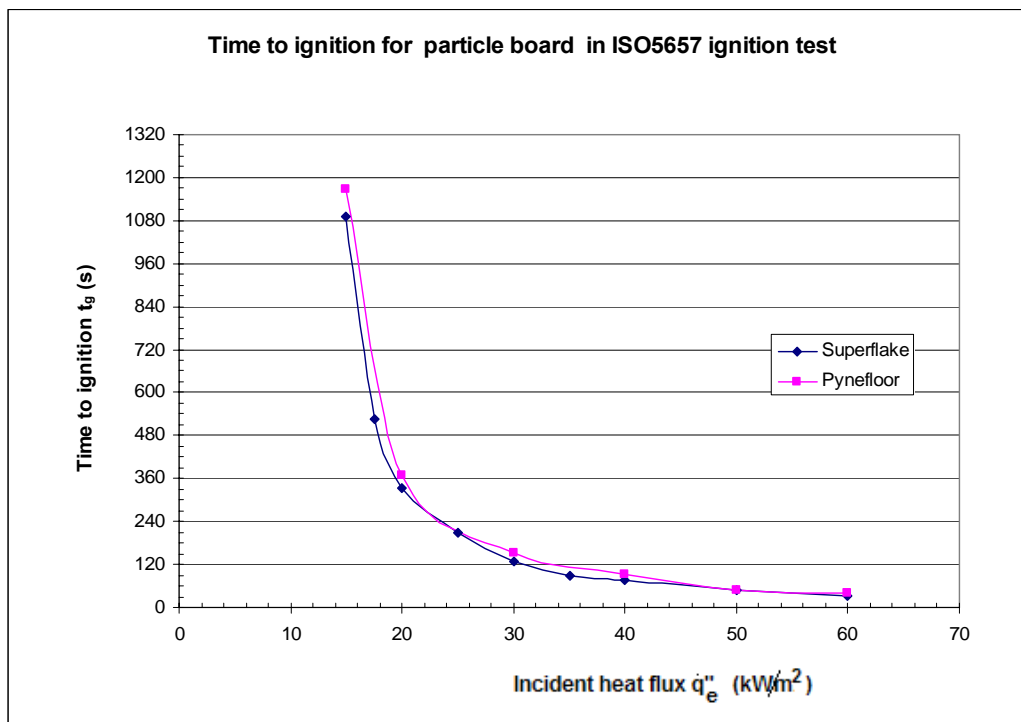


Figure 52: Ignition time for 2 brands of particle board in ISO 5657 apparatus.

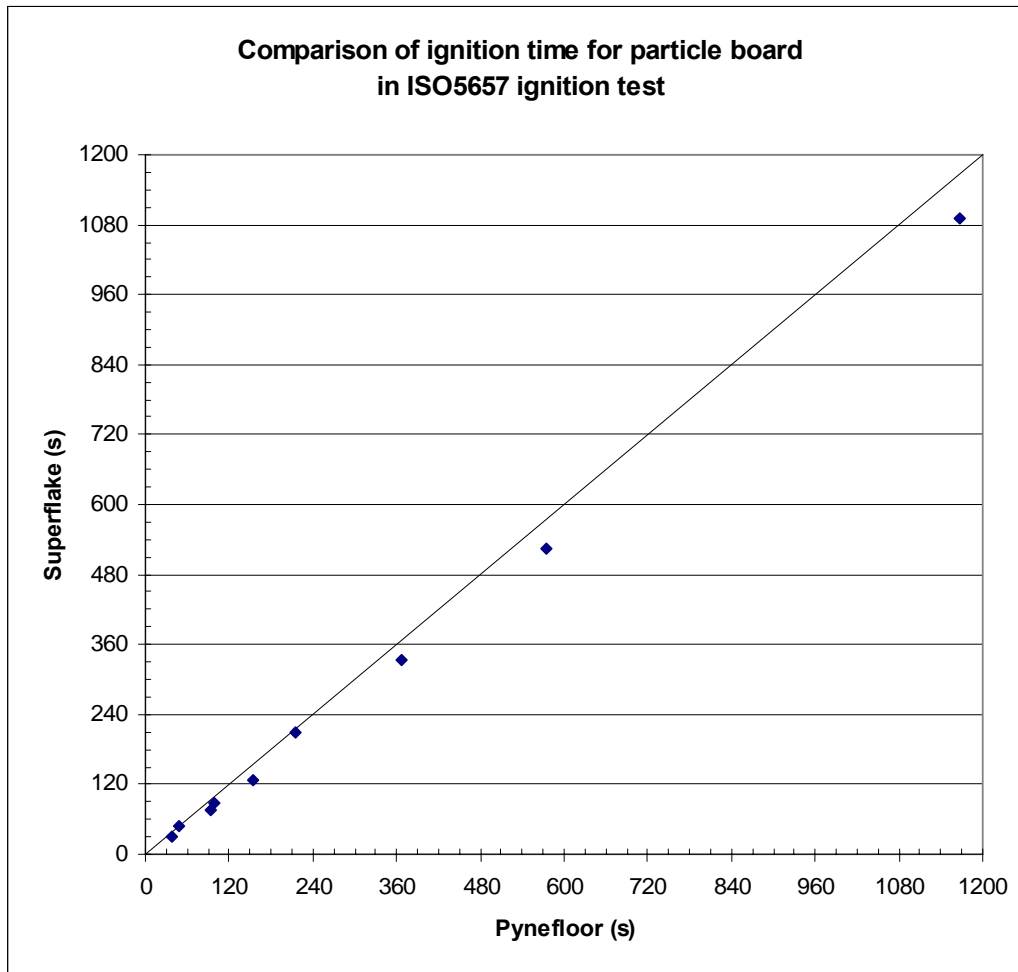


Figure 53: Comparison of ignition times for particle board

There is a difference between the 2 brands, but it is small and appears to be approximately in proportion to the product density., where the higher density material (Pynefloor) has a longer time to ignition at any given heat flux level.

The results of the ignition tests for Pynefloor are shown in Figure 54, where the minimum flux for ignition ($\dot{q}_{ig,min}$) is 13.75kW/m² for the ISO 5657 ignition tests. The LIFT and RIFT gave higher values for the minimum ignition flux, in line with the expected findings. The results for Superflake (Figure 55) are similar.

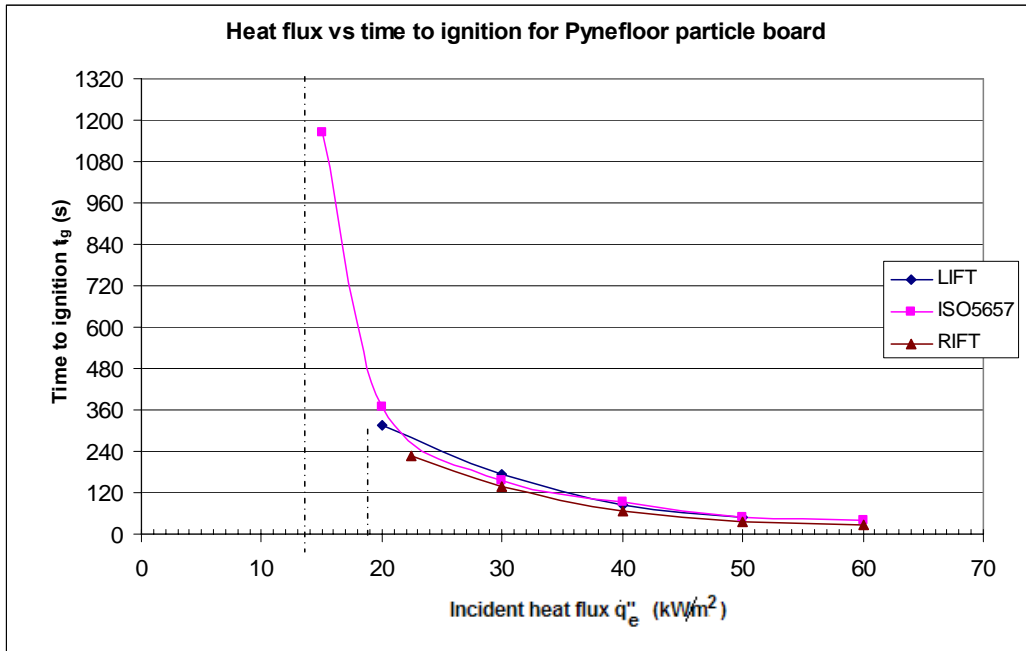


Figure 54: Time to ignition for Pynefloor particle board

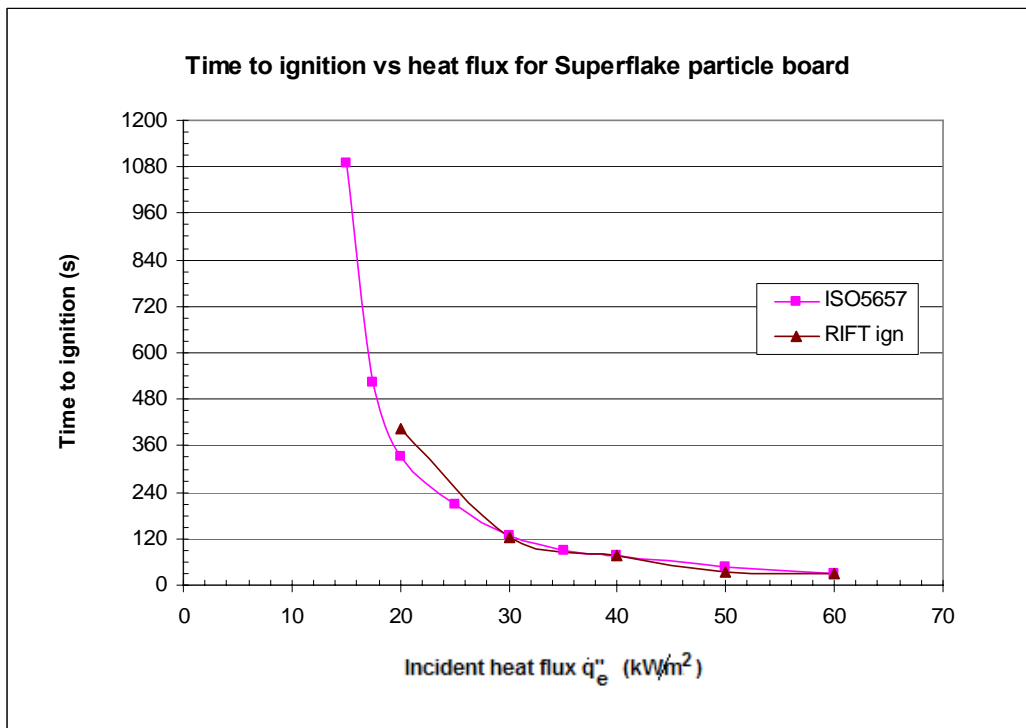


Figure 55: Time to ignition for Superflake particle board

The ignition parameters for Pynefloor from the different tests are given in Figure 56. The effect of the different ignition tests on the ignition parameter value “ b ”, which is the slope of the best fit line can be seen, as well as the preheating time t^* , where $(t^*)^{1/2}$ is the intercept where the ignition parameter line crosses $\dot{q}_e'' / \dot{q}_{ig,min}'' = 1$.

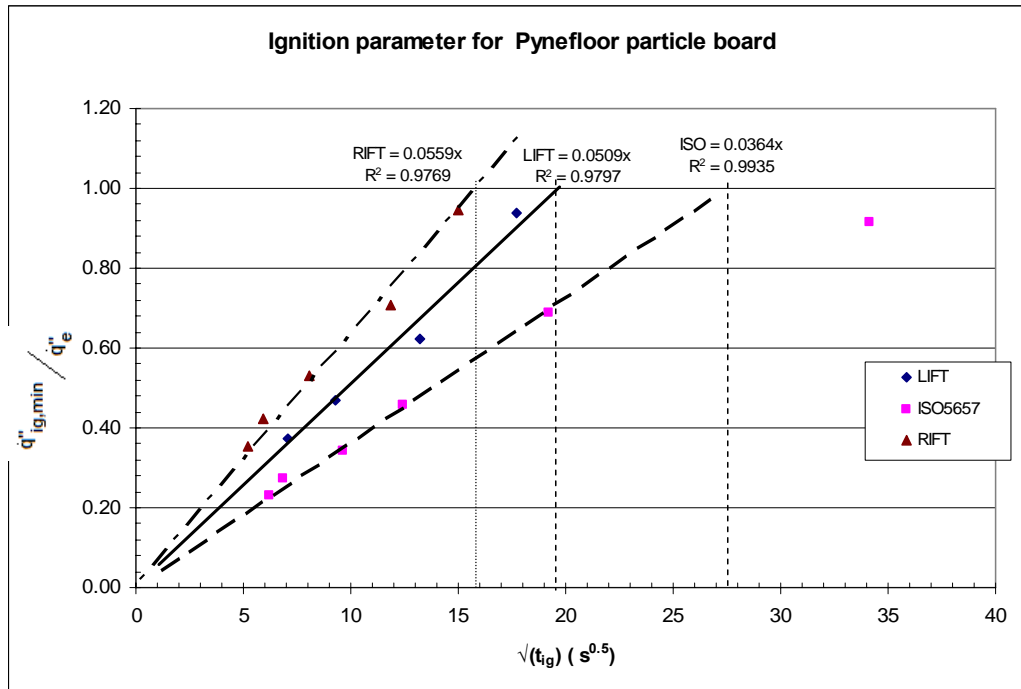


Figure 56: Ignition parameter for Pynefloor particle board

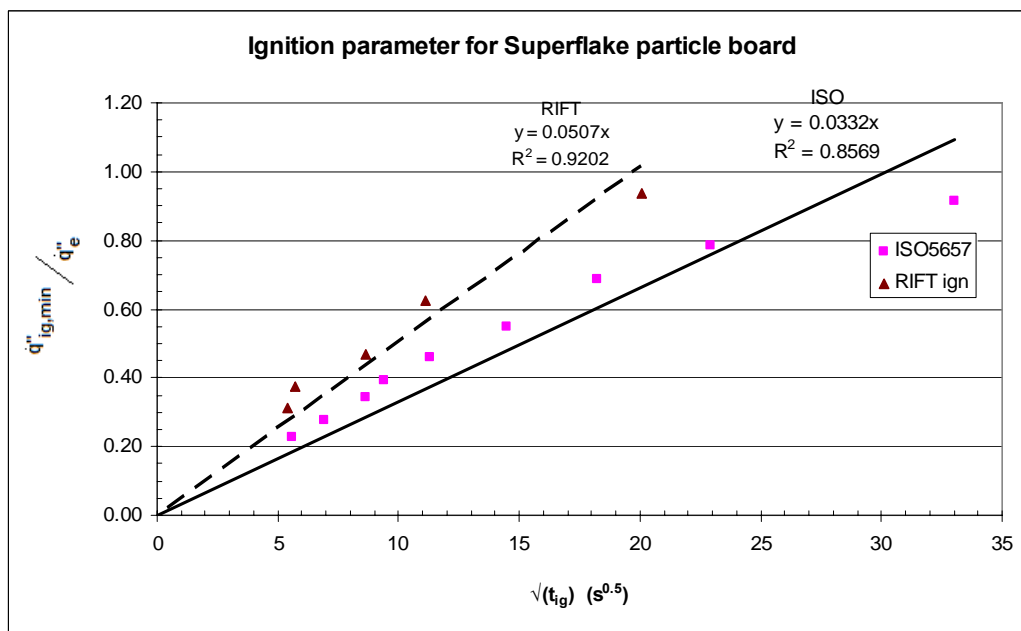


Figure 57: Ignition parameter for Superflake particle board

The critical ignition flux for the two brands of particle board (Figure 58 for Pynefloor, and Figure 59 for Superflake) gives very similar results.

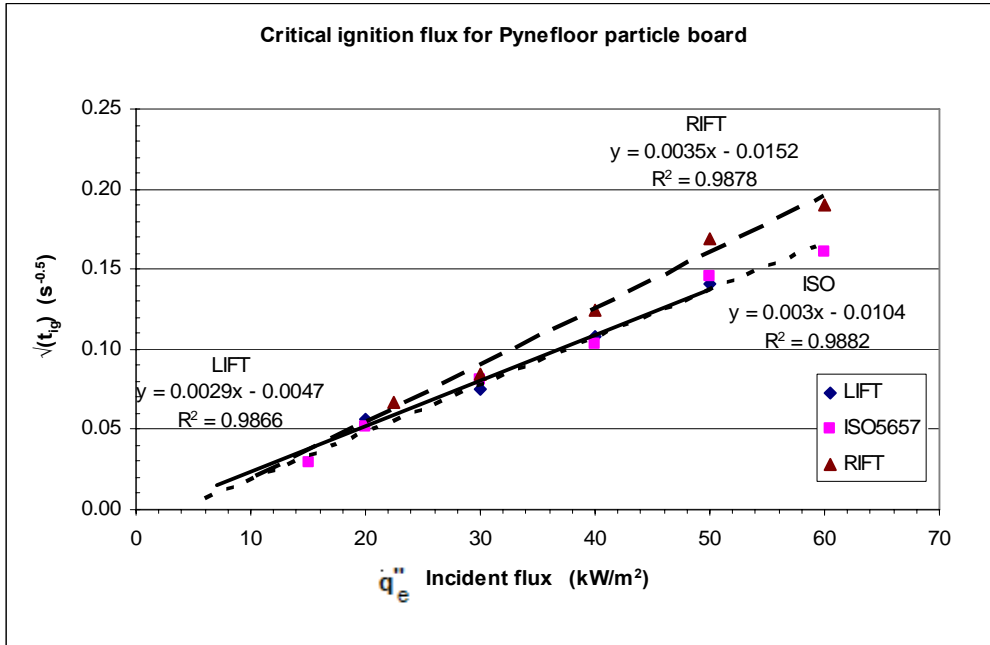


Figure 58: Critical ignition flux for Pynefloor particle board

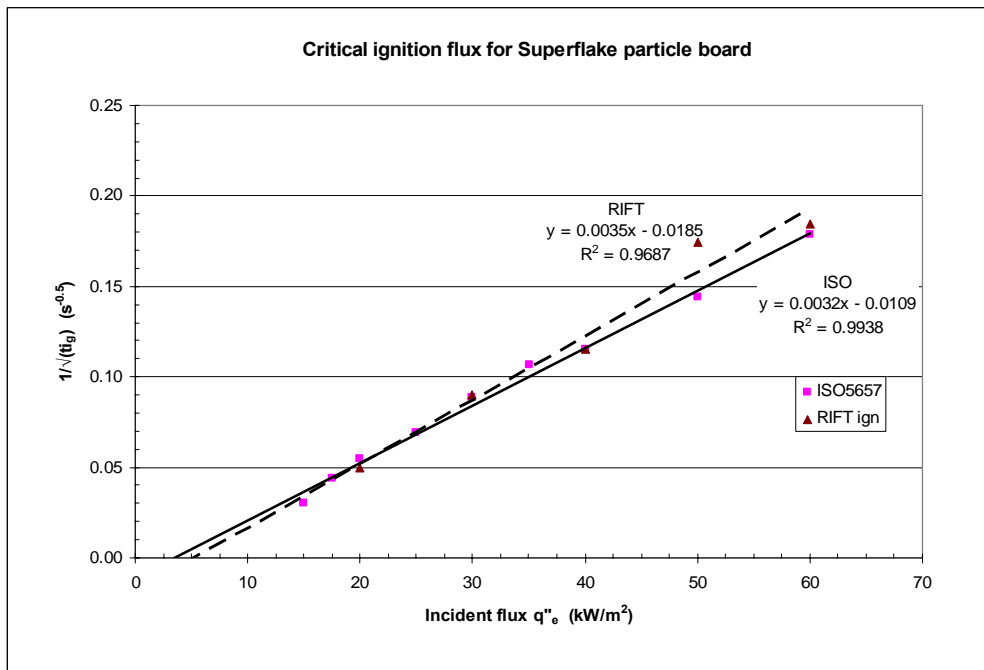


Figure 59: Critical ignition flux for Superflake particle board

As a comparison between Janssen's ignition theory and that of Quintiere, the critical ignition flux q_{crit}'' is shown in Figure 58 and Figure 60. Typically, Janssen's correlation gives a slightly higher value for the critical ignition flux; due to the steeper slope of the data fit line. In this case the values for the Quintiere model and the Janssen's correlation are 5.5 and 6 kW/m² respectively for Pynefloor particle board. The Quintiere model give 3.4kW/m² for Superflake, against 5.8kW/m² for the Janssen's' model for the same material.

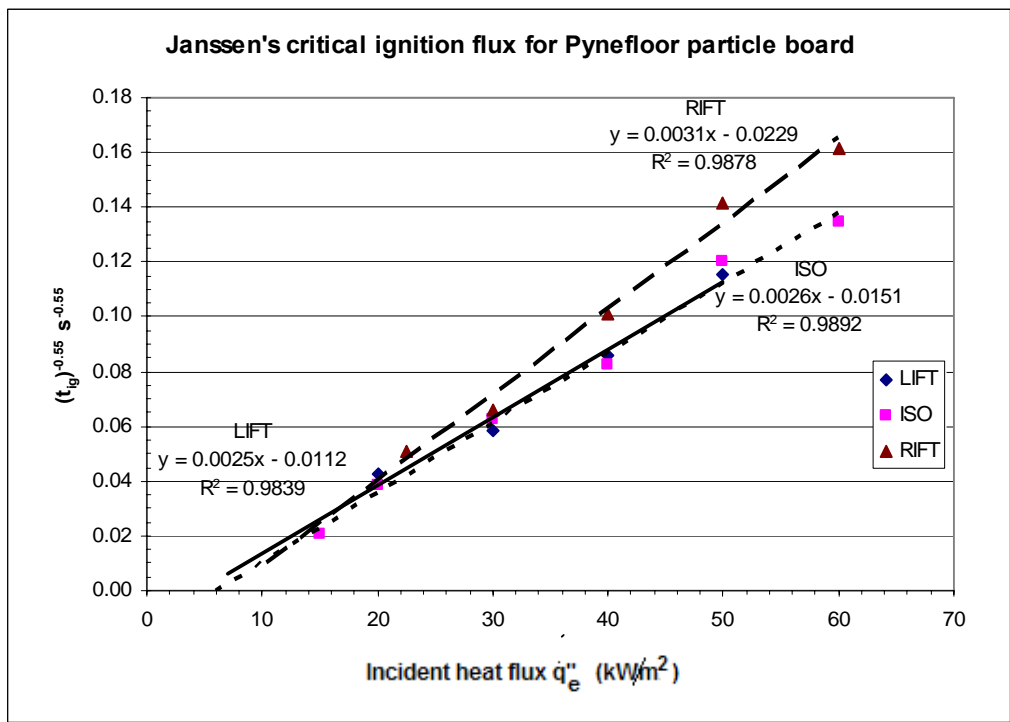


Figure 60: Janssen's critical ignition flux for Pynefloor particle board

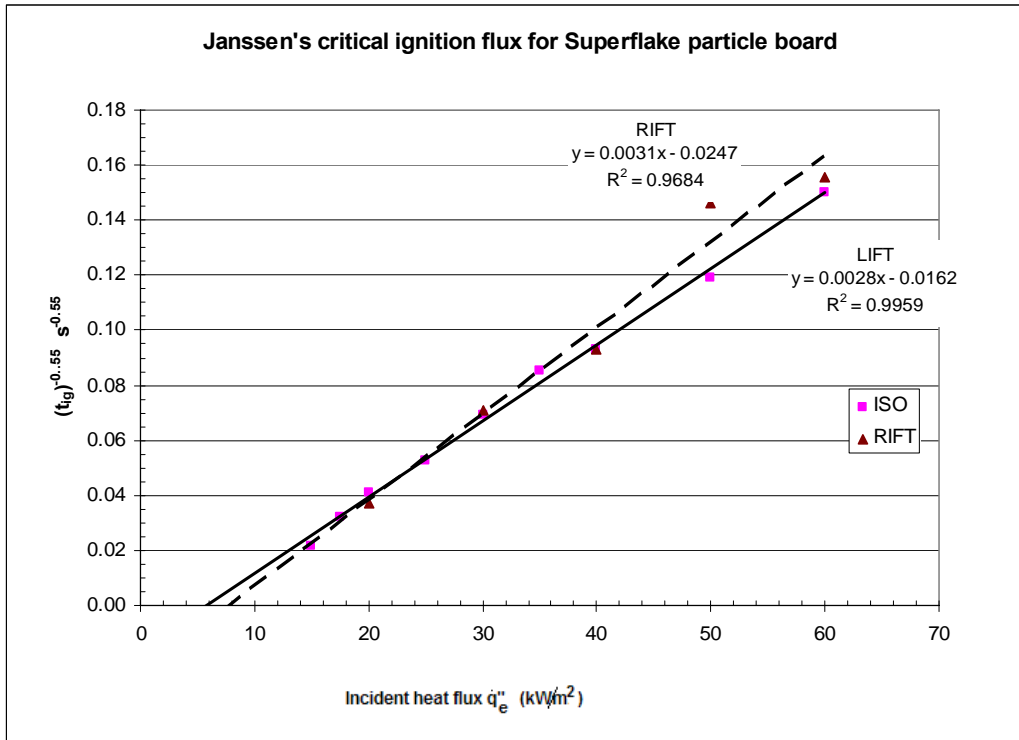


Figure 61: Janssen's critical ignition flux for Superflake particle board

8.2.2 Flame spread for particle board

Flame spread in RIFT

A preheat time of 80 seconds was used for the low preheat tests. The t^* time of 755 seconds from the ISO 5657 ignition was used for the full preheat time for the RIFT tests, and the t^* time of 386 seconds from the LIFT ignition test was used for the LIFT flame spread tests.

A comparison of the flame spread between the 2 brands of particle board in the RIFT shows a minor difference in the flame spread rate (Figure 62 and Figure 63), which affects the final flame spread properties. This reflects the ignition test results, where the Superflake board had a shorter time to ignition at for any given heat flux. From the flame spread theory, this would give a faster flame spread rate, as shown here.

Given that particle board is a common material used in flame spread testing, this shows the limitation in comparing “equivalent” materials.

The effect of preheating the material on the variation of the flame spread rate measured in the RIFT can be seen by comparing Figure 62 and Figure 63. It can also

be seen in the amount of data scatter in the flame spread correlation (Figure 64) when compared to the same material which is fully preheated (Figure 65).

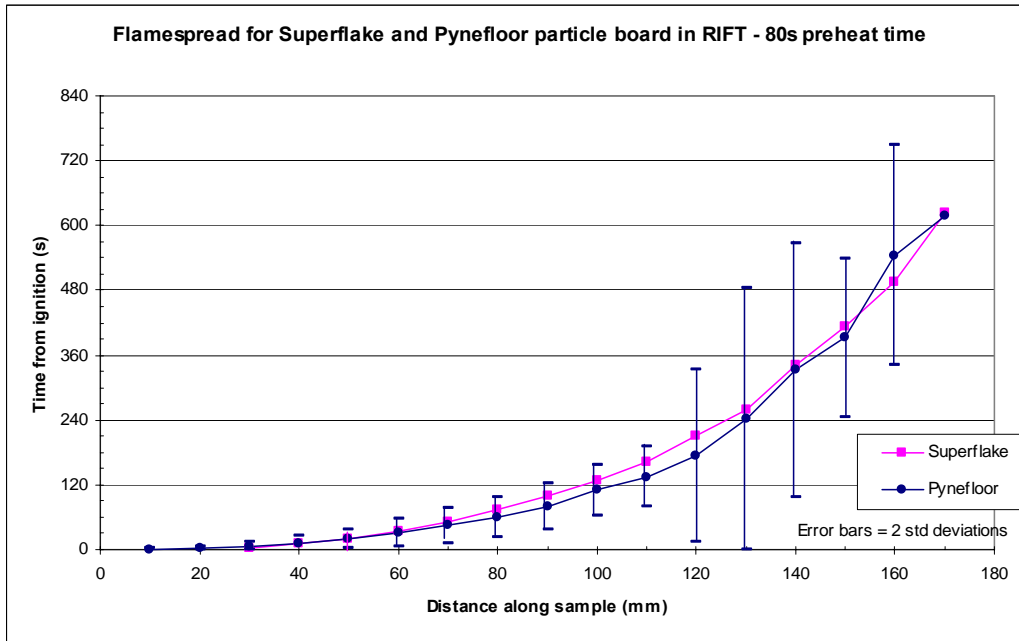


Figure 62: Comparison of flame spread of 2 brands of particle board – low preheat time

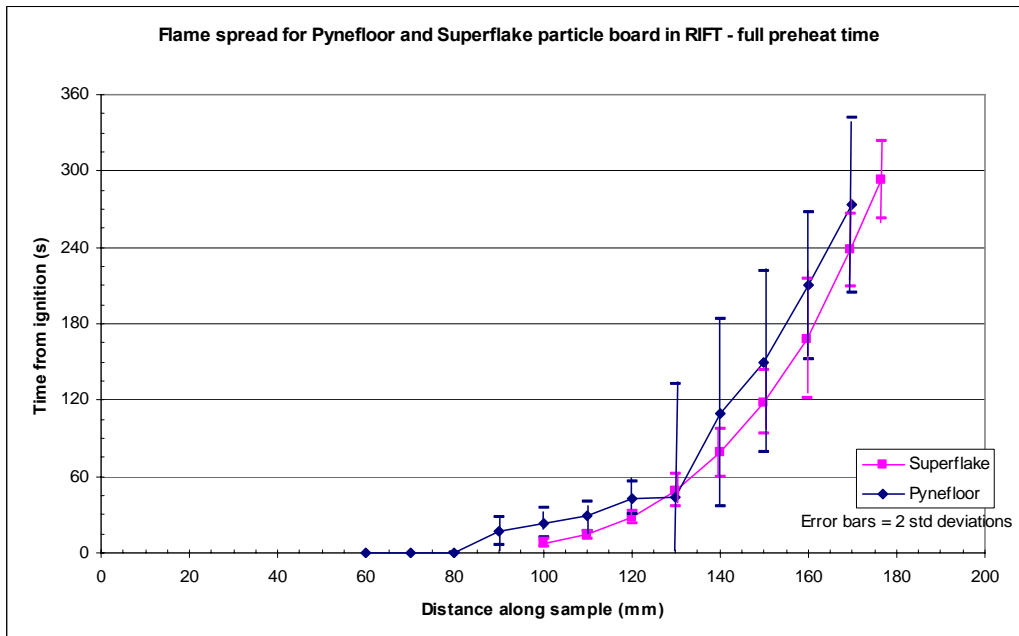


Figure 63: Comparison of flame spread for 2 brands of particle board - full preheat time

The flame spread correlation for the Pynefloor in the RIFT is affected by outliers at the end of the test (Figure 65) – i.e. at the period of low flame spread rate. Without

these, the results would be a better match to those obtained in the LIFT (Figure 68). The Superflake board was not tested in the LIFT as there was insufficient material to conduct a full suite of LIFT tests.

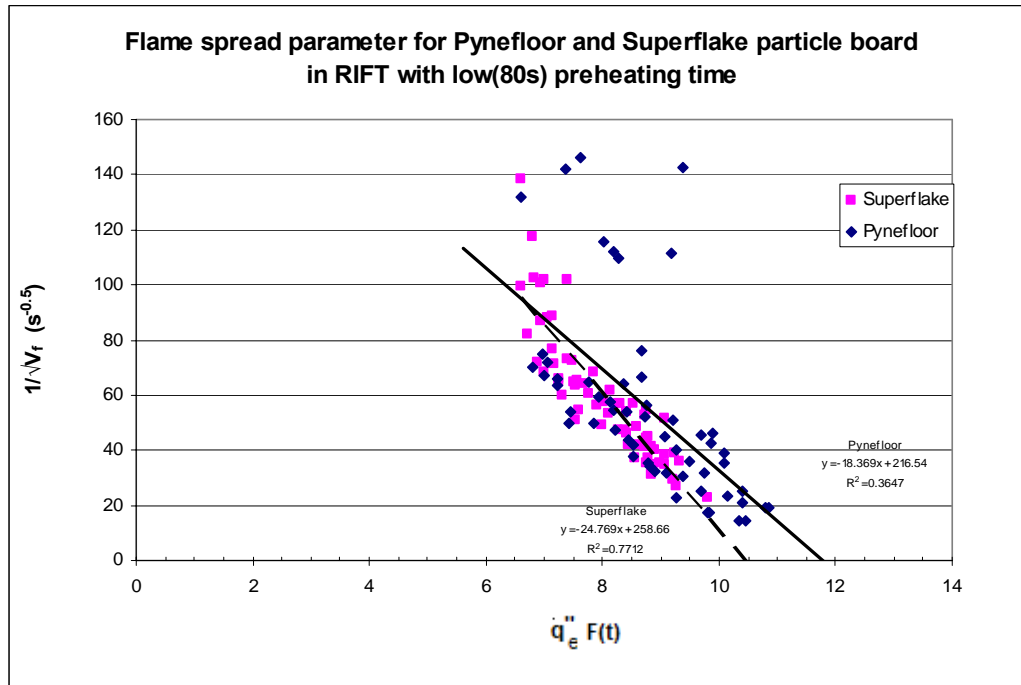


Figure 64: Flame spread parameter for Superflake and Pynefloor particle board in RIFT with a 80s preheat time.

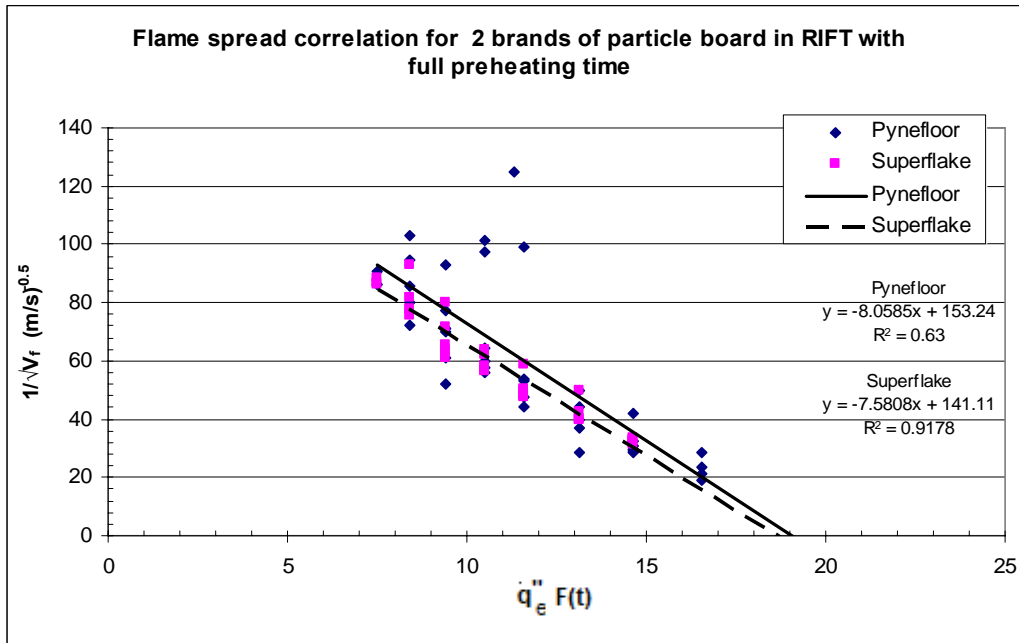


Figure 65: Flame spread correlation for 20mm Particle board in RIFT with full pre-heating time.

Flame spread for particle board in the LIFT

The LIFT was set to the flux profile shown in Figure 66 and the samples preheated for the preheating time based on the LIFT ignition results of $t^* = 386$ seconds prior to ignition.

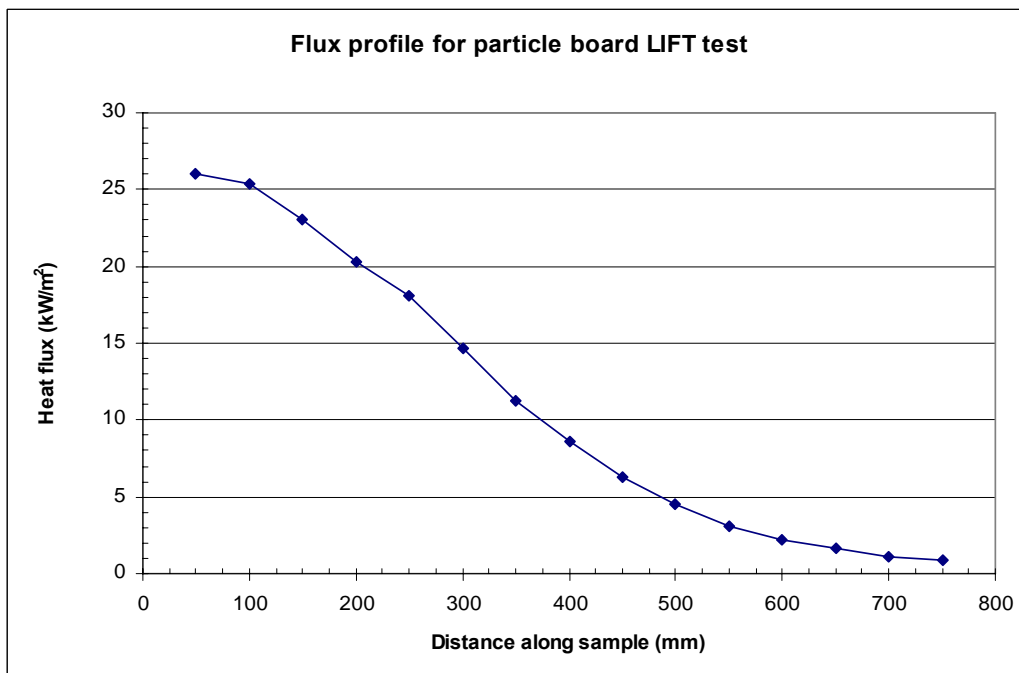


Figure 66: Heat flux profile for LIFT flame spread tests on particle board

The resulting flame spread along the sample is shown in Figure 67.

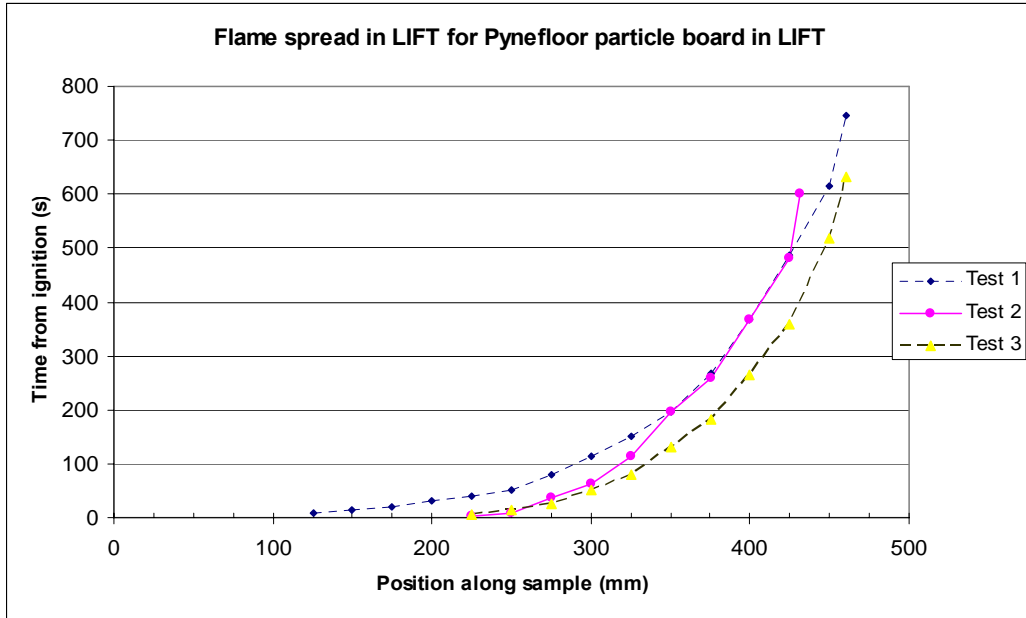


Figure 67: Flame spread in LIFT for Pynefloor particle board

The resulting flame spread correlation for Pynefloor is compared to the same material in the LIFT in Figure 68, where the value of the minimum flux for flame spread is similar, but the RIFT gives a lower correlated value of the minimum ignition flux. In both tests, the material was fully preheated, with the RIFT test using the ISO 5657 ignition test data, and the LIFT using the ignition data from the LIFT ignition tests.

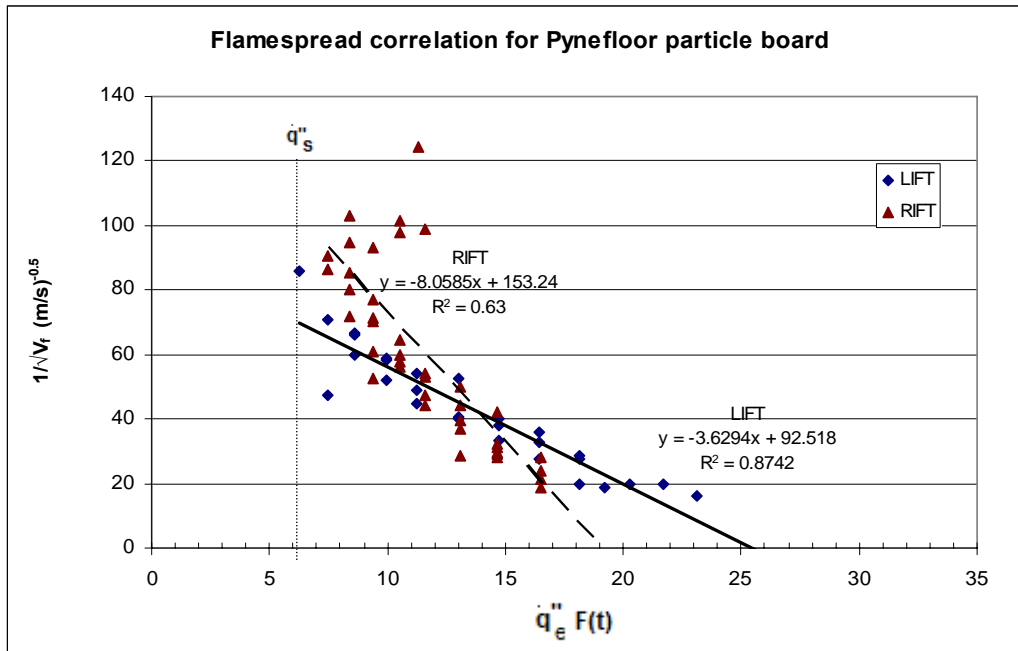


Figure 68: Flame spread correlation for 20mm Pynefloor particle board in LIFT and RIFT

8.3 Plywood

All samples were from a single sheet of IPL “Tuffply” 17mm untreated Radiata Pine C/D grade plywood. The smooth (C grade) face was used for the ignition and flame spread tests.

8.3.1 Ignition of plywood

The time to ignition for varying flux levels is shown in Figure 69.

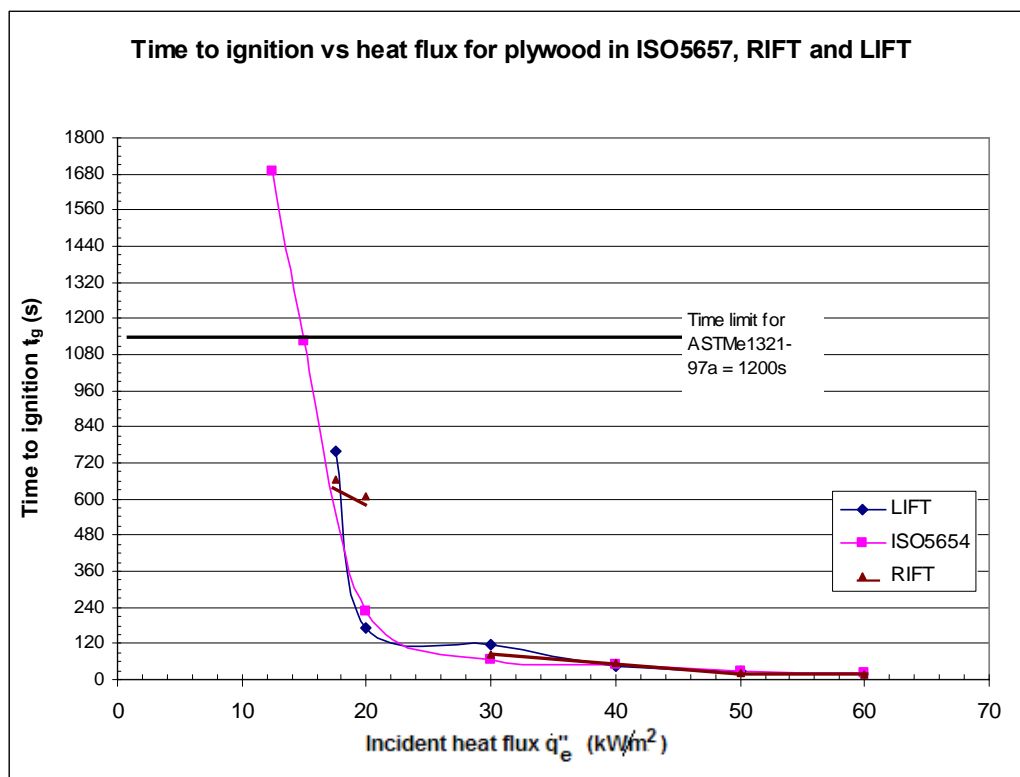


Figure 69: Time to ignition for 17mm plywood

As can be seen in Figure 69, the fact that the sample does not ignite within the time limit does not mean that the minimum ignition flux is the lowest point that ignition will occur. In the case of this ignition test, the sample had a glowing spot before finally igniting, and there was considerable charring.

The critical ignition flux (Figure 70) for plywood by the 3 ignition methods gave a range of results from 4.6kW/m² to 10kW/m², compared with 13.75kW/m² for the

minimum ignition flux in the ISO 5657 test and 16.25kW/m² for the RIFT and LIFT ignition tests.

The chart for the ignition parameter (Figure 71) shows less spread of the results than with the particle board (Figure 56), largely due to the minimum ignition flux being similar for all test methods. Values above $\dot{q}_{ig,min}'' / \dot{q}_e'' < 0.8$ were ignored to improve the data fit.

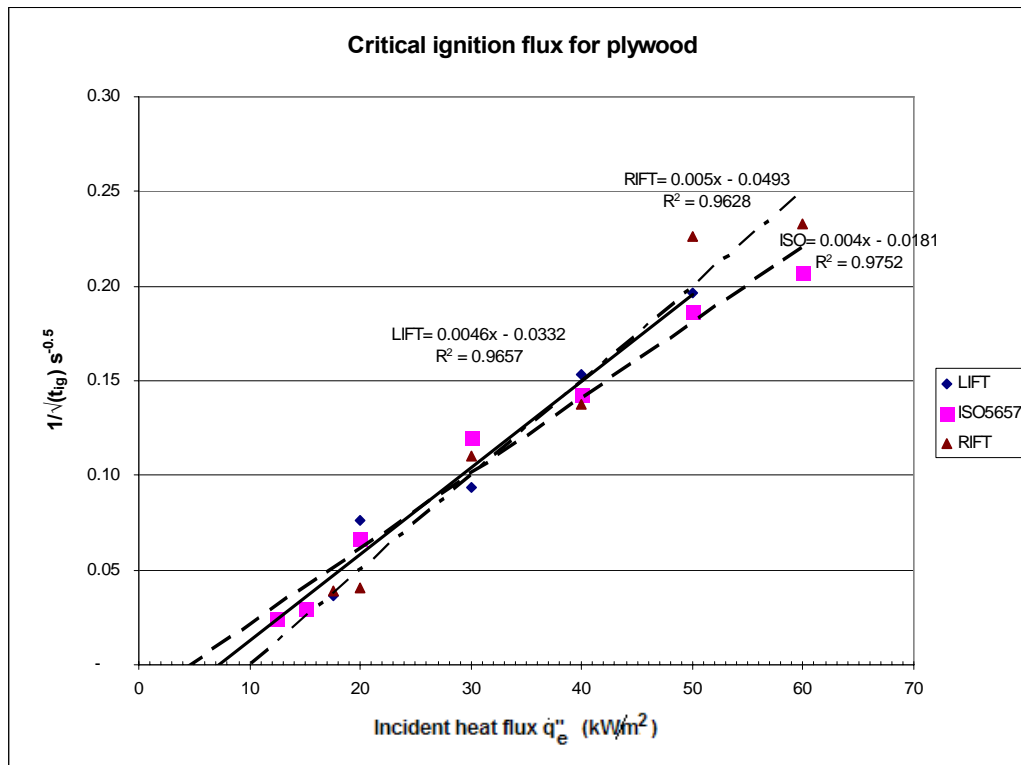


Figure 70: Critical ignition flux for plywood

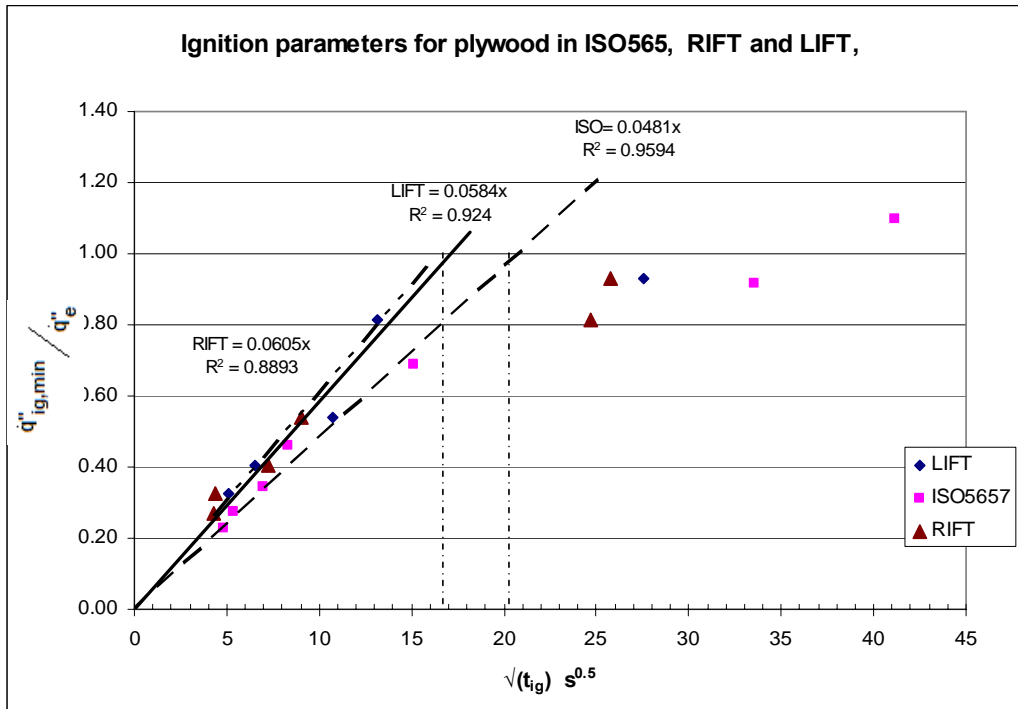


Figure 71: Ignition parameter for plywood

8.3.2 Flame spread of plywood

Flame spread in RIFT

The flame spread in the RIFT shows the expected behaviour, with the preheated sample having a faster flame spread rate, due to the higher initial surface temperature. The low preheat time was approximately 65 seconds., compared with the preheat time for the LIFT at 293 seconds, and the full preheat time for the RIFT , based on the ISO 5657 ignition data of 432 seconds.

The flame spread along the sample is given in Figure 72, showing the effect of preheating on the flame spread rate and the extent of flame spread. The flame spread rate is sufficiently slow compared with the preheating time that the sample can preheat to equilibrium at the extent of flame spread. The extent of flame spread along the sample is therefore the same in both cases. The velocity of the flame front is less for the sample which is not preheated, reflecting the lower initial surface temperature prior to ignition.

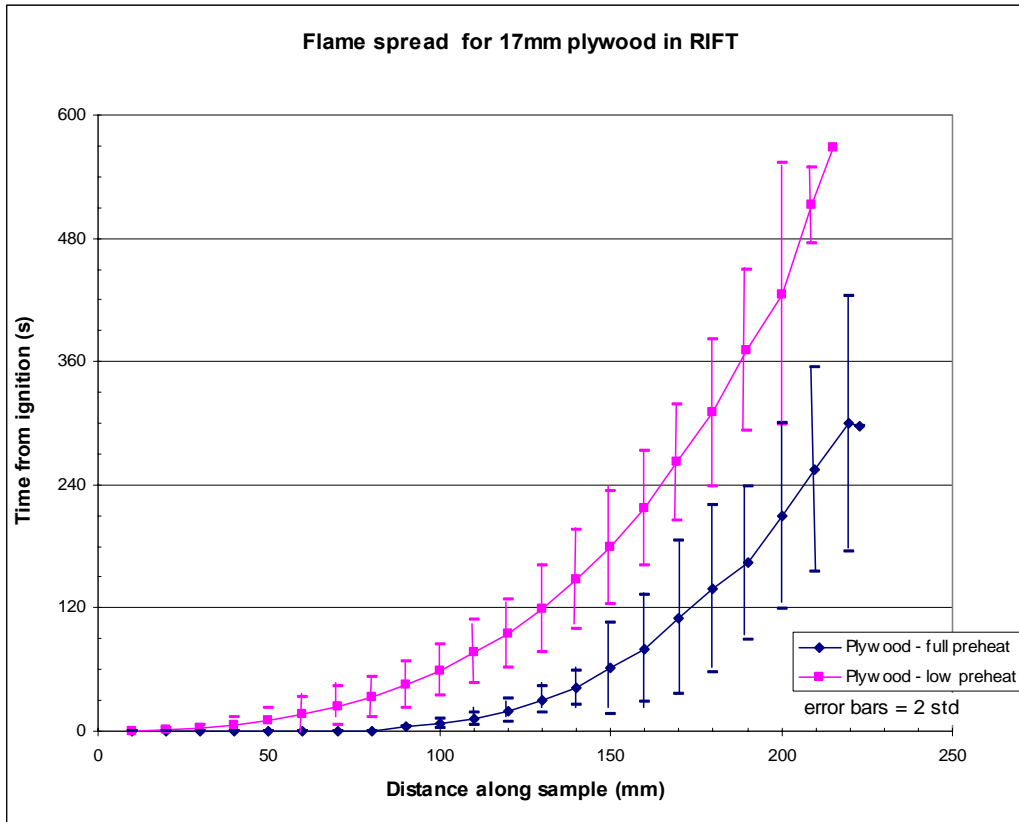


Figure 72: Flame spread of 17mm plywood in RIFT

Both 9mm and 17mm plywood were tested without a preheating period, to check if the material thickness had any significant effect on the flame spread. In this case, the difference in the flame spread is within the limits of error and there is no significant difference (Figure 73). Different materials and a long preheating time may alter this result, if the material thickness is less than the thermal penetration depth.

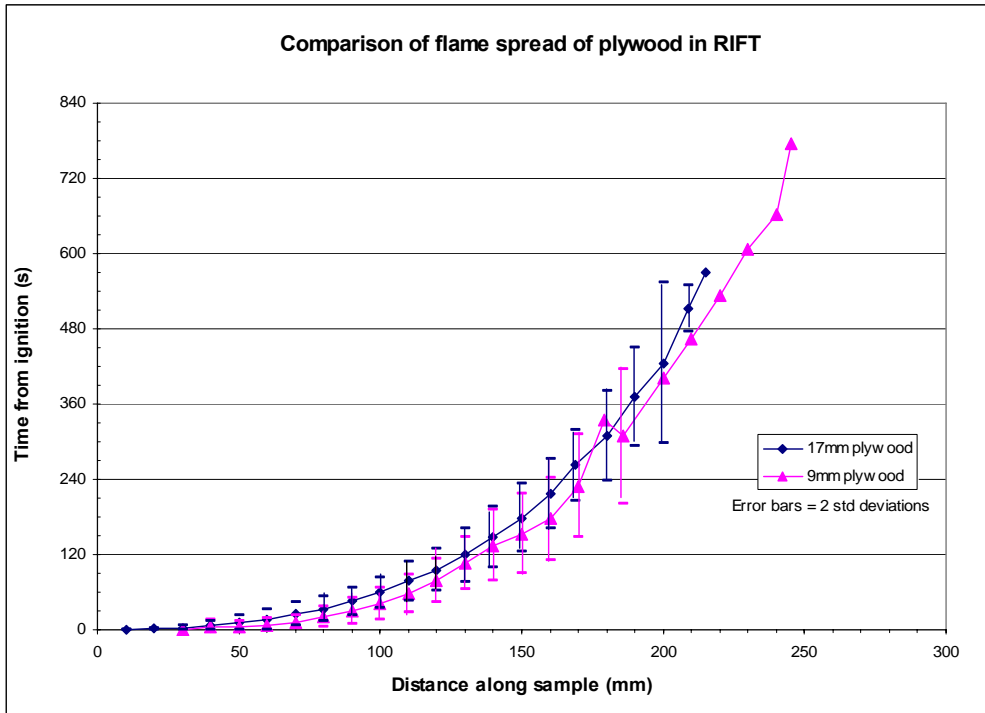


Figure 73: Comparison of flame spread with different thicknesses of plywood

The resulting flame spread correlation from the RIFT flame spread tests is shown in Figure 74.

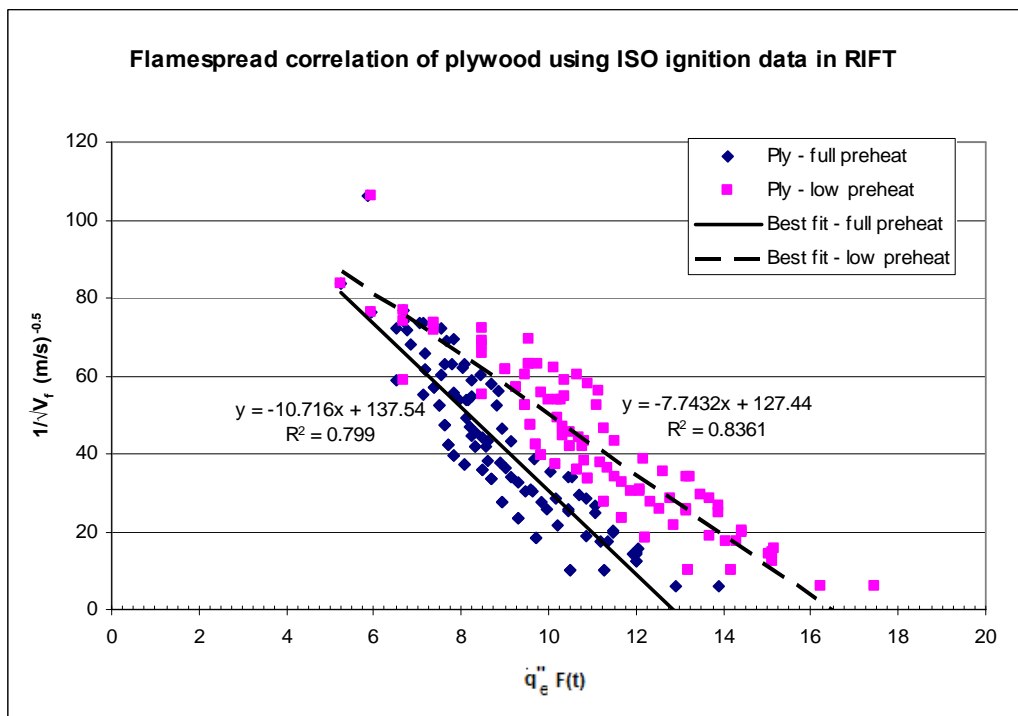


Figure 74: Flame spread correlation for 17mm plywood in RIFT

Flame spread in LIFT

The flame spread tests in the LIFT used the heat flux profile shown in Figure 75 with the resulting flame spread along the sample shown in Figure 76.

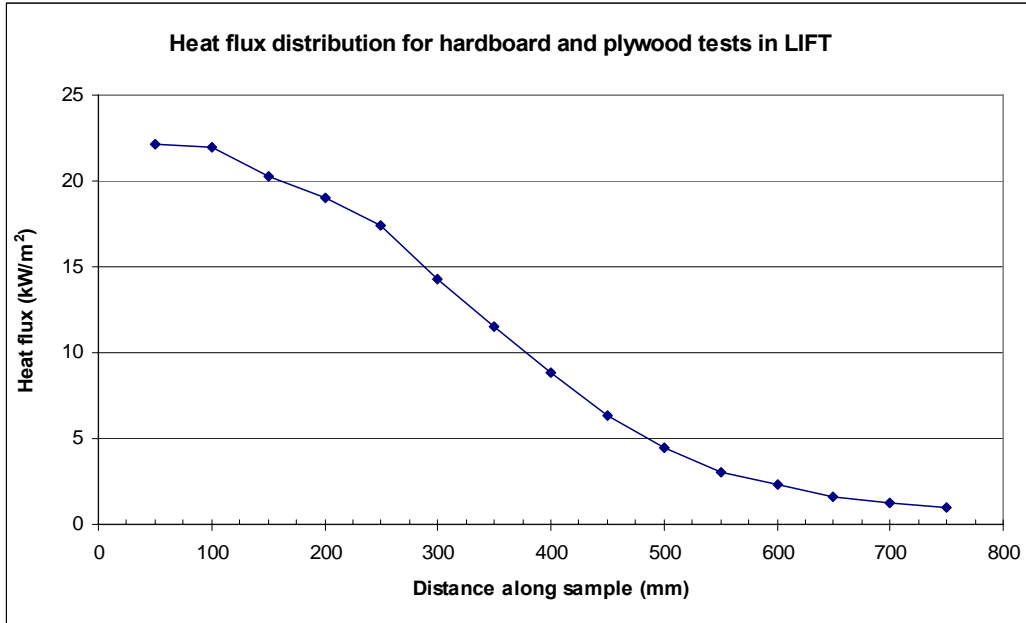


Figure 75: LIFT heat flux profile for plywood and hardboard flame spread tests

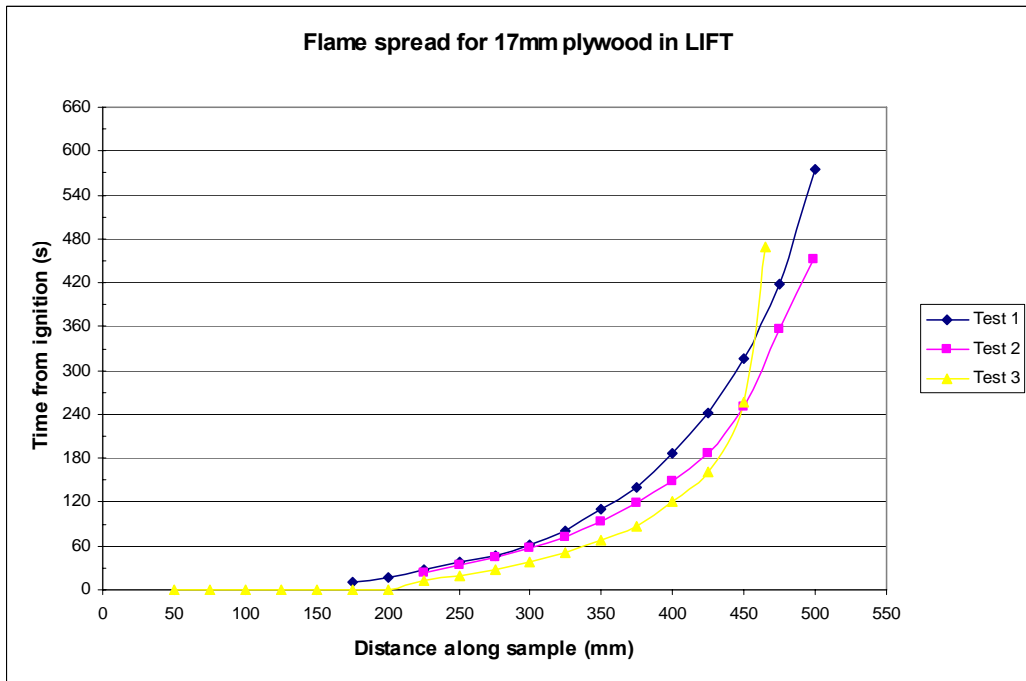


Figure 76: Flame spread for 17mm plywood in LIFT

The flame spread correlation (Figure 77 and Figure 78) shows that the RIFT and LIFT gave similar results, however the RIFT has more data scatter than the LIFT.

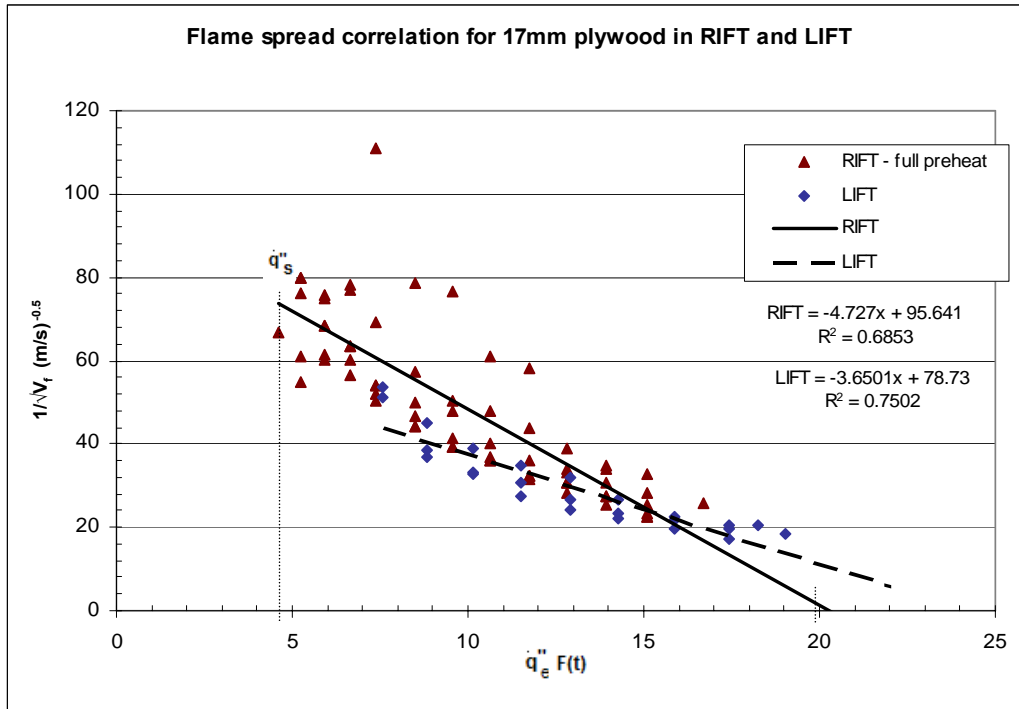


Figure 77: Flame spread correlation for 17mm plywood in RIFT and LIFT

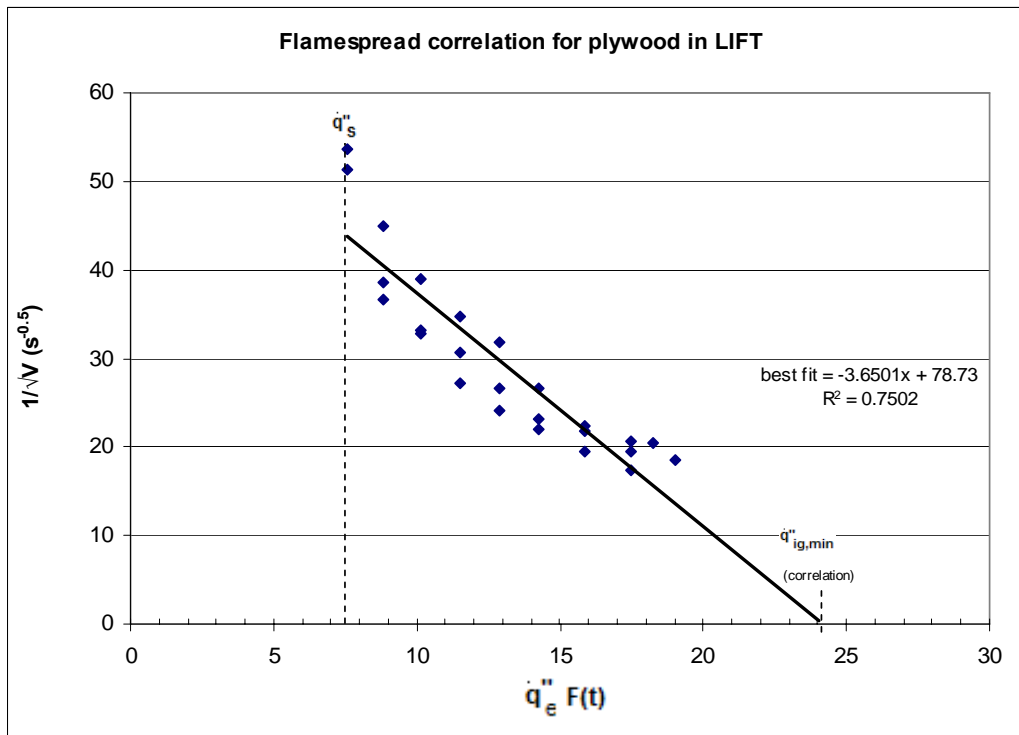


Figure 78: Flame spread correlation for plywood in LIFT

8.4 Hardboard

The material used here was a generic unbranded material from a builders supply merchant, with a thickness of 5mm.

8.4.1 Ignition of hardboard

The sample in the ISO 5657 ignition test was backed with 20mm lightweight Kaoboard low density insulating board. The RIFT ignition test used 12mm lightweight Kaoboard. The LIFT uses a higher density CaSi board, and this may affect any time to ignition comparison, as the material is physically thin in comparison to the other materials tested. Attempts to calculate the thermal thickness of the hardboard showed to much variation to be successful. Quintiere and Harkleroad (1984) found little difference attributable to the density of the backing board – the expected result for a thermally thick material.

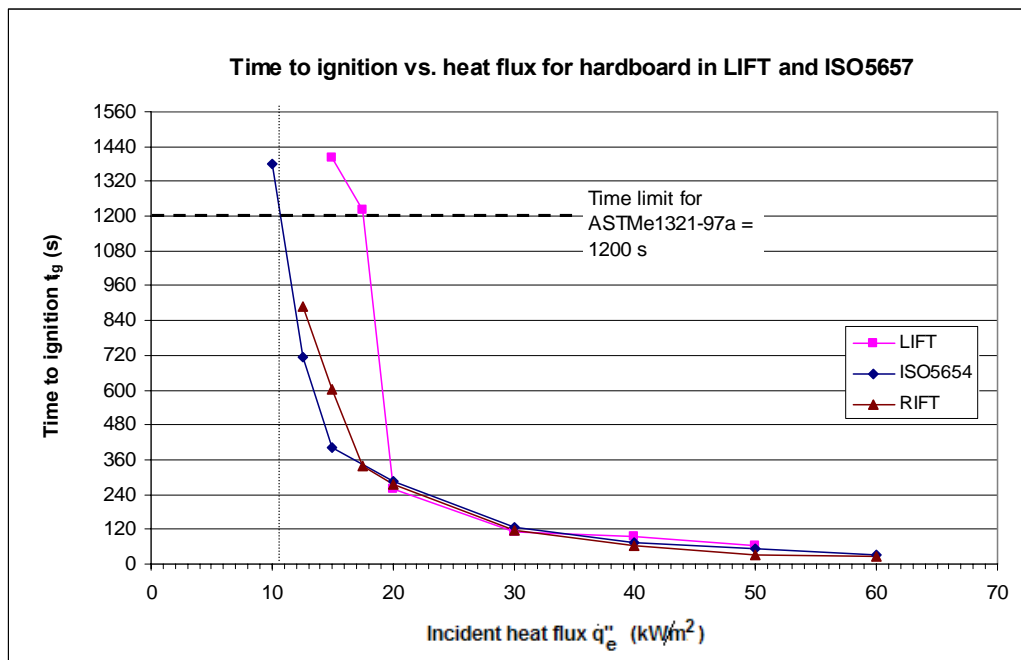


Figure 79: Time to ignition of hardboard

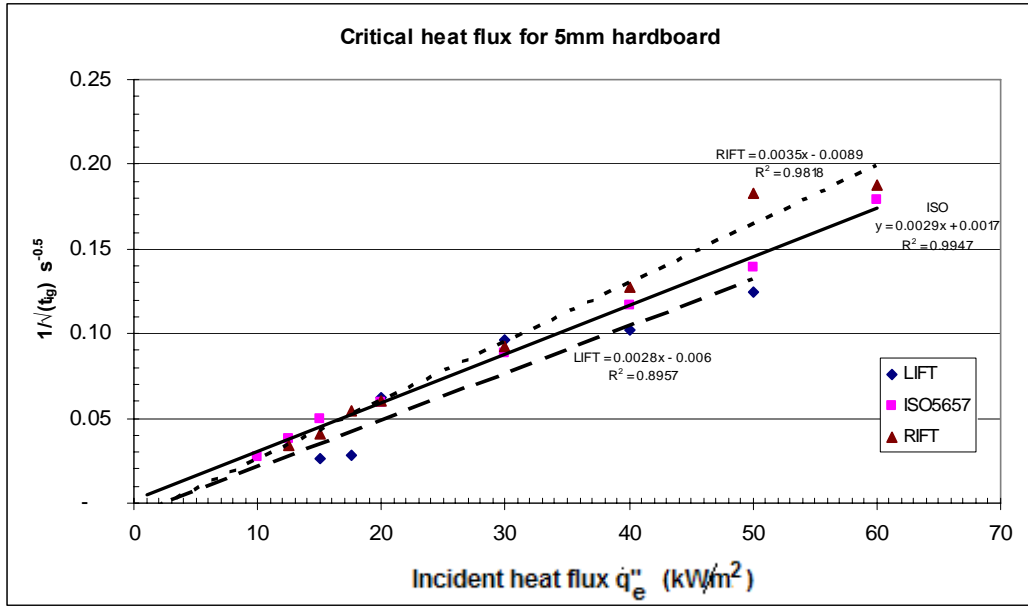


Figure 80: Critical heat flux for hardboard

The ignition parameter (Figure 81) shows considerable spread between the LIFT and ISO ignition results. The calculated preheat time t^* from the ISO 5657 ignition tests of 944 seconds is unrealistically long, as the material chars and collapses before this time can be achieved in the flame spread test. The ignition test conducted in the RIFT gave a preheat time of 977 seconds, compared with the LIFT calculated preheating time of 375s.

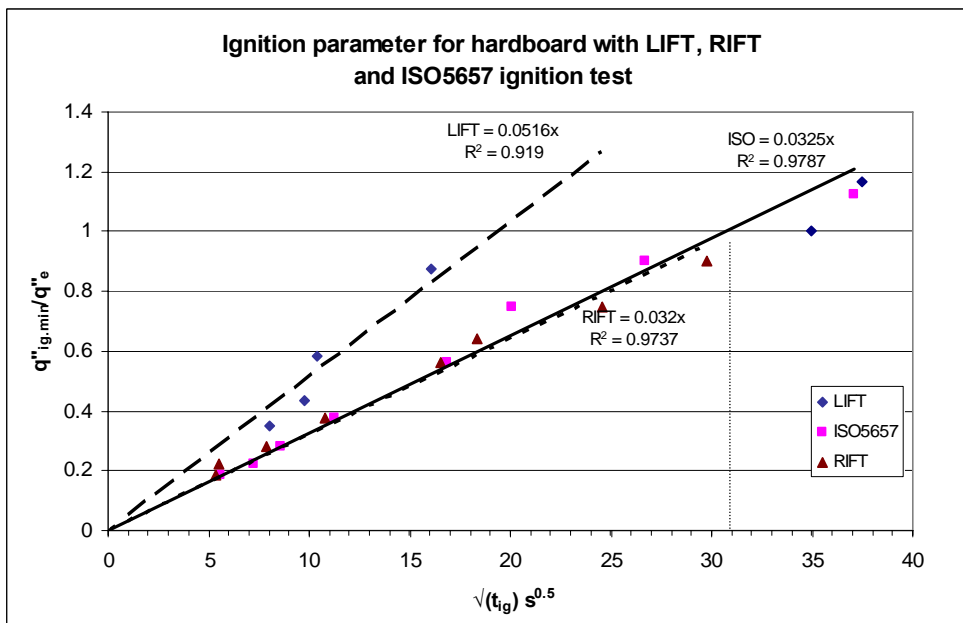


Figure 81: Ignition parameters for hardboard

8.4.2 Flame spread of hardboard

Flame spread of hardboard in the RIFT

Five repeat runs were conducted with hardboard in the RIFT, and they produced consistent flame spread results between runs in the RIFT and LIFT (Figure 83 and Figure 86), in spite of the behaviour of the material during preheating and burning. The material cracks behind the flame front area (Figure 82) which allows the pyrolised material to open and potentially allow flames to the rear of the sample.

With low preheat times, the area of the flame front appears to be unaffected until after the flame has passed and it does not appear to affect the flame spread correlation (Figure 85). The correlation is less accurate with more scatter when the material is given the full preheat time (Figure 87), possibly due to both the material cracking and increasing thermal penetration of the material, making the assumption that the material is thermally thick less valid.

A particular problem is the long preheat time dictated by the RIFT and ISO 5657 ignition results and the calculated ignition parameter (Figure 81) was unobtainable in the RIFT, as the sample charred to such an extent that pieces of the sample fell out and the sample self ignited. The preheating time used was therefore the time calculated from the LIFT ignition tests.

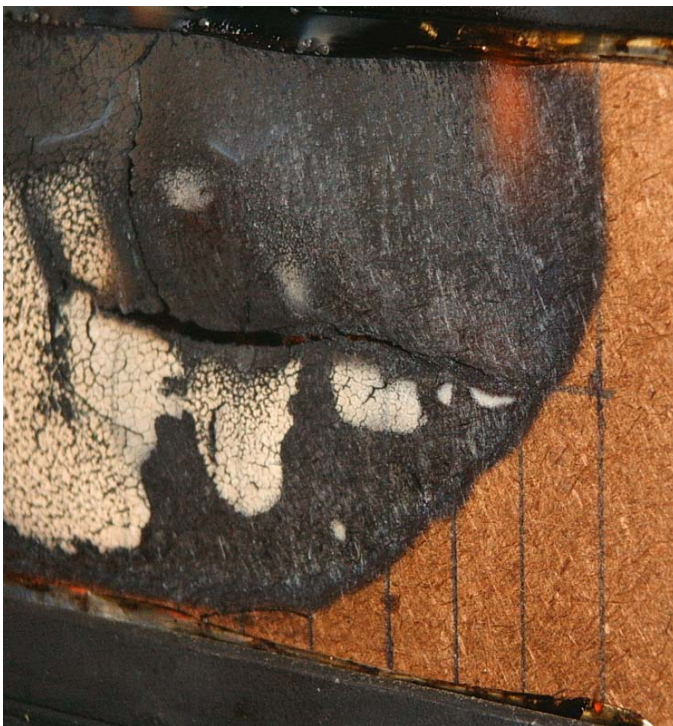


Figure 82: Cracking behind the flame front on hardboard

The consistent flame spread performance during the initial part of the flame spread test gives a good correlation result (Figure 85), with less data scatter for low preheat times, unlike the other products tested; where the data scatter is greater with a low preheat time. The data scatter in the correlation also increases significantly at the end of the flame spread test, possibly due to thermal penetration, and the material cracking and flames getting behind the sample.

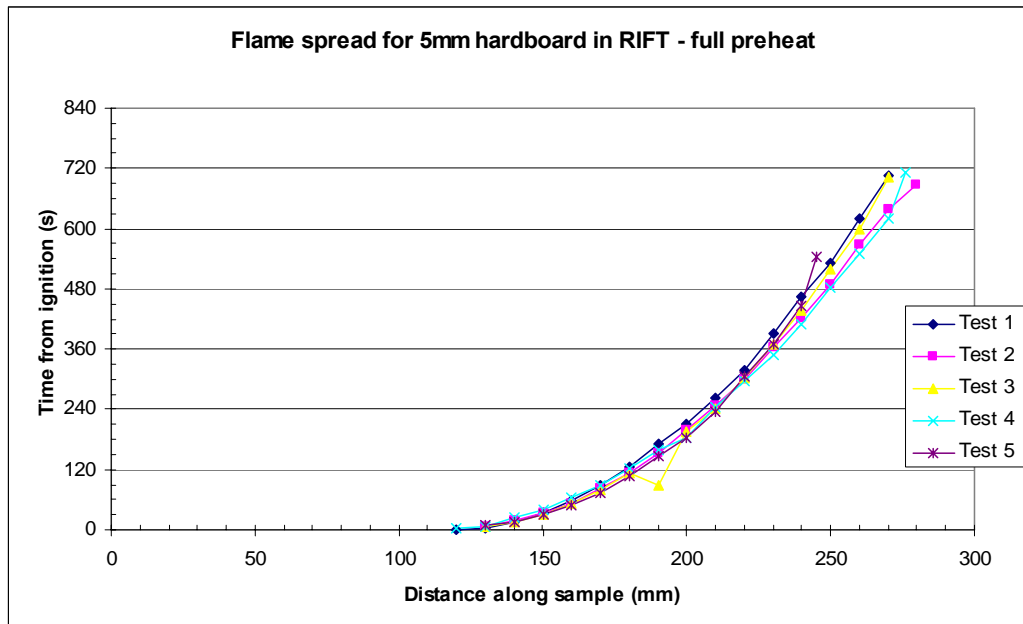


Figure 83: Flame spread of hardboard in RIFT – full preheat time

Comparing the flame spread for the different preheating times shows the expected behaviour, where the preheated sample has a higher flame spread rate (Figure 84).

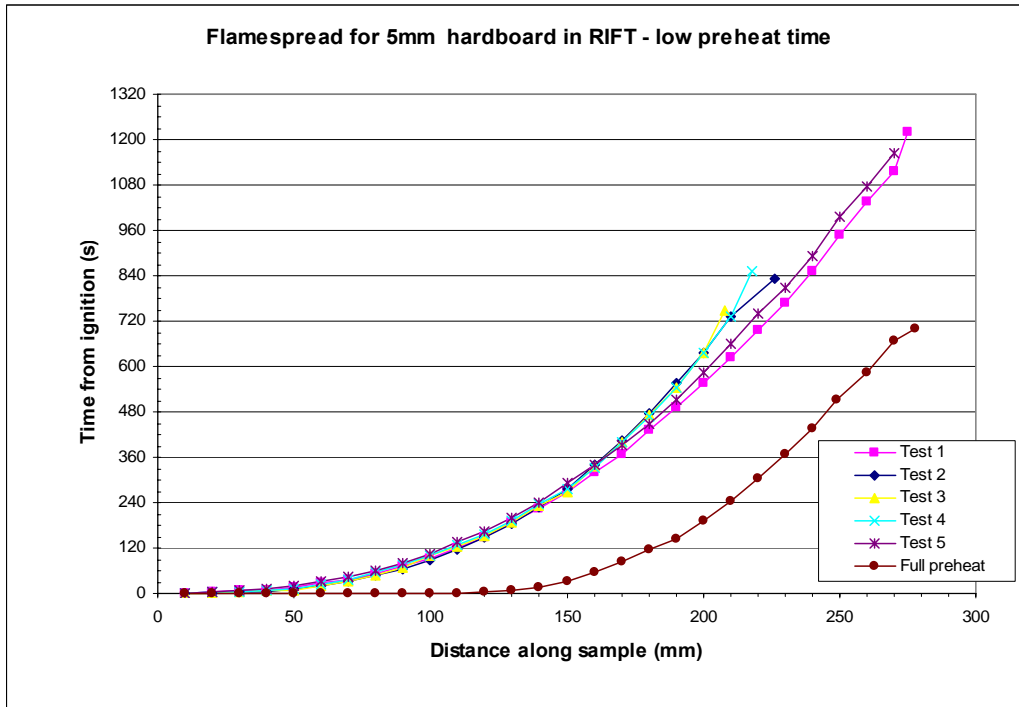


Figure 84: Flame spread for hardboard in RIFT – low preheat time

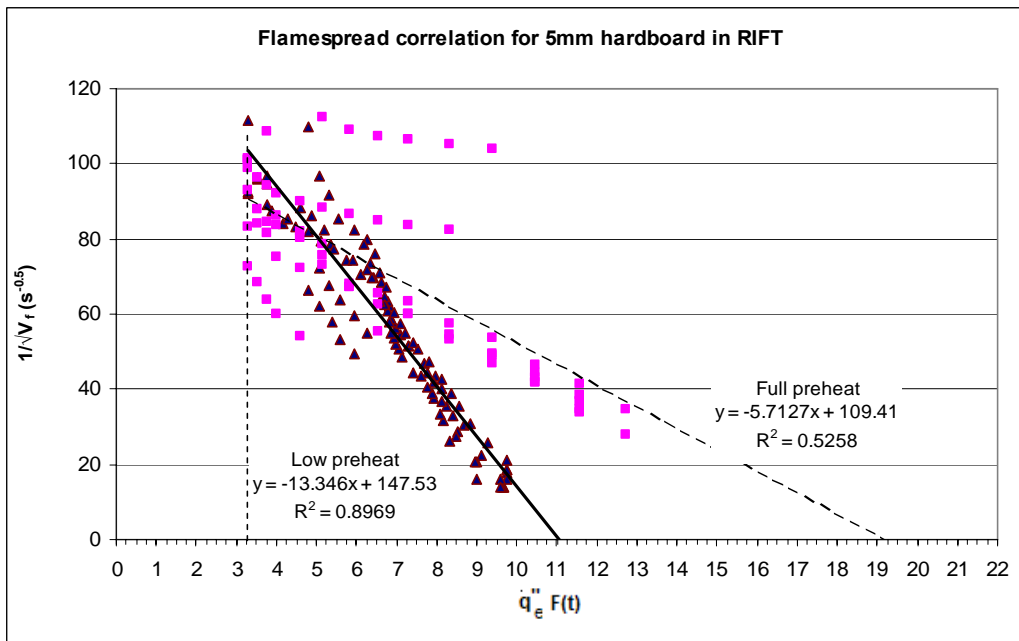


Figure 85: Flame spread correlation for hardboard in RIFT

The flame spread correlation for the RIFT with a full preheat period is compared to the results from the LIFT in Figure 87.

Flame spread for hardboard in the LIFT

The heat flux distribution for the LIFT tests is shown in Figure 75, and the resulting flame spread for hardboard in the RIFT is given in Figure 86.

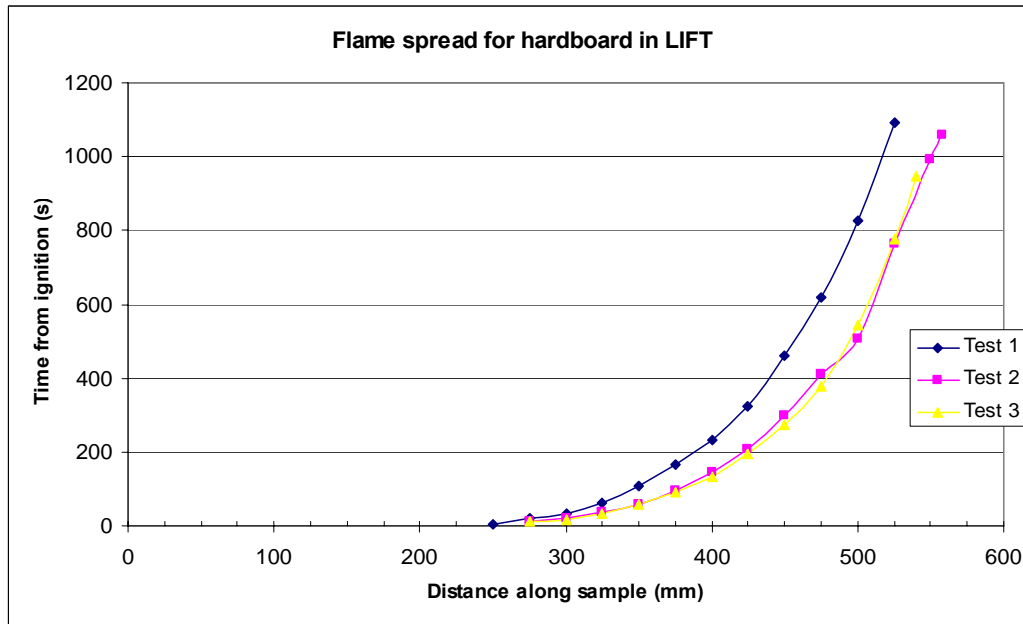


Figure 86: Flame spread of hardboard in LIFT

The results for the flame spread correlation from the RIFT closely match those for the LIFT (Figure 87), although the LIFT results have much less data scatter.

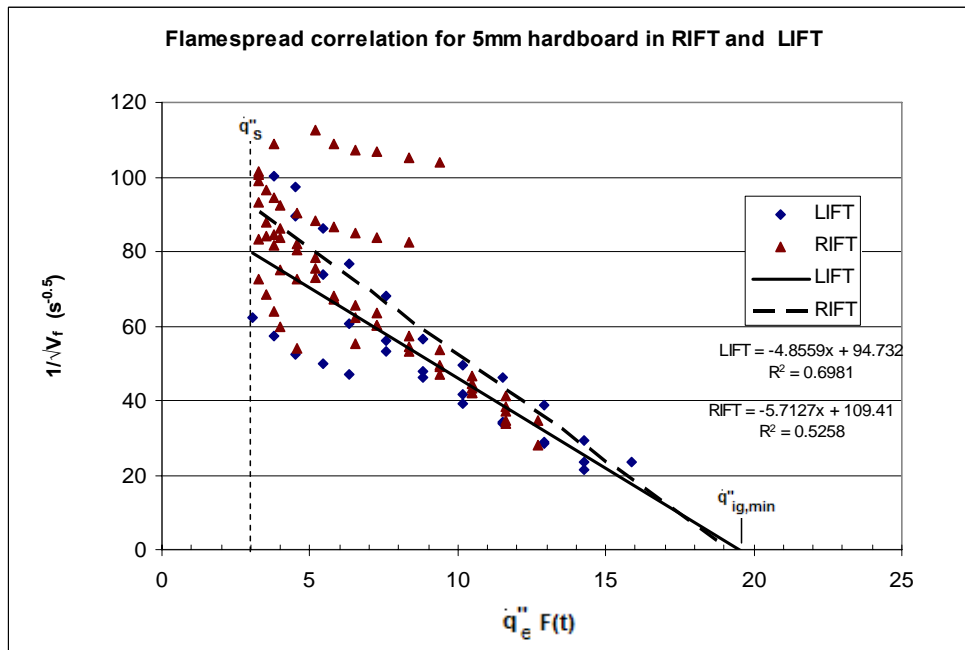


Figure 87: Flame spread correlation for hardboard in RIFT and LIFT

8.4.3 Melteca

The flame spread of two samples of melamine sheet products were compared in the RIFT to determine the variation between materials. One was a generic white Melteca faced board, using a MDF substrate, manufactured by Fletcher Wood Panels, and sold through builder's merchants and panel suppliers. The other was "Regal" brand shelving with a particle board substrate, sold as prefinished and clashed boards in hardware and builders supplies.

Only the Melteca- MDF sheet was tested in the LIFT, due to the amount of material available from the shelving product. The results from the RIFT tests and the Melteca-MDF results from the LIFT indicated that further testing in the LIFT of the Melteca – particle board material was not required due to the inconsistent flame spread results.

The ignition and flame spread behaviour of Melteca shown in Figure 88 is typical. The facing material starts to bubble at relatively low heat fluxes, insulating the substrate material. The flame front only progresses as the facing peels off or the bubbles split, allowing the pyrolised substrate to escape, and this gives erratic flame spread rates and ignition times.



Figure 88: Flame spread behaviour of Melteca faced board

8.4.4 Ignition of Melteca faced boards

The addition of the melamine (Melteca) facing affects the ignition and hence the flame spread of the samples. The facing board bubbles and chars at lower flux levels than the underlying material, thus insulating the underlying substrate, however it does not ignite easily. The substrate pyrolyzes and as the surface bubbles split, the gas escapes and can ignite. As a result, at low flux levels, the ignition time can become erratic. This behaviour also affects the flame spread, giving erratic flame spread results.

The insulating property of the facing material is apparent when comparing the ignition flux to that of the bare substrate material.

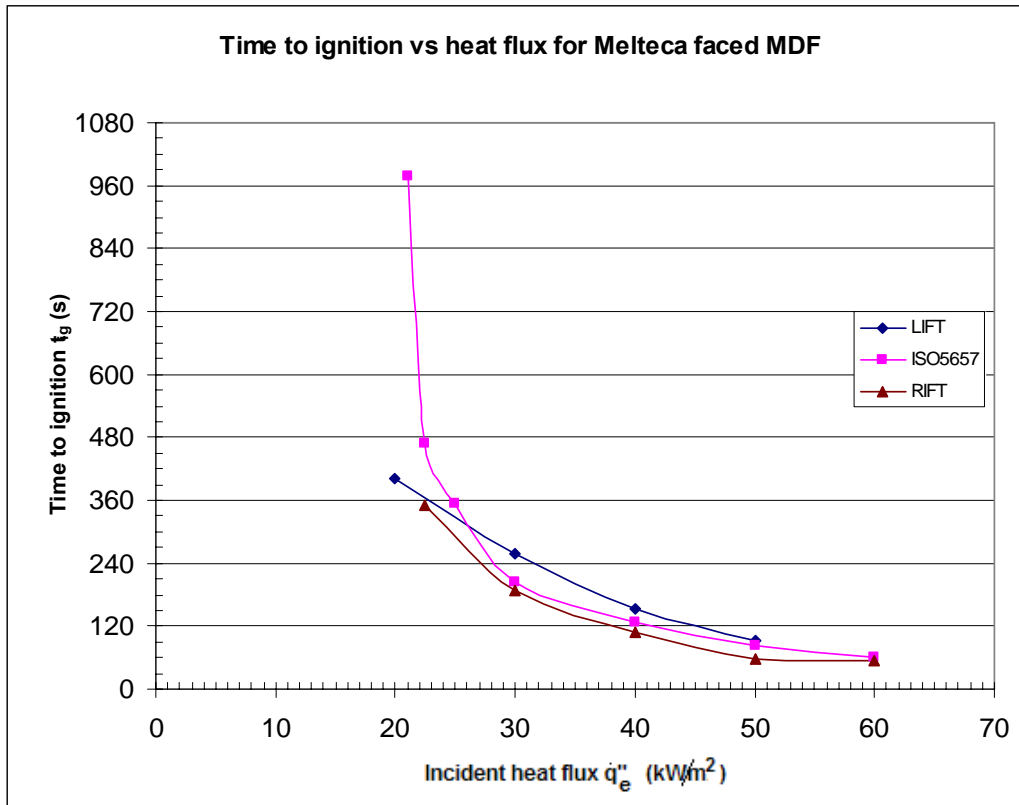


Figure 89: Time to ignition vs. heat flux of Melteca/MDF board

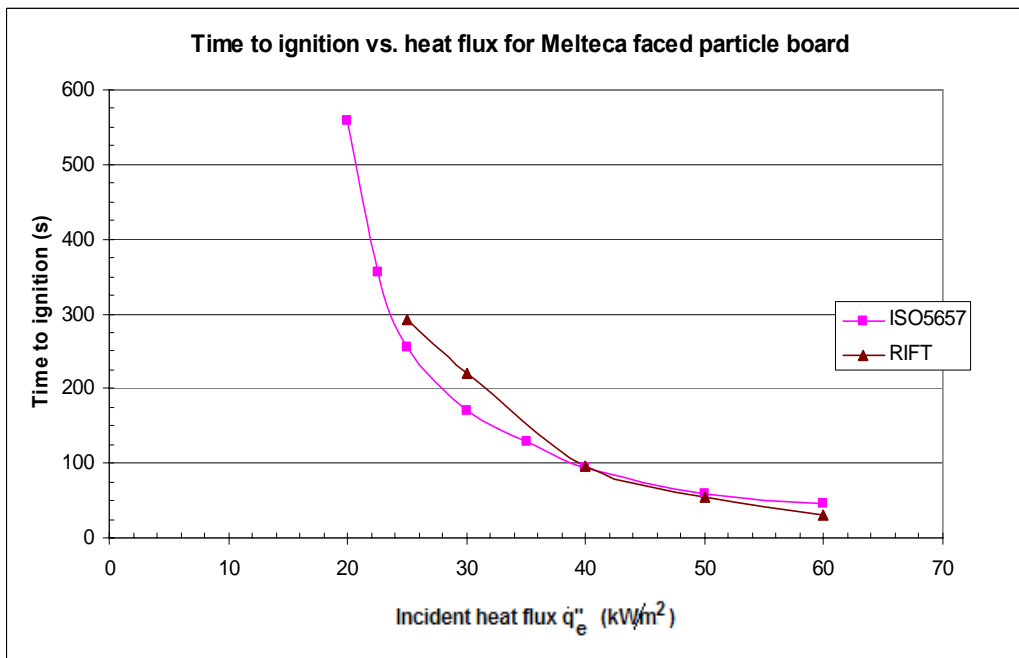


Figure 90: Time to ignition for Melteca faced particle board

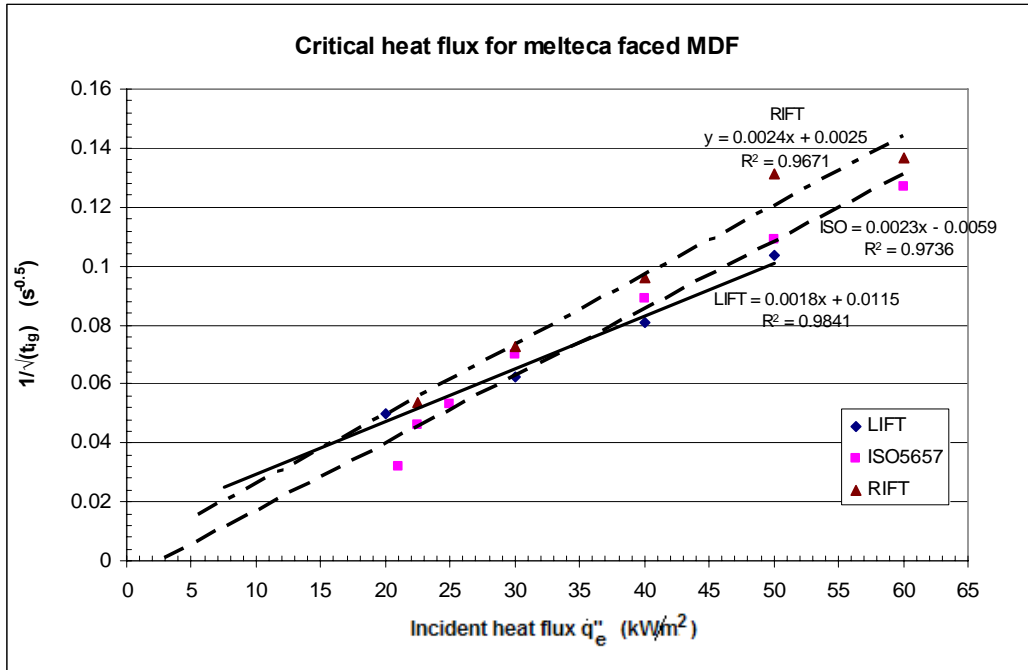


Figure 91: Critical ignition flux for Melteca faced MDF

The results are given in Appendix 3.

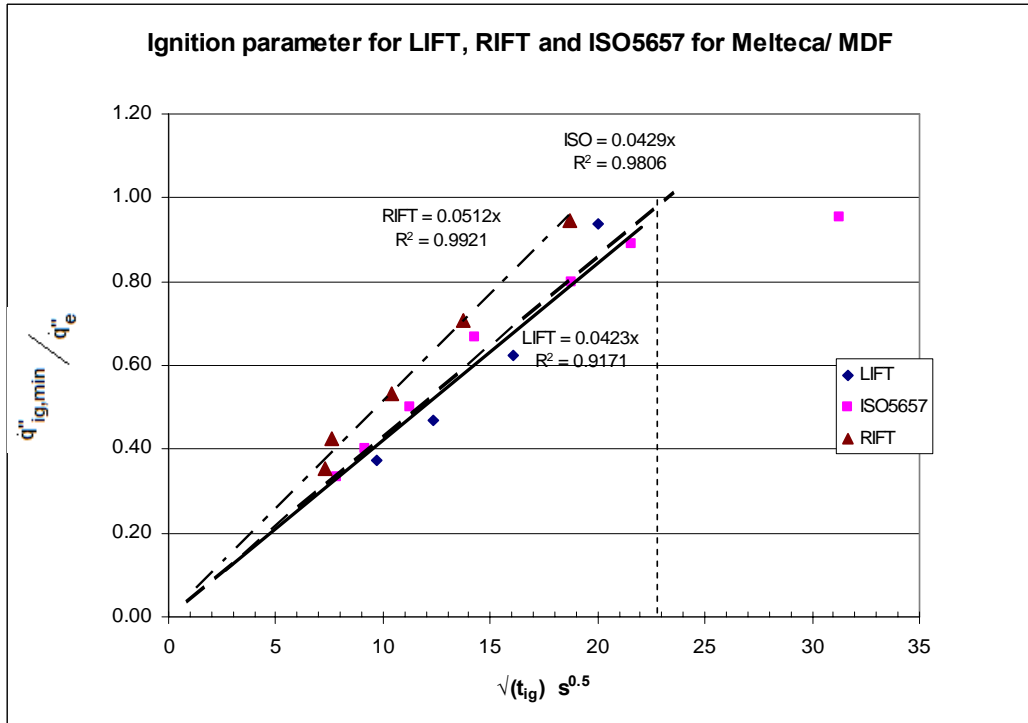


Figure 92: Ignition parameter for Melteca/ MDF board

Comparison of ignition results between two substrate materials

Comparing the time to ignition of the two Melteca boards with the different substrate materials (Figure 93) shows that the particle board based material ignited faster than the MDF based board, and this is reflected in the flame spread rate, as discussed in the following section.

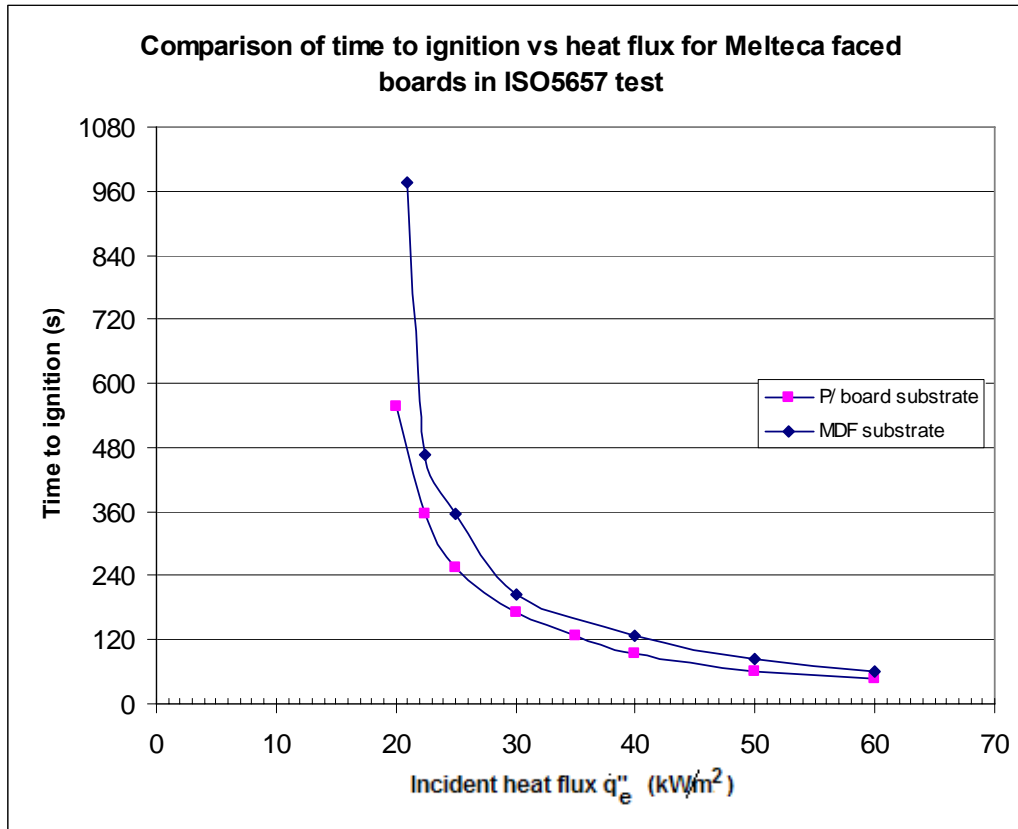


Figure 93: Time to ignition vs. heat flux for Melteca faced boards

8.4.5 Flame spread of Melteca

Flame spread in RIFT

Six samples of each material were tested in the RIFT, both with a preheating period and with no preheating prior to ignition. It was not possible to derive a flame spread correlation for Melteca faced boards in the RIFT with no preheating, as there was no linearity and it was not possible to fit a line to the data. The effect of the substrate can be seen in Figure 94, where the MDF based board has a slower flame spread rate than the particle board based material, reflecting the ignition results.

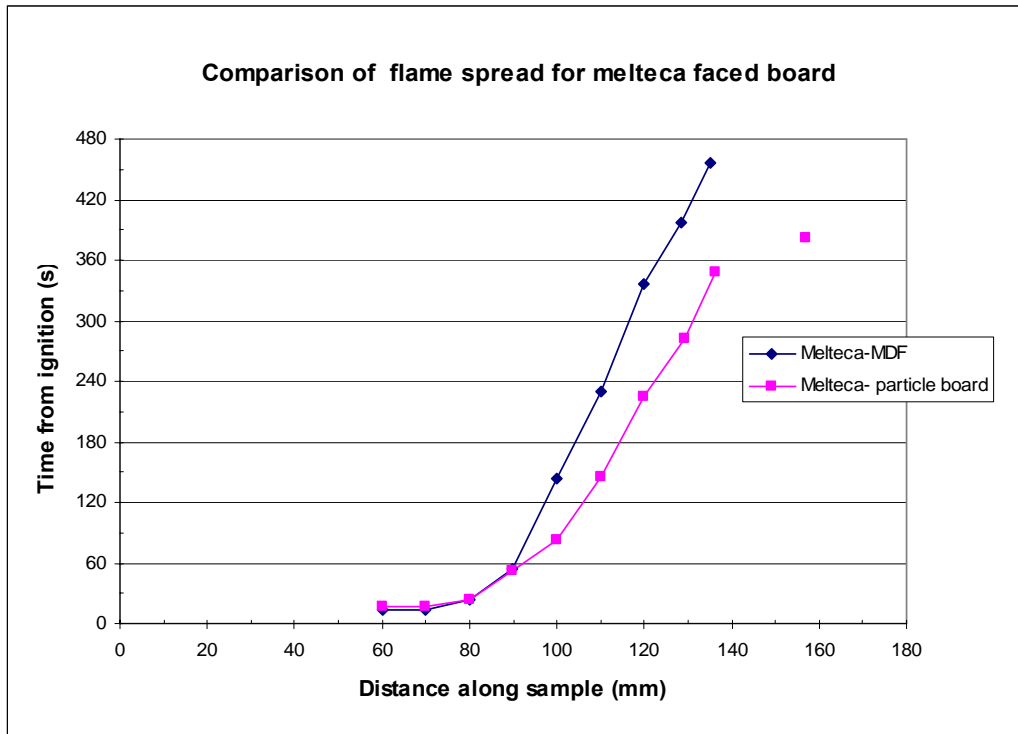


Figure 94: Flame spread of Melteca faced boards in RIFT

The difference between the two board types is greater than that of the substrate alone, indicating that the surface material is having a greater effect, as seen in Figure 95, where the time to a point on the sample for Melteca faced boards (MDF and particle board substrate) and for the MDF and particle board (Pynefloor) alone. This could be a factor of the manufacturer of the boards, as the facing material was not controlled and the boards come from different manufacturers.

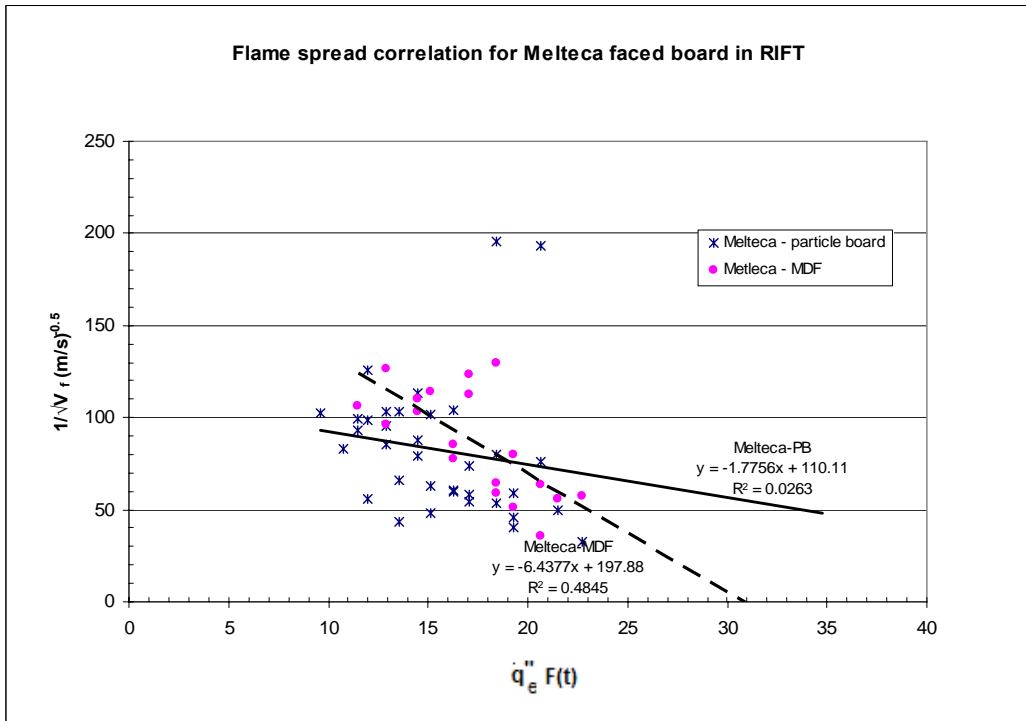


Figure 96: Flame spread correlation for Melteca faced board in RIFT

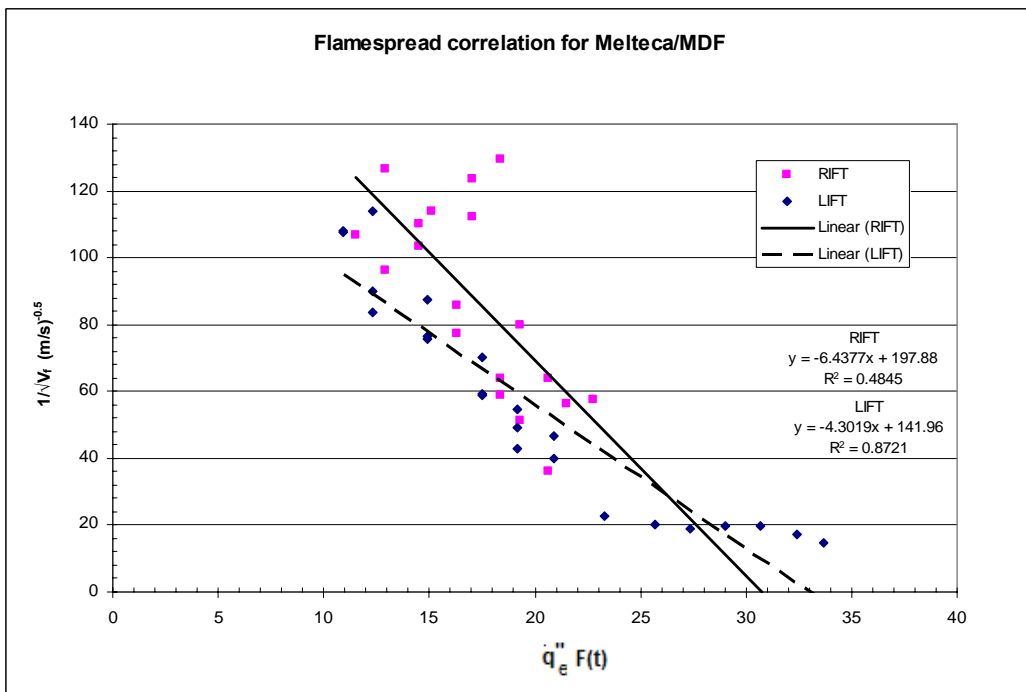


Figure 97: Flame spread correlation for Melteca/ MDF

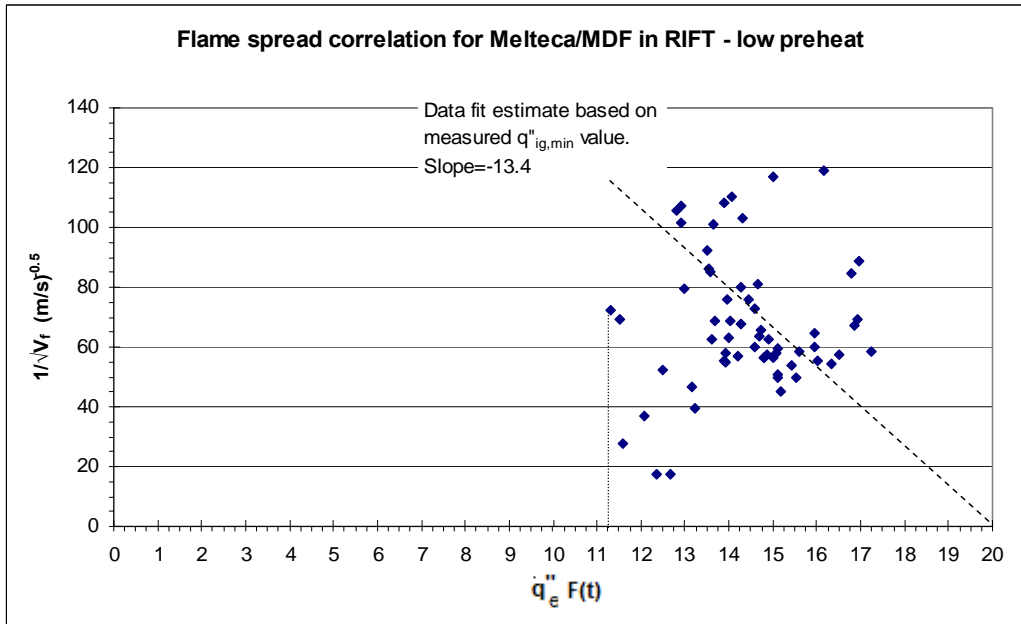


Figure 98: Flame spread correlation for Melteca-MDF with a low preheating period

Flame spread of Melteca faced boards in LIFT

The heat flux profile used in the LIFT test of Melteca- MDF is shown in Figure 99. The flame spread results for Melteca-MDF (Figure 97 and Figure 100) shows less data scatter than the same material in the RIFT. This is due to the larger scale of the LIFT test, making the variation due to the burning behaviour of the facing material less significant.

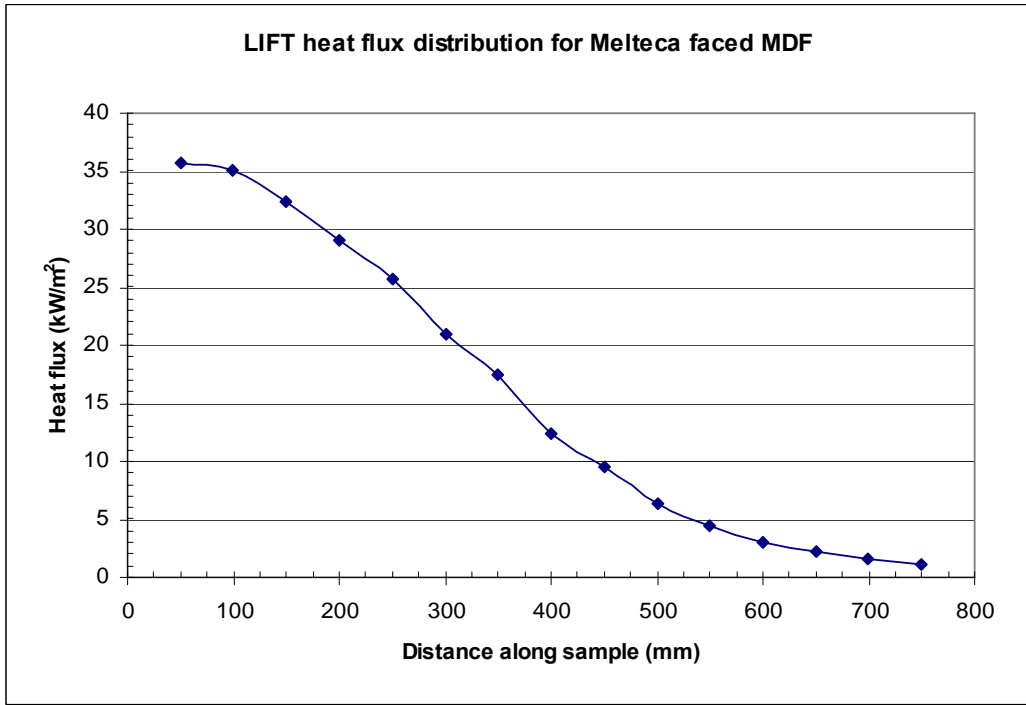


Figure 99: LIFT heat flux profile for Melteca faced MDF flame spread test

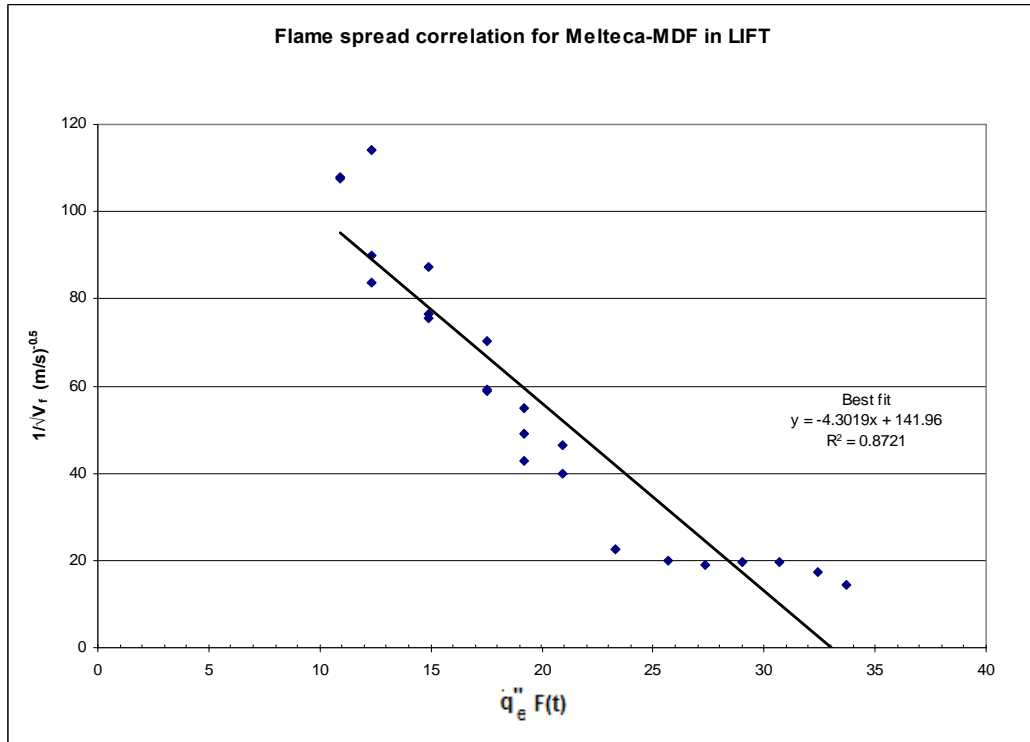


Figure 100: Flame spread correlation for Melteca-MDF in LIFT

9 Material test results for natural timbers

Natural timbers showed greater variation in the results between tests of identical materials than for manufactured boards, due to the greater variation in the material from the grain, knots or other features in the timber. The flame spread rates along the sample are generally higher for natural timbers than for the manufactured boards.

9.1 New Zealand Beech

9.1.1 Ignition of Beech

The time to ignition for New Zealand Beech is shown in Figure 101, which shows greater variation in the time to ignition, than the other timber products (e.g. particle board Figure 54 and Figure 55) especially at low flux levels,

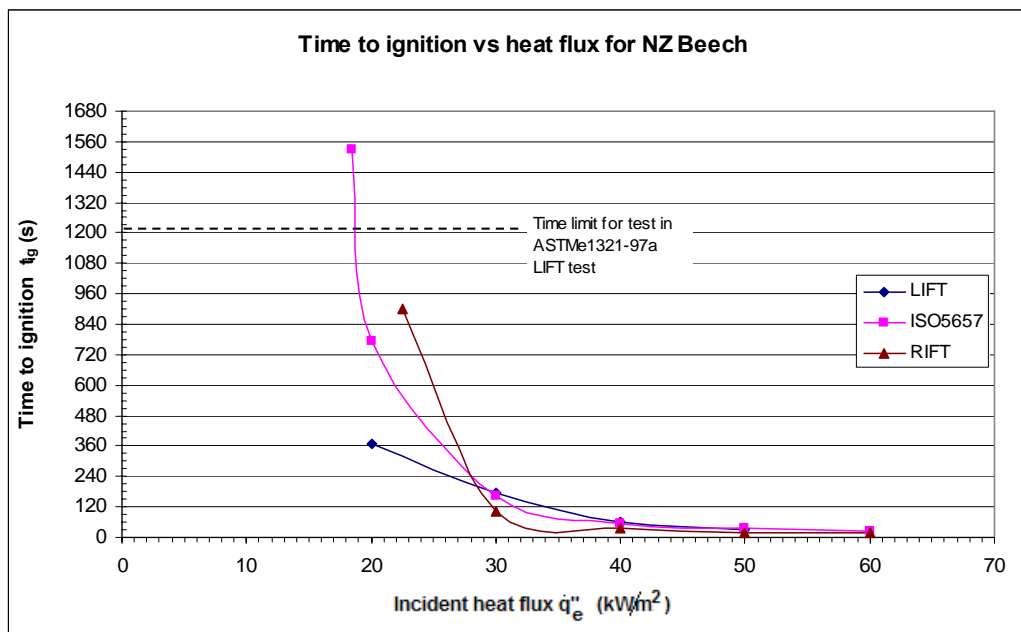


Figure 101: Time to ignition vs. heat flux for NZ Beech

The ignition parameter from ASTM E 1321-97a is shown below in Figure 102. While the ignition parameter results for the ISO 5657 and LIFT tests were similar at $0.050 \text{ s}^{0.5}$ for the ISO 5657 results, and $0.053 \text{ s}^{0.5}$ for the LIFT, the RIFT showed a wide

variation, due to the higher minimum ignition flux and shorter times to ignition than produced by the other methods.

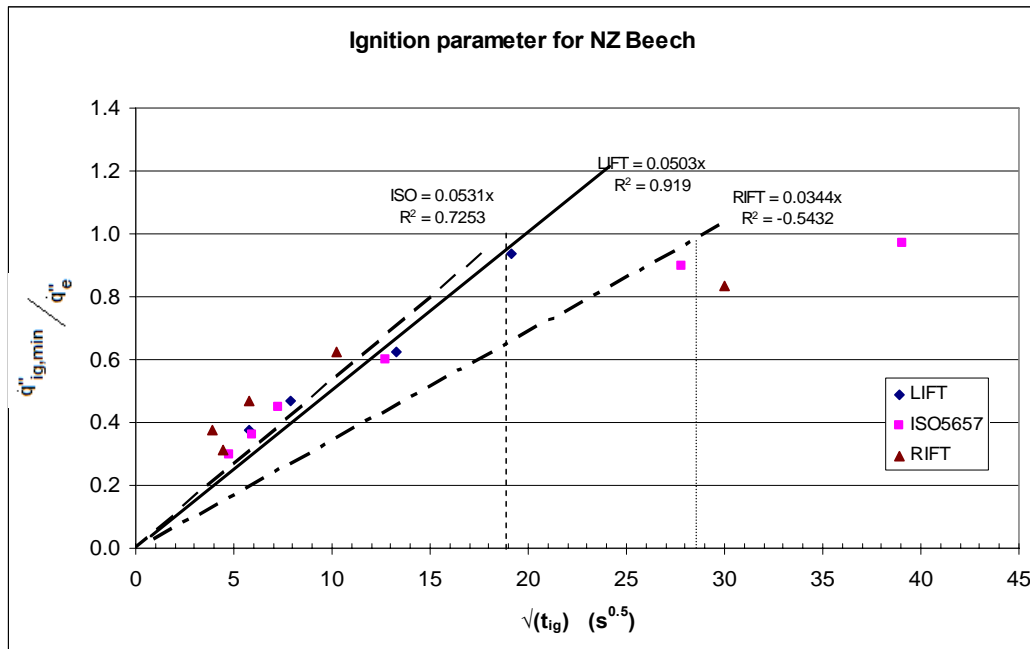


Figure 102: Ignition parameter for Beech

The ISO 5657 and LIFT gave similar results for the critical ignition flux (Figure 103) and there is greater variation for the critical flux calculated from the RIFT ignition test.

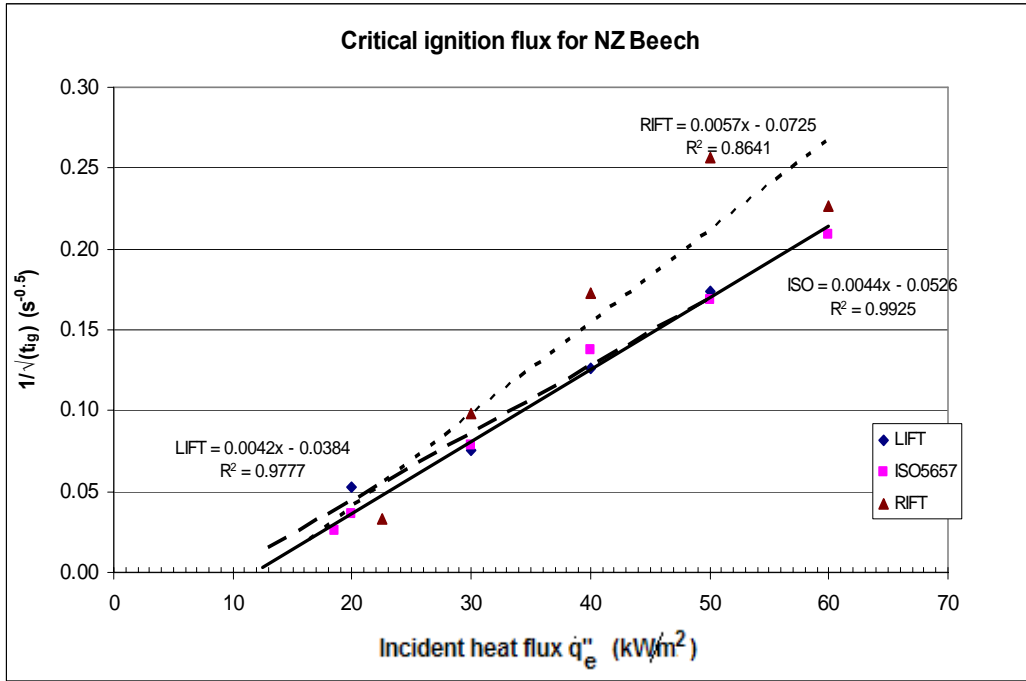


Figure 103: Critical ignition flux for NZ Beech

9.1.2 Flame spread of Beech

Flame spread of NZ Beech in the RIFT

The flame spread showed wide variations between runs in the RIFT, whether or not it was preheated prior to ignition (Figure 104 and Figure 105) and the flame spread in the RIFT was less consistent than in the LIFT (Figure 108). The low preheat time was 55 seconds, against a full preheat time for the RIFT of 844 seconds, and 395 seconds for the LIFT, using the ignition data from the LIFT ignition tests for this material.

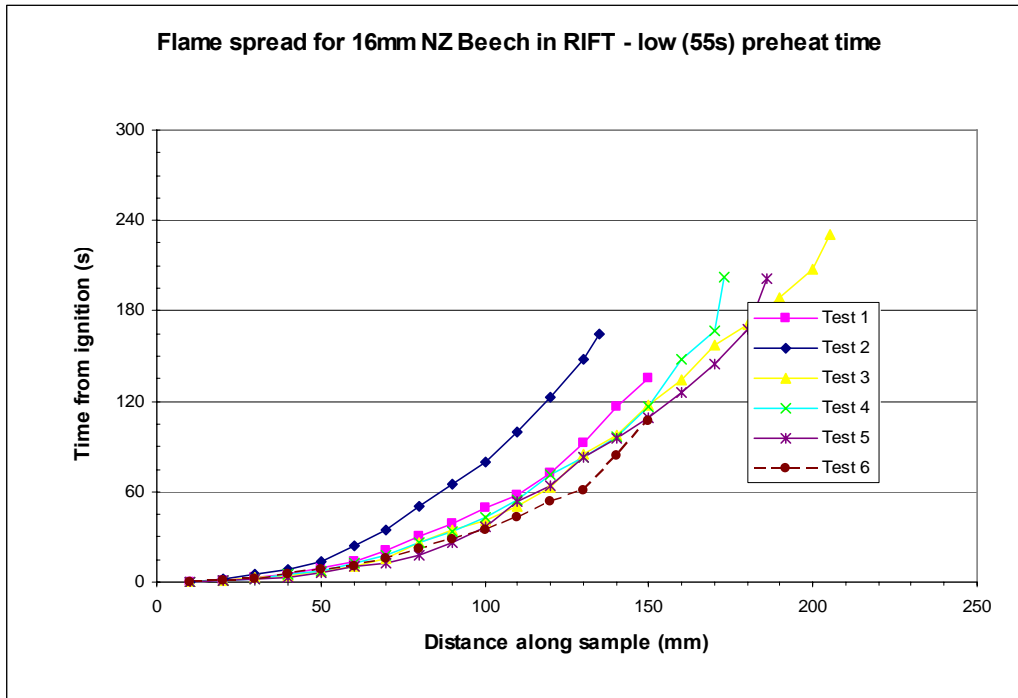


Figure 104: Flame spread of Beech in RIFT with 55 second preheating period

The extent of flame spread is less if the material is not preheated and hence the experimental value for the minimum heat flux for flame spread is higher than for a fully preheated sample. As can be seen from time to reach each point on the sample in Figure 104, the rate of flame spread was very rapid in comparison to the other materials tested, indicating that the flame spread was faster than the surface of the material could reach the minimum ignition temperature, hence the extent of flame spread is less when the material has not been preheated fully prior to ignition.

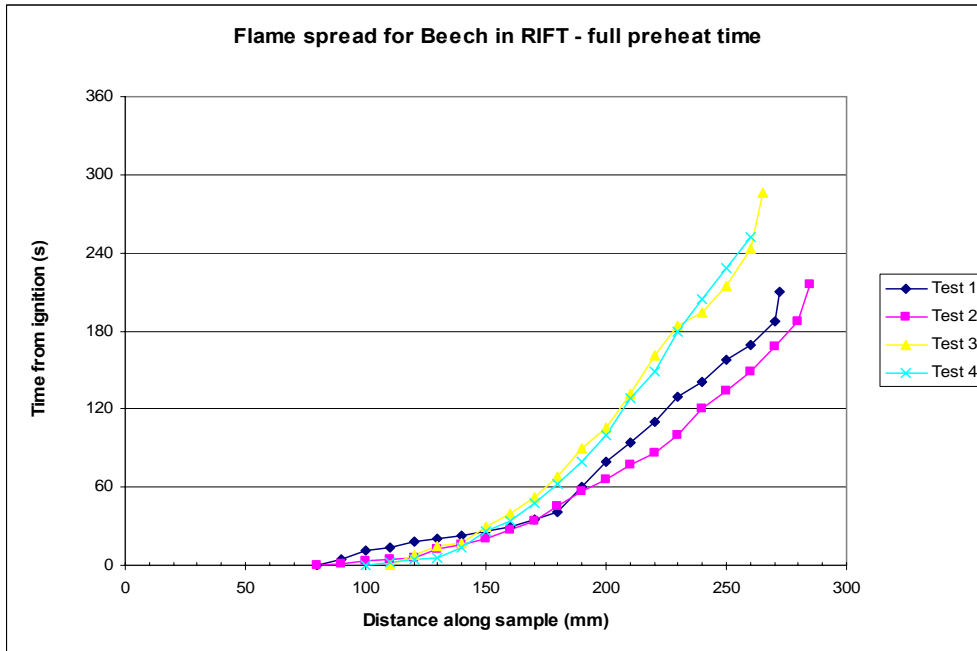


Figure 105: Flame spread for Beech in RIFT with full preheat

The effect that the ignition data has on the flame correlation is shown in Figure 106, where the same flame velocity measurements are used, but with the “*b*” value and thermal equilibrium time “*t*^{*}” from the ignition tests in the RIFT and ISO 5657 ignition apparatus.

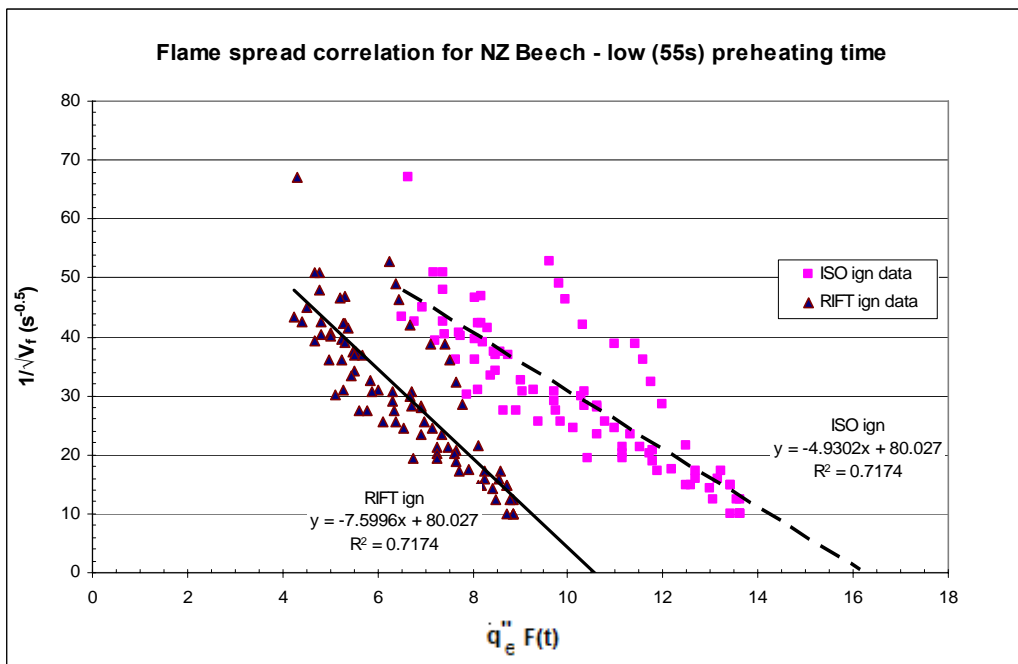


Figure 106: Flame spread correlation for NZ Beech in RIFT - low preheat time

The flame spread correlation for the RIFT with the full preheating period is compared with the LIFT in Figure 110.

Flame spread of NZ Beech in the LIFT

The heat flux profile used for the LIFT tests of NZ Beech is shown in Figure 107.

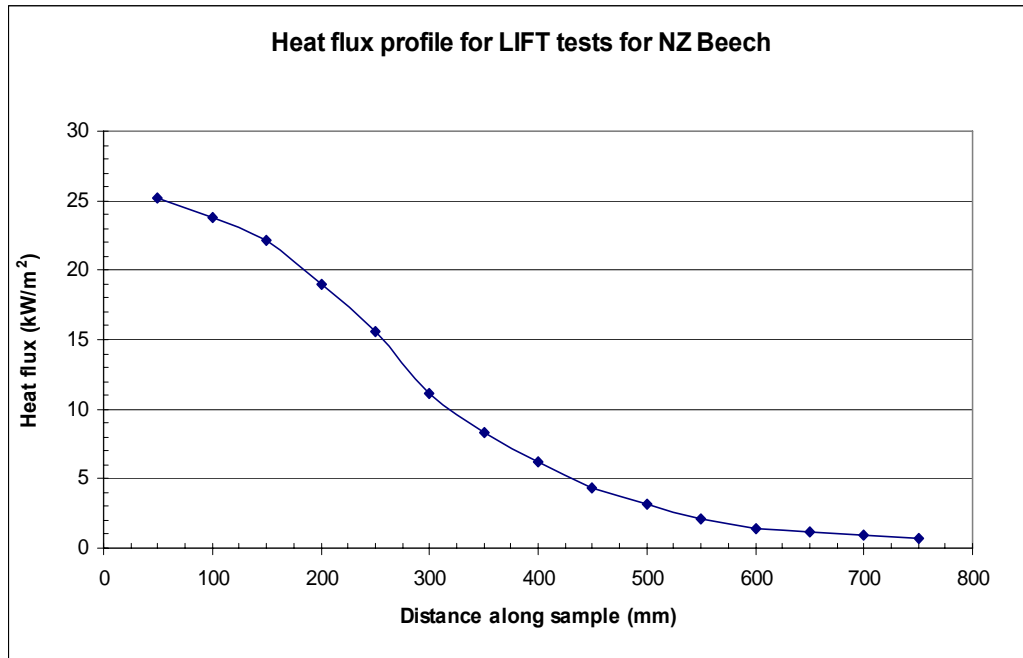


Figure 107: Heat flux profile for LIFT tests for NZ Beech

The flame spread along the sample (Figure 108) showed much less variation than for the same material in the RIFT (Figure 105).

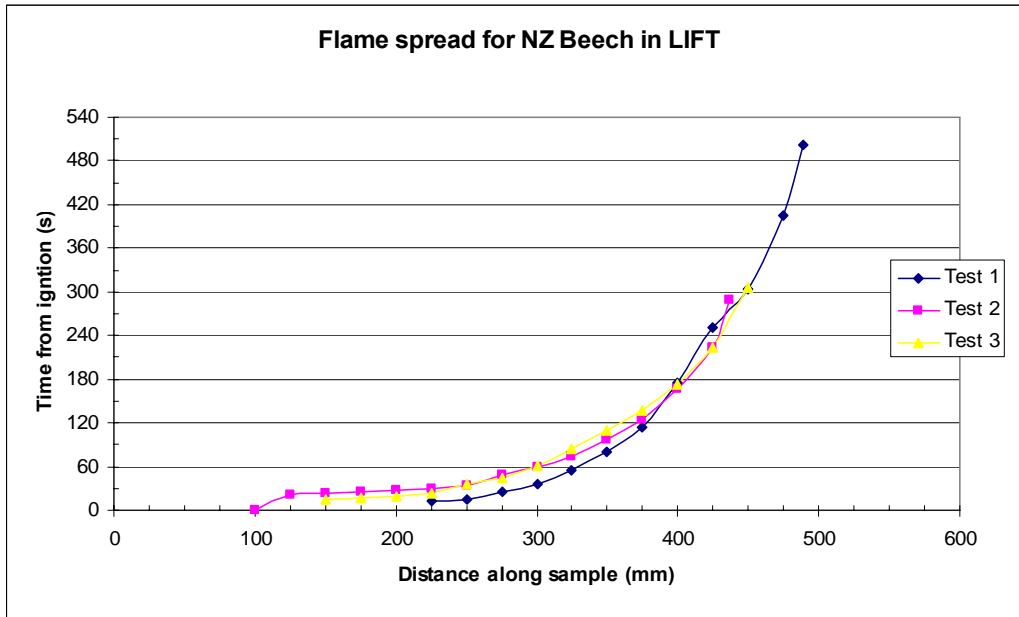


Figure 108: Flame spread for NZ Beech in LIFT

The resulting flame spread correlation, shown in Figure 109 shows some curvature in the fit of the data, indicating that the material may not have reached thermal equilibrium, despite being preheated to the time given by the ignition results.

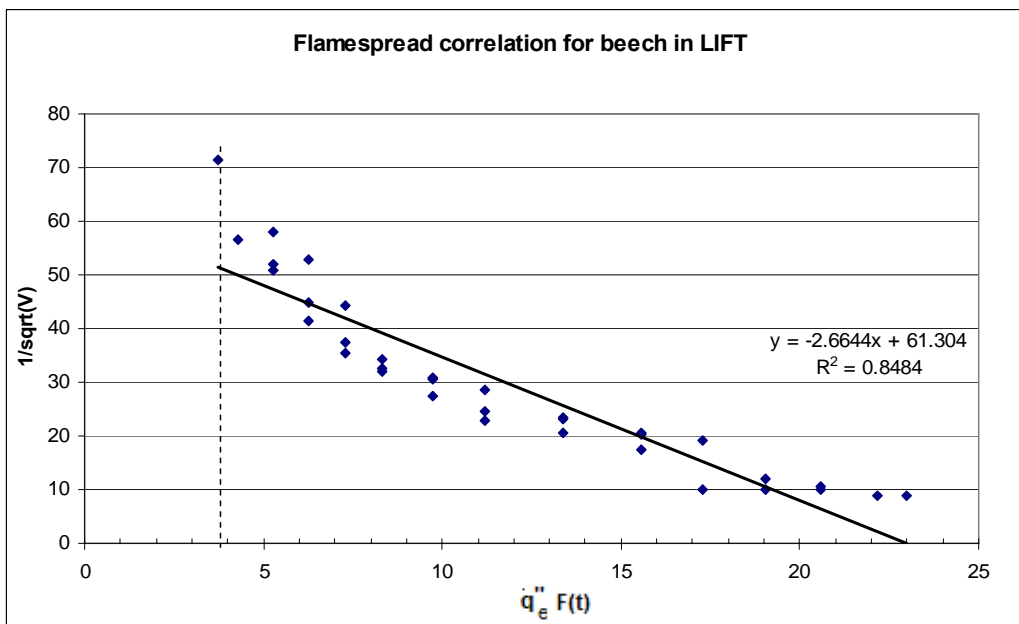


Figure 109: Flame spread correlation for NZ Beech in LIFT

The RIFT and LIFT gave similar results for the flame spread correlation (Figure 110) at 74.8 for the RIFT and 58.3 for the LIFT, although the RIFT has more scatter in the

data, shown by the lower R^2 value. The results for the correlated values for the minimum heat flux for flame spread and the minimum ignition flux are similar with both methods.

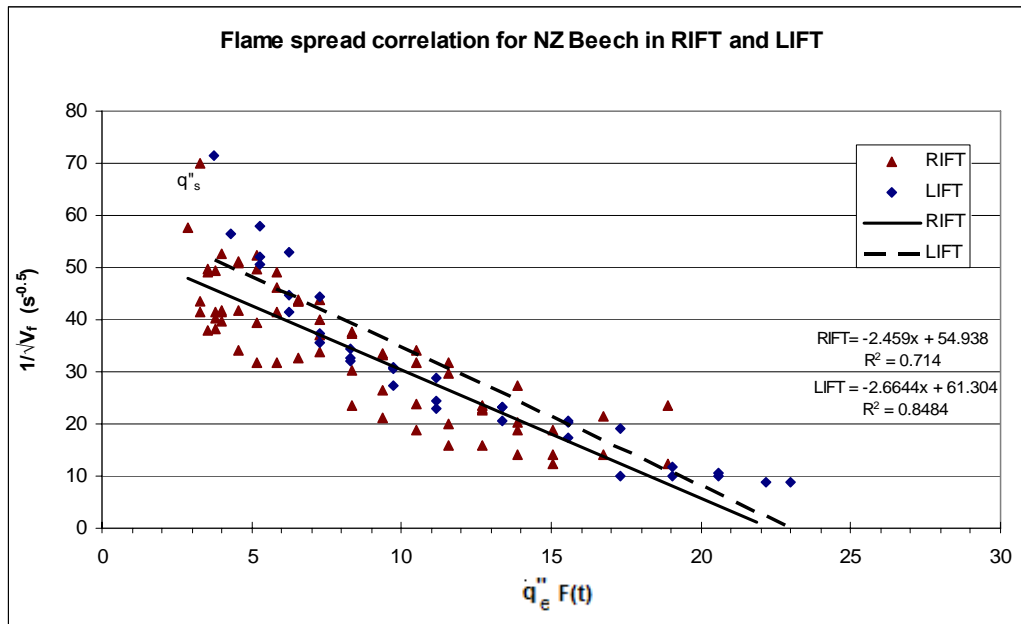


Figure 110: Flame spread correlation of Beech in RIFT and LIFT.

9.2 *Macrocarpa*

9.2.1 Ignition of Macrocarpa

The three ignition test methods produced similar results for Macrocarpa (Figure 111), with the LIFT having longer times to ignition at low heat flux levels.

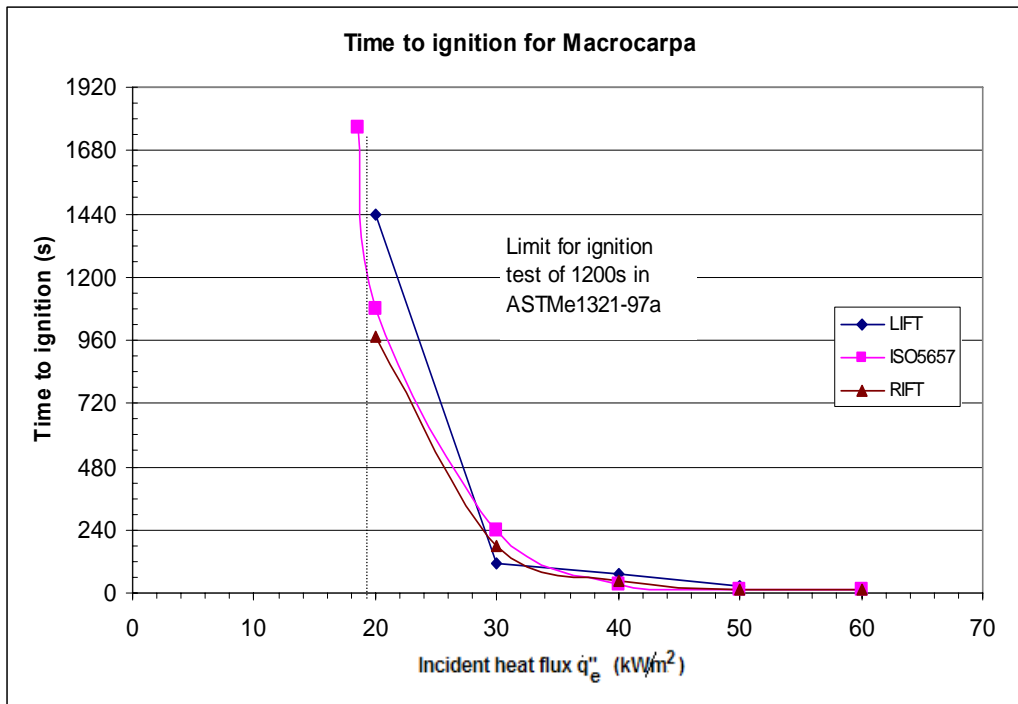


Figure 111: Time to ignition for Macrocarpa

The ignition parameter (Figure 112) and the critical ignition flux (Figure 113) show much more scatter in the data than the manufactured boards, such as MDF (Figure 46 and Figure 45) or particle board (Figure 56 - Figure 59).

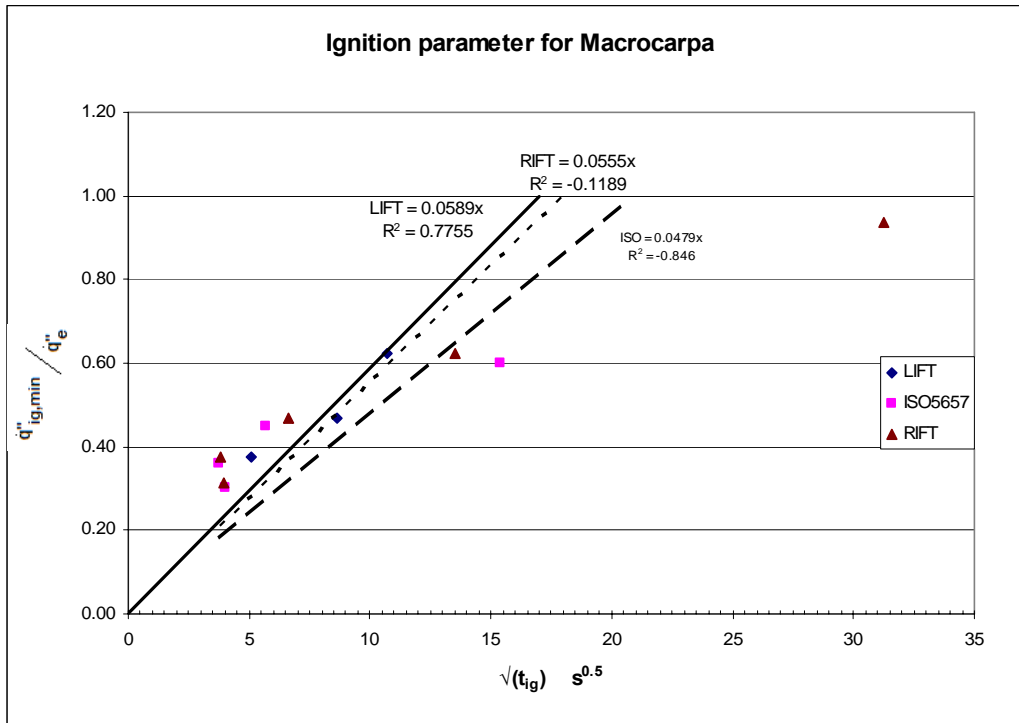


Figure 112: Ignition parameter for Macrocarpa

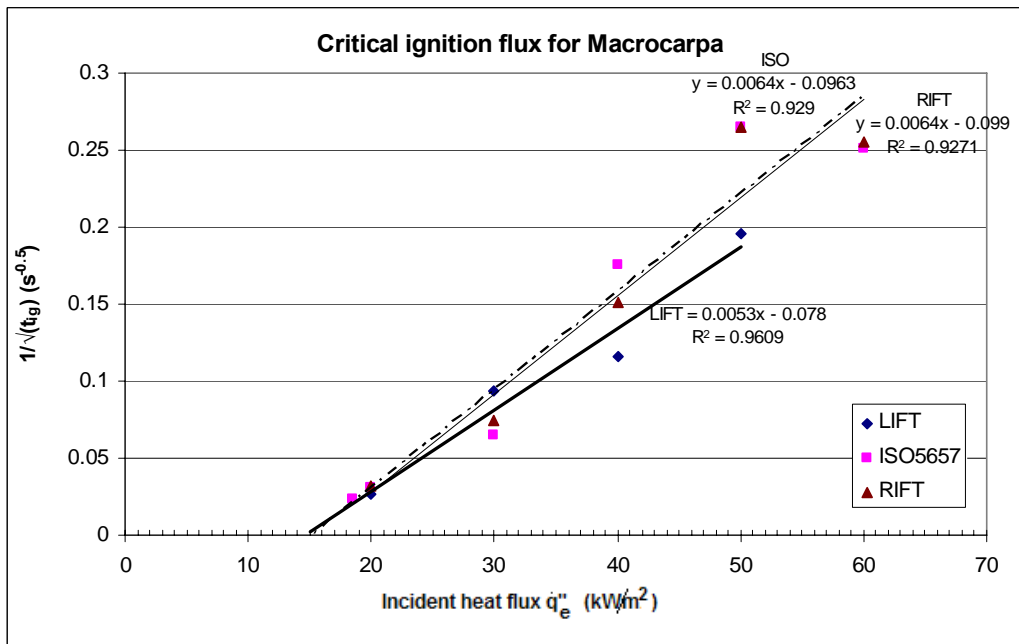


Figure 113: Critical heat flux for Macrocarpa

9.2.2 Flame spread of Macrocarpa

The resinous streaks in Macrocarpa can make the flame spread erratic, as the flame front can tend to follow a resin streak on the face of the timber, rather than spreading evenly over the face of the material. This gives more erratic flame spread than for a more consistent material, seen in the variation of the flame spread results between runs in Figure 115 and Figure 117.

The preheating time was 40 seconds for the low preheating tests, and 436 seconds for a full preheating time in the RIFT, based on the ISO 5657 ignition tests, and 288 seconds for the LIFT ignition tests

Flame spread in RIFT

The flame spread for Macrocarpa showed wide variation between tests of the same material under the same conditions (Figure 114 and Figure 115), particularly towards the end of the sample.

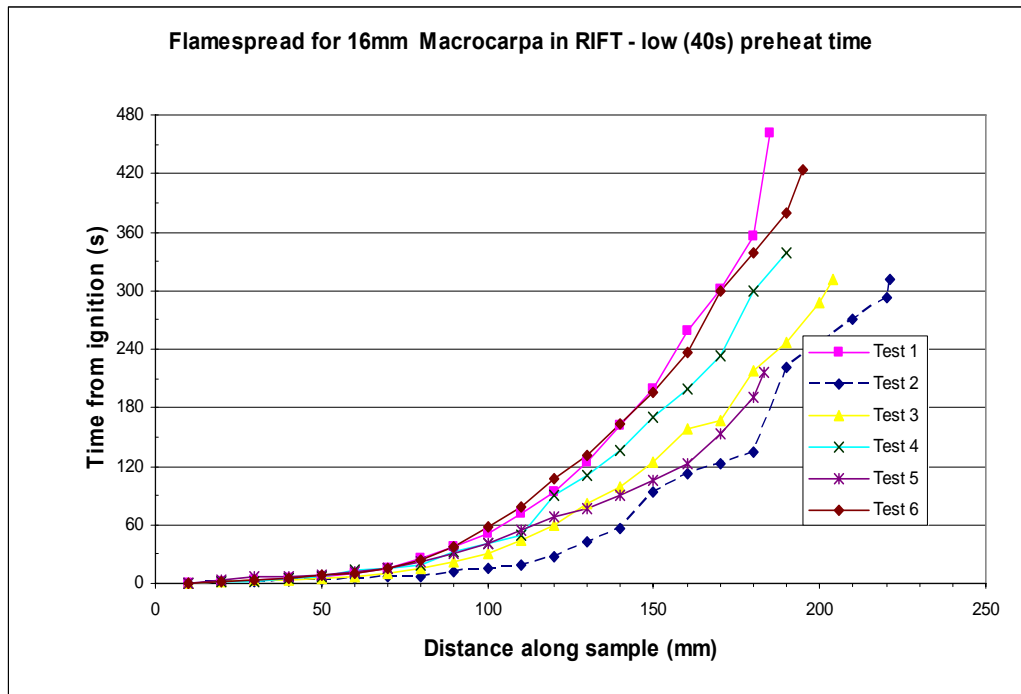


Figure 114: Flame spread of Macrocarpa in RIFT with low (40s) preheat time

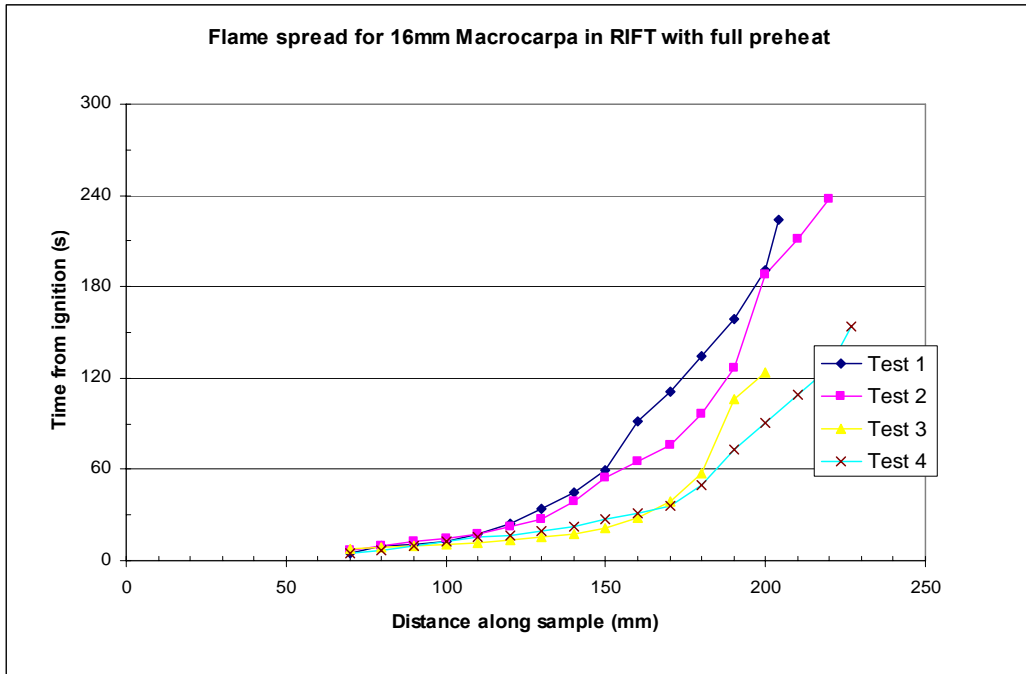


Figure 115: Flame spread of Macrocarpa in RIFT – full preheat of 436 seconds

The resulting flame spread correlation for the RIFT results shows a lot of data scatter and the linear fit is a relatively poor match (Figure 116). The fit of the data, shown by the R^2 values seen on the chart, improves with preheating the sample prior to ignition, but is still poor.

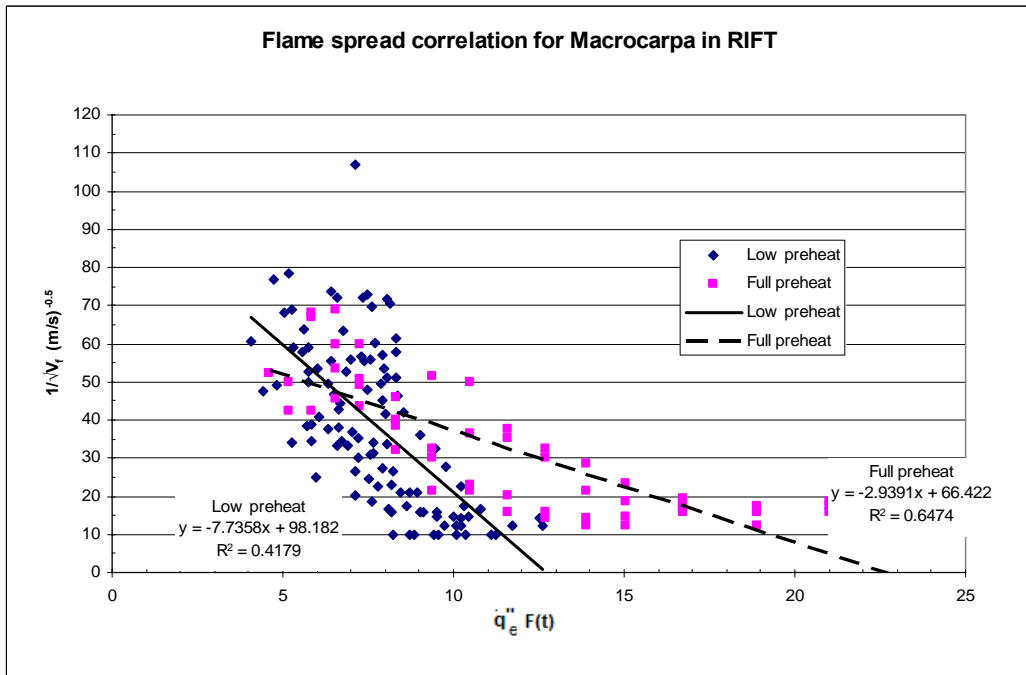


Figure 116: Flame spread correlation for Macrocarpa in RIFT

Flame spread of Macrocarpa in LIFT

The flame spread for Macrocarpa in the LIFT showed similar variation between tests to the samples in the RIFT.

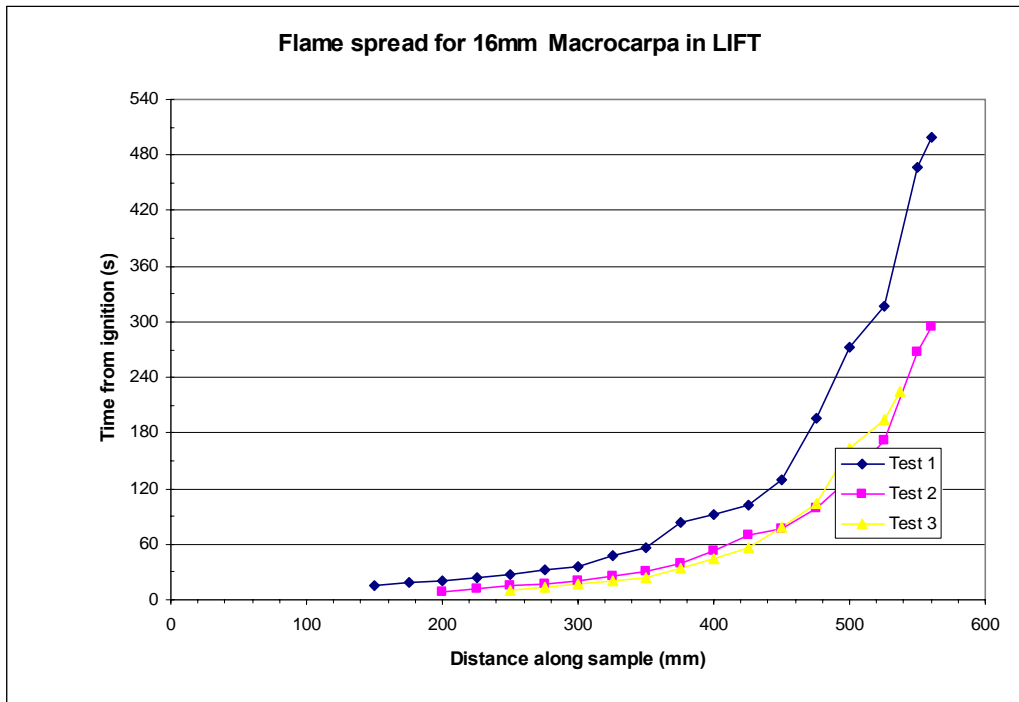


Figure 117: Flame spread for Macrocarpa in LIFT

The curve to the LIFT results in the flame spread correlation (Figure 118) indicates that the material was not preheated sufficiently, based on the work by Quintiere (1981), despite the preheating time coming from the LIFT ignition results.

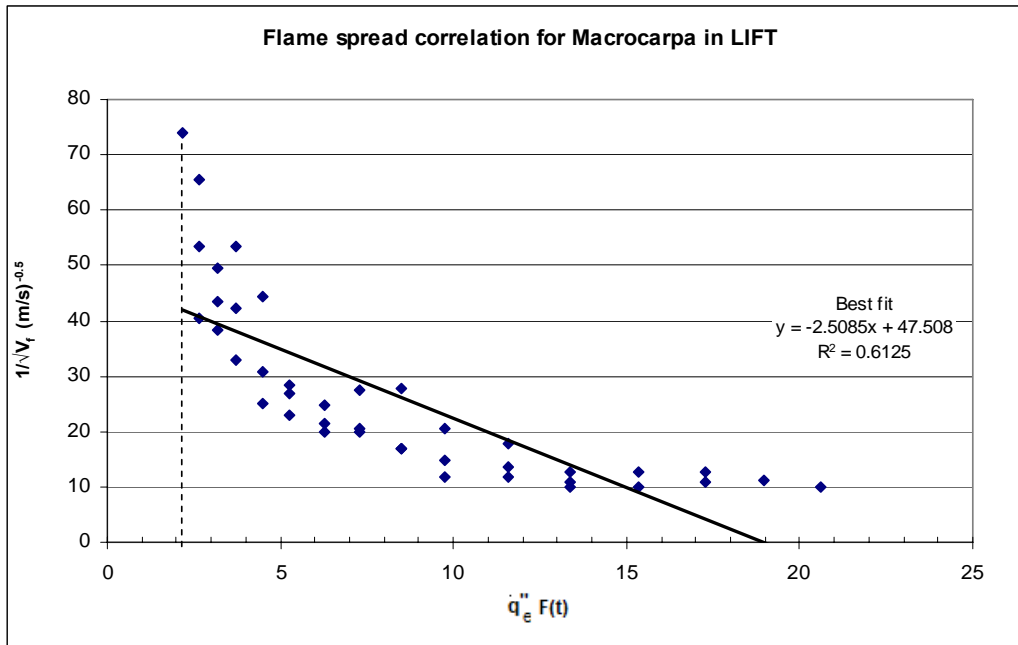


Figure 118: Flame spread correlation for Macrocarpa in LIFT

The comparison of the RIFT and LIFT results (Figure 119) for the flame spread correlation shows the RIFT gives a higher value for the correlated value of the minimum ignition flux $q''_{ig,min}$ although the flame spread modulus C (the slope of the best fit line) is similar. In this case, the value of the minimum flux for spread q''_s is higher for the RIFT than the LIFT.

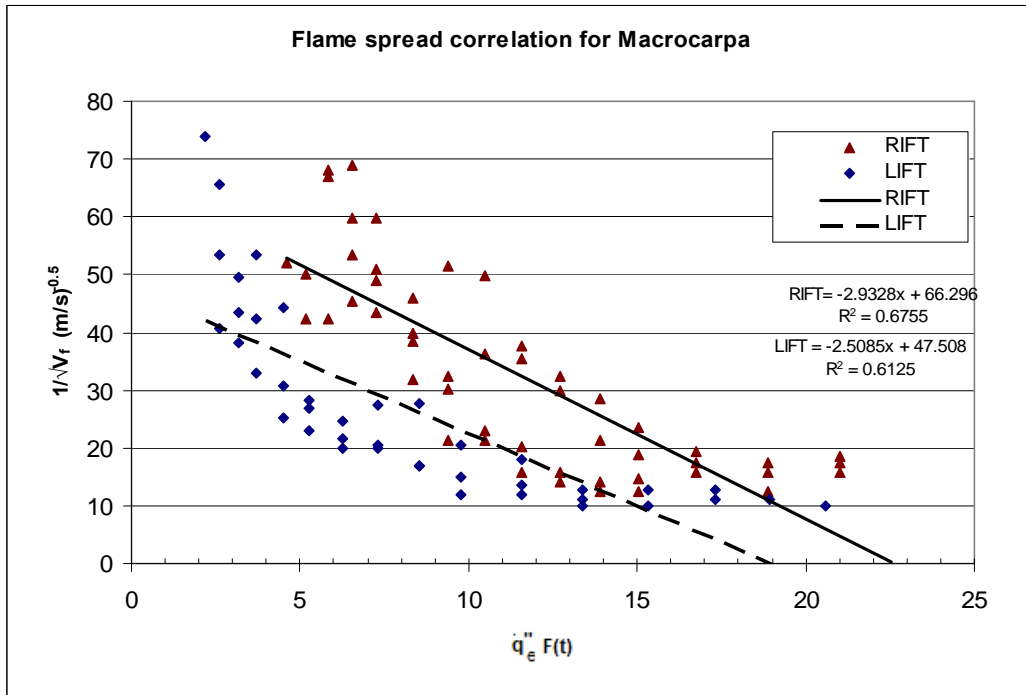


Figure 119: Flame spread correlation for Macrocarpa

9.3 Radiata Pine

9.3.1 Ignition of Radiata Pine

The time to ignition for the three ignition test methods is given in Figure 120, where the ISO 5657 and RIFT gave similar results. As can be seen in the results, in some cases, the material still ignited after the limiting ignition test period. During the course of the test, the material noticeably charred over the long test intervals, with some surface cracking. Localised surface hot spots formed, where an area around 2cm across would be glowing, when the rest of the sample showed no signs of heating.

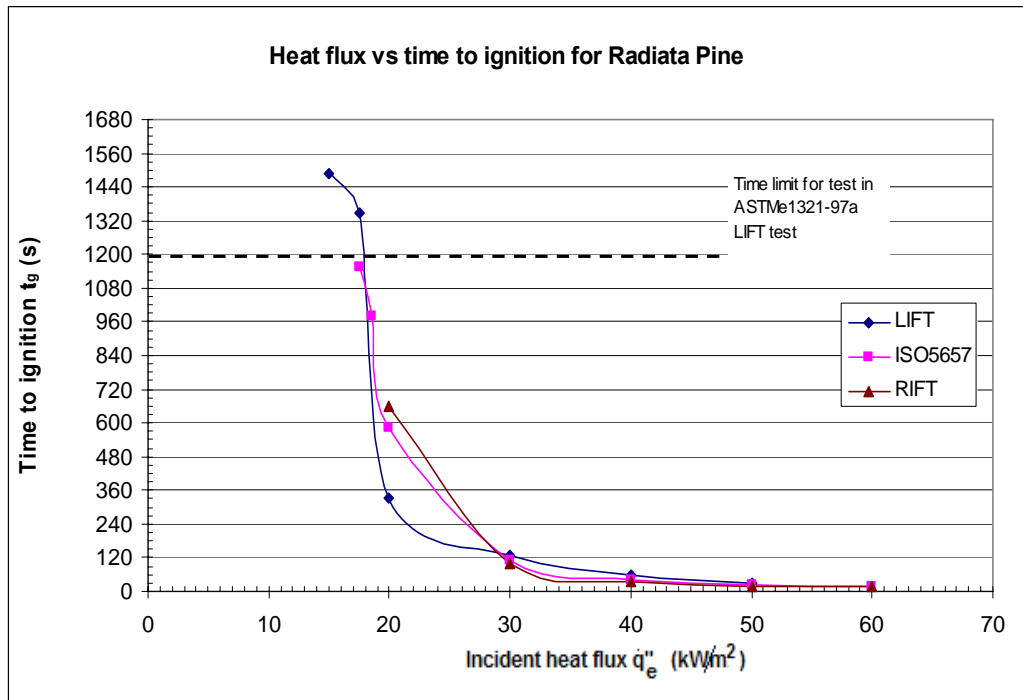


Figure 120: Time to ignition of Radiata Pine

The three methods gave similar results for the critical ignition flux (Figure 121).

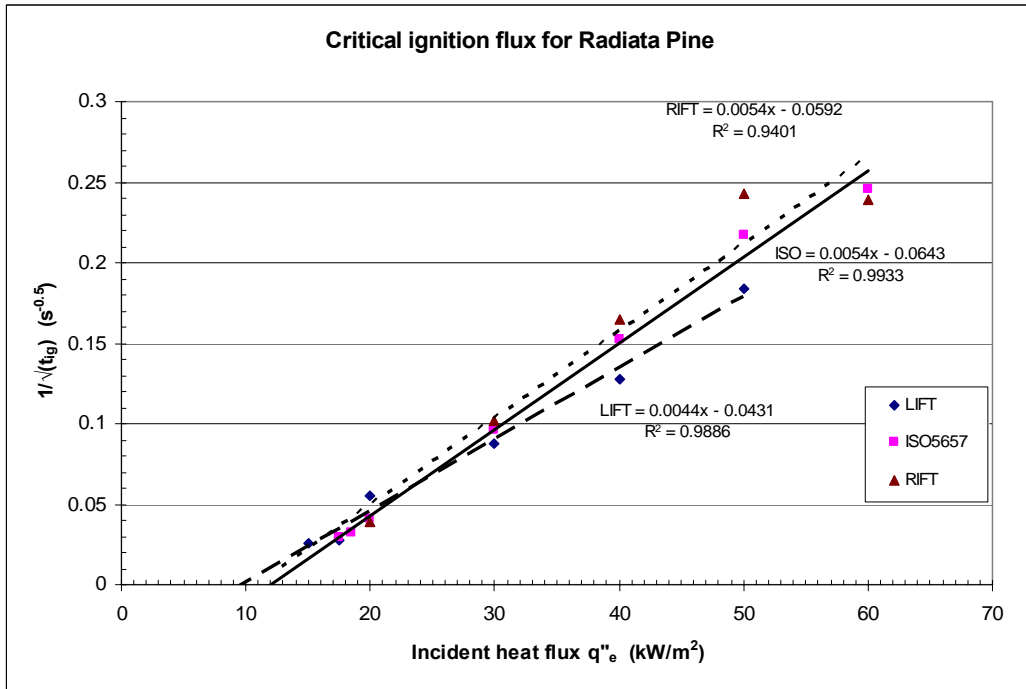


Figure 121: Critical ignition flux for Radiata Pine

The ignition parameter chart (Figure 122) shows that the three different methods gave widely different values for the equilibrium time t^* despite eliminating the values for

$$\frac{q''_{ig,min}}{q_e} < 0.8 \text{ for calculating the data fit.}$$

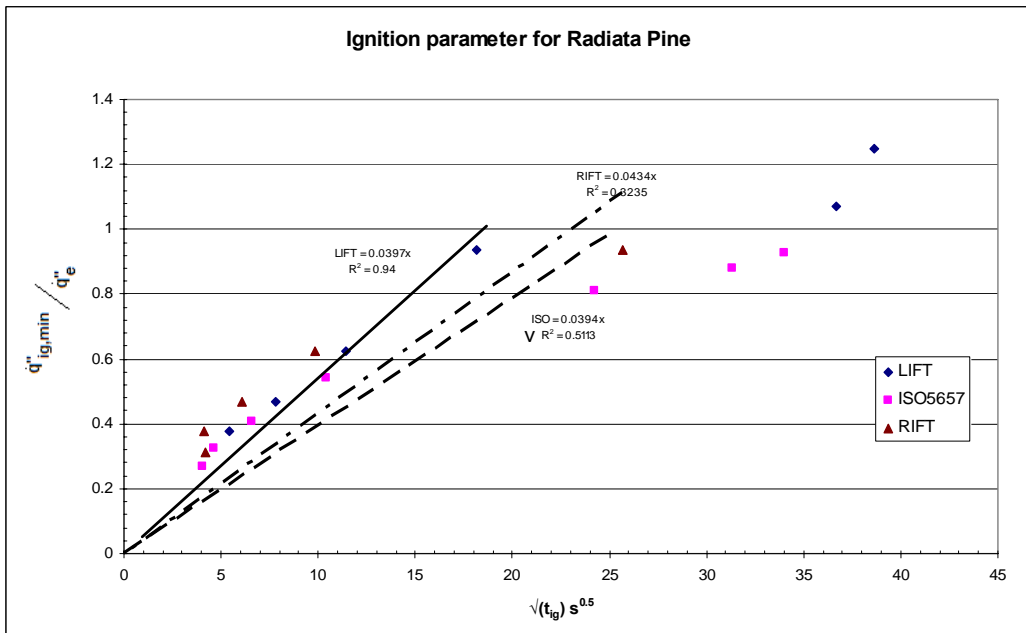


Figure 122: Ignition parameter for Radiata Pine

9.3.2 Flame spread of Radiata Pine

The low preheat time for the flame spread tests was 40 seconds. The full preheat time was 643 seconds in the RIFT and 341 seconds in the LIFT. Radiata Pine noticeably charred during the preheating period, and the area up to 180mm along the sample was difficult to ignite just by using the pilot flame.

Flame spread of Radiata Pine in RIFT

The flame spread along the Radiata Pine samples in the RIFT is shown in Figure 123 and Figure 124. The effect of preheating of the sample can be seen in Figure 125 - the preheated sample has a larger flame spread distance, with a lower time to reach each point on the sample, giving a higher flame front velocity.

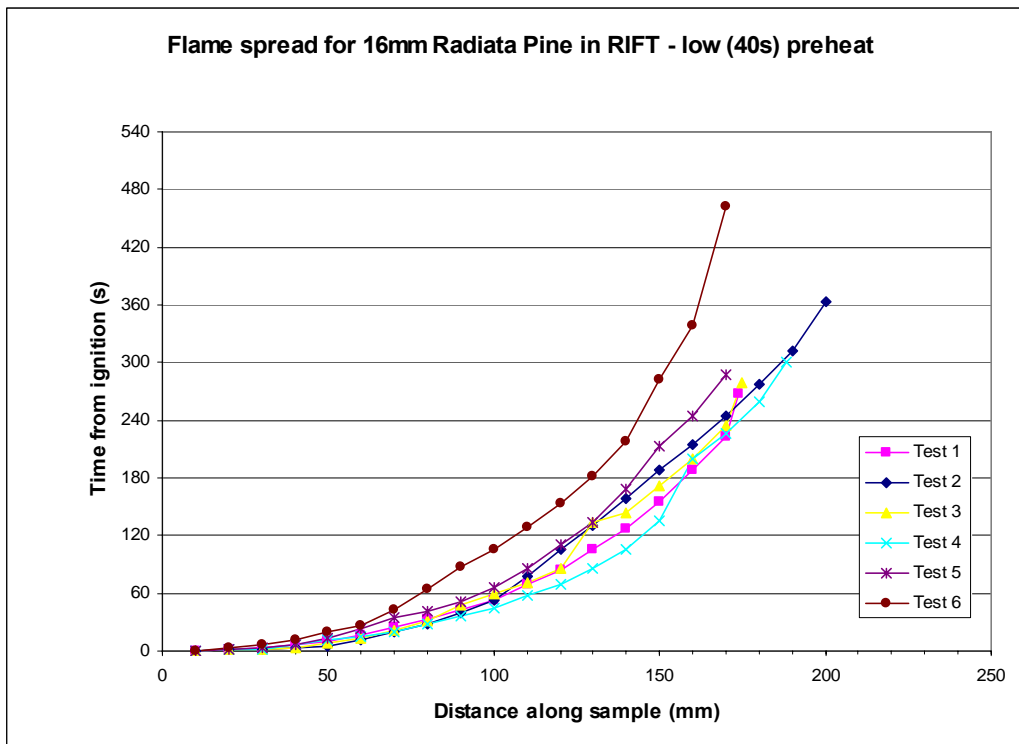


Figure 123: Flame spread for Radiata Pine in RIFT – low (40s) preheat

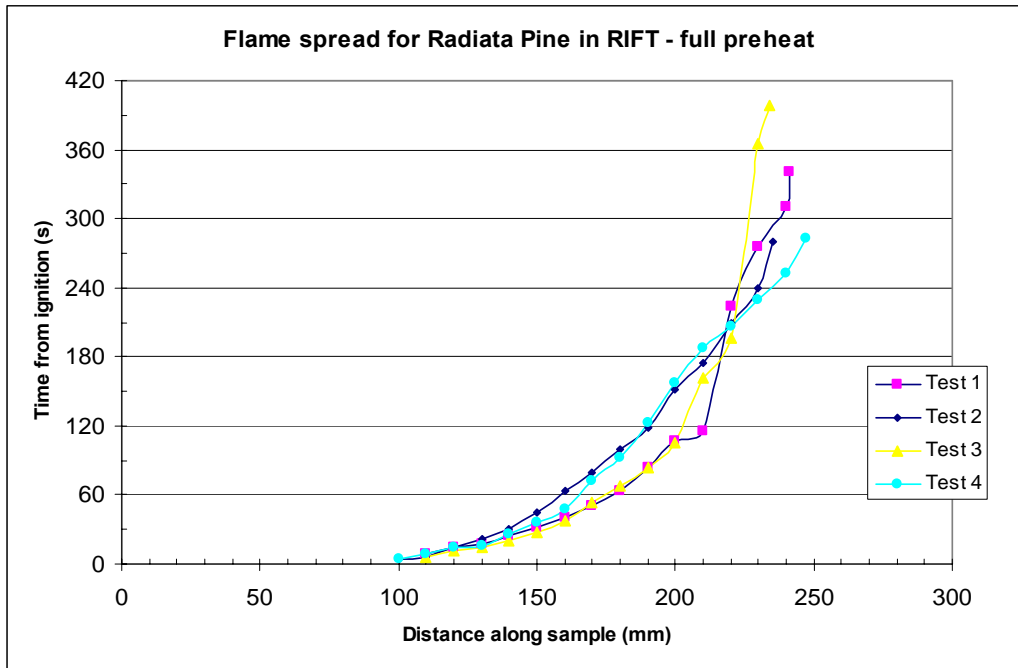


Figure 124: Flame spread for Radiata Pine in RIFT - full preheat

The effect of preheating on the flame spread can be seen in Figure 125, where preheating increases the flame spread rate.

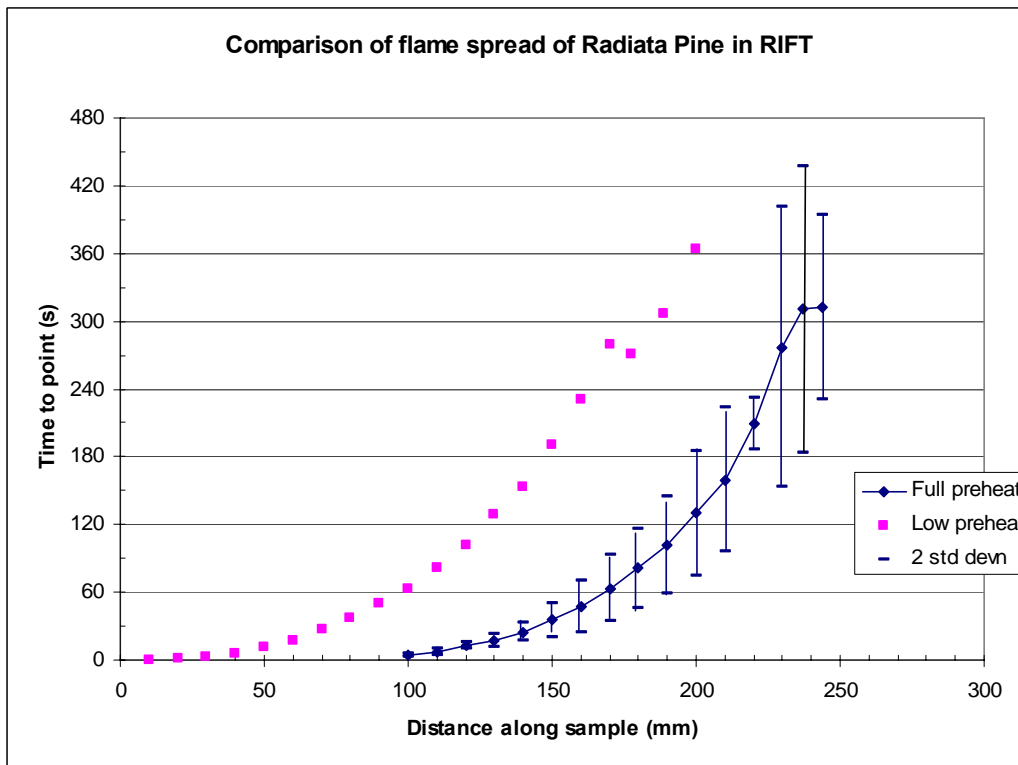


Figure 125: Comparison of flame spread of Radiata Pine

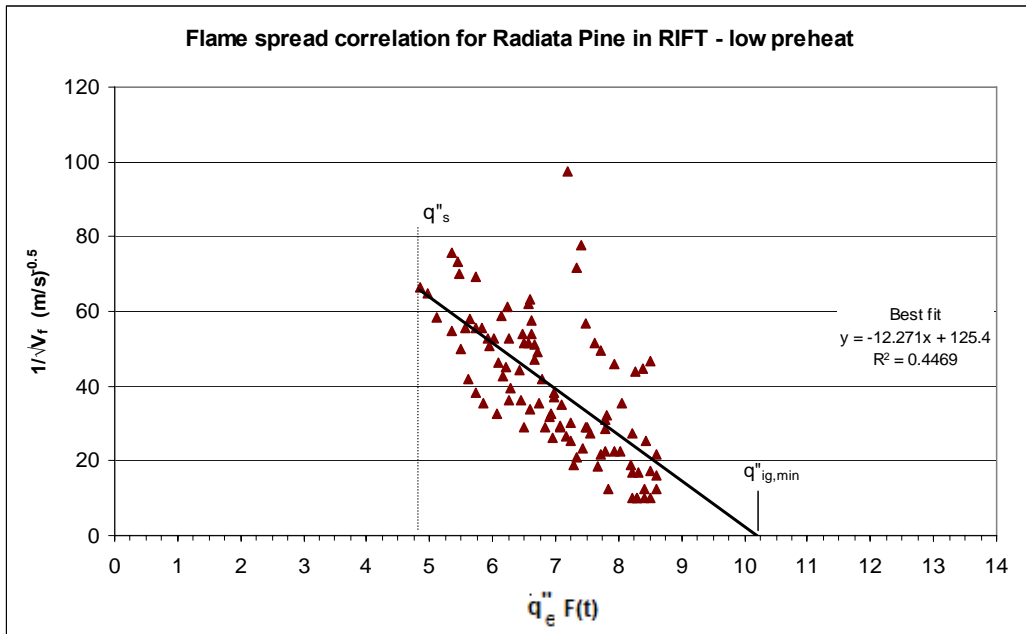


Figure 126: Flame spread correlation for Radiata Pine in RIFT – low preheat time

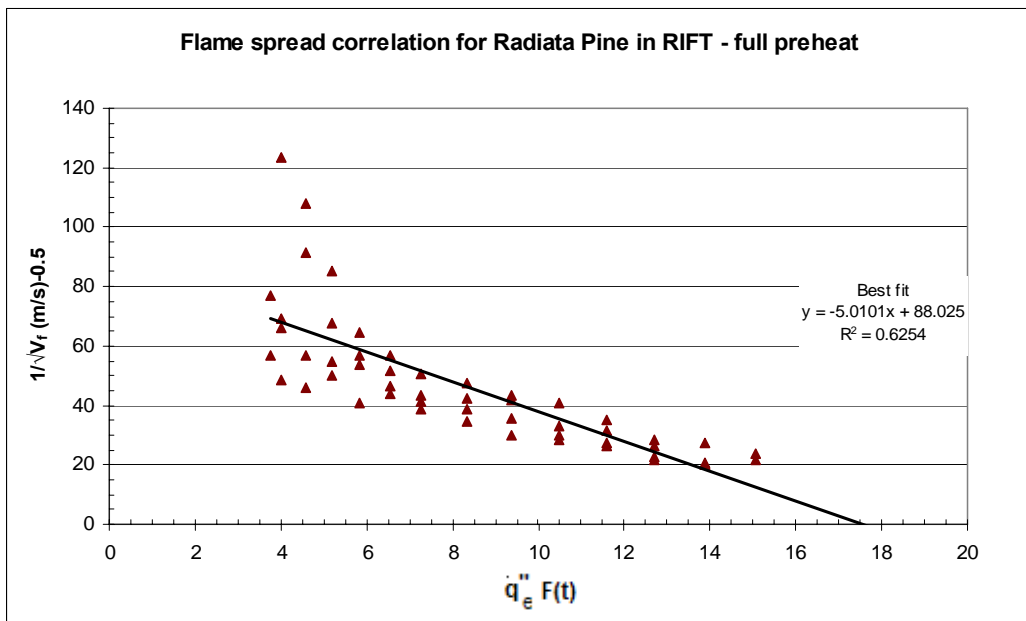


Figure 127: Flame spread correlation for Radiata Pine in RIFT - full preheat

Flame spread for Radiata Pine in LIFT

The heat flux distribution for the flame spread tests in the LIFT is the same as that for Rimu, shown in Figure 135.

The flame spread rate (Figure 128) for Radiata pine shows less variation than some of the other material tested, such as Macrocarpa (Figure 117) or Beech (Figure 108).

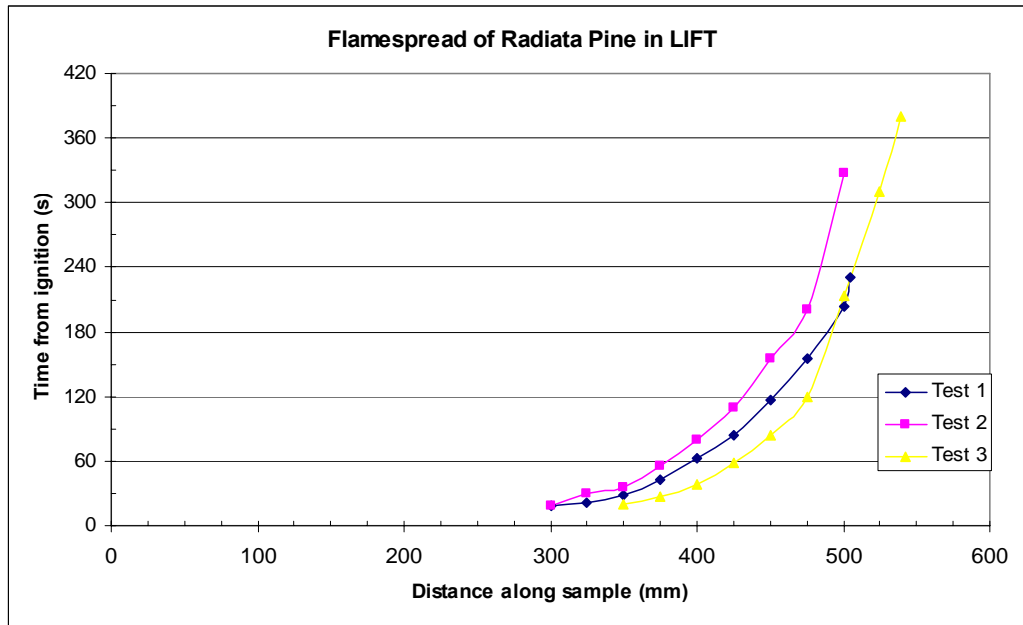


Figure 128: Flame spread of Radiata Pine in LIFT

The more consistent flame spread behaviour (when compared to macrocarpa) gives a more accurate correlation for the flame spread (Figure 127) with less scatter in the data.

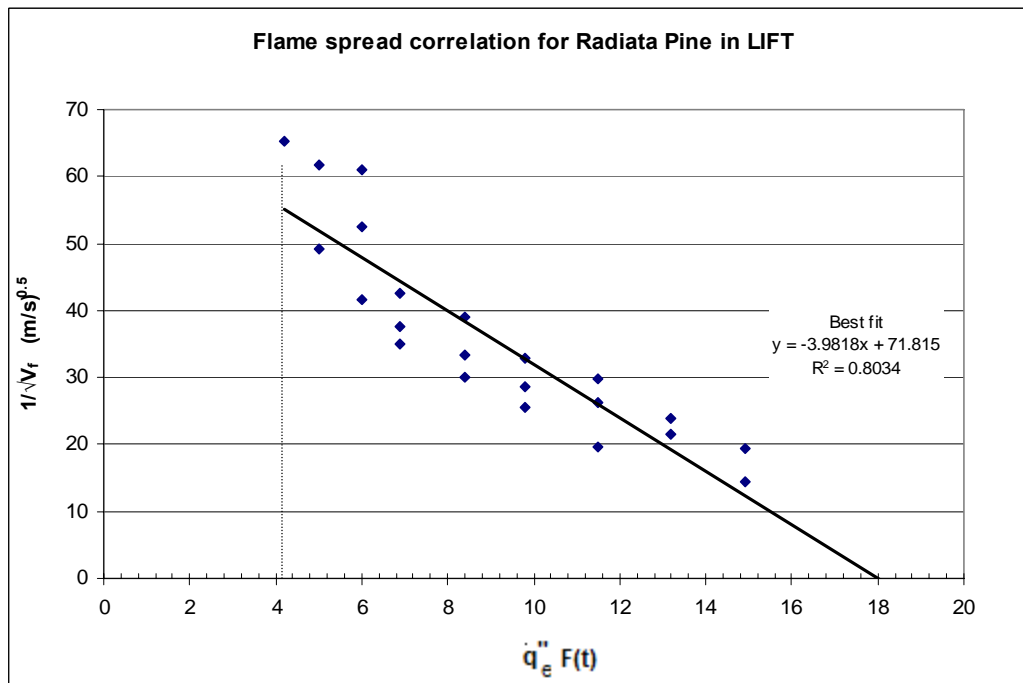


Figure 129: Flame spread correlation for Radiata Pine in LIFT

The RIFT gives a similar match for the flame spread correlation (Figure 130) but with more data scatter, shown by the lower R^2 value.

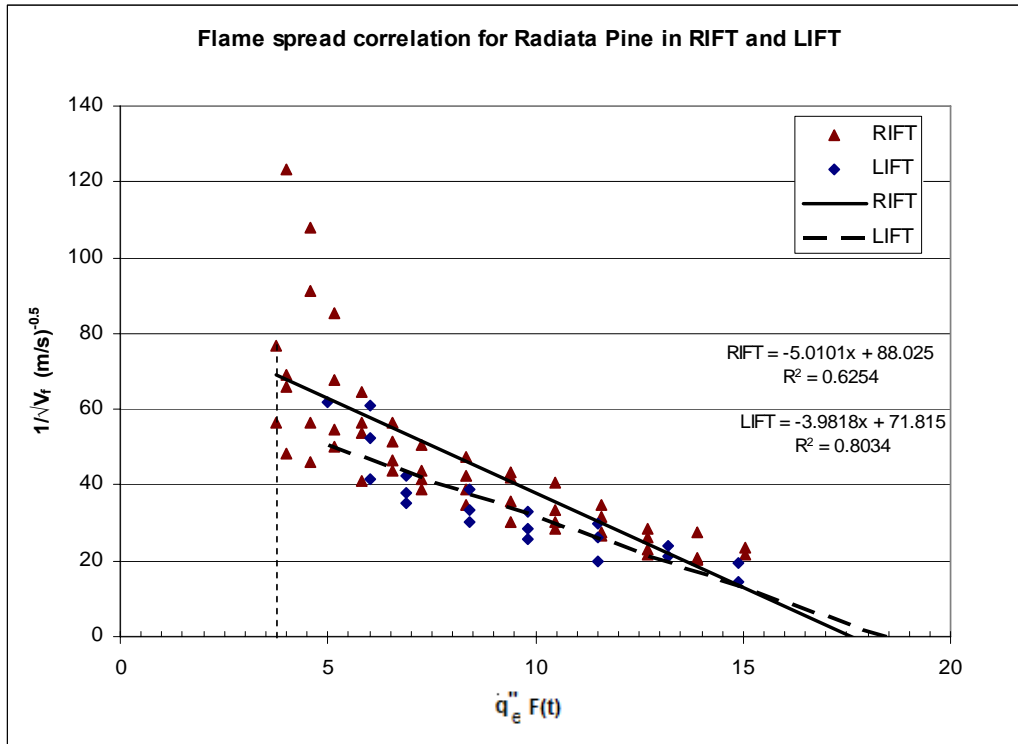


Figure 130: Flame spread correlation for RIFT and LIFT

9.4 Rimu

9.4.1 Ignition of Rimu

The time to ignition for Rimu is shown in Figure 131. Rimu charred less than the softer woods such as Radiata Pine, but the samples tended to bow during the low heat flux tests, where the sample was exposed to long heating periods. It did not appear to have had a significant effect on the ignition results.

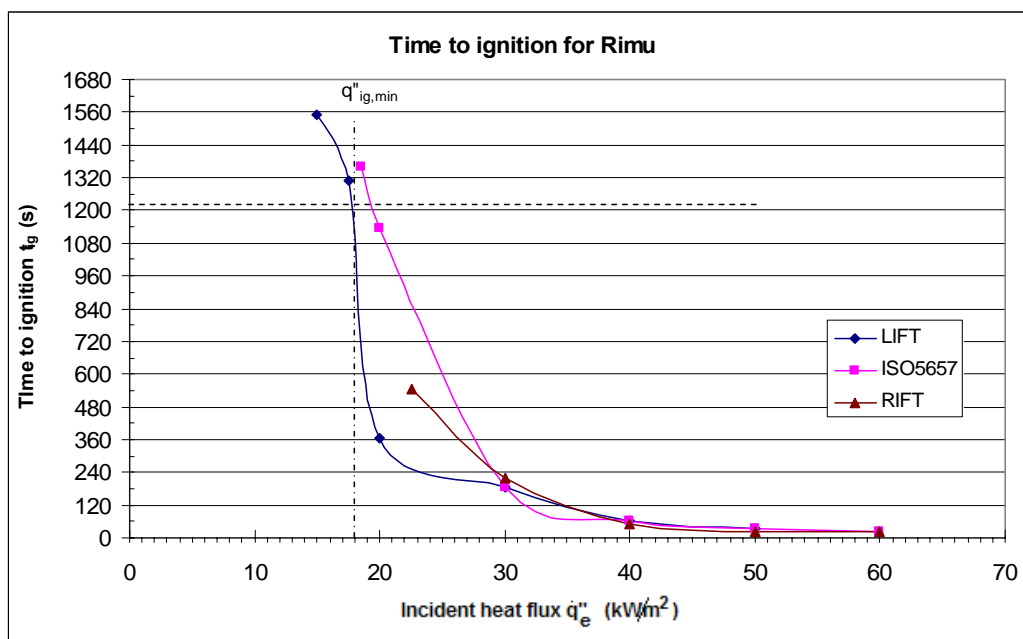


Figure 131: Time to ignition of Rimu

The resulting critical ignition flux (Figure 132) shows all the test methods gave similar results. The spread of the data was typical of the timber products tested.

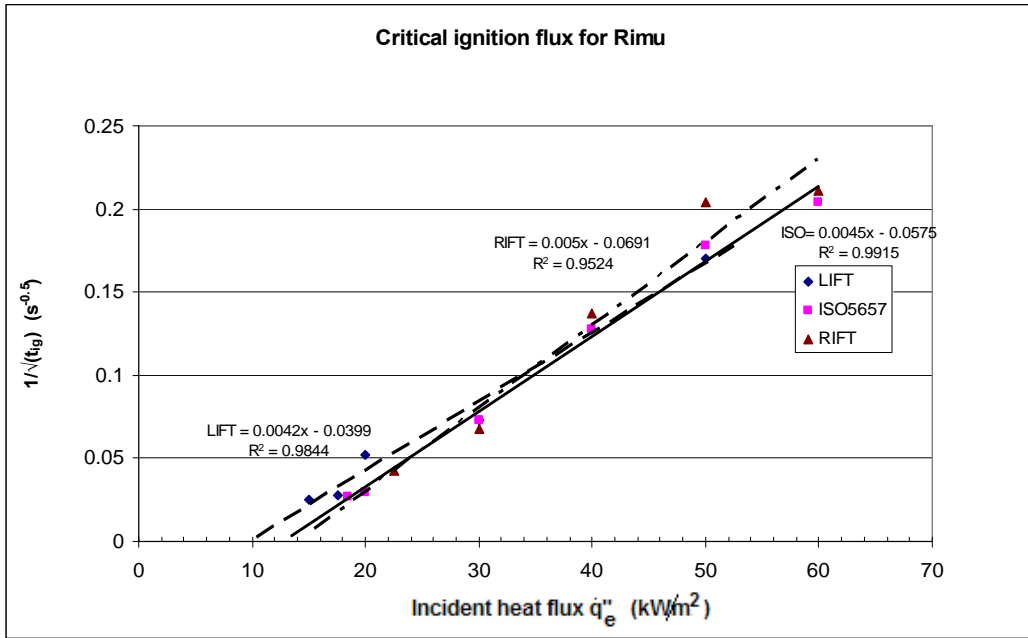


Figure 132: Critical ignition flux for Rimu

The fit of the ignition parameter for Rimu (Figure 133) required some data reduction. Most noticeably, the results for the RIFT ignition tests have significantly worse fit, given by the lower R^2 value, than those of the other methods.

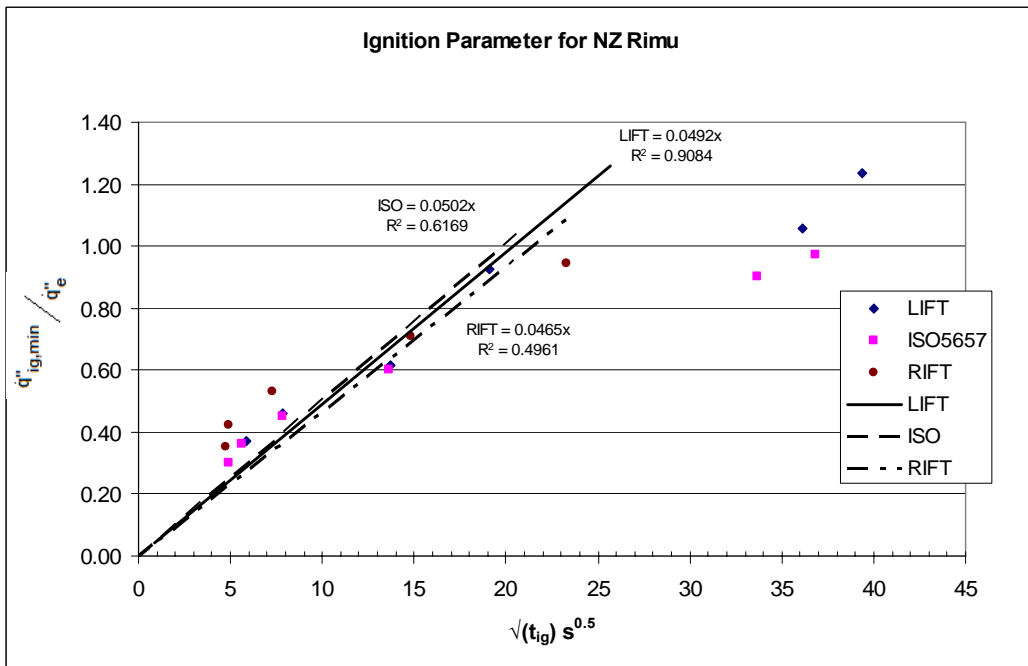


Figure 133: Ignition parameter of Rimu

9.4.2 Flame spread of Rimu

Flame spread for Rimu in the RIFT

There was insufficient flame spread in the RIFT with a full preheat period to get accurate data. The extent of flame spread was in the order of 130mm; however the initial 90-100mm was unusable, due to excessive charring. In this respect the extent of flame spread is similar to the case with a low preheat period (Figure 134). The low preheat period ranged from 67-80 seconds. The range was due to the time taken to get the sample to ignite after the preheating period. The full preheating period was 397 seconds, based on the ISO 5657 ignition data, or 395 seconds based on the LIFT ignition tests.

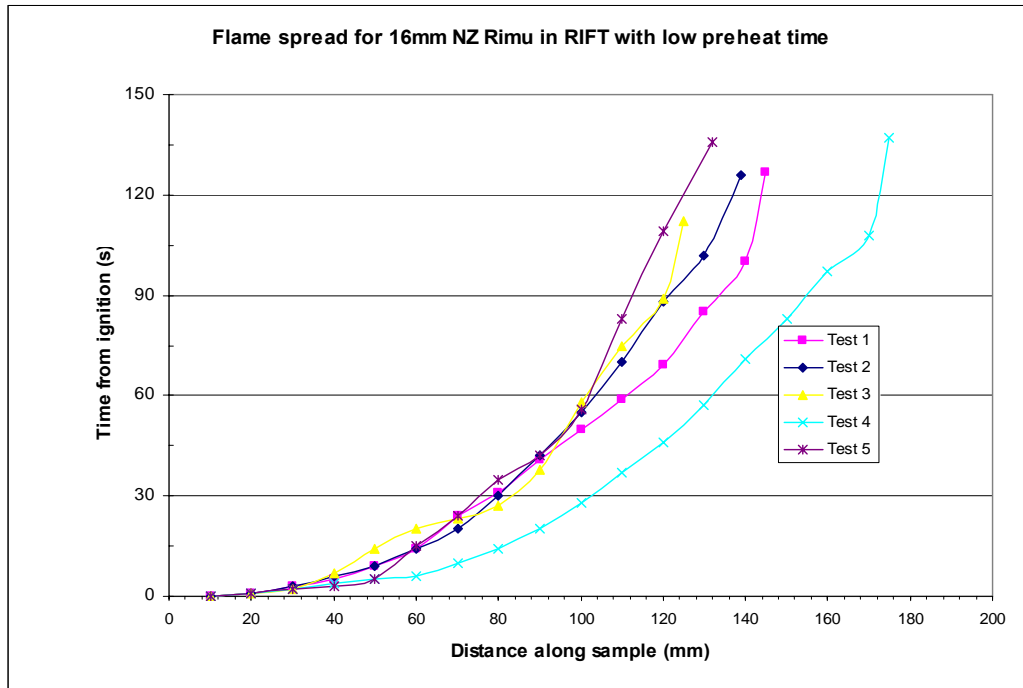


Figure 134: Flame spread along NZ Rimu in RIFT with a low preheat time of 67-80 seconds

Flame spread for Rimu in the LIFT

With the flux profile used in the flame spread tests in the LIFT, given in Figure 135, the resulting flame spread is given in Figure 136. The extent of flame spread in the LIFT results (Figure 136) shows significant variation, covering a range of over 125mm. Comparing this with the flux profile in Figure 135 gives a flux required for

flame spread (\dot{q}_s) of between 5-10kW/m². This material would have benefited from more tests to give a more accurate estimate of the average value. The flux required for spread from the correlations (Figure 137 and Figure 138) is similar although generally lower than that based on the extent of flame spread. Both the RIFT and LIFT gave similar values for the correlated values for the minimum heat flux for flame spread, despite the lack of preheating in the tests with the RIFT.

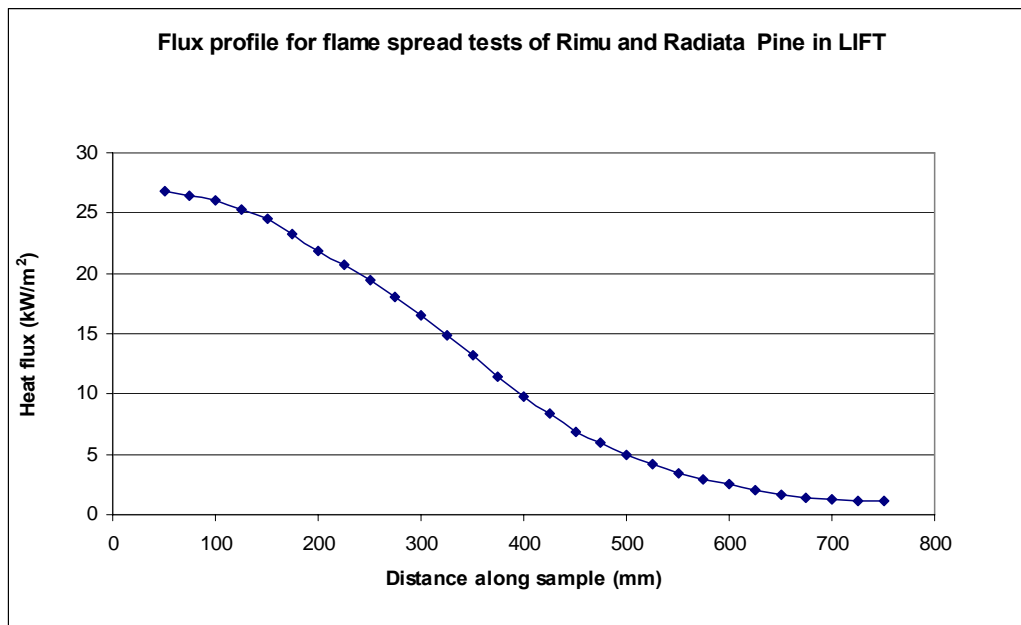


Figure 135: Flux profile of LIFT flame spread test for Rimu and Radiata Pine

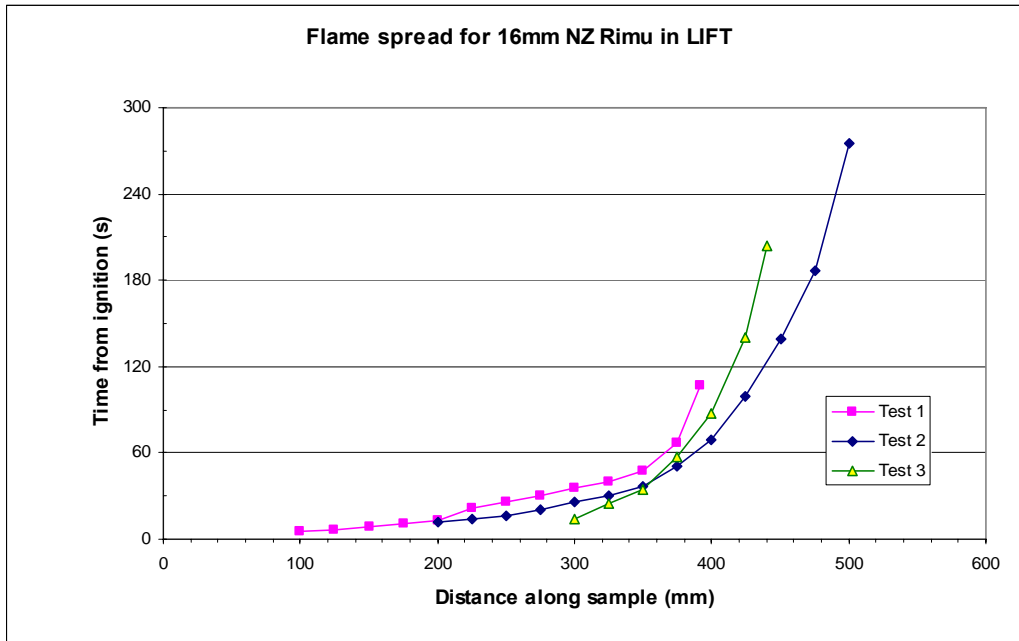


Figure 136: Flame spread for Rimu in LIFT

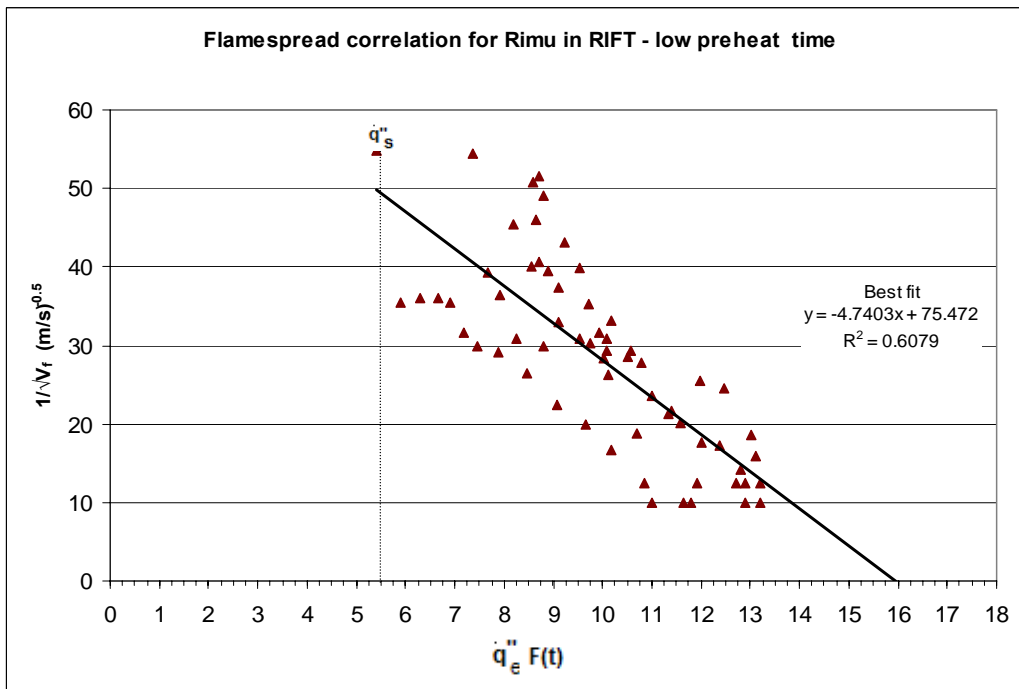


Figure 137: Flame spread correlation for Rimu in RIFT with ISO 5657 ignition “b” value – 67-90 seconds preheat time

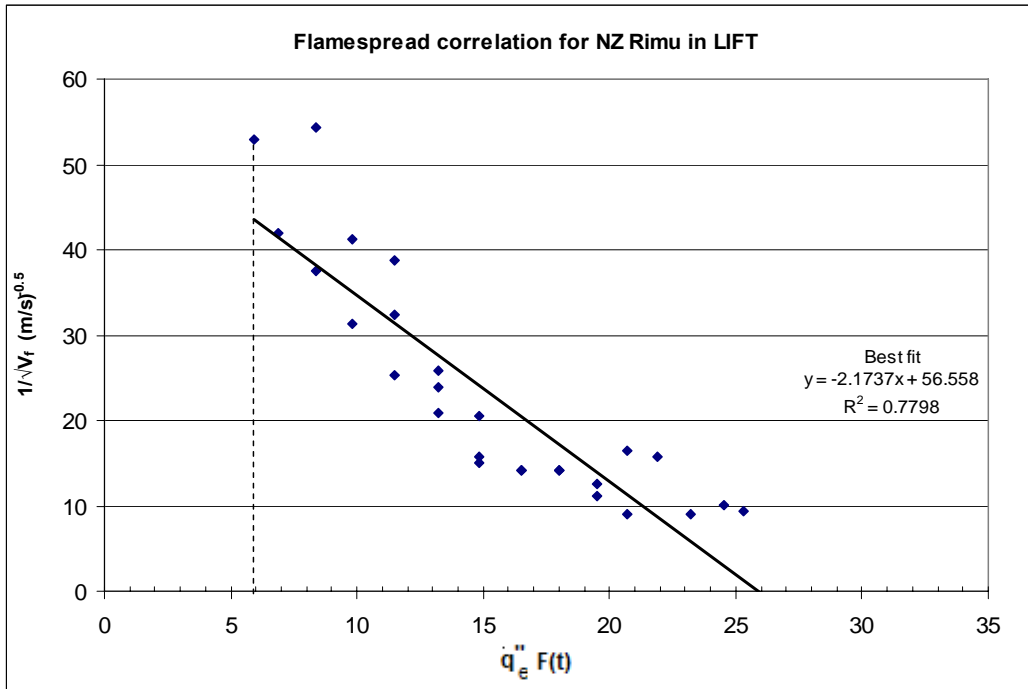


Figure 138: Flame spread correlation for Rimu in LIFT

10 Discussion of results

10.1 *Equipment specific issues*

10.1.1 LIFT

The tests conducted for this report were the first results from the new LIFT testing machine at the University of Canterbury. In general, after initial teething problems, it performed well; however there are some improvements which can be made for future work

The limitation for the upper heat flux is dictated by the air supply. The air compressor which feeds the LIFT burner is also used for the air supply for other parts of the building. Using an 8cfm compressor in parallel with the main supply improved the consistency, and showed that over $\dot{q}_{50mm} = 60\text{kW/m}^2$ was possible; however the air supply was not consistent enough for extended running over 50kW/m^2 . There are a number of alternatives. Another compressor could be mounted in parallel to provide additional capacity, or the burner can be redesigned to run on a lower pressure. The current burner design, seen in Figure 13, uses a 25mm square supply backbone with 6mm feeder tubes to the rear of the burner box, and semi circular baffles and Kaowool inside the burner box to distribute the gas evenly across the burner face. Replacing this with a larger tube would allow the air supply pressure to be reduced and a forward curve centrifugal fan could then be used for the air supply. If this is controlled with a variable frequency drive with RPM readout, then the air supply volume can be calibrated to the fan speed.

While the gas supply is controlled via a mass flow controller, the air supply is currently set with a variable pressure regulator and gauge, with a ball valve allowing additional restriction to be added to the regulator to stop fluctuation. The gauge is sufficient for crude adjustment, but the final mixture is set by the operator, based on the appearance of the flames from the panel and the required flux output. A highly precise adjustment has not proven to be necessary in practice, however easily repeatable settings would make the setup and changes to the flux levels faster and more consistent from run to run. This can be achieved with the current setup by using a 350-500 litre/min mass flow controller on the air supply, or changing to a variable speed fan with tachometer as described above.

Changing the burner system or modifying the manifold would also allow the burner to run at slightly lower flux levels than can currently be achieved. With flux levels less than $q_{50mm} = 25\text{kW/m}^2$ the heating of the face of the burner becomes uneven, with a cooler section noticeable in the centre. An extra series of gas feed pipes into this area from the gas manifold backbone would help to reduce this problem.

The measurement of the heat flux is critical to accurate results. Due to the narrower angle of 15 degrees when compared with the RIFT, as well as the larger scale, with a shallower flux profile, this tends to be less critical than the RIFT. The positioning of the holes in the LIFT measuring template are specified with a 2mm tolerance. This is easily achievable when making the template, however it was noticed with use that the holes tended to wear and chip. The flux gauge was bent to allow it to be clamped to the rail behind the sample holder. A dedicated holder which would ensure that the face of the flux gauge was parallel with the face of the measuring template and not canted would give more consistent results. As the 50mm position is used the most, making extra templates with just this hole or reinforcing this hole to prevent wear is recommended.

While the calibration curve was within specification over the extent of the flame spread, it was outside the limit at the cold end of the sample. Some further adjustment of the apparatus may improve the match to the standard curve, however, this appears to be a common problem as it was reported by Nisted (1991) and Babrauskas and Wetterlund (1999). Pauner (2003) also reported the same issues with the IMO 653/ASTM E 1317 round robin tests, which use the same equipment and calibration curve. At low flux levels, the errors in measurement become critical, and although the measurement results deviate from the standard value by a large percentage, the absolute value is low, and may approach the limits of accuracy of the measurements and the effect of variation from the burner. Robertson and Ohlemiller (1995) conducted tests to improve the consistency of measurements of the ASTM E 1317 marine finishes test at low flux levels. The error in measurements increased along the sample due to the effect of the convective boundary layer over the face of the sample. Their recommendation was that the face of the flux meter is proud of the surface of the measuring template to avoid the boundary layer. In practice, this is difficult as the refractory board is fragile and a thinner board will not last. The flux meter head

imposes a maximum thickness of the template board of 12mm in order for the face to be level with the template and not shielded inside the hole.

The observation of the flame front in the LIFT is either directly via marks on the sample or via the observation mirror and viewing rake. Measuring the flame front by observing the progress directly is easier and more accurate, as the flame front is ill defined at the initial stages, and can be difficult to see in the mirror, and errors are compounded by the effect of parallax and the width of the pins. . A problem shared by both the RIFT and the LIFT for directly observing the flame front is the charring of the material during preheating. Lines marked in pen disappear, but those done with a graphite pencil can often still be distinguished even though the surface of the material has blackened.

In order to increase the resolution and the number of data points collected, Dietenberger (1995) used a system where a pointer was moved via a hand crank parallel with the sample, in line with the flame front. The pointer was connected to a potentiometer and a data acquisition system, so that data collection is continuous and more automated with less chance of error. A modification for the University of Canterbury LIFT along these lines is recommended.

10.1.2 RIFT

Some of the comments noted for the LIFT also apply to the RIFT. The issue of the template holes wearing is more pronounced on the RIFT, as the combination of the smaller scale, the rapid decay of the flux profile and steeper angle between the element face and the sample makes the setup and calibration both more difficult and more critical. The rapid decay of the heat flux along the sample makes location of the measuring holes critical, as a small change in the position can make a large change in the actual heat flux. It is reasonably straightforward to get the location of the sample holder and the angle consistent between different experiment setups by measuring from the face of the cone calorimeter element, and the changeover time from the cone calorimeter in the horizontal position to the RIFT is usually between 15-20 minutes. Modifying the apparatus to use templates and locating stops would reduce this source of error further and make the changeover faster.

It is important when measuring the heat flux that the face of the heat flux gauge is parallel with the face of the template. This is easier than in the LIFT, as the operator can see the front face of the template. Due to the steeper 60° sample angle of the RIFT

against the 15° angle of the LIFT, small errors in holding the flux gauge in place can have a large effect. A mounting frame to provide consistency would reduce this error. The accuracy of the data can be increased by increasing the number of reading points, preferably to every 10mm, which would coincide with the data collection points along the sample. This is not possible with a single template, due to the proximity of the holes. It can be achieved using 3 templates, with measuring holes at 30mm centres, and each template is offset by 10mm from the other templates.

Samples mounted in the LIFT are preset in a sample holder, which is slid into position. The RIFT as used in these experiments had a fixed frame, into which the sample and backing board was slid into place. This has the advantage of being easier to setup the sample, and makes tearing the foil backing less likely, and makes positioning the sample into place more consistent and faster.

The RIFT sample holder frame is mounted on an angle bracket, which allows the frame to pivot to change the sample angle, without changing the distance from the cone element. This forms a flange along the bottom of the sample holder, seen in Figure 38. This affects the airflow over the face of the sample, seen visually during the ignition tests from the behaviour of the smoke emitted from the sample. The ledge disrupts the airflow, reducing the cooling from the convective airflow – a flange is mounted on the bottom of the ASTM E 1621 ICAL intermediate scale calorimeter samples for the same reason (Babrauskas 2003). In the case of the RIFT, it decreases the time to ignition to close to that of the ISO 5657 ignition tests, where it would be expected to be higher due to the orientation. The minimum ignition flux is also increased. The effect of this is discussed in detail in the following sections; however it appears that the RIFT with the flange as currently constructed is not suitable for conducting the ignition tests which form part of the flame spread experiments.

The charring of the initial part of the sample in the flame spread tests obliterates the surface marks on the face of the sample. A series of pins as markers (Figure 139) was used to monitor the flame spread rate. Generally it was found that if the surface was too heavily charred, so that the pencil marks were no longer visible, then flame spread would be too rapid for accurate measurement, or the material would no longer ignite. In addition the error due to parallax and the width of the pins was too large given the scale of the sample and measuring positions to be generally worthwhile



Figure 139: Marker pins in RIFT

10.2 *Comparison of LIFT, ISO 5657 and RIFT ignition results*

The differences in the details between the apparatus, regarding sample size, orientation, pilot and heating source, etc are expected to affect the ignition results, and hence the values subsequently calculated.

The RIFT has a ledge at the front as part of the mounting frame and this affects the convective flow across the face of the sample. The ASTM E 1623 ICAL intermediate scale calorimeter uses such a ledge to prevent convective cooling of the exposed sample surface, as the ignition time results are otherwise far greater than those produced by other methods (Babrauskas, 2003). As the radiative component of the heat transfer coefficient is expected to be unaffected by the ledge, it appears that the RIFT as used in these experiments appears to have a lower convective coefficient h_c than the LIFT. This gives a correspondingly reduced heat loss from the face of the sample, and consequently the RIFT has shorter ignition times than the LIFT. The ASTM E 1321-97a standard specifies that the LIFT has a heat transfer coefficient of $0.015 \text{ kW/m}^2\text{K}$, including the convective component, although Dietenberger (1996) found the heat transfer coefficient was much higher at the hot end of the sample. This

was due to the effect of turbulence induced by the gas burner, and was a function of the heat flux at the point, and the convection coefficient varied along the sample.

The heat transfer coefficient for the cone calorimeter is approximately $0.010 \text{ kW/m}^2\text{K}$ (Janssens et al, 2003), and Babrauskas and Wetterlund (1999) used a value from other research of $0.0115 \text{ kW/m}^2\text{K}$. Babrauskas (2003) gives the convection coefficient for the cone calorimeter in the vertical position as 20% higher than in the horizontal position, or $0.012 \text{ kW/m}^2\text{K}$. Diitenberger (1995b) found that it was a function of the received heat flux, in the same manner as the LIFT. The RIFT would therefore be expected to have longer ignition times than the ISO 5657 apparatus, due to the orientation, in the same manner as the LIFT. Since the ignition times for the RIFT were similar to the ISO ignition test results, as discussed in more detail below in section 10.2.2, then this implies that the convection coefficient for the RIFT is similar to the ISO ignitability apparatus.

The effect of the larger sample size in the LIFT is expected to be less of a cause for the difference in results. The main difference in the heat loss from the surface between a LIFT and RIFT sample is convective, and the convective coefficient $h_c \propto (\text{sample height})^{1/4}$ (Babrauskas, 2003).

10.2.1 The effect of data reduction of ignition data

As noted in section 3.4.2, the data reduction undertaken can greatly affect the results of the test, by affecting the preheating time t^* and the ignition parameter b , from the slope of the fitted data points. As given in Equation (32), the thermal equilibrium time t^* equals $[1/(\text{ignition parameter } b)]^2$, a small change in the fit of the data points leads to excessively long or short preheating times. The effect of insufficient preheating is a curvature in the flame spread correlation, and a poorer linear data fit. The points which are discarded as being a poor fit are generally obvious, and the process given in section 3.4.2 appears to give consistent results.

This is an area recognised by others (Babrauskas and Wetterlund, 1999) as an area which is unclear within the standard, and a definite procedure should be included in future revisions for consistency and clarity.

10.2.2 Time to ignition

The time to ignition between the ISO 5657 apparatus and the LIFT (Figure 140) follows the expected behaviour shown by Diitenberger (1995), where the ignition

times are longer in the LIFT than the ISO 5657 test, although not as marked, as the average difference is 4.3% in these tests. While the difference is greater at lower flux levels, the scatter of the results is also greater, and this tends to hide the trend at flux levels less than 30kW/m². This is also noted by Babrauskas (2003).

Shields, Silcock and Murray (1993) investigated the time to ignition for particle board, plywood and spruce softwood in the horizontal and vertical positions in the ISO 5657 ignition apparatus and in the cone calorimeter, as well as inverted in the ISO 5657 apparatus. The cone calorimeter and the ISO 5657 apparatus produced similar ignition results. In all cases, where the sample was in the vertical orientation, the ignition times were significantly increased for flux levels between 20 and 40 kW/m².

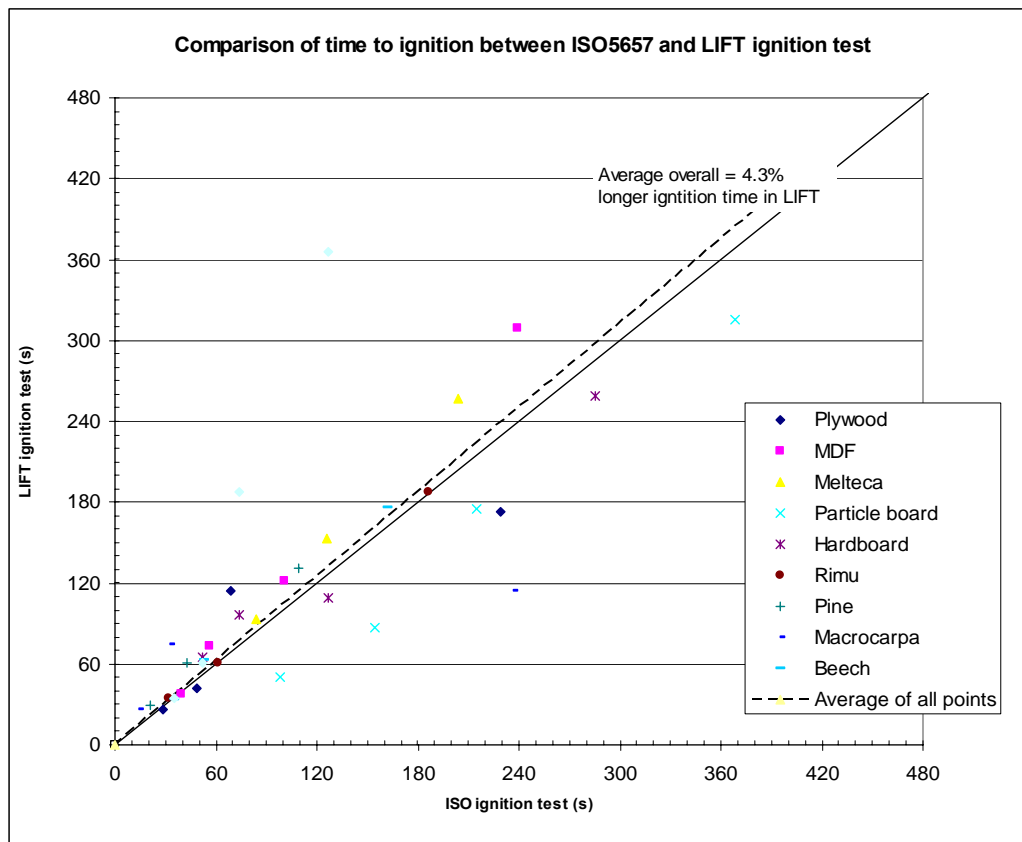


Figure 140: Comparison of time to ignition for ISO 5657 and LIFT ignition test

The trend is similar with the RIFT vs. the LIFT, with the LIFT having higher times to ignition than the RIFT (Figure 141). The time to ignition for the RIFT and ISO 5657 are similar (Figure 142)

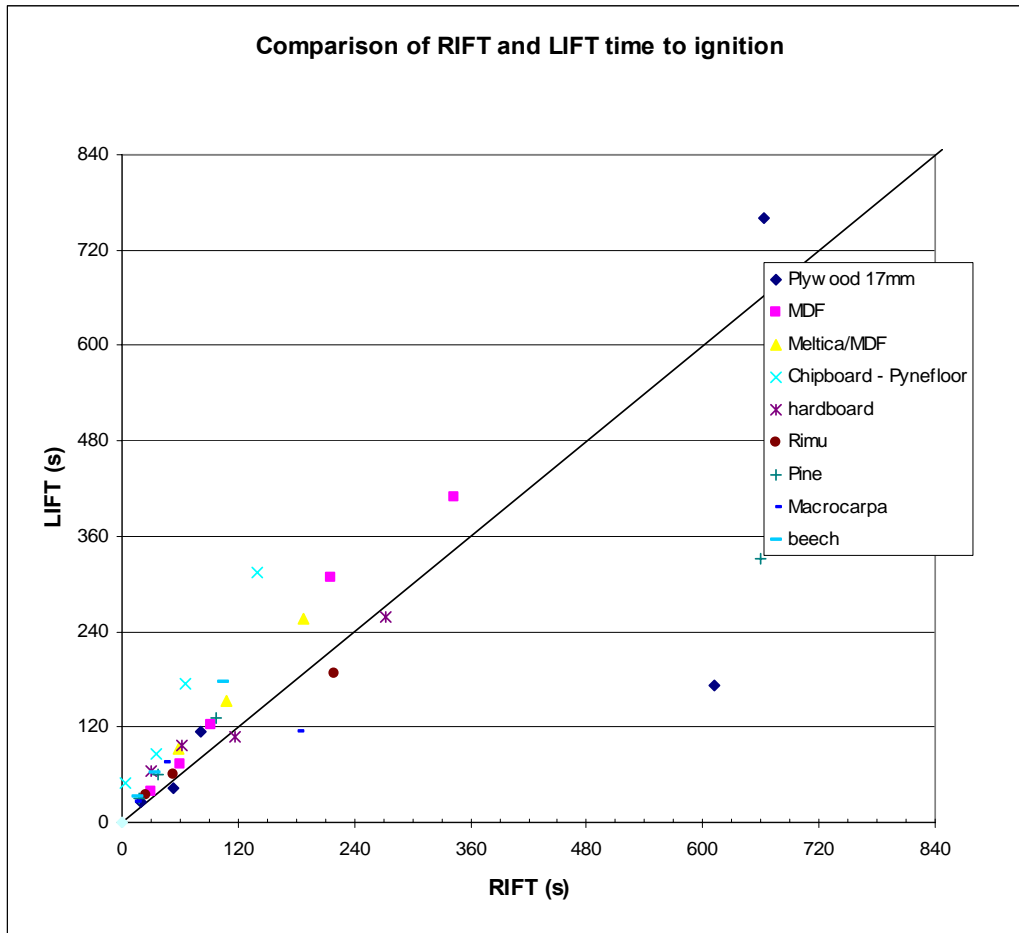
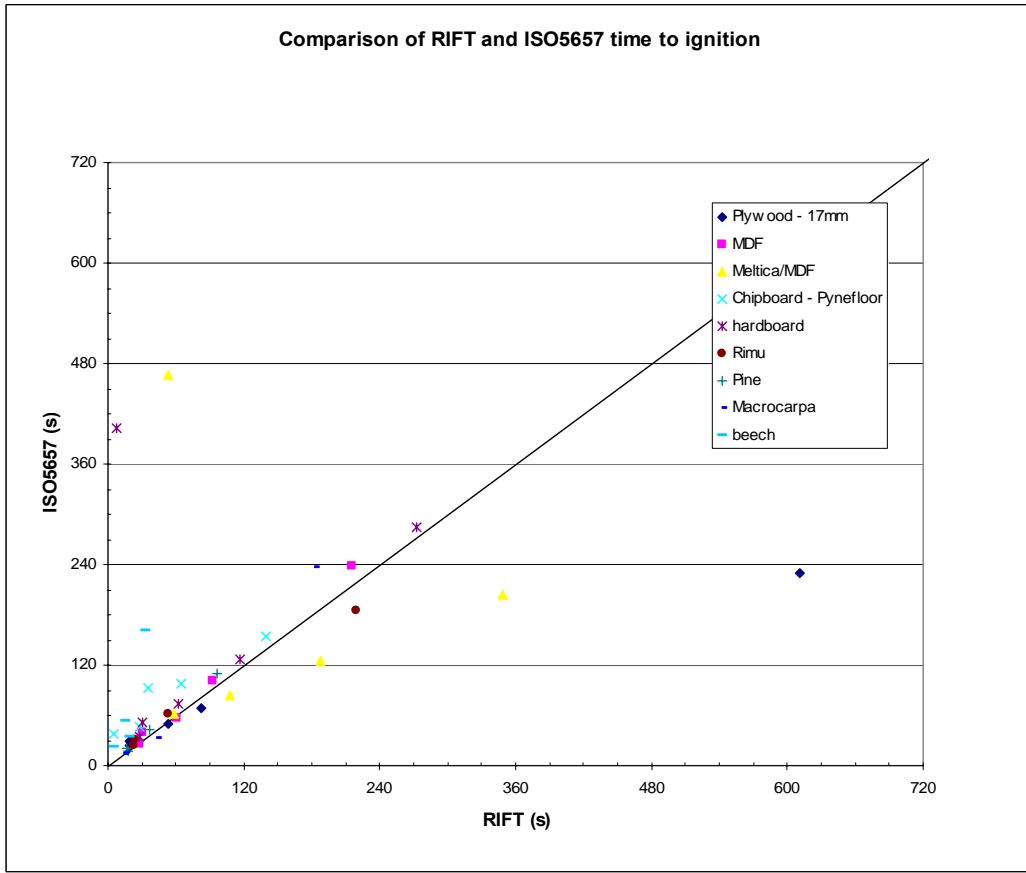


Figure 141: Comparison of time to ignition for tests in RIFT and LIFT



10.2.3 Thermal inertia $k\rho c$

The thermal inertia is compared in Figure 143, where the differences between the types of apparatus are apparent. The ISO 5657 apparatus produces higher thermal inertial values than the LIFT. The RIFT shows much more variation and spread compared with the other methods, giving more inconsistent results when it is applied to calculate the flame spread parameter.

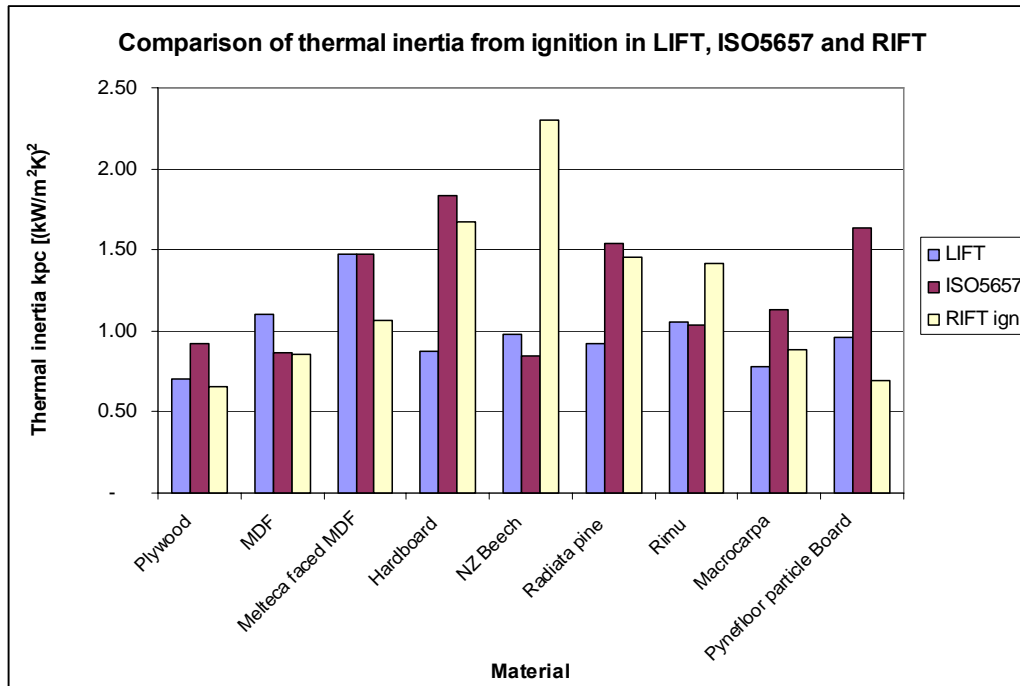


Figure 143: Comparison of thermal inertia ($k\rho c$) in LIFT, ISO 5657 and RIFT

10.2.4 Minimum ignition flux

The minimum ignition flux is compared in Figure 144, where the ISO 5657 ignition test gives a consistently lower value for $\dot{q}_{ig,\min}$ than the LIFT. The RIFT is generally greater than or equal to the LIFT values.

As a comparison, Dietenberger (1996) found that the minimum ignition flux for redwood was 4kW/m^2 greater in the LIFT when compared to the cone calorimeter in the horizontal position. Given that the ISO 5657 and cone calorimeter tests give similar results for the minimum ignition flux (Babrauskas, 2003), then the values from

ignition tests in the LIFT would be expected to be higher than those obtained in the ISO 5657 ignition tests. This can be seen in Figure 144.

The higher minimum ignition flux for the RIFT ignition, combined with the lower ignition times gives a higher ignition parameter value “b”, which affects the final flame spread parameter Φ value.

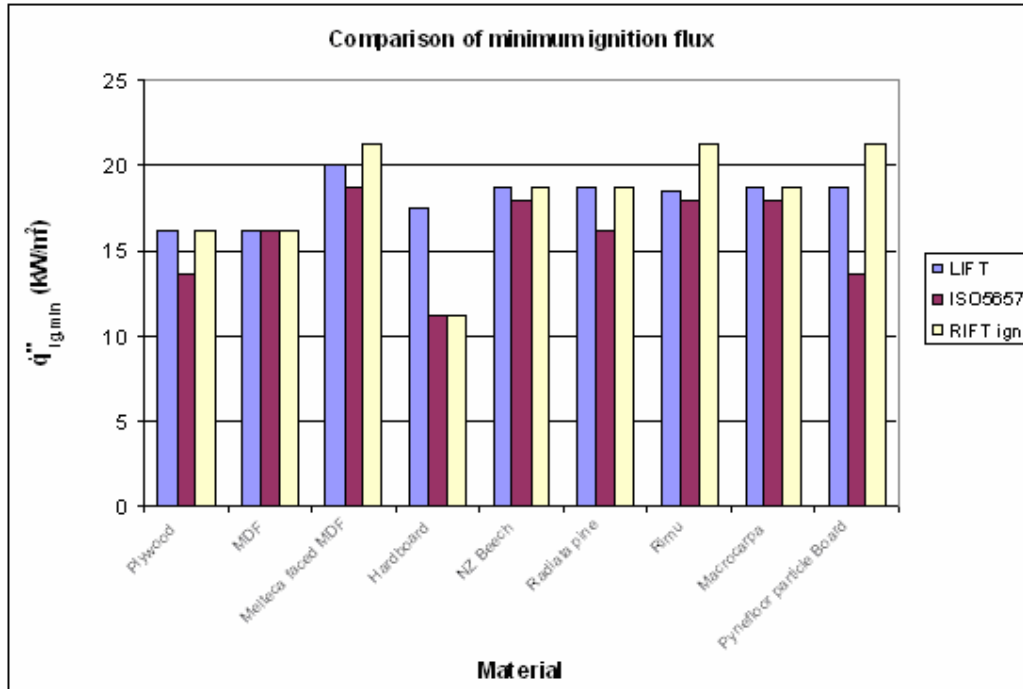


Figure 144: Comparison of minimum ignition flux $q''_{ig,min}$

10.2.5 Comparison of correlation values and measured minimum ignition flux $q''_{ig,min}$

The comparison of the correlated value and the measured value for the minimum ignition flux ($q''_{ig,min}$) is shown below for both the RIFT (Figure 145) and the LIFT (Figure 146). The values of the minimum ignition flux from the flame spread correlation, given in the procedure in Section 3.4.4, are consistently higher than the

experimental values. Babrauskas and Wetterlund (1999) also noted this finding with their results, where they used the LIFT for both the ignition tests and flame spread.

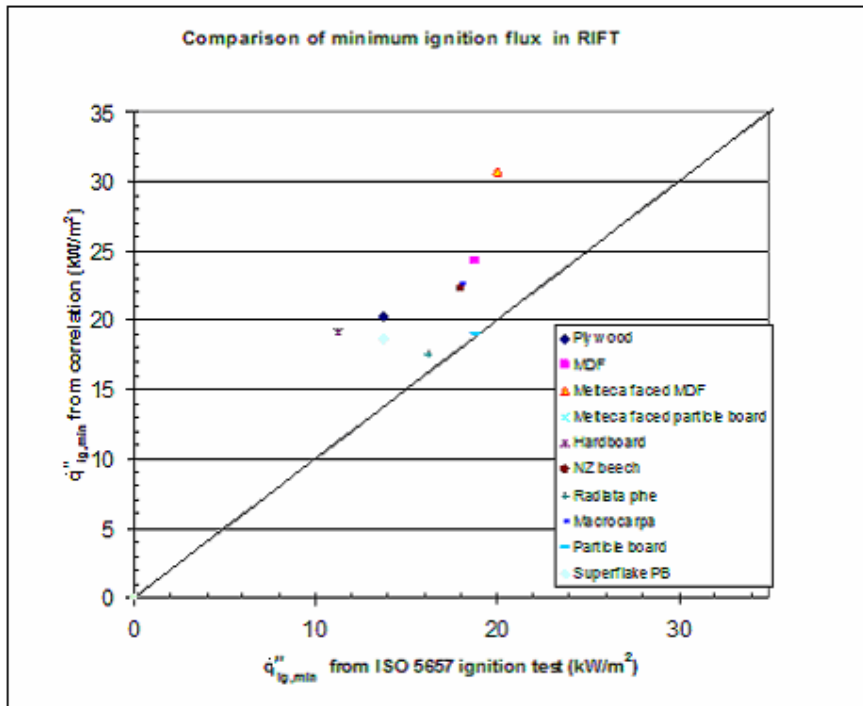


Figure 145: Comparison of RIFT flame spread correlation and ISO 5657 ignition test results for minimum ignition flux $q''_{ig,min}$

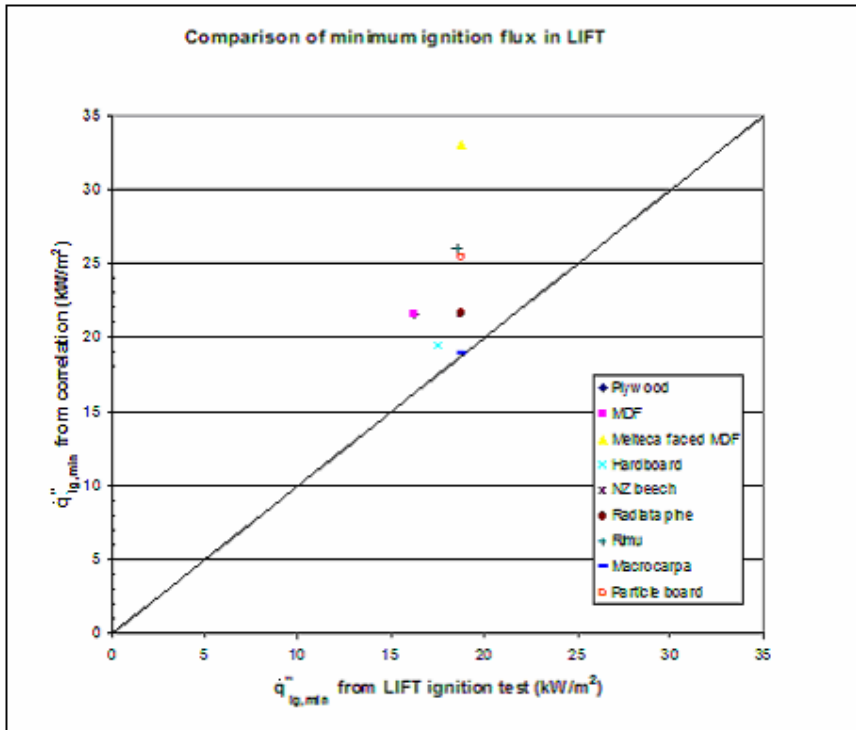


Figure 146: Comparison of LIFT correlation and LIFT ignition test results for minimum ignition flux

10.2.6 Apparatus and flame spread

It is apparent when looking at the flux distribution in the RIFT in Section 6.2, reproduced below in Figure 147, that the apparatus is limited to materials with a relatively low value for the minimum flux required for flame spread (\dot{q}_s), in order to get sufficient flame spread along the sample.

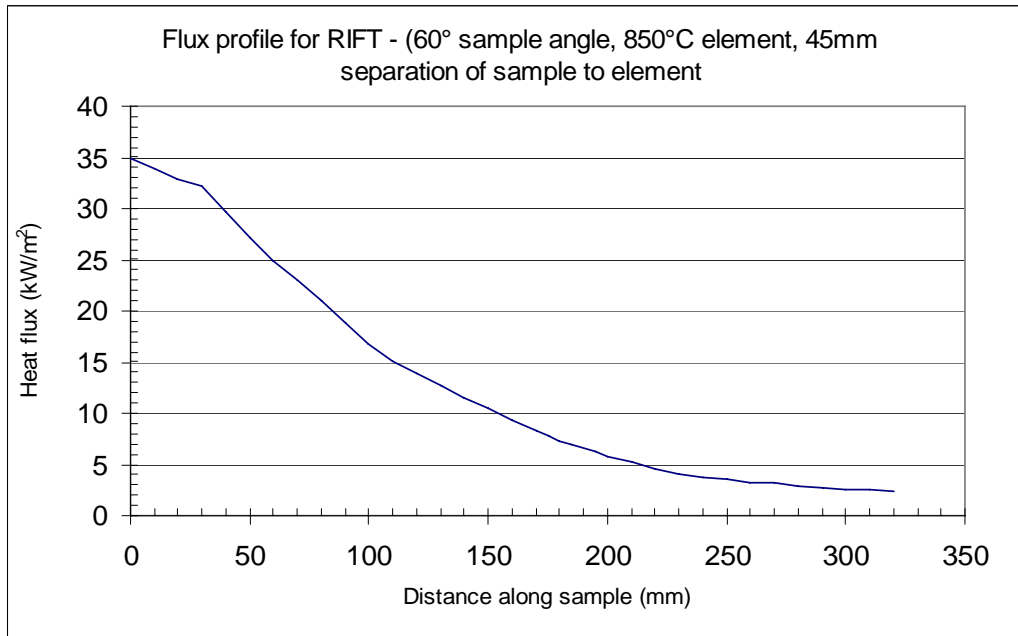


Figure 147: RIFT irradiance curve

As the initial 80mm of most timber based samples in the RIFT was unusable for the flame spread test due to excessive charring during the preheat period, the practical limit in order to get sufficient data is around $\dot{q}_s = 7\text{kW/m}^2$, giving flame spread measurements along to 180mm from the hot end of the sample. The rapid decay of the flux profile around this point makes the measurement of the flame spread velocity more difficult, as there is a significant change between each measuring point. Samples with a lower flame spread parameter Φ , which consequently have a lower flame spread velocity, will give more accurate results.

It is important that the markings on the sample match their position. A small variation of the actual position against the expected position (with the measured heat flux) will introduce errors in the RIFT measurements, due to the more rapid decay of the flux profile and the smaller resolution. As the LIFT has a shallower flux profile and a

longer sample area, it is not as critical in this regard. A tolerance of $\pm 2\text{mm}$ is listed for the LIFT. The LIFT uses a sample holder which is slid into place against a stop, allowing it to maintain the positioning, whereas the RIFT as currently designed has the sample slide directly into a sample holder frame, giving less consistent positioning, due to the effect of the aluminium foil backing bunching at the ends of the sample. The separate frame allows this to be taken into account when the sample is setup in the sample, so it can be zeroed accurately prior to insertion.

10.2.7 Comparison of ignition parameter “b”

The ignition parameter “b”, calculated from the ignition data, depends on the minimum ignition flux $\dot{q}_{ig,min}''$, which has been shown to be dependent on the ignition apparatus, as well as the data reduction, as excluding data points can make a significant difference to the final value. As a result, the value of the ignition parameter can be expected to vary between the ignition methods used. Figure 148 shows that the data from the LIFT tests tends to give slightly higher ignition parameter values for the materials tested. This is expected to be largely due to the higher $\dot{q}_{ig,min}''$ values that this ignition test gives compared with the ISO 5657 test.

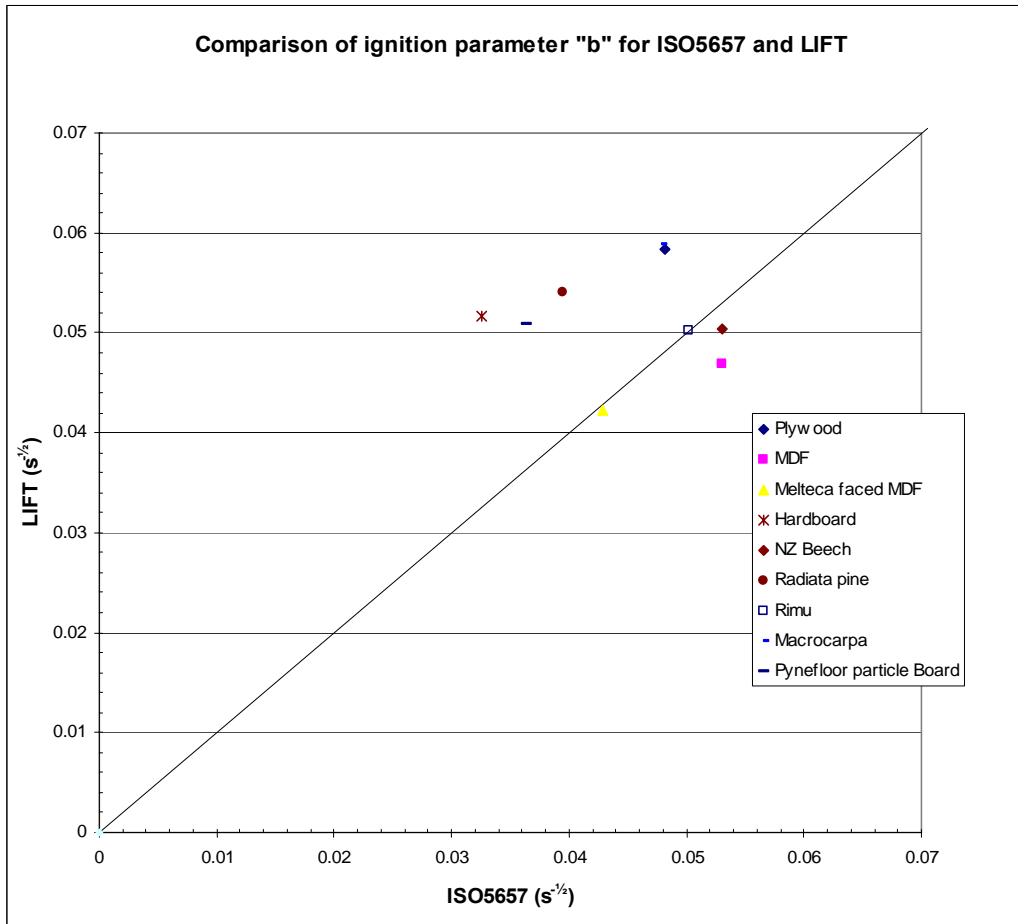


Figure 148: Comparison of ignition parameter "b" in ISO 5657 and LIFT

10.2.8 Flame spread parameter Φ

From equation (34), reproduced below in equation (46), the flame spread parameter depends on the ignition parameter "b" value. As noted previously, this can vary depending on the data reduction used, and the experimental apparatus. The effect this has can be seen by a 10% change in the ignition parameter value in the range of the materials tested, which leads to approximately a 17% reduction in the resulting flame spread parameter.

$$\phi = \frac{4}{\pi (Cb)^2} \quad (46)$$

Generally the flame spread parameters calculated from the RIFT tests are higher than those from the same material in the LIFT (Figure 149). The results based on the ISO 5657 ignition data show less scatter than those on the RIFT ignition tests, reflecting the variation in the ignition results using the RIFT for ignition testing.

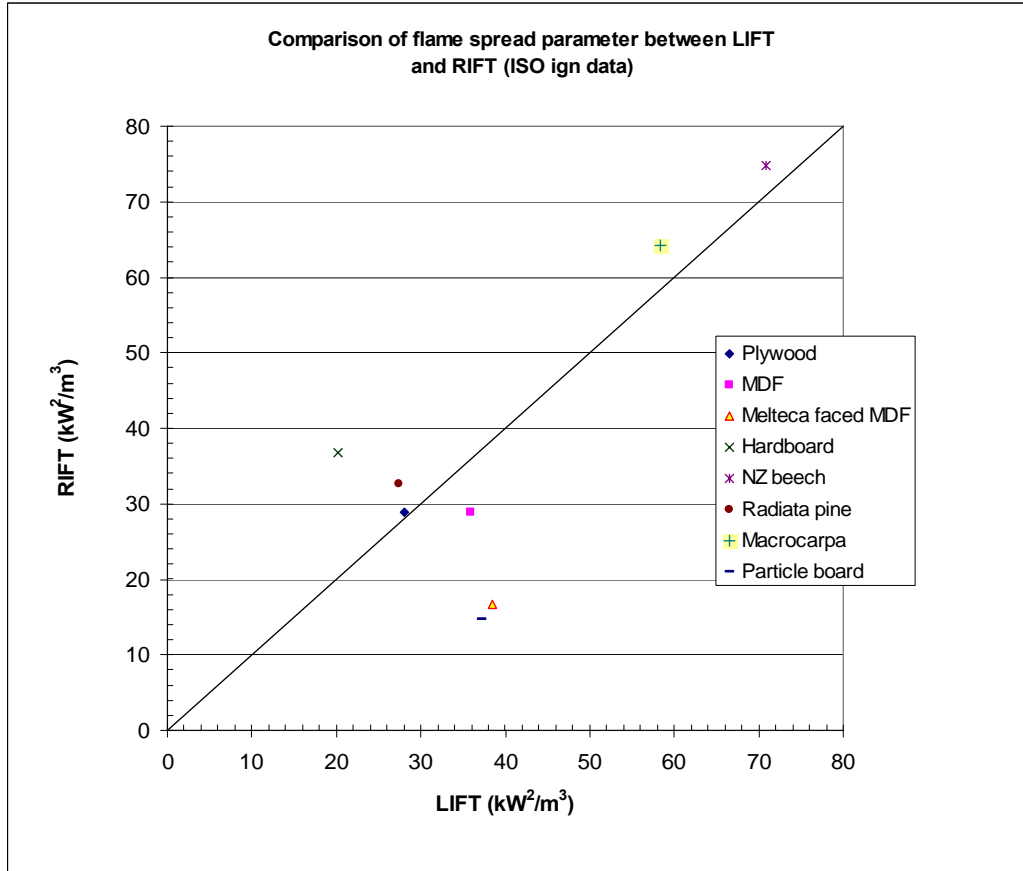


Figure 149: Comparison between flame spread parameter for LIFT and RIFT (using ISO 5657 ign data for RIFT)

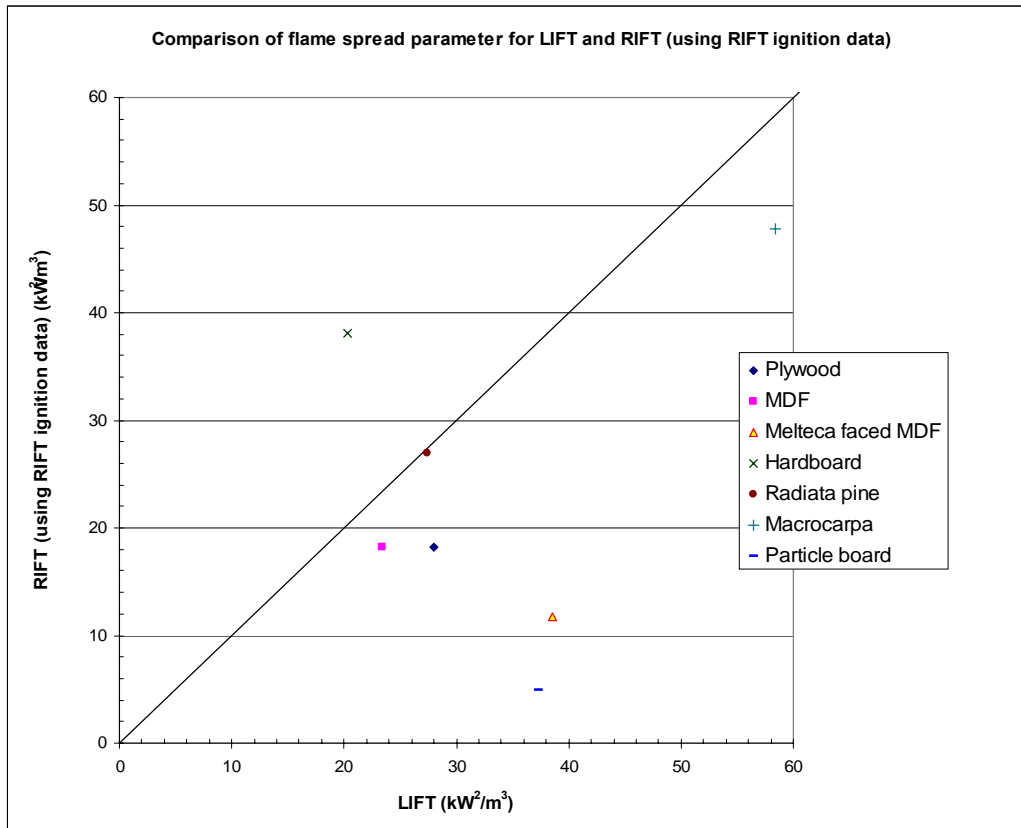


Figure 150: Comparison of flame spread parameter for LIFT and RIFT (using RIFT ignition data)

10.2.9 Minimum heat flux for flame spread

A limiting factor to the RIFT test is the minimum flux required for flame spread (\dot{q}_s), as if this value is too high, then there is insufficient flame spread distance to give accurate results. The results are generally comparable for the LIFT and RIFT (Figure 151). The outliers of Rimu and Melteca faced MDF are largely because the flame spread stops in the area where the profile is rapidly diminishing with a change of 4kW/m^2 over the 25mm measuring interval of the flux measuring template, so a small error in the location can have a large effect on the final outcome.

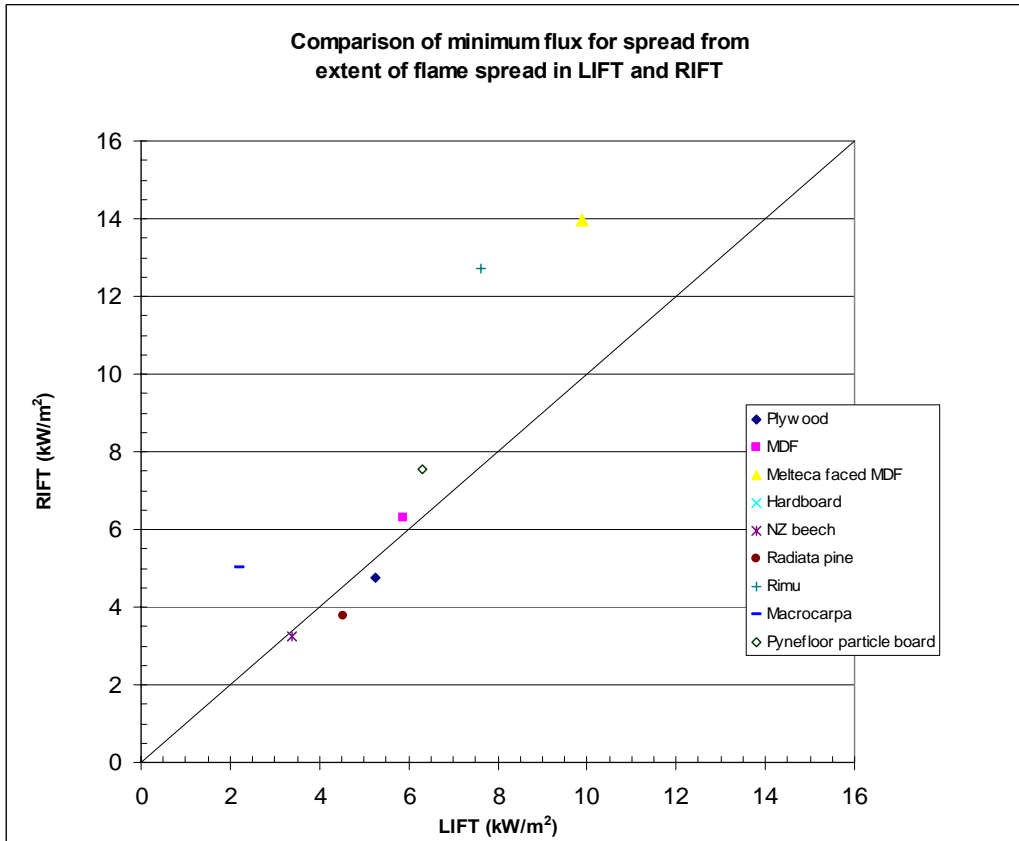


Figure 151: Comparison of minimum flux for flame spread \dot{q}_s'' in LIFT and RIFT

The results where there is a closer match are for materials where $\dot{q}_s'' < 7\text{kW/m}^2$, giving a practical limit to the RIFT test for materials to get comparable results. This limit does depend on the flame spread behaviour of the material, and the effect of charring due to the preheating. If the flame spread rate is sufficiently low, and data can be obtained over the area that is normally too heavily charred to ignite easily, then it may be possible to get useable data above this level. The value for the experimental minimum heat flux for flame spread \dot{q}_s'' is still going to have significant error due to the rapid change in the flux profile in the RIFT in this area.

Given that the minimum flux for spread is not known until the material is tested, an estimate of the likelihood of success of the RIFT flame spread test is necessary from the ignition tests. A comparison of the minimum ignition flux and the flux required for spread shows a poor correlation (Figure 152), however the products for which no flame spread results were possible (the Melteca faced boards, and Rimu) all have highest minimum ignition flux. This indicates there is an approximate limit for the

minimum ignition flux of $q_{ig,min} < 18 - 19 \text{ kW/m}^2$ for a successful flame spread test in the RIFT.

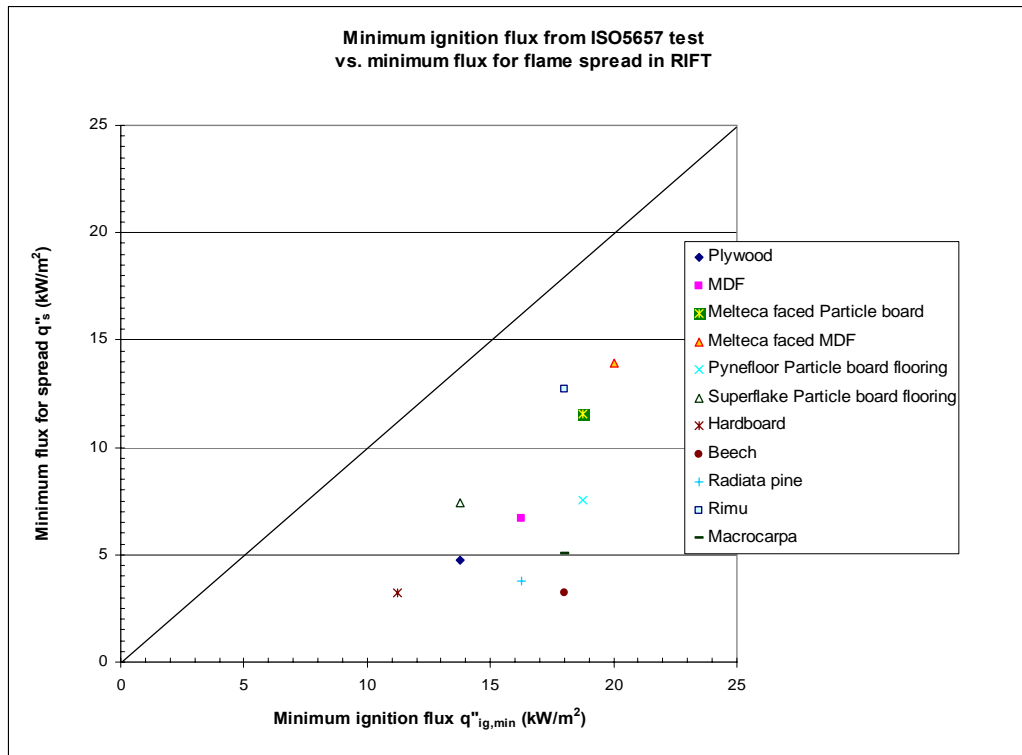


Figure 152: Minimum ignition flux from ISO 5657 test vs. minimum flux for spread for RIFT

10.3 Material and operational differences

10.3.1 Effect of preheating

Quintiere (1981, 1983, 1984), and the resulting ASTM LIFT standard calls for the material to be preheated so that the surface reaches equilibrium, and hence the time transient function $F(t) = 1$, simplifying the data reduction. It is also justified for fire modelling as the walls are expected to be heated by the fire in the compartment and it gives a more conservative approach as the calculated flame spread velocity will be higher. The process of preheating the material changes the material properties, such as drying the moisture from the wood, and charring or melting the material. These changes are not constant along the sample – the charring of the sample occurs at the hot end of the sample, where as the cold end is close to room temperature. With excessive preheating times the material can char to such an extent that the material

can no longer be ignited. This problem occurred with hardboard in the RIFT, which had a longer preheating time than in the LIFT due to the results of the ISO ignition test. The material charred to such an extent that it cracked and fell out or self ignited, so the shorter LIFT preheating time was used. This issue also occurred for the tests conducted by Nisted (1991) where some materials would not ignite when tested with the standard preheating period, so only half the preheat period was used on those materials.

Babrauskas (1999) reports that some of the materials tested, which covered a wider range of material types than these tests, gave more consistent results when no preheating period was used. The results from these tests indicate the opposite for these materials, with the flame spread rate and the correlations showing far more variation than when the material is preheated fully, for example, the results for particle board given in Figure 62 - Figure 65.

The issue of charring of the material during the preheating period makes the first 80mm in the RIFT, and 150-200mm in the LIFT effectively useless for flame spread measurements. The material is above the minimum ignition flux, so that the flame spread travels across the material in this region almost instantly.

The effect of preheating on the flame spread correlation and the slope of the data points, from which the flame spread parameter is calculated, is shown in Figure 153. The slope, which equates to the flame spread modulus C , decreases as the material is preheated until equilibrium is reached (i.e. $F(t)=1$), due to the scaling effect of the $F(t)$ time transient function.

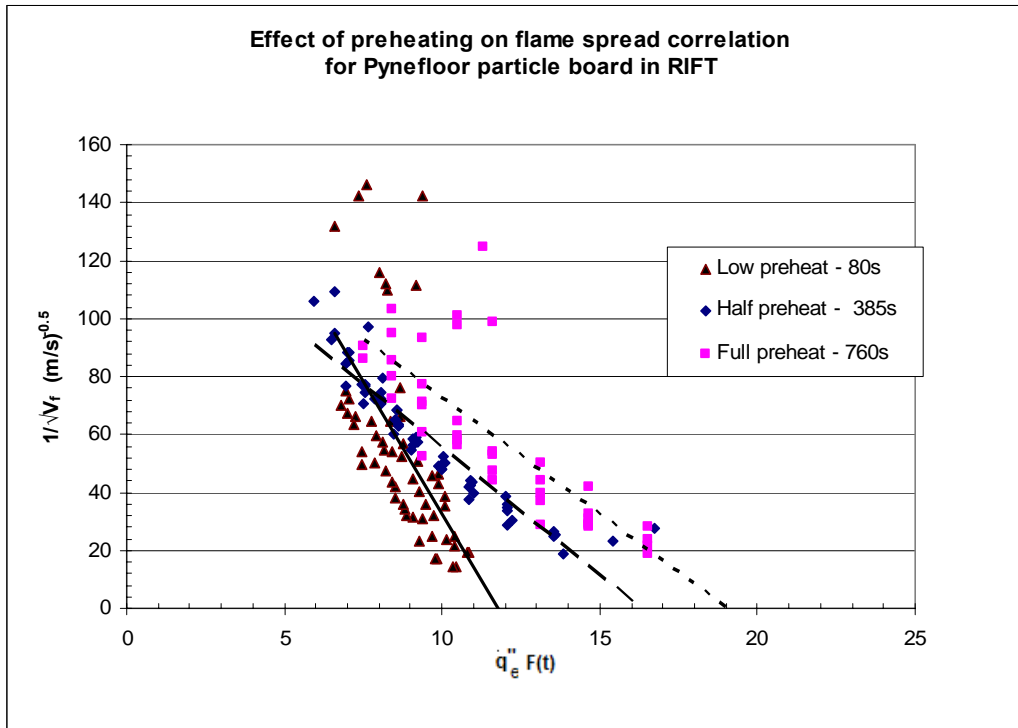


Figure 153: Effect of preheating on the flame spread correlation for Pynefloor in RIFT

The preheat times for Figure 153 were approximately 80 seconds, 385 and 760 seconds, where 755 seconds was the calculated time for the surface to reach equilibrium from the ISO 5657 ignition tests.

10.3.2 Effect of substrates on Melteca and facings on boards

It is apparent from the tests on the Melteca faced boards, outlined in Section 8.4.3 that having a layer with a higher minimum ignition flux over the comparatively more flammable substrate gives inconsistent results in the LIFT tests (, and these results are worse in the RIFT (Figure 97 and Figure 98) due to the smaller scale and more rapid decay of the flux profile.

10.3.3 Effect of thickness

There is a limitation on the theory given in the ASTM E 1321 LIFT standard that the material is assumed to be thermally thick. As an illustration of the effect of the sample thickness on the ignition time, 9mm and 17mm plywood with a 12mm lightweight Kaoboard insulated backing board were compared with ignition in the RIFT (Figure 154). At high heat fluxes, the time to ignition is the approximately the same, regardless of the thickness, as the thermal penetration depth is less than the sample

thickness. As the time to ignition increases, the thermal penetration is greater than the thickness of the thin sample, and as the backing board is a good insulator, there is little heat loss from the back of the sample into the backing board, hence the sample tends to become thermally thin, the sample temperature increases and the ignition time is less. With the thicker sample, there is still heat loss into the unheated part of the sample, leading to a longer ignition time.

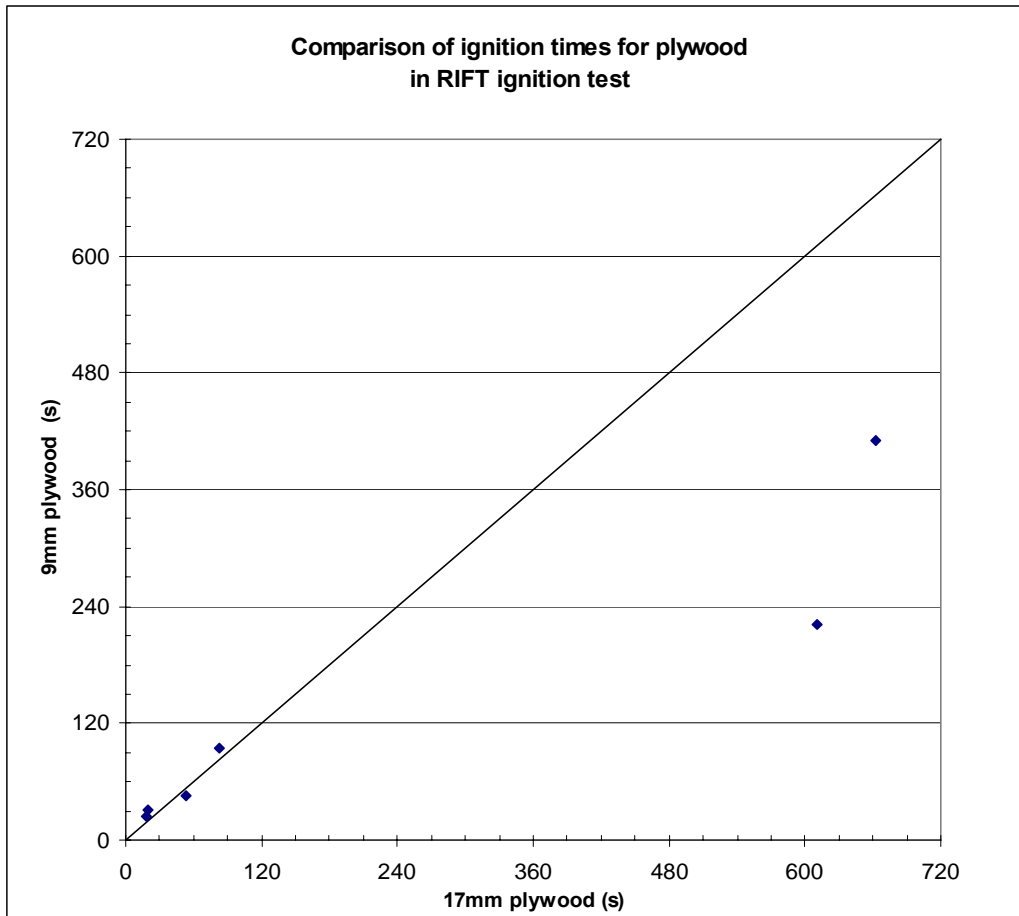


Figure 154: Comparison of ignition times for plywood in RIFT test

10.4 *Proposal for improved apparatus*

The objective of this research report was to investigate alternative methods to the ASTM LIFT for measuring flame spread properties. While the RIFT shows some success, the limitation on suitable materials in order to get sufficient and consistent flame spread data rules out the use of the RIFT for a lot of cases.

During the fabrication and use of the LIFT, it became apparent that it would be possible to reduce the size and cost of the apparatus and increase the control of the radiant panel by using modern elements and thermocouple controllers.

The flux profile over the first 150mm of the sample is almost constant, allowing the LIFT to be used ignition testing. If this section was eliminated, then the length of the sample can be reduced without reducing the resolution of the flame spread section. This can be achieved by changing the offset of the panel to the sample so that the level section of the flux profile is shorter. The panel size can therefore also be reduced. The ignition tests can still be done if the radiant panel can turn to be parallel with the face of the sample, and is on a slide, similar to the University of Canterbury LIFT, so that the spacing between the sample and the elements can be changed.

The major change would be to use thermocouple controlled radiant electric elements. These are capable of reaching 1000°C within 3 minutes and give a black body radiant spectrum. The thermocouple controllers will give an output with far less variation than that of the gas panel, and the temperature across the face will be more uniform.

One limitation is that the electrical elements cannot produce the same output as the gas panel, with the current supply of 20A/phase giving $\dot{q}_{50mm} = 50\text{kW/m}^2$. This is primarily an issue for the ignition tests where higher heat fluxes are required. Having the element bank able to move closer to the sample will allow higher heat fluxes for ignition.

This should allow for a testing method which is only slightly bigger than the ISO 5657 ignition testing apparatus. This compares with the 1.7m*0.9m footprint of the LIFT testing apparatus.

The initial work is to make a full scale replacement of the LIFT gas panel, which can also be used as a reduced scale panel by eliminating some of the elements as required.

This allows the effect of scale to be determined, and would easily allow the use the current LIFT apparatus for direct comparison. The full scale radiant panel measures 490mm x 300mm and uses 15 Elstein SHTS elements. Each element measures 95mm square and is mounted at 100mm centres, and has a maximum continuous temperature of 900°C and an output of 800W. This would give a $\dot{q}_{50mm} = 56\text{kW/m}^2$ at the standard LIFT layout, as shown in Appendix 2.

11 Comparison of data with published literature

There is little published data available from LIFT flame spread tests, reflecting the narrower focus of the test when compared to the cone calorimeter. As can be seen from the results, the variations between nominally similar materials can be significant if the preheating time is not adequate to get the material to equilibrium before ignition. Even within materials of the same type or source, the variation can be significant.

There is a greater availability of ignition data for materials, some of which is summarised in Babrauskas (2003). Again, nominally identical materials can give different results for the same properties, depending on the testing apparatus, procedure and correlations or ignition theory used (Babrauskas, 2003)

Comparisons have to be treated with caution, since apart from the materials used within the tests conducted for this report, they were not controlled. The materials often have a different base for the same nominal material. As an example the material basis is given as Douglas fir or Southern Pine for much of the literature which uses US construction plywood, and European plywood tests where the material details are specified are birch based. New Zealand plywood is generally Radiata Pine, other than specialty furniture and marine plywood.

There is little data on NZ native timbers, other than that published by Ngu (2002) and Henderson (1998). The complete list of thermal properties and comparisons is given in Appendix 5. The list of properties from the literature is limited to those approximately the same as those tested for this report, in regard to material composition and surface finish.

Not all the results can be compared, as much of the literature does not give the data

for values such as $\dot{q}_{ig,min}$.

11.1 Comparison of Ignition results with published literature

11.1.1 Thermal inertia ($k\rho c$)

The thermal inertia from the ignition tests generally compares well with the published data, as shown in Figure 155 - Figure 156 and Appendix 5

The thermal inertia plays a direct part in the flame spread calculation, given in equation (33). As can be seen from the results, there can be significant variation even with the same material, due to the correlations used and the effect of different testing methods. The detail of each material is given in Appendix 5 if it was specified in the original reference.

The round-robin test report by Fowell of the LIFT apparatus, reported that a 2:1 spread of results was not uncommon, despite testing the same material, using the same methods in different laboratories.

The thermal inertia for plywood could be expected to vary more than more homogeneous materials, due to the presence of voids in the material from bonding the ply. As this plywood was rated C/D grade, then some internal voids could be expected

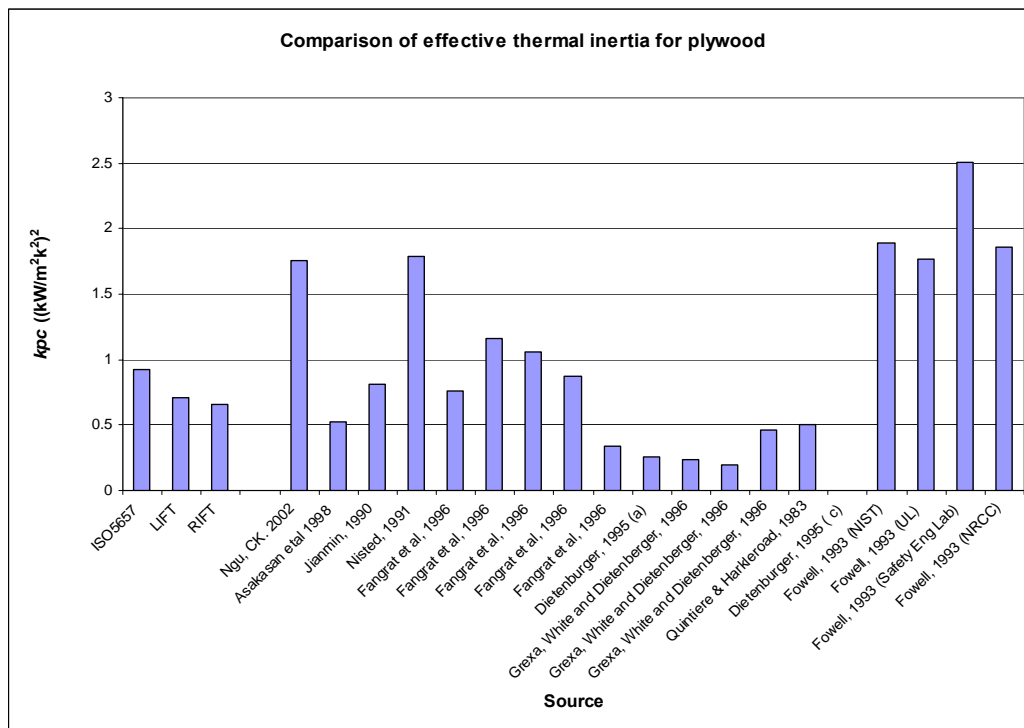


Figure 155: Comparison of thermal inertia of plywood

Particle board and fibreboard products, such as MDF and hardboard show much more consistent results than plywood, due to the more homogeneous nature of the material. Despite being made from the same base material, there is a significant difference between the thermal inertia of Pynefloor and Superflake particle board and between the results from different test methods on the same material.

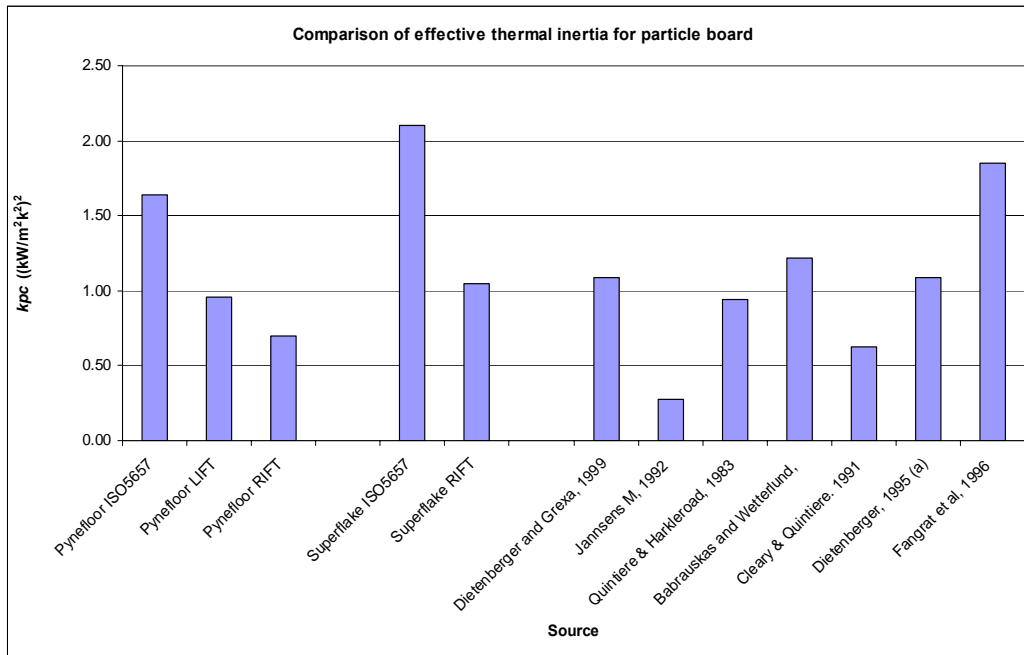


Figure 156: Comparison of thermal inertia of particle board

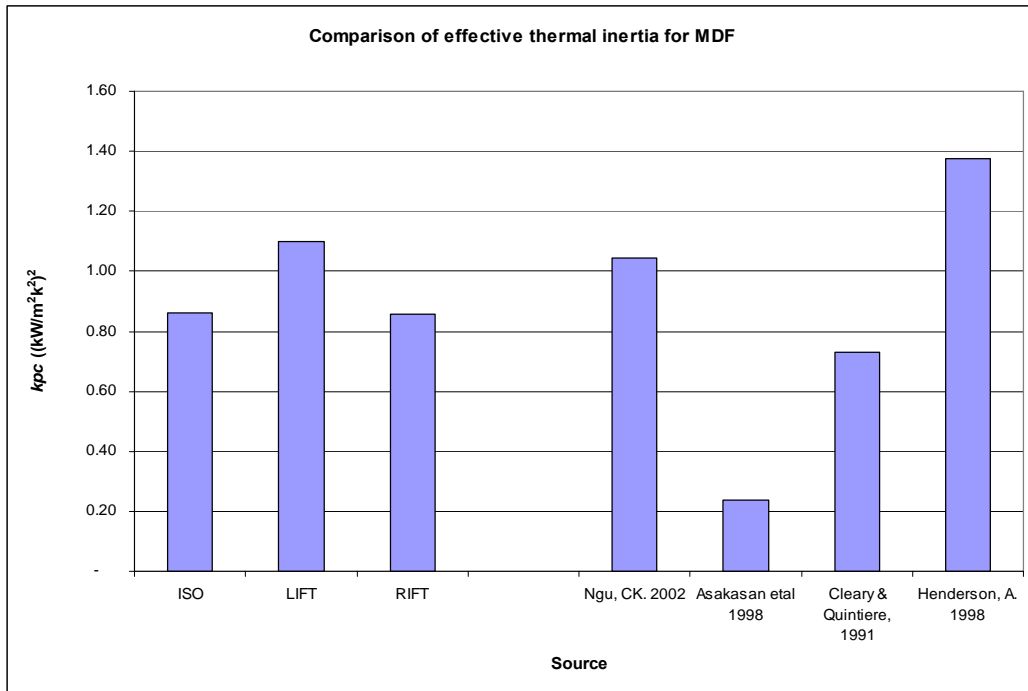


Figure 157: Comparison of thermal inertia of MDF

Since the definition of “hardboard” is not necessarily clearly defined, then some variation can be expected for this material (Figure 158). The results for Dietenberger come from a report on siding materials, so it may not be “hardboard” of the same type as tested in this report.

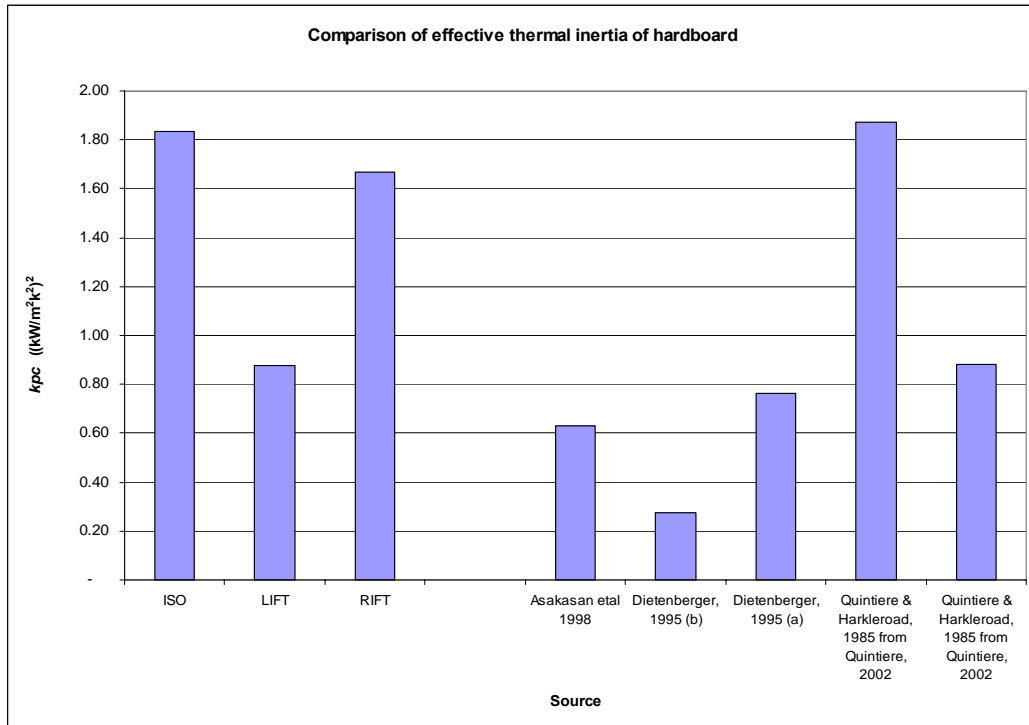


Figure 158: Comparison of thermal inertia of hardboard

When the thermal inertia for natural timbers is compared, there is much more variation.

The value for thermal inertia from Moghtaderi et al. (1997) for Radiata Pine, shown in Figure 159, is for US grown specimens at 15% moisture content. The others are for New Zealand grown Radiata Pine, and the results for Henderson (1998) were at 11% moisture content, and both were measured in the cone calorimeter.

Henderson (1998) got identical results for thermal inertia and ignition temperature for Rimu heart wood and sapwood, although the critical ignition flux was 20% higher for the heart wood over the sap wood.

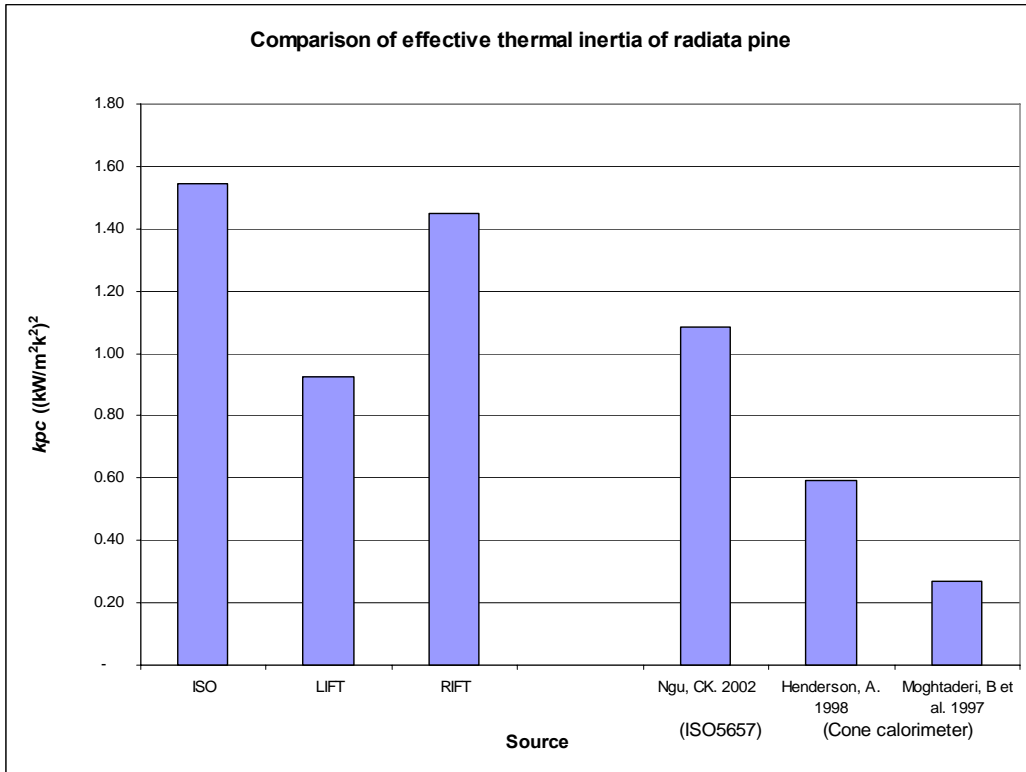


Figure 159: Comparison of thermal inertia of Radiata (Monterey) Pine

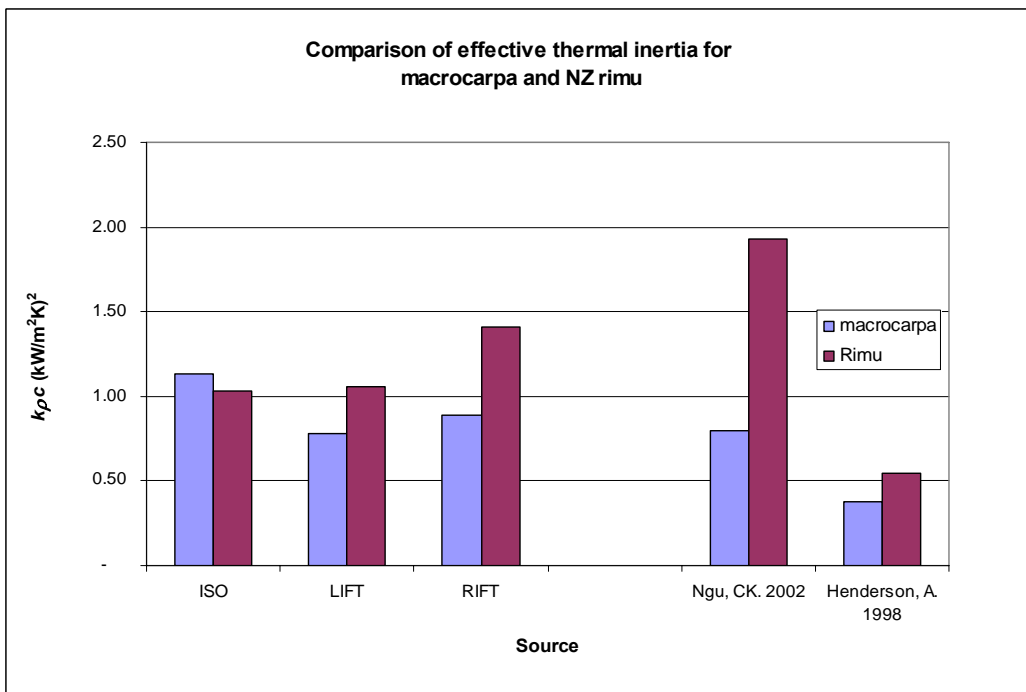


Figure 160: Comparison of thermal inertial of Macrocarpa and NZ Rimu

11.2 Comparison of published flame spread results

The significant effect of preheating on the results for the flame spread parameter has been covered previously in Section 10.3.1.

The results from Huynh (2003) should be taken with care, as the correlation obtained by Huynh of the flame spread results was poor, and the material was not preheated.

The results from Jinmen (1990) was calculated using the data given in the report by Jinmen as the flame spread parameter was not specifically stated as an outcome.

11.2.1 Flame spread parameter

The results for plywood show that the flame spread parameter results in these tests on New Zealand Radiata based plywood are generally higher than the published values in the literature for plywood.

The non-preheated results in the RIFT are comparable with those obtained by Huynh (2002), who also used Radiata pine plywood without preheating.

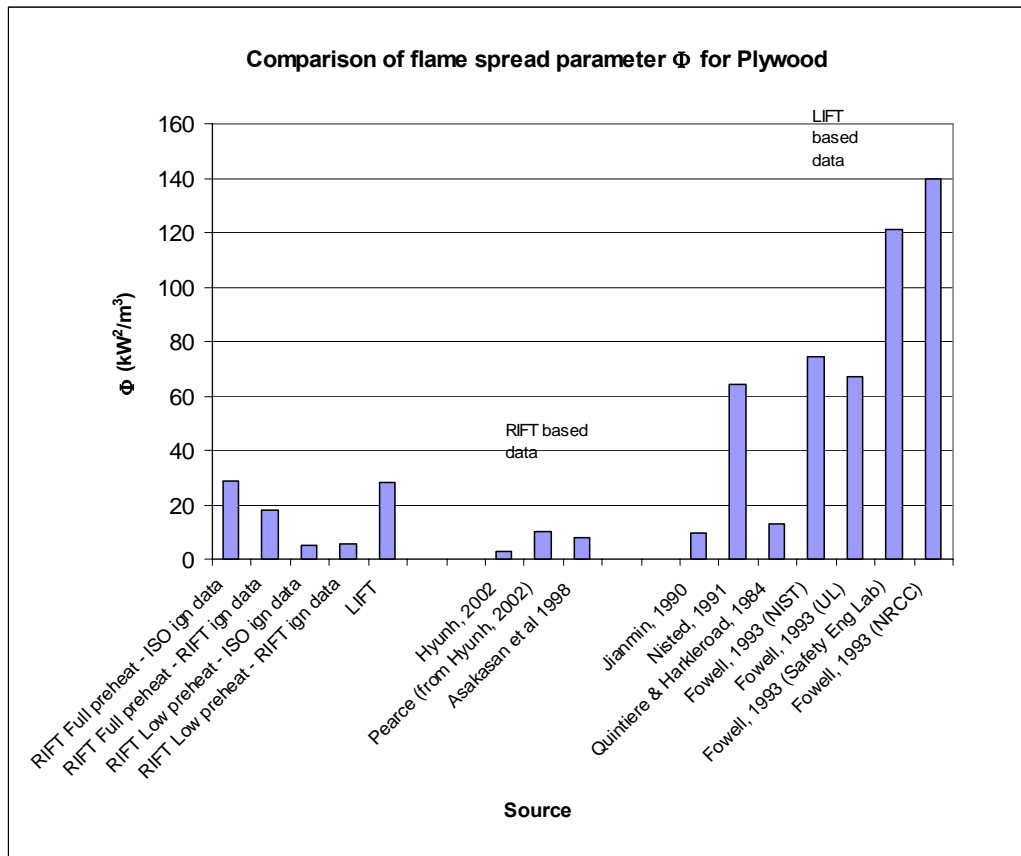


Figure 161: Flame spread parameter for plywood

The results for medium density fibreboard (Figure 162) show that the flame spread parameter for this material is greatly affected by the preheating time. Fibreboard is an ill-defined material, as it can cover a range of materials made from wood fibre, including low density ceiling panel material as well as medium and high density fibreboard, and the material specified as “fibreboard” by Azhakesan et al (1998) is not clearly defined as MDF. No density information was available in the original publication, and a comment was made that the value they obtained was lower than expected, and this value was expected to be around 13 kW²/m³.

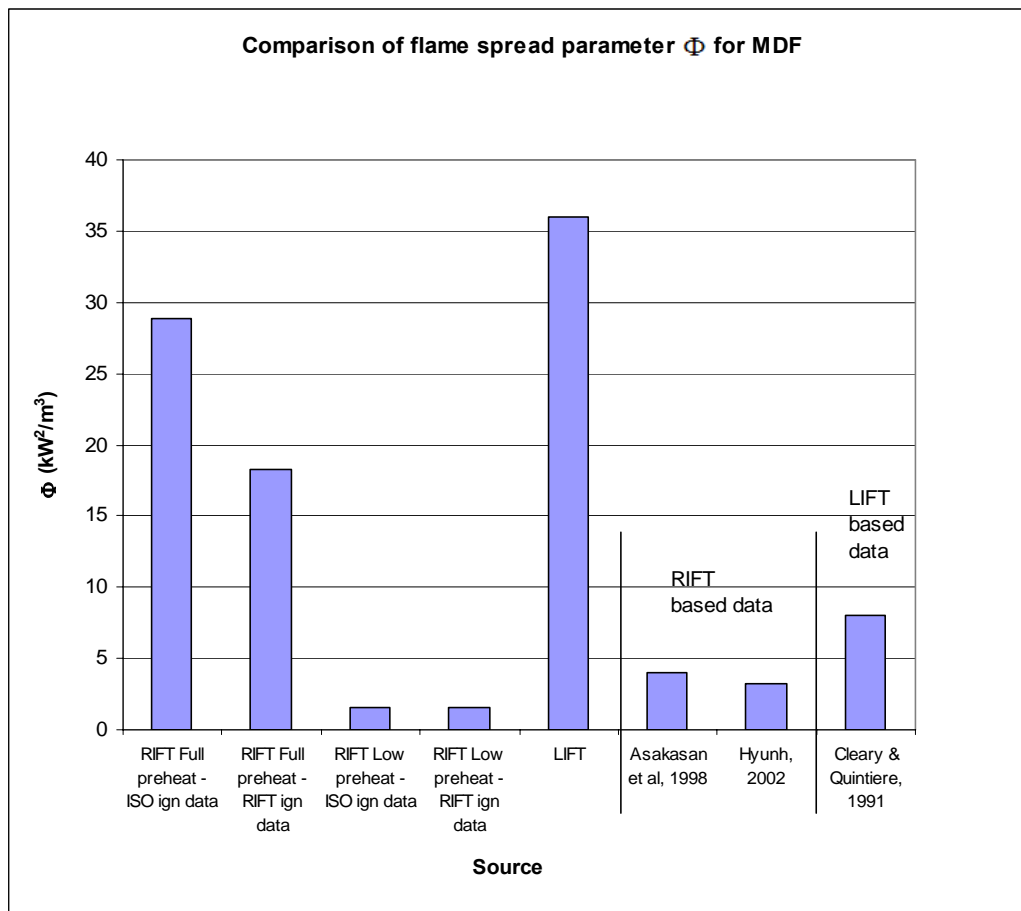


Figure 162: Comparison of flame spread parameter for MDF

Particle board is a commonly tested material in the LIFT literature, and much of the initial work on developing the theory was based on results for this material (Quintiere et al, 1981, 1983, 1984)

The results for the RIFT are similar to the published data, but significantly less than the results from the LIFT with the same material.

The results for a low preheating period are similar to Huynh (2002), which were also not preheated.

The particle board used by Cleary (1991), Quintiere and Harkleroad (1984) and Babrauskas (1999) were Douglas Fir based, as opposed to the results from these tests, and Huynh (2002), which were all Radiata Pine based.

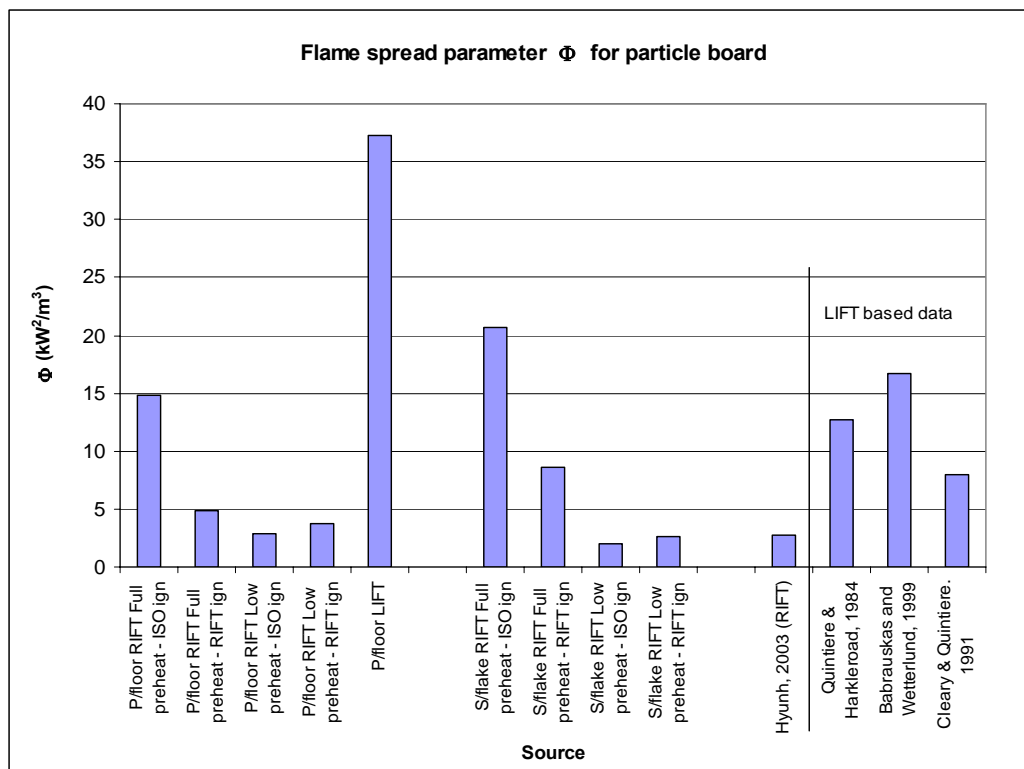


Figure 163: Flame spread parameter for particle board

12 Conclusions

A full-scale ASTM E 1321 Lateral ignition and Flame Transport (LIFT) apparatus was constructed and a reduced scale ignition and flame spread apparatus (RIFT) was built to fit the cone calorimeter in the vertical position. A series of lateral flame spread tests with 9 different types of timber based products were conducted, and Quintiere's flame spread model was applied to the results to obtain material properties. These materials included plywood, medium density fibreboard (MDF), hardboard, particle board flooring, Melteca covered MDF, Radiata Pine, NZ Rimu, Macrocarpa and New Zealand Beech. Further limited tests were conducted on Melteca covered particle board, and a second brand of particle board.

As only timber based products were tested, the conclusions regarding the suitability of the RIFT can only be in relation to these materials. Other materials may give different results from those obtained in these tests.

Test methodology

These tests were based on the procedures given in the ASTM standard, and were conducted using common materials with both sets of equipment, so the results could be compared. Ignition tests were conducted in the LIT, RIFT and ISO 5657 ignitability apparatus. The flame spread tests in the RIFT were done with a preheating period, as required by the ASTM standard, and also without the preheating period, to gauge the effect of preheating on the results.

The effect of sample preheating

If the sample was not preheated to equilibrium before the flame spread test, the resulting values for the flame spread parameter are lower than with a fully preheated sample. This reflects the lower flame front velocity across the sample due to the greater difference between the surface temperature and the material ignition temperature. Non preheated samples also had more scatter in the correlation results, and the extent of flame spread was less than for preheated samples, if the flame spread was faster than the material in ahead of the flame front could reach equilibrium. This gives a higher value for the heat flux required for flame spread (\dot{q}_s) than is actually

achievable, hence in a fire situation, where some preheating can be expected, the flame front will spread further than anticipated.

For comparable values to the LIFT, the testing method must be the same, so preheating is required in the RIFT in the same manner as the LIFT results.

The reduced scale flame test method

The RIFT method of flame spread testing has been shown to be successful for measuring flame spread properties; however, there are limitations on materials which can be reliably tested. These limitations are dictated by the smaller scale, such that the effects of errors on the results are more pronounced. The shape of the flux distribution profile along the sample has a sharp decay due to the directionality of the cone element, which leads to insufficient flame spread for accurate results for materials

where the flux required for flame spread $\dot{q}_s > 7 \text{ kW/m}^2$. This equates to a maximum

limit in the minimum flux for ignition $\dot{q}_{ig,min}$ of 18-19 kW/m^2 , although this limit is not clearly defined. It was not possible to get flame spread results for Rimu, yet Macrocarpa gave acceptable results, despite both materials having the same value of $\dot{q}_{ig,min}$.

Allied to the limitation of suitable materials dictated above, the material behaviour during flame spread is more critical. The smaller scale increases the effect of errors and erratic burning behaviour. The tests for Melteca covered MDF showed that the erratic behaviour caused by the Melteca facing meant that no reliable correlation was possible in the RIFT, even though a result was obtained in the LIFT.

Using the RIFT for the ignition tests proved to give inconsistent results and this most likely due to the design of the apparatus, which disrupts the airflow over the face of the sample. The ignition results which gave the best results when combined with the RIFT flame spread data came from the tests in the ISO 5657 ignitability apparatus.

A view factor calculation was developed for the RIFT, based on earlier work by Huynh (2002), and compared against experimental findings. The simplifications in the view factor model led to results that were consistently too low against the experimental findings, although the match of the shape of the resulting curve was good.

Flame spread parameter

The LIFT gives values for the ignition parameter “ b ”, used in calculating the flame spread parameter values, which are generally higher than those obtained in the ISO 5657 ignition test, leading to higher values for the flame spread parameter Φ for similar flame spread test results.

The flame spread parameter Φ calculated from the results in the RIFT, using the ISO ignition data is generally comparable to those obtained in the LIFT, although on average, the value tends to be higher than the value obtained in the LIFT. The more erratic ignition results for ignition tests in the RIFT give a wide variation in the flame spread parameter results, and this ignition method is not recommended.

The values for the minimum flux for heat spread are comparable between the RIFT and the LIFT, for values which are under the recommended limit for successful RIFT tests.

Ignition tests in the ISO 5657 apparatus generally gave faster times to ignition than the same material in the LIFT, with a difference of 4% overall. This difference is expected, but the magnitude of the difference is less than other tests in the literature. To get a more definitive result would require more ignition tests.

Generally, the flame spread correlation gave the expected results for the minimum ignition flux against the experimental values. The correlated value is higher than the experimental values, in line with the findings of Quintiere et al, 1983.

The University of Canterbury LIFT apparatus and future developments

This report also gives the first results of the new LIFT testing machine, built at the University of Canterbury in the first half of 2005. After initial teething problems, it has proven to give a consistent output. The burner is running on LPG, rather than methane, originally specified in the ASTM standard, due to problems with supply of methane or natural gas.

Due to the limitations imposed by LPG on the lowest flux levels possible by the burner, the burner position is adjustable using a 7/8” leadscrew to allow the burner to be positioned further away from the sample for lower flux levels during ignition tests. This has proven to be successful, achieving a minimum flux level at the sample face of 11kW/m^2 , and the lead screw allows for consistent positioning and fine adjustment.

The current air supply limits the burner output to a maximum sustained output of 50kW/m^2 at the sample face, although tests have shown that over 60kW/m^2 is possible if the air supply is available.

A modification to the design is proposed, using a thermocouple controlled radiant electric panel instead of the gas burner, which will give a more consistent output, and greater control than the gas panel can provide. Allied to this is a proposed intermediate/ bench scale test apparatus, which will give the same sample resolution and flame spread testing flux profile, yet allow the use of a smaller and less expensive apparatus than the current LIFT.

References

Anon. Elstein SHTS IR elements http://www.elstein.de/english/index_shts.htm.
Accessed 02-11-2005

Anon. Index of Species Information - species: Cupressus Macrocarpa. US Dept of Agriculture. US Forest Service. <http://www.fs.fed.us/database/feis/plants/tree/cupmac/>
Accessed 14-01-2006

Anon. Superflake materials safety data sheet. Fletcher Wood Panels, New Zealand.
Issued 1 December 2004

Anon. Production of Planted Production Forest Rough Sawn Timber for Year Ended 31 March 2004 for All Species. Ministry of Agriculture and Forestry, New Zealand. <http://www.maf.govt.nz/statistics/primaryindustries/forestry/production/annual-sawn-timber-highlights/aprodplantspec.htm>. Accessed 14-11-2005

Anon; Pynefloor Materials Safety Data sheet. Fletcher Wood Panels, New Zealand.
Issued 1 December 2004 <http://www.fwp.co.nz/pdf/products/Pynefloor%20MSDS.pdf>

Azhakesan, A. Shields, T. Silcock, G. Ignition and opposed flow flame spread using a reduced scale attachment to the cone calorimeter. Fire Technology, Vol 14, No. 2. 1998.

Azhakesan, A. Shields, T. Silcock, G. Combustibility parameters for enclosure lining materials obtained during surface flame spread using reduced scale ignition and flame spread technique. Fire Technology, Vol 34, No.3. 1998.

Azhakesan, A. Shields, T. Silcock, G. On the nature, influence and magnitude of flame heat transfer during surface flame spread. Fire Safety Journal, Vol 35. pp189 - 222. 2000.

ASTM E 1623 Standard Test Method for Determination of Fire and Thermal Parameters of Materials, Products, and Systems Using an Intermediate Scale

Calorimeter. American Society of Testing and Materials, ASTM International, West Conshohocken, PA. USA. 2004.

ASTM E 1354. Standard test method for heat and visible smoke release rates for materials using an oxygen consumption calorimeter. American Society of Testing and Materials, ASTM International, West Conshohocken, PA. USA. 2004.

ADJE1317. Adjunct to ASTM E 1321-97a. American Society of Testing and Materials, ASTM International, West Conshohocken, PA. USA. 2004.

ASTM E 1317-97a. Standard Test Method for Flammability of Marine Surface Finishes. American Society of Testing and Materials, ASTM International, West Conshohocken, PA. USA. 1997

Babrauskas, V. Cone calorimeter annotated bibliography 1982-1991, technote 1296. National Institute of Standards and Technology. Gaithersburg, 1991.

Babrauskas, V. Ten years of heat release research with the cone calorimeter. National Institute of Standards and Technology. Gaithersburg, MD. USA. 1992. Also available from <http://www.doctorfire.com/cone>

Babrauskas, V. Flame fluxes in opposed flow flame spread; a review of the literature. SP report 1995:06, SP Swedish National Testing and Research Institute, Sweden. 1995.

Babrauskas, V., Ignition of Wood: A Review of the State of the Art. Interflam 2001, Interscience Communications Ltd., London. 2001. pp. 71-88

Babrauskas, V. The cone calorimeter. Section 3, Chapter 3. SFPE Handbook of Fire Protection Engineering, 3rd edition. Editor Beyler C et al. Publ. NFPA, Quincy, MA. 2002.

Babrauskas, V. Ignition Handbook. Fire Science Publishers, Fire Science and Technology, Inc, Issaquah, WA, USA. 2003

Babrauskas, V. Wetterlund, I. Comparative data from LIFT and cone calorimeter tests on 6 products, including flame flux measurements. SP report 1999:14, SP Swedish National Testing and Research Institute, Sweden. 1999

Beyler, Craig L. Hunt, Sean P. Lattimer, Brian Y. Prediction of ISO 9705 Room/Corner Test Results. Volume 1. CGR/DC-215-99-I. Coast Guard Research and Development Centre, Groton CT, USA. November 1999. <http://stinet.dtic.mil/cgi-bin/GetTRDoc?AD=A378408&Location=U2&doc=GetTRDoc.pdf>

Cleary, T. Flammability Characterization with the LIFT Apparatus and the Cone Calorimeter. Fire Retardant Chemicals Association. Technical and Marketing Issues Impacting the Fire Safety of Building and Construction and Home Furnishings Applications. Spring Conference, 1992. Orlando, FL, Publ. Technomic Publishing Co., Lancaster, PA, 99-115 pp, 1992. <http://fire.nist.gov/bfrlpubs/fire92/art046.html>

Cleary, T. Quintiere, J. Framework for Utilizing Fire Property Tests - NISTIR 4619 .International Association for Fire Safety Science. Fire Safety Science. Proceedings. 3rd International Symposium. July 8-12, 1991, Edinburgh, Scotland, Publ. Elsevier Applied Science, New York, Editors Cox, G.; Langford, B. pp 647-656, 1991. <http://fire.nist.gov/bfrlpubs/fire91/art009.html>.

Comeford, J. The spectral distribution of radiant energy of a gas fired radiant panel and some diffusion flames. Combustion and Flame, vol 18, pp 125-132. 1972

Delichatsios, MA. A new interpretation of data from LIFT (Lateral Ignition and Flame Transport) apparatus and modifications for creeping flame spread. Interflam 99. Interscience Communications Ltd., London. 1999

Dietenberger, M. Protocol for Ignitability, Lateral Flame Spread, and Heat Release Rate Using Lift Apparatus. Nelson, G., editor. Fire and polymers II. Materials and tests for hazard prevention: Proceedings of 208th National meeting of the American Chemical Society; 1994 August 21-26; Washington, DC. ACS symposium series 599.

Washington, DC: American Chemical Society, 1995A. Chapter 29.
<http://www.fpl.fs.fed.us/documnts/pdf1995/diete95c.pdf>

Dietenberger, M. Experimental and analytical protocol for ignitability of common materials. Fire and Materials Journal, vol 19, pp89-94. 1995B.
www.fpl.fs.fed.us/documnts/pdf1995/diete95b.pdf

Dietenberger, M. Ignitability Analysis of Siding Materials Using Modified Protocol for Lift Apparatus. Fire and Materials, VOL. 20, 115-121. 1996A.
www.fpl.fs.fed.us/documnts/pdf1996/diete96a.pdf

Dietenberger, M. Ignitability analysis using the cone calorimeter and lift apparatus Proceedings of the International Conference on Fire Safety: July 22-26, 1996, Columbus, OH. Volume 22. pp 189-197. 1996B
<http://www.treesearch.fs.fed.us/pubs/8878>

Drysdale, D. An introduction to fire dynamics, 2nd edition. J Wiley & sons, Chichester, UK. March 2003.

Fowell, A. Interlaboratory test program on ASTM E 1321: Standard test method for measuring material ignition and flame spread properties. Second edition, American Society of Testing and Materials, ASTM International, West Conshohocken, PA. USA. November 1994

Grand AF, Mehrafza, M. Evaluation of the effectiveness of fire resistant durable agents on residential siding using an ICAL based testing protocol. Fire and materials 2001. 7th international conference and exhibition. Proceedings. Interscience communications limited. January 22-24, 2001, San Antonio, Texas, USA. pp 241-248, 2001.

Goransson, U. Using the cone calorimeter to predict flame spread. Nordtest project 882-90. SP Report AR1991:32. Fire Technology, Boras, Sweden, 1990

Hagge, M. Bryden, K, Dietenberger, M. Effects of backing board materials on wood combustion. Wood & fire safety : proceedings, 5th international scientific conference, April 18-22, 2004 . Faculty of Wood Sciences and Technology, Technical University of Zvolen, Slovak Republic. pp51-58.2004. <http://www.treesearch.fs.fed.us/pubs/7019>

Henderson, A. Predicting Ignition Time Under Transient Heat Flux Using Results from Constant Flux Experiments. University of Canterbury, Christchurch, New Zealand . 1998

Hilado, C. Flammability test methods handbook. Technomic Publishing Co. Westport, Conn, USA. 1973

Howell, J. A catalog of radiation heat transfer view factors, 2nd edition. <http://www.me.utexas.edu/~howell/index.html>. Accessed 14-01-2006

Huynh. CK. Flame spread measurements of New Zealand timber using a modified cone calorimeter. University of Canterbury, Christchurch, New Zealand. 2003.

ISO 5657 – 1986. Method of Measuring the Ignitability of Products Subjected to Thermal Irradiance. International Organisation of Standards, Geneva, Switzerland 1986

ISO5660. Reaction to fire tests – heat release rate, smoke production and mass loss rate – part 1. Cone calorimeter method. International Organisation of Standards, Geneva, Switzerland. 2002

ISO 9705. Full scale room fire test for surface finishes. International Organisation of Standards, Geneva, Switzerland. 1993

Janssens, M. Fire test and evaluation methods. APEC Timber and Fire conference, BRANZ New Zealand. Wellington 2005. <http://www.branz.co.nz/branzltd/pdfs/MarcJanssens.pdf>

Janssens, M. L.; Kimble, J.; Murphy, D. Computer Tools to Determine Material Properties for Fire Growth Modelling From Cone Calorimeter Data. Fire and

Materials 2003. 8th International Conference. Conference Papers. Proceedings. .January 27-28, 2003, San Francisco, CA, pp 377-387, 2003. Interscience Communications Limited, New York. USA
<http://fire.nist.gov/bfrlpubs/fire03/art044.html>

Jianmin, Q. Prediction of flame spread test results using the test data from the cone calorimeter. SP Report 1990:38. Fire Technology, Boras, Sweden, 1990

Leung, C. Yuen W. Chow. W. A practical model of flame spreading over materials. Proceedings of the 6th ASME-JSME Thermophysics Conference, March 16-23, Hawaii, USA. 2003. http://www.engineering.ucsb.edu/~yuen/current_paper/TED-AJ03-128.pdf

Ngu. Ignition of New Zealand timber University of Canterbury, Christchurch, New Zealand. 2002

Nisted, T. Flame spread experiments in bench scale: project 5 of the Eurfic fire research programme. Dantest. Denmark. April 1991

Karlsson, B and Quintiere, J. Enclosure Fire Dynamics. CRC Press, Boca Raton, Florida. USA. 2000

Pauner, MA. Nordic Round Robin and Investigation on IMO Resolution A. 653 (16) TR 529. Nordtest. Finland. April 2003.

Pease, T. "A study of surface flame spread using a modified cone calorimeter". Undergraduate final year project. Department of Chemical Engineering. University of Newcastle, Australia. 2001

Perrin, M. A comparison between cone calorimeter and LIFT flame spread data. Undergraduate final year project. Department of Chemical Engineering. University of Newcastle, Australia. 2002

Persson, B. On the prediction of lateral flame spread based on cone calorimeter data. SP Report 1993:28. Fire Technology, Boras, Sweden, 1993

Quintiere, J. A simplified theory for generalizing results from a radiant panel rate of flame spread apparatus. Fire and Materials, Vol 5, No. 2. 1981

Quintiere, J. Harkleroad. Walton, D. Measurement of flame spread properties. Combustion Science and Technology, Vol 32. pp 67-89. 1983

Quintiere, J. Harkleroad, M. New concepts for Measuring flame Spread Properties NBSIR 84-2943. National Institute of Standards and Technology. Gathersburg, MD. USA. November 1984.

Quintiere, J. Principles of fire behaviour. Delmar publishers, USA. 1998

Quintiere, J. Surface flame spread. Chapter 12, Section 2, SFPE Handbook of Fire Protection Engineering, 3rd edition. Editor Beyler C et al. Publ. NFPA, Quincy, MA. 2002

Rasbash, D. Ramachandran, G. Kandola, B. Watts, J. law. M. Evaluation of fire safety. J Wiley and Sons, Chichester, UK. 2004.

Robertson, A. Ohlemiller, T. Low heat flux measurements: some predictions. Fire Safety Journal, Vol. 25, No. 2, 109-124, September 1995

Shields, T. Silcock, G. Murray, J. The effects of geometry and ignition mode on ignition times obtained using a cone calorimeter and ISO ignitability apparatus. Fire and Materials, Vol 17, pp 25-32. 1993

Shields TJ. Silcock, G. Murray, J. Evaluating ignition data using the flux time product. Fire and Materials, Vol 18. pp 243-354. 1993

Spearpoint, M. Huynh, M. Moghtaderi, B. Merryweather, G. Flame spread measurements of New Zealand timber using an adaptation of the cone calorimeter.

APEC Timber and Fire conference, Wellington, New Zealand, 2005.
<http://www.branz.co.nz/branzltd/pdfs/MichaelSpearpoint.pdf>

Smith, S. Effects of moisture on combustion characteristics of live California chaparral and Utah foliage. A thesis submitted to the faculty of Brigham Young University in partial fulfilment of the requirements for the degree of Master of Science. Department of Chemical Engineering Brigham Young University, Utah, USA. August 2005

Simpson, W and TenWolde, A. Physical properties and moisture relations of wood. Ch. 3. Wood handbook - Wood as an engineering material. Gen. Tech. Rep. FPL-GTR-113. Forest Products Laboratory Madison, WI: U.S. Department of Agriculture, Forest Service, Forest Products Laboratory. 1999

White, R and Dietenberger, M. Fire Safety. Ch 17, Wood handbook - Wood as an engineering material. Gen. Tech. Rep. FPL-GTR-113. Forest Products Laboratory Madison, WI: U.S. Department of Agriculture, Forest Service, Forest Products Laboratory. 1999

White, R and Dietenberger, M. Cone Calorimeter evaluation of wood products. 15th Annual conference on flame retardancy 2004.
http://www.fpl.fs.fed.us/documnts/pdf2004/fpl_2004_white002.pdf (accessed Jan 2006)

Wilson MT; Dlugogorski BZ and Kennedy EM, “Uniformity of Radiant Heat Fluxes in Cone Calorimeter”, Process Safety and Environmental Protection Group, The University of Newcastle, Callaghan, Australia, 7th Symposium in Fires Science in Worcester, USA, 2002.

Younquist, J. Wood based products and panel products. Chapter 10. Wood handbook - Wood as an engineering material. Gen. Tech. Rep. FPL-GTR-113. Forest Products Laboratory, Madison, WI: U.S. Department of Agriculture, Forest Service, Forest Products Laboratory. 1999

Appendix 1: Procedure for operating University of Canterbury LIFT

The gas supply to the main radiant panel is controlled by a mass flow controller, and the compressed air supply is adjusted through an air regulator and ball valve (Figure 164). The ball valve allows the regulator to be used in the optimum range by providing a bulk adjustment to the output restriction. Without the ball valve set to give a minimum of 6-8 psi on the gauge, the regulator will fluctuate. The limiting flux output without preloading the regulator is where $q_{50mm}^{\prime\prime} < \text{approximately } 26\text{kW/m}^2$. Closing the ball valve part way loads up the regulator to 6-8psi and gives a stable output.

The pilot burner uses a mass flow controller for the air supply, and a separate LPG supply.

Starting the LIFT panel

- Insert the measurement template into the sample holder and fit the flux gauge in the 50mm position, so the face of the flux gauge is level and parallel with the face of the template.
- Turn on the water supply to the flux gauge.
- Close the ball valve so the air is turned off.
- Turn on gas and ignite the panel and set the gas output to the desired value on the mass flow controller by adjusting the set point adjustment (Figure 165).
- Slowly open the ball valve and adjust the air supply with the regulator and ball valve so that the regulator reads a minimum of 8 psi. Leave the mixture slightly rich, shown by the yellow flame tips, until the temperature and flux output has stabilised. As the burner heats up, it tends towards a leaner gas mixture and can flash back inside the burner.

Adjustments are made by either increasing the gas flow or decreasing the air so that gas mixture is rich during the flux alteration, so it doesn't flash back inside the burner. Once the burner is stable, which usually takes around 5 minutes, then the gas mixture can be adjusted for a neutral mix. Monitor the flux meter for a further time of approximately 5 minutes to ensure that it is stable.

Extinguish the radiant panel by turning off the air supply first and then the gas supply



Figure 164: Regulator and ball valve.

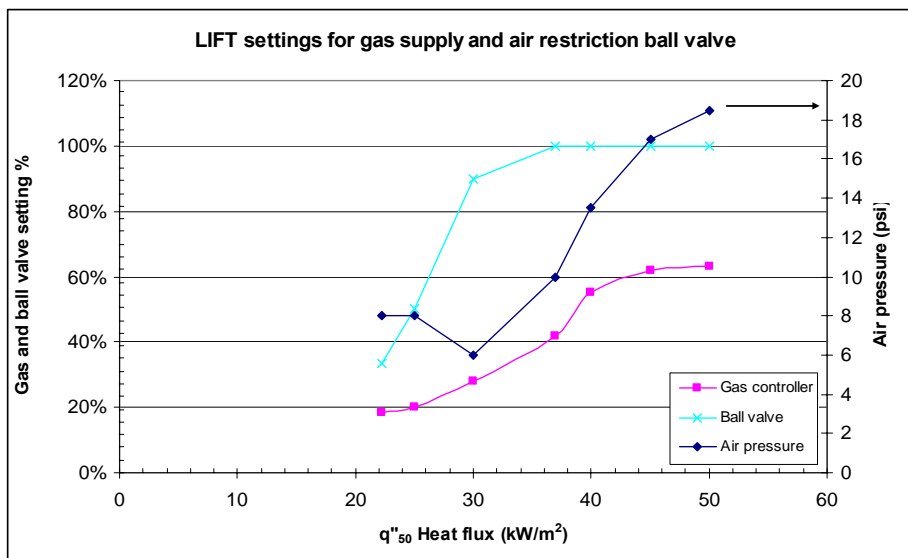


Figure 165: LIFT settings

Setting the pilot flame

Set the air supply flow rate to minimum and turn off the pilot air supply mass flow controller and turn on the pilot burner gas supply and ignite the pilot flame. Turn on the air supply and adjust the gas needle valve and regulator and air supply to give a blue pilot flame approximately 180mm long. The flame mixture usually has to be slightly rich to be stable with the air turbulence during an ignition test. Once the pilot flame is set, further adjustment is not usually required.

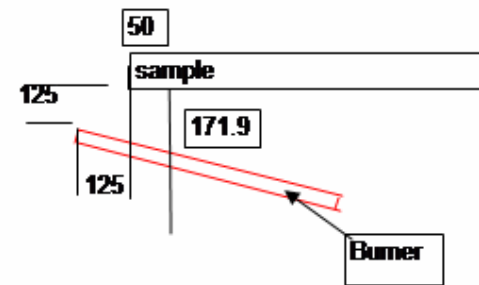
Appendix 2: Electrical power and current requirements for an electric LIFT radiant panel

Angle of sample to element

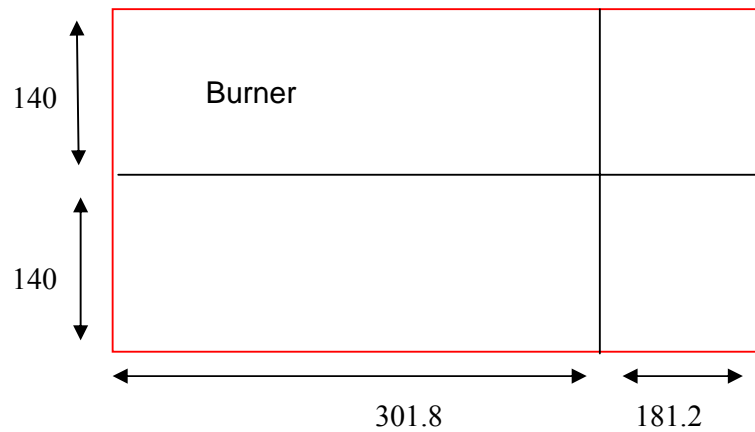
15 deg

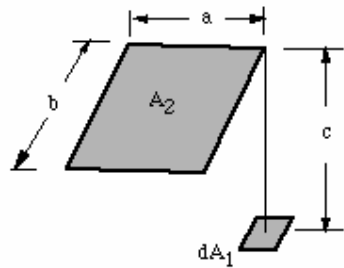
Flux at 50mm point on sample

50.5 kW/m²



Standard LIFT panel dimensions:





$$F_{d1-2} = \frac{1}{2\pi} \left\{ \frac{A}{(1+A^2)^{1/2}} \tan^{-1} \left[\frac{B}{(1+A^2)^{1/2}} \right] + \frac{B}{(1+B^2)^{1/2}} \tan^{-1} \left[\frac{A}{(1+B^2)^{1/2}} \right] \right\}$$

From: Howell, <http://www.me.utexas.edu/~howell/index.html>

Area of panel segment (in line with 50mm point)

A1 = A2	0.042252 m ²
a3=a4	0.025368 m ²
Panel width	0.28 m
Panel length	0.483 m
Element temp	1140.5 K

Stefan-Boltzman const. σ

5.67E-08 Wm²/K⁴

Emissivity ϵ

0.99 (from Wilson et al for a cone calorimeter element)

$$\dot{q}_{A1:A2} = F \cdot \sigma \epsilon \cdot (T)^4$$

a	0.140 m
b	0.302 m
c	0.172 m

$F_{(A1,A2)}$ (View factor)

0.147

$q_{A1:A2}$

13979 W/m²

$q_{A3:A4} = F \cdot \sigma \epsilon (T)^4$

a

0.14 m

b

0.181 m

c

0.172 m

$F_{(A3,A4)}$ (View factor)

0.128

$q_{A3:A4}$

12143 W/m²

$q_e =$

52243

Radiation received at point (angled 15 deg)

50463 W/m² received at point

Radiation on sample

50.5 kW/m² at 50mm sampling point

Element emitted heat flux

95.0 kW/m² emitted from surface of element

Element area

0.135 m²

Element power

12.8 kW

current (240v)

54 Amps if electrically powered at 240v

Appendix 3: Results of material tests

Ignition test results

MDF – 18mm	LIFT	ISO 5657-1986	Ngu (ISO 5657)	Ignition in RIFT	
Ignition parameter b	0.047	0.053	0.043	0.053	$s^{0.5}$
intercept of ignition parameter graph $(t^*)^{0.5}$	21	19	23	19	$s^{0.5}$
Preheat time t^*	456	355	544	357	sec
Critical ignition flux q_{crit}	3.4	3.7	4.7	-0.3	kW/m^2
Thermal inertia kpc	1.10	0.86	1.04	0.86	$(kW/m^2K)^2$
Minimum ignition flux $q_{ig,min}$	16.25	16.25	13.5	16.25	kW/m^2
Heat transfer coefficient at ignition h	0.044	0.044	0.039	0.043	kW/m^2K
Ignition temperature T_{ig}	391	391	348	391	$^{\circ}C$
Plywood - 17mm	LIFT	ISO 5657-1986	Ngu (ISO 5657)	Ignition in RIFT	
Ignition parameter b	0.058	0.048	0.034	0.061	$s^{0.5}$
intercept of ignition parameter graph $(t^*)^{0.5}$	17	21	29	17	$s^{0.5}$
Preheat time t^*	293	432	870	273	sec
Critical ignition flux q_{crit}	7.2	4.6	7.2	9.9	kW/m^2
Thermal inertia kpc	0.71	0.93	1.76	0.66	$(kW/m^2K)^2$
Minimum ignition flux q_{crit}	16.3	13.8	12.0	16.3	kW/m^2

Heat transfer coefficient at ignition h	0.044	0.041	0.040	0.043	kW/m ² K
Ignition temperature T_{ig}	391	352	321	391	°C
Melteca faced MDF	LIFT	ISO 5657-1986	Ignition in RIFT		
Ignition parameter b	0.0423	0.0429	0.051		s ^{0.5}
intercept of ignition parameter graph $(t^*)^{0.5}$	24	23	19.5		s ^{0.5}
Preheat time t^*	560	542	382		sec
Critical ignition flux q_{crit}	-6.44	2.58	1.06		kW/m ²
Thermal inertia kpc	1.475	1.474	1.07		(kW/m ² K) ²
Minimum ignition flux $q_{ig,min}$	18.75	20	21.25		kW/m ²
Heat transfer coefficient at ignition h	0.045	0.046	0.047		kW/m ² K
Ignition temperature T_{ig}	440	425	454		°C
Melteca/ Particle board	LIFT	ISO 5657-1986	Ignition in RIFT		
Ignition parameter b	Not tested	0.044	0.057		s ^{0.5}
intercept of ignition parameter graph $(t^*)^{0.5}$	Not tested	22.6	17.5		s ^{0.5}
Preheat time t^*	Not tested	512	308		sec
Critical ignition flux q_{crit}	Not tested	2.00	10.1		kW/m ²
Thermal inertia kpc	Not tested	1.27	0.97		(kW/m ² K) ²
Minimum ignition flux $q_{ig,min}$	Not tested	18.75	23.75		kW/m ²
Heat transfer coefficient at ignition h	Not tested	0.044	0.050		kW/m ² K
Ignition temperature T_{ig}	Not tested	425	478		°C

Pynefloor particle Board	LIFT	ISO 5657-1986		
Ignition parameter b	0.0509	0.0364	0.063	$s^{0.5}$
intercept of ignition parameter graph $(t^*)^{0.5}$	19.6	27.5	16	$s^{0.5}$
Preheat time t^*	385.6	754.6	250	sec
Critical ignition flux q_{crit}	1.7	3.5	4.3	kW/m^2
Thermal inertia kpc	0.96	1.64	0.70	$(kW/m^2K)^2$
Minimum ignition flux $q_{ig,min}$	18.75	13.75	21.25	kW/m^2
Heat transfer coefficient at ignition h	0.044	0.041	0.047	kW/m^2K
Ignition temperature T_{ig}	425	352	454	$^{\circ}C$
Superflake particle board	LIFT	ISO 5657-1986	Ignition in RIFT	
Ignition parameter b	Not tested	0.0327	0.05	$s^{0.5}$
intercept of ignition parameter graph $(t^*)^{0.5}$	Not tested	30.6	19.72	$s^{0.5}$
Preheat time t^*	Not tested	935	389	sec
Critical ignition flux q_{crit}	Not tested	3.44	5.24	kW/m^2
Thermal inertia kpc	Not tested	2.11	1.05	$(kW/m^2K)^2$
Minimum ignition flux $q_{ig,min}$	Not tested	13.75	18.75	kW/m^2
Heat transfer coefficient at ignition h	Not tested	0.042	0.05	kW/m^2K
Ignition temperature T_{ig}	Not tested	352	424.87	$^{\circ}C$

Hardboard	LIFT	ISO 5657-1986	Ignition in RIFT		
Ignition parameter b	0.052	0.033	0.032		$s^{0.5}$
intercept of ignition parameter graph $(t^*)^{0.5}$	19	31	31.3		$s^{0.5}$
Preheat time t^*	375	944	977		sec
Critical ignition flux q_{crit}	2.172	- 0.588	2.6		kW/m^2
Thermal inertia kpc	0.88	1.83	1.67		$(kW/m^2K)^2$
Minimum ignition flux $q_{ig,min}$	17.5	11.25	11.25		kW/m^2
Heat transfer coefficient at ignition h	0.043	0.039	0.037		kW/m^2K
Ignition temperature T_{ig}	409	307	307		$^{\circ}C$
NZ Beech	LIFT	ISO 5657-1986	Ngu (ISO 5657)	Ignition in RIFT	
Ignition parameter b	0.050	0.053	0.025	0.034	$s^{0.5}$
intercept of ignition parameter graph $(t^*)^{0.5}$	20	19	40	29.1	$s^{0.5}$
Preheat time t^*	395	355	1,618	844	sec
Critical ignition flux q_{crit}	9.24	11.83	11.14	12.8	kW/m^2
Thermal inertia kpc	0.98	0.85	3.27	2.30	$(kW/m^2K)^2$
Minimum ignition flux $q_{ig,min}$	18.75	18	12	18.75	kW/m^2
Heat transfer coefficient at ignition h	0.044	0.043	0.040	0.046	kW/m^2K
Ignition temperature T_{ig}	425	415	321	425	$^{\circ}C$

Radiata Pine	LIFT	ISO 5657-1986	Ngu (ISO 5657)	Ignition in RIFT	
Ignition parameter b	0.054	0.039	0.047	0.043	$s^{0.5}$
intercept of ignition parameter graph $(t^*)^{0.5}$	18	25	21	23	$s^{0.5}$
Preheat time t^*	341	643	460	531	sec
Critical ignition flux q_{crit}	9.7	12.0	7.8	10.9	kW/m^2
Thermal inertia kpc	0.92	1.54	1.08	1.45	$(kW/m^2K)^2$
Minimum ignition flux $q_{ig,min}$	18.75	16.25	15.5	18.75	kW/m^2
Heat transfer coefficient at ignition h	0.046	0.043	0.043	0.046	kW/m^2K
Ignition temperature T_{ig}	425	391	380	425	$^{\circ}C$
Rimu	LIFT	ISO 5657-1986	Ngu (ISO 5657)	Ignition in RIFT	
Ignition parameter b	0.050	0.050	0.033	0.047	$s^{0.5}$
intercept of ignition parameter graph $(t^*)^{0.5}$	20	20	30	21.5	$s^{0.5}$
Preheat time t^*	395	397	893	462	sec
Critical ignition flux q_{crit}	9.62	12.75	7.52	13.9	kW/m^2
Thermal inertia kpc	1.06	1.03	1.93	1.41	$(kW/m^2K)^2$
Minimum ignition flux $q_{ig,min}$	18.5	18	13.5	21.25	kW/m^2
Heat transfer coefficient at ignition h	0.046	0.045	0.041	0.049	kW/m^2K
Ignition temperature T_{ig}	422	415	348	454	$^{\circ}C$

Macrocarpa	LIFT	ISO 5657-1986	Ngu (ISO 5657)	Ignition in RIFT	
Ignition parameter b	0.059	0.048	0.055	0.056	$s^{0.5}$
intercept of ignition parameter graph $(t^*)^{0.5}$	17	21	18	18.0	$s^{0.5}$
Preheat time t^*	288	436	337	325	sec
Critical ignition flux q_{crit}	14.7	15.2	12.9	15.6	kW/m^2
Thermal inertia kpc	0.78	1.13	0.79	0.89	$(kW/m^2K)^2$
Minimum ignition flux $q_{ig,min}$	18.75	18	15.5	18.75	kW/m^2
Heat transfer coefficient at ignition h	0.046	0.045	0.043	0.046	kW/m^2K
Ignition temperature T_{ig}	425	415	380	425	$^{\circ}C$

Ignition test data

**Plywood -
17mm**

ISO 5657		RIFT		LIFT	
Heat flux (kW/m ²)	Time to ignition (s)	Heat flux (kW/m ²)	Time to ignition (s)	Heat flux (kW/m ²)	Time to ignition (s)
10	no ignition	12.5	No ign	12.5	No ign
12.5	1690	15	No ign	15	No ign
15	1125	17.5	663	17.5	760
20	229	20	611	20	173
30	69	30	82	30	114.7
40	49	40	52.8	40	42.4
50	28.7	50	19.5	50	26
60	23.3	60	18.5		

Medium Density fibreboard (MDF)

ISO 5657		RIFT		LIFT	
Heat flux (kW/m ²)	Time to ignition (s)	Heat flux (kW/m ²)	Time to ignition (s)	Heat flux (kW/m ²)	Time to ignition (s)
15	no ignition	17.5	343	15	No ign
17.5	723	20	215	17.5	760
20	239	30	92	20	173
30	101	40	60.5	30	114.7
40	56.4	50	30	40	42.4
50	39.2	60	28	50	26
60	25.4				

Melteca / MDF

ISO 5657		RIFT		LIFT	
Heat flux (kW/m ²)	Time to ignition (s)	Heat flux (kW/m ²)	Time to ignition (s)	Heat flux (kW/m ²)	Time to ignition (s)
20	No ign	20	No ign	17.5	No ign
21	977	22.5	349	20	401
22.5	467	30	188	30	257
25	354	40	108	40	153
30	204	50	58.1	50	93.5
40	126	60	53.4		
50	84				
60	62				

Melteca / particle board shelving

ISO 5657		RIFT		LIFT	
Heat flux (kW/m ²)	Time to ignition (s)	Heat flux (kW/m ²)	Time to ignition (s)	Heat flux (kW/m ²)	Time to ignition (s)
17.5	No ign	22.5	No ign		Not tested
20	558	25	292		
22.5	356	30	221		
25	255	40	95		
30	170	50	54.2		
35	128	60	30.2		
40	93				
50	59				
60	45.4				

Pynefloor particle board

ISO 5657	
Heat flux (kW/m ²)	Time to ignition (s)
12.5	No ign
15	1166
17.5	575
20	368
25	215
30	154
35	98
40	93
50	47
60	38.4

RIFT	
Heat flux (kW/m ²)	Time to ignition (s)
20	No Ign
22.5	226
30	140
40	64.8
50	35
60	27.5

LIFT	
Heat flux (kW/m ²)	Time to ignition (s)
17.5	No ign
20	315
30	175
40	86.5
50	50.5

Superflake particle board

ISO 5657	
Heat flux (kW/m ²)	Time to ignition (s)
12.5	No ign
15	1090
17.5	525
20	333
25	210
30	128
35	88
40	75
50	48
60	31.4

RIFT	
Heat flux (kW/m ²)	Time to ignition (s)
17.5	No ign
20	404
30	123
40	75
50	33
60	39.4

LIFT	
Heat flux (kW/m ²)	Time to ignition (s)
	Not tested

Hardboard

ISO 5657		RIFT		LIFT	
Heat flux (kW/m ²)	Time to ignition (s)	Heat flux (kW/m ²)	Time to ignition (s)	Heat flux (kW/m ²)	Time to ignition (s)
10	1378	12.5	886	15	1403
12.5	712	15	605	17.5	1223
15	402	17.5	338	20	259
20	285	20	273	30	108.5
30	127	30	117	40	96
40	74	40	62	50	64.5
50	52	50	30		
60	35	60	28.4		

Rimu

ISO 5657		RIFT		LIFT	
Heat flux (kW/m ²)	Time to ignition (s)	Heat flux (kW/m ²)	Time to ignition (s)	Heat flux (kW/m ²)	Time to ignition (s)
17.5	No ign	20	No ign	15	1549
18.5	1358	22.5	544	17.5	1308
20	1134	30	219.5	20	366
30	186	40	53	30	187.5
40	61	50	24.1	40	61
50	31.5	60	22.4	50	34.4
60	24				

Pine

	ISO 5657		RIFT		LIFT
Heat flux (kW/m ²)	Time to ignition (s)	Heat flux (kW/m ²)	Time to ignition (s)	Heat flux (kW/m ²)	Time to ignition (s))
15	No ign	17.5	No ign	15	1490
17.5	1154	20	660	17.5	1348
18.5	982	30	96.6	20	331
20	586	40	37	30	131
30	109	50	16.9	40	61
40	43	60	17.5	50	29.5
50	21.3				
60	16.6				

Macrocarpa

	ISO 5657		RIFT		LIFT
Heat flux (kW/m ²)	Time to ignition (s)	Heat flux (kW/m ²)	Time to ignition (s)	Heat flux (kW/m ²)	Time to ignition (s))
17.5	No ign	17.5	No ign	17.5	No ign
18.5	1767	20	976	20	1439
20	1077	30	182	30	114
30	237	40	43.6	40	74.5
40	32.5	50	14.3	50	26
50	14.2	60	15.4		
60	15.9				

NZ Beech

	ISO 5657		RIFT		LIFT	
Heat flux (kW/m ²)	Time to ignition (s)		Heat flux (kW/m ²)	Time to ignition (s)	Heat flux (kW/m ²)	Time to ignition (s)
17.5	glowing at 1800		20	No ign	17.5	No ign
18.5	1526		22.5	901	20	366
20	774		30	104	30	176.4
30	162		40	33.5	40	62.5
40	52.8		50	15.2	50	33.2
50	35		60	19.5		
60	23					

Appendix 4 Flame spread results

12.1 Summary of flame spread results

Plywood	<i>RIFT (using RIFT ignition data) - 17mm</i>	<i>RIFT (using ISO ignition data) - 17mm</i>	<i>RIFT (using RIFT ignition data) - 17mm</i>	<i>RIFT (using ISO 5657 ignition data) - 17mm</i>	<i>LIFT</i>
-	low preheat time	low preheat time	Full preheat time	Full preheat time	Full preheat time
Flame spread modulus C	7.74	10.72	4.37	4.37	3.7
Flame spread parameter Φ	5.80	4.79	18.23	28.84	28.0
" $q_{ig,min}$ (ignition test)	16.25	13.75	16.25	13.75	16.3
" $q_{ig,min}$ (correlation)	16.46	12.83	20.23	20.23	21.6
" q_s (correlation)	5.25	5.25	4.62	4.62	5.4
" q_s (from extent of flame spread)	6.47 <i>Std Dev 1.32</i>	6.47 <i>Std Dev1.32</i>	4.74 <i>Std Dev0.33</i>	4.74 <i>Std Dev 0.33</i>	5.3 <i>Std Dev 0.65</i>
Medium Density Fibreboard (MDF)	<i>RIFT - 18mm MDF with ISO ign data</i>	<i>RIFT - 18mm MDF with RIFT ignition data</i>	<i>RIFT - 18mm MDF with ISO ign data</i>	<i>RIFT - 18mm MDF with RIFT ignition data</i>	<i>LIFT</i>
	Low preheating time	Low preheating time	Full preheating time	Full preheating time	Full preheating time
Flame spread modulus C	17.01	17.10	4.9	4.9	4.0
Flame spread parameter Φ	1.56	1.55	18.6	18.5	36.0
" $q_{ig,min}$ (ignition test)	16.25	16.25	16.3	16.3	16.3
" $q_{ig,min}$ (correlation)	14.85	14.82	24.3	24.3	23.6

q_s'' (correlation)	8.67	8.67	6.7	6.7	6.0
q_s'' (from extent of flame spread)	8.23 <i>Std Dev 0.26</i>	8.23 <i>Std Dev 0.26</i>	6.3 <i>Std Dev0.2</i>	6.3 <i>Std Dev 0.2</i>	5.9 <i>Std Dev 0.4</i>
Melteca faced Particle board	<i>RIFT (using ISO 5657 ignition data)</i>	<i>RIFT (Using RIFT ign data)</i>	<i>RIFT (Using RIFT ign data)</i>	<i>RIFT (Using ISO 5657 ign data)</i>	<i>LIFT</i>
	Low preheat time	Low preheat time	Full preheat time	Full preheat time	Full preheat time
Flame spread modulus C	2.76	2.72	1.78	1.78	Not tested
Flame spread parameter Φ	90.72	65.54	154.28	206.73	Not tested
$q_{ig,min}''$ (ignition test)	18.75	23.75	23.75	18.75	Not tested
$q_{ig,min}''$ (correlation)	36.60	39.26	62.01	62.01	Not tested
q_s'' (correlation)	11.30	11.30	9.61	9.61	Not tested
q_s'' (from extent of flame spread)	12.41 <i>Std Dev 1.18</i>	12.41 <i>Std Dev 1.18</i>	11.57 <i>Std Dev1.38</i>	11.57 <i>Std Dev 1.38</i>	Not tested
Melteca faced MDF	<i>RIFT (using ISO 5657 ignition data)</i>	<i>RIFT (Using RIFT ign data)</i>	<i>RIFT (Using RIFT ign data)</i>	<i>RIFT (Using ISO 5657 ign data)</i>	<i>LIFT</i>
	Low preheat time	Low preheat time	Full preheat time	Full preheat time	Full preheat time
Flame spread modulus C	13.40	2.32	6.44	6.44	4.3
Flame spread parameter Φ	3.85	90.36	11.74	16.67	38.5
$q_{ig,min}''$ (ignition test)	20.00	21.25	21.25	20.00	18.8
$q_{ig,min}''$ (correlation)	20.00	46.10	30.74	30.74	33.0
q_s'' (correlation)	11.30	12.91	11.48	11.48	10.9
q_s'' (from extent of flame spread)	14.16 <i>Std Dev 1.63</i>	14.16 <i>Std Dev 1.63</i>	13.96 <i>Std Dev 1.78</i>	13.96 <i>Std Dev 1.78</i>	9.9 <i>Std Dev 0.16</i>

	<i>RIFT - with ISO 5657</i>	<i>RIFT - with RIFT</i>	<i>RIFT - with ISO 5657</i>	<i>RIFT – with RIFT</i>	
Pynefloor Particle board flooring	<i>ign data</i>	<i>ignition data</i>	<i>ignition data</i>	<i>ignition data</i>	<i>LIFT</i>
	Low preheating time	Low preheating time	Full preheating time	Full preheating time	Full preheating time
Flame spread modulus C	19.5	9.3	8.1	8.1	3.6
Flame spread parameter Φ	2.8	3.7	14.8	4.9	37.3
$q_{ig,min}^{\prime\prime}$ (ignition test)	0.0	0.0	18.8	21.3	0.0
$q_{ig,min}^{\prime\prime}$ (correlation)	11.8	20.2	19.0	19.0	25.5
$q_s^{\prime\prime}$ (correlation)	6.6	8.4	7.5	7.5	6.2
$q_s^{\prime\prime}$ (from extent of flame spread)	8.7	8.7	7.6	7.6	6.3
	<i>Std Dev 0.74</i>	<i>Std Dev 0.74</i>	<i>Std Dev 0.61</i>	<i>Std Dev 0.61</i>	<i>Std Dev 0.73</i>
	<i>RIFT - 20mm particle board with ISO 5657</i>	<i>RIFT - 20mm particle board with RIFT</i>	<i>RIFT - 20mm particle board with ISO 5657</i>	<i>RIFT - with RIFT</i>	
Superflake Particle board	<i>ign data</i>	<i>ignition data</i>	<i>ignition data</i>	<i>ignition data</i>	<i>LIFT</i>
	Low preheating time	Low preheating time	Full preheating time	Full preheating time	Full preheating time
Flame spread modulus C	24.77	13.79	7.58	7.58	Not Tested
Flame spread parameter Φ	1.94	2.61	20.71	8.62	Not tested
$q_{ig,min}^{\prime\prime}$ (ignition test)	13.75	18.75	13.75	18.75	Not tested
$q_{ig,min}^{\prime\prime}$ (correlation)	10.44	16.70	18.61	18.61	Not tested
$q_s^{\prime\prime}$ (correlation)	6.60	8.39	7.48	7.48	Not tested
$q_s^{\prime\prime}$ (from extent of flame spread)	9.75	9.75	7.41	7.41	Not tested
	<i>Std Dev 1.58</i>	<i>Std Dev 1.58</i>	<i>Std Dev 0.71</i>	<i>Std Dev 0.71</i>	

Hardboard	<i>RIFT (using ISO ignition data</i>	<i>RIFT (Using RIFT ign data</i>	<i>RIFT (using ISO ignition data</i>	<i>RIFT (Using RIFT ign data</i>	<i>LIFT</i>
	Low preheat time	Low preheat time	Full preheat time	Full preheat time	Full preheat time
Flame spread modulus C	13.3	13.6	5.7	5.7	4.9
Flame spread parameter Φ	6.7	6.7	36.8	38.1	20.3
$q_{ig,min}''$ (ignition test)	11.3	11.3	11.3	11.3	17.5
$q_{ig,min}''$ (correlation)	11.1	10.9	19.2	19.2	19.5
q_s'' (correlation)	3.3	3.3	3.3	3.3	3.1
q_s'' (from extent of flame spread)	4.1	4.1	3.2	3.2	3.4
	<i>Std Dev 0.9</i>	<i>Std Dev 0.9</i>	<i>Std Dev 0.3</i>	<i>Std Dev 0.3</i>	<i>Std Dev 0.4</i>
NZ Beech	<i>RIFT (using ISO ignition data</i>	<i>RIFT (Using RIFT ign data</i>	<i>RIFT (using ISO ignition data</i>	<i>RIFT (Using RIFT ign data</i>	<i>LIFT</i>
	Low preheat time	Low preheat time	Full preheat time	Full preheat time	Full preheat time
Flame spread modulus C	4.7	7.3	2.5	2.5	2.7
Flame spread parameter Φ	20.2	20.2	74.8	177.7	70.9
$q_{ig,min}''$ (ignition test)	18.0	18.75	18.00	18.75	18.75
$q_{ig,min}''$ (correlation)	16.2	10.5	22.3	22.3	23.7
q_s'' (correlation)	6.5	4.2	2.9	2.9	3.7
q_s'' (from extent of flame spread)	9.6	9.6	3.3	3.3	4.8
	<i>Std Dev 2.0</i>	<i>Std Dev 2.0</i>	<i>Std Dev 0.3</i>	<i>Std Dev 0.3</i>	<i>Std Dev 0.9</i>

Radiata Pine	<i>RIFT (using ISO ignition data</i>	<i>RIFT (Using RIFT ign data</i>	<i>RIFT (Using ISO 5657 ign data</i>	<i>RIFT (Using RIFT ign data)</i>	<i>LIFT</i>
	Low preheat time	Low preheat time	Full preheat time	Full preheat time	Full preheat time
Flame spread modulus C	12.3	11.1	5.0	5.0	4.0
Flame spread parameter Φ	5.4	5.4	32.6	26.9	27.4
$q_{ig,min}''$ (ignition test)	16.25	18.75	16.25	18.75	18.75
$q_{ig,min}''$ (correlation)	10.2	11.2	17.6	17.6	18.0
q_s'' (correlation)	4.9	5.3	3.8	3.8	4.2
q_s'' (from extent of flame spread)	7.5	7.5	3.8	3.8	4.5
	<i>Std Dev</i> 1.0	<i>Std Dev</i> 1.0	<i>Std Dev</i> 0.1	<i>Std Dev</i> 0.1	<i>Std Dev</i> 0.7
Rimu	<i>RIFT (using ISO ignition data</i>	<i>RIFT (Using RIFT ign data</i>	<i>RIFT (using ISO ignition data</i>	<i>RIFT (Using RIFT ign data</i>	<i>LIFT</i>
	Low preheat time	Low preheat time	Full preheat time	Full preheat time	Full preheat time
Flame spread modulus C	4.7	5.1	Insufficient flame spread	Insufficient flame spread	2.2
Flame spread parameter Φ	22.5	22.5	-	-	106
$q_{ig,min}''$ (ignition test)	18.0	21.25	18.0	21.25	18.5
$q_{ig,min}''$ (correlation)	15.9	14.8	Insufficient flame spread	Insufficient flame spread	26.0
q_s'' (correlation)	5.4	5.0	Insufficient flame spread	Insufficient flame spread	6.0
q_s'' (from extent of flame spread)	11.7	11.7			7.6
	<i>Std Dev</i> 2.3	<i>std Dev</i> 2.3	12.7	12.7	<i>Std Dev</i> 2.7

Macrocarpa	<i>RIFT (using ISO 5657 ignition data)</i>	<i>RIFT (Using RIFT ign data)</i>	<i>RIFT (Using ISO 5657 ign data)</i>	<i>RIFT (Using RIFT ign data)</i>	<i>LIFT</i>
	Low preheating time	Low preheating time	Full preheat time	Full preheat time	Full preheating time
Flame spread modulus C	7.7	6.9	2.9	2.9	2.5
Flame spread parameter Φ	9.3	8.6	64.5	48.0	58.3
$q_{ig,min}''$ (ignition test)	18.0	18.8	18.0	18.8	18.8
$q_{ig,min}''$ (correlation)	12.7	14.5	22.6	22.6	18.9
q_s'' (correlation)	4.1	4.6	4.6	4.6	2.2
q_s'' (from extent of flame spread)	6.1 <i>Std Dev 1.0</i>	6.1 <i>Std Dev 1.0</i>	5.0 <i>Std Dev 0.8</i>	5.0 <i>Std Dev 0.8</i>	2.2 <i>Std Dev 0.2</i>

12.2 Flame spread data and correlation results

Plywood, 17mm

Flame Front Position x	Time to position x t (s)	time from ignition (s)	Σt	Σx	$\Sigma(t^2)$	$\Sigma(t.x)$	V_f	V_f	$F(t)$	\dot{q}_e	$\dot{q}_e.F(t)$	$1/\sqrt{V_f}$
LIFT Plywood Test 1	Ignition Time	295					m/s	mm/s		kW/m ²		(m/s) ^{-0.5}
50												
75												
100												
125												
150												
175	305	10							1.000	19.66	19.66	
200	312	17	939	600	294053	881721	188225	0.0029	2.9110	1.000	19.05	18.535
225	322	27	967	675	311917	935089	218100	0.0024	2.3792	1.000	18.25	20.502
250	333	38	996	750	330854	992016	249475	0.0026	2.6099	1.000	17.45	19.574
275	341	46	1030	825	353906	1060900	283825	0.0021	2.1088	1.000	15.86	21.776
300	356	61	1073	900	384393	1151329	322775	0.0014	1.4189	1.000	14.28	26.547
325	376	81	1138	975	432948	1295044	371100	0.0010	0.9868	1.000	12.89	31.833
350	406	111	1218	1050	496308	1483524	427800	0.0008	0.8333	1.000	11.50	34.641
375	436	141	1323	1125	586293	1750329	498000	0.0007	0.6579	1.000	10.17	38.987
400	481	186	1454	1200	709826	2114116	584125	0.0005	0.4931	1.000	8.83	45.033
425	537	242	1630	1275	894274	2656900	696025	0.0004	0.3790	1.000	7.59	51.365
450	612	317	1862	1350	1171282	3467044	842300	0.0003	0.2820	1.000	6.35	59.545
475	713	418								1.000	5.42	5.42
500	870	575										

<i>Flame Front Position x</i>	<i>Time to position x t (s)</i>	<i>Time from ignition (s)</i>	Σt	Σx	$\Sigma(t^2)$	$\Sigma(t)^2$	$\Sigma(t.x)$	V_f	V_f	$F(t)$	\dot{q}_e	$\dot{q}_e.F(t)$	$1/\sqrt{V_f}$
LIFT Plywood Test 2	Ignition Time	307						m/s		kW/m ²		(m/s) ^{-0.5}	(m/s) ^{-0.5}
50													
75													
100													
125													
150													
175													
200													
225	319	24								1.000	18.25	18.25	
250	328	33	987	750	324945	974169	247275	0.0024	2.3649	1.000	17.45	17.45	20.563
275	340	45	1021	825	347793	1042441	281400	0.0020	1.9989	1.000	15.86	15.86	22.367
300	353	58	1060	900	374898	1123600	318675	0.0019	1.8510	1.000	14.28	14.28	23.243
325	367	72	1108	975	409842	1227664	360975	0.0014	1.4098	1.000	12.89	12.89	26.633
350	388	93	1169	1050	456629	1366561	410325	0.0011	1.0598	1.000	11.50	11.50	30.717
375	414	119	1245	1125	518189	1550025	468250	0.0009	0.9082	1.000	10.17	10.17	33.183
400	443	148	1338	1200	599006	1790244	536875	0.0007	0.7418	1.000	8.83	8.83	36.716
425	481	186	1470	1275	725726	2160900	627325	0.0005	0.4746	1.000	7.59	7.59	45.904
450	546	251	1678	1350	953278	2815684	759350	0.0003	0.2888	1.000	6.35	6.35	58.845
475	651	356	1945	1424	1281421	3783025	928177	0.0002	0.2425	1.000	5.42	5.42	64.214
499	748	453								1.000	4.53	4.53	

<i>Flame Front Position x</i>	<i>Time to position x t (s)</i>	<i>Time from ignition (s)</i>	Σt	Σx	$\Sigma(t^2)$	$\Sigma(t)^2$	$\Sigma(t.x)$	V_f	V_f	$F(t)$	\dot{q}_e	$\dot{q}_e.F(t)$	$1/\sqrt{V_f}$
LIFT Plywood Test 3	Ignition Time	295						m/s		kW/m ²		(m/s) ^{-0.5}	(m/s) ^{-0.5}
50													
75													
100													
125													
150													
175													
200													
225	307	12								1.000	18.25	18.25	
250	314	19	943	750	296529	889249	236125	0.0033	3.3284	1.000	17.45	17.45	17.333
275	322	27	969	825	313169	938961	266950	0.0026	2.6099	1.000	15.86	15.86	19.574
300	333	38	1001	900	334289	1002001	300900	0.0021	2.0785	1.000	14.28	14.28	21.934
325	346	51	1041	975	361649	1083681	339050	0.0017	1.7180	1.000	12.89	12.89	24.126
350	362	67	1091	1050	397449	1190281	382775	0.0013	1.3432	1.000	11.50	11.50	27.286
375	383	88	1160	1125	449958	1345600	436325	0.0009	0.9300	1.000	10.17	10.17	32.791
400	415	120	1255	1200	527763	1575025	503850	0.0007	0.6716	1.000	8.83	8.83	38.588
425	457	162	1424	1275	685778	2027776	608625	0.0003	0.3476	1.000	7.59	7.59	53.635
450	552	257	1772	1340	1095722	3139984	797420	0.0001	0.1208	1.000	6.35	6.35	90.983
465	763	468								1.000	5.79	5.79	

<i>Flame Front Position x</i>	<i>Time to position x t (s)</i>	<i>time from ignition (s)</i>	Σt	Σx	$\Sigma(t^2)$	$\Sigma(t)^2$	$\Sigma(t.x)$	V_f	$F(t)$	$\dot{q}_{.e}''$	$\dot{q}_{.e}'' F(t)$
RIFT – 9mm plywood low preheat time Test 1	Ignition Time	66						m/s		kW/m ²	
10											
20											
30											
40											
50	66	0							0.320	27.20	
60	78	12	227	180	17329	51529	13790	0.0011	0.348	24.94	8.68
70	83	17	254	210	21622	64516	17930	0.0013	0.359	22.89	8.22
80	93	27	279	240	26147	77841	22520	0.0010	0.380	20.84	7.92
90	103	37	309	270	32027	95481	28010	0.0010	0.400	18.76	7.50
100	113	47	346	300	40278	119716	34870	0.0007	0.419	16.68	6.99
110	130	64	399	330	54005	159201	44320	0.0005	0.449	15.08	6.77
120	156	90	483	360	80045	233289	58630	0.0003	0.492	13.96	6.87
130	197	131	591	390	119789	349281	77650	0.0002	0.553	12.83	7.10
140	238	172	699	420	165149	488601	98530	0.0003	0.608	11.74	7.14
150	264	198	785	450	206429	616225	118200	0.0004	0.640	10.65	6.81
160	283	217	899	480	273689	808201	144720	0.0002	0.663	9.56	6.33
170	352	286	1357	510	725277	1841449	235080	0.0000	0.739	8.47	6.26
180	722	656							1.000	7.39	7.39

<i>Flame Front Position x</i>	<i>Time to position x</i> <i>t (s)</i>	<i>time from ignition</i> <i>(s)</i>	Σt	Σx	$\Sigma(t^2)$	$\Sigma(t)^2$	$\Sigma(t.x)$	V_f	$F(t)$	\dot{q}_e	$\dot{q}_e.F(t)$
RIFT – 9mm plywood low preheat time Test 2	Ignition Time	81s						m/s		kW/m ²	
10											
20											
30											
40	81	0							0.355	29.67	
50	85	4	257	150	22067	66049	12950	0.0020	0.363	27.20	9.88
60	91	10	271	180	24531	73441	16360	0.0020	0.376	24.94	9.37
70	95	14	285	210	27107	81225	20030	0.0025	0.384	22.89	8.79
80	99	18	299	240	29851	89401	24020	0.0020	0.392	20.84	8.17
90	105	24	318	270	33822	101124	28770	0.0013	0.404	18.76	7.57
100	114	33	346	300	40150	119716	34820	0.0009	0.421	16.68	7.02
110	127	46	386	330	50150	148996	42770	0.0006	0.444	15.08	6.70
120	145	64	441	360	65715	194481	53340	0.0005	0.474	13.96	6.62
130	169	88	512	390	88790	262144	67090	0.0004	0.512	12.83	6.57
140	198	117	589	420	117049	346921	82990	0.0004	0.554	11.74	6.51
150	222	141	671	450	151489	450241	101180	0.0004	0.587	10.65	6.25
160	251	170							0.624	9.56	5.97

<i>Flame Front Position x</i>	<i>Time to position x</i> <i>t (s)</i>	<i>time from ignition</i> <i>(s)</i>	Σt	Σx	$\Sigma(t^2)$	$\Sigma(t)^2$	$\Sigma(t.x)$	V_f	$F(t)$	\dot{q}_e	$\dot{q}_e.F(t)$
RIFT – 9mm plywood low preheat time Test 3	Ignition Time	69s						m/s		kW/m ²	
10											
20											
30											

40												
50												
60	69	0							0.327	24.94		
70	72	3	216	210	15570	46656	15180	0.0033	0.334	22.89	7.65	
80	75	6	229	240	17533	52441	18420	0.0019	0.341	20.84	7.11	
90	82	13	252	270	21374	63504	22880	0.0010	0.357	18.76	6.69	
100	95	26	287	300	27849	82369	28980	0.0007	0.384	16.68	6.41	
110	110	41	339	330	39081	114921	37680	0.0005	0.413	15.08	6.23	
120	134	65	400	360	54392	160000	48460	0.0004	0.456	13.96	6.37	
130	156	87	471	390	75053	221841	61700	0.0004	0.492	12.83	6.31	
140	181	112	540	420	98306	291600	76070	0.0004	0.530	11.74	6.22	
150	203	134	603	450	121931	363609	90830	0.0005	0.561	10.65	5.98	
160	219	150	666	480	148706	443556	106970	0.0005	0.583	9.56	5.57	
170	244	175	742	510	185338	550564	126740	0.0003	0.615	8.47	5.21	
180	279	210	842	535	239138	708964	150715	0.0002	0.658	7.39	4.86	
185	319	250							0.704	7.02	4.94	

<i>Flame Front Position x</i>	<i>Time to position x t (s)</i>	<i>time from ignition (s)</i>	Σt	Σx	$\Sigma(t^2)$	$\Sigma(t)^2$	$\Sigma(t.x)$	V_f	$F(t)$	\dot{q}_e	$\dot{q}_e.F(t)$
RIFT – 9mm plywood low preheat time Test 4	Ignition Time	66s						m/s		kW/m ²	

10												
20												
30	66	0										
40	75	9	218	120	15910	47524	8830	0.0016	0.341	29.67	10.12	
50	77	11	231	150	17795	53361	11590	0.0050	0.346	27.20	9.40	
60	79	13	239	180	19059	57121	14400	0.0032	0.350	24.94	8.73	

70	83	17	248	210	20526	61504	17430	0.0028	0.359	22.89	8.22
80	86	20	262	240	22934	68644	21060	0.0019	0.365	20.84	7.61
90	93	27	280	270	26246	78400	25350	0.0013	0.380	18.76	7.13
100	101	35	305	300	31171	93025	30680	0.0011	0.396	16.68	6.60
110	111	45	338	330	38398	114244	37430	0.0008	0.415	15.08	6.26
120	126	60	393	360	52533	154449	47610	0.0004	0.442	13.96	6.17
130	156	90	452	390	69112	204304	59200	0.0004	0.492	12.83	6.31
140	170	104	512	420	87832	262144	71980	0.0007	0.514	11.74	6.03
150	186	120	563	450	106345	316969	84820	0.0005	0.537	10.65	5.72
160	207	141	683	480	161545	466489	110320	0.0002	0.567	9.56	5.42
170	290	224	841	510	245285	707281	144340	0.0001	0.671	8.47	5.68
180	344	278	1019	533	350661	#####	181675	0.0001	0.731	7.39	5.40
183	385	319							0.773	7.17	5.54

<i>Flame Front Position x</i>	<i>Time to position x t (s)</i>	<i>time from ignition (s)</i>	Σt	Σx	$\Sigma(t^2)$	$\Sigma(t)^2$	$\Sigma(t.x)$	V_f	$F(t)$	\dot{q}_{e}''	$\dot{q}_{e}'' \cdot F(t)$
RIFT – 9mm plywood low preheat time Test 5	Ignition Time	67s						m/s		kW/m ²	

10											
20											
30											
40											
50	67	0	140	150	9818	19600	7730	0.0002	0.323	27.20	8.77
60	73	6	221	180	16379	48841	13400	0.0014	0.337	24.94	8.39
70	81	14	245	210	20171	60025	17330	0.0011	0.355	22.89	8.12
80	91	24	276	240	25658	76176	22310	0.0009	0.376	20.84	7.83
90	104	37	313	270	33021	97969	28440	0.0007	0.402	18.76	7.54

100	118	51	359	300	43509	128881	36230	0.0006	0.428	16.68	7.14
110	137	70	417	330	58937	173889	46310	0.0005	0.461	15.08	6.95
120	162	95	482	360	78502	232324	58300	0.0004	0.501	13.96	7.00
130	183	116	556	390	104254	309136	72770	0.0004	0.533	12.83	6.84
140	211	144	634	420	135610	401956	89330	0.0004	0.572	11.74	6.72
150	240	173	723	450	176105	522729	109060	0.0003	0.610	10.65	6.50
160	272	205	825	480	229553	680625	132730	0.0003	0.650	9.56	6.21
170	313	246	951	510	305909	904401	162610	0.0002	0.697	8.47	5.91
180	366	299	1102	540	410854	1214404	199460	0.0002	0.754	7.39	5.57
190	423	356	1257	570	531909	1580049	239850	0.0002	0.810	6.66	5.40
200	468	401	1423	600	680977	2024929	285690	0.0002	0.852	5.93	5.06
210	532	465	1600	630	862048	2560000	337320	0.0002	0.909	5.25	4.77
220	600	533	1805	660	1095953	3258025	398510	0.0001	0.965	4.62	4.46
230	673	606	2003	690	1345829	4012009	461990	0.0002	1.022	3.99	4.08
240	730	663	2246	715	1696478	5044516	536525	0.0001	1.000	3.74	3.74
245	843	776							1.000	3.62	3.62

<i>Flame Front Position x</i>	<i>Time to position x t (s)</i>	<i>Time from ignition (s)</i>	Σt	Σx	$\Sigma(t^2)$	$\Sigma(t)^2$	$\Sigma(t.x)$	V_f	$F(t)$	\dot{q}_e	$\dot{q}_e.F(t)$
RIFT – 9mm plywood low preheat time Test 6	Ignition Time	66s						m/s		kW/m ²	
10											
20											
30											
40											
50											
60	67	0						0.0002	0.323	24.94	
70	78	11	239	210	19409	57121	17000	0.0007	0.348	22.89	7.96

80	94	27	281	240	26801	78961	22790	0.0006	0.382	20.84	7.96
90	109	42	330	270	36846	108900	30030	0.0006	0.411	18.76	7.72
100	127	60	381	300	49035	145161	38460	0.0006	0.444	16.68	7.41
110	145	78	435	330	63723	189225	48210	0.0006	0.474	15.08	7.15
120	163	96	503	360	85619	253009	60860	0.0004	0.503	13.96	7.02
130	195	128	586	390	116578	343396	76830	0.0003	0.550	12.83	7.06
140	228	161	713	419	174109	508369	100480	0.0002	0.595	11.74	6.98
149	290	223							0.671	10.75	7.22

Flame Front Position x	Time to position x t (s)	Time from ignition (s)	Σt	Σx	$\Sigma(t^2)$	$\Sigma(t)^2$	$\Sigma(t.x)$	V_f	$F(t)$	\dot{q}_e	$\dot{q}_e.F(t)$
RIFT – 17mm plywood low preheat time Test 1	Ignition Time	69						m/s		kW/m ²	
10	69	0								37.09	
20	69.5	0.5	208	60	14422	43264	4165	0.0300	0.401	34.62	13.89
30	69.5	0.5	209	90	14561	43681	6275	0.0300	0.401	32.14	12.89
40	70	1	213	120	15059	45156	8535	0.0049	0.403	29.67	11.94
50	73	4	219	150	16005	47961	11010	0.0033	0.411	27.20	11.18
60	76	7	234	180	18330	54756	14160	0.0015	0.419	24.94	10.46
70	85	16	253	210	21465	64009	17870	0.0012	0.444	22.89	10.15
80	92	23	280	240	26298	78400	22580	0.0011	0.461	20.84	9.62
90	103	34	310	270	32298	96100	28130	0.0009	0.488	18.76	9.16
100	115	46	350	300	41258	122500	35290	0.0007	0.516	16.68	8.61
110	132	63	397	330	53149	157609	44020	0.0006	0.553	15.08	8.34
120	150	81	454	360	69508	206116	54880	0.0005	0.589	13.96	8.22
130	172	103	520	390	91288	270400	68080	0.0004	0.631	12.83	8.10
140	198	129	600	420	121688	360000	84580	0.0003	0.677	11.74	7.95
150	230	161	704	450	168280	495616	106380	0.0003	0.730	10.65	7.77
160	276	207	815	480	224557	664225	131190	0.0003	0.799	9.56	7.64
170	309	240	946	510	301978	894916	161670	0.0002	0.846	8.47	7.17
180	361	292	1082	540	395546	1170724	195790	0.0002	0.914	7.39	6.75
190	412	343	1194	570	477306	1425636	227460	0.0003	0.977	6.66	6.50
200	421	352	1401	598	669609	1962801	280624	0.0001	0.987	5.93	5.85
208	568	499								5.39	

Flame Front Position x	<i>Time to position x t (s)</i>	<i>Time from ignition (s)</i>	Σt	Σx	$\Sigma(t^2)$	$\Sigma(t)^2$	$\Sigma(t.x)$	V_f	$F(t)$	\dot{q}_e	$\dot{q}_e.F(t)$
	Ignition Time	50						m/s		kW/m ²	
10	50	0							0.340	37.09	
20	52	2	155	60	8013	24025	3130	0.0064	0.347	34.62	12.01
30	53	3	159	90	8429	25281	4790	0.0100	0.350	32.14	11.26
40	54	4	162	120	8750	26244	6500	0.0100	0.354	29.67	10.49
50	55	5	169	150	9541	28561	8510	0.0029	0.357	27.20	9.70
60	60	10	181	180	10981	32761	10970	0.0018	0.373	24.94	9.29
70	66	16	201	210	13581	40401	14220	0.0013	0.391	22.89	8.95
80	75	25	229	240	17725	52441	18540	0.0009	0.417	20.84	8.68
90	88	38	264	270	23570	69696	24020	0.0008	0.451	18.76	8.47
100	101	51	305	300	31401	93025	30780	0.0007	0.484	16.68	8.06
110	116	66	349	330	41081	121801	38700	0.0006	0.518	15.08	7.81
120	132	82	400	360	53984	160000	48360	0.0006	0.553	13.96	7.71
130	152	102	461	390	71857	212521	60380	0.0004	0.593	12.83	7.61
140	177	127	536	420	97282	287296	75590	0.0004	0.640	11.74	7.51
150	207	157	626	450	132742	391876	94550	0.0003	0.692	10.65	7.37
160	242	192	732	480	181502	535824	117880	0.0003	0.748	9.56	7.15
170	283	233							0.809	8.47	

Flame Front Position x	<i>Time to position x t (s)</i>	<i>Time from ignition (s)</i>	Σt	Σx	$\Sigma(t^2)$	$\Sigma(t)^2$	$\Sigma(t.x)$	V_f	$F(t)$	\dot{q}_e	$\dot{q}_e.F(t)$
	Ignition Time	69						m/s		kW/m ²	
10	50	0							0.340	37.09	
20	52	2	155	60	8013	24025	3130	0.0064	0.347	34.62	12.01
30	53	3	159	90	8429	25281	4790	0.0100	0.350	32.14	11.26
40	54	4	162	120	8750	26244	6500	0.0100	0.354	29.67	10.49
50	55	5	169	150	9541	28561	8510	0.0029	0.357	27.20	9.70

60	60	10	181	180	10981	32761	10970	0.0018	0.373	24.94	9.29
70	66	16	201	210	13581	40401	14220	0.0013	0.391	22.89	8.95
80	75	25	229	240	17725	52441	18540	0.0009	0.417	20.84	8.68
90	88	38	264	270	23570	69696	24020	0.0008	0.451	18.76	8.47
100	101	51	305	300	31401	93025	30780	0.0007	0.484	16.68	8.06
110	116	66	349	330	41081	121801	38700	0.0006	0.518	15.08	7.81
120	132	82	400	360	53984	160000	48360	0.0006	0.553	13.96	7.71
130	152	102	461	390	71857	212521	60380	0.0004	0.593	12.83	7.61
140	177	127	536	420	97282	287296	75590	0.0004	0.640	11.74	7.51
150	207	157	626	450	132742	391876	94550	0.0003	0.692	10.65	7.37
160	242	192	732	480	181502	535824	117880	0.0003	0.748	9.56	7.15
170	283	233	859	510	250209	737881	146950	0.0002	0.809	8.47	6.86
180	334	284	999	539	337569	998001	180428	0.0002	0.879	7.39	6.50
189	382	332							0.940	6.73	

Flame Front Position x	Time to position x t (s)	Time from ignition (s)	Σt	Σx	$\Sigma(t^2)$	$\Sigma(t)^2$	$\Sigma(tx)$	V_f	$F(t)$	\dot{q}_e	$\dot{q}_e \cdot F(t)$
RIFT – 17mm plywood low preheat time Test 4	Ignition Time	69						m/s		kW/m ²	
10	50	0							0.340	37.09	
20	52	2	156	60	8120	24336	3160	0.0050	0.347	34.62	12.01
30	54	4	164	90	8984	26896	4980	0.0032	0.354	32.14	11.36
40	58	8	173	120	10001	29929	6990	0.0028	0.366	29.67	10.87
50	61	11	186	150	11574	34596	9390	0.0021	0.376	27.20	10.22
60	67	17	204	180	13986	41616	12390	0.0013	0.394	24.94	9.82
70	76	26	229	210	17661	52441	16220	0.0011	0.419	22.89	9.60
80	86	36	259	240	22581	67081	20930	0.0010	0.446	20.84	9.30
90	97	47	297	270	29801	88209	27010	0.0007	0.474	18.76	8.89
100	114	64	343	300	39829	117649	34650	0.0006	0.514	16.68	8.57

110	132	82	395	330	52621	156025	43800	0.0006	0.553	15.08	8.34
120	149	99	456	360	70250	207936	55150	0.0005	0.587	13.96	8.20
130	175	125	531	390	95675	281961	69610	0.0003	0.636	12.83	8.17
140	207	157	615	420	127763	378225	86680	0.0003	0.692	11.74	8.13
150	233	183	708	450	168962	501264	106810	0.0003	0.734	10.65	7.82
160	268	218	807	480	219749	651249	129850	0.0003	0.788	9.56	7.53
170	306	256	901	510	272389	811801	153760	0.0003	0.842	8.47	7.13
180	327	277							0.870	7.39	

Flame Front Position x	Time to position x t (s)	Time from ignition (s)	Σt	Σx	$\Sigma(t^2)$	$\Sigma(t)^2$	$\Sigma(t.x)$	V_f	$F(t)$	\dot{q}_e	$\dot{q}_e.F(t)$
		69									
10	50	0							0.340	37.09	
20	52.5	2.5	158	60	8281	24806	3200	0.0040	0.349	34.62	12.07
30	55	5	168	90	9381	28056	5100	0.0026	0.357	32.14	11.47
40	60	10	184	120	11386	33856	7500	0.0014	0.373	29.67	11.06
50	69	19	205	150	14137	42025	10410	0.0012	0.400	27.20	10.87
60	76	26	227	180	17261	51529	13750	0.0015	0.419	24.94	10.46
70	82	32	247	210	20421	61009	17420	0.0015	0.436	22.89	9.97
80	89	39	271	240	24645	73441	21860	0.0011	0.454	20.84	9.46
90	100	50	304	270	31146	92416	27620	0.0008	0.481	18.76	9.03
100	115	65	352	300	41994	123904	35570	0.0005	0.516	16.68	8.61
110	137	87	406	330	55710	164836	45050	0.0005	0.563	15.08	8.49
120	154	104	469	360	74169	219961	56690	0.0005	0.597	13.96	8.33
130	178	128	545	390	100769	297025	71440	0.0003	0.642	12.83	8.24
140	213	163	638	420	138062	407044	90010	0.0003	0.702	11.74	8.24

150	247	197	750	450	190478	562500	113270	0.0003	0.756	10.65	8.05
160	290	240	880	480	262758	774400	141760	0.0002	0.819	9.56	7.83
170	343	293	1027	510	356985	1054729	175630	0.0002	0.891	8.47	7.55
180	394	344	1188	540	476286	1411344	214920	0.0002	0.955	7.39	7.06
190	451	401	1357	570	620781	1841449	259010	0.0002	1.000	6.66	6.66
200	512	462							1.000	5.93	
<i>Flame Front Position x</i>	<i>Time to position x t (s)</i>	<i>Time from ignition (s)</i>	Σt	Σx	$\Sigma(t^2)$	$\Sigma(t)^2$	$\Sigma(t.x)$	V_f	$F(t)$	\dot{q}_e	$\dot{q}_e.F(t)$
RIFT – 17mm plywood low preheat time Test 6	Ignition Time	69						m/s		kW/m ²	
10	51	0							0.344	37.09	
20	52	1	158	60	8330	24964	3200	0.0046	0.347	34.62	12.01
30	55	4	167	90	9329	27889	5090	0.0024	0.357	32.14	11.47
40	60	9	182	120	11114	33124	7400	0.0017	0.373	29.67	11.06
50	67	16	204	150	14018	41616	10370	0.0012	0.394	27.20	10.71
60	77	26	234	180	18518	54756	14270	0.0009	0.422	24.94	10.53
70	90	39	267	210	24029	71289	18920	0.0009	0.456	22.89	10.45
80	100	49	305	240	31325	93025	24650	0.0008	0.481	20.84	10.03
90	115	64	345	270	40125	119025	31350	0.0007	0.516	18.76	9.68
100	130	79	397	300	53229	157609	40070	0.0005	0.549	16.68	9.15
110	152	101	455	330	69933	207025	50480	0.0005	0.593	15.08	8.94
120	173	122	531	360	95469	281961	64260	0.0004	0.633	13.96	8.83
130	206	155	615	390	128061	378225	80580	0.0003	0.691	12.83	8.86
140	236	185	715	420	172661	511225	100770	0.0003	0.739	11.74	8.68
150	273	222	818	450	225706	669124	123430	0.0003	0.795	10.65	8.46
160	309	258	934	480	293914	872356	150230	0.0003	0.846	9.56	8.08

170	352	301	1065	510	382601	1134225	182000	0.0002	0.903	8.47	7.65
180	404	353	1216	540	498720	1478656	219960	0.0002	0.967	7.39	7.15
190	460	409	1378	570	639012	1898884	262920	0.0002	1.000	6.66	6.66
200	514	463	1550	600	807572	2402500	311160	0.0002	1.000	5.93	5.93
210	576	525	1710	625	980372	2924100	357060	0.0001	1.000	5.25	5.25
215	620	569							1.000	4.94	

Flame Front Position x	Time to position x t (s)	Time from ignition (s)	Σt	Σx	$\Sigma(t^2)$	$\Sigma(t)^2$	$\Sigma(t.x)$	V_f	$F(t)$	\dot{q}_e	$\dot{q}_e \cdot F(t)$
--------------------------	------------------------------	------------------------	------------	------------	---------------	---------------	---------------	-------	--------	-------------	------------------------

RIFT – 17mm plywood full preheat time Test 1

	Ignition Time							m/s		kW/m ²	
	291										
10	0	0									
20	0	0									
30	0	0									
40	0	0									
50	0	0									
60	0	0									
70	0	0									
80	0	0									
90	296	5								18.76	
100	301	10	906	300	273698	820836	90730	0.0015	1.000	16.68	16.68
110	309	18	932	330	289766	868624	102730	0.0009	1.000	15.08	15.08
120	322	31	964	360	310054	929296	115920	0.0008	1.000	13.96	13.96
130	333	42	1000	390	333598	1000000	130230	0.0009	1.000	12.83	12.83
140	345	54	1071	420	384363	1147041	150540	0.0003	1.000	11.74	11.74
150	393	102	1155	450	447363	1334025	173970	0.0003	1.000	10.65	10.65
160	417	126	1249	480	521059	1560001	200300	0.0004	1.000	9.56	9.56
170	439	148	1323	510	584699	1750329	225410	0.0004	1.000	8.47	8.47
180	467	176	1399	540	653859	1957201	252360	0.0004	1.000	7.39	7.39
190	493	202	1498	570	750582	2244004	285330	0.0003	1.000	6.66	6.66
200	538	247	1624	598	884142	2637376	324614	0.0002	1.000	5.93	5.93

208	593	302							1.000	5.39		
<i>Flame Front Position x</i>	<i>Time to position x t (s)</i>	<i>Time from ignition (s)</i>	Σt	Σx	$\Sigma(t^2)$	$\Sigma(t)^2$	$\Sigma(t.x)$	V_f	$F(t)$	\dot{q}_{e}''	$\dot{q}_{e}'' . F(t)$	
RIFT – 17mm plywood full preheat time Test 2	Ignition Time	329						m/s		kW/m ²		
10	0	0										
20												
30												
40												
50												
60												
70												
80												
90												
100	337	8							1.000	16.68		
110	340	11	1026	330	350970	1052676	112980	0.0015	1.000	15.08	15.08	
120	349	20	1048	360	366282	1098304	125950	0.0011	1.000	13.96	13.96	
130	359	30	1079	390	388323	1164241	140490	0.0009	1.000	12.83	12.83	
140	371	42	1115	420	414747	1243225	156360	0.0008	1.000	11.74	11.74	
150	385	56	1159	450	448275	1343281	174170	0.0006	1.000	10.65	10.65	
160	403	74	1276	480	548778	1628176	205190	0.0002	1.000	9.56	9.56	
170	488	159	1408	510	667842	1982464	240500	0.0002	1.000	8.47	8.47	
180	517	188	1497	540	747497	2241009	269500	0.0001	1.000	7.39	7.39	
190	492	163	1538	570	789194	2365444	292340	0.0002	1.000	6.66	6.66	
200	529	200	1588	600	843394	2521744	318350	0.0003	1.000	5.93	5.93	
210	567	238	1699	630	964939	2886601	357530	0.0003	1.000	5.25	5.25	
220	603	274	1796	653	1076974	3225616	391328	0.0002	1.000	4.62	4.62	

Flame Front Position x	Time to position x t (s)	Time from ignition (s)	Σt	Σx	$\Sigma(t^2)$	$\Sigma(t)^2$	$\Sigma(tx)$	V_f	$F(t)$	\dot{q}_{e}''	$\dot{q}_{e}'' \cdot F(t)$
223	626	297							1.000	4.43	
RIFT – 17mm plywood full preheat time Test 3											
	Ignition Time	432									
10											
20											
30											
40											
50											
60											
70											
80											
90											
100	435	3							1.000	16.68	
110	442	10	1328	330	587990	1763584	146240	0.0012	1.000	15.08	15.08
120	451	19	1358	360	614990	1844164	163190	0.0009	1.000	13.96	13.96
130	465	33	1397	390	650987	1951609	181910	0.0007	1.000	12.83	12.83
140	481	49	1449	420	700595	2099601	203240	0.0005	1.000	11.74	11.74
150	503	71	1511	450	762099	2283121	227110	0.0004	1.000	10.65	10.65
160	527	95	1584	480	837654	2509056	253950	0.0004	1.000	9.56	9.56
170	554	122	1673	510	935109	2798929	285060	0.0003	1.000	8.47	8.47
180	592	160	1795	540	1078581	3222025	324050	0.0002	1.000	7.39	7.39
190	649	217	1955	570	1281461	3822025	372670	0.0002	1.000	6.66	6.66
200	714	282	2126	600	1513166	4519876	426340	0.0002	1.000	5.93	5.93
210	763	331	2306	630	1779206	5317636	485410	0.0002	1.000	5.25	5.25

Flame Front Position x	Time to position x t (s)	Time from ignition (s)	Σt	Σx	$\Sigma(t^2)$	$\Sigma(t)^2$	$\Sigma(t.x)$	V_f	$F(t)$	\dot{q}_{e}''	$\dot{q}_{e}'' . F(t)$
220	829	397							1.000	4.62	
RIFT – 17mm plywood full preheat time Test 4	Ignition Time	455						m/s		kW/m ²	
10	0	0									
20	0	0									
30	0	0									
40	0	0									
50	0	0									
60	0	0									
70	0	0									
80	0	0									
90	0	0									
100	462	7								16.68	
110	467	12	1402	330	655262	1965604	154330	0.0018	1.000	15.08	15.08
120	473	18	1420	360	672218	2016400	170530	0.0015	1.000	13.96	13.96
130	480	25	1442	390	693250	2079364	187620	0.0012	1.000	12.83	12.83
140	489	34	1469	420	719521	2157961	205860	0.0010	1.000	11.74	11.74
150	500	45	1505	450	755377	2265025	226020	0.0007	1.000	10.65	10.65
160	516	61	1550	480	801412	2402500	248340	0.0006	1.000	9.56	9.56
170	534	79	1609	510	863893	2588881	273960	0.0005	1.000	8.47	8.47
180	559	104	1678	540	939862	2815684	302550	0.0004	1.000	7.39	7.39
190	585	130	1766	570	1041590	3118756	336170	0.0003	1.000	6.66	6.66
200	622	167	1864	600	1160758	3474496	373520	0.0003	1.000	5.93	5.93
210	657	202	1961	630	1283657	3845521	412410	0.0003	1.000	5.25	5.25
220	682	227							1.000	4.62	

<i>Flame Front Position x</i>	<i>Time to position x t (s)</i>	<i>Time from ignition (s)</i>	Σt	Σx	$\Sigma(t^2)$	$\Sigma(t)^2$	$\Sigma(t.x)$	V_f	$F(t)$	\dot{q}_{e}''	$\dot{q}_{e}'' \cdot F(t)$
RIFT – 17mm plywood full preheat time Test 5	Ignition Time	432						m/s		kW/m ²	
10	0	0									
20	0	0									
30	0	0									
40	0	0									
50	0	0									
60	0	0									
70	0	0									
80	0	0									
90	0	0									
100	439	7								16.68	
110	443	11	1331	330	590571	1771561	146510	0.0020	1.000	15.08	15.08
120	449	17	1350	360	607614	1822500	162150	0.0013	1.000	13.96	13.96
130	458	26	1375	390	630389	1890625	178940	0.0011	1.000	12.83	12.83
140	468	36	1405	420	658229	1974025	196910	0.0010	1.000	11.74	11.74
150	479	47	1441	450	692501	2076481	216410	0.0008	1.000	10.65	10.65
160	494	62	1483	480	733577	2199289	237590	0.0006	1.000	9.56	9.56
170	510	78	1537	510	788225	2362369	261680	0.0005	1.000	8.47	8.47
180	533	101	1611	540	866813	2595321	290560	0.0003	1.000	7.39	7.39
190	568	136	1714	570	982482	2937796	326460	0.0002	1.000	6.66	6.66
200	613	181	1842	600	1135314	3392964	369330	0.0002	1.000	5.93	5.93
210	661	229	2006	629	1348514	4024036	421718	0.0002	1.000	5.25	5.25
219	732	300							1.000	4.68	

Flame Front Position x	Time to position x t (s)	Time from ignition (s)	Σt	Σx	$\Sigma(t^2)$	$\Sigma(t)^2$	$\Sigma(t.x)$	V_f	$F(t)$	\dot{q}_{e}''	$\dot{q}_{e}'' . F(t)$
RIFT – 17mm plywood full preheat time Test 6	Ignition Time	432						m/s		kW/m ²	
10	0	0									
20	0	0									
30	0	0									
40	0	0									
50	0	0									
60	0	0									
70	0	0									
80	0	0									
90	0	0									
100	439	7							1.000	16.68	
110	443	11	1331	330	590571	1771561	146510	0.0020	1.000	15.08	15.08
120	449	17	1350	360	607614	1822500	162150	0.0013	1.000	13.96	13.96
130	458	26	1375	390	630389	1890625	178940	0.0011	1.000	12.83	12.83
140	468	36	1405	420	658229	1974025	196910	0.0010	1.000	11.74	11.74
150	479	47	1441	450	692501	2076481	216410	0.0008	1.000	10.65	10.65
160	494	62	1483	480	733577	2199289	237590	0.0006	1.000	9.56	9.56
170	510	78	1537	510	788225	2362369	261680	0.0005	1.000	8.47	8.47
180	533	101	1611	540	866813	2595321	290560	0.0003	1.000	7.39	7.39
190	568	136	1714	570	982482	2937796	326460	0.0002	1.000	6.66	6.66
200	613	181	1842	600	1135314	3392964	369330	0.0002	1.000	5.93	5.93
210	661	229	2006	629	1348514	4024036	421718	0.0002	1.000	5.25	5.25
219	732	300							1.000	4.68	

Medium Density Fibreboard (MDF)

<i>Flame Front Position x</i>	<i>Time to position x t (s)</i>	<i>Time from ignition (s)</i>	Σt	Σx	$\Sigma(t^2)$	$\Sigma(t)^2$	$\Sigma(t.x)$	V_f	$F(t)$	\dot{q}_e	$\dot{q}_e.F(t)$	$1/\sqrt{V_f}$
LIFT – 18mm MDF Test 1	Ignition Time	479						m/s		kW/m ²		(m/s) ^{-0.5}
50	479											
75	479											
100	479											
125	479											
150	479											
175	479											
200	479											
225	482	3								18.54		
250	488	9	1462	750	712532	2137444	365750	0.0049	1.000	17.25	17.25	14.236
275	492	13	1510	825	761108	2280100	416300	0.0010	1.000	15.85	15.85	31.992
300	530	51	1598	900	854740	2553604	481500	0.0006	1.000	14.45	14.45	41.050
325	576	97	1746	975	1022276	3048516	570200	0.0005	1.000	12.84	12.84	47.113
350	640	161	1924	1050	1242640	3701776	676700	0.0004	1.000	11.23	11.23	51.389
375	708	229	2159	1125	1568585	4661281	813900	0.0003	1.000	9.64	9.64	58.888
400	811	332	2461	1200	2046349	6056521	990250	0.0002	1.000	8.05	8.05	68.574
425	942	463	2887	1275	2831041	8334769	1235050	0.0002	1.000	7.01	7.01	80.850
450	1134	655	3308	1335	3691144	10942864	1477370	0.0001	1.000	5.97	5.97	90.534
460	1232	753							1.000	5.56	5.56	

Flame Front Position x	Time to position x t (s)	Time from ignition (s)	Σt	Σx	$\Sigma(t^2)$	$\Sigma(t)^2$	$\Sigma(t.x)$	V_f	$F(t)$	q_e''	$q_e'' \cdot F(t)$	$1/\sqrt{V_f \cdot x}$
LIFT – 18mm MDF Test 2	Ignition Time	478						m/s		kW/m ²		(m/s) ^{-0.5}
50	478											
75	478											
100	478											
125	478											
150	478											
175	478											
200	478											
225	478											
250	478											
275	487	9								15.85		
300	515	37	1558	900	811530	2427364	469125	0.0007	1.000	14.45	14.45	37.367
325	556	78	1678	975	942810	2815684	547650	0.0005	1.000	12.84	12.84	42.980
350	607	129	1850	1050	1149554	3422500	650775	0.0004	1.000	11.23	11.23	51.602
375	687	209	2098	1125	1486834	4401604	791675	0.0003	1.000	9.64	9.64	63.137
400	804	326	2418	1200	1977714	5846724	973200	0.0002	1.000	8.05	8.05	69.289
425	927	449	2820	1266	1712770	7952400	738325	0.0005	1.000	7.01	7.01	45.570
441	1089	611							1.000	6.35	6.35	
Flame Front Position x	Time to position t	time from ignition	Σt	Σx	$\Sigma(t^2)$	$\Sigma(t)^2$	$\Sigma(t.x)$	V	$F(t)$	q''	$q'' \cdot F(t)$	$1/\sqrt{V}$
LIFT – 18mm MDF Test 3	Ignition Time	455s						m/s		kW/m ²		(m/s) ^{-0.5}
50	455											
75	455											
100	455											

125	455												
150	455												
175	455												
200	455												
225	455												
250	455												
275	466	11									15.85		
300	487	32	1478	900	729950	2184484	444875	0.0008	1.000	14.45	14.45	34.823	
325	525	70	1589	975	845723	2524921	518675	0.0006	1.000	12.84	12.84	42.597	
350	577	122	1740	1050	1015598	3027600	611825	0.0004	1.000	11.23	11.23	47.590	
375	638	183	1950	1125	1280198	3802500	735200	0.0003	1.000	9.64	9.64	56.698	
400	735	280	2232	1200	1685150	4981824	898325	0.0002	1.000	8.05	8.05	66.648	
425	859	404	2618	1275	1278106	6853924	659075	0.0005	1.000	7.01	7.01	47.107	
450	1024	569	2992	1332	1786457	8952064	825875	0.0004	1.000	5.97	5.97	48.815	
457	1109	654							1.000	5.69	5.69		

Flame Front Position x	Time t (s)	Time to position	Σt	Σx	$\Sigma(t^2)$	$\Sigma(t)^2$	$\Sigma(t.x)$	V_f	$F(t)$	\dot{q}_e	$\dot{q}_e.F(t)$	$1/\sqrt{V_f}$
		Ignition Time	69s					m/s		kW/m ²	(m/s) ^{-0.5}	
10	69	0								34.0		
20	69	0	207	60	14283	42849	4140	#DIV/0!	0.441	33.1	14.57	
30	69	0	207	90	14283	42849	6210	#DIV/0!	0.441	32.5	14.31	
40	69	0	211	120	14851	44521	8480	0.0038	0.441	30.0	13.22	16.330
50	73	4	226	150	17146	51076	11450	0.0012	0.453	27.5	12.48	28.363
60	84	15	256	180	22186	65536	15620	0.0008	0.486	25.3	12.31	36.197
70	99	30	301	210	30781	90601	21410	0.0006	0.528	23.4	12.33	41.326
80	118	49	356	240	43046	126736	28880	0.0005	0.576	21.4	12.33	44.740
90	139	70	428	270	62486	183184	39050	0.0004	0.625	19.2	11.99	51.846
100	171	102	516	300	90998	266256	52270	0.0003	0.694	16.9	11.75	57.899
110	206	137	626	330	133678	391876	69640	0.0003	0.761	15.0	11.45	62.559

120	249	180	751	360	192053	564001	91020	0.0002	0.837	13.5	11.29	67.104
130	296	227	893	390	270721	797449	117080	0.0002	0.913	11.9	10.90	70.386
140	348	279	1052	420	375184	11067604	148400	0.0002	0.990	10.8	10.72	74.897
150	408	339	1243	450	524737	1545049	187840	0.0001	1.000	9.7	9.72	83.626
160	487	418							1.000	8.7	8.67	

Flame Front Position x	Time to position t (s)	time from ignition	Σt	Σx	$\Sigma(t^2)$	$\Sigma(t)^2$	$\Sigma(t.x)$	V_f	$F(t)$	\dot{q}_e	$\dot{q}_e.F(t)$	$1/\sqrt{V_f}$
	Ignition Time	60s						m/s	kW/m ²			(m/s) ^{-0.5}
										34.9		
10	60	0							0.411	34.0	13.96	
20	61	1	184	60	11290	33856	3710	0.0064	0.414	33.1	13.70	12.472
30	63	3	190	90	12046	36100	5750	0.0039	0.421	32.5	13.67	15.916
40	66	6	203	120	13801	41209	8230	0.0017	0.431	30.0	12.93	24.246
50	74	14	227	150	17401	51529	11560	0.0009	0.456	27.5	12.57	32.708
60	87	27	263	180	23449	69169	16060	0.0007	0.495	25.3	12.53	37.448
70	102	42	306	210	31662	93636	21720	0.0007	0.536	23.4	12.52	38.730
80	117	57	355	240	42589	126025	28740	0.0006	0.574	21.4	12.28	41.326
90	136	76	422	270	60746	178084	38500	0.0004	0.619	19.2	11.86	51.603
100	169	109	498	300	84306	248004	50370	0.0003	0.690	16.9	11.68	53.607
110	193	133	594	330	119634	352836	65970	0.0003	0.737	15.0	11.08	56.653
120	232	172	704	360	168914	495616	85340	0.0002	0.808	13.5	10.90	65.669
130	279	219	842	390	241226	708964	110450	0.0002	0.886	11.9	10.58	70.386
140	331	271	999	420	338723	998001	140960	0.0002	0.965	10.8	10.45	74.199
150	389	329	1183	450	475251	1399489	178770	0.0002	1.000	9.7	9.72	81.439
160	463	403	1341	320	369171	1798281	133020	0.0000	1.000	8.7	8.67	151.590
164	489	429							1.000	8.1	8.08	

Flame Front Position x	Time to position	time from ignition	Σt	Σx	$\Sigma(t^2)$	$\Sigma(t)^2$	$\Sigma(t.x)$	V_f	$F(t)$	q_e	$q_e.F(t)$	$1/\sqrt{V_f}$
	x	t (s)										
MDF-RIFT - low preheat ISO ign data test 3			Ignition Time	59s				m/s		kW/m ²		(m/s) ^{-0.5}
10	59	0							0.407	34.0		
20	59	0	177	60	10443	31329	3540	#DIV/0!	0.407	33.1	13.47	!
30	59	0	183	90	11187	33489	5550	0.0025	0.407	32.5	13.23	20.000
40	65	6	199	120	13331	39601	8120	0.0012	0.428	30.0	12.83	28.577
50	75	16	228	150	17594	51984	11630	0.0009	0.459	27.5	12.65	34.008
60	88	29	266	180	23978	70756	16240	0.0007	0.498	25.3	12.60	37.448
70	103	44	310	210	32514	96100	22010	0.0006	0.538	23.4	12.58	39.377
80	119	60	360	240	43814	129600	29150	0.0006	0.579	21.4	12.39	41.884
90	138	79	422	270	60430	178084	38440	0.0004	0.623	19.2	11.94	48.199
100	165	106	499	300	84685	249001	50480	0.0003	0.681	16.9	11.54	53.894
110	196	137	598	330	121810	357604	66500	0.0003	0.743	15.0	11.17	60.193
120	237	178	713	360	172985	508369	86400	0.0002	0.817	13.5	11.02	64.814
130	280	221	847	390	243469	717409	111040	0.0002	0.888	11.9	10.60	68.255
140	330	271	1001	420	340181	1002001	141250	0.0002	0.964	10.8	10.44	74.620
150	391	332	1199	450	490265	1437601	181330	0.0001	1.000	9.7	9.72	86.465
160	478	419	1397	370	388761	1951609	140290	0.0001	1.000	8.7	8.67	90.437
164	528	469							1.000	8.1	8.08	
MDF-RIFT - low preheat ISO ign data test 4			Ignition Time	66s				m/s		kW/m ²		(m/s) ^{-0.5}
10	66	0							0.431	34.0		
20	67	1		60	13469	0	4040	0.0003	0.434	33.1	14.36	57.740
30	68	2		90	14013	0	6180	0.0004	0.437	32.5	14.20	47.618
40	70	4	212	120	15000	44944	8540	0.0032	0.444	30.0	13.32	17.638
50	74	8	230	150	17772	52900	11660	0.0012	0.456	27.5	12.57	29.439

60	86	20	260	180	22872	67600	15860	0.0008	0.492	25.3	12.46	36.091
70	100	34	304	210	31320	92416	21600	0.0006	0.530	23.4	12.39	40.104
80	118	52	355	240	42693	126025	28770	0.0005	0.576	21.4	12.33	43.017
90	137	71	422	270	60582	178084	38470	0.0004	0.621	19.2	11.90	49.911
100	167	101	502	300	85862	252004	50810	0.0003	0.686	16.9	11.61	55.229
110	198	132	602	330	123262	362404	66920	0.0003	0.746	15.0	11.23	59.289
120	237	171	714	360	173214	509796	86490	0.0002	0.817	13.5	11.02	63.654
130	279	213	853	390	247579	727609	111890	0.0002	0.886	11.9	10.58	71.012
140	337	271	1010	420	346646	1020100	142550	0.0002	0.974	10.8	10.55	75.830
150	394	328	1257	450	545481	1580049	190440	0.0001	1.000	9.7	9.72	99.730
160	526	460	1460	473	723512	2131600	231280	0.0001	1.000	8.7	8.67	109.287
163	540	474							1.000	8.2	8.23	

Flame Front Position x	Time to position t (s)	time from ignition	Σt	Σx	$\Sigma(t^2)$	$\Sigma(t)^2$	$\Sigma(t.x)$	V_f	$F(t)$	\dot{q}_e	$\dot{q}_e.F(t)$	$1/\sqrt{V_f}$
MDF-RIFT - low preheat ISO ign data test 5												
10	61	0						0.414	34.0	14.08		
20	62	1	187	60	11661	34969	3770	0.0064	0.418	33.1	13.81	12.472
30	64	3	195	90	12701	38025	5920	0.0027	0.424	32.5	13.78	19.272
40	69	8	207	120	14333	42849	8380	0.0020	0.441	30.0	13.22	22.361
50	74	13	229	150	17633	52441	11620	0.0011	0.456	27.5	12.57	29.967
60	86	25	259	180	22673	67081	15790	0.0008	0.492	25.3	12.46	35.365
70	99	38	305	210	31597	93025	21690	0.0006	0.528	23.4	12.33	41.610
80	120	59	360	240	44082	129600	29220	0.0005	0.581	21.4	12.44	45.826
90	141	80	432	270	63522	186624	39390	0.0004	0.630	19.2	12.07	50.759
100	171	110	513	300	89523	263169	51900	0.0003	0.694	16.9	11.75	54.772
110	201	140	614	330	128206	376996	68250	0.0003	0.752	15.0	11.31	59.820
120	242	181	731	360	181909	534361	88590	0.0002	0.825	13.5	11.13	65.991
130	288	227	875	390	260533	765625	114780	0.0002	0.900	11.9	10.75	71.900
140	345	284	1037	420	365185	1075369	146340	0.0002	0.985	10.8	10.67	76.162

150	404	343	1230	450	513602	1512900	185860	0.0001	1.000	9.7	9.72	82.703
160	481	420	1439	472	701493	2070721	227308	0.0001	1.000	8.7	8.67	111.487
162	554	493							1.000	8.4	8.37	

Flame Front Position x	Time to position x	time from ignition	Σt	Σx	$\Sigma(t^2)$	$\Sigma(t)^2$	$\Sigma(t.x)$	V_f	$F(t)$	\dot{q}_e	$\dot{q}_e.F(t)$	$1/\sqrt{V_f}$
	t (s)							m/s	kW/m ²			(m/s) ^{-0.5}
MDF-RIFT - low preheat. ISO ign data test 6	Ignition Time	68s										
10	68	0							0.437	34.0	14.86	
20	68.5	0.5	206	60	14077	42230	4120	0.0200	0.439	33.1	14.52	7.071
30	69	1	208	90	14353	43056	6240	0.0129	0.441	32.5	14.31	8.819
40	70	2	215	120	15437	46225	8670	0.0024	0.444	30.0	13.32	20.237
50	76	8	237	150	18957	56169	12060	0.0009	0.462	27.5	12.74	33.381
60	91	23	271	180	24873	73441	16540	0.0007	0.506	25.3	12.82	37.448
70	104	36	315	210	33497	99225	22340	0.0007	0.541	23.4	12.64	38.147
80	120	52	366	240	45380	133956	29660	0.0005	0.581	21.4	12.44	43.770
90	142	74	433	270	63805	187489	39480	0.0004	0.632	19.2	12.12	50.656
100	171	103	515	300	90209	265225	52100	0.0003	0.694	16.9	11.75	54.782
110	202	134	614	330	128126	376996	68240	0.0003	0.754	15.0	11.34	59.289
120	241	173	725	360	178409	525625	87800	0.0002	0.824	13.5	11.11	63.252
130	282	214	857	390	249161	734449	112340	0.0002	0.891	11.9	10.64	68.350
140	334	266	1012	420	347896	1024144	142820	0.0002	0.969	10.8	10.50	75.595
150	396	328	1196	450	485528	1430416	180720	0.0002	1.000	9.7	9.72	81.290
160	466	398	1389	475	651701	1929321	220915	0.0001	1.000	8.7	8.67	93.171
165	527	459							1.000	7.9	7.93	

<i>Flame Front Position x</i>	<i>Time to position x - t (s)</i>	<i>time from ignition</i>	Σt	Σx	$\Sigma(t^2)$	$\Sigma(t)^2$	$\Sigma(t.x)$	V_f	$F(t)$	$\dot{q}_{.e}$	$\dot{q}_{.e}.F(t)$	$1/\sqrt{V_f}$
MDF – RIFT –Full preheat Test 1	Ignition Time	364s						m/s		kW/m ²		(m/s) ^{-0.5}
10												
20												
30												
40												
50												
60												
70												
80												
90												
100	369	5							1.000	16.9		
110	382	18	1154	330	444494	1331716	127280	0.0006	1.000	15.0	15.04	41.610
120	403	39	1221	360	498429	1490841	147060	0.0004	1.000	13.5	13.49	52.387
130	436	72	1317	390	580989	1734489	171960	0.0003	1.000	11.9	11.95	61.384
140	478	114	1441	420	696309	2076481	202650	0.0002	1.000	10.8	10.83	67.520
150	527	163	1593	450	851957	2537649	240050	0.0002	1.000	9.7	9.72	74.309
160	588	224	1774	480	1057754	3147076	285160	0.0002	1.000	8.7	8.67	81.318
170	659	295	1969	510	1301309	3876961	336070	0.0001	1.000	7.7	7.68	81.902
180	722	358								6.7		

<i>Flame Front Position x</i>	<i>Time to position x t (s)</i>	<i>time from ignition</i>	Σt	Σx	$\Sigma(t^2)$	$\Sigma(t)^2$	$\Sigma(t.x)$	V_f	$F(t)$	q_e	$q_e.F(t)$	$1/\sqrt{V_f}$
MDF – RIFT –Full preheat Test 2	Ignition Time	357s						m/s		kW/m ²		(m/s) ^{-0.5}
10												
20												
30												
40												
50												
60												
70												
80												
90												
100	365	8								16.9		
110	382	25	1149	330	440753	1320201	126760	0.0005	1.000	15.0	15.04	43.059
120	402	45	1222	360	499372	1493284	147200	0.0003	1.000	13.5	13.49	53.630
130	438	81	1313	390	577177	1723969	171400	0.0003	1.000	11.9	11.95	59.584
140	473	116	1434	420	689102	2056356	201610	0.0002	1.000	10.8	10.83	65.530
150	523	166	1574	450	831342	2477476	237150	0.0002	1.000	9.7	9.72	72.484
160	578	221	1742	480	1018494	3034564	279900	0.0002	1.000	8.7	8.67	76.870
170	641	284	1920	340	744965	3686400	201450	0.0000	1.000	7.7	7.68	173.086
180	701	344	2091	535	1463283	4372281	373715	0.0001	1.000	6.7	6.70	84.507
185	749	392								6.2		
MDF – RIFT –Full preheat Test 3	Ignition Time	359s						m/s		kW/m ²		(m/s) ^{-0.5}
10												
20												
30												

40												
50												
60												
70												
80												
90												
100	365	6							1.000	16.9		
110	378	19	1165	330	454193	1357225	128720	0.0003	1.000	15.0	15.04	55.955
120	422	63	1257	360	529817	1580049	151630	0.0003	1.000	13.5	13.49	62.985
130	457	98	1374	390	631958	1887876	179350	0.0003	1.000	11.9	11.95	60.432
140	495	136	1476	420	728450	2178576	207310	0.0003	1.000	10.8	10.83	58.053
150	524	165	1592	450	847930	2534464	239580	0.0003	1.000	9.7	9.72	63.131
160	573	214	1734	370	602905	3006756	170280	0.0001	1.000	8.7	8.67	95.726
170	637	278	1910	510	1224098	3648100	325970	0.0002	1.000	7.7	7.68	79.688
180	700	341	2085	535	1455273	4347225	372670	0.0001	1.000	6.7	6.70	85.644
185	748	389								6.2		

<i>Flame Front Position x</i>	<i>Time to position x t (s)</i>	<i>time from ignition</i>	Σt	Σx	$\Sigma(t^2)$	$\Sigma(t)^2$	$\Sigma(t.x)$	V_f	$F(t)$	" \dot{q}_e	" $\dot{q}_e.F(t)$	$1/\sqrt{V_f}$
MDF – RIFT –Full preheat Test 4	Ignition Time	358s						m/s		kW/m ²		(m/s) ^{-0.5}

10
20
30
40
50
60
70
80
90
100

366 8

16.9

110	380	22	1148	330	439960	1317904	126640	0.0005	1.000	15.0	15.04	42.774
120	402	44	1213	360	491765	1471369	146070	0.0004	1.000	13.5	13.49	50.656
130	431	73	1304	390	569206	1700416	170210	0.0003	1.000	11.9	11.95	58.985
140	471	113	1423	420	679043	2024929	200120	0.0002	1.000	10.8	10.83	67.220
150	521	163	1573	450	830843	2474329	237050	0.0002	1.000	9.7	9.72	74.264
160	581	223	1735	480	1009691	3010225	278720	0.0002	1.000	8.7	8.67	74.897
170	633	275	1903	510	1212971	3621409	324590	0.0002	1.000	7.7	7.68	73.501
180	689	331	2046	534	1399586	4186116	364846	0.0002	1.000	6.7	6.70	80.027
184	724	366							1.000	6.3		

<i>Flame Front Position x</i>	<i>Time to position x t (s)</i>	<i>time from ignition</i>	Σt	Σx	$\Sigma(t^2)$	$\Sigma(t)^2$	$\Sigma(t.x)$	V_f	$F(t)$	" \dot{q}_e	" $\dot{q}_e.F(t)$	$1/\sqrt{V_f}$
MDF – RIFT –Full preheat Test 5	Ignition Time	367s						m/s		kW/m ²		(m/s) ^{-0.5}

10												
20												
30												
40												
50												
60												
70												
80												
90												
100	377	10							1.000	16.9		
110	395	28	1189	330	472043	1413721	131190	0.0005	1.000	15.0	15.04	44.796
120	417	50	1266	360	536030	1602756	152510	0.0003	1.000	13.5	13.49	54.896
130	454	87	1370	390	629006	1876900	178920	0.0002	1.000	11.9	11.95	64.133
140	499	132	1504	420	758718	2262016	211530	0.0002	1.000	10.8	10.83	69.702
150	551	184	1664	450	929598	2768896	250750	0.0002	1.000	9.7	9.72	75.944
160	614	247	1848	480	1147086	3415104	297000	0.0002	1.000	8.7	8.67	81.268
170	683	316	2050	509	1410494	4202500	349137	0.0001	1.000	7.7	7.68	85.539

179	753	386							1.000	6.5		
<i>Flame Front Position x</i>	<i>Time to position x t (s)</i>	<i>time from ignition</i>	Σt	Σx	$\Sigma(t^2)$	$\Sigma(t)^2$	$\Sigma(t.x)$	V_f	$F(t)$	$\dot{q}_{.e}$	$\dot{q}_{.e}.F(t)$	$1/\sqrt{V_f}$
MDF – RIFT –Full preheat Test 6	Ignition Time	358s						m/s		kW/m ²		(m/s) ^{-0.5}
10												
20												
30												
40												
50												
60												
70												
80												
90												
100	366	8							1.000	16.9		
110	381	23	1151	330	442333	1324801	126990	0.0005	1.000	15.0	15.04	43.910
120	404	46	1219	360	496733	1485961	146810	0.0004	1.000	13.5	13.49	51.628
130	434	76	1328	390	591672	1763584	173500	0.0002	1.000	11.9	11.95	66.566
140	490	132	1454	420	709356	2114116	204520	0.0002	1.000	10.8	10.83	69.602
150	530	172	1606	450	864396	2579236	241860	0.0002	1.000	9.7	9.72	69.602
160	586	228	1788	480	1075880	3196944	287500	0.0001	1.000	8.7	8.67	84.886
170	672	314	1972	510	1304776	3888784	336520	0.0002	1.000	7.7	7.68	81.560
180	714	356	2160	540	1560456	4665600	389820	0.0002	1.000	6.7	6.70	71.784
190	774	416							1.000	6.0		

Flame Front Position x	Time to position x t (s)	Melteca/ MDF										
		time from ignition	Σt	Σx	$\Sigma(t^2)$	$\Sigma(t)^2$	$\Sigma(t.x)$	V_f	$F(t)$	\dot{q}_e	$\dot{q}_e.F(t)$	$1/\sqrt{V_f}$
LIFT Melteca /MDF- test 1		Ignition Time	498s					m/s		kW/m ²		(m/s) ^{-0.5}
50												
75									0.000	35.4	0.00	
100									0.000	35.0	0.00	
125									0.000	33.7	0.00	
150									0.000	32.4	0.00	
175									0.000	30.7	0.00	
200									0.000	29.0	0.00	
225									0.000	27.4	0.00	
250									0.000	25.7	0.00	
275									0.000	23.3	0.00	
300	518	20							0.962	20.9	20.10	
325	569	71	1697	975	964185	2879809	553825	0.0005	1.000	19.2	19.20	42.980
350	610	112	1966	1050	1315230	3865156	693550	0.0002	1.000	17.5	17.50	70.183
375	787	289	2286	1125	1781790	5225796	864225	0.0002	1.000	14.9	14.90	75.594
400	889	391	2840	1200	2764586	8065600	1145425	0.0001	1.000	12.3	12.30	89.829
425	1164	666	3463	1270	4133317	11992369	1477750	0.0001	1.000	10.9	10.90	107.545
445	1410	912							1.000	9.8	9.78	
LIFT Melteca /MDF- test 2		Ignition Time	518s					m/s		kW/m ²		(m/s) ^{-0.5}
50												
75												
100	563	45							1.000	35.0	35.00	
125	566	48	1702	375	965654	2896804	213000	0.00475	1.000	33.7	33.70	14.514

150	573	55	1720	450	986246	2958400	258375	0.00333	1.000	32.4	32.40	17.333
175	581	63	1746	525	1016354	3048516	306025	0.00261	1.000	30.7	30.70	19.574
200	592	74	1773	600	1048025	3143529	355075	0.00261	1.000	29.0	29.00	19.574
225	600	82	1802	675	1082564	3247204	405900	0.00277	1.000	27.4	27.35	19.013
250	610	92	1830	750	1116500	3348900	458000	0.00250	1.000	25.7	25.70	20.000
275	620	102	1865	825	1159725	3478225	513500	0.00197	1.000	23.3	23.30	22.509
300	635	117	1969	900	1297421	3876961	593050	0.00046	1.000	20.9	20.90	46.589
325	714	196	2134	975	1529246	4553956	697300	0.00033	1.000	19.2	19.20	54.798
350	785	267	2387	1050	1914565	5697769	839800	0.00028	1.000	17.5	17.50	59.323
375	888	370	2743	1125	2549669	7524049	1035750	0.00017	1.000	14.9	14.90	76.459
400	1070	552	3196	1200	3466088	10214416	1287150	0.00014	1.000	12.3	12.30	83.688
425	1238	720	3826	1265	4981868	14638276	1622070	0.00009	1.000	10.9	10.90	108.058
440	1518	1000							1.000	10.1	10.06	

<i>Flame Front Position</i> x	<i>Time to position</i> $x \quad t \text{ (s)}$	<i>time from ignition</i>	Σt	Σx	$\Sigma(t^2)$	$\Sigma(t)^2$	$\Sigma(t.x)$	V_f	$F(t)$	" q_e	" $q_e.F(t)$	$1/V_f$
LIFT Melteca /MDF- test 3		Ignition Time	60					m/s		kW/m ²		(m/s) ^{-0.5}
50												
75									0.000	35.4		
100									0.000	35.0		
125									0.000	33.7		
150									0.000	32.4		
175									0.000	30.7		
200									0.000	29.0		
225									0.000	27.4		
250									0.000	25.7		
275	580	62							1.000	23.3		
300	605	87	1842	900	1134074	3392964	554525	0.0006	1.000	20.9	20.90	40.039
325	657	139	1987	975	1323299	3948169	648775	0.0004	1.000	19.2	19.20	49.135
350	725	207	2210	1050	1642858	4884100	777775	0.0003	1.000	17.5	17.50	58.888

375	828	310	2638	1125	2388434	6959044	998250	0.0001	1.000	14.9	14.90	87.402
400	1085	567	3383	1200	4023709	11444689	1369250	0.0001	1.000	12.3	12.30	114.062
425	1470	952							1.000	10.9	10.90	
445	1675	1157							1.000	9.8	9.78	

Flame Front Position x	Time to position x t (s)	time from ignition	Σt	Σx	$\Sigma(t^2)$	$\Sigma(t)^2$	$\Sigma(t.x)$	V_f	$F(t)$	\dot{q}_e	$\dot{q}_e \cdot F(t)$	$1/\sqrt{V_f}$
RIFT Melteca/MDF low preheat-test 1	Ignition Time	75s						m/s		kW/m ²		(m/s) ^{-0.5}
10	75	0							0.372	34.25	12.74	
20	78	3	234	60	18270	54756	4740	0.0033	0.379	33.40	12.67	17.321
30	81	6	243	90	19701	59049	7350	0.0033	0.386	31.99	12.36	17.321
40	84	9	260	120	22642	67600	10540	0.0013	0.394	29.45	11.59	27.860
50	95	20	351	150	45665	123201	18430	0.0002	0.418	27.00	11.30	72.284
60	172	97	472	180	80634	222784	29420	0.0002	0.563	24.80	13.97	76.114
70	205	130	628	210	134610	394384	44750	0.0003	0.615	22.75	13.98	63.132
80	251	176	756	240	195026	571536	61430	0.0002	0.680	20.62	14.03	68.932
90	300	225	896	270	272026	802816	81580	0.0002	0.744	18.39	13.67	68.577
100	345	270	1069	300	388801	1142761	108140	0.0002	0.797	16.28	12.99	79.721
110	424	349	1331	330	614645	1771561	148580	0.0001	0.884	14.50	12.82	105.439
120	562	487							1.000	12.91	12.91	

Flame Front Position x	Time to position t	time from ignition	Σt	Σx	$\Sigma(t^2)$	$\Sigma(t)^2$	$\Sigma(t.x)$	V	$F(t)$	q''	$q'' \cdot F(t)$	$1/\sqrt{V}$
RIFT Melteca/MDF low preheat-test 2	Ignition Time	48s						m/s		kW/m ²		(m/s) ^{-0.5}
10	48	0								34.25		
20	76	28	227	60	18689	51529	5090	0.00036	0.374	33.40	12.50	52.443
30	103	55	321	90	36549	103041	10290	0.00030	0.436	31.99	13.94	57.761
40	142	94	415	120	59673	172225	17270	0.00030	0.512	29.45	15.07	58.139

50	170	122	505	150	86313	255025	25760	0.00039	0.560	27.00	15.12	50.578
60	193	145	595	180	119973	354025	36320	0.00032	0.596	24.80	14.79	56.292
70	232	184	683	210	157637	466489	48460	0.00030	0.654	22.75	14.88	57.388
80	258	210	786	240	208004	617796	63520	0.00031	0.690	20.62	14.22	56.899
90	296	248	948	270	309416	898704	86680	0.00014	0.739	18.39	13.58	85.095
100	394	346	1218	300	521636	1483524	124120	0.00009	0.852	16.28	13.88	108.135
110	528	480	1522	330	794020	2316484	169480	0.00009	0.987	14.50	14.30	103.010
120	600	552	1848	359	1157184	3415104	222960	0.00010	1.000	12.91	12.91	101.790
129	720	672							1.000	12.97	12.97	

<i>Flame Front Position x</i>	<i>Time to position x t (s)</i>	<i>time from ignition</i>	Σt	Σx	$\Sigma(t^2)$	$\Sigma(t)^2$	$\Sigma(t.x)$	V_f	$F(t)$	q_e	$q_e \cdot F(t)$	$1/\sqrt{V_f}$
RIFT Melteca/MDF- low preheat-test 3		Ignition Time	60s					m/s		kW/m ²		(m/s) ^{-0.5}
10	60	0										
20	94	34	275	60	27077	75625	6110	0.0003	0.416	33.40	13.90	55.348
30	121	61	358	90	43926	128164	11230	0.0004	0.472	31.99	15.11	49.583
40	143	83	453	120	70811	205209	18800	0.0003	0.513	29.45	15.12	59.508
50	189	129	558	150	107246	311364	28730	0.0002	0.590	27.00	15.94	64.547
60	226	166	664	180	148798	440896	40440	0.0003	0.645	24.80	16.01	55.267
70	249	189	758	210	193166	574564	53630	0.0003	0.677	22.75	15.41	53.716
80	283	223	859	240	249019	737881	69500	0.0003	0.722	20.62	14.89	62.621
90	327	267	985	270	327643	970225	89570	0.0002	0.776	18.39	14.28	67.845
100	375	315	1172	300	468454	1373584	118630	0.0001	0.831	16.28	13.54	86.067
110	470	410	1389	330	657461	1929321	154480	0.0001	0.931	14.50	13.50	92.160
120	544	484	1633	353	899997	2666689	193117	0.0001	1.000	12.91	12.91	107.124
123	619	559							1.000	13.35	13.35	

<i>Flame Front Position x</i>	<i>Time to position x t (s)</i>	<i>time from ignition</i>	Σt	Σx	$\Sigma(t^2)$	$\Sigma(t)^2$	$\Sigma(t.x)$	V_f	$F(t)$	\dot{q}_e	$\dot{q}_e \cdot F(t)$	$1/\sqrt{V_f}$
RIFT Melteca/MDF- low preheat-test 4	Ignition Time	60s						m/s		kW/m ²		(m/s) ^{-0.5}
10	60	0	153	30	12249	23409	2460	0.0002	0.333	34.64	11.52	69.142
20	93	33	273	60	26649	74529	6060	0.0003	0.414	33.67	13.94	54.863
30	120	60	355	90	43213	126025	11140	0.0004	0.470	33.00	15.52	49.583
40	142	82	448	120	69160	200704	18580	0.0003	0.512	30.46	15.59	58.500
50	186	126	518	150	90860	268324	26380	0.0003	0.586	27.92	16.35	54.365
60	190	130	596	180	119096	355216	36100	0.0005	0.592	25.63	15.17	45.071
70	220	160	664	210	149016	440896	47120	0.0003	0.637	23.57	15.01	56.605
80	254	194	779	240	205941	606841	63170	0.0002	0.684	21.51	14.72	65.625
90	305	245	928	270	293702	861184	84670	0.0002	0.750	19.28	14.46	75.990
100	369	309	1208	300	514342	1459264	123090	0.0001	0.825	17.05	14.06	110.419
110	534	474	1526	329	809446	2328676	169777	0.0001	0.992	15.14	15.02	117.028
119	623	563							1.000	15.14	15.14	
RIFT Melteca/MDF- low preheat-test 5	Ignition Time	65s						m/s		kW/m ²		(m/s) ^{-0.5}
10	65	0										
20	105	40	297	60	31379	88209	6560	0.0003	0.440	33.67	14.81	56.454
30	127	62	406	90	57430	164836	12870	0.0003	0.484	33.00	15.97	60.008
40	174	109	491	120	82505	241081	20270	0.0003	0.566	30.46	17.25	58.346
50	190	125	599	150	121601	358801	30560	0.0003	0.592	27.92	16.53	57.269
60	235	170	705	180	169725	497025	43200	0.0002	0.658	25.63	16.87	67.082
70	280	215	846	210	243186	715716	60180	0.0002	0.718	23.57	16.93	69.327
80	331	266	1031	240	364361	1062961	83880	0.0001	0.781	21.51	16.81	84.687

90	420	355	1238	270	523130	1532644	112980	0.0001	0.880	19.28	16.97	88.610
100	487	422	1563	298	843905	2442969	157348	0.0001	0.947	17.05	16.15	118.971
108	656	591							1.000	17.05	17.05	

<i>Flame Front Position x</i>	<i>Time to position x t (s)</i>	<i>time from ignition</i>	Σt	Σx	$\Sigma(t^2)$	$\Sigma(t)^2$	$\Sigma(t.x)$	V_f	$F(t)$	q_e	$q_e \cdot F(t)$	$1/\sqrt{V_f}$
RIFT Melteca/MDF- low preheat-test 6		Ignition Time	60s					m/s		kW/m ²		(m/s) ^{-0.5}
10	60											
20	70	70	217	60	16069	47089	4610	0.0007	0.359	33.67	12.09	37.152
30	87	87	258	90	22670	66564	8050	0.0006	0.400	33.00	13.22	39.431
40	101	101	317	120	34411	100489	13100	0.0005	0.431	30.46	13.14	46.667
50	129	129	408	150	58526	166464	21170	0.0003	0.488	27.92	13.62	62.813
60	178	178	515	180	91589	265225	31690	0.0002	0.573	25.63	14.68	63.452
70	208	208	635	210	136949	403225	45160	0.0003	0.619	23.57	14.60	59.820
80	249	249	770	240	203234	592900	62650	0.0002	0.677	21.51	14.58	73.034
90	313	313	943	270	305131	889249	86190	0.0002	0.760	19.28	14.65	81.253
100	381	381	1135	300	437611	1288225	114780	0.0002	0.838	17.05	14.29	80.052
110	441	441	1398	330	671418	1954404	155730	0.0001	0.902	15.14	13.65	101.147
120	576	576							1.000	13.54		

<i>Flame Front Position x</i>	<i>Time to position x t (s)</i>	<i>time from ignition</i>	Σt	Σx	$\Sigma(t^2)$	$\Sigma(t)^2$	$\Sigma(t.x)$	V_f	$F(t)$	\dot{q}_e	$\dot{q}_e.F(t)$	$1/\sqrt{V_f}$
RIFT – Melteca/MDF full preheat, test 1	Ignition Time	550						m/s		kW/m ²		(m/s) ^{-0.5}
10												
20												
30												
40												
50												
60	564	14							1.000	24.80		
70	579	29	1768	210	1043962	3125824	124370	0.0003	1.000	22.75	22.75	57.555
80	625	75	1864	240	1161466	3474496	149930	0.0002	1.000	20.62	20.62	63.835
90	660	110	2193	270	1650689	4809249	200200	0.0001	1.000	18.39	18.39	129.699
100	908	358							1.000	16.28		
RIFT – Melteca/MDF full preheat, test 2	Ignition Time	571						m/s		kW/m ²		(m/s) ^{-0.5}
10	0	0										
20	0	0										
30	0	0										
40	0	0										
50	0	0										
60	0	0										
70	579	8							1.000	22.75		
80	592	21	1776	240	1051730	3154176	142340	0.00077	1.000	20.62	20.62	36.056
90	605	34	1851	270	1144205	3426201	167210	0.00029	1.000	18.39	18.39	58.723
100	654	83	2006	300	1351750	4024036	202020	0.00014	1.000	16.28	16.28	85.599
110	747	176	2268	330	1737414	5143824	251610	0.00009	1.000	14.50	14.50	103.475

	120	867	296	2539	360	2165323	6446521	306460	0.00011	1.000	12.91	12.91	96.229
	130	925	354	2820	385	2664098	7952400	363070	0.00009	1.000	11.48	11.48	106.611
	135	1028	457							1.000	11.72		
	<i>Flame Front Position x</i>	<i>Time to position x t (s)</i>	<i>time from ignition</i>	Σt	Σx	$\Sigma(t^2)$	$\Sigma(t)^2$	$\Sigma(t.x)$	V_f	$F(t)$	\dot{q}_{e}	$\dot{q}_{e}.F(t)$	$1/\sqrt{V_f}$
RIFT – Melteca/MDF full preheat, test 3	Ignition Time	557							m/s		kW/m ²		(m/s) ^{-0.5}
	10	0	0										
	20	0	0										
	30	0	0										
	40	0	0										
	50	0	0										
	60	0	0										
	70	0	0										
	80	566	9							1.000	20.62		
	90	610	53	1824	270	1112360	3326976	164980	0.0002	1.000	18.39	18.39	64.088
	100	648	91	1983	300	1317629	3932289	199450	0.0002	1.000	16.28	16.28	77.269
	110	725	168	2255	330	1723453	5085025	250390	0.0001	1.000	14.50	14.50	110.254
	120	882	325	2604	357	2297558	6780816	312209	0.0001	1.000	12.91	12.91	126.420
	127	997	440							1.000	13.10	13.10	
	<i>Flame Front Position x</i>	<i>Time to position x t (s)</i>	<i>time from ignition</i>	Σt	Σx	$\Sigma(t^2)$	$\Sigma(t)^2$	$\Sigma(t.x)$	V_f	$F(t)$	\dot{q}_{e}	$\dot{q}_{e}.F(t)$	$1/\sqrt{V_f}$
RIFT – Melteca/MDF full preheat, test 4	Ignition Time	549							m/s		kW/m ²		(m/s) ^{-0.5}
	10	0	0										
	20	0	0										
	30	0	0										
	40	0	0										
	50	0	0										

60	0	0										
70	555	6							1.000	23.57		
80	559	10	1720	240	987742	2958400	138110	0.0003	1.000	21.51	21.51	56.163
90	606	57	1849	270	1147573	3418801	167660	0.0002	1.000	19.28	19.28	79.863
100	684	135	2138	300	1554196	4571044	216220	0.0001	1.000	17.05	17.05	112.291
110	848	299	2467	330	2061185	6086089	273880	0.0001	1.000	15.14	15.14	113.770
120	935	386							1.000	13.54		
<i>Flame Front Position x</i>	<i>Time to position x t (s)</i>	<i>time from ignition</i>	Σt	Σx	$\Sigma(t^2)$	$\Sigma(t)^2$	$\Sigma(t.x)$	V_f	$F(t)$	\dot{q}_e	$\dot{q}_e.F(t)$	$1/V_f$
RIFT – Melteca/MDF full preheat, test 5	Ignition Time	565						m/s		kW/m ²		(m/s) ^{-0.5}
10	0	0										
20	0	0										
30	0	0										
40	0	0										
50	0	0										
60	0	0										
70	0	0										
80	571	6							1.000	21.51		
90	579	14	1767	270	1041971	3122289	159490	0.0004	1.000	19.28	19.28	51.245
100	617	52	2036	300	1421530	4145296	206210	0.0001	1.000	17.05	17.05	123.432
110	840	275							1.000	15.14		

Melteca/ particle board												
<i>Flame Front Position x</i>	<i>Time to position x t (s)</i>	<i>time from ignition</i>	Σt	Σx	$\Sigma(t^2)$	$\Sigma(t)^2$	$\Sigma(t.x)$	V_f	$F(t)$	\dot{q}_e	$\dot{q}_e.F(t)$	$1/\sqrt{V_f}$
Melteca/PB low preheat ISO ign data RIFT - Test 1	Ignition Time	60						m/s		kW/m ²		(m/s) ^{-0.5}
10	60	0							0.332	34.25	11.38	
20	66	6	204	60	14040	41616	4260	0.0011	0.349	33.40	11.64	30.551
30	78	18	233	90	18361	54289	7220	0.0009	0.379	31.99	12.12	33.922
40	89	29	289	120	28889	83521	12000	0.0004	0.405	29.45	11.92	48.819
50	122	62	368	150	47454	135424	19080	0.0003	0.474	27.00	12.80	58.318
60	157	97	477	180	78737	227529	29380	0.0003	0.538	24.80	13.33	61.708
70	198	138	585	210	116753	342225	41680	0.0003	0.604	22.75	13.73	60.568
80	230	170	693	240	162329	480249	56110	0.0003	0.651	20.62	13.42	57.899
90	265	205	895	270	283125	801025	82250	0.0001	0.698	18.39	12.84	97.367
100	400	340	1121	300	438161	1256641	114010	0.0001	0.858	16.28	13.97	100.472
110	456	396	1355	330	616937	1836025	150040	0.0002	0.916	14.50	13.28	70.558
120	499	439	1513	360	768301	2289169	182580	0.0002	0.958	12.91	12.37	71.707
130	558	498							1.000	11.48	11.48	
Melteca/PB low preheat ISO ign data RIFT - Test 2	Ignition Time	60						m/s		kW/m ²		(m/s) ^{-0.5}
10	60	0							0.332	34.25	11.38	
20	69	9	204	60	13986	41616	4230	0.00132	0.356	33.40	11.90	27.568
30	75	15	231	90	17955	53361	7110	0.00107	0.372	31.99	11.88	30.551
40	87	27	272	120	25294	73984	11230	0.00055	0.400	29.45	11.78	42.516
50	110	50	341	150	40405	116281	17620	0.00035	0.450	27.00	12.15	53.716

60	144	84	426	180	62420	181476	26180	0.00032	0.515	24.80	12.77	55.764
70	172	112	523	210	93169	273529	37240	0.00032	0.563	22.75	12.80	56.240
80	207	147	643	240	142129	413449	52360	0.00021	0.617	20.62	12.73	68.467
90	264	204	825	270	237861	680625	75720	0.00013	0.697	18.39	12.82	86.449
100	354	294	1078	300	406612	1162084	109760	0.00010	0.807	16.28	13.14	99.105
110	460	400	1337	330	610445	1787569	148760	0.00012	0.920	14.50	13.34	92.910
120	523	463	1602	355	868290	2566404	190735	0.00009	0.981	12.91	12.66	104.910
125	619	559								13.22		

<i>Flame Front Position x</i>	<i>Time to position x t (s)</i>	<i>time from ignition</i>	Σt	Σx	$\Sigma(t^2)$	$\Sigma(t)^2$	$\Sigma(t.x)$	V_f	$F(t)$	" $\dot{q}_{.e}$	" $\dot{q}_{.e}.F(t)$	$1/\sqrt{V_f}$
Melteca/PB low preheat ISO ign data RIFT - Test 3	Ignition Time	60						m/s		kW/m ²		(m/s) ^{-0.5}
10	60	0										
20	76	16	223	60	16945	49729	4730	0.0007	0.374	33.40	12.49	36.952
30	87	27	270	90	24794	72900	8410	0.0006	0.400	31.99	12.80	39.919
40	107	47	323	120	35659	104329	13340	0.0005	0.444	29.45	13.07	45.843
50	129	69	400	150	54986	160000	20570	0.0003	0.487	27.00	13.16	53.846
60	164	104	480	180	78506	230400	29380	0.0003	0.549	24.80	13.63	54.234
70	187	127	591	210	119465	349281	42130	0.0003	0.587	22.75	13.35	63.225
80	240	180	723	240	180185	522729	58930	0.0002	0.665	20.62	13.71	73.833
90	296	236	887	270	268417	786769	80940	0.0002	0.738	18.39	13.57	74.499
100	351	291	1116	300	430778	1245456	113330	0.0001	0.804	16.28	13.09	95.039
110	469	409	1349	330	623003	1819801	150170	0.0001	0.929	14.50	13.47	95.995
120	529	469	1642	360	914538	2696164	198790	0.0001	0.987	12.91	12.73	95.069
130	644	584	1854	381	1158338	3437316	236411	0.0001	1.000	11.48	11.48	114.829
131	681	621								11.90		

Flame Front Position x	Time to position x t (s)	time from ignition	Σt	Σx	$\Sigma(t^2)$	$\Sigma(t)^2$	$\Sigma(t.x)$	V_f	$F(t)$	\dot{q}_e	$\dot{q}_e.F(t)$	$1/\sqrt{V_f}$
	Ignition Time											
Melteca/PB low preheat ISO ign data RIFT - Test 4												
	63							m/s		kW/m ²		(m/s) ^{-0.5}
10	63	0	145	30	10693	21025	2270	0.0002	0.341	34.64	11.80	67.034
20	82	19	236	60	18974	55696	5000	0.0007	0.388	33.67	13.08	38.204
30	91	28	279	90	26241	77841	8610	0.0008	0.409	33.00	13.51	35.000
40	106	43	319	120	34401	101761	13070	0.0006	0.442	30.46	13.46	39.377
50	122	59	373	150	47145	139129	19040	0.0005	0.474	27.92	13.23	44.395
60	145	82	433	180	63465	187489	26420	0.0005	0.517	25.63	13.24	46.920
70	166	103	513	210	89385	263169	36480	0.0003	0.553	23.57	13.03	53.998
80	202	139	640	240	142344	409600	52260	0.0002	0.610	21.51	13.12	74.039
90	272	209	793	270	216549	628849	72540	0.0002	0.708	19.28	13.64	76.976
100	319	256	959	300	311169	919681	96860	0.0002	0.766	17.05	13.06	69.287
110	368	305	1127	330	430785	1270129	125180	0.0002	0.823	15.14	12.46	78.249
120	440	377	1369	360	643745	1874161	166210	0.0001	0.900	13.54	12.19	99.284
130	561	498	1640	390	916642	2689600	215190	0.0001	1.000	11.95	11.95	100.523
140	639	576	1916	415	1235698	3671056	266210	0.0001	1.000	10.78	10.78	101.617
145	716	653								10.78		
Melteca/PB low preheat ISO ign data RIFT - Test 5												
	60							m/s		kW/m ²		(m/s) ^{-0.5}
10	60	0										
20	81	21	245	60	20977	60025	5340	0.0005	0.386	33.67	13.00	46.920
30	104	44	297	90	29921	88209	9220	0.0006	0.437	33.00	14.44	40.877
40	112	52	344	120	39744	118336	14000	0.0008	0.454	30.46	13.83	35.277

50	128	68	414	150	59204	171396	21320	0.0003	0.485	27.92	13.55	57.809
60	174	114	496	180	84296	246016	30420	0.0003	0.566	25.63	14.50	58.913
70	194	134	582	210	113708	338724	41140	0.0005	0.598	23.57	14.08	44.721
80	214	154	654	240	143948	427716	52840	0.0004	0.628	21.51	13.50	51.441
90	246	186	752	270	191576	565504	68460	0.0003	0.673	19.28	12.97	62.784
100	292	232	892	300	271096	795664	90280	0.0002	0.733	17.05	12.50	73.753
110	354	294	1075	330	394621	1155625	119620	0.0001	0.807	15.14	12.22	82.889
120	429	369	1365	358	648081	1863225	164916	0.0001	0.889	13.54	12.03	115.454
128	582	522								13.54		

Flame Front Position x	Time to position x t (s)	time from ignition	Σt	Σx	$\Sigma(t^2)$	$\Sigma(t)^2$	$\Sigma(t.x)$	V_f	$F(t)$	\dot{q}_e	$\dot{q}_e.F(t)$	$1/\sqrt{V_f}$	
	Ignition Time												60s
Melteca/PB low preheat ISO ign data RIFT - Test 6	10	60											
	20	79	79	228	60	17762	51984	4850	0.0007	0.381	33.67	12.84	38.685
	30	89	89	269	90	24363	72361	8290	0.0009	0.405	33.00	13.36	33.212
	40	101	101	318	120	34506	101124	13110	0.0005	0.431	30.46	13.13	45.234
	50	128	128	419	150	62685	175561	21840	0.0002	0.485	27.92	13.55	68.406
	60	190	190	536	180	100008	287296	33060	0.0002	0.591	25.63	15.15	68.659
	70	218	218	667	210	150705	444889	47380	0.0003	0.633	23.57	14.93	59.083
	80	259	259	793	240	214461	628849	64420	0.0002	0.690	21.51	14.85	70.310
	90	316	316	945	270	303837	893025	86160	0.0002	0.763	19.28	14.70	74.507
	100	370	370	1107	300	413997	1225449	111750	0.0002	0.825	17.05	14.07	72.467
	110	421	421	1364	330	642470	1860496	152070	0.0001	0.880	15.14	13.32	104.821
	120	573	573								13.54		

Flame Front Position x	Time to position t (s)	time from ignition	Σt	Σx	$\Sigma(t^2)$	$\Sigma(t)^2$	$\Sigma(t.x)$	V_f	$F(t)$	\dot{q}_e	$\dot{q}_e.F(t)$	$1/\sqrt{V_f}$
RIFT – Melteca/part bd – full preheat – test 1												
10												
20												
30												
40												
50												
60	567	17							1.000	24.80		
70	577	27	1732	210	1000162	2999824	121450	0.0010	1.000	22.75	22.75	32.416
80	588	38	1839	240	1132949	3381921	148090	0.0002	1.000	20.62	20.62	76.266
90	674	124	1969	270	1299869	3876961	178400	0.0002	1.000	18.39	18.39	79.646
100	707	157	2129	300	1513629	4532641	213640	0.0003	1.000	16.28	16.28	60.946
110	748	198	2307	330	1785257	5322249	255220	0.0001	1.000	14.50	14.50	87.785
120	852	302	2508	355	2109872	6290064	298020	0.0001	1.000	12.91	12.91	103.113
125	908	358								13.22		
RIFT – Melteca/part bd – full preheat – test 2												
Flame Front Position x	Time to position t (s)	time from ignition	Σt	Σx	$\Sigma(t^2)$	$\Sigma(t)^2$	$\Sigma(t.x)$	V_f	$F(t)$	\dot{q}_e	$\dot{q}_e.F(t)$	$1/\sqrt{V_f}$
		Ignition Time	542					m/s		kW/m ²		(m/s) ^{-0.5}
10		0										
20		0										
30		0										
40		0										
50		0										
60		0										
70		0							0.000	22.75		

80	560	18	1146	240	656996	1313316	97540	0.00003	1.000	20.62	20.62	193.417
90	586	44	1764	270	1038920	3111696	159340	0.00034	1.000	18.39	18.39	53.948
100	618	76	1862	300	1158284	3467044	186920	0.00028	1.000	16.28	16.28	60.123
110	658	116	2014	330	1359532	4056196	222740	0.00016	1.000	14.50	14.50	78.881
120	738	196	2198	360	1620812	4831204	265200	0.00014	1.000	12.91	12.91	85.027
130	802	260	2423	385	1967537	5870929	312025	0.00010	1.000	11.48	11.48	99.192
135	883	341								11.72		

Flame Front Position x	Time to position x t (s)	Time from ignition	Σt	Σx	$\Sigma(t^2)$	$\Sigma(t)^2$	$\Sigma(t.x)$	V_f	$F(t)$	\dot{q}_e	$\dot{q}_e.F(t)$	$1/\sqrt{V_f}$
			Ignition Time				m/s		kW/m ²	(m/s) ^{-0.5}		
RIFT – Melteca/part bd – full preheat – test 3		545										
10												
20												
30												
40												
50												
60												
70												
80									0.000	20.62		
90	572	27	1182	270	699284	1397124	112480	0.0000	1.000	18.39	18.39	195.681
100	610	65	1947	300	1284509	3790809	196630	0.0001	1.000	16.28	16.28	104.077
110	765	220	2239	330	1703821	5013121	248830	0.0001	1.000	14.50	14.50	113.604
120	864	319	2577	360	2230425	6640929	311070	0.0001	1.000	12.91	12.91	95.763
130	948	403	2841	389	2704041	8071281	369951	0.0001	1.000	11.48	11.48	93.179
139	1029	484							1.000	11.53		

Flame Front Position x	Time to position x t (s)	Time from ignition	Σt	Σx	$\Sigma(t^2)$	$\Sigma(t)^2$	$\Sigma(t.x)$	V_f	$F(t)$	\dot{q}_{e}	$\dot{q}_{e}.F(t)$	$1/\sqrt{V_f}$
								m/s		kW/m ²		(m/s) ^{-0.5}
RIFT – Melteca/part bd – full preheat – test 4			Ignition Time	545								
10												
20												
30												
40												
50												
60												
70												
80	559	14							1.000	21.51		
90	583	38	1743	270	1013571	3038049	157290	0.0005	1.000	19.28	19.28	45.981
100	601	56	1863	300	1162131	3470769	187260	0.0002	1.000	17.05	17.05	73.655
110	679	134	2084	330	1468658	4343056	231270	0.0001	1.000	15.14	15.14	101.643
120	804	259	2371	360	1896001	5621641	286610	0.0001	1.000	13.54	13.54	102.879
130	888	343	2694	383	2438964	7257636	345186	0.0001	1.000	11.95	11.95	125.604
133	1002	457							1.000	11.95		
RIFT – Melteca/part bd – full preheat – test 5			Ignition Time	613								
10												
20												
30												
40												

50												
60												
70												
80	625	12							1.000	21.51		
90	639	26	1921	270	1230595	3690241	173210	0.0006	1.000	19.28	19.28	40.104
100	657	44	1991	300	1322995	3964081	199660	0.0003	1.000	17.05	17.05	54.028
110	695	82	2088	330	1456370	4359744	230470	0.0003	1.000	15.14	15.14	62.864
120	736	123	2213	360	1636245	4897369	266430	0.0002	1.000	13.54	13.54	65.991
130	782	169	2390	385	1913604	5712100	307700	0.0001	1.000	11.95	11.95	98.655
135	872	259							1.000	11.95		

Flame Front Position x	Time to position x t (s)	Time from ignition	Σt	Σx	$\Sigma(t^2)$	$\Sigma(t)^2$	$\Sigma(t.x)$	V_f	$F(t)$	\dot{q}_e	$\dot{q}_e.F(t)$	$1/\sqrt{V_f}$
RIFT – Melteca/part bd – full preheat – test 6	Ignition Time	543						m/s		kW/m ²		(m/s) ^{-0.5}
10												
20												
30												
40												
50												
60												
70	551	8							1.000	23.57		
80	576	33	1728	240	996578	2985984	138740	0.0004	1.000	21.51	21.51	50.000
90	601	58	1821	270	1107713	3316041	164570	0.0003	1.000	19.28	19.28	58.987
100	644	101	1912	300	1220826	3655744	191860	0.0003	1.000	17.05	17.05	58.318
110	667	124	2002	330	1337106	4008004	220690	0.0004	1.000	15.14	15.14	48.480
120	691	148	2061	360	1416579	4247721	247680	0.0005	1.000	13.54	13.54	43.205
130	703	160	2141	390	1529699	4583881	278890	0.0003	1.000	11.95	11.95	55.720
140	747	204	2285	420	1749443	5221225	321220	0.0001	1.000	10.78	10.78	82.731
150	835	292	2507	447	2110859	6285049	375055	0.0001	1.000	9.61	9.61	102.362

157

925

382

9.02

Hardboard

<i>Flame Front Position</i> x	<i>Time to position x</i> t (s)	<i>time from ignition</i>	Σt	Σx	$\Sigma(t^2)$	$\Sigma(t)^2$	$\Sigma(t.x)$	V_f	V_f	$F(t)$	\dot{q}_e	$\dot{q}_e.F(t)$	$1/\sqrt{V_f}$
LIFT – Hardboard – test 1	Ignition Time	606						m/s	mm/s	kW/m ²	(m/s) ^{-0.5}		
50	0	0											
75	0	0									22.05		
100	0	0									21.94		
125	0	0									21.10		
150	0	0									20.27		
175	0	0									19.66		
200	0	0									19.05		
225	0	0									18.25		
250	612	6								1.000	17.45	17.45	
275	626	20	1878	825	1176020	3526884	517150	0.0018	1.7857	1.000	15.86	15.86	23.664
300	640	34	1933	900	1246365	3736489	580925	0.0012	1.1800	1.000	14.28	14.28	29.112
325	667	61	2021	975	1364285	4084441	658675	0.0007	0.6596	1.000	12.89	12.89	38.936
350	714	108	2155	1050	1553761	4644025	756925	0.0005	0.4650	1.000	11.50	11.50	46.374
375	774	168	2325	1125	1809441	5405625	874950	0.0004	0.4064	1.000	10.17	10.17	49.603
400	837	231	2542	1200	2166406	6461764	1020725	0.0003	0.3144	1.000	8.83	8.83	56.399
425	931	325	2834	1275	2703686	8031556	1210175	0.0002	0.2160	1.000	7.59	7.59	68.036
450	1066	460	3223	1350	3506193	10387729	1457725	0.0002	0.1691	1.000	6.35	6.35	76.903
475	1226	620	3726	1425	4695788	13883076	1779050	0.0001	0.1351	1.000	5.42	5.42	86.033
500	1434	828	4359	1500	6446033	19000881	2191325	0.0001	0.1052	1.000	4.50	4.50	97.498
525	1699	1093								1.000	3.79	3.79	

<i>Flame Front Position</i> x	<i>Time to position x</i> t (s)	<i>time from ignition</i>	Σt	Σx	$\Sigma(t^2)$	$\Sigma(t)^2$	$\Sigma(t.x)$	V_f	V_f	$F(t)$	\dot{q}_e	$\dot{q}_e.F(t)$	$1/\sqrt{V_f}$
LIFT – Hardboard	Ignition	608						m/s		kW/m ²	(m/s) ^{-0.5}		

– test 2		Time												
50	0	0												
75	0	0										22.05		
100	0	0										21.94		
125	0	0										21.10		
150	0	0										20.27		
175	0	0										19.66		
200	0	0										19.05		
225	0	0										18.25		
250	0	0										17.45		
275	617	11								1.000	15.86	15.86		
300	626	20	1887	900	1187301	3560769	566775	0.0018	1.7857	1.000	14.28	14.28	23.664	
325	644	38	1936	975	1250168	3748096	630200	0.0012	1.2458	1.000	12.89	12.89	28.331	
350	666	60	2010	1050	1348292	4040100	704900	0.0009	0.8794	1.000	11.50	11.50	33.722	
375	700	94	2117	1125	1497557	4481689	796000	0.0006	0.5805	1.000	10.17	10.17	41.505	
400	751	145	2265	1200	1716597	5130225	908850	0.0004	0.4370	1.000	8.83	8.83	47.837	
425	814	208	2472	1275	2049246	6110784	1054500	0.0003	0.3166	1.000	7.59	7.59	56.200	
450	907	301	1721	925	1485245	2961841	754100	0.0004	0.4487	1.000	6.35	6.35	47.206	
475	1015	409	1922	1000	1852874	3694084	890275	0.0004	0.4016	1.000	5.42	5.42	49.899	
500	1111	505	2126	1075	2264546	4519876	1037625	0.0004	0.3639	1.000	4.50	4.50	52.421	
525	1369	763	2480	1150	3108482	6150400	1274225	0.0003	0.3057	1.000	3.79	3.79	57.192	
550	1597	991	2966	1225	4424570	8797156	1597075	0.0003	0.2587	1.000	3.08	3.08	62.179	
558	1665	1059										2.96		
<i>Flame Front Position</i> x	<i>Time to position x</i> t (s)	<i>time from ignition</i>	Σt	Σx	$\Sigma(t^2)$	$\Sigma(t)^2$	$\Sigma(t.x)$	V_f	V_f	$F(t)$	\dot{q}_e	$\dot{q}_e.F(t)$	$1/V_f$	
LIFT – Hardboard	Ignition													
– test 3	Time	610						m/s	mm/s		kW/m ²			
50														
75														
100														

125													
150													
175													
200													
225													
250													
275	617	11								1.000	15.86	15.86	
300	622	16	1877	900	1174617	3523129	563625	0.0022	2.1814	1.000	14.28	14.28	21.411
325	638	32	1923	975	1233497	3697929	626000	0.0012	1.2002	1.000	12.89	12.89	28.865
350	663	57	1997	1050	1331029	3988009	700400	0.0009	0.8566	1.000	11.50	11.50	34.167
375	696	90	2099	1125	1471585	4405801	789050	0.0006	0.6450	1.000	10.17	10.17	39.376
400	740	134	2238	1200	1675220	5008644	897850	0.0005	0.4672	1.000	8.83	8.83	46.264
425	802	196	2422	1275	1965204	5866084	1032850	0.0004	0.3556	1.000	7.59	7.59	53.030
450	880	274	2666	1350	2385860	7107556	1204250	0.0003	0.2729	1.000	6.35	6.35	60.537
475	984	378	3012	1425	3060560	9072144	1437400	0.0002	0.1835	1.000	5.42	5.42	73.821
500	1148	542	3514	1500	4196084	12348196	1766950	0.0001	0.1243	1.000	4.50	4.50	89.678
525	1382	776	4082	1565	5636532	16662724	2137630	0.0001	0.0995	1.000	3.79	3.79	100.259
540	1552	946								1.000	3.36		

Flame Front Position x	Time to position x t (s)	time from ignition	Σt	Σx	$\Sigma(t^2)$	$\Sigma(t)^2$	$\Sigma(t.x)$	V_f	$F(t)$	\dot{q}_e	$\dot{q}_e.F(t)$	$1/\sqrt{V_f}$
	Ignition Time	80						m/s		kW/m ²		(m/s) ^{-0.5}
10	80	0							0.291	33.88		
20	83	3	250	60	20858	62500	5070	0.0028	0.296	32.87	9.75	18.772
30	87	7	259	90	22379	67081	7830	0.0032	0.304	32.16	9.76	17.638
40	89	9	272	120	24706	73984	10970	0.0020	0.307	29.67	9.11	22.278
50	96	16	292	150	28586	85264	14780	0.0011	0.319	27.17	8.66	30.246
60	107	27	321	180	34589	103041	19480	0.0009	0.337	24.95	8.40	33.166
70	118	38	359	210	43329	128881	25400	0.0007	0.354	22.99	8.13	36.952
80	134	54	405	240	55289	164025	32750	0.0006	0.377	21.03	7.92	41.884

90	153	73	459	270	70949	210681	41690	0.0005	0.403	18.88	7.60	43.589
100	172	92	525	300	92993	275625	52970	0.0004	0.427	16.73	7.14	48.772
110	200	120	602	330	122484	362404	66800	0.0003	0.460	15.06	6.93	53.862
120	230	150	699	360	165261	488601	84570	0.0003	0.494	13.89	6.85	58.903
130	269	189	803	390	217677	644809	105130	0.0003	0.534	12.71	6.78	60.857
140	304	224	922	420	286578	850084	129880	0.0002	0.567	11.59	6.58	63.410
150	349	269	1054	450	375018	1110916	159070	0.0002	0.608	10.48	6.37	69.702
160	401	321	1198	480	483306	1435204	192670	0.0002	0.652	9.39	6.12	70.386
170	448	368	1360	510	622626	1849600	232300	0.0002	0.689	8.33	5.74	74.423
180	511	431	1531	540	789009	2343961	276820	0.0002	0.736	7.27	5.35	78.743
190	572	492	1720	570	994074	2958400	328060	0.0002	0.778	6.55	5.10	79.386
200	637	557	1915	600	1231389	3667225	384340	0.0001	0.821	5.83	4.79	81.866
210	706	626	2118	630	1504830	4485924	446160	0.0001	0.865	5.17	4.47	83.066
220	775	695	2329	660	1818165	5424241	513800	0.0001	0.906	4.58	4.15	84.273
230	848	768	2557	690	2192085	6538249	589700	0.0001	0.948	3.99	3.78	89.262
240	934	854	2809	720	2646189	7890481	675950	0.0001	0.995	3.77	3.75	94.629
250	1027	947	3079	750	3177009	9480241	771590	0.0001	1.000	3.54	3.54	95.919
260	1118	1038	3341	780	3735069	11162281	870350	0.0001	1.000	3.29	3.29	92.014
270	1196	1116	3614	805	4370340	13060996	971100	0.0001	1.000	3.29	3.29	111.413
275	1300	1220							1.000	3.09	3.09	

Flame Front Position x	Time to position x t (s)	time from ignition	Σt	Σx	$\Sigma(t^2)$	$\Sigma(t)^2$	$\Sigma(t.x)$	V_f	$F(t)$	q_e	$q_e.F(t)$	$1/V_f$
RIFT – Hardboard – low preheat – ISO ign data – test 2												
10	80	0							0.291	33.88		
20	82	2	246	60	20180	60516	4960	0.0050	0.295	32.87	9.69	14.142
30	84	4	252	90	21176	63504	7600	0.0050	0.298	32.16	9.59	14.142
40	86	6	262	120	22916	68644	10560	0.0023	0.302	29.67	8.95	20.817
50	92	12	279	150	26061	77841	14100	0.0013	0.312	27.17	8.48	27.568
60	101	21	305	180	31209	93025	18500	0.0010	0.327	24.95	8.16	31.675

70	112	32	342	210	39386	116964	24220	0.0007	0.344	22.99	7.92	37.702
80	129	49	386	240	50210	148996	31210	0.0006	0.370	21.03	7.78	40.626
90	145	65	442	270	65890	195364	40170	0.0005	0.392	18.88	7.40	44.395
100	168	88	509	300	87665	259081	51410	0.0004	0.422	16.73	7.06	50.578
110	196	116	592	330	118624	350464	65720	0.0003	0.456	15.06	6.86	54.813
120	228	148	687	360	159569	471969	83110	0.0003	0.491	13.89	6.82	57.899
130	263	183	798	390	215402	636804	104530	0.0003	0.528	12.71	6.71	62.985
140	307	227	927	420	290867	859329	130720	0.0002	0.570	11.59	6.61	68.603
150	357	277	1086	450	399782	1179396	164050	0.0002	0.615	10.48	6.44	76.043
160	422	342	1263	480	539789	1595169	203350	0.0002	0.669	9.39	6.28	79.694
170	484	404	986	340	418740	972196	150600	0.0004	0.716	8.33	5.97	49.363
180	555	475	1121	370	549005	1256641	183820	0.0004	0.767	7.27	5.58	53.441
190	635	555	1274	400	718306	1623076	223070	0.0003	0.820	6.55	5.37	57.725
200	718	638	1440	430	926318	2073600	267730	0.0003	0.872	5.83	5.08	61.917
210	812	732	1619	460	1182789	2621161	318570	0.0002	0.927	5.17	4.80	66.295
226	911	831							0.982	4.23	4.15	

<i>Flame Front Position</i> x	<i>Time to position x</i> t (s)	<i>time from ignition</i>	Σt	Σx	$\Sigma(t^2)$	$\Sigma(t)^2$	$\Sigma(t.x)$	V_f	$F(t)$	\dot{q}_e	$\dot{q}_e.F(t)$	$1/\sqrt{V_f}$
RIFT – Hardboard – low preheat – ISO ign data – test 3	Ignition Time	69						m/s		kW/m ²		(m/s) ^{-0.5}
10	80	0							0.291	33.88		
20	82	2	246	60	20180	60516	4960	0.0050	0.295	32.87	9.69	14.142
30	84	4	253	90	21349	64009	7640	0.0039	0.298	32.16	9.59	15.916
40	87	7	260	120	22546	67600	10450	0.0039	0.304	29.67	9.01	15.916
50	89	9	275	150	25291	75625	13870	0.0015	0.307	27.17	8.34	26.247
60	99	19	299	180	30043	89401	18160	0.0009	0.324	24.95	8.08	33.212
70	111	31	339	210	38763	114921	24030	0.0007	0.343	22.99	7.88	38.987
80	129	49	390	240	51462	152100	31590	0.0005	0.370	21.03	7.78	44.202
90	150	70	459	270	71541	210681	41820	0.0004	0.399	18.88	7.53	50.759

100	180	100	533	300	96109	284089	53830	0.0004	0.437	16.73	7.30	51.628
110	203	123	617	330	128365	380689	68410	0.0004	0.464	15.06	6.98	52.151
120	234	154	707	360	168865	499849	85510	0.0003	0.498	13.89	6.91	57.933
130	270	190	818	390	226252	669124	107140	0.0002	0.535	12.71	6.80	63.351
140	314	234	932	420	292600	868624	131260	0.0003	0.577	11.59	6.69	62.621
150	348	268	1080	450	394424	1166400	163040	0.0002	0.607	10.48	6.36	73.537
160	418	338	869	370	306437	755161	125260	0.0003	0.665	9.39	6.25	55.007
170	481	401	1017	400	420009	1034289	156910	0.0003	0.714	8.33	5.95	59.422
180	554	474	1170	430	556502	1368900	192290	0.0002	0.766	7.27	5.57	63.835
190	625	545	1335	460	721877	1782225	232510	0.0002	0.814	6.55	5.33	67.790
200	718	638	1522	490	938190	2316484	280250	0.0002	0.872	5.83	5.08	72.420
208	828	748							0.936	5.30	4.97	

Flame Front Position x	Time to position x t (s)	time from ignition	Σt	Σx	$\Sigma(t^2)$	$\Sigma(t)^2$	$\Sigma(t.x)$	V_f	$F(t)$	q_e	$q_e.F(t)$	$1/V_f$
	Ignition Time	66						m/s		kW/m ²		(m/s) ^{-0.5}
RIFT – Hardboard – low preheat – ISO ign data – test 4												
10	80	0							0.291	33.88		
20	83	3	248	60	20514	61504	5010	0.0039	0.296	32.87	9.75	15.916
30	85	5	255	90	21683	65025	7690	0.0050	0.300	32.16	9.65	14.142
40	87	7	265	120	23443	70225	10680	0.0023	0.304	29.67	9.01	20.817
50	93	13	283	150	26827	80089	14310	0.0012	0.314	27.17	8.53	28.577
60	103	23	314	180	33182	98596	19090	0.0008	0.330	24.95	8.24	35.590
70	118	38	356	210	42758	126736	25240	0.0006	0.354	22.99	8.13	40.026
80	135	55	409	240	56485	167281	33100	0.0005	0.378	21.03	7.95	43.669
90	156	76	470	270	74602	220900	42740	0.0005	0.406	18.88	7.67	46.920
100	179	99	544	300	100058	295936	54930	0.0004	0.435	16.73	7.28	51.628
110	209	129	626	330	132366	391876	69450	0.0003	0.470	15.06	7.09	54.317
120	238	158	719	360	174309	516961	86910	0.0003	0.502	13.89	6.97	56.184

130	272	192	825	390	229853	680625	108020	0.0003	0.537	12.71	6.82	62.189
140	315	235	943	420	299945	889249	132860	0.0002	0.578	11.59	6.70	64.814
150	356	276	1083	450	395705	1172889	163420	0.0002	0.614	10.48	6.43	69.919
160	412	332	1247	480	525921	1555009	200750	0.0002	0.661	9.39	6.20	78.526
170	479	399	1439	510	699489	2070721	245990	0.0001	0.712	8.33	5.93	82.465
180	548	468	1652	540	920370	2729104	298820	0.0001	0.762	7.27	5.54	85.483
190	625	545	1889	570	1203585	3568321	360590	0.0001	0.814	6.55	5.33	91.758
200	716	636	2154	600	1564250	4639716	432680	0.0001	0.871	5.83	5.08	96.970
210	813	733	2460	628	2040386	6051600	516888	0.0001	0.928	5.17	4.80	109.663
218	931	851							0.993	4.70	4.67	

Flame Front Position x	Time to position x t (s)	time from ignition	Σt	Σx	$\Sigma(t^2)$	$\Sigma(t)^2$	$\Sigma(t.x)$	V_f	$F(t)$	\dot{q}_e	$\dot{q}_e.F(t)$	$1/\sqrt{V_f}$
	Ignition Time	67						m/s		kW/m ²		(m/s) ^{-0.5}
RIFT – Hardboard – low preheat – ISO ign data – test 5												
10	80	0							0.291	33.88		
20	83	3	250	60	20858	62500	5070	0.0028	0.296	32.87	9.75	18.772
30	87	7	262	90	22922	68644	7950	0.0022	0.304	32.16	9.76	21.257
40	92	12	279	120	26033	77841	11290	0.0015	0.312	29.67	9.26	25.720
50	100	20	303	150	30785	91809	15340	0.0010	0.325	27.17	8.84	30.950
60	111	31	336	180	37946	112896	20410	0.0008	0.343	24.95	8.55	35.440
70	125	45	377	210	47827	142129	26690	0.0007	0.364	22.99	8.37	38.759
80	141	61	427	240	61427	182329	34520	0.0006	0.386	21.03	8.13	42.514
90	161	81	488	270	80398	238144	44370	0.0004	0.413	18.88	7.80	47.532
100	186	106	563	300	107173	316969	56850	0.0004	0.444	16.73	7.42	52.513
110	216	136	648	330	141768	419904	71880	0.0003	0.478	15.06	7.20	54.772
120	246	166	744	360	186696	553536	89940	0.0003	0.510	13.89	7.09	57.525
130	282	202	847	390	241801	717409	110840	0.0003	0.547	12.71	6.95	60.417
140	319	239	972	420	318926	944784	136970	0.0002	0.581	11.59	6.74	67.023
150	371	291	1110	450	415802	1232100	167510	0.0002	0.627	10.48	6.57	71.074
160	420	340	1265	480	538717	1600225	203430	0.0002	0.667	9.39	6.26	71.792

170	474	394	1424	510	681976	2027776	243180	0.0002	0.709	8.33	5.90	74.166
180	530	450	1598	540	858412	2553604	288840	0.0002	0.749	7.27	5.45	77.517
190	594	514	1789	570	1075961	3200521	341260	0.0001	0.793	6.55	5.20	82.195
200	665	585	2001	600	1345625	4004001	401680	0.0001	0.839	5.83	4.89	86.047
210	742	662	2228	630	1666830	4963984	469440	0.0001	0.886	5.17	4.59	88.320
220	821	741	2451	660	2013149	6007401	540680	0.0001	0.932	4.58	4.27	85.536
230	888	808	2682	690	2409314	7193124	618380	0.0001	0.970	3.99	3.87	87.381
240	973	893	2936	720	2890898	8620096	706510	0.0001	1.000	3.77	3.77	96.828
250	1075	995	3206	750	3443318	10278436	803350	0.0001	1.000	3.54	3.54	96.346
260	1158	1078	3479	780	4049105	12103441	906250	0.0001	1.000	3.29	3.29	92.479
270	1246	1166							1.000	3.29	3.29	

<i>Flame Front Position x</i>	<i>Time to position x t (s)</i>	<i>time from ignition</i>	Σt	Σx	$\Sigma(t^2)$	$\Sigma(t)^2$	$\Sigma(t.x)$	V_f	$F(t)$	\dot{q}_e	$\dot{q}_e \cdot F(t)$	$1/\sqrt{V_f}$
RIFT – hardboard – Full preheat – test 1	Ignition Time	985						m/s		kW/m ²		(m/s) ^{-0.5}
10												
20												
30												
40												
50												
60												
70												
80												
90												
100												
110												
120	986	1							1.000	13.89		
130	989	4	2975	390	2950317	8850625	386890	0.0013	1.000	12.71	12.71	27.860
140	1000	15	3007	420	3014445	9042049	421270	0.0007	1.000	11.59	11.59	38.447

150	1018	33	3061	450	3124173	9369721	459580	0.0005	1.000	10.48	10.48	46.572
160	1043	58	3136	480	3279798	9834496	502330	0.0003	1.000	9.39	9.39	53.519
170	1075	90	3227	510	3473355	10413529	549250	0.0003	1.000	8.33	8.33	57.454
180	1109	124	3339	540	3719531	11148921	601820	0.0002	1.000	7.27	7.27	63.482
190	1155	170	3459	570	3991931	11964681	658070	0.0002	1.000	6.55	6.55	65.628
200	1195	210	3597	600	4317059	12938409	720320	0.0002	1.000	5.83	5.83	68.015
210	1247	262	3744	630	4678238	14017536	787310	0.0002	1.000	5.17	5.17	73.153
220	1302	317	3924	660	5140838	15397776	864560	0.0002	1.000	4.58	4.58	80.263
230	1375	390	4127	690	5688329	17032129	950690	0.0001	1.000	3.99	3.99	86.026
240	1450	465	4343	720	6297449	18861649	1043750	0.0001	1.000	3.77	3.77	84.591
250	1518	533	4572	750	6979640	20903184	1144540	0.0001	1.000	3.54	3.54	87.949
260	1604	619	4813	780	7736621	23164969	1253110	0.0001	1.000	3.29	3.29	93.006
270	1691	706								3.29		

<i>Flame Front Position x</i>	<i>Time to position x t (s)</i>	<i>time from ignition</i>	Σt	Σx	$\Sigma(t^2)$	$\Sigma(t)^2$	$\Sigma(t.x)$	V_f	$F(t)$	\dot{q}_e	$\dot{q}_e . F(t)$	$1/\sqrt{V_f}$
RIFT – hardboard – Full preheat – test 2	Ignition Time	987						m/s		kW/m ²		(m/s) ^{-0.5}
10												
20												
30												
40												
50												
60												
70												
80												
90												
100												
110												
120												
130	993	6								12.71	0.00	#DIV/0!
140	1004	17	3017	420	3034465	9102289	422650	0.0007	1.000	11.59	11.59	36.952

150	1020	33	3063	450	3127937	9381969	459800	0.0006	1.000	10.48	10.48	41.884
160	1039	52	3127	480	3260545	9778129	500800	0.0004	1.000	9.39	9.39	49.343
170	1068	81	2107	340	2220145	4439449	347800	0.0001	1.000	8.33	8.33	82.411
180	1101	114	2169	370	2352825	4704561	379740	0.0001	1.000	7.27	7.27	83.614
190	1140	153	2241	400	2511801	5022081	414780	0.0001	1.000	6.55	6.55	84.991
200	1186	199	2326	430	2706196	5410276	453800	0.0001	1.000	5.83	5.83	86.589
210	1233	246	2419	460	2926885	5851561	496130	0.0001	1.000	5.17	5.17	88.303
220	1286	299	2519	490	3174085	6345361	541850	0.0001	1.000	4.58	4.58	90.111
230	1350	363	2636	520	3476296	6948496	593420	0.0001	1.000	3.99	3.99	92.186
240	1408	421	2758	550	3804964	7606564	648420	0.0001	1.000	3.77	3.77	94.289
250	1477	490	2885	580	4163993	8323225	707170	0.0001	1.000	3.54	3.54	96.441
260	1556	569	3033	610	4602665	9199089	773810	0.0001	1.000	3.29	3.29	98.890
270	1626	639	3182	640	5065012	10125124	843580	0.0001	1.000	3.29	3.29	101.280
280	1674	687								2.89		

<i>Flame Front Position x</i>	<i>Time to position x t (s)</i>	<i>time from ignition</i>	Σt	Σx	$\Sigma(t^2)$	$\Sigma(t)^2$	$\Sigma(t.x)$	V_f	$F(t)$	\dot{q}_{e}	$\dot{q}_{e} .F(t)$	$1/\sqrt{V_f}$
RIFT – hardboard – Full preheat – test 3	Ignition Time	987						m/s		kW/m ²		(m/s) ^{-0.5}
10												
20												
30												
40												
50												
60												
70												
80												
90												
100												
110												
120												
130	994	7								12.71		

140	1001	14	3012	420	3024326	9072144	421910	0.0008	1.000	11.59	11.59	34.766
150	1017	30	3056	450	3113734	9339136	458770	0.0005	1.000	10.48	10.48	43.142
160	1038	51	2055	370	2111733	4223025	318630	0.0001	1.000	9.39	9.39	103.931
170	1066	79	2104	400	2213800	4426816	347300	0.0001	1.000	8.33	8.33	105.149
180	1100	113	2166	430	2346356	4691556	379220	0.0001	1.000	7.27	7.27	106.678
190	1077	90	2177	460	2369929	4739329	402630	0.0001	1.000	6.55	6.55	107.149
200	1182	195	2259	490	2557053	5103081	441030	0.0001	1.000	5.83	5.83	108.992
210	1227	240	2409	520	2902653	5803281	494070	0.0001	1.000	5.17	5.17	112.494
220	1290	303	3503	550	4141825	12271009	659790	0.0003	1.000	4.58	4.58	54.129
230	1358	371	3636	580	4484408	13220496	724580	0.0003	1.000	3.99	3.99	59.901
240	1423	436	3787	610	4881129	14341369	794700	0.0002	1.000	3.77	3.77	63.872
250	1505	518	3950	640	5334438	15602500	871070	0.0002	1.000	3.54	3.54	68.585
260	1585	598	4135	670	5869275	17098225	955550	0.0002	1.000	3.29	3.29	72.783
270	1691	704								3.29		

Flame Front Position x	Time to position x t (s)	time from ignition	Σt	Σx	$\Sigma(t^2)$	$\Sigma(t)^2$	$\Sigma(t.x)$	V_f	$F(t)$	" $\dot{q}_{.e}$	" $\dot{q}_{.e} . F(t)$	$I/\sqrt{V_f}$
	Ignition Time	982						m/s		kW/m ²		(m/s) ^{-0.5}
10												
20												
30												
40												
50												
60												
70												
80												
90												
100												
110												

120	986	4									13.89	
130	988	6	2980	390	2960376	8880400	387600	0.0008	1.000	12.71	12.71	34.833
140	1006	24	3016	420	3032664	9096256	422580	0.0006	1.000	11.59	11.59	41.255
150	1022	40	3073	450	3148545	9443329	461340	0.0005	1.000	10.48	10.48	44.395
160	1045	63	3137	480	3281409	9840769	502400	0.0004	1.000	9.39	9.39	49.004
170	1070	88	3219	510	3455741	10361961	547820	0.0003	1.000	8.33	8.33	54.524
180	1104	122	3316	540	3667880	10995856	597600	0.0003	1.000	7.27	7.27	60.031
190	1142	160	3410	570	3877876	11628100	648500	0.0003	1.000	6.55	6.55	55.418
200	1164	182	3532	600	4162136	12475024	707240	0.0002	1.000	5.83	5.83	67.212
210	1226	244	3668	630	4491256	13454224	771420	0.0002	1.000	5.17	5.17	75.595
220	1278	296	3835	660	4907921	14707225	844750	0.0002	1.000	4.58	4.58	72.458
230	1331	349	4000	690	5339726	16000000	921130	0.0002	1.000	3.99	3.99	75.215
240	1391	409	4186	720	5849738	17522596	1005970	0.0001	1.000	3.77	3.77	81.677
250	1464	482	4388	750	6428266	19254544	1098420	0.0001	1.000	3.54	3.54	84.273
260	1533	551	4600	780	7062994	21160000	1197390	0.0001	1.000	3.29	3.29	83.367
270	1603	621	4829	806	7785947	23319241	1298658	0.0001	1.000	3.29	3.29	100.786
276	1693	711								3.05		

<i>Flame Front Position x</i>	<i>Time to position x t (s)</i>	<i>time from ignition</i>	Σt	Σx	$\Sigma(t^2)$	$\Sigma(t)^2$	$\Sigma(t.x)$	V_f	$F(t)$	\dot{q}_{e}''	$\dot{q}_{e}'' \cdot F(t)$	$1/\sqrt{V_f}$
RIFT – hardboard – Full preheat – test 5	Ignition Time	1054						m/s		kW/m ²		(m/s) ^{-0.5}

- 10
- 20
- 30
- 40
- 50
- 60
- 70
- 80
- 90

100												
110												
120												
130	1062	8								12.71		
140	1069	15	3215	420	3445661	10336225	450320	0.0009	1.000	11.59	11.59	33.889
150	1084	30	3257	450	3536633	10608049	488900	0.0006	1.000	10.48	10.48	41.975
160	1104	50	3316	480	3666256	10995856	531000	0.0005	1.000	9.39	9.39	46.969
170	1128	74	3392	510	3836800	11505664	577200	0.0004	1.000	8.33	8.33	53.095
180	1160	106	3488	540	4057984	12166144	628560	0.0003	1.000	7.27	7.27	60.123
190	1200	146	3598	570	4318244	12945604	684400	0.0003	1.000	6.55	6.55	62.457
200	1238	184	3728	600	4636744	13897984	746500	0.0002	1.000	5.83	5.83	67.352
210	1290	236	3888	630	5046344	15116544	817700	0.0002	1.000	5.17	5.17	78.385
220	1360	306	4074	660	5541476	16597476	897620	0.0001	1.000	4.58	4.58	81.881
230	1424	370	4284	690	6127376	18352656	986720	0.0001	1.000	3.99	3.99	83.768
240	1500	446	4522	715	6831380	20448484	1079030	0.0001	1.000	3.77	3.77	108.757
245	1598	544								3.66		

<i>Flame Front Position x</i>	Particle board											
	<i>Time to position x t</i> (s)	<i>time from ignition</i>	Σt	Σx	$\Sigma(t^2)$	$\Sigma(t)^2$	$\Sigma(t.x)$	V_f	$F(t)$	\dot{q}_e	$\dot{q}_e.F(t)$	$1/\sqrt{V_f}$
LIFT-Pynefloor particle Board – test 1	Ignition Time	396						m/s		kW/m ²		(m/s) ^{-0.5}
50												
75												
100												
125	404	8							1.000	24.24		
150	409	13	1230	450	504386	1512900	184825	0.0038	1.000	23.10	23.10	16.267
175	417	21	1254	525	524354	1572516	219925	0.0026	1.000	21.67	21.67	19.574
200	428	32	1282	600	548042	1643524	256900	0.0025	1.000	20.25	20.25	20.033
225	437	41	1311	675	573069	1718721	295425	0.0028	1.000	19.18	19.18	18.974
250	446	50	1358	750	615510	1844164	340450	0.0012	1.000	18.11	18.11	28.813
275	475	79	1432	825	685662	2050624	395425	0.0008	1.000	16.40	16.40	36.125
300	511	115	1533	900	785955	2350089	461700	0.0007	1.000	14.70	14.70	37.947
325	547	151	1650	975	910794	2722500	538275	0.0006	1.000	12.98	12.98	40.332
350	592	196	1804	1050	1091898	3254416	634350	0.0004	1.000	11.27	11.27	49.034
375	665	269	2019	1125	1373333	4076361	761375	0.0003	1.000	9.94	9.94	58.503
400	762	366	2311	1200	1804325	5340721	929875	0.0002	1.000	8.62	8.62	66.325
425	884	488	2658	1275	2386244	7064964	1135900	0.0002	1.000	7.44	7.44	70.717
450	1012	616	3039	1335	3112049	9235521	1356880	0.0001	1.000	6.25	6.25	86.096
460	1143	747							1.000	5.89		
LIFT-Pynefloor particle Board – test 2	Ignition Time	391						m/s		kW/m ²		(m/s) ^{-0.5}
50	391											

75	391											
100	391											
125	391											
150	391											
175	391											
200	391											
225	395	4							1.000	19.18		
250	400	9	1223	750	499209	1495729	306575	0.0013	1.000	18.11	18.11	27.692
275	428	37	1281	825	548393	1640961	353600	0.0009	1.000	16.40	16.40	32.575
300	453	62	1386	900	643418	1920996	417725	0.0006	1.000	14.70	14.70	40.039
325	505	114	1546	975	805978	2390116	505825	0.0004	1.000	12.98	12.98	52.416
350	588	197	1743	1050	1023269	3038049	613675	0.0003	1.000	11.27	11.27	54.040
375	650	259	1996	1125	1342808	3984016	752750	0.0003	1.000	9.94	9.94	59.017
400	758	367	2280	1200	1757448	5198400	917550	0.0002	1.000	8.62	8.62	66.641
425	872	481	2622	1256	1334948	6874884	673800	0.0004	1.000	7.44	7.44	47.504
431	992	601							1.000	7.15		

<i>Flame Front Position x</i>	<i>Time to position x t (s)</i>	<i>time from ignition</i>	Σt	Σx	$\Sigma(t^2)$	$\Sigma(t)^2$	$\Sigma(t.x)$	V_f	$F(t)$	$\dot{q}_{e,0}$	$\dot{q}_{e,0}.F(t)$	$1/\sqrt{V_f}$
LIFT-Pynefloor particle Board – test 3	Ignition Time	393						m/s		kW/m ²		(m/s) ^{-0.5}
50												
75												
100												
125												
150												
175												
200												
225	400	7								19.18		
250	407	14	1226	750	501210	1503076	306975	0.0026	1.000	18.11	18.11	19.717
275	419	26	1269	825	537459	1610361	349875	0.0013	1.000	16.40	16.40	27.325
300	443	50	1336	900	596486	1784896	402175	0.0009	1.000	14.70	14.70	33.256

325	474	81	1440	975	694454	2073600	470000	0.0006	1.000	12.98	12.98	40.336
350	523	130	1572	1050	828830	2471184	552725	0.0005	1.000	11.27	11.27	44.951
375	575	182	1755	1125	1035803	3080025	661475	0.0004	1.000	9.94	9.94	52.199
400	657	264	1985	1200	1329283	3940225	798450	0.0003	1.000	8.62	8.62	59.727
425	753	360	2321	1275	998658	5387041	992775	-0.00001	1.000	7.44	7.44	
450	911	518	2689	1335	1396930	7230721	1201475	0.00000	1.000	6.25	6.25	
460	1025	632							1.000	5.89		

Flame Front Position x	Time to position x	time from ignition	Σt	Σx	$\Sigma(t^2)$	$\Sigma(x^2)$	$\Sigma(t \cdot x)$	V_f	$F(t)$	\dot{q}_e	$\dot{q}_e \cdot F(t)$	$1/\sqrt{V_f}$
	t (s)							m/s	kW/m ²			(m/s) ^{-0.5}
RIFT – pynefloor particle board	Ignition Time											
– low preheat – ISO ign data	75											
– test 1		75								33.82		
10	75	0										
20	77	2	231	60	17795	53361	4660	0.0050	0.319	32.76	10.46	14.142
30	79	4	237	90	18731	56169	7150	0.0050	0.324	31.96	10.34	14.142
40	81	6	250	120	20902	62500	10110	0.0016	0.328	29.56	9.68	24.985
50	90	15	271	150	24661	73441	13740	0.0011	0.345	27.16	9.38	30.836
60	100	25	300	180	30200	90000	18200	0.0010	0.364	24.97	9.09	31.623
70	110	35	335	210	37725	112225	23700	0.0008	0.382	22.98	8.77	35.590
80	125	50	380	240	48750	144400	30750	0.0006	0.407	20.99	8.54	41.975
90	145	70	440	270	65550	193600	40050	0.0004	0.438	18.76	8.22	47.532
100	170	95	510	300	87950	260100	51500	0.0004	0.475	16.53	7.85	50.000
110	195	120	593	330	118909	351649	65810	0.0003	0.508	14.65	7.45	54.022
120	228	153	698	360	165634	487204	84560	0.0002	0.550	13.12	7.21	63.568
130	275	200	821	390	228733	674041	107630	0.0002	0.604	11.59	7.00	67.104
140	318	243	966	420	315878	933156	136220	0.0002	0.649	10.50	6.81	70.175
150	373	298	1314	450	628382	1726596	200150	0.0001	0.703	9.40	6.61	131.635
160	623	548	1667	475	977499	2778889	266345	0.0000	0.909	8.39	7.63	145.962
165	671	596							0.943	7.94		

Flame Front Position x	Time to position x t (s)	time from ignition	Σt	Σx	$\Sigma(t^2)$	$\Sigma(x^2)$	$\Sigma(t.x)$	V_f	$F(t)$	\dot{q}_{e}	$\dot{q}_{e} \cdot F(t)$	$1/\sqrt{V_f}$
RIFT – pynefloor particle board – low preheat – ISO ign data – test 2	Ignition Time	65						m/s		kW/m ²		(m/s) ^{-0.5}
10	65	0								33.82		
20	68	3	204	60	13890	41616	4140	0.0033	0.300	32.76	9.83	17.321
30	71	6	213	90	15141	45369	6450	0.0033	0.307	31.96	9.80	17.321
40	74	9	226	120	17078	51076	9140	0.0019	0.313	29.56	9.26	22.949
50	81	16	249	150	20873	62001	12650	0.0010	0.328	27.16	8.90	32.094
60	94	29	279	180	26213	77841	16970	0.0009	0.353	24.97	8.81	34.008
70	104	39	320	210	34536	102400	22680	0.0007	0.371	22.98	8.53	37.922
80	122	57	368	240	45864	135424	29820	0.0005	0.402	20.99	8.44	43.609
90	142	77	449	270	69273	201601	41040	0.0003	0.434	18.76	8.14	57.358
100	185	120	521	300	92025	271441	52620	0.0003	0.495	16.53	8.19	54.502
110	194	129	608	330	124302	369664	67320	0.0004	0.507	14.65	7.43	49.559
120	229	164	703	360	168477	494209	85220	0.0002	0.551	13.12	7.23	65.952
130	280	215	842	390	241730	708964	110500	0.0002	0.609	11.59	7.06	72.115
140	333	268	1005	420	342953	1010025	141820	0.0002	0.664	10.50	6.97	74.869
150	392	327							0.721	9.40		

<i>Flame Front Position x</i>	<i>Time to position x t (s)</i>	<i>time from ignition</i>	Σt	Σx	$\Sigma(t^2)$	$\Sigma(t)^2$	$\Sigma(t.x)$	V_f	$F(t)$	\dot{q}_{e}''	$\dot{q}_{e}'' \cdot F(t)$	$1/\sqrt{V_f}$
RIFT – pynefloor particle board – low preheat – ISO ign data – test 3	Ignition Time	71						m/s		kW/m ²		(m/s) ^{-0.5}
10	71	0							0.307	33.82		
20	76	5	227	60	17217	51529	4630	0.0022	0.317	32.76	10.40	21.257
30	80	9	244	90	19920	59536	7440	0.0016	0.326	31.96	10.41	24.944
40	88	17	272	120	24960	73984	11120	0.0008	0.341	29.56	10.09	35.277
50	104	33	310	150	32484	96100	15800	0.0007	0.371	27.16	10.08	38.759
60	118	47	362	180	44340	131044	22080	0.0005	0.395	24.97	9.87	42.774
70	140	69	419	210	59445	175561	29760	0.0005	0.431	22.98	9.90	46.372
80	161	90	483	240	78645	233289	39060	0.0005	0.462	20.99	9.69	45.826
90	182	111	555	270	103989	308025	50460	0.0004	0.491	18.76	9.21	50.759
100	212	141	640	300	138584	409600	64640	0.0003	0.530	16.53	8.76	56.605
110	246	175	752	330	191896	565504	83540	0.0002	0.571	14.65	8.37	64.342
120	294	223	1012	360	369736	1024144	123700	0.0001	0.624	13.12	8.19	112.010
130	472	401	1280	390	573416	1638400	168600	0.0001	0.791	11.59	9.17	111.361
140	514	443	1572	420	830376	2471184	221220	0.0002	0.825	10.50	8.66	76.365
150	586	515	1749	441	1028793	3059001	257859	0.0001	0.881	9.40	8.28	109.870
151	649	578							0.927	9.30		

<i>Flame Front Position x</i>	<i>Time to position x t (s)</i>	<i>time from ignition</i>	Σt	Σx	$\Sigma(t^2)$	$\Sigma(t)^2$	$\Sigma(t.x)$	V_f	$F(t)$	$\dot{q}_{\cdot e}$	$\dot{q}_{\cdot e} \cdot F(t)$	$1/\sqrt{V_f}$
RIFT – pynefloor particle board	Ignition Time							m/s		kW/m ²		(m/s) ^{-0.5}
– low preheat – ISO ign data – test 4	80											
10	80	0							0.326	33.82		
20	82	2	249	60	20693	62001	5050	0.0027	0.330	32.76	10.80	19.272
30	87	7	258	90	22214	66564	7810	0.0027	0.340	31.96	10.85	19.272
40	89	9	273	120	24899	74529	11020	0.0018	0.343	29.56	10.15	23.664
50	97	17	295	150	29211	87025	14950	0.0010	0.359	27.16	9.74	31.833
60	109	29	329	180	36419	108241	20000	0.0008	0.380	24.97	9.49	36.091
70	123	43	373	210	46891	139129	26430	0.0006	0.404	22.98	9.28	40.104
80	141	61	427	240	61579	182329	34560	0.0005	0.432	20.99	9.07	44.796
90	163	83	499	270	84475	249001	45450	0.0004	0.465	18.76	8.72	52.258
100	195	115	579	300	113435	335241	58480	0.0003	0.508	16.53	8.40	53.948
110	221	141	680	330	156562	462400	75490	0.0003	0.541	14.65	7.93	59.328
120	264	184	789	360	210953	622521	95510	0.0002	0.591	13.12	7.76	64.435
130	304	224	1171	390	525721	1371241	155620	0.0000	0.635	11.59	7.36	142.295
140	603	523	1551	420	870761	2405601	220540	0.0000	0.894	10.50	9.38	142.348
150	644	564	1938	450	1255826	3755844	291580	0.0002	0.924	9.40	8.68	66.384
160	691	611	2145	474	1548317	4601025	340000	0.0001	0.957	8.39	8.03	115.901
164	810	730							1.000	8.03		

<i>Flame Front Position x</i>	<i>Time to position x t (s)</i>	<i>time from ignition</i>	Σt	Σx	$\Sigma(t^2)$	$\Sigma(t)^2$	$\Sigma(t.x)$	V_f	$F(t)$	$\dot{q}_{\cdot e}$	$\dot{q}_{\cdot e} \cdot F(t)$	$1/\sqrt{V_f}$
RIFT – pynefloor particle board												
– low preheat – ISO ign data												
– test 5												
	Ignition Time	82						m/s		kW/m ²		(m/s) ^{-0.5}
10	82	0							0.330	33.82		
20	85	3	258	60	22230	66564	5250	0.0021	0.336	32.76	10.99	21.602
30	91	9	270	90	24342	72900	8190	0.0021	0.347	31.96	11.10	21.602
40	94	12	283	120	26721	80089	11390	0.0028	0.353	29.56	10.43	18.772
50	98	16	303	150	30761	91809	15320	0.0011	0.360	27.16	9.79	30.486
60	111	29	335	180	37801	112225	20380	0.0007	0.384	24.97	9.58	37.448
70	126	44	379	210	48361	143641	26840	0.0006	0.409	22.98	9.39	39.377
80	142	60	428	240	61640	183184	34580	0.0006	0.434	20.99	9.10	41.255
90	160	78	493	270	82245	243049	44860	0.0004	0.460	18.76	8.64	50.075
100	191	109	571	300	110481	326041	57700	0.0003	0.503	16.53	8.32	54.782
110	220	138	670	330	151962	448900	74380	0.0003	0.540	14.65	7.91	58.519
120	259	177	789	360	211581	622521	95580	0.0002	0.586	13.12	7.69	67.281
130	310	228	938	390	299342	879844	123040	0.0002	0.641	11.59	7.43	74.227
140	369	287	1114	420	421486	1240996	157210	0.0002	0.699	10.50	7.34	79.098
150	435	353	1327	450	598915	1760929	200590	0.0001	0.759	9.40	7.14	88.048
160	523	441	1570	473	837298	2464900	248686	0.0001	0.833	8.39	6.99	116.745
163	612	530							0.901	8.12		
RIFT – pynefloor particle board												
– low preheat – ISO ign data												
– test 6												
	Ignition Time	78						m/s		kW/m ²		(m/s) ^{-0.5}
10	78	0							0.322	33.82		

20	81	2.5	242	60	19453	58322	4880	0.0040	0.327	32.76	10.70	15.811
30	83	5	252	90	21113	63252	7620	0.0026	0.332	31.96	10.60	19.720
40	88	10	266	120	23658	70756	10760	0.0017	0.341	29.56	10.09	24.608
50	95	17	285	150	27173	81225	14390	0.0014	0.355	27.16	9.64	26.458
60	102	24	310	180	32198	96100	18780	0.0011	0.368	24.97	9.18	30.246
70	113	35	335	210	37573	112225	23630	0.0011	0.387	22.98	8.89	30.246
80	120	42	367	240	45125	134689	29570	0.0009	0.399	20.99	8.37	32.998
90	134	56	410	270	56692	168100	37260	0.0005	0.421	18.76	7.90	42.774
100	156	78	475	300	76517	225625	48010	0.0004	0.455	16.53	7.52	50.656
110	185	107	563	330	107845	316969	62590	0.0003	0.495	14.65	7.26	57.586
120	222	144	666	360	150590	443556	80660	0.0003	0.542	13.12	7.12	60.828
130	259	181	790	390	211846	624100	103570	0.0002	0.586	11.59	6.79	66.200
140	309	231	940	420	300946	883600	132730	0.0002	0.640	10.50	6.72	75.332
150	372	294							0.702	9.40		

Test 1 - half preheat

Flame Front Position x	Time to position x	time from ignition	Σt	Σx	$\Sigma(t^2)$	$\Sigma(t)^2$	$\Sigma(t.x)$	V_f	$F(t)$	\dot{q}_e	$\dot{q}_e.F(t)$	$I/\sqrt{V_f}$
	t (s)											
RIFT – Pynefloor particle board	Ignition Time	386										
– half preheat – ISO ign data – test 1								m/s		kW/m ²		(m/s) ^{-0.5}
10												
20												
30												
40												
50	390	4										
60	392	6							0.72	24.97		
70	400	14	1199	210	479313	1437601	84080	0.0013	0.73	22.98	16.73	27.406
80	407	21	1217	240	493749	1481089	97460	0.0019	0.73	20.99	15.41	22.949
90	410	24	1231	270	505145	1515361	110860	0.0028	0.74	18.76	13.83	18.772
100	414	28	1251	300	521825	1565001	125270	0.0011	0.74	16.53	12.25	30.486
110	427	41	1286	330	551750	1653796	141770	0.0006	0.75	14.65	11.02	39.540
120	445	59	1348	360	606930	1817104	162250	0.0004	0.77	13.12	10.08	50.075

130	476	90	1432	390	685722	2050624	186820	0.0003	0.79	11.59	9.21	57.481
140	511	125	1542	420	795722	2377764	216670	0.0003	0.82	10.50	8.64	62.985
150	555	169	1680	450	946142	2822400	253030	0.0002	0.86	9.40	8.06	72.017
160	614	228	1834	480	1127246	3363556	294540	0.0002	0.90	8.39	7.57	74.227
170	665	279	2044	510	1404446	4177936	348990	0.0001	0.94	7.48	7.02	88.403
180	765	379	2275	540	1741475	5175625	411300	0.0001	1.00	6.57	6.57	95.063
190	845	459							1.00	5.93	5.93	

Flame Front Position x	Time to position x	time from ignition	Σt	Σx	$\Sigma(t^2)$	$\Sigma(t)^2$	$\Sigma(t.x)$	V_f	$F(t)$	\dot{q}_e	$\dot{q}_e.F(t)$	$1/\sqrt{V_f}$
	t (s)							m/s		kW/m ²		(m/s) ^{-0.5}
RIFT – Pynefloor particle board	Ignition											
– half preheat – ISO ign data – test 2	Time	385										
10												
20												
30												
40												
50												
60												
70												
80	386	1							0.715	20.99		
90	392	7	1178	270	462660	1387684	106160	0.0014	0.721	18.76	13.52	26.547
100	400	15	1212	300	490064	1468944	121480	0.0007	0.728	16.53	12.04	38.545
110	420	35	1258	330	528244	1582564	138760	0.0005	0.746	14.65	10.93	43.609
120	438	53	1326	360	587268	1758276	159600	0.0004	0.762	13.12	10.00	49.497
130	468	83	1411	390	665893	1990921	184100	0.0003	0.788	11.59	9.13	57.984
140	505	120	1534	420	788770	2353156	215690	0.0002	0.818	10.50	8.59	68.664
150	561	176	1697	450	967907	2879809	255810	0.0002	0.862	9.40	8.10	79.536
160	631	246	1895	475	1207091	3591025	301105	0.0001	0.914	8.39	7.68	97.376
165	703	318							0.965	7.94	7.66	

<i>Flame Front Position x</i>	<i>Time to position x t (s)</i>	<i>time from ignition</i>	Σt	Σx	$\Sigma(t^2)$	$\Sigma(t)^2$	$\Sigma(t.x)$	V_f	$F(t)$	\dot{q}_e	$\dot{q}_e.F(t)$	$1/\sqrt{V_f}$
RIFT – Pynefloor particle board – half preheat – ISO ign data – test 3	Ignition Time	386						m/s		kW/m ²		(m/s) ^{-0.5}
10												
20												
30												
40												
50												
60												
70												
80	389	3							0.718	20.99		
90	393	7	1183	270	466571	1399489	106590	0.0016	0.722	18.76	13.54	24.944
100	401	15	1209	300	487475	1461681	121120	0.0009	0.729	16.53	12.05	33.575
110	415	29	1252	330	523122	1567504	138070	0.0006	0.742	14.65	10.87	42.111
120	436	50	1312	360	574842	1721344	157900	0.0004	0.760	13.12	9.98	48.019
130	461	75	1400	390	655626	1960000	182670	0.0003	0.782	11.59	9.06	58.497
140	503	117	1518	420	772446	2304324	213450	0.0002	0.816	10.50	8.57	68.297
150	554	168	1671	450	936921	2792241	251760	0.0002	0.857	9.40	8.05	74.580
160	614	228	1839	480	1134153	3381921	295410	0.0002	0.902	8.39	7.57	76.494
170	671	285	2052	510	1415526	4210704	350370	0.0001	0.943	7.48	7.05	88.406
180	767	381	2323	538	1821755	5396329	418510	0.0001	1.000	6.57	6.57	109.437
188	885	499							1.000	6.06	6.06	

<i>Flame Front Position x</i>	<i>Time to position x t (s)</i>	<i>time from ignition</i>	Σt	Σx	$\Sigma(t^2)$	$\Sigma(t)^2$	$\Sigma(t.x)$	V_f	$F(t)$	\dot{q}_e	$\dot{q}_e.F(t)$	$1/\sqrt{V_f}$
RIFT – Pynefloor particle board – half preheat – ISO ign data – test 4	Ignition Time	386						m/s		kW/m ²		(m/s) ^{-0.5}
10												
20												

30												
40												
50												
60												
70												
80												
90	392	6							0.721	18.76	-6.82	
100	401	15	1210	300	488354	1464100	121250	0.0008	0.729	16.53	12.05	35.814
110	417	31	1255	330	525659	1575025	138410	0.0006	0.743	14.65	10.89	42.514
120	437	51	1317	360	579227	1734489	158500	0.0004	0.761	13.12	9.99	48.094
130	463	77	1400	390	655338	1960000	182630	0.0003	0.783	11.59	9.08	56.409
140	500	114	1510	420	763578	2280100	212240	0.0002	0.814	10.50	8.54	64.960
150	547	161	1648	450	910410	2715904	248210	0.0002	0.851	9.40	8.00	71.120
160	601	215	1795	480	1079019	3222025	288200	0.0002	0.892	8.39	7.49	70.786
170	647	261	1986	510	1324454	3944196	338990	0.0001	0.926	7.48	6.93	84.240
180	738	352	2203	540	1632377	4853209	398250	0.0001	0.989	6.57	6.50	92.530
190	818	432	2461	565	2032793	6056521	464735	0.0001	1.000	5.93	5.93	105.792
195	905	519							1.000	5.61	5.61	

<i>Flame Front Position x</i>	<i>Time to position x t (s)</i>	<i>time from ignition</i>	Σt	Σx	$\Sigma(t^2)$	$\Sigma(t \cdot x)$	V_f	$F(t)$	\dot{q}_{e}	$\dot{q}_{e} \cdot F(t)$	$1/\sqrt{V_f}$
RIFT – Pynefloor particle board – half preheat – ISO ign data – test 5	Ignition Time	389					m/s		kW/m ²		(m/s) ^{-0.5}

10
20
30
40
50
60
70
80

90	396	7							0.724	18.76	13.59	#DIV/0!
100	401	12	1209	300	487361	1461681	121060	0.0012	0.729	16.53	12.05	28.940
110	412	23	1242	330	514586	1542564	136900	0.0007	0.739	14.65	10.83	37.702
120	429	40	1300	360	564466	1690000	156470	0.0004	0.754	13.12	9.89	49.091
130	459	70	1377	390	633843	1896129	179610	0.0003	0.780	11.59	9.04	54.772
140	489	100	1479	420	731763	2187441	207780	0.0003	0.805	10.50	8.45	60.277
150	531	142	1612	450	871546	2598544	242830	0.0002	0.839	9.40	7.88	72.169
160	592	203	1774	480	1056226	3147076	285040	0.0002	0.886	8.39	7.43	77.463
170	651	262	1953	510	1278365	3814209	333190	0.0002	0.929	7.48	6.95	76.811
180	710	321							0.970	6.57		

Flame Front Position x	Time to position x t (s)	time from ignition	Σt	Σx	$\Sigma(t^2)$	$\Sigma(t)^2$	$\Sigma(t.x)$	V_f	$F(t)$	\dot{q}_e	$\dot{q}_e.F(t)$	$1/\sqrt{V_f}$
	Ignition Time	387						m/s		kW/m ²		(m/s) ^{-0.5}
10												
20												
30												
40												
50												
60												
70												
80	389	-371							0.718	20.99	15.07	
90	395	-365	1186	270	468950	1406596	106870	0.0015	0.723	18.76	13.57	25.520
100	402	-358	1215	300	492353	1476225	121730	0.0008	0.730	16.53	12.07	34.766
110	418	-342	1261	330	530809	1590121	139100	0.0005	0.744	14.65	10.91	44.395
120	441	-319	1332	360	592934	1774224	160390	0.0004	0.764	13.12	10.03	52.674
130	473	-287	1424	390	678310	2027776	185810	0.0003	0.792	11.59	9.18	58.788

140	510	-250	1536	420	789638	2359296	215840	0.0002	0.822	10.50	8.63	63.305
150	553	-207	1672	450	936790	2795584	251790	0.0002	0.856	9.40	8.05	70.558
160	609	-151	1835	480	1129619	3367225	294800	0.0002	0.898	8.39	7.54	77.517
170	673	-87	2015	507	1361099	4060225	341591	0.0001	0.944	7.48	7.06	85.339
177	733	-27							0.986	6.84	6.74	

Flame Front Position x RIFT – Pynefloor particle board – full preheat – test 1	Time to positio n x t (s)	time from ignition	Σt	Σx	$\Sigma(t^2)$	$\Sigma(t)^2$	$\Sigma(t.x)$	V_f	$F(t)$	\dot{q}_e	$\dot{q}_e.F(t)$	$1/\sqrt{V_f}$
	Ignition Time							m/s		kW/m ²		(m/s) ^{-0.5}
		760										
10												
20												
30												
40												
50												
60												
70												
80												
90	778	18							1.00	18.76		
100	785	25	2352	300	1844030	5531904	235310	0.0018	1.00	16.53	16.53	23.741
110	789	29	2374	330	1878746	5635876	261290	0.0012	1.00	14.65	14.65	28.363
120	800	40	2415	360	1944797	5832225	290170	0.0005	1.00	13.12	13.12	44.174
130	826	66	2482	390	2055012	6160324	323220	0.0004	1.00	11.59	11.59	52.960
140	856	96	2579	420	2219621	6651241	361770	0.0003	1.00	10.50	10.50	59.820
150	897	137	2725	450	2482129	7425625	409910	0.0002	1.00	9.40	9.40	77.240
160	972	212	2912	480	2837242	8479744	467380	0.0001	1.00	8.39	8.39	85.451
170	1043	283	3089	502	3186109	9541921	517558	0.0001	1.00	7.48	7.48	90.661
172	1074	314							1.00	7.30		

Flame Front Position x	Time to position t (s)	time from ignition	Σt	Σx	$\Sigma(t^2)$	$\Sigma(t)^2$	$\Sigma(t.x)$	V_f	$F(t)$	q_e	$q_e.F(t)$	$1/\sqrt{V_f}$
	Ignition Time	760s						m/s		kW/m ²		(m/s) ^{-0.5}
RIFT – Pynefloor particle board – full preheat – test 2												
10												
20												
30												
40												
50												
60												
70												
80												
90												
100	791	31							1.000	16.53		
110	796	36	2394	330	1910546	5731236	263500	0.0012	1.000	14.65	14.65	28.940
120	807	47	2426	360	1962194	5885476	291390	0.0007	1.000	13.12	13.12	36.952
130	823	63	2481	390	2052779	6155361	322970	0.0004	1.000	11.59	11.59	47.482
140	851	91	2563	420	2191851	6568969	359480	0.0003	1.000	10.50	10.50	57.665
150	889	129	2665	450	2370147	7102225	400490	0.0003	1.000	9.40	9.40	60.835
160	925	165	2804	480	2626046	7862416	449650	0.0002	1.000	8.39	8.39	72.033
170	990	230	2988	510	2987054	8928144	509440	0.0001	1.000	7.48	7.48	86.235
180	1073	313							1.000	6.57		
RIFT – Pynefloor particle board – full preheat – test 3												
	Ignition Time	760						m/s		kW/m ²		(m/s) ^{-0.5}

10												
20												
30												
40												
50												
60												
70												
80												
90	784	24							1.000	18.76		
100	788	28	2365	300	1864449	5593225	236590	0.0022	1.000	16.53	16.53	21.257
110	793	33	2387	330	1899429	5697769	262750	0.0010	1.000	14.65	14.65	30.972
120	806	46	2423	360	1957461	5870929	291070	0.0006	1.000	13.12	13.12	39.540
130	824	64	2475	390	2042637	6125625	322140	0.0005	1.000	11.59	11.59	44.202
140	845	85	2554	420	2176226	6522916	358170	0.0003	1.000	10.50	10.50	56.113
150	885	125	2735	450	2507275	7480225	411850	0.0001	1.000	9.40	9.40	93.095
160	1005	245	2929	475	2872771	8579041	464985	0.0001	1.000	8.39	8.39	103.304
165	1039	279							1.000	7.94		
<i>Flame Front Position x</i>	<i>Time to position x t (s)</i>	<i>time from ignition</i>	Σt	Σx	$\Sigma(t^2)$	$\Sigma(t)^2$	$\Sigma(t.x)$	V_f	$F(t)$	\dot{q}_{e}	$\dot{q}_{e} \cdot F(t)$	$1/\sqrt{V_f}$
RIFT – Pynefloor particle board – full preheat – test 4	Ignition Time	771						m/s		kW/m ²		(m/s) ^{-0.5}
10												
20												
30												
40												
50												
60												
70												

Flame Front Position x	Time to position x t (s)	time from ignition	Σt	Σx	$\Sigma(t^2)$	$\Sigma(t)^2$	$\Sigma(t.x)$	V_f	$F(t)$	" $q_{.e}$	" $q_{.e} . F(t)$	$1/\sqrt{V_f}$
80												
90												
100	793	22							1.000	16.53		
110	797	26	2399	330	1918539	5755201	264050	0.0012	1.000	14.65	14.65	29.439
120	809	38	2413	360	1940939	5822569	289660	0.0012	1.000	13.12	13.12	28.752
130	807	36	2570	390	2215846	6604900	335550	0.0001	1.000	11.59	11.59	99.004
140	954	183	2750	420	2539486	7562500	386820	0.0001	1.000	10.50	10.50	101.236
150	989	218	2950	450	2902286	8702500	443030	0.0004	1.000	9.40	9.40	52.353
160	1007	236							1.000	8.39		
RIFT – Pynefloor particle board – full preheat – test 5	Ignition Time	760						m/s		kW/m ²		(m/s) ^{-0.5}
10												
20												
30												
40												
50												
60												
70												
80												
90	773	13							1.000	18.76		
100	776	16	2329	300	1808105	5424241	232970	0.0028	1.000	16.53	16.53	18.772
110	780	20	2351	330	1842601	5527201	258800	0.0009	1.000	14.65	14.65	32.498
120	795	35	2294	360	1757386	5262436	274670	-0.0002	1.000	13.12	13.12	#NUM!
130	719	-41	2368	390	1878302	5607424	308430	0.0001	0.976	11.59	11.32	124.606
140	854	94	2464	420	2040158	6071296	346680	0.0001	1.000	10.50	10.50	97.625

<i>Flame Front Position x</i>	<i>Time to position x t (s)</i>	<i>time from ignition</i>	Σt	Σx	$\Sigma(t^2)$	$\Sigma(t)^2$	$\Sigma(t.x)$	V_f	$F(t)$	q_e	$q_e \cdot F(t)$	$1/\sqrt{V_f}$
RIFT – Pynefloor particle board – full preheat – test 6	Ignition Time	760						m/s		kW/m ²		(m/s) ^{-0.5}
150	891	131	2698	450	2431406	7279204	405690	0.0002	1.000	9.40	9.40	71.100
160	953	193	2857	479	2728259	8162449	457327	0.0002	1.000	8.39	8.39	80.124
169	1013	253								7.57		
10												
20												
30												
40												
50												
60												
70												
80												
90	772	12							1.000	18.76		
100	779	19	2339	300	1823769	5470921	234060	0.0012	1.000	16.53	16.53	28.358
110	788	28	2379	330	1887129	5659641	262020	0.0006	1.000	14.65	14.65	41.996
120	812	52	2438	360	1982532	5943844	293060	0.0004	1.000	13.12	13.12	50.013
130	838	78	2520	390	2118488	6350400	328180	0.0003	1.000	11.59	11.59	53.948
140	870	110	2628	420	2305544	6906384	368740	0.0002	1.000	10.50	10.50	64.543
150	920	160	2758	450	2540324	7606564	414680	0.0002	1.000	9.40	9.40	70.005
160	968	208	2969	479	2951985	8814961	475569	0.0001	1.000	8.39	8.39	94.857
169	1081	321							1.000	7.57		

Flame Front Position x		Superflake particle board											
		Time to position t Ignition Time	time from ignition	Σt	Σx	$\Sigma(t^2)$	$\Sigma(t)^2$	$\Sigma(t.x)$	V	F(t)	q''	$q''*F(t)$	$1/\sqrt{V}$
RIFT – Superflake PB – low preheat – ISO ign data – test 1			82						m/s		kW/m ²		(m/s) ^{-0.5}
10											33.82		
20											32.76		
30	89	7									31.96		
40	95	13	288	120	27762	82944	11670	0.0013	0.319	29.56	9.42	27.568	
50	104	22	318	150	34002	101124	16140	0.0008	0.334	27.16	9.06	35.000	
60	119	37	359	180	43473	128881	21860	0.0006	0.357	24.97	8.91	40.026	
70	136	54	430	210	63282	184900	30660	0.0003	0.381	22.98	8.76	54.259	
80	175	93	493	240	82245	243049	39900	0.0004	0.433	20.99	9.08	51.682	
90	182	100	571	270	109545	326041	51780	0.0005	0.441	18.76	8.28	47.086	
100	214	132	642	300	139436	412164	64840	0.0003	0.479	16.53	7.91	56.569	
110	246	164	757	330	194521	573049	84100	0.0002	0.513	14.65	7.52	64.981	
120	297	215	890	359	269134	792100	107463	0.0002	0.564	13.12	7.40	72.904	
129	347	265							0.609	11.75	7.16		
Flame Front Position x		Time to position x t (s)	time from ignition	Σt	Σx	$\Sigma(t^2)$	$\Sigma(t)^2$	$\Sigma(t.x)$	V_f	F(t)	q''_e	$q''_e.F(t)$	$1/\sqrt{V_f}$
RIFT – Superflake PB – low preheat – ISO ign data – test 2		Ignition Time	82						m/s		kW/m ²		(m/s) ^{-0.5}
10											34.88		
20											33.82		
30											32.76		
40	82										31.96		
50	93	11									29.56		
60	100	18	309	150	32105	95481	15680	0.0008	0.327	27.16	8.88	34.766	
60	116	34	343	180	39585	117649	20850	0.0007	0.352	24.97	8.80	36.952	

70	127	45	393	210	52085	154449	27850	0.0006	0.369	22.98	8.47	42.078
80	150	68	447	240	67529	199809	36190	0.0005	0.401	20.99	8.41	46.406
90	170	88	518	270	90604	268324	47100	0.0004	0.426	18.76	8.00	49.216
100	198	116	597	300	120545	356409	60290	0.0003	0.460	16.53	7.61	54.337
110	229	147	707	330	170045	499849	78590	0.0002	0.495	14.65	7.25	64.663
120	280	198	840	360	240402	705600	101820	0.0002	0.547	13.12	7.18	71.414
130	331	249	994	390	334650	988036	130250	0.0002	0.595	11.59	6.90	71.765
140	383	301	1177	420	470619	1385329	166100	0.0001	0.640	10.50	6.72	81.847
150	463	381	1424	450	695142	2027776	215550	0.0001	0.704	9.40	6.62	99.271
160	578	496	1748	320	548453	3055504	161930	0.0001	0.786	8.39	6.60	138.446
167	707	625							0.870	7.76	6.74	

Flame Front Position x	Time to position x	time from ignition	Σt	Σx	$\Sigma(t^2)$	$\Sigma(t)^2$	$\Sigma(tx)$	V_f	$F(t)$	\dot{q}_e	$\dot{q}_e \cdot F(t)$	$1/\sqrt{V_f}$
	t (s)											
RIFT – Superflake PB – low preheat – ISO ign data – test 3	Ignition Time	83						m/s		kW/m ²		(m/s) ^{-0.5}
10										33.82		
20										32.76		
30	83	0								31.96		
40	91	8								29.56		
50	97	14	302	150	30686	91204	15330	0.0008	0.322	27.16	8.75	35.181
60	114	31	342	180	39566	116964	20860	0.0006	0.349	24.97	8.72	41.231
70	131	48	394	210	52358	155236	27930	0.0006	0.374	22.98	8.60	41.839
80	149	66	455	240	69987	207025	36840	0.0004	0.399	20.99	8.38	47.162
90	175	92	530	270	95262	280900	48270	0.0003	0.433	18.76	8.12	53.454
100	206	123	629	300	134565	395641	63630	0.0003	0.469	16.53	7.76	60.643
110	248	165	740	330	185736	547600	82200	0.0002	0.515	14.65	7.55	63.272
120	286	203	869	360	255525	755161	105150	0.0002	0.553	13.12	7.26	66.130
130	335	252	1053	390	380645	1108809	138350	0.0001	0.599	11.59	6.94	86.966
140	432	349	1257	420	538949	1580049	177530	0.0001	0.680	10.50	7.14	88.958
150	490	407	1507	442	768949	2271049	222900	0.0001	0.724	9.40	6.81	117.204

152

585

502

0.791

9.20

7.28

*Flame Front Position x**Time to position x
t (s)**time from ignition* Σt Σx $\Sigma(t^2)$ $\Sigma(t)^2$ $\Sigma(t.x)$ V_f $F(t)$ \dot{q}_e $\dot{q}_e.F(t)$ $1/\sqrt{V_f}$ **RIFT – Superflake PB – low preheat
– ISO ign data – test 4**Ignition
Time

82

m/s

kW/m²(m/s)^{-0.5}

10

33.82

20

32.76

30

82

0

31.96

40

91

9

272

120

24806

73984

11050

0.0012

0.312

29.56

9.22

29.172

50

99

17

300

150

30182

90000

15190

0.0010

0.325

27.16

8.84

30.950

60

110

28

335

180

37777

112225

20370

0.0007

0.343

24.97

8.56

36.952

70

126

44

381

210

49001

145161

27020

0.0006

0.367

22.98

8.44

41.884

80

145

63

459

240

72245

210681

37340

0.0003

0.394

20.99

8.27

57.051

90

188

106

528

270

94394

278784

48020

0.0003

0.448

18.76

8.41

54.148

100

195

113

616

300

127658

379456

62050

0.0004

0.457

16.53

7.55

51.048

110

233

151

695

330

163603

483025

77170

0.0003

0.499

14.65

7.32

60.031

120

267

185

825

360

231203

680625

99920

0.0002

0.534

13.12

7.01

68.588

130

325

243

1057

390

393139

1117249

139390

0.0001

0.590

11.59

6.84

102.303

140

465

383

1309

420

591211

1713481

185200

0.0001

0.705

10.50

7.40

101.663

150

519

437

1579

443

839611

2493241

233985

0.0001

0.745

9.40

7.00

102.038

153

595

513

0.798

9.10

7.26

*Flame Front Position x**Time to position x
t (s)**time from ignition* Σt Σx $\Sigma(t^2)$ $\Sigma(t)^2$ $\Sigma(t.x)$ V_f $F(t)$ \dot{q}_e $\dot{q}_e.F(t)$ $1/\sqrt{V_f}$ **RIFT – Superflake PB – low preheat
– ISO ign data – test 5**Ignition
Time

82

m/s

kW/m²(m/s)^{-0.5}

10

33.82

20

82

32.76

30

88

6

262

90

22932

68644

7960

0.0020

0.307

31.96

9.81

22.509

40

92

10

282

120

26612

79524

11420

0.0013

0.314

29.56

9.27

27.255

50	102	20	311	150	32557	96721	15800	0.0008	0.330	27.16	8.97	35.590
60	117	35	355	180	42589	126025	21640	0.0006	0.354	24.97	8.83	41.326
70	136	54	409	210	56521	167281	29020	0.0005	0.381	22.98	8.76	44.164
80	156	74	475	240	76321	225625	38470	0.0004	0.409	20.99	8.57	48.656
90	183	101	559	270	106225	312481	50950	0.0003	0.442	18.76	8.30	56.798
100	220	138	652	300	143890	425104	65860	0.0003	0.485	16.53	8.02	57.586
110	249	167	772	330	202210	595984	85750	0.0002	0.516	14.65	7.56	65.387
120	303	221	907	360	279835	822649	109900	0.0002	0.569	13.12	7.47	72.805
130	355	273	1079	390	395075	1164241	141450	0.0002	0.616	11.59	7.14	76.991
140	421	339	1285	420	562347	1651225	181440	0.0001	0.671	10.50	7.04	88.048
150	509	427	1486	443	745458	2208196	220358	0.0001	0.738	9.40	6.94	100.750
153	556	474							0.771	9.10	7.02	

Flame Front Position x	Time to position x t (s)	time from ignition	Σt	Σx	$\Sigma(t^2)$	$\Sigma(t)^2$	$\Sigma(t.x)$	V_f	$F(t)$	\dot{q}_e	$\dot{q}_e.F(t)$	$1/\sqrt{V_f}$
	Ignition Time											
RIFT – Superflake PB – low preheat – ISO ign data – test 6		82						m/s		kW/m ²		(m/s) ^{-0.5}
10										33.82		
20										32.76		
30	82	0	175	90	15373	30625	6180	0.0002	0.296	31.96	9.47	74.521
40	93	11	283	120	27037	80089	11580	0.0008	0.315	29.56	9.32	36.197
50	108	26	324	150	35442	104976	16500	0.0007	0.340	27.16	9.23	38.730
60	123	41	368	180	45562	135424	22370	0.0007	0.363	24.97	9.06	38.086
70	137	55	422	210	60142	178084	29930	0.0005	0.383	22.98	8.80	44.740
80	162	80	492	240	82262	242064	39920	0.0004	0.416	20.99	8.74	53.016
90	193	111	582	270	115022	338724	53030	0.0003	0.454	18.76	8.52	57.029
100	227	145	689	300	161139	474721	69660	0.0003	0.493	16.53	8.15	61.758
110	269	187	816	330	226290	665856	90690	0.0002	0.536	14.65	7.86	68.297
120	320	238	939	360	297261	881721	113490	0.0002	0.585	13.12	7.68	64.349
130	350	268							0.612	11.59	7.09	

<i>Flame Front Position x</i>	<i>Time to position x t (s)</i>	<i>time from ignition</i>	Σt	Σx	$\Sigma(t^2)$	$\Sigma(t)^2$	$\Sigma(t.x)$	V_f	$F(t)$	\dot{q}_e	$\dot{q}_e.F(t)$	$1/V_f$
RIFT – Superflake Particle Board Full preheat – test 1	Ignition Time	699						m/s		kW/m ²		(m/s) ^{-0.5}
10												
20												
30												
40												
50												
60												
70												
80												
90												
100	706	7							0.869	16.53		
110	711	12	2139	330	1525241	4575321	235450	0.0012	0.872	14.65	12.78	28.940
120	722	23	2175	360	1577369	4730625	261310	0.0006	0.879	13.12	11.53	39.919
130	742	43	2235	390	1666289	4995225	291040	0.0004	1.000	11.59	11.59	49.775
140	771	72	2322	420	1799486	5391684	325750	0.0003	1.000	10.50	10.50	58.053
150	809	110	2432	450	1974826	5914624	365610	0.0002	1.000	9.40	9.40	63.680
160	852	153	2587	478	2237861	6692569	413238	0.0001	1.000	8.39	8.39	81.964
168	926	227							1.000	7.66		
RIFT – Superflake Particle Board Full preheat – test 2	Ignition Time	755						m/s		kW/m ²		(m/s) ^{-0.5}
10												
20												
30												

40												
50												
60												
70												
80												
90												
100	763	8								16.53		
110	771	16	2318	330	1791266	5373124	255190	0.0009	1.000	14.65	14.65	32.708
120	784	29	2357	360	1852301	5555449	283150	0.0006	1.000	13.12	13.12	39.540
130	802	47	2420	390	1953416	5856400	315100	0.0004	1.000	11.59	11.59	50.649
140	834	79	2514	420	2109644	6320196	352720	0.0003	1.000	10.50	10.50	61.900
150	878	123	2648	450	2342536	7011904	398220	0.0002	1.000	9.40	9.40	71.638
160	936	181	2814	320	1646980	7918596	281460	0.0000	1.000	8.39	8.39	230.386
170	1000	245	2990	505	2987012	8940100	504210	0.0001	1.000	7.48	7.48	88.385
175	1054	299							1.000	7.02		

<i>Flame Front Position x</i>	<i>Time to position x t (s)</i>	<i>time from ignition</i>	Σt	Σx	$\Sigma(t^2)$	$\Sigma(t)^2$	$\Sigma(t.x)$	V_f	$F(t)$	\dot{q}_{e}	$\dot{q}_{e}.F(t)$	$1/V_f$
RIFT – Superflake Particle Board Full preheat – test 3	Ignition Time	755						m/s		kW/m ²		(m/s) ^{-0.5}

10												
20												
30												
40												
50												
60												
70												
80												
90												
100	761	6							1.000	16.53		
110	769	14	2312	330	1782006	5345344	254530	0.0009	1.000	14.65	14.65	32.708

120	782	27	2351	360	1842885	5527201	282430	0.0006	1.000	13.12	13.12	39.540
130	800	45	2409	390	1935453	5803281	313620	0.0004	1.000	11.59	11.59	47.749
140	827	72	2493	420	2073885	6215049	349680	0.0003	1.000	10.50	10.50	57.761
150	866	111	2595	450	2247489	6734025	390000	0.0003	1.000	9.40	9.40	61.254
160	902	147	2783	479	2593785	7745089	445755	0.0001	1.000	8.39	8.39	92.835
169	1015	260							1.000	7.57		

<i>Flame Front Position x</i>	<i>Time to position x t (s)</i>	<i>time from ignition</i>	Σt	Σx	$\Sigma(t^2)$	$\Sigma(t)^2$	$\Sigma(t.x)$	V_f	$F(t)$	\dot{q}_{e}''	$\dot{q}_{e}'' . F(t)$	$1/\sqrt{V_f}$
RIFT – Superflake Particle Board Full preheat – test4	Ignition Time	755						m/s		kW/m ²		(m/s) ^{-0.5}
10												
20												
30												
40												
50												
60												
70												
80												
90												
100	762	7							1.000	16.53		
110	769	14	2314	330	1785094	5354596	254750	0.0009	1.000	14.65	14.65	32.998
120	783	28	2368	360	1870306	5607424	284630	0.0004	1.000	13.12	13.12	49.780
130	816	61	2451	390	2004849	6007401	319320	0.0003	1.000	11.59	11.59	58.755
140	852	97	2565	420	2196369	6579225	359910	0.0002	1.000	10.50	10.50	63.770
150	897	142	2714	448	2461738	7365796	406300	0.0002	1.000	9.40	9.40	80.080
158	965	210							1.000	8.60		

<i>Flame Front Position x</i>	<i>Time to position x t (s)</i>	<i>time from ignition</i>	Σt	Σx	$\Sigma(t^2)$	$\Sigma(t)^2$	$\Sigma(t.x)$	V_f	$F(t)$	\dot{q}_{e}''	$\dot{q}_{e}'' . F(t)$	$1/\sqrt{V_f}$
RIFT – Superflake Particle Board Full preheat – test 5	Ignition Time	756						m/s		kW/m ²		(m/s) ^{-0.5}
10												
20												
30												
40												
50												
60												
70												
80												
90												
100	765	9	1535	300	1178125	2356225	161200	0.0000	1.000	16.53	16.53	225.837
110	770	14	2321	330	1795921	5387041	255520	0.0009	1.000	14.65	14.65	33.853
120	786	30	2362	360	1860332	5579044	283800	0.0006	1.000	13.12	13.12	42.514
130	806	50	2424	390	1959656	5875776	315580	0.0004	1.000	11.59	11.59	48.094
140	832	76	2507	420	2097021	6285049	351610	0.0003	1.000	10.50	10.50	56.409
150	869	113	2619	450	2290109	6859161	393710	0.0002	1.000	9.40	9.40	65.787
160	918	162	2770	480	2564174	7672900	444340	0.0002	1.000	8.39	8.39	75.746
170	983	227	2933	505	2874037	8602489	494590	0.0001	1.000	7.48	7.48	86.790
175	1032	276							1.000	7.02		
RIFT – Superflake Particle Board Full preheat – test 6	Ignition Time	755						m/s		kW/m ²		(m/s) ^{-0.5}
10												
20												
30												
40												

50												
60												
70												
80												
90												
100	765	10							1.000	16.53		
110	771	16	2320	330	1794322	5382400	255390	0.0010	1.000	14.65	14.65	31.512
120	784	29	2358	360	1853906	5560164	283280	0.0006	1.000	13.12	13.12	40.234
130	803	48	2418	390	1950026	5846724	314810	0.0004	1.000	11.59	11.59	48.772
140	831	76	2501	420	2087059	6255001	350780	0.0003	1.000	10.50	10.50	56.716
150	867	112	2609	450	2272171	6806881	392150	0.0002	1.000	9.40	9.40	63.351
160	911	156	2763	480	2551835	7634169	443260	0.0002	1.000	8.39	8.39	77.635
170	985	230	2956	510	2923746	8737936	504010	0.0001	1.000	7.48	7.48	86.314
180	1060	305							1.000	6.57		

Radiata Pine													
<i>Flame Front Position x</i>	<i>Time to position x (s)</i>	<i>t</i>	<i>time from ignition</i>	Σt	Σx	$\Sigma(t^2)$	$\Sigma(t)^2$	$\Sigma(t.x)$	V_f	$F(t)$	\dot{q}_e	$\dot{q}_e.F(t)$	$1/V_f$
LIFT – Radiata Pine test 1			Ignition Time	635					m/s		kW/m ²		(m/s) ^{-0.5}
50													
75													
100													
125													
150													
175													
200													
225													
250													
275													
300	653		18							1.000	16.50		
325	656		21	1972	975	1296314	3888784	641150	0.0047	1.000	14.90	14.90	14.514
350	663		28	1997	1050	1329589	3988009	699500	0.0022	1.000	13.20	13.20	21.433
375	678		43	2038	1125	1385062	4153444	765100	0.0015	1.000	11.50	11.50	26.137
400	697		62	2094	1200	1462454	4384836	838625	0.0012	1.000	9.80	9.80	28.661
425	719		84	2168	1275	1568274	4700224	922775	0.0009	1.000	8.40	8.40	33.387
450	752		117	2261	1350	1706565	5112121	1019225	0.0007	1.000	6.90	6.90	37.714
475	790		155	2380	1425	1891848	5664400	1132650	0.0006	1.000	6.00	6.00	41.566
500	838		203	2493	1480	2074569	6215049	1231075	0.0004	1.000	5.00	5.00	49.143
505	865		230								4.84		
LIFT – Radiata Pine test 2			Ignition Time	639					m/s		kW/m ²		(m/s) ^{-0.5}
50													
75													

100												
125												
150												
175												
200												
225												
250												
275												
300	657	18							1.000	16.50		
325	669	30	2001	975	1334835	4004001	650775	0.0027	1.000	14.90	14.90	19.322
350	675	36	2039	1050	1386211	4157521	714300	0.0018	1.000	13.20	13.20	23.880
375	695	56	2089	1125	1455611	4363921	784475	0.0011	1.000	11.50	11.50	29.706
400	719	80	2163	1200	1560987	4678569	866550	0.0009	1.000	9.80	9.80	32.931
425	749	110	2262	1275	1708398	5116644	963225	0.0007	1.000	8.40	8.40	38.987
450	794	155	2383	1350	1897037	5678689	1074625	0.0005	1.000	6.90	6.90	42.662
475	840	201	2601	1425	2271125	6765201	1239800	0.0003	1.000	6.00	6.00	60.933
500	967	328							1.000	5.00		

<i>Flame Front Position x</i>	<i>Time to position x (s)</i>	<i>t</i>	<i>time from ignition</i>	Σt	Σx	$\Sigma(t^2)$	$\Sigma(t \cdot x)$	V_f	$F(t)$	\dot{q}_{e}	$\dot{q}_{e} \cdot F(t)$	$1/V_f$
LIFT – Radiata Pine test 3	Ignition Time	655						m/s		kW/m ²		(m/s) ^{-0.5}

50
75
100
125
150
175
200
225
250
275

300												
325												
350	675	20								13.20		
375	682	27	2051	1125	1402385	4206601	769600	0.0026	1.000	11.50	11.50	19.717
400	694	39	2090	1200	1456556	4368100	836800	0.0015	1.000	9.80	9.80	25.560
425	714	59	2147	1275	1537553	4609609	913600	0.0011	1.000	8.40	8.40	30.062
450	739	84	2228	1350	1656542	4963984	1004125	0.0008	1.000	6.90	6.90	35.117
475	775	120	2382	1425	1900170	5673924	1134675	0.0004	1.000	6.00	6.00	52.420
500	868	213	2608	1500	2285274	6801664	1308750	0.0003	1.000	5.00	5.00	61.649
525	965	310	2868	1564	2755874	8225424	1498490	0.0002	1.000	4.20	4.20	65.228
539	1035	380								3.75		

Flame Front Position x	Time to position x	time from ignition	Σt	Σx	$\Sigma(t^2)$	$\Sigma(t)^2$	$\Sigma(t.x)$	V_f	$F(t)$	\dot{q}_e	$\dot{q}_e.F(t)$	$1/\sqrt{V_f}$
	t (s)											
RIFT – Pine- low preheat ISO ign data- test 1	Ignition Time	43						m/s		kW/m ²		(m/s) ^{-0.5}
10	42	0							0.256	33.88		
20	43	1	129	60	5549	16641	2600	0.0100	0.259	32.87	8.50	10.000
30	44	2	132	90	5810	17424	3980	0.0100	0.262	32.16	8.41	10.000
40	45	3	136	120	6170	18496	5470	0.0064	0.264	29.67	7.85	12.472
50	47	5	145	150	7043	21025	7330	0.0023	0.270	27.17	7.34	20.817
60	53	11	161	180	8739	25921	9800	0.0014	0.287	24.95	7.16	26.547
70	61	19	184	210	11430	33856	13050	0.0012	0.308	22.99	7.08	29.172
80	70	28	213	240	15345	45369	17250	0.0009	0.330	21.03	6.94	32.514
90	82	40	247	270	20649	61009	22480	0.0008	0.357	18.88	6.74	35.365
100	95	53	297	300	30149	88209	30080	0.0005	0.384	16.73	6.43	44.308
110	120	78	363	330	45329	131769	40460	0.0004	0.432	15.06	6.50	51.506
120	148	106	440	360	65888	193600	53320	0.0004	0.480	13.89	6.66	51.040
130	172	130	521	390	91889	271441	68260	0.0004	0.517	12.71	6.57	51.554
140	201	159	603	420	122885	363609	85000	0.0003	0.559	11.59	6.48	53.852
150	230	188	688	450	159350	473344	103760	0.0004	0.598	10.48	6.26	52.926
160	257	215	773	480	200745	597529	124240	0.0004	0.632	9.39	5.93	52.926
170	286	244	862	510	249606	743044	147160	0.0003	0.667	8.33	5.56	55.716
180	319	277	959	540	308873	919681	173300	0.0003	0.704	7.27	5.12	58.318
190	354	312	1079	570	391913	1164241	205880	0.0002	0.742	6.55	4.86	66.373
200	406	364							0.794	5.83	4.63	

Flame Front Position x	Time to position x	time from ignition	Σt	Σx	$\Sigma(t^2)$	$\Sigma(t)^2$	$\Sigma(t.x)$	V_f	$F(t)$	\dot{q}_{e}	$\dot{q}_{e} . F(t)$	$1/\sqrt{V_f}$	
	t (s)												
RIFT – Radiata Pine- low preheat ISO ign data- test 2	Ignition Time	42						m/s		kW/m ²		(m/s) ^{-0.5}	
	10	43	0						0.259	33.88			
	20	44	1	133	60	5901	17689	2690	0.0064	0.262	32.87	8.60	12.472
	30	46	3	139	90	6453	19321	4220	0.0039	0.267	32.16	8.60	15.916
	40	49	6	148	120	7326	21904	5990	0.0028	0.276	29.67	8.19	18.772
	50	53	10	161	150	8691	25921	8150	0.0020	0.287	27.17	7.80	22.509
	60	59	16	180	180	10914	32400	10950	0.0013	0.303	24.95	7.56	27.568
	70	68	25	203	210	13881	41209	14380	0.0012	0.325	22.99	7.48	29.172
	80	76	33	230	240	17796	52900	18580	0.0011	0.344	21.03	7.23	30.062
	90	86	43	258	270	22388	66564	23420	0.0010	0.366	18.88	6.90	31.623
	100	96	53	294	300	29156	86436	29660	0.0008	0.386	16.73	6.46	36.374
	110	112	69	335	330	37889	112225	37160	0.0006	0.417	15.06	6.28	39.377
	120	127	84	387	360	50577	149769	46800	0.0006	0.444	13.89	6.17	42.622
	130	148	105	445	390	66933	198025	58280	0.0005	0.480	12.71	6.10	46.372
	140	170	127	517	420	90405	267289	72890	0.0004	0.514	11.59	5.96	50.656
	150	199	156	601	450	122325	361201	90770	0.0003	0.556	10.48	5.83	55.716
	160	232	189	697	480	164181	485809	112190	0.0003	0.601	9.39	5.64	57.881
	170	266	223	808	504	220680	652864	136280	0.0002	0.643	8.33	5.36	75.541
174	310	267							0.694	7.91			

Flame Front Position x	Time to position x	time from ignition	Σt	Σx	$\Sigma(t^2)$	$\Sigma(t)^2$	$\Sigma(t.x)$	V_f	$F(t)$	\dot{q}_{e}	$\dot{q}_{e} . F(t)$	$1/\sqrt{V_f}$
	t (s)											
RIFT – Radiata Pine- low preheat ISO ign data- test 3	Ignition Time	40						m/s		kW/m ²		(m/s) ^{-0.5}
	10	40	0						0.249	33.88		
	20	41	1	123	60	5045	15129	2480	0.0100	0.252	32.87	8.30

30	42	2	126	90	5294	15876	3800	0.0100	0.256	32.16	8.22	10.000
40	43	3	133	120	5917	17689	5380	0.0029	0.259	29.67	7.67	18.559
50	48	8	145	150	7069	21025	7360	0.0018	0.273	27.17	7.42	23.484
60	54	14	163	180	8941	26569	9910	0.0015	0.290	24.95	7.23	25.520
70	61	21	186	210	11678	34596	13190	0.0012	0.308	22.99	7.08	29.306
80	71	31	220	240	16506	48400	17870	0.0007	0.332	21.03	6.99	37.152
90	88	48	259	270	22785	67081	23600	0.0007	0.370	18.88	6.98	38.267
100	100	60	299	300	30065	89401	30130	0.0009	0.394	16.73	6.59	33.922
110	111	71	337	330	38197	113569	37330	0.0008	0.415	15.06	6.26	36.197
120	126	86	411	360	58473	168921	49950	0.0003	0.443	13.89	6.14	58.635
130	174	134	484	390	80008	234256	63500	0.0003	0.520	12.71	6.61	57.576
140	184	144	570	420	109076	324900	80180	0.0005	0.535	11.59	6.20	45.190
150	212	172	636	450	136400	404496	95960	0.0004	0.574	10.48	6.01	52.915
160	240	200	726	480	177620	527076	116780	0.0003	0.611	9.39	5.73	55.764
170	274	234	833	505	234437	693889	140805	0.0002	0.653	8.33	5.44	73.376
175	319	279							0.704	7.80		

Flame Front Position x	Time to position x	time from ignition	Σt	Σx	$\Sigma(t^2)$	$\Sigma(t)^2$	$\Sigma(t.x)$	V_f	$F(t)$	$q_{.e}$	$q_{.e} . F(t)$	$1/\sqrt{V_f}$
	t (s)											
RIFT – Pine- low preheat ISO ign data- test 4	Ignition Time	40						m/s		kW/m ²		(m/s) ^{-0.5}
10	40	0							0.249	33.88		
20	41	1	123	60	5045	15129	2480	0.0100	0.252	32.87	8.30	10.000
30	42	2	129	90	5561	16641	3920	0.0036	0.256	32.16	8.22	16.733
40	46	6	140	120	6584	19600	5700	0.0020	0.267	29.67	7.93	22.509
50	52	12	153	150	7845	23409	7740	0.0021	0.284	27.17	7.73	21.602
60	55	15	166	180	9210	27556	10030	0.0028	0.292	24.95	7.29	18.772
70	59	19	182	210	11130	33124	12870	0.0015	0.303	22.99	6.96	26.116
80	68	28	203	240	13881	41209	16410	0.0012	0.325	21.03	6.84	29.172

90	76	36	229	270	17625	52441	20780	0.0012	0.344	18.88	6.49	29.172
100	85	45	258	300	22410	66564	26010	0.0009	0.363	16.73	6.08	32.514
110	97	57	292	330	28734	85264	32370	0.0008	0.388	15.06	5.85	35.365
120	110	70	333	360	37385	110889	40250	0.0007	0.414	13.89	5.74	38.147
130	126	86	381	390	49001	145161	49880	0.0006	0.443	12.71	5.62	41.884
140	145	105	446	420	67526	198916	62930	0.0004	0.475	11.59	5.50	49.911
150	175	135	559	450	108771	312481	84790	0.0002	0.522	10.48	5.46	70.035
160	239	199	680	480	158502	462400	109710	0.0002	0.610	9.39	5.72	69.287
170	266	226	804	510	217278	646416	137280	0.0003	0.643	8.33	5.36	54.863
180	299	259	906	538	276438	820836	163148	0.0002	0.682	7.27	4.96	64.849
188	341	301							0.728	6.70		

Flame Front Position x	Time to position x	time from ignition	Σt	Σx	$\Sigma(t^2)$	$\Sigma(t)^2$	$\Sigma(t.x)$	V_f	$F(t)$	q_e	$q_e \cdot F(t)$	$1/\sqrt{V_f}$	
	t (s)												
RIFT – Radiata Pine- low preheat ISO ign data- test 5	Ignition Time	40						m/s		kW/m ²		(m/s) ^{-0.5}	
	10	40	0						0.249	33.88			
	20	42	2	125	60	5213	15625	2530	0.0064	0.256	32.87	8.40	12.472
	30	43	3	132	90	5822	17424	4010	0.0036	0.259	32.16	8.31	16.733
	40	47	7	143	120	6867	20449	5820	0.0020	0.270	29.67	8.02	22.509
	50	53	13	163	150	8987	26569	8310	0.0012	0.287	27.17	7.80	28.577
	60	63	23	190	180	12254	36100	11610	0.0010	0.313	24.95	7.81	32.416
	70	74	34	219	210	16169	47961	15520	0.0010	0.339	22.99	7.80	30.950
	80	82	42	247	240	20481	61009	19930	0.0012	0.357	21.03	7.51	29.172
	90	91	51	279	270	26241	77841	25350	0.0008	0.376	18.88	7.10	35.000
	100	106	66	323	300	35393	104329	32650	0.0006	0.406	16.73	6.79	41.975
	110	126	86	382	330	49612	145924	42460	0.0005	0.443	15.06	6.67	46.969
	120	150	110	450	360	68652	202500	54480	0.0004	0.483	13.89	6.70	48.990
	130	174	134	532	390	96040	283024	69740	0.0003	0.520	12.71	6.61	54.118
	140	208	168	635	420	137549	403225	89690	0.0003	0.569	11.59	6.59	63.052
	150	253	213	745	450	187929	555025	112510	0.0003	0.627	10.48	6.57	61.992

160	284	244	864	480	251594	746496	138980	0.0003	0.664	9.39	6.24	61.094
170	327	287							0.713	8.33		

Flame Front Position x	Time to position x t (s)	time from ignition	Σt	Σx	$\Sigma(t^2)$	$\Sigma(t)^2$	$\Sigma(t.x)$	V_f	$F(t)$	\dot{q}_{e}	$\dot{q}_{e} \cdot F(t)$	$1/\sqrt{V_f}$
	Ignition Time											
RIFT – Radiata Pine- low preheat ISO ign data- test 6		40						m/s		kW/m ²		(m/s) ^{-0.5}
10	40	0							0.249	33.88		
20	43	3	129	60	5565	16641	2640	0.0033	0.259	32.87	8.50	17.321
30	46	6	141	90	6669	19881	4320	0.0021	0.267	32.16	8.60	21.602
40	52	12	157	120	8301	24649	6410	0.0015	0.284	29.67	8.43	25.520
50	59	19	178	150	10674	31684	9050	0.0013	0.303	27.17	8.23	27.406
60	67	27	209	180	14859	43681	12780	0.0008	0.323	24.95	8.05	35.277
70	83	43	255	210	22403	65025	18230	0.0005	0.359	22.99	8.26	43.770
80	105	65	315	240	34043	99225	25640	0.0005	0.404	21.03	8.50	46.904
90	127	87	377	270	48179	142129	34330	0.0005	0.444	18.88	8.39	44.796
100	145	105	441	300	65715	194481	44520	0.0005	0.475	16.73	7.94	45.981
110	169	129	508	330	87222	258064	56370	0.0004	0.513	15.06	7.72	49.501
120	194	154	585	360	115481	342225	70730	0.0004	0.549	13.89	7.62	51.506
130	222	182	674	390	153484	454276	88260	0.0003	0.587	12.71	7.47	56.716
140	258	218	802	420	219532	643204	113280	0.0002	0.633	11.59	7.34	71.629
150	322	282	958	450	313132	917764	144900	0.0002	0.707	10.48	7.41	77.517
160	378	338	1203	480	499577	1447209	194290	0.0001	0.767	9.39	7.20	97.408
170	503	463							0.884	8.33		

Flame Front Position x	Time to position x t (s)	time from ignition	Σt	Σx	$\Sigma(t^2)$	$\Sigma(t)^2$	$\Sigma(t.x)$	V_f	$F(t)$	\dot{q}_{e}	$\dot{q}_{e} \cdot F(t)$	$1/\sqrt{V_f}$
	Ignition Time											
RIFT – Radiata Pine – full preheat – test 1		643						m/s		kW/m ²		(m/s) ^{-0.5}

20												
30												
40												
50												
60												
70												
80												
90												
100												
110	652	9							1.000	15.06		
120	657	14	1969	360	1292353	3876961	236360	0.0024	1.000	13.89	13.89	20.207
130	660	17	1984	390	1312138	3936256	258020	0.0019	1.000	12.71	12.71	22.949
140	667	24	2002	420	1336114	4008004	280430	0.0013	1.000	11.59	11.59	27.406
150	675	32	2025	450	1367003	4100625	303910	0.0013	1.000	10.48	10.48	28.284
160	683	40	2051	480	1402363	4206601	328340	0.0011	1.000	9.39	9.39	30.062
170	693	50	2083	510	1446587	4338889	354350	0.0008	1.000	8.33	8.33	34.801
180	707	64	2127	540	1508627	4524129	383200	0.0006	1.000	7.27	7.27	41.445
190	727	84	2184	570	1590878	4769856	415390	0.0005	1.000	6.55	6.55	46.406
200	750	107	2235	600	1665593	4995225	447310	0.0006	1.000	5.83	5.83	40.877
210	758	115	2375	630	1888753	5640625	499920	0.0001	1.000	5.17	5.17	85.458
220	867	224	2543	660	2168977	6466849	561060	0.0001	1.000	4.58	4.58	91.381
230	918	275	2738	690	2502622	7496644	630600	0.0002	1.000	3.99	3.99	65.952
240	953	310	2855	711	2719189	8151025	677004	0.0002	1.000	3.77	3.77	76.874
241	984	341								3.74		

Flame Front Position x	Time to position x		Σt	Σx	$\Sigma(t^2)$	$\Sigma(t)^2$	$\Sigma(t.x)$	V_f	$F(t)$	\dot{q}_e	$\dot{q}_e \cdot F(t)$	$1/\sqrt{V_f}$
	t	time from ignition										
RIFT – Radiata Pine – full preheat – test 2	Ignition Time	644						m/s		kW/m ²		(m/s) ^{-0.5}

10
20
30

40												
50												
60												
70												
80												
90												
100	648	4							1.000	16.73		
110	650	6	1956	330	1275368	3825936	215260	0.0018	1.000	15.06	15.06	23.664
120	658	14	1973	360	1297689	3892729	236910	0.0013	1.000	13.89	13.89	27.406
130	665	21	1997	390	1329465	3988009	259770	0.0012	1.000	12.71	12.71	28.358
140	674	30	2028	420	1371222	4112784	284160	0.0008	1.000	11.59	11.59	35.000
150	689	45	2070	450	1428846	4284900	310830	0.0006	1.000	10.48	10.48	40.676
160	707	63	2120	480	1498746	4494400	339550	0.0006	1.000	9.39	9.39	41.839
170	724	80	2174	510	1576074	4726276	369940	0.0006	1.000	8.33	8.33	42.448
180	743	99	2229	540	1656869	4968441	401600	0.0005	1.000	7.27	7.27	43.589
190	762	118	2300	570	1764718	5290000	437520	0.0004	1.000	6.55	6.55	51.603
200	795	151	2376	600	1883430	5645376	475770	0.0003	1.000	5.83	5.83	53.607
210	819	175	2468	630	2032102	6091024	518870	0.0003	1.000	5.17	5.17	54.628
220	854	210	2556	660	2179766	6533136	562960	0.0003	1.000	4.58	4.58	56.651
230	883	239	2661	685	2362781	7080921	608110	0.0002	1.000	3.99	3.99	69.310
235	924	280								3.88		

Flame Front Position x	Time to		Σt	Σx	$\Sigma(t^2)$	$\Sigma(t)^2$	$\Sigma(t.x)$	V_f	$F(t)$	\dot{q}_e	$\dot{q}_e \cdot F(t)$	$1/\sqrt{V_f}$
	position x (s)	t time from ignition										
RIFT – Radiata Pine – full preheat – test 3	Ignition Time	40						m/s		kW/m ²		(m/s) ^{-0.5}

10
20
30
40
50

60
70
80
90
100
110
120
130
140
150
160
170
180
190
200
210
220
230
234

649	6										15.06		
654	11	1960	360	1280566	3841600	235280	0.0024	1.000	13.89	13.89	20.207		
657	14	1974	390	1298934	3896676	256710	0.0021	1.000	12.71	12.71	21.602		
663	20	1991	420	1321459	3964081	278880	0.0014	1.000	11.59	11.59	26.547		
671	28	2015	450	1353571	4060225	302430	0.0011	1.000	10.48	10.48	30.062		
681	38	2048	480	1398418	4194304	327930	0.0008	1.000	9.39	9.39	35.590		
696	53	2088	510	1453698	4359744	355260	0.0007	1.000	8.33	8.33	38.730		
711	68	2133	540	1517013	4549689	384240	0.0007	1.000	7.27	7.27	38.730		
726	83	2186	570	1593598	4778596	415720	0.0005	1.000	6.55	6.55	43.910		
749	106	2280	600	1736102	5198400	456790	0.0002	1.000	5.83	5.83	64.651		
805	162	2393	630	1912947	5726449	503430	0.0002	1.000	5.17	5.17	67.747		
839	196	2652	660	2368010	7033104	585470	0.0001	1.000	4.58	4.58	107.918		
1008	365	2889	684	2805749	8346321	660248	0.0001	1.000	3.99	3.99	123.264		
1042	399												

<i>Flame Front Position x</i>	<i>Time to position x (s)</i>	<i>time from ignition</i>	Σt	Σx	$\Sigma(t^2)$	$\Sigma(t)^2$	$\Sigma(t.x)$	V_f	$F(t)$	\dot{q}_e	$\dot{q}_e \cdot F(t)$	$1/\sqrt{V_f}$
RIFT – Radiata Pine – full preheat – test 4	Ignition Time	40						m/s		kW/m ²		(m/s) ^{-0.5}

10
20
30
40
50
60
70
80

90												
100	649	5								16.73		
110	652	8	1959	330	1279269	3837681	215580	0.0021	1.000	15.06	15.06	21.602
120	658	14	1970	360	1293668	3880900	236480	0.0023	1.000	13.89	13.89	20.817
130	660	16	1988	390	1317464	3952144	258560	0.0015	1.000	12.71	12.71	26.247
140	670	26	2010	420	1346900	4040100	281600	0.0010	1.000	11.59	11.59	31.623
150	680	36	2042	450	1390164	4169764	306520	0.0009	1.000	10.48	10.48	33.212
160	692	48	2088	480	1453920	4359744	334440	0.0005	1.000	9.39	9.39	43.205
170	716	72	2145	510	1534689	4601025	365100	0.0004	1.000	8.33	8.33	47.469
180	737	93	2220	540	1644114	4928400	400110	0.0004	1.000	7.27	7.27	50.759
190	767	123	2305	570	1773059	5313025	438590	0.0003	1.000	6.55	6.55	56.605
200	801	157	2399	600	1920451	5755201	480440	0.0003	1.000	5.83	5.83	56.605
210	831	187	2482	630	2054662	6160324	521710	0.0004	1.000	5.17	5.17	49.911
220	850	206	2554	660	2175190	6522916	562300	0.0005	1.000	4.58	4.58	45.895
230	873	229	2620	690	2289238	6864400	603070	0.0004	1.000	3.99	3.99	48.480
240	897	253	2697	717	2426067	7273809	645039	0.0003	1.000	3.77	3.77	56.662
247	927	283							1.000	3.61		

Flame Front Position x	Macrocarpa											
	Time to position x t (s)	time from ignition	Σt	Σx	$\Sigma(t^2)$	$\Sigma(t)^2$	$\Sigma(t.x)$	V_f	$F(t)$	\dot{q}_e	$\dot{q}_e.F(t)$	$1/V_f$
LIFT – Macrocarpa Test 1	Ignition Time	291						m/s		kW/m ²		(m/s) ^{-0.5}
50												
75												
100												
125												
150	306	15							1.000	21.80	21.80	
175	309	18	926	525	285838	857476	162175	0.0099	1.000	20.60	20.60	10.066
200	311	20	935	600	291427	874225	187150	0.0080	1.000	18.95	18.95	11.155
225	315	24	945	675	297707	893025	212825	0.0063	1.000	17.29	17.29	12.649
250	319	28	957	750	305315	915849	239450	0.0063	1.000	15.33	15.33	12.649
275	323	32	969	825	313019	938961	266675	0.0063	1.000	13.37	13.37	12.649
300	327	36	988	900	325502	976144	296775	0.0031	1.000	11.56	11.56	17.938
325	338	47	1013	975	342277	1026169	329750	0.0024	1.000	9.75	9.75	20.502
350	348	57	1060	1050	375224	1123600	371900	0.0013	1.000	8.52	8.52	27.702
375	374	83	1105	1125	407669	1221025	415250	0.0013	1.000	7.28	7.28	27.478
400	383	92	1151	1200	441801	1324801	460900	0.0025	1.000	6.28	6.28	20.033
425	394	103	1198	1275	479166	1435204	510100	0.0012	1.000	5.27	5.27	28.371
450	421	130	1302	1350	569646	1695204	588225	0.0005	1.000	4.50	4.50	44.374
475	487	196	1471	1425	731379	2163841	702275	0.0004	1.000	3.72	3.72	53.336
500	563	272	1657	1500	922587	2745649	831500	0.0004	1.000	3.18	3.18	49.567
525	607	316	1928	1575	1259982	3717184	1017075	0.0002	1.000	2.63	2.63	65.509
550	758	467	2155	1635	1567113	4644025	1177975	0.0002	1.000	2.18	2.18	73.882
560	790	499							1.000	1.96	1.96	

<i>Flame Front Position x</i>	<i>Time to position x t (s)</i>	<i>time from ignition</i>	Σt	Σx	$\Sigma(t^2)$	$\Sigma(t)^2$	$\Sigma(t.x)$	V_f	$F(t)$	\dot{q}_{e}	$\dot{q}_{e}.F(t)$	$1/V_f$
LIFT – Macrocarpa Test 2	Ignition Time	280						m/s		kW/m ²		(m/s) ^{-0.5}
50										25.20		
75										24.51		
100										23.75		
125										22.99		
150										21.80		
175										20.60		
200	289	9							1.000	18.95		
225	292	12	876	675	255810	767376	197250	0.0083	1.000	17.29	17.29	10.954
250	295	15	884	750	260498	781456	221125	0.0099	1.000	15.33	15.33	10.066
275	297	17	892	825	265234	795664	245425	0.0099	1.000	13.37	13.37	10.066
300	300	20	903	900	271845	815409	271125	0.0054	1.000	11.56	11.56	13.663
325	306	26	917	975	280357	840889	298300	0.0045	1.000	9.75	9.75	14.853
350	311	31	937	1050	292757	877969	328300	0.0035	1.000	8.52	8.52	16.959
375	320	40	963	1125	309345	927369	361650	0.0024	1.000	7.28	7.28	20.563
400	332	52	1002	1200	335124	1004004	401550	0.0016	1.000	6.28	6.28	24.658
425	350	70	1039	1275	360173	1079521	442200	0.0019	1.000	5.27	5.27	23.071
450	357	77	1086	1350	393590	1179396	489425	0.0016	1.000	4.50	4.50	25.134
475	379	99	1147	1425	440011	1315609	546175	0.0009	1.000	3.72	3.72	33.051
500	411	131	1242	1500	516866	1542564	622825	0.0007	1.000	3.18	3.18	38.307
525	452	172	1410	1575	672434	1988100	743650	0.0003	1.000	2.63	2.63	53.506
550	547	267							1.000	2.18	2.18	

<i>Flame Front Position x</i>	<i>Time to position x t (s)</i>	<i>time from ignition</i>	Σt	Σx	$\Sigma(t^2)$	$\Sigma(t)^2$	$\Sigma(t.x)$	V_f	$F(t)$	$\dot{q}_{.e}$	$\dot{q}_{.e}.F(t)$	$1/\sqrt{V_f}$
LIFT – Macrocarpa Test 3	Ignition Time	289						m/s		kW/m ²		(m/s) ^{-0.5}
50										25.20		
75										24.51		
100										23.75		
125										22.99		
150										21.80		
175										20.60		
200										18.95		
225										17.29		
250	300	11							1.000	15.33		
275	303	14	909	825	275445	826281	250125	0.0083	1.000	13.37	13.37	10.954
300	306	17	919	900	281545	844561	275875	0.0071	1.000	11.56	11.56	11.872
325	310	21	929	975	287705	863041	302100	0.0071	1.000	9.75	9.75	11.872
350	313	24	946	1050	298398	894916	331425	0.0035	1.000	8.52	8.52	16.886
375	323	34	969	1125	313187	938961	363875	0.0025	1.000	7.28	7.28	20.000
400	333	44	1002	1200	334934	1004004	401375	0.0022	1.000	6.28	6.28	21.508
425	346	57	1047	1275	366029	1096209	445850	0.0014	1.000	5.27	5.27	26.747
450	368	79	1107	1350	409589	1225449	499325	0.0011	1.000	4.50	4.50	30.680
475	393	104	1214	1425	495082	1473796	578775	0.0006	1.000	3.72	3.72	42.380
500	453	164	1330	1500	593914	1768900	667275	0.0005	1.000	3.18	3.18	43.378
525	484	195	1451	1562	703661	2105401	756618	0.0006	1.000	2.63	2.63	40.566
537	514	225							1.000	2.42	2.42	

<i>Flame Front Position x</i>	<i>Time to position x t (s)</i>	<i>time from ignition</i>	Σt	Σx	$\Sigma(t^2)$	$\Sigma(t)^2$	$\Sigma(t.x)$	V_f	$F(t)$	$\dot{q}_{.e}$	$\dot{q}_{.e}.F(t)$	$1/\sqrt{V_f}$
RIFT – Macrocarpa Low preheat – ISO ign- Test 1	Ignition Time	63						m/s		kW/m ²		(m/s) ^{-0.5}
10	50	0								33.88		

20	51	1	153	60	7805	23409	3080	0.0100	0.342	32.87	11.25	10.000
30	52	2	156	90	8114	24336	4700	0.0100	0.346	32.16	11.11	10.000
40	53	3	159	120	8429	25281	6380	0.0100	0.349	29.67	10.35	10.000
50	54	4	162	150	8750	26244	8120	0.0100	0.352	27.17	9.57	10.000
60	55	5	165	180	9077	27225	9920	0.0100	0.355	24.95	8.87	10.000
70	56	6	168	210	9410	28224	11780	0.0100	0.359	22.99	8.24	10.000
80	57	7	175	240	10229	30625	14060	0.0029	0.362	21.03	7.61	18.559
90	62	12	184	270	11318	33856	16640	0.0024	0.377	18.88	7.12	20.207
100	65	15	196	300	12830	38416	19670	0.0028	0.386	16.73	6.46	18.772
110	69	19	211	330	14915	44521	23330	0.0016	0.398	15.06	5.99	24.944
120	77	27	238	360	19154	56644	28790	0.0008	0.420	13.89	5.84	34.431
130	92	42	276	390	25842	76176	36180	0.0007	0.460	12.71	5.84	38.730
140	107	57	343	420	40649	117649	48540	0.0004	0.496	11.59	5.75	52.489
150	144	94	413	450	58429	170569	62500	0.0003	0.575	10.48	6.02	53.473
160	162	112	479	480	76909	229441	76930	0.0007	0.610	9.39	5.73	38.447
170	173	123	520	510	90398	270400	88630	0.0009	0.630	8.33	5.25	33.922
180	185	135	630	540	138138	396900	114390	0.0002	0.652	7.27	4.74	76.792
190	272	222	754	570	196418	568516	144380	0.0002	0.790	6.55	5.18	78.562
200	297	247	889	600	264593	790321	178280	0.0004	0.826	5.83	4.81	49.004
210	320	270	959	630	307573	919681	201840	0.0004	0.857	5.17	4.43	47.438
220	342	292	1023	651	349685	1046529	222221	0.0003	0.886	4.58	4.06	60.505
221	361	311							0.910	4.52	4.12	

<i>Flame Front Position x</i>	<i>Time to position x t (s)</i>	<i>time from ignition</i>	Σt	Σx	$\Sigma(t^2)$	$\Sigma(t)^2$	$\Sigma(t.x)$	V_f	$F(t)$	\dot{q}_e	$\dot{q}_e.F(t)$	$1/V_f$
RIFT – Macrocarpa Low preheat – ISO ign- Test 2	Ignition Time	50						m/s		kW/m ²		(m/s) ^{-0.5}
10	63	0								33.88		
20	64	1	193	60	12421	37249	3890	0.0064	0.383	32.87	12.60	12.472
30	66	3	198	90	13076	39204	5980	0.0050	0.389	32.16	12.52	14.142
40	68	5	203	120	13741	41209	8150	0.0064	0.395	29.67	11.72	12.472
50	69	6	210	150	14714	44100	10550	0.0036	0.398	27.17	10.82	16.733

60	73	10	221	180	16331	48841	13360	0.0020	0.409	24.95	10.21	22.509
70	79	16	240	210	19314	57600	16950	0.0013	0.426	22.99	9.79	27.568
80	88	25	267	240	23985	71289	21570	0.0009	0.449	21.03	9.45	32.514
90	100	37	302	270	30740	91204	27440	0.0008	0.479	18.88	9.05	36.091
100	114	51	349	300	41221	121801	35250	0.0006	0.512	16.73	8.56	42.111
110	135	72	406	330	55870	164836	45090	0.0005	0.557	15.06	8.38	46.372
120	157	94	479	360	77843	229441	58000	0.0004	0.600	13.89	8.34	51.191
130	187	124	568	390	109794	322624	74510	0.0003	0.655	12.71	8.33	57.984
140	224	161	673	420	153789	452929	94970	0.0003	0.717	11.59	8.31	61.239
150	262	199	808	450	222504	652864	122180	0.0002	0.776	10.48	8.12	70.586
160	322	259	948	480	304824	898704	152700	0.0002	0.860	9.39	8.07	71.784
170	364	301	1105	510	411741	1221025	188820	0.0002	0.914	8.33	7.62	69.850
180	419	356	1307	535	582633	1708249	234240	0.0001	0.981	7.27	7.13	106.818
185	524	461							1.000	6.91	6.91	

<i>Flame Front Position x</i>	<i>Time to position x t (s)</i>	<i>time from ignition</i>	Σt	Σx	$\Sigma(t^2)$	$\Sigma(t)^2$	$\Sigma(t.x)$	V_f	$F(t)$	" q_e	" $q_e.F(t)$	$1/\sqrt{V_f}$
RIFT – Macrocarpa Low preheat – ISO ign- Test 3	Ignition Time	40						m/s		kW/m ²		(m/s) ^{-0.5}
10	40	0								33.88		
20	41	1	124	60	5130	15376	2510	0.0064	0.307	32.87	10.09	12.472
30	43	3	128	90	5466	16384	3870	0.0064	0.314	32.16	10.10	12.472
40	44	4	132	120	5810	17424	5300	0.0100	0.318	29.67	9.43	10.000
50	45	5	135	150	6077	18225	6770	0.0100	0.321	27.17	8.73	10.000
60	46	6	141	180	6641	19881	8510	0.0036	0.325	24.95	8.11	16.733
70	50	10	152	210	7752	23104	10740	0.0020	0.339	22.99	7.79	22.509
80	56	16	168	240	9480	28224	13560	0.0017	0.359	21.03	7.54	24.495
90	62	22	188	270	11880	35344	17060	0.0014	0.377	18.88	7.12	26.547
100	70	30	217	300	15969	47089	21930	0.0008	0.401	16.73	6.71	34.431
110	85	45	254	330	21926	64516	28230	0.0007	0.442	15.06	6.65	38.086
120	99	59	305	360	31667	93025	36960	0.0005	0.477	13.89	6.62	42.774
130	121	81	358	390	43486	128164	46930	0.0005	0.527	12.71	6.70	44.280

140	138	98	423	420	60581	178929	59650	0.0005	0.563	11.59	6.53	46.705
150	164	124	501	450	85541	251001	75760	0.0003	0.614	10.48	6.43	55.427
160	199	159	570	480	109346	324900	91630	0.0004	0.676	9.39	6.35	49.321
170	207	167	664	510	149014	440896	113470	0.0003	0.689	8.33	5.74	58.926
180	258	218	751	540	191209	564001	135970	0.0002	0.770	7.27	5.60	63.731
190	286	246	871	570	255289	758641	166180	0.0003	0.810	6.55	5.31	59.083
200	327	287	965	594	312629	931225	191548	0.0002	0.866	5.83	5.05	68.160
204	352	312							0.899	5.57	5.00	

<i>Flame Front Position x</i>	<i>Time to position x t (s)</i>	<i>time from ignition</i>	Σt	Σx	$\Sigma(t^2)$	$\Sigma(t)^2$	$\Sigma(t.x)$	V_f	$F(t)$	q_e	$q_e.F(t)$	$1/V_f$
RIFT – Macrocarpa Low preheat – ISO ign- Test 4	Ignition Time	40						m/s		kW/m ²		(m/s) ^{-0.5}
10	40	0								33.88		
20	41	1	123	60	5045	15129	2480	0.0100	0.307	32.87	10.09	10.000
30	42	2	128	90	5470	16384	3880	0.0046	0.311	32.16	9.99	14.720
40	45	5	134	120	5998	17956	5410	0.0039	0.321	29.67	9.54	15.916
50	47	7	145	150	7043	21025	7330	0.0023	0.328	27.17	8.93	20.817
60	53	13	155	180	8043	24025	9380	0.0023	0.349	24.95	8.70	20.817
70	55	15	166	210	9198	27556	11670	0.0039	0.355	22.99	8.17	15.916
80	58	18	185	240	11573	34225	14970	0.0010	0.365	21.03	7.68	31.123
90	72	32	211	270	15109	44521	19220	0.0009	0.407	18.88	7.68	34.178
100	81	41	243	300	19845	59049	24480	0.0011	0.431	16.73	7.21	30.000
110	90	50	301	330	31561	90601	33600	0.0004	0.455	15.06	6.85	52.696
120	130	90	370	360	47500	136900	45000	0.0003	0.546	13.89	7.59	55.777
130	150	110	456	390	70376	207936	59740	0.0004	0.587	12.71	7.46	48.094
140	176	136	537	420	97997	288369	75790	0.0003	0.636	11.59	7.37	55.427
150	211	171	627	450	133097	393129	94690	0.0003	0.696	10.48	7.29	56.651
160	240	200	724	480	176650	524176	116460	0.0003	0.742	9.39	6.97	55.716
170	273	233	853	510	247729	727609	146010	0.0002	0.792	8.33	6.60	72.060
180	340	300	992	540	333770	984064	179620	0.0002	0.883	7.27	6.43	73.643

	190	379	339						0.933	6.55		
<i>Flame Front Position x</i>	<i>Time to position x t (s)</i>	<i>time from ignition</i>	Σt	Σx	$\Sigma(t^2)$	$\Sigma(t)^2$	$\Sigma(t.x)$	V_f	$F(t)$	\dot{q}_e	$\dot{q}_e.F(t)$	$1/\sqrt{V_f}$
RIFT – Macrocarpa Low preheat – ISO ign- Test 5	Ignition Time	40						m/s		kW/m ²		(m/s) ^{-0.5}
10	40	0								33.88		
20	43	3	129	60	5565	16641	2640	0.0033	0.314	32.87	10.33	17.321
30	46	6	136	90	6174	18496	4120	0.0046	0.325	32.16	10.45	14.720
40	47	7	142	120	6726	20164	5710	0.0064	0.328	29.67	9.74	12.472
50	49	9	148	150	7314	21904	7450	0.0039	0.335	27.17	9.11	15.916
60	52	12	156	180	8130	24336	9420	0.0033	0.346	24.95	8.62	17.321
70	55	15	169	210	9573	28561	11930	0.0019	0.355	22.99	8.17	22.949
80	62	22	187	240	11769	34969	15110	0.0013	0.377	21.03	7.94	27.406
90	70	30	213	270	15305	45369	19360	0.0010	0.401	18.88	7.57	30.950
100	81	41	246	300	20486	60516	24850	0.0008	0.431	16.73	7.21	35.440
110	95	55	284	330	27250	80656	31510	0.0007	0.467	15.06	7.03	36.751
120	108	68	320	360	34378	102400	38620	0.0009	0.498	13.89	6.91	33.348
130	117	77	355	390	42253	126025	46370	0.0009	0.518	12.71	6.59	33.348
140	130	90	392	420	51614	153664	55160	0.0007	0.546	11.59	6.33	37.448
150	145	105	438	450	64494	191844	66030	0.0006	0.577	10.48	6.04	40.676
160	163	123	502	480	85230	252004	80810	0.0004	0.612	9.39	5.74	50.075
170	194	154	587	510	117105	344569	100460	0.0003	0.667	8.33	5.56	57.933
180	230	190	681	533	156585	463761	121411	0.0002	0.727	7.27	5.29	68.972
183	257	217							0.768	7.06		
<i>Flame Front Position x</i>	<i>Time to position x t (s)</i>	<i>time from ignition</i>	Σt	Σx	$\Sigma(t^2)$	$\Sigma(t)^2$	$\Sigma(t.x)$	V_f	$F(t)$	\dot{q}_e	$\dot{q}_e.F(t)$	$1/\sqrt{V_f}$
RIFT – Macrocarpa Low preheat – ISO ign- Test 6	Ignition Time	40						m/s		kW/m ²		(m/s) ^{-0.5}
10	40	0								33.88		

20	42	2	126	60	5300	15876	2560	0.0050	0.311	32.87	10.21	14.142
30	44	4	131	90	5725	17161	3960	0.0064	0.318	32.16	10.22	12.472
40	45	5	137	120	6265	18769	5520	0.0046	0.321	29.67	9.54	14.720
50	48	8	143	150	6829	20449	7200	0.0039	0.332	27.17	9.02	15.916
60	50	10	154	180	7940	23716	9320	0.0023	0.339	24.95	8.45	20.817
70	56	16	170	210	9732	28900	12040	0.0014	0.359	22.99	8.24	26.547
80	64	24	198	240	13316	39204	16060	0.0009	0.383	21.03	8.06	33.575
90	78	38	240	270	19784	57600	21940	0.0006	0.423	18.88	7.99	41.445
100	98	58	295	300	29849	87025	29910	0.0005	0.474	16.73	7.93	45.281
110	119	79	364	330	45374	132496	40530	0.0004	0.523	15.06	7.87	49.666
120	147	107	437	360	65011	190969	52960	0.0004	0.581	13.89	8.07	51.040
130	171	131	522	390	92466	272484	68430	0.0003	0.627	12.71	7.96	53.607
140	204	164	611	420	126553	373321	86190	0.0003	0.684	11.59	7.93	57.011
150	236	196	716	450	173488	512656	108120	0.0003	0.736	10.48	7.71	60.123
160	276	236	852	480	247472	725904	137360	0.0002	0.796	9.39	7.47	72.748
170	340	300	994	510	334660	988036	170000	0.0002	0.883	8.33	7.36	72.183
180	378	338	1138	540	434884	1295044	205640	0.0002	0.932	7.27	6.78	63.272
190	420	380	1261	565	533653	1590121	238125	0.0002	0.982	6.55	6.43	75.328
195	463	423								6.19		

<i>Flame Front Position x</i>	<i>Time to position x t (s)</i>	<i>time from ignition</i>	Σt	Σx	$\Sigma(t^2)$	$\Sigma(t)^2$	$\Sigma(t.x)$	V_f	$F(t)$	\dot{q}_e	$\dot{q}_e \cdot F(t)$	$1/V_f$
RIFT – Macrocarpa – full preheat – test 1	Ignition Time	436						m/s		kW/m ²		(m/s) ^{-0.5}
10												
20												
30												
40												
50												
60												
70	441	5							1.000	22.99		

80	446	10	1334	240	593206	1779556	106780	0.0029	1.000	21.03	21.03	18.559
90	447	11	1342	270	600326	1800964	120810	0.0064	1.000	18.88	18.88	12.472
100	449	13	1350	300	607526	1822500	135070	0.0027	1.000	16.73	16.73	19.272
110	454	18	1363	330	619317	1857769	150040	0.0018	1.000	15.06	15.06	23.484
120	460	24	1384	360	638616	1915456	166240	0.0012	1.000	13.89	13.89	28.577
130	470	34	1411	390	663861	1990921	183640	0.0010	1.000	12.71	12.71	32.416
140	481	45	1446	420	697286	2090916	202690	0.0008	1.000	11.59	11.59	35.440
150	495	59	1504	450	755170	2262016	226070	0.0004	1.000	10.48	10.48	49.780
160	528	92	1570	480	823018	2464900	251720	0.0004	1.000	9.39	9.39	51.603
170	547	111	1645	510	902893	2706025	280070	0.0005	1.000	8.33	8.33	45.895
180	570	134	1712	540	978134	2930944	308640	0.0004	1.000	7.27	7.27	49.004
190	595	159	1792	570	1072054	3211264	341050	0.0003	1.000	6.55	6.55	53.519
200	627	191	1882	594	1182754	3541924	373090	0.0002	1.000	5.83	5.83	68.216
204	660	224								5.57		

<i>Flame Front Position x</i>	<i>Time to position x t (s)</i>	<i>time from ignition</i>	Σt	Σx	$\Sigma(t^2)$	$\Sigma(x^2)$	$\Sigma(t.x)$	V_f	$F(t)$	" $q_{.e}$	" $q_{.e} . F(t)$	$1/\sqrt{V_f}$
RIFT – Macrocarpa – full preheat – test 2	Ignition Time	438						m/s		kW/m ²		(m/s) ^{-0.5}
10												
20												
30												
40												
50												
60												
70	445	7							1.000	22.99		
80	448	10	1344	240	602130	1806336	107580	0.0033	1.000	21.03	21.03	17.321
90	451	13	1352	270	609314	1827904	121730	0.0039	1.000	18.88	18.88	15.916
100	453	15	1360	300	616546	1849600	136050	0.0039	1.000	16.73	16.73	15.916
110	456	18	1369	330	624745	1874161	150660	0.0028	1.000	15.06	15.06	18.772
120	460	22	1381	360	635761	1907161	165810	0.0022	1.000	13.89	13.89	21.257
130	465	27	1402	390	655354	1965604	182430	0.0011	1.000	12.71	12.71	29.967

140	477	39	1435	420	686803	2059225	201180	0.0007	1.000	11.59	11.59	37.544
150	493	55	1473	450	723587	2169729	221210	0.0008	1.000	10.48	10.48	36.374
160	503	65	1510	480	760254	2280100	241810	0.0010	1.000	9.39	9.39	32.416
170	514	76	1551	510	802361	2405601	263980	0.0006	1.000	8.33	8.33	39.919
180	534	96	1613	540	868577	2601769	290850	0.0004	1.000	7.27	7.27	50.888
190	565	127	1725	570	996257	2975625	328670	0.0002	1.000	6.55	6.55	69.015
200	626	188	1840	600	1132302	3385600	368840	0.0002	1.000	5.83	5.83	66.981
210	649	211	1951	630	1270053	3806401	410210	0.0004	1.000	5.17	5.17	50.053
220	676	238							1.000	4.58		

<i>Flame Front Position x</i>	<i>Time to position x t (s)</i>	<i>time from ignition</i>	Σt	Σx	$\Sigma(t^2)$	$\Sigma(t)^2$	$\Sigma(t.x)$	V_f	$F(t)$	$q_{.e}$	$q_{.e} \cdot F(t)$	$1/\sqrt{V_f}$
RIFT – Macrocarpa – full preheat – test 3	Ignition Time	438						m/s		kW/m ²		(m/s) ^{-0.5}
10												
20												
30												
40												
50												
60												
70	446	8							1.000	22.99		
80	447	9	1341	240	599429	1798281	107300	0.0100	1.000	21.03	21.03	10.000
90	448	10	1344	270	602114	1806336	120980	0.0100	1.000	18.88	18.88	10.000
100	449	11	1347	300	604805	1814409	134720	0.0100	1.000	16.73	16.73	10.000
110	450	12	1351	330	608405	1825201	148640	0.0064	1.000	15.06	15.06	12.472
120	452	14	1356	360	612920	1838736	162760	0.0050	1.000	13.89	13.89	14.142
130	454	16	1362	390	618356	1855044	177100	0.0050	1.000	12.71	12.71	14.142
140	456	18	1369	420	624733	1874161	191710	0.0039	1.000	11.59	11.59	15.916
150	459	21	1381	450	635773	1907161	207250	0.0019	1.000	10.48	10.48	22.949
160	466	28	1402	480	655366	1965604	224500	0.0011	1.000	9.39	9.39	30.246
170	477	39	1438	510	689710	2067844	244750	0.0007	1.000	8.33	8.33	38.447
180	495	57	1516	540	768490	2298256	273550	0.0003	1.000	7.27	7.27	59.909

<i>Flame Front Position x</i>	<i>Time to position x t (s)</i>	<i>time from ignition</i>	Σt	Σx	$\Sigma(t^2)$	$\Sigma(t)^2$	$\Sigma(t.x)$	V_f	$F(t)$	$q_{.e}$	$q_{.e} . F(t)$	$1/\sqrt{V_f}$
RIFT – Macrocarpa – full preheat – test 4	Ignition Time	443						m/s		kW/m ²		(m/s) ^{-0.5}
10												
20												
30												
40												
50												
60												
70	448	5								22.99		
80	450	7	1351	240	608413	1825201	108130	0.0039	1.000	21.03	21.03	15.916
90	453	10	1359	270	615645	1846881	122370	0.0033	1.000	18.88	18.88	17.321
100	456	13	1368	300	623826	1871424	136860	0.0033	1.000	16.73	16.73	17.321
110	459	16	1375	330	630217	1890625	151290	0.0046	1.000	15.06	15.06	14.720
120	460	17	1381	360	635725	1907161	165750	0.0064	1.000	13.89	13.89	12.472
130	462	19	1387	390	641269	1923769	180360	0.0039	1.000	12.71	12.71	15.916
140	465	22	1397	420	650569	1951609	195660	0.0024	1.000	11.59	11.59	20.207
150	470	27	1409	450	661801	1985281	211440	0.0022	1.000	10.48	10.48	21.257
160	474	31	1423	480	675017	2024929	227770	0.0022	1.000	9.39	9.39	21.257
170	479	36	1446	510	697166	2090916	246010	0.0010	1.000	8.33	8.33	31.954
180	493	50	1488	540	738746	2214144	268210	0.0005	1.000	7.27	7.27	43.434
190	516	73	1543	570	794461	2380849	293580	0.0005	1.000	6.55	6.55	45.389
200	534	91	1602	600	856116	2566404	320760	0.0006	1.000	5.83	5.83	42.426
210	552	109	1656	630	914760	2742336	348120	0.0006	1.000	5.17	5.17	42.426
220	570	127	1719	657	986013	2954961	376839	0.0004	1.000	4.58	4.58	52.099
227	597	154								4.17		

Flame Front Position x	Time to position x t (s)	time from ignition	Rimu										
			Σt	Σx	$\Sigma(t^2)$	$\Sigma(t)^2$	$\Sigma(t.x)$	V_f	$F(t)$	\dot{q}_e	$\dot{q}_e.F(t)$	$1/\sqrt{V_f}$	
LIFT Rimu test 1	Ignition Time	715							m/s		kW/m ²		(m/s) ^{-0.5}
50											#N/A		
75											26.45		
100	720	5								1.000	26.10	26.10	
125	721	6	2165	375	1562417	4687225	270725	0.0115	1.000	1.000	25.30	25.30	9.309
150	724	9	2171	450	1571093	4713241	325775	0.0099	1.000	1.000	24.50	24.50	10.066
175	726	11	2178	525	1581236	4743684	381250	0.0125	1.000	1.000	23.20	23.20	8.944
200	728	13	2191	600	1600229	4800481	438475	0.0040	1.000	1.000	21.90	21.90	15.802
225	737	22	2206	675	1622234	4866436	496675	0.0037	1.000	1.000	20.70	20.70	16.517
250	741	26	2223	750	1647275	4941729	555950	0.0063	1.000	1.000	19.50	19.50	12.649
275	745	30	2237	825	1668107	5004169	615425	0.0049	1.000	1.000	18.00	18.00	14.236
300	751	36	2251	900	1689051	5067001	675550	0.0049	1.000	1.000	16.50	16.50	14.236
325	755	40	2269	975	1716195	5148361	737725	0.0040	1.000	1.000	14.85	14.85	15.776
350	763	48	2300	1050	1763718	5290000	805675	0.0018	1.000	1.000	13.20	13.20	23.872
375	782	67	2367	1117	1869377	5602689	882524	0.0007	1.000	1.000	11.50	11.50	38.703
392	822	107							1.000	1.000	10.34	10.34	
LIFT Rimu test 2	Ignition Time	717							m/s		kW/m ²		(m/s) ^{-0.5}
50													
75													
100													
125													
150													
175													

200	729	12							1.000	21.90	21.90	
225	731	14	2193	675	1603091	4809249	493525	0.0125	1.000	20.70	20.70	8.944
250	733	16	2201	750	1614819	4844401	550400	0.0080	1.000	19.50	19.50	11.155
275	737	20	2213	825	1632507	4897369	608825	0.0049	1.000	18.00	18.00	14.236
300	743	26	2227	900	1653227	4959529	668350	0.0049	1.000	16.50	16.50	14.236
325	747	30	2244	975	1678574	5035536	729575	0.0044	1.000	14.85	14.85	15.015
350	754	37	2269	1050	1716349	5148361	794675	0.0023	1.000	13.20	13.20	20.870
375	768	51	2308	1125	1776136	5326864	866300	0.0016	1.000	11.50	11.50	25.364
400	786	69	2370	1200	1873476	5616900	949200	0.0010	1.000	9.80	9.80	31.305
425	816	99	2458	1275	2016388	6041764	1046400	0.0007	1.000	8.35	8.35	37.544
450	856	139	2576	1350	2215808	6635776	1161400	0.0006	1.000	6.90	6.90	42.010
475	904	187	2752	1425	2534016	7573504	1310600	0.0004	1.000	5.95	5.95	52.900
500	992	275							1.000	5.00	5.00	

<i>Flame Front Position x</i>	<i>Time to position x t (s)</i>	<i>time from ignition</i>	Σt	Σx	$\Sigma(t^2)$	$\Sigma(t)^2$	$\Sigma(t.x)$	V_f	$F(t)$	\dot{q}_{e}	$\dot{q}_{e}.F(t)$	$1/V_f$
Ignition												
LIFT Rimu test 3	Time	736						m/s		kW/m ²		(m/s) ^{-0.5}
50												
75												
100												
125												
150												
175												
200												
225												
250												
275												
300	750	14							1.000	16.50	16.50	
325	761	25	2282	975	1736062	5207524	742175	0.0024	1.000	14.85	14.85	20.502
350	771	35	2325	1050	1802411	5405625	814550	0.0015	1.000	13.20	13.20	25.884
375	793	57	2387	1125	1900619	5697769	896425	0.0010	1.000	11.50	11.50	32.376

<i>Flame Front Position x</i>	<i>Time to position x t (s)</i>	<i>time from ignition</i>	Σt	Σx	$\Sigma(t^2)$	$\Sigma(t)^2$	$\Sigma(t.x)$	V_f	$F(t)$	\dot{q}_e	$\dot{q}_e . F(t)$	$1/\Delta V_f$
RIFT – Rimu – Low preheat – ISO ign data – Test 1	Ignition Time	80						m/s		kW/m ²		(m/s) ^{-0.5}
400	823	87	2492	1200	2073554	6210064	998875	0.0006	1.000	9.80	9.80	41.261
425	876	140	2639	1265	2328305	6964321	1115100	0.0003	1.000	8.35	8.35	54.376
440	940	204							1.000	7.48	7.48	
10	60	0								33.88		
20	61	1	184	60	11290	33856	3710	0.0064	0.392	32.87	12.89	12.472
30	63	3	189	90	11915	35721	5710	0.0050	0.399	32.16	12.82	14.142
40	65	5	197	120	12955	38809	7940	0.0032	0.405	29.67	12.01	17.638
50	69	9	208	150	14462	43264	10490	0.0022	0.417	27.17	11.33	21.257
60	74	14	227	180	17293	51529	13770	0.0013	0.432	24.95	10.78	27.889
70	84	24	249	210	20813	62001	17600	0.0012	0.460	22.99	10.58	29.306
80	91	31	276	240	25538	76176	22250	0.0012	0.479	21.03	10.07	29.306
90	101	41	302	270	30582	91204	27370	0.0011	0.505	18.88	9.53	30.836
100	110	50	330	300	36462	108900	33180	0.0011	0.527	16.73	8.81	30.000
110	119	59	358	330	42902	128164	39570	0.0011	0.548	15.06	8.25	30.836
120	129	69	393	360	51827	154449	47420	0.0008	0.570	13.89	7.92	36.374
130	145	85	434	390	63266	188356	56730	0.0006	0.605	12.71	7.68	39.377
140	160	100	492	415	81594	242064	68365	0.0003	0.635	11.59	7.36	54.502
145	187	127							0.687	11.59	7.96	

<i>Flame Front Position x</i>	<i>Time to position x t (s)</i>	<i>time from ignition</i>	Σt	Σx	$\Sigma(t^2)$	$\Sigma(t)^2$	$\Sigma(t.x)$	V_f	$F(t)$	\dot{q}_{e}	$\dot{q}_{e}.F(t)$	$1/\sqrt{V_f}$
RIFT – Rimu – Low preheat – ISO ign data – Test 2			Ignition Time	80				m/s		kW/m ²		(m/s) ^{-0.5}
10	63	0								33.88		
20	64	1	193	60	12421	37249	3890	0.0064	0.402	32.87	13.20	12.472
30	66	3	199	90	13213	39601	6020	0.0039	0.408	32.16	13.12	15.916
40	69	6	207	120	14301	42849	8340	0.0033	0.417	29.67	12.37	17.321
50	72	9	218	150	15874	47524	10980	0.0024	0.426	27.17	11.58	20.207
60	77	14	232	180	18002	53824	14030	0.0018	0.441	24.95	10.99	23.484
70	83	20	253	210	21467	64009	17870	0.0012	0.457	22.99	10.52	28.577
80	93	30	281	240	26563	78961	22700	0.0009	0.484	21.03	10.18	33.212
90	105	42	316	270	33598	99856	28690	0.0008	0.514	18.88	9.71	35.365
100	118	55	356	300	42638	126736	35880	0.0007	0.545	16.73	9.12	37.448
110	133	70	402	330	54414	161604	44550	0.0006	0.579	15.06	8.72	40.676
120	151	88	449	360	67715	201601	54200	0.0006	0.617	13.89	8.57	40.104
130	165	102	505	389	85747	255025	65841	0.0005	0.645	12.71	8.20	45.339
139	189	126							0.690	12.71	8.77	
RIFT – Rimu – Low preheat – ISO ign data – Test 3			Ignition Time	69				m/s		kW/m ²		(m/s) ^{-0.5}
10	63	0								33.88		
20	64	1	192	60	12290	36864	3860	0.0100	0.402	32.87	13.20	10.000
30	65	2	199	90	13221	39601	6030	0.0029	0.405	32.16	13.02	18.559
40	70	7	212	120	15054	44944	8600	0.0017	0.420	29.67	12.46	24.608
50	77	14	230	150	17718	52900	11630	0.0015	0.441	27.17	11.97	25.520
60	83	20	246	180	20214	60516	14850	0.0021	0.457	24.95	11.41	21.602
70	86	23	259	210	22385	67081	18200	0.0028	0.466	22.99	10.71	18.772

80	90	27	277	240	25697	76729	22310	0.0012	0.476	21.03	10.02	28.363
90	101	38	312	270	32942	97344	28390	0.0006	0.505	18.88	9.53	39.919
100	121	58	360	300	43886	129600	36370	0.0005	0.552	16.73	9.24	43.059
110	138	75	411	330	56789	168921	45520	0.0006	0.590	15.06	8.88	39.431
120	152	89	465	355	72773	216225	55295	0.0004	0.619	13.89	8.59	50.845
125	175	112							0.664	13.89	9.22	

<i>Flame Front Position x</i>	<i>Time to position x t (s)</i>	<i>time from ignition</i>	Σt	Σx	$\Sigma(t^2)$	$\Sigma(t)^2$	$\Sigma(t.x)$	V_f	$F(t)$	q_e	$q_e.F(t)$	$1/V_f$
RIFT – Rimu – Low preheat – ISO ign data – Test 4	Ignition Time	66						m/s		kW/m ²		(m/s) ^{-0.5}
10	60	0								33.88		
20	61	1	183	60	11165	33489	3680	0.0100	0.392	32.87	12.89	10.000
30	62	2	187	90	11661	34969	5640	0.0064	0.395	32.16	12.71	12.472
40	64	4	191	120	12165	36481	7670	0.0064	0.402	29.67	11.92	12.472
50	65	5	195	150	12677	38025	9770	0.0100	0.405	27.17	11.00	10.000
60	66	6	201	180	13481	40401	12110	0.0036	0.408	24.95	10.18	16.733
70	70	10	210	210	14732	44100	14780	0.0025	0.420	22.99	9.66	20.000
80	74	14	224	240	16776	50176	18020	0.0020	0.432	21.03	9.08	22.509
90	80	20	242	270	19620	58564	21920	0.0014	0.449	18.88	8.48	26.547
100	88	28	265	300	23553	70225	26670	0.0012	0.471	16.73	7.88	29.172
110	97	37	291	330	28389	84681	32190	0.0011	0.494	15.06	7.45	30.000
120	106	46	320	360	34334	102400	38600	0.0010	0.517	13.89	7.18	31.675
130	117	57	354	390	42086	125316	46270	0.0008	0.543	12.71	6.90	35.440
140	131	71	391	420	51299	152881	55000	0.0008	0.575	11.59	6.66	36.091
150	143	83	431	450	62259	185761	64910	0.0008	0.600	10.48	6.29	36.091
160	157	97	468	480	73322	219024	75130	0.0008	0.629	9.39	5.91	35.440
170	168	108	522	505	91682	272484	88155	0.0003	0.651	8.33	5.42	54.740
175	197	137							0.705	7.80	5.50	

<i>Flame Front Position x</i>	<i>Time to position x t (s)</i>	<i>time from ignition</i>	Σt	Σx	$\Sigma(t^2)$	$\Sigma(t)^2$	$\Sigma(t.x)$	V_f	$F(t)$	\dot{q}_{e}	$\dot{q}_{e}.F(t)$	$1/\sqrt{V_f}$
RIFT – Rimu – Low preheat – ISO ign data – Test 5	Ignition Time	67						m/s		kW/m ²		(m/s) ^{-0.5}
10	50	0								33.88		
20	51	1	153	60	7805	23409	3080	0.0100	0.359	32.87	11.79	10.000
30	52	2	156	90	8114	24336	4700	0.0100	0.362	32.16	11.64	10.000
40	53	3	160	120	8538	25600	6430	0.0064	0.366	29.67	10.84	12.472
50	55	5	173	150	10059	29929	8770	0.0015	0.372	27.17	10.12	26.247
60	65	15	194	180	12726	37636	11830	0.0011	0.405	24.95	10.10	30.836
70	74	24	224	210	16926	50176	15880	0.0010	0.432	22.99	9.93	31.675
80	85	35	251	240	21165	63001	20260	0.0011	0.463	21.03	9.74	30.246
90	92	42	283	270	26925	80089	25680	0.0009	0.482	18.88	9.09	32.998
100	106	56	331	300	37389	109561	33510	0.0005	0.517	16.73	8.65	46.029
110	133	83	398	330	54206	158404	44310	0.0004	0.579	15.06	8.72	51.481
120	159	109	478	362	77566	228484	58262	0.0004	0.633	13.89	8.79	49.071
132	186	136							0.685	12.71		

There was insufficient flame spread for a full –preheat result for Rimu in the RIFT

		NZ Beech										
Flame Front Position x	Time to position x t (s)	time from ignition	Σt	Σx	$\Sigma(t^2)$	$\Sigma(t)^2$	$\Sigma(t.x)$	V_f	$F(t)$	\dot{q}_e	$\dot{q}_e.F(t)$	$1/\sqrt{V_f}$
LIFT – Beech – Test 1		Ignition Time						m/s	kW/m ²		(m/s) ^{-0.5}	
50		415										
75												
100												
125												
150												
175												
200												
225	427	12							1.000	17.29	17.29	
250	429	14	1296	750	559970	1679616	324325	0.0033	1.000	15.55	15.55	17.365
275	440	25	1319	825	580141	1739761	363250	0.0024	1.000	13.37	13.37	20.502
300	450	35	1359	900	616061	1846881	408425	0.0017	1.000	11.19	11.19	24.467
325	469	54	1415	975	668477	2002225	461025	0.0011	1.000	9.75	9.75	30.484
350	496	81	1493	1050	744761	2229049	524025	0.0008	1.000	8.32	8.32	34.392
375	528	113	1615	1125	874081	2608225	608000	0.0005	1.000	7.28	7.28	44.356
400	591	176	1786	1200	1072954	3189796	717875	0.0004	1.000	6.25	6.25	52.803
425	667	252	1976	1275	1309694	3904576	842975	0.0004	1.000	5.27	5.27	50.723
450	718	303	2206	1350	1634454	4866436	996550	0.0003	1.000	4.29	4.29	56.543
475	821	406	2457	1414	2032289	6036849	1161977	0.0002	1.000	3.72	3.72	71.521
489	918	503							1.000	3.72		

<i>Flame Front Position x</i>	<i>Time to position x t (s)</i>	<i>time from ignition</i>	Σt	Σx	$\Sigma(t^2)$	$\Sigma(t)^2$	$\Sigma(t.x)$	V_f	$F(t)$	\dot{q}_{e}''	$\dot{q}_{e}'' \cdot F(t)$	$1/\sqrt{V_f}$
LIFT – Beech – Test 2		Ignition Time	397					m/s		kW/m ²		(m/s) ^{-0.5}
50												
75												
100	416	1	834	300	347780	695556	93850	0.00009	1.000	23.82	23.82	
125	418	21	1254	375	524180	1572516	156850	0.01250	1.000	22.99	22.99	8.944
150	420	23	1260	450	529208	1587600	189100	0.01250	1.000	22.16	22.16	8.944
175	422	25	1267	525	535109	1605289	221850	0.00987	1.000	20.60	20.60	10.066
200	425	28	1274	600	541038	1623076	254925	0.00987	1.000	19.04	19.04	10.066
225	427	30	1282	675	547854	1643524	288575	0.00987	1.000	17.29	17.29	10.066
250	430	33	1302	750	565254	1695204	325950	0.00242	1.000	15.55	15.55	20.331
275	445	48	1332	825	591774	1774224	366975	0.00184	1.000	13.37	13.37	23.286
300	457	60	1373	900	628715	1885129	412550	0.00192	1.000	11.19	11.19	22.826
325	471	74	1422	975	674726	2022084	463075	0.00133	1.000	9.75	9.75	27.470
350	494	97	1487	1050	738361	2211169	521725	0.00098	1.000	8.32	8.32	31.989
375	522	125	1579	1125	833489	2493241	593850	0.00072	1.000	7.28	7.28	37.367
400	563	166	1706	1200	975094	2910436	684875	0.00050	1.000	6.25	6.25	44.715
425	621	224	1870	1262	1173206	3496900	788907	0.00030	1.000	5.27	5.27	57.881
437	686	289							1.000	5.27		
LIFT test 3		Ignition Time	397					m/s		kW/m ²		(m/s) ^{-0.5}
50												
75												
100												
125												

150	412	15							1.000	22.16		
175	413	16	1242	525	514202	1542564	217475	0.0089	1.000	20.60	20.60	10.583
200	417	20	1250	600	520858	1562500	250175	0.0071	1.000	19.04	19.04	11.872
225	420	23	1270	675	537778	1612900	286150	0.0028	1.000	17.29	17.29	19.018
250	433	36	1294	750	558370	1674436	324025	0.0023	1.000	15.55	15.55	20.687
275	441	44	1333	825	592651	1776889	367225	0.0018	1.000	13.37	13.37	23.359
300	459	62	1382	900	637486	1909924	415625	0.0012	1.000	11.19	11.19	28.707
325	482	85	1448	975	700054	2096704	471800	0.0010	1.000	9.75	9.75	30.993
350	507	110	1524	1050	775598	2322576	534725	0.0009	1.000	8.32	8.32	32.575
375	535	138	1612	1125	868174	2598544	606075	0.0008	1.000	7.28	7.28	35.569
400	570	173	1725	1200	995525	2975625	692125	0.0006	1.000	6.25	6.25	41.445
425	620	223	1893	1275	1203509	3583449	807850	0.0004	1.000	5.27	5.27	52.102
450	703	306							1.000	4.29		
<i>Flame Front Position x</i>	<i>Time to position x t (s)</i>	<i>time from ignition</i>	Σt	Σx	$\Sigma(t^2)$	$\Sigma(x^2)$	$\Sigma(t.x)$	V_f	$F(t)$	\dot{q}_{e}	$\dot{q}_{e}.F(t)$	$1/\sqrt{V_f}$
RIFT – Beech	Ignition Time											
–												
Low preheat - test 1		55						m/s		kW/m ²		(m/s) ^{-0.5}
10	55	0								33.88		
20	56	1	169	60	9525	28561	3410	0.0064	0.397	32.87	13.05	12.472
30	58	3	174	90	10100	30276	5260	0.0050	0.404	32.16	13.00	14.142
40	60	5	182	120	11060	33124	7340	0.0032	0.411	29.67	12.19	17.638
50	64	9	193	150	12457	37249	9740	0.0022	0.424	27.17	11.54	21.257
60	69	14	209	180	14633	43681	12660	0.0017	0.441	24.95	11.00	24.608
70	76	21	230	210	17762	52900	16260	0.0012	0.463	22.99	10.64	28.358
80	85	30	255	240	21837	65025	20580	0.0011	0.489	21.03	10.29	30.000
90	94	39	283	270	26877	80089	25660	0.0011	0.514	18.88	9.71	30.836
100	104	49	311	300	32421	96721	31290	0.0011	0.541	16.73	9.05	30.836
110	113	58	344	330	39714	118336	38070	0.0009	0.564	15.06	8.50	34.178

120	127	72	387	360	50507	149769	46780	0.0006	0.598	13.89	8.30	41.445
130	147	92	445	390	66979	198025	58290	0.0005	0.643	12.71	8.18	46.969
140	171	116	508	420	86950	258064	71550	0.0005	0.694	11.59	8.04	46.472
150	190	135								10.48		

<i>Flame Front Position x</i>	<i>Time to position x t (s)</i>	<i>time from ignition</i>	Σt	Σx	$\Sigma(t^2)$	$\Sigma(t)^2$	$\Sigma(t.x)$	V_f	$F(t)$	\dot{q}_{e}''	$\dot{q}_{e}'' \cdot F(t)$	$1/\sqrt{V_f}$
RIFT – Beech												
–	Ignition											
Low preheat - test 2	Time							m/s		kW/m²		(m/s)^{-0.5}
	55	0										
10	55	0							0.394	33.88		
20	57	2	172	60	9874	29584	3490	0.0039	0.401	32.87	13.17	15.916
30	60	5	180	90	10818	32400	5460	0.0033	0.411	32.16	13.22	17.321
40	63	8	192	120	12330	36864	7770	0.0021	0.421	29.67	12.49	21.602
50	69	14	211	150	14971	44521	10710	0.0012	0.441	27.17	11.98	28.577
60	79	24	238	180	19102	56644	14490	0.0010	0.472	24.95	11.77	32.416
70	90	35	274	210	25366	75076	19440	0.0008	0.503	22.99	11.57	36.197
80	105	50	315	240	33525	99225	25500	0.0007	0.544	21.03	11.44	38.730
90	120	65	360	270	43650	129600	32700	0.0007	0.581	18.88	10.97	38.730
100	135	80	410	300	56650	168100	41350	0.0006	0.617	16.73	10.31	41.975
110	155	100	468	330	73934	219024	51910	0.0005	0.661	15.06	9.95	46.406
120	178	123	536	360	96918	287296	64800	0.0004	0.708	13.89	9.83	49.004
130	203	148	601	385	121293	361201	77450	0.0004	0.756	12.71	9.61	52.679
135	220	165							0.787	12.71		

Flame Front Position x	Time to position x t (s)	time from ignition	Σt	Σx	$\Sigma(t^2)$	$\Sigma(t)^2$	$\Sigma(t.x)$	V_f	$F(t)$	\dot{q}_{e}''	$\dot{q}_{e}'' \cdot F(t)$	$1/\sqrt{V_f}$
RIFT – Beech												
–												
Low preheat - test 3		60						m/s		kW/m ²		(m/s) ^{-0.5}
10	60	0							0.411	33.88		
20	61	1	184	60	11290	33856	3710	0.0064	0.414	32.87	13.62	12.472
30	63	3	188	90	11786	35344	5670	0.0064	0.421	32.16	13.54	12.472
40	64	4	194	120	12554	37636	7800	0.0046	0.424	29.67	12.59	14.720
50	67	7	202	150	13626	40804	10170	0.0028	0.434	27.17	11.80	18.772
60	71	11	214	180	15306	45796	12930	0.0022	0.447	24.95	11.15	21.257
70	76	16	233	210	18213	54289	16460	0.0013	0.463	22.99	10.64	27.889
80	86	26	257	240	22197	66049	20750	0.0011	0.492	21.03	10.35	30.836
90	95	35	282	270	26622	79524	25530	0.0013	0.517	18.88	9.76	27.568
100	101	41	306	300	31326	93636	30750	0.0013	0.533	16.73	8.92	27.568
110	110	50	334	330	37430	111556	36960	0.0009	0.557	15.06	8.38	33.348
120	123	63	378	360	48254	142884	45710	0.0006	0.588	13.89	8.17	42.292
130	145	85	426	390	61118	181476	55730	0.0006	0.639	12.71	8.12	42.292
140	158	98	480	420	77318	230400	67520	0.0006	0.667	11.59	7.73	40.234
150	177	117	529	450	93929	279841	79710	0.0006	0.706	10.48	7.40	42.448
160	194	134	588	480	116054	345744	94480	0.0005	0.739	9.39	6.94	44.889
170	217	157	642	510	138086	412164	109510	0.0005	0.782	8.33	6.51	43.434
180	231	171							0.806	7.27		
RIFT – Beech												
–												
Low preheat - test 4		60						m/s		kW/m ²		(m/s) ^{-0.5}
10	60	0							0.411	33.88		

20	61	1	183	60	11165	33489	3680	0.0100	0.414	32.87	13.62	10.000
30	62	2	188	90	11790	35344	5680	0.0046	0.418	32.16	13.44	14.720
40	65	5	194	120	12558	37636	7810	0.0039	0.428	29.67	12.69	15.916
50	67	7	205	150	14043	42025	10330	0.0023	0.434	27.17	11.80	20.817
60	73	13	218	180	15902	47524	13190	0.0018	0.453	24.95	11.31	23.484
70	78	18	237	210	18809	56169	16720	0.0015	0.469	22.99	10.77	25.720
80	86	26	258	240	22316	66564	20800	0.0013	0.492	21.03	10.35	28.284
90	94	34	283	270	26841	80089	25640	0.0012	0.514	18.88	9.71	29.172
100	103	43	312	300	32670	97344	31410	0.0009	0.539	16.73	9.01	32.514
110	115	55	349	330	40995	121801	38670	0.0007	0.569	15.06	8.57	37.544
120	131	71	389	360	50835	151321	46960	0.0007	0.607	13.89	8.43	37.544
130	143	83	431	390	62259	185761	56290	0.0008	0.635	12.71	8.06	36.091
140	157	97	476	420	76074	226576	66970	0.0006	0.665	11.59	7.71	40.775
150	176	116	541	450	98889	292681	81660	0.0004	0.704	10.48	7.37	51.041
160	208	148	611	480	125769	373321	98270	0.0004	0.765	9.39	7.19	51.041
170	227	167	697	503	163437	485809	117196	0.0002	0.799	8.33	6.66	67.198
173	262	202							0.859	8.33		

Flame Front Position x	Time to position x t (s)	time from ignition	Σt	Σx	$\Sigma(t^2)$	$\Sigma(t)^2$	$\Sigma(t.x)$	V_f	$F(t)$	\dot{q}_e	$\dot{q}_e.F(t)$	$1/\sqrt{V_f}$
RIFT – Beech												
–												
Low preheat - test 5												
10	60	0							0.411	33.88		
20	61	1	183	60	11165	33489	3680	0.0100	0.414	32.87	13.62	10.000
30	62	2	186	90	11534	34596	5600	0.0100	0.418	32.16	13.44	10.000
40	63	3	191	120	12169	36481	7680	0.0046	0.421	29.67	12.49	14.720
50	66	6	200	150	13366	40000	10080	0.0024	0.431	27.17	11.71	20.207
60	71	11	210	180	14726	44100	12670	0.0027	0.447	24.95	11.15	19.272
70	73	13	222	210	16454	49284	15610	0.0027	0.453	22.99	10.42	19.272

80	78	18	237	240	18809	56169	19090	0.0015	0.469	21.03	9.86	25.720
90	86	26	261	270	22889	68121	23680	0.0010	0.492	18.88	9.29	30.950
100	97	37	296	300	29574	87616	29870	0.0007	0.523	16.73	8.74	36.952
110	113	53	334	330	37554	111556	37010	0.0007	0.564	15.06	8.50	36.952
120	124	64	380	360	48594	144400	45900	0.0007	0.591	13.89	8.20	39.186
130	143	83	422	390	59850	178084	55170	0.0006	0.635	12.71	8.06	39.703
140	155	95	467	420	73035	218089	65640	0.0008	0.661	11.59	7.66	36.091
150	169	109	510	450	87182	260100	76810	0.0006	0.690	10.48	7.23	39.431
160	186	126	560	480	105182	313600	89960	0.0006	0.724	9.39	6.79	42.448
170	205	145							0.760	8.33		

<i>Flame Front Position x</i>	<i>Time to position x t (s)</i>	<i>time from ignition</i>	Σt	Σx	$\Sigma(t^2)$	$\Sigma(t)^2$	$\Sigma(t.x)$	V_f	$F(t)$	\dot{q}_{e}''	$\dot{q}_{e}'' \cdot F(t)$	$1/\sqrt{V_f}$
RIFT – Beech	Ignition Time	60s						m/s		kW/m²		(m/s)^{-0.5}
– Low preheat - test 6												
10	60	0							0.411	33.88		
20	61	1	183	60	11165	33489	3680	0.0100	0.414	32.87	13.62	10.000
30	62	2	188	90	11790	35344	5680	0.0046	0.418	32.16	13.44	14.720
40	65	5	195	120	12693	38025	7860	0.0033	0.428	29.67	12.69	17.321
50	68	8	204	150	13890	41616	10260	0.0033	0.438	27.17	11.89	17.321
60	71	11	215	180	15441	46225	12980	0.0024	0.447	24.95	11.15	20.207
70	76	16	229	210	17541	52441	16140	0.0018	0.463	22.99	10.64	23.484
80	82	22	246	240	20244	60516	19800	0.0017	0.480	21.03	10.11	24.495
90	88	28	265	270	23493	70225	23980	0.0015	0.498	18.88	9.40	25.520
100	95	35	286	300	27378	81796	28750	0.0013	0.517	16.73	8.65	27.406
110	103	43	312	330	32630	97344	34510	0.0010	0.539	15.06	8.11	30.950
120	114	54	338	360	38246	114244	40740	0.0011	0.567	13.89	7.87	30.246
130	121	61	379	390	48373	143641	49570	0.0006	0.584	12.71	7.42	40.524
140	144	84	432	420	63266	186624	60940	0.0004	0.637	11.59	7.38	47.958
150	167	107							0.686	10.48		

<i>Flame Front Position x</i>	<i>Time to position x t (s)</i>	<i>time from ignition</i>	Σt	Σx	$\Sigma(t^2)$	$\Sigma(t)^2$	$\Sigma(t.x)$	V_f	$F(t)$	\dot{q}_e	$\dot{q}_e.F(t)$	$1/V_f$
RIFT – Beech – full preheat - test 1	Ignition Time	841						m/s		kW/m ²		(m/s) ^{-0.5}
10										33.88		
20										32.87	0.00	
30										32.16	0.00	
40										29.67	0.00	
50										27.17	0.00	
60										24.95	0.00	
70										22.99	0.00	
80	842	0							0.999	21.03	21.01	
90	847	5	2542	270	2153982	6461764	228890	0.0018	1.000	18.88	18.88	23.484
100	853	11	2556	300	2177754	6533136	255690	0.0021	1.000	16.73	16.73	21.602
110	856	14	2569	330	2199945	6599761	282660	0.0028	1.000	15.06	15.06	18.772
120	860	18	2579	360	2217105	6651241	309550	0.0028	1.000	13.89	13.89	18.772
130	863	21	2588	390	2232594	6697744	336490	0.0039	1.000	12.71	12.71	15.916
140	865	23	2596	420	2246418	6739216	363490	0.0039	1.000	11.59	11.59	15.916
150	868	26	2605	450	2262033	6786025	390820	0.0028	1.000	10.48	10.48	18.772
160	872	30	2617	480	2282937	6848689	418810	0.0022	1.000	9.39	9.39	21.257
170	877	35	2632	510	2309202	6927424	447550	0.0018	1.000	8.33	8.33	23.484
180	883	41	2662	540	2362422	7086244	479410	0.0007	1.000	7.27	7.27	36.914
190	902	60	2706	570	2441534	7322436	514520	0.0005	1.000	6.55	6.55	43.589
200	921	79	2759	600	2537941	7612081	552140	0.0006	1.000	5.83	5.83	41.326
210	936	94	2809	630	2630641	7890481	590200	0.0006	1.000	5.17	5.17	39.377
220	952	110	2859	660	2725241	8173881	629330	0.0006	1.000	4.58	4.58	41.884
230	971	129	2906	690	2815434	8444836	668690	0.0006	1.000	3.99	3.99	39.703
240	983	141	2954	720	2909130	8726116	709250	0.0007	1.000	3.77	3.77	38.267
250	1000	158							1.000	3.54	3.54	

Flame Front Position x	Time to position x t (s)	time from ignition	Σt	Σx	$\Sigma(t^2)$	$\Sigma(t)^2$	$\Sigma(t.x)$	V_f	$F(t)$	\dot{q}_{e}	$\dot{q}_{e}.F(t)$	$1/\sqrt{V_f}$
RIFT – Beech – full preheat - test 2	Ignition Time	841						m/s		kW/m ²		(m/s) ^{-0.5}
10												
20												
30												
40												
50												
60												
70												
80	847	0							1.000	21.03	21.03	
90	848	1	2545	270	2159013	6477025	229080	0.0064	1.000	18.88	18.88	12.472
100	850	3	2550	300	2167508	6502500	255040	0.0050	1.000	16.73	16.73	14.142
110	852	5	2555	330	2176013	6528025	281080	0.0064	1.000	15.06	15.06	12.472
120	853	6	2564	360	2191394	6574096	307750	0.0024	1.000	13.89	13.89	20.237
130	859	12	2575	390	2210259	6630625	334850	0.0020	1.000	12.71	12.71	22.509
140	863	16	2589	420	2234339	6702921	362540	0.0025	1.000	11.59	11.59	20.000
150	867	20	2604	450	2260334	6780816	390710	0.0018	1.000	10.48	10.48	23.741
160	874	27	2622	480	2291726	6874884	419660	0.0014	1.000	9.39	9.39	26.458
170	881	34	2647	510	2335701	7006609	450170	0.0011	1.000	8.33	8.33	30.246
180	892	45	2677	540	2389041	7166329	482090	0.0009	1.000	7.27	7.27	33.922
190	904	57	2709	570	2446449	7338681	514920	0.0009	1.000	6.55	6.55	32.514
200	913	66	2741	600	2504561	7513081	548400	0.0010	1.000	5.83	5.83	31.675
210	924	77	2770	630	2557834	7672900	581900	0.0010	1.000	5.17	5.17	31.675
220	933	86	2804	660	2621074	7862416	617110	0.0009	1.000	4.58	4.58	34.178
230	947	100	2847	690	2702387	8105409	655150	0.0006	1.000	3.99	3.99	41.445
240	967	120	2895	720	2794259	8381025	695140	0.0006	1.000	3.77	3.77	41.445
250	981	134	2944	750	2889466	8667136	736290	0.0007	1.000	3.54	3.54	38.086
260	996	149	2992	780	2984602	8952064	778260	0.0006	1.000	3.29	3.29	41.326
270	1015	168	3045	810	3091397	9272025	822530	0.0005	1.000	3.29	3.29	43.589

<i>Flame Front Position x</i>	<i>Time to position x t (s)</i>	<i>time from ignition</i>	Σt	Σx	$\Sigma(t^2)$	$\Sigma(t)^2$	$\Sigma(t.x)$	V_f	$F(t)$	\dot{q}_e	$\dot{q}_e.F(t)$	$1/\sqrt{V_f}$
RIFT – Beech – full preheat - test 3	Ignition Time	848						m/s		kW/m ²		(m/s) ^{-0.5}
10	0	0										
20	0	0										
30	0	0										
40	0	0										
50	0	0										
60	0	0										
70	0	0										
80	0	0										
90	0	0										
100	0	0										
110	848	0	1704	330	1450984	2901912	195940	0.0000	1.000	15.06	15.06	237.777
120	855.5	7.5	2567	360	2195753	6586922	308130	0.0013	1.000	13.89	13.89	27.386
130	863	15	2584	390	2224874	6674472	335950	0.0019	1.000	12.71	12.71	22.980
140	865	17	2606	420	2263878	6791236	364990	0.0011	1.000	11.59	11.59	29.740
150	878	30	2631	450	2307653	6922161	394880	0.0009	1.000	10.48	10.48	34.008
160	888	40	2666	480	2369428	7107556	426780	0.0009	1.000	9.39	9.39	33.212
170	900	52	2704	510	2437600	7311616	459960	0.0007	1.000	8.33	8.33	37.544
180	916	68	2754	540	2528900	7584516	496100	0.0005	1.000	7.27	7.27	43.770
190	938	90	2808	570	2629016	7884864	533900	0.0005	1.000	6.55	6.55	43.770
200	954	106	2872	600	2750360	8248384	574820	0.0005	1.000	5.83	5.83	46.257
210	980	132	2943	630	2888597	8661249	618580	0.0004	1.000	5.17	5.17	52.466
220	1009	161	3021	660	3043505	9126441	665140	0.0004	1.000	4.58	4.58	51.103

230	1032	184	3083	690	3168869	9504889	709420	0.0006	1.000	3.99	3.99	41.658
240	1042	194	3137	720	3280757	9840769	753190	0.0006	1.000	3.77	3.77	40.188
250	1063	215	3196	750	3406014	10214416	799490	0.0004	1.000	3.54	3.54	49.666
260	1091	243	3288	775	3606206	10810944	849920	0.0002	1.000	3.29	3.29	70.137
265	1134	286							1.000	3.29	3.29	
<i>Flame Front Position x</i>	<i>Time to position x t (s)</i>	<i>time from ignition</i>	Σt	Σx	$\Sigma(t^2)$	$\Sigma(t)^2$	$\Sigma(t.x)$	V_f	$F(t)$	\dot{q}_{e}	$\dot{q}_{e}.F(t)$	$1/\sqrt{V_f}$
RIFT – Beech – full preheat - test 4	Ignition Time	841						m/s		kW/m ²		(m/s) ^{-0.5}
10										33.88		
20												
30												
40												
50												
60												
70												
80												
90												
100	847	0	1696	300	1438210	2876416	178090	0.0000	1.000	16.73	16.73	237.628
110	849	2	2547	330	2162411	6487209	280210	0.0050	1.000	15.06	15.06	14.142
120	851	4	2553	360	2172611	6517809	306400	0.0050	1.000	13.89	13.89	14.142
130	853	6	2565	390	2193131	6579225	333550	0.0018	1.000	12.71	12.71	23.664
140	861	14	2587	420	2231059	6692569	362380	0.0010	1.000	11.59	11.59	31.833
150	873	26	2615	450	2279611	6838225	392450	0.0010	1.000	10.48	10.48	31.833
160	881	34	2649	480	2339315	7017201	424060	0.0009	1.000	9.39	9.39	33.575
170	895	48	2685	510	2403467	7209225	456730	0.0007	1.000	8.33	8.33	37.417
180	909	62	2731	540	2486635	7458361	491900	0.0006	1.000	7.27	7.27	40.104
190	927	80	2783	570	2582419	7745089	529150	0.0005	1.000	6.55	6.55	43.609
200	947	100	2849	600	2706763	8116801	570280	0.0004	1.000	5.83	5.83	49.216
210	975	128	2918	630	2839450	8514724	613270	0.0004	1.000	5.17	5.17	49.666

220	996	149	2997	660	2995317	8982009	659850	0.0004	1.000	4.58	4.58	50.759
230	1026	179	3073	690	3149293	9443329	707340	0.0004	1.000	3.99	3.99	52.513
240	1051	204	3152	720	3312902	9935104	756970	0.0004	1.000	3.77	3.77	49.501
250	1075	228	3225	750	3468027	10400625	806730	0.0004	1.000	3.54	3.54	48.990
260	1099	252							1.000	3.29	3.29	

Appendix 5

Comparison with published results in the literature

Plywood	Source	Test	Thickness (mm)	$q_{ig,min}$ (kW/m ²)	q_{crit} (kW/m ²)	b (s ^{-0.5})	t^* (s)	T_{ig} (°C)	h (kW/m ² K)	kpc ((kW/m ² k ²) ²)	
Radiata Pine	ISO	ISO 5657	17	13.75	4.6	0.048	432	352	0.041	0.93	
Radiata Pine	LIFT	LIFT	17	16.25	7.2	0.058	293	391	0.044	0.71	
Radiata Pine	RIFT	RIFT	17	16.25	9.9	0.061	273	391	0.043	0.66	
Radiata Pine	Ngu, CK. 2002	ISO 5657	20	12.00	7.2	0.034	870	321	0.040	1.76	
Birch 9-ply	Azhakesan et al 1998	Cone		10.7		0.0387	655	386		0.526	
Birch faced	Jianmin, 1990	Cone	9	14		0.051	383	389		0.8106	
"Ordinary" plywood	Nisted, 1991	LIFT	12	16.3		0.0369	733	392		1.7871	
Japanese plywood - 8.1% MC	Fangrat et al, 1996	Cone	18		11.5			328	0.038	0.762	Janssens correlation
Japanese plywood - 7.7%MC	Fangrat et al, 1996	Cone	12		7.8			264	0.033	1.157	Janssens correlation
Japanese plywood - 8.2%MC	Fangrat et al, 1996	Cone	9		8.5			277	0.039	1.057	Janssens correlation
Japanese plywood - 8.2%MC	Fangrat et al, 1996	Cone	5.5		9.6			298	0.036	0.877	Janssens correlation
US plywood	Fangrat et al, 1996	Cone	11.2		14.5			372	0.028	0.334	Janssens correlation
Douglas fir (NIST)	Fowell 1993	LIFT	unspecified	14.7		0.0343	851	372		1.89	Round robin test – all Fowell's results used the same material but tested at different labs.
Douglas fir (UL)	Fowell 1993	LIFT	unspecified	17.5		0.0383	681	408		1.77	
Douglas fir (Safety eng lab)	Fowell 1993	LIFT	unspecified	17.0		0.032	974	402		2.51	

Douglas fir (NRCC)	Fowell 1993	LIFT	unspecified	14.0		0.0337	880	363		1.86	LIFT protocol used for results.
Douglas fir	Dietenberger, 1995 (c)	LIFT	6.55	17	12.1	0.095		335	0.048		Modified protocol & Janssens correlation
Douglas fir	Dietenberger, 1995 (a)	Unspecified	unspecified					336		0.254	
Douglas fir -5 layers	Grexa, White and Dietenberger, 1996	Cone	11.5		13.6			355	0.036	0.236	Janssens correlation
Douglas fir -3 layers	Grexa, White and Dietenberger, 1996	Cone	12		15.2			369	0.037	0.194	Janssens correlation
Oak veneer ply - 5 layers	Grexa, White and Dietenberger, 1996	Cone	13		8.9			279	0.030	0.465	Janssens correlation
unspecified	Quintiere & Harkleroad, 1983	LIFT	6.3-12.7	16				390		0.46-0.54	
MDF	<i>Source</i>	<i>Test</i>	<i>Thickness (mm)</i>	<i>q_{ig,min} (kW/m²)</i>	<i>q_{crit} (kW/m²)</i>	<i>b (s^{-0.5})</i>	<i>t* (s)</i>	<i>T_{ig} (°C)</i>	<i>h (kW/m²K)</i>	<i>kpc ((kW/m²k²)²)</i>	
"Customwood" MDF	ISO	ISO 5657	18	16.25	15.2	0.053	432	352	0.044	0.86	
"Customwood" MDF	LIFT	LIFT	18	16.25	14.7	0.047	293	391	0.044	1.10	
"Customwood" MDF	RIFT	RIFT	18	16.25	15.6	0.053	273	391	0.043	0.86	
	Ngu, CK. 2002	ISO 5657	20	13.50	12.9	0.043	870	348	0.039	1.04	
	Asakasan etal 1998	Cone	unspecified		7.7	0.046	486	334		0.238	
	Cleary & Quintiere, 1991	Unspecified	unspecified					361		0.732	
	Henderson, A. 1998	Cone	unspecified		1.6			330		1.377	

Melteca faced MDF	Source	Test	Thickness (mm)	$q_{ig,min}$ (kW/m ²)	q_{crit} (kW/m ²)	b (s ^{-0.5})	t^* (s)	T_{ig} (°C)	h (kW/m ² K)	kpc ((kW/m ² k ²) ²)
	ISO	ISO 5657	18	18.75	2.58	0.043	542	425	0.046	1.47
	LIFT	LIFT	18	20.00	6.44	0.042	560	440	0.045	1.47
	RIFT	RIFT	18	21.25	1.06	0.051	382	454	0.047	1.07
Melteca faced particle board	Source	Test	Thickness (mm)	$q_{ig,min}$ (kW/m ²)	q_{crit} (kW/m ²)	b (s ^{-0.5})	t^* (s)	T_{ig} (°C)	h (kW/m ² K)	kpc ((kW/m ² k ²) ²)
"Regal" brand shelving	ISO	ISO 5657	18	18.75	2.00	0.044	512	425	0.044	1.27
"Regal" brand shelving	RIFT	RIFT	18	23.75	10.1	0.057	308	478	0.050	0.97
	Asakasan et al 1998	Cone	unspecified		16.6	0.0402	576	463		0.575
	Cleary & Quintiere, 1991	LIFT	unspecified					483		0.804
Hardboard	Source	Test	Thickness (mm)	$q_{ig,min}$ (kW/m ²)	q_{crit} (kW/m ²)	b (s ^{-0.5})	t^* (s)	T_{ig} (°C)	h (kW/m ² K)	kpc ((kW/m ² k ²) ²)
	ISO	ISO 5657	5	11.25	0.59	0.033	944	307	0.039	1.83
	LIFT	LIFT	5	17.50	2.17	0.052	375	409	0.043	0.88
	RIFT	RIFT	5	11.25	2.57	0.032	977	307	0.037	1.67
	Azhakesan et al 1998	Cone	unspecified		11.1	0.0384	665	392		0.629
	Dietenberger, 1995 (b)	Cone	6		16.5			393	0.0389	0.277
	Dietenberger, 1995 (a)	Cone	unspecified					281		0.763
	Quintiere & Harkleroad, 1984	LIFT	6.35	10				298		1.87

	Quintiere & Harkleroad, 1984	LIFT	3.2	14				365		0.88	
NZ Beech	<i>Source</i>	<i>Test</i>	<i>Thickness (mm)</i>	" $q_{ig,min}$ (kW/m ²)	" q_{crit} (kW/m ²)	b (s ^{-0.5})	t^* (s)	T_{ig} (°C)	h (kW/m ² K)	kpc (kW/m ² k ²) ²	
	ISO	ISO 5657	16	18.00	11.83	0.053	355	415	0.043	0.85	
	LIFT	LIFT	16	18.75	9.24	0.050	395	425	0.044	0.98	
	RIFT	RIFT	16	18.75	12.77	0.034	844	425	0.046	2.30	
	Ngu, CK. 2002	ISO 5657	20	12.00	11.14	0.025	1618	321.33	0.040	3.27	
US Beech	Grexa, White Dietenberger, 1996	Cone	15		13.7			358	0.0358	0.508	
Radiata Pine (Monterey Pine)	<i>Source</i>	<i>Test</i>	<i>Thickness (mm)</i>	" $q_{ig,min}$ (kW/m ²)	" q_{crit} (kW/m ²)	b (s ^{-0.5})	t^* (s)	T_{ig} (°C)	h (kW/m ² K)	kpc (kW/m ² k ²) ²	
	ISO	ISO 5657	16	16.25	12.01	0.039	643	391	0.043	1.54	
	LIFT	LIFT	16	18.75	9.71	0.054	341	425	0.046	0.92	
	RIFT	RIFT	16	18.75	10.93	0.043	531	425	0.046	1.45	
	Ngu, CK. 2002	ISO 5657	20	15.50	7.78	0.047	460	380.17	0.043	1.08	
15% moisture content	Moghtaderi, B et al. 1997	Cone	unspecified							0.269	In Babrauskas 2003
11% moisture content	Henderson, A. 1998	Cone	unspecified		10.8			340		0.593	

Rimu	Source	Test	Thickness (mm)	$q_{ig,min}$ (kW/m ²)	q_{crit} (kW/m ²)	b (s ^{-0.5})	t^* (s)	T_{ig} (°C)	h (kW/m ² K)	kpc ((kW/m ² k ²) ²)	
	ISO	ISO 5657	16	18.00	12.75	0.050	397	415	0.045	1.03	
	LIFT	LIFT	16	18.50	9.62	0.050	395	422	0.046	1.06	
	RIFT	RIFT	16	21.25	13.88	0.047	462	454	0.049	1.41	
	Ngu, CK. 2002	ISO 5657	20	13.50	7.52	0.033	893	348	0.041	1.93	
10% MC	Henderson, A. 1998	Cone			10.4			355		0.548	In Babrauskas 2003
Heart - 10%MC	Henderson, A. 1998	Cone			12.6			355		0.548	In Babrauskas 2003
Macrocarpa	Source	Test	Thickness (mm)	$q_{ig,min}$ (kW/m ²)	q_{crit} (kW/m ²)	b (s ^{-0.5})	t^* (s)	T_{ig} (°C)	h (kW/m ² K)	kpc ((kW/m ² k ²) ²)	
	ISO	ISO 5657	16	18.00	15.16	0.048	436	415	0.045	1.13	
	LIFT	LIFT	16	18.75	14.68	0.059	288	425	0.046	0.78	
	RIFT	RIFT	16	18.75	15.57	0.056	325	425	0.046	0.89	
	Ngu, CK. 2002	ISO 5657	20	15.50	12.89	0.055	337	380	0.043	0.79	
	Henderson, A. 1998	Cone			11.1			402		0.376	
Particle board	Source	Test	Thickness (mm)	$q_{ig,min}$ (kW/m ²)	q_{crit} (kW/m ²)	b (s ^{-0.5})	t^* (s)	T_{ig} (°C)	h (kW/m ² K)	kpc ((kW/m ² k ²) ²)	
Pynefloor Rad. Pine flooring PB	Pynefloor ISO 5657	ISO 5657	20	13.75	3.5	0.036	755	352	0.041	1.64	
Pynefloor Rad. Pine flooring PB	Pynefloor LIFT	LIFT	20	18.75	1.7	0.051	386	425	0.044	0.96	
Pynefloor Rad. Pine flooring PB	Pynefloor RIFT	RIFT	20	21.25	4.3	0.063	250	454	0.047	0.70	

Superflake PB	Superflake ISO	ISO 5657	20	13.75	3.44	0.032	934	352	0.042	2.10	
Superflake PB	Superflake RIFT	RIFT	20	18.75	5.2	0.051	389	425	0.046	1.05	
	Dietenberger and Grexa, 1999	cone						257		1.09	
7% MC - species unspecified	Janssens M, 1992	LIFT	13	20				422	0.0431	0.277	In Babrauskas 2003
Douglas fir	Quintiere & Harkleroad, 1984	LIFT	12.7	16				382		0.94	
Douglas Fir	Dillon, S & Hamins, A. 2003	LIFT	12.8	16							In Babrauskas 2003
	Babrauskas and Wetterlund (1999),	LIFT	19	10		0.0346	836	319	0.0338	1.215	
	Cleary & Quintiere. 1991	Unspecified	Unspecified					405		0.626	
	Dietenberger, 1995 (a)	Unspecified	Unspecified					529.7		1.09	
"US particle board" 7.1% MC	Fangrat et al, 1996	Cone	12.9		3			145	0.02751	1.8	